

"One-pot" synthesis of (-)-oseltamivir,
"three-pot" synthesis of spirooxyindole
alkaloids, and mechanistic investigation of
organocatalyzed Michael addition of aldehydes
into nitroalkenes

著者	MUKAIYAMA Takasuke
学位授与機関	Tohoku University
学位授与番号	11301甲第16005号
URL	http://hdl.handle.net/10097/58839

博士論文

**”One-pot” synthesis of (–)-Oseltamivir,
“three-pot” synthesis of spirooxyindole alkaloids,
and mechanistic investigation of organocatalyzed
Michael addition of aldehydes into nitroalkenes**

(有機分子触媒を用いる不斉マイケル反応を利用したオセルタミビ
ルの 1 ポット合成及びスピロオキシインドールアルカロイド類の
3 ポット合成)

向山 貴祐

平成 26 年

”One-pot” synthesis of (–)-Oseltamivir,
“three-pot” synthesis of spirooxyindole alkaloids,
and mechanistic investigation of organocatalyzed
Michael addition of aldehydes into nitroalkenes

Takasuke Mukaiyama

2014

Acknowledgements

First and foremost, I would like to sincerely acknowledge my advisor, Prof. Yujiro Hayashi (Tohoku University) for his guidance during this study. I learned a lot of things such as logical thinking for manuscript writing, problem solving skills, and coaching. I believe these newly established skills will contribute to the success of my future career.

I would like to express my sincere appreciation to Prof. Dieter Seebach (ETH Zurich) for significant discussions regarding the mechanistic study of the Michael reaction of α -alkoxyaldehydes with nitroalkenes. It was my greatest honor working with him at the ETH Zurich. I became more enthusiastic in chemistry to see your passion and attitude for chemistry.

I am particular indebted to Prof. Hayato Ishikawa (Kumamoto University) for significant experiment and discussion for the synthesis of (–)-Oseltamivir, Dr. Tadafumi Uchimaru (Advanced Industrial Science and Technology) for conducting calculation study of enamines, and Dr. Hiroyuki Koshino (RIKEN) for JBCA NMR analysis.

I am grateful to all staffs in the Hayashi laboratory (Tohoku University), including Prof. Martin J. Lear, Prof. Itaru Sato, Prof. Shuji Yamashita, Prof. Kotaro Iwasaki, and Ms. Michiko Fukushima for their great support.

I would express my hearty thanks to all co-workers on this study, especially, Mr. Kento Ogata (Tohoku University) for his dedication to the synthesis of spirooxyindole alkaloids.

I also would express my hearty thanks to Dr. Albert K Beck, Dr. Xiaoyu Sun, and Dr. Nirupam Purkayastha for supporting me not only research but also life at the ETH Zurich.

My special thanks are due to Prof. Junichiro Yamaguchi (Nagoya University) for keeping me motivated by many encouraging messages.

Finally, I would like to thank to Mr. Shigenobu Umemiya (Hayashi lab) and all past and current members of the Hayashi laboratory.

Dedication

This dissertation is dedicated to my family; my parents, Mr. Mitsunori Mukaiyama and Ms. Naoko Mukaiyama; my parents in law, Mr. Tsuyoshi Kimoto and Ms. Yoshiko Kimoto; and my wife Emi Mukaiyama. Without their understanding, encouraging, and valuable supports, this work would never have been completed.

Contents

Chapter 1 Introduction

Chapter 2 One-pot synthesis of (–)-Oseltamivir and mechanistic insights into organocatalyzed Michael reaction

- 2-1 Synthetic plan
- 2-2 Michael reaction of α -alkoxyaldehyde with *cis*-nitroalkene
- 2-3 One-pot synthesis of (–)-Oseltamivir
- 2-4 Mechanistic insights into organocatalyzed Michael reaction
 - 2-4-1 Background of asymmetric organocatalyzed Michael reaction of aldehyde with nitroalkene
 - 2-4-2 Strange stereoselectivity in the organocatalyzed Michael reaction
 - 2-4-3 The geometry of enamine
 - 2-4-4 The reactivity of enamine toward *trans*-nitroalkene
 - 2-4-5 The reactivity of enamine toward *cis*-nitroalkene
 - 2-4-6 Michael reaction of α -alkoxyaldehyde with other *cis*-Michael acceptor
 - 2-4-7 Transition state models
- 2-5 Conclusion

Chapter 3 Asymmetric Michael addition of nitromethane to 2-oxoindoline-3-ylidene acetaldehyde and three “one-pot” sequential synthesis of (–)-Horsfiline and (–)-Coerulescine

- 3-1 Retrosynthesis
- 3-2 Synthesis of 2-oxoindoline-3-ylidene acetaldehyde
- 3-3 Construction of all-carbon quaternary stereogenic centers
- 3-4 Determination of absolute configuration of Michael product
- 3-5 Three “one-pot” sequential synthesis of (*R*)-Horsfiline and (*R*)-Coerulescine
- 3-6 Determination of absolute configuration of (–)-Coerulescine
- 3-7 Conclusion

Chapter 4 Conclusion

Experimental section

List of publications

Publications in doctoral thesis

Chapter 2

“One-pot synthesis of (–)-Oseltamivir and mechanistic insights into organocatalyzed Michael reaction”

T. Mukaiyama, H. Ishikawa, H. Koshino, Y. Hayashi

Chem. Eur. J. **2013**, *19*, 17789.

“Stoichiometric Reactions of Enamines Derived from Diphenylprolinol Silyl Ethers with Nitro Olefins and Lessons for the Corresponding Organocatalytic Conversions – a Survey”

D. Seebach, S. Xiaoyu, M. O. Ebert, W. B. Schweizer, N. Purkayastha, A. K. Beck, J. Duschmalé, H. Wennemers, **T. Mukaiyama**, M. Benohoud, Y. Hayashi, M. Reiher

Helv. Chim. Acta **2013**, *96*, 799.

Chapter 3

“Asymmetric organocatalyzed Michael addition of nitromethane to 2-oxoindoline-3-ylidene acetaldehyde and three “one-pot” sequential synthesis of (–)-horsfiline and (–)-coerulescine”

T. Mukaiyama, K. Ogata, I. Sato, Y. Hayashi

Chem. Eur. J. in press

Other publications

“Diphenylprolinol silyl ether catalyzed asymmetric Michael reaction of nitroalkanes and β,β -disubstituted α,β -unsaturated aldehydes for the construction of all-carbon quaternary stereogenic centers”

Y. Hayashi, Y. Kawamoto, M. Honda, D. Okamura, S. Umemiya, Y. Noguchi, **T. Mukaiyama**, I. Sato

Chem. Eur. J. in press

“Diarylprolinol in an asymmetric, direct cross-aldol reaction with alkynyl aldehydes”

Y. Hayashi, M. Kojima, Y. Yasui, Y. Kanda, **T. Mukaiyama**, H. Shomura, D. Nakamura, Ritmaleni, I. Sato

ChemCatChem. **2013**, *5*, 2887.

“Optimisation of a novel series of selective CNS penetrant CB₂ agonists”

C. Watson, D. R. Owen, D. Harding, K. Kon-I, M. L. Lewis, H. Mason, M. Matsumizu, **T. Mukaiyama**, M. Rodriguez-Lens, A. Shima, M. Takeuchi, I. Tran, T. Young

Bioorg. & Med. Chem. Lett. **2011**, *21*, 4284.

“First asymmetric total synthesis of Synerazol, an antifungal antibiotic, and determination of its absolute stereochemistry”

Y. Hayashi, M. Shoji, **T. Mukaiyama**, H. Gotoh, S. Yamaguchi, M. Nakata, H. Kakeya, H. Osada

J. Org. Chem. **2005**, *70*, 5643.

“Asymmetric Total Synthesis of Pseurotin A”

Y. Hayashi, M. Shoji, S. Yamaguchi, **T. Mukaiyama**, J. Yamaguchi, H. Kakeya, H. Osada

Org. Lett. **2003**, *5*, 2287.

“Asymmetric Total Synthesis of (–)-Azaspiroene, a Novel Angiogenesis Inhibitor”

Y. Hayashi, M. Shoji, J. Yamaguchi, K. Sato, S. Yamaguchi, **T. Mukaiyama**, K. Sakai, H. Kakeya, H. Osada

J. Am. Chem. Soc. **2002**, *124*, 12078-12079.

Abbreviations

Ac	acetyl
Ar	aryl
aq.	aqueous
Bn	benzyl
Boc	<i>t</i> -butoxycarbonyl
Bu	butyl
ca.	circa
cat.	catalyst
Cbz	carboxybenzyl
COSY	correlation spectroscopy
DBU	1,8-diazabicyclo[5.4.0]undec-7-ene
DMF	<i>N,N</i> -dimethylformamide
dr	diastereomer ratio
EDC	1-ethyl-3-(3-dimethylaminopropyl)carbodiimide
ee	enantiomeric excess
Et	ethyl
eq.	equivalent
h	hours
HMBC	heteronuclear multiple bond correlation
HOBT	hydroxybenzotriazole
HSQC	heteronuclear single quantum coherence
<i>i</i>	iso
JBCA	J-based configuration analysis
lit.	literature
Me	methyl
min	minutes
MS	Molecular Sieves
<i>n</i>	normal
Nap	naphthyl
NBS	<i>N</i> -bromosuccinimide
NMM	<i>N</i> -methymorpholine
NMR	nuclear magnetic resonance

NOESY	nuclear overhauser effect spectroscopy
<i>p</i> -	para-
Ph	phenyl
Py	pyridine
rt	room temperature
<i>t</i>	tertiary
TBAT	tetrabutylammonium difluorophenylsilicate
TBDPS	tertiarybutyldiphenylsilyl
TFA	trifluoroacetic acid
TFAA	trifluoroacetic anhydride
THF	tetrahydrofuran
TIPS	triisopropylsilyl
TMS	trimethylsilyl
Tol	toluene
TS	transition state

Chapter 1. Introduction

We have received much benefit from the pharmaceutical products to live healthier and longer. A number of pharmaceutical products possess a chiral center, which generates mirror image of isomers called enantiomer. The biological activity is typically different between one isomer and the other isomer in enantiomer. For instance, (*R*)-thalidomide possesses sedative activity while (*S*)-thalidomide shows teratogenesis (Figure 1). This resulted fatal birth defects crisis in the late 1950s and early 1960s all over the world.

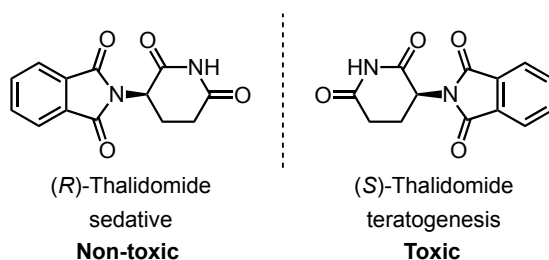


Figure 1. (*R*) and (*S*)-Thalidomide and biological activity

The selective preparation of desired enantiomer is a challenging task in the field of organic chemistry as chemical reaction usually gives 1:1 mixture of (*R*) and (*S*) isomers without selectivity. The complexes of transition metals with chiral ligands have contributed for the development of enantioselective reaction to generate enantio-enriched compounds.^[1] The metal catalysts are highly active, in other words, they are sensitive against moisture and air. The special equipment such as glove box is necessary to handle the metal catalyst. The metal waste is harmful for the environment. In addition, contamination of heavy metal residue in the final product often causes a problem, as the heavy metal possesses toxicity. Recently, the shortage of rare metal and increase of price have become worldwide problem, affecting the production of metal catalyst. Therefore, the development of new catalyst, playing a complementary role with a metal catalyst, is required to secure the production of enantio-enriched products in the world.

Organocatalysts are expected to solve the above-mentioned problem. Organocatalyst is constituted by elements such as carbon, nitrogen, hydrogen, sulfur, and so on, not including any metal. Since List, Barbas III and Lerner have discovered that intermolecular aldol reaction of acetone with aldehydes can be catalyzed by proline,^[2] one of amino acids, the field of organocatalyst is rapidly growing.^[3] Benefits of organocatalyst are as follows; 1) insensitive to moisture and air, 2) operationally easy to handle, 3) non toxic, 4) inexpensive. The organocatalysts have been contributing for the development of novel asymmetric reactions to generate enantio-enriched compounds.

On the other hand, the development of environmentally benign methods is a current key topic in chemistry. When synthesizing molecules we need to consider both efficiency and sustainability, as indicated by terminology such as atom economy,^[4] and step economy.^[5]

Atom economy is the conversion efficiency of a chemical process in terms of all atoms involved, which was proposed by Trost.^[4] The concept of atom economy is shown in Figure 2. When all atoms in the starting materials (**A**, **B**, and **C**) are incorporated in the product without the generation of waste, it is regarded as high atom economy (eq. 1). On the other hand, when waste **D** is generated, it is regarded as low atom economy (eq. 2). High atom economy is regarded as an important chemical process from the point of view of environmental concern as the high atom economy chemical process hardly generates a chemical wastes.

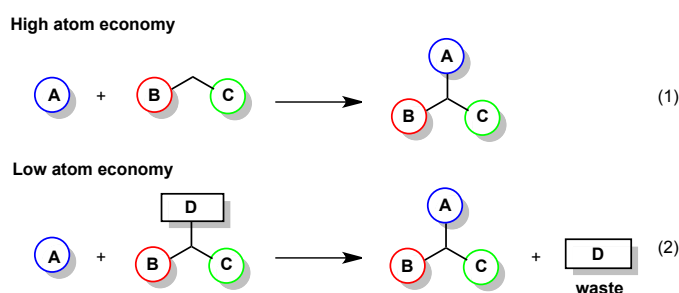


Figure 2. Concept of atom economy

Step economy is a terminology proposed by Wender.^[5] The number of reaction steps affects to the efficiency of a synthetic route. The number of reaction step is shorter, the synthetic route is more efficient in terms of cost and time. Ideally, complex molecules would be synthesized in short number of steps.

In addition to these terminologies, our group proposed “pot economy”.^[6] The synthetic method to conduct several transformations in a single vessel is called “one-pot” reaction. Since several transformations and bond formations can be achieved in a single vessel, it cuts several purification operations, and minimizes chemical wastes, enabling a shorter total production time. Thus, a “one-pot” reaction can also be regarded as environmentally benign, and “pot economy” should be considered when planning a synthesis.

Our group has applied the concept of “pot-economy” to the synthesis of several biologically active compounds. In 2009, our group reported a sequential synthesis of (–)-Oeltamivir by three “one-pot” operations,^[7] which was modified into two “one-pot” sequences in 2010.^[8] We also reported the “one-pot” synthesis of ABT-341^[9] and the synthesis of prostaglandin E₁ methyl ester in three “one-pot” operations.^[6]

The “one-pot” reaction is environmentally benign method and has a potential to reduce a number of reaction steps, enabling the synthesis of complex molecules easier compared with

previous way. Therefore, I aimed to develop an efficient synthetic method of chiral molecules, which possess interesting biological activity, by applying “one-pot” reaction with the construction of stereogenic centers by organocatalyzed asymmetric reaction. (–)-Oseltamivir (1-1), (–)-Horsfiline (1-2), and (–)-Coerulescine (1-3), were selected as a target molecules (Figure 3).

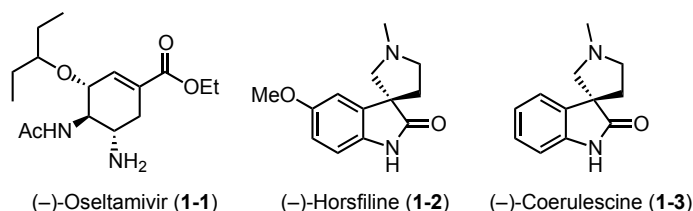


Figure 3. (–)-Oseltamivir (1-1), (–)-Horsfiline (1-2), and (–)-Coerulescine (1-3)

1-1. “One-pot” synthesis of (–)-Oseltamivir (Chapter 2)

(–)-Oseltamivir phosphate (Tamiflu®), a neuraminidase inhibitor, is one of the most effective drugs that has been extensively used for the treatment of influenza (Figure 4). For this reason, many synthetic chemists have investigated its effective preparation, and a large number of synthetic methods have been reported.^[10] Although 62 synthetic methods have been reported including Corey,^[11] Shibasaki,^[12] Fukuyama,^[13] and Trost^[14] to date, a robust and efficient preparation method is still required to produce sufficient quantity of (–)-Oseltamivir for worldwide use.

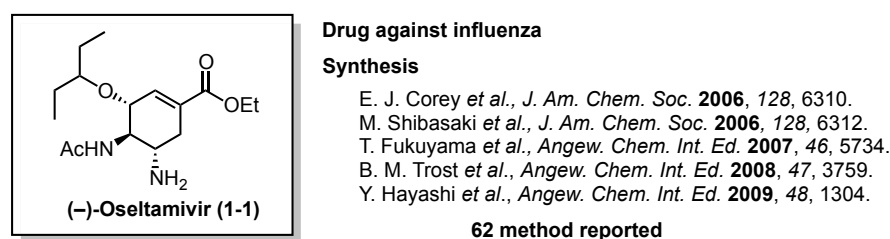
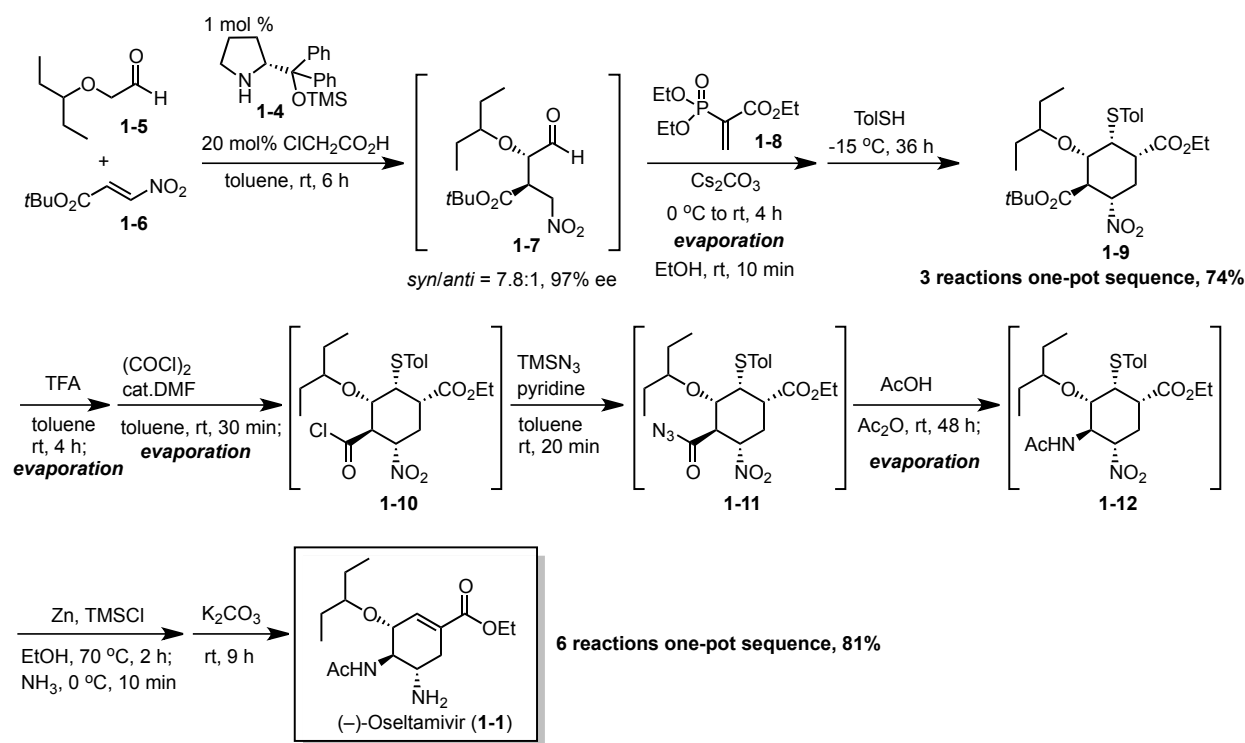


Figure 4. (–)-Oseltamivir

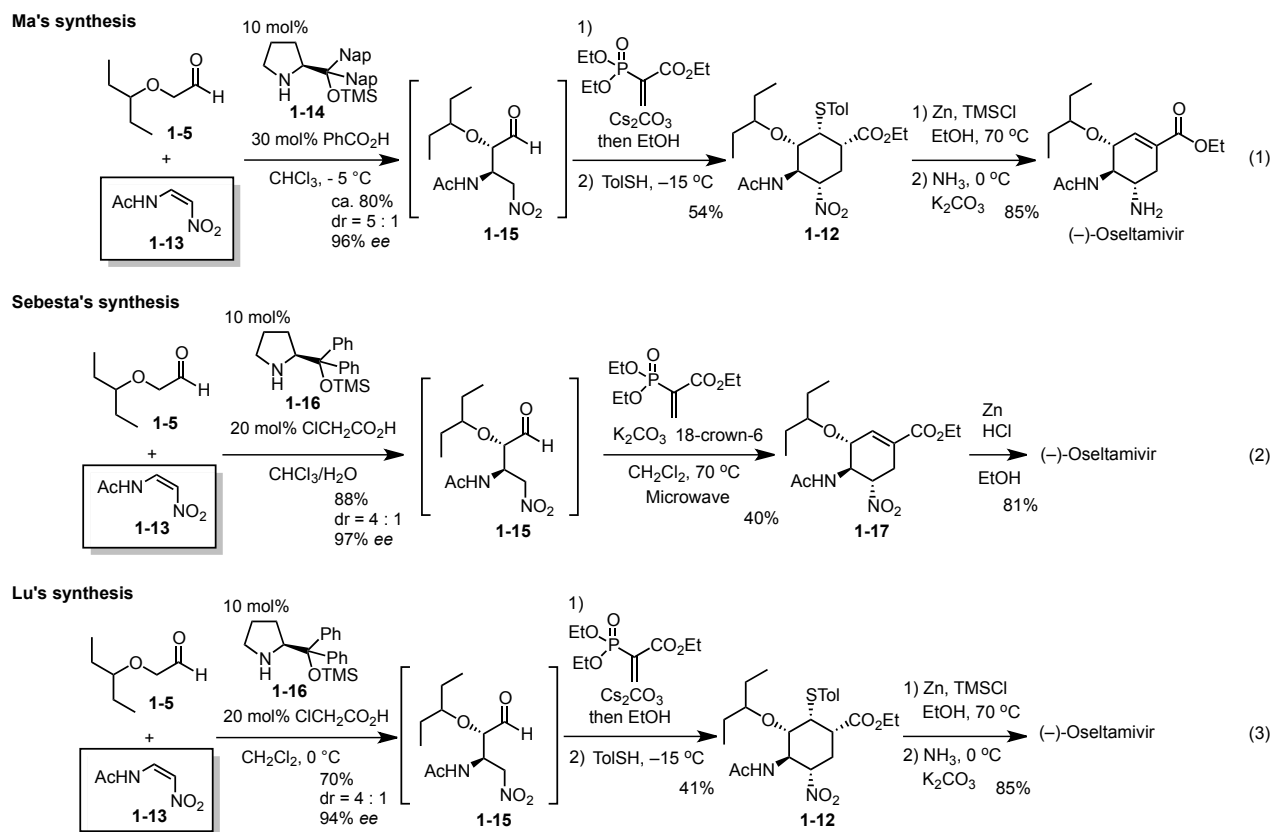
Previously, Dr. Ishikawa in our group developed three “one-pot” sequential synthesis of (–)-Oseltamivir (1) in 2009,^[7] which was modified into two “one-pot” sequential synthesis in 2010.^[8] In the two “one-pot” synthesis of 1-1, the first one-pot sequence started by the Michael reaction of α -alkoxyaldehyde 1-5 and *trans*-nitroalkene 1-6, as catalyzed by (*R*)-diphenylprolinol silyl ether 1-4, the organocatalyst of which has been developed by our group^[15] and that of Jørgensen,^[16] independently (Scheme 1). Without isolation, the generated Michael product 1-7 was treated with the ethyl acrylate derivative 1-8. After evaporation, the addition of toluenethiol afforded the cyclohexane 1-9 with control of five consecutive chiral

centers. The next, second one-pot sequence started by trifluoroacetic acid hydrolysis of the *tert*-butylester. Subsequently, the acid chloride **1-10** was generated, which was followed by Curtius rearrangement via the acyl azide **1-11** to generate the acetamide **1-12**. The nitro group was reduced to a primary amine, and retro-Michael reaction of the toluenethiol group furnished **1-1**. Solvent exchange was employed three times in the second “one-pot” sequence, even though the reaction sequences were carried out in the same vessel. Clearly, it would be synthetically and operationally more ideal if the evaporation process and solvent exchange could be omitted in the “one-pot” operation. This would thus enable a reduction in solvent wastage, production time, and cost.



Scheme 1. Two “one-pot” sequential synthesis of (-)-Oseltamivir (**1-1**)

After publication of the “one-pot” synthesis of (-)-Oseltamivir, Ma,^[17] Sebesta^[18] and Lu^[19] have independently reported the synthesis of (-)-Oseltamivir in a short number of steps via a similar route to ours (Scheme 2). The key change to our original route is that they all employed (*Z*)-*N*-2-nitroethenylacetamide **1-13** as a starting material. This more conveniently possesses an aminoacetyl group instead of a (*E*)-*tert*-butyl-3-nitropropenoate **1-6** and importantly avoids a potentially explosive Curtius rearrangement of an acyl azide intermediate **1-11**.



Scheme 2. Synthesis of (-)-Oseltamivir using *cis*-nitroalkene **1-13**

When I repeated the key Michael reaction between α -alkoxyaldehyde **1-5** and (*Z*)-*N*-2-nitroethenylacetamide **1-13** in CHCl_3 in the presence of PhCO_2H , catalyzed by diphenylprolinol silyl ether **1-16**, the yield and diastereoselectivity was low. Given this result and to avoid environmentally unfriendly solvents (e.g., CHCl_3 and CH_2Cl_2) for large-scale production, we set out to determine reliable conditions, under which the desired aldehyde-nitroalkene Michael adduct would be obtained in good yield with excellent diastereo- and enantio-selectivities. Moreover, we aimed to realize a completely “one-pot” sequential synthesis of (-)-Oseltamivir (**1-1**) without any evaporation or solvent exchange by the optimization of all subsequent reactions. During our investigation into the organocatalyzed Michael reactions, including those between α -alkoxylaldehydes and *cis*-nitroalkenes, we found that an acid additive is important to improve both selectivity and reactivity issues, which promoted us to investigate the effect of acid.

In the chapter 2, the successful realization of a completely “one-pot” synthesis of (-)-Oseltamivir (**1-1**) without any solvent exchange, along with several new findings about the effect of acid and course of the Michael reaction will be discussed.

1-2. Three “one-pot” sequential synthesis of (–)-Horsfiline and (–)-Coerulescine (Chapter 3)

The concept of “one-pot” was extended to the synthesis of spirooxyindole alkaloids. (–)-Horsfiline (**1-2**) and (–)-Coerulescine (**1-3**) are spirooxyindole alkaloids that have been isolated from *Horsfieldia superba* in 1991 by Bodo’s group^[20] and from *Pharalis coerulescens* in 1998 by Colegate’s group (Figure 5).^[21] The spirooxyindole alkaloids show a variety of biological activities; for instance, (–)-Horsfiline (**1-2**) is used as an intoxicating snuff substance,^[20] Spirotryprostatin A (**1-18**) inhibits G2/M progression of mammalian tsFT210 cells,^[22] and Strychnofoline (**1-19**) inhibits various cell lines.^[23] Due to such diverse bioactivities, spirooxyindole derivatives have become attractive targets for drug discovery.^[24]

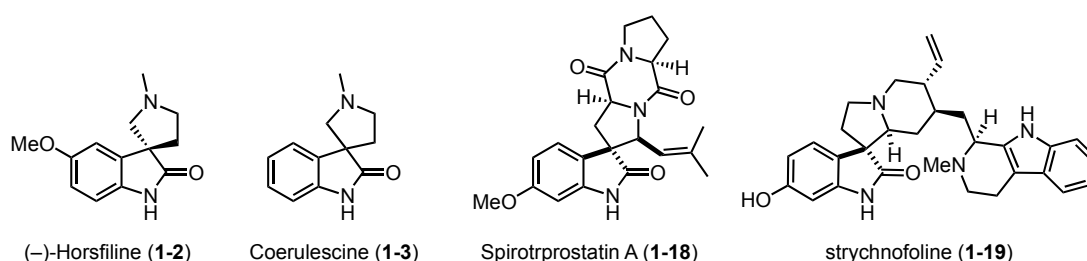


Figure 5. Structure of spirooxyindole alkaloids

We aimed to develop an efficient synthesis of both (–)-Horsfiline (**1-2**) and (–)-Coerulescine (**1-3**) via a common spirocyclic intermediate. Here, the main challenge was to construct the all-carbon, quaternary spirocyclic carbon stereocenter in a catalytic enantioselective fashion. Although several methods have been reported for the synthesis of racemic horsfiline and coerulescine,^[25] there are five reports and one report for the synthesis of enantio-enriched horsfiline and coerulescine, respectively (Figure 6). For the synthesis of enantio-enriched horsfiline, Borschberg’s group employed a diastereoselective oxidative rearrangement of a chiral tetrahydro- β -carboline and determined the absolute configuration by synthesizing both enantiomers (eq. 1).^[26] Palmisano’s group used a diastereoselective 1,3-dipolar cycloaddition of a chiral ester auxiliary with *N*-methylazomethine ylide (eq. 2).^[27] An asymmetric nitro olefination by Fuji’s group (eq. 3),^[28] a palladium catalyzed asymmetric allylic alkylation by Trost’s group (eq. 4),^[29] and an enantioselective phase-transfer catalytic allylation by Park’s group (eq. 5),^[30] have also been employed to construct the all-carbon quaternary stereogenic centers. Except for Park’s group synthesis, all routes require around 10 steps and total yield is low (eq. 1, 2, 3, 4). In addition, catalytic asymmetric reaction is reported only two examples and enantioselectivity of constructing the asymmetric quaternary carbon center is not perfect (eq. 4, 5).

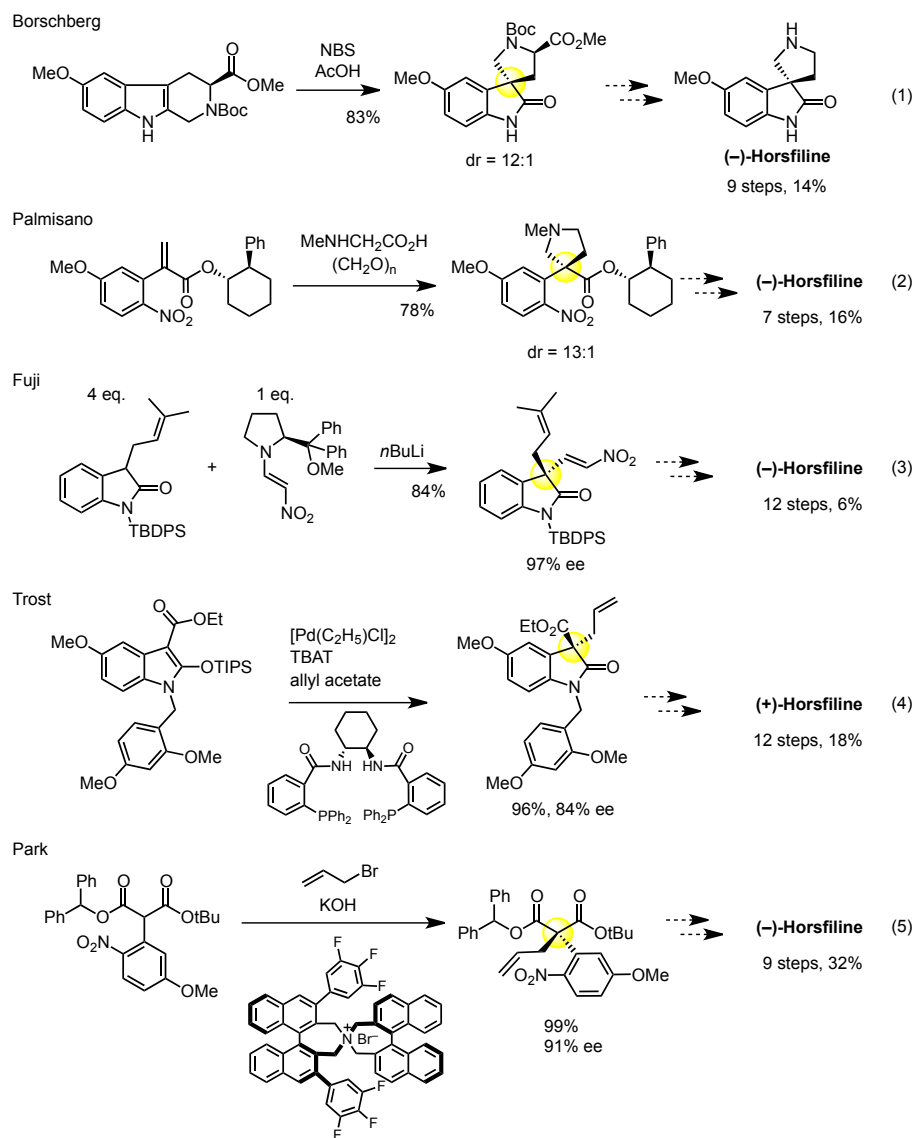


Figure 6. Construction of all-carbon quaternary stereogenic centers

The enantio-enriched (*S*)-coerulescine has also been synthesized in the total synthesis of phalarine by Danishefsky's group.^[31] They also report an optical rotation of -0.55 for (*S*)-Coerulescine, although no solvent was specified. Thus, the absolute configuration of (-)-Coerulescine (**1-3**) still remains to be determined unambiguously.

Pertinent to the current targets, we have not only developed the synthesis of α,β -unsaturated aldehyde from acetaldehyde and arylaldehydes (Figure 7, eq. 1),^[32] but also developed the enantioselective conjugate addition of nitromethane to α,β -unsaturated aldehydes using diphenylprolinol silyl ether.^[33] Recently, we also reported Michael addition of nitromethane or nitroethane to β,β -disubstituted- α,β -unsaturated aldehydes to construct all-carbon quaternary stereogenic centers in excellent enantioselective manner (Figure 7, eq. 2).^[34] We envisioned that these methodologies should be applicable to the synthesis of horsfiline and coerulescine. We

selected an isatin derivative and acetaldehyde as suitable starting materials to synthesize the 2-oxoindoline-3-ylidene acetaldehyde (Figure 3, eq. 3, step 1). If the Michael addition of nitromethane to 2-oxoindoline-3-ylidene acetaldehyde proceeds, the all-carbon quaternary stereogenic centers would be constructed (Figure 3, eq. 3, step 2).^[35]

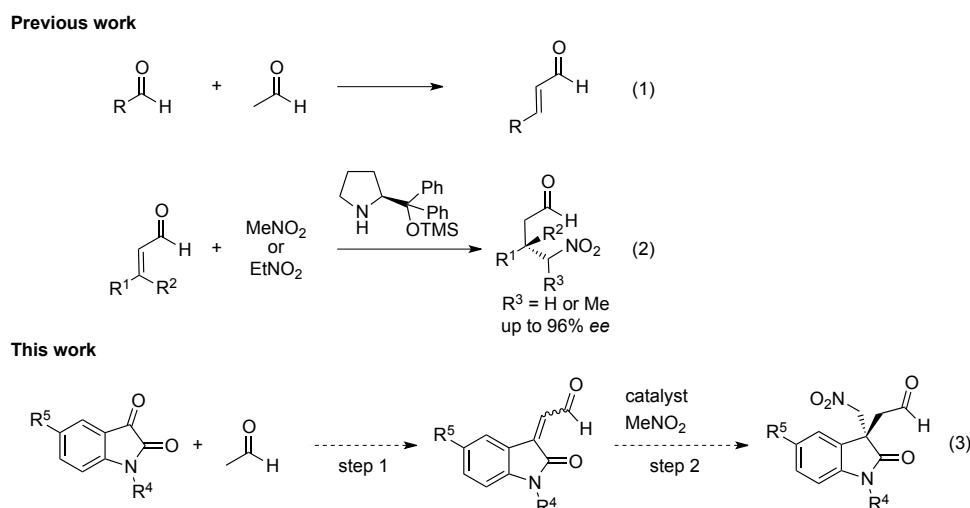


Figure 7. Synthesis of α,β -unsaturated aldehyde and construction of quaternary carbon center

In chapter 3, the three “one-pot” sequential synthesis of both (–)-Horsfiline (**1-2**) and (–)-Coerulescine (**1-3**) will be described. Key reactions are as follows, 1) the synthesis of 2-oxoindoline-3-ylidene acetaldehyde from acetaldehyde and an isatin derivative, and 2) the organocatalyzed Michael addition of nitromethane to 2-oxoindoline-3-ylidene acetaldehyde to construct the all-carbon quaternary stereogenic centers with excellent enantioselectivity. Furthermore, we synthesized (*S*)-Coerulescine according to Danishefsky’s route to verify the small optical rotation of Coerulescine and define the solvent for optical rotation comparison. In this way, we determined the absolute configuration of (–)-Coerulescine to be (*R*).

References and notes

- [1] Review see; M. Shibasaki, H. Sasai, T. Arai, *Angew. Chem. Int. Ed.* **1997**, *36*, 1236.
- [2] B. List, R. A. Lerner, C. F. Barbas III, *J. Am. Chem. Soc.* **2000**, *122*, 2395.
- [3] Reviews, see: a) *Asymmetric Organocatalysis 1: Lewis Base and Acid Catalysts in Science of Synthesis*, ed. By B. List, Georg Thieme Verlag KG, Stuttgart, **2012**; b) *Asymmetric Organocatalysis 2: Bronsted Base and Acid Catalysts, and Additional Topics in Science of Synthesis*, ed. By K. Maruoka, Georg Thieme Verlag KG, Stuttgart, **2012**.
- [4] B. M. Trost, *Science* **1991**, *254*, 1471.
- [5] P. A. Wender, V. A. Verma, T. J. Paxton, T. H. Pillow, *Acc. Chem. Res.* **2008**, *41*, 40.
- [6] Y. Hayashi, S. Umemiya, *Angew. Chem. Int. Ed.* **2013**, *52*, 3450.
- [7] H. Ishikawa, T. Suzuki, Y. Hayashi, *Angew. Chem. Int. Ed.* **2009**, *48*, 1304.
- [8] H. Ishikawa, T. Suzuki, H. Orita, T. Uchimar, Y. Hayashi, *Chem. Eur. J.* **2010**, *16*, 12616.
- [9] H. Ishikawa, M. Honma, Y. Hayashi, *Angew. Chem. Int. Ed.* **2011**, *50*, 2824.
- [10] a) J. C. Rohloff, K. M. Kent, M. J. Postich, M. W. Becker, H. H. Chapman, D.E. Kelly, W. Lew, M.S. Louie, L.R. McGee, E.J. Prisbe, L. M. Schultze, R. H. Yu, L. J. Zhang, *J. Org. Chem.* **1998**, *63*, 4545; b) M. Federspiel, R. Fischer, M. Hennig, H.-J. Mair, T. Oberhauser, G. Rimm-ler, T. Albiez, J. Bruhin, H. Estermann, C. Gandert, V. Gçckel, S. Gçtzç, U. Hoffmann, G. Huber, G. Janatsch, S. Lauper, O. Rçckel-Ståbler, R. Trussardi, A. G. Zwahlen, *Org. Process Res. Dev.* **1999**, *3*, 266; c) M. Karpf, R. Trussardi, *J. Org. Chem.* **2001**, *66*, 2044; d) S. Abrecht, M. Karpf, R. Trussardi, B. Wirz, EP 1127872 A1, 2001; *Chem. Abstr.* **2001**, *135*, 195452; e) U. Zutter, H. Iding, B. Wirz, EP 1146036 A2, 2001; *Chem. Abstr.* **2001**, *135*, 303728; f) P. J. Harrington, J. D. Brown, T. Foderaro, R. C. Hughes, *Org. Process Res. Dev.* **2004**, *8*, 86; g) S. Abrecht, P. Har- rington, H. Iding, M. Karpf, R. Trussardi, B. Wirz, U. Zutter, *Chimia* **2004**, *58*, 621; h) Y.-Y. Yeung, S. Hong, E. J. Corey, *J. Am. Chem. Soc.* **2006**, *128*, 6310; i) Y. Fukuta, T. Mita, N. Fukuda, M. Kanai, M. Shibasaki, *J. Am. Chem. Soc.* **2006**, *128*, 6312; j) X. Cong, Z.-J. Yao, *J. Org. Chem.* **2006**, *71*, 5365; k) S. Abrecht, M. C. Federspiel, H. Es- termann, R. Fischer, M. Karpf, H.-J. Mair, T. Oberhauser, G. Rimm- ler, R. Trussardi, U. Zutter, *Chimia* **2007**, *61*, 93; l) N. Satoh, T. Akiba, S. Yokoshima, T. Fukuyama, *Angew. Chem.* **2007**, *119*, 5836; *Angew. Chem. Int. Ed.* **2007**, *46*, 5734; m) J.-J. Shie, J.-M. Fang, S.-Y. Wang, K.-C. Tsai, Y.-S. E. Cheng, A.-S. Yang, S.-C. Hsiao, C.-Y. Su, C.-H. Wong, *J. Am. Chem. Soc.* **2007**, *129*, 11892; n) T. Mita, N. Fukuda, F. X. Roca, M. Kanai, M. Shibasaki, *Org. Lett.* **2007**, *9*, 259; o) K. M. Bromfield, H. GradØn, D. P. Hagberg, T. Olsson, N. Kann, *Chem. Commun.* **2007**, 3183; p) K. Yamatsugu, S. Kamijo, Y. Suto, M. Kanai, M. Shaibasaki, *Tetrahedron Lett.* **2007**, *48*, 1403; q) U. Zutter, H. Iding, P. Spurr, B. Wirz, *J. Org. Chem.* **2008**, *73*, 4895; r) B. M. Trost,

T. Zhang, *Angew. Chem.* **2008**, *120*, 3819; *Angew. Chem. Int. Ed.* **2008**, *47*, 3759; s) J.-J. Shie, J.-M. Fang, C.-H. Wong, *Angew. Chem.* **2008**, *120*, 5872; *Angew. Chem. Int. Ed.* **2008**, *47*, 5788; t) M. Matveenko, M. G. Banwell, A. C. Willis, *Tetrahedron Lett.* **2008**, *49*, 7018; u) N. T. Kipassa, H. Okamura, K. Kina, T. Hamada, T. Iwagawa, *Org. Lett.* **2008**, *10*, 815; v) L.-D. Nie, X.-X. Shi, K. H. Ko, W.-D. Lu, *J. Org. Chem.* **2009**, *74*, 3970 ; w) T. Mandai, T. Oshitari, *Synlett* **2009**, 783; x) T. Oshitari, T. Mandai, *Synlett* **2009**, 787; y) H. Sun, Y.-J. Lin, Y.-L. Wu, Y. Wu, *Synlett* **2009**, 2473; z) K. Yamatsugu, L. Yin, S. Kamijo, Y. Kimura, M. Kanai, M. Shibasaki, *Angew. Chem.* **2009**, *121*, 1090; *Angew. Chem. Int. Ed.* **2009**, *48*, 1070; aa) B. Sullivan, I. Carrera, M. Drouin, T. Hudlicky, *Angew. Chem.* **2009**, *121*, 4293; *Angew. Chem. Int. Ed.* **2009**, *48*, 4229; ab) M. Karpf, R. Trussardi, *Angew. Chem.* **2009**, *121*, 5871; *Angew. Chem. Int. Ed.* **2009**, *48*, 5760; ac) N. Satoh, T. Akiba, S. Yokoshima, T. Fukuyama, *Tetrahedron* **2009**, *65*, 3239; ad) L.-D. Nie, X.-X. Shi, *Tetrahedron : Asymmetry* **2009**, *20*, 124; ae) K. Yamatsugu, M. Kanai, M. Shibasaki, *Tetrahedron* **2009**, *65*, 6017; af) H. Osato, I. L. Jones, A. Chen, C. L. L. Chai, *Org. Lett.* **2010**, *12*, 60; ag) L. Werner, A. Machara, T. Hudlicky, *Adv. Synth. Catal.* **2010**, *352*, 195; ah) A. Kamimura, T. Nakano, *J. Org. Chem.* **2010**, *75*, 3133; ai) J. Weng, Y.-B. Li, R.-B. Wang, F.-Q. Li, C. Liu, A. S. C. Chan, G. Lu, *J. Org. Chem.* **2010**, *75*, 3125; aj) J. Ma, Y. Zhao, S. Ng, J. Zhang, J. Zeng, A. Than, P. Chen, X.-W. Liu, *Chem. Eur. J.* **2010**, *16*, 4533; ak) P. Wichienukul, S. Akkarasamiyo, N. Kongkathip, B. Kongkathip, *Tetrahedron Lett.* **2010**, *51*, 3208; al) J. S. Ko, J. E. Keum, S. Y. Ko, *J. Org. Chem.* **2010**, *75*, 7006; am) S. Raghavan, V. S. Babu, *Tetrahedron* **2011**, *67*, 2044; an) B. M. Trost, T. Zhang, *Chem. Eur. J.* **2011**, *17*, 3630; ao) T. Tanaka, Q. Tan, H. Kawakubo, M. Hayashi, *J. Org. Chem.* **2011**, *76*, 5477; ap) L.-D. Nie, X.-X. Shi, N. Quan, F.-F. Wang, X. Lu, *Tetrahedron: Asymmetry* **2011**, *22*, 1692; aq) L. Werner, A. Machara, B. Sullivan, I. Carrera, M. Moser, D. R. Adams, T. Hudlicky, *J. Org. Chem.* **2011**, *76*, 10050; ar) M. Trajkovic, Z. Ferjancic, R. N. Saicic, *Org. Biomol. Chem.* **2011**, *9*, 6927; as) N. Chuanopparat, N. Kongkathip, B. Kongkathip, *Tetrahedron Lett.* **2012**, *53*, 6209; at) T.-J. Cheng, S. Weinheimer, E. B. Tarbet, J.-T. Jan, Y.-S. Cheng, J.-J. Shie, C.-L. Chen, C.-A. Chen, W.-C. Hsieh, P.-W. Huang, *J. Med. Chem.* **2012**, *55*, 8657; au) H.-S. Oh, H.-Y. Kang, *J. Org. Chem.* **2012**, *77*, 8792; av) N. Chuanopparat, N. Kongkathip, B. Kongkathip, *Tetrahedron* **2012**, *68*, 6803; aw) L.-D. Nie, W. Ding, X.-X. Shi, N. Quan, X. Lu, *Tetrahedron Asymmetry* **2012**, *23*, 742; ax) V. Rawat, S. Dey, A. Sudalai, *Org. Biomol. Chem.* **2012**, *10*, 3988; ay) D. S. Gunasekera, *Synlett* **2012**, *23*, 573; az) H.-K. Kim, K.-J. J. Park, *Tetrahedron Lett.* **2012**, *53*, 1561; ba) M. Trajkovic, Z. Ferjancic, R. N. Saicic, *Synthesis* **2013**, *45*, 389; bb) K. Alagiri, M. Furutachi, K. Yamatsugu, N. Kumagai, T. Watanabe, M. Shibasaki, *J. Org. Chem.* **2013**, *78*, 4019; bc) L.

- D. Nie, F. F. Wang, W. Ding, X. X. Shi, X. Lu, *Tetrahedron Asymmetry* **2013**, *24*, 638; bd) H. Ishikawa, T. Suzuki, Y. Hayashi, *Angew. Chem.* **2009**, *121*, 1330; *Angew. Chem. Int. Ed.* **2009**, *48*, 1304; be) H. Ishikawa, T. Suzuki, H. Orita, T. Uchimaru, Y. Hayashi, *Chem. Eur. J.* **2010**, *16*, 12616; bf) H. Ishikawa, B. P. Bondzic, Y. Hayashi, *Eur. J. Org. Chem.* **2011**, *30*, 6020; bg) T. Mukaiyama, H. Ishikawa, H. Koshino, Y. Hayashi, *Chem. Eur. J.* **2013**, *19*, 17789; bh) S. Zhu, S. Yu, Y. Wang, D. Ma, *Angew. Chem.* **2010**, *122*, 4760; *Angew. Chem. Int. Ed.* **2010**, *49*, 4656; bi) J. Rehpuk, M. Hut'ka, A. Latika, H. Brath, A. Almassy, V. Hajzer, J. Durmis, S. Toma, R. Sebesta, *Synthesis* **2012**, *44*, 2424; bj) J. Weng, Y.-B. Li, R.-B. Wang, G. Lu, *ChemCatChem* **2012**, *4*, 1007. Review, see: bk) V. Farina, J. D. Brown, *Angew. Chem.* **2006**, *118*, 7488; *Angew. Chem. Int. Ed.* **2006**, *45*, 7330; bl) M. Shibasaki, M. Kanai, *Eur. J. Org. Chem.* **2008**, 1839; bm) J. Magano, *Chem. Rev.* **2009**, *109*, 4398; bn) J. Andraos, *Org. Process Res. Dev.* **2009**, *13*, 161; bo) J. Magano, *Tetrahedron* **2011**, *67*, 7875; bp) M. Shibasaki, M. Kanai, K. Yamatsugu, *Isr. J. Chem.* **2011**, *51*, 316.
- [11] Y. -Y. Yeung, S. Hong, E. J. Corey, *J. Am. Chem. Soc.* **2006**, *128*, 6310.
- [12] Y. Fukuta, T. Mita, N. Fukuda, M. Kanai, M. Shibasaki, *J. Am. Chem. Soc.* **2006**, *128*, 6312.
- [13] N. Satoh, T. Akiba, S. Yokoshima, T. Fukuyama, *Angew. Chem. Int. Ed.* **2007**, *36*, 5734.
- [14] B. M. Trost, T. Zhang, *Angew. Chem. Int. Ed.* **2008**, *47*, 3759.
- [15] Y. Hayashi, H. Gotoh, T. Hayashi, M. Shoji, *Angew. Chem. Int. Ed.* **2005**, *44*, 4212.
- [16] M. Marigo, T. C. Wabnitz, D. Fielenbach, K. A. Jørgensen, *Angew. Chem. Int. Ed.* **2005**, *44*, 794.
- [17] S. Zhu, S. Yu, Y. Wang, D. Ma, *Angew. Chem. Int. Ed.* **2010**, *49*, 4656.
- [18] a) J. Rehpuk, M. Hut'ka, A. Latika, H. Brath, A. Almassy, V. Hajzer, J. Durmis, S. Toma, R. Sebesta, *Synthesis* **2012**, *44*, 2424; b) V. Hajzer, A. Latika, J. Durmis, R. Sebesta, *Helv. Chim. Acta* **2012**, *95*, 2421.
- [19] J. Weng, Y.-B. Li, R.-B. Wang, G. Lu, *ChemCatChem* **2012**, *4*, 1007.
- [20] A. Jossang, P. Jossang, H. A. Hadi, T. Sévenet, B. Bodo, *J. Org. Chem.* **1991**, *56*, 6527.
- [21] N. Anderton, P. A. Cockrum, S. M. Colegate, J. A. Edgar, K. Flower, I. Vit, R. I. Willing, *Phytochemistry* **1998**, *48*, 437.
- [22] a) C. B. Cui, H. Kakeya, H. Osada, *Tetrahedron* **1996**, *52*, 12651; b) C. B. Cui, H. Kakeya, H. Osada, *J. Antibiot.* **1996**, *49*, 832.
- [23] O. Dideberg, J. Lamotte-Brasseur, L. Dupont, H. Campsteyn, M. Vermeire, L. Angenot, *Acta Crystallogr. Sect. B* **1977**, *33*, 1796.
- [24] Review see, C. V. Galliford, K. A. Scheidt, *Angew. Chem. Int. Ed.* **2007**, *46*, 8748.
- [25] a) K. Jones, J. Wilkinson, *J. Chem. Soc. Chem. Commun.* **1992**, 1767; b) S. Bascop, J. Sapi,

- J. Laronze, J. Levy, *Heterocycles* **1994**, *38*, 725; c) C. Fischer, C. Meyers, E. M. Carreira, *Helv. Chim. Acta* **2000**, *83*, 1175; d) M. Somei, K. Noguchi, R. Yamagami, Y. Kawada, K. Yamada, F. Yamada, *Heterocycles* **2000**, *53*, 7; e) U. K. Syam Kumar, H. Illa, H. Junjappa, *Org. Lett.* **2001**, *3*, 4193; f) N. Selvakumar, A. M. Azhagan, D. Srinivas, G. G. Krishna, *Tetrahedron Lett.* **2002**, *43*, 9175; g) D. E. Lizos, J. A. Murphy, *Org. Biomol. Chem.* **2003**, *1*, 117; h) J. A. Murphy, R. Tripoli, T. A. Khan, U. W. Mali, *Org. Lett.* **2005**, *7*, 3287; i) M. Y. Chang, C.-L. Pai, Y.-H. Kung, *Tetrahedron Lett.* **2005**, *46*, 8463; j) J. D. White, Y. Li, C. David, D. C. Ihle, *J. Org. Chem.* **2010**, *75*, 3569; k) N. Deppermann, H. Thomanek, A. H. G. P. Prenzel, W. Maison, *J. Org. Chem.* **2010**, *75*, 5994; l) J. E. Thomson, A. F. Kyle, K. B. Ling, R. Siobhan, S. R. Smith, A. M. Z. Slawin, A. D. Smith, *Tetrahedron* **2010**, *66*, 3801; m) M. G. Kulkarni, A. P. Dhondge, S. W. Chavhan, A. S. Borhade, Y. B. Shaikh, D. R. Birhade, M. P. Desai, N. R. Dhattrak, Beilstein *J. Org. Chem.* **2010**, *6*, 876, n) J. Hsieh, A. Cheng, J. Fu, T. Kang, *Org. Biomol. Chem.* **2012**, *10*, 6404; o) M. Gormen, R. L. Goff, A. M. Lawson, A. Daïch, S. Comesse, *Tetrahedron Lett.* **2013**, *54*, 2174; p) R. L. Goff, A. M. Lawson, A. Daïch, S. Comesse, *Org. Biomol. Chem.* **2013**, *11*, 1818. Review see: C. Marti, E. M. Carreira, *Eur. J. Org. Chem.* **2003**, *12*, 2209.
- [26] C. Pellegrini, C. Strässler, M. Weber, H. J. Borschberg, *Tetrahedron Asymmetry* **1994**, *5*, 1979.
- [27] G. Cravotto, G. B. Giovenzana, T. Pilati, M. Sisti, G. Palmisano, *J. Org. Chem.* **2001**, *66*, 8447.
- [28] G. Lakshmaiah, T. Kawabata, M. Shang, K. Fuji, *J. Org. Chem.* **1999**, *64*, 1699.
- [29] B. M. Trost, M. K. Brennan, *Org. Lett.* **2006**, *8*, 2027.
- [30] S. Hong, M. Jung, Y. Park, M. W. Ha, C. Park, M. Lee, H. Park, *Chem. Eur. J.* **2013**, *19*, 9599.
- [31] a) C. Li, C. Chan, A. C. Heimann, S. J. Danishefsky, *Angew. Chem. Int. Ed.* **2007**, *46*, 1444; b) C. Li, C. Chan, A. C. Heimann, S. J. Danishefsky, *Angew. Chem. Int. Ed.* **2007**, *46*, 1448.
- [32] Manuscript in preparation
- [33] H. Gotoh, D. Okamura, H. Ishikawa, Y. Hayashi, *Org. Lett.* **2007**, *9*, 5307.
- [34] Y. Hayashi, Y. Kawamoto, M. Honda, D. Okamura, S. Umemiya, Y. Noguchi, T. Mukaiyama, I. Sato, submitted
- [35] During our investigation, the organocatalyzed Michael addition of indoles and malonates to 2-oxoindoline-3-ylidene acetaldehyde was reported: a) R. Liu, J. Zhang, *Org. Lett.* **2013**, *15*, 2266; b) R. Liu, J. Zhang, *Chem. Eur. J.* **2013**, *19*, 7319.

Chapter 2. One-pot synthesis of (–)-Oseltamivir and mechanistic insights into organocatalyzed Michael reaction

In the previous two “one-pot” synthesis of (–)-Oseltamivir, solvent exchange was employed even though the reaction sequences were carried out in the same vessel.^[1] Clearly, it would be synthetically and operationally more ideal if the evaporation process and solvent exchange could be omitted in the “one-pot” operation. This would thus enable a reduction in solvent wastage, production time, and cost. Therefore, I planned to develop a completely “one-pot” synthesis of (–)-Oseltamivir without any evaporation and solvent exchange. This should contribute not only reduction of chemical waste but also shortening reaction steps to realize environmentally benign synthesis of (–)-Oseltamivir.

2-1 Synthetic plan

(–)-Oseltamivir would be obtained by reduction of nitro group on cyclohexane **2-2**, which is derived from addition of toluenethiol onto cyclohexene **2-3** (Figure 1). The cyclohexene **2-3** would be constructed by Michael reaction and intramolecular Horner-Wadsworth-Emmons reactions of Michael adduct **2-4** with ethyl acrylate derivative. The Michael adduct **2-4** would be synthesized by organocatalyzed Michael reaction of pentan-3-yloxyacetaldehyde (**2-5**) and (*Z*)-*N*-2-nitroethenylacetamide (**2-6**). The challenge is to perform all reactions in a same reaction vessel without the change of solvent.

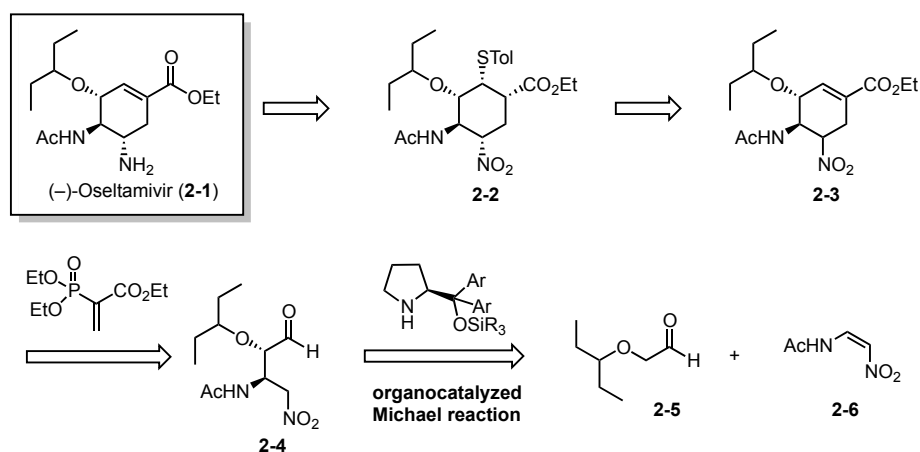


Figure 1. Retrosynthetic analysis of (–)-Oseltamivir

2-2 Michael reaction of α -alkoxyaldehyde with *cis*-nitroalkene

First, Michael reaction of pentan-3-yloxyacetaldehyde (**2-5**) and (*Z*)-*N*-2-nitroethenylacetamide (**2-6**), catalyzed by the (*S*)-diphenylprolinol silyl ether **2-7**, was investigated (Table 1).

As mentioned in the introduction, Ma obtained the products **2-4/2-8** in approximately 80% yield with good diastereoselectivity (**2-4/2-8** = 5:1) using PhCO₂H as an additive and CHCl₃ as the solvent.^[2] Sebesta used CHCl₃/H₂O as the solvent system and chloroacetic acid as an additive, and obtained good yield (88%) with good diastereo-selectivity (**2-4/2-8** = 81:19) for **2-4/2-8**.^[3] Lu employed CH₂Cl₂ as the solvent and chloroacetic acid as an additive, which afforded good yield and selectivity (**2-4/2-8** = 4:1).^[4]

However, when we performed the reaction in CHCl₃ in the presence of PhCO₂H, the NMR spectra of the crude mixture were not clean and the yield and diastereoselectivity were low. As this is the first step of a “one-pot” multi-step reaction sequence, the first reaction needs to be supremely clean with high yield and selectivity. Halogenated solvents should be substituted with non-halogenated ones for scale up. In our previous two “one-pot” synthesis of (–)-Oseltamivir,^[1] toluene gave a good result in terms of both yield and selectivity. As nitroalkene **2-6** was scarcely soluble in toluene, chlorobenzene and CH₃CN were found to be suitable candidates, both being acceptable solvents for large scale production. As we know that an acid is effective in this type of Michael reaction,^[5] we investigated several acids in either CH₃CN or chlorobenzene (Table 1).

Although the reaction proceeds in CH₃CN, the reaction was slow even in the presence of acid, and afforded the product with low diastereoselectivity (entries 1, 2). Contrary to CH₃CN, chlorobenzene was found to be the solvent of choice. In the presence of PhCO₂H, the reaction was fast, but resulted in low diastereoselectivity (entry 3). While the reaction was relatively slow in the presence of chloroacetic acid, the optimal acid in our previous synthesis of (–)-Oseltamivir in chlorinated solvents,^[1] an excellent diastereoselectivity was obtained in chlorobenzene (entry 4). The best result was obtained with HCO₂H in chlorobenzene (entry 5). The reaction was complete within 45 minutes, affording the product in good yield with excellent diastereo- and enantio-selectivities. The reaction also proceeded in the presence of 5 mol% of the organocatalyst (entry 6). The gram-scale synthesis was realized with good yield and diastereoselectivity (entry 7). The key points for scale up are, 1) slow addition of the α -alkoxyaldehyde **5** to suppress self-condensation, 2) control of the reaction temperature at 20 °C to maintain high diastereoselectivity. Better diastereoselectivity was observed at 0 °C and 10 °C, but yield was lower. On the other hand, better yield was observed at 28 °C, but diastereoselectivity was 5:1 (**2-4/2-8**). It should be noted that the nitroalkene **2-6** partially

dissolves in chlorobenzene, and the initial heterogeneous solution gradually becomes clear as the reaction proceeds to completion.

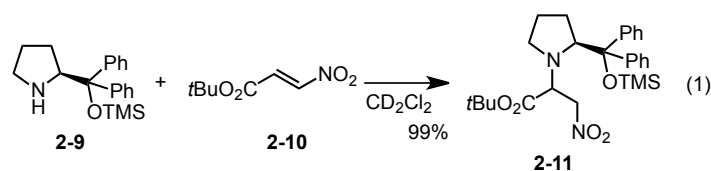
The stability of the Michael product **2-4** is noteworthy. As the Michael adduct possesses an acidic α -proton, epimerization can readily occur. For instance, the diastereomeric ratio was observed to decrease during evaporation and chromatographic (silica-gel) operations. Thus, it is a great advantage to carry out the reaction in a one-pot process. Operations such as evaporation, solvent exchange, and isolation tend to reduce the overall diastereoselectivity.

Table 1: Asymmetric Michael reaction of pentan-3-yloxyacetaldehyde **2-5** and (*Z*)-*N*-2-nitroethenylacetamide **2-6** catalyzed by diphenylprolinol silyl ether **2-7**^[a,f]

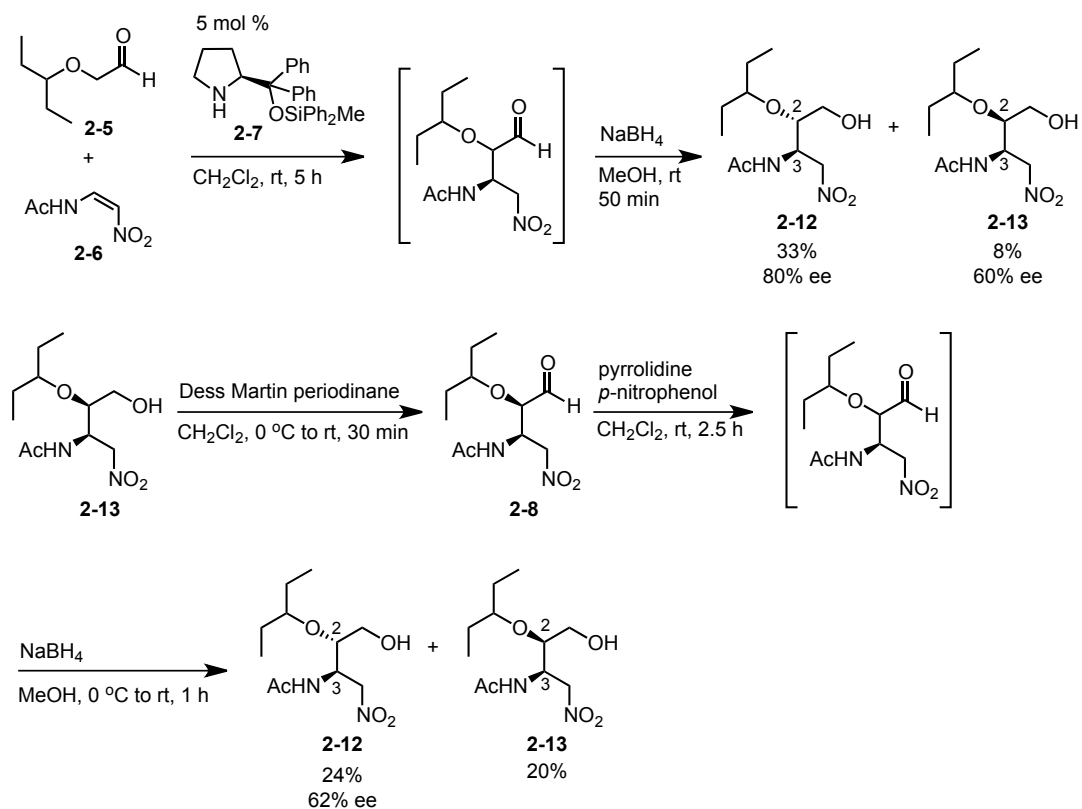
Entry	Solvent	Acid	Time [h]	NMR Yield [%] ^[b]	2-4 : 2-8 ^[c]	Ee (%) ^[d]
1	CH ₃ CN	PhCO ₂ H	2	90	1.3:1	
2	CH ₃ CN	ClCH ₂ CO ₂ H	16	90	3.6:1	
3	C ₆ H ₅ Cl	PhCO ₂ H	0.5	80	2.7:1	
4	C ₆ H ₅ Cl	ClCH ₂ CO ₂ H	2	80	9:1	
5	C ₆ H ₅ Cl	HCO ₂ H	0.75	90	9:1	99
6 ^[e]	C ₆ H ₅ Cl	HCO ₂ H	4	85	9:1	
7 ^[f]	C ₆ H ₅ Cl	HCO ₂ H	1.5	80	7.1:1	

[a] Unless stated otherwise, reactions were performed by employing α -alkoxyaldehyde **2-5** (0.60 mmol), nitroalkene **2-6** (0.30 mmol), acid-additive (30 mol%), catalyst **2-7** (10 mol%), and solvent (1 ml) at room temperature for the indicated time. [b] Calculated yield from ¹H NMR of reaction mixture. [c] Determined by ¹H NMR analysis of reaction mixture. [d] Optical purity of the major isomer was determined by HPLC analysis on chiral phase of the corresponding *p*-nitrobenzoyl ester derivative. The *p*-nitrobenzoyl ester was obtained by reduction of **2-4** to alcohol, followed by formation of *p*-nitrobenzoyl ester. [e] 5 mol % of catalyst **2-7** was employed. [f] α -Alkoxyaldehyde **2-5** (2.25 g, 17.3 mmol) in ClC₆H₅ (5 ml) was slowly

added (60 min) to the mixture of nitroalkene **2-6** (1.5 g, 11.5 mmol), acid-additive (0.17 ml, 4.6 mmol, 40 mol %), and catalyst **2-7** (517 mg, 1.15 mmol, 10 mol%) in ClC₆H₅ (42 ml) at 20 °C. The internal temperature of the reaction mixture was kept at 20 °C. The conversion was 46% and **2-4**:**2-8** was 9:1 at 30 min. [f] Although the crude NMR of the reaction mixture using diphenylprolinol trimethylsilyl (TMS) ether **2-9** was relatively dirty, the corresponding bulky silyl ether, such as the diphenylmethylsilyl (DPMS) ether **2-7** developed by Seebach,^[6] proceeded in a clean manner as determined by NMR. As the catalyst adduct **2-11** was observed in the stoichiometric reaction between the TMS-catalyst **2-9** and (*E*)-*tert*-butyl-3-nitropropenoate (**2-10**) (eq. 1),^[7] a similar addition reaction could proceed between TMS-catalyst **2-9** and *cis*-nitroalkene **2-6**. This unproductive side reaction could be responsible for the unfavourable results. By employing the bulky Ph₂MeSi catalyst **2-7** instead of the TMS catalyst **2-9**, this side reaction would be suppressed to afford a clean reaction.



The absolute configuration of the major stereoisomer **2-4** of the Michael reaction of **2-5** with **2-6** was (2*S*, 3*R*) by the catalytic use of (*S*)-diphenylprolinol silyl ether, which was determined after conversion to (–)-Oseltamivir (*vide infra*). This determination is also consistent with the observations of Ma,^[2] Sebesta^[3] and Lu.^[4] The absolute configuration of the minor isomer **2-8**, however, was not known. This identification would be important to understand the reaction mechanism. In order to obtain the minor isomer **2-8** in sufficient amounts, the reaction was thus performed without an acid additive to decrease the diastereoselectivity (Scheme 1). The (2*S*, 3*R*)-isomer **2-12** and **2-13** were obtained in 33% and 8% yield, respectively, after reduction with NaBH₄. The enantioselectivity of these isomers were determined to be 80% ee, and 60% ee, respectively. This result indicates that an acid additive increases not only the yield and diastereoselectivity, but also the enantioselectivity. The reason will be discussed later. Alcohol **2-13** was oxidized with Dess-Martin periodinane to aldehyde **2-8**, which was isomerized with pyrrolidine in the presence of *p*-nitrophenol and reduced with NaBH₄ to afford **2-12** and **2-13** in 24% and 20% yield, respectively. Next, HPLC analysis on chiral phase was investigated. Compound **2-12** generated after isomerization, showed the same retention time as (2*S*, 3*R*)-**2-12** generated from **2-5** and **2-6**. Thus, the absolute configuration of **2-13** was determined to be (2*R*, 3*R*), therefore the absolute configuration of **2-8** was determined to be (2*R*, 3*R*). Transition state models to rationalize the stereochemical results will be discussed later.



Scheme 1. Determination of absolute configuration of minor isomer **2-13**

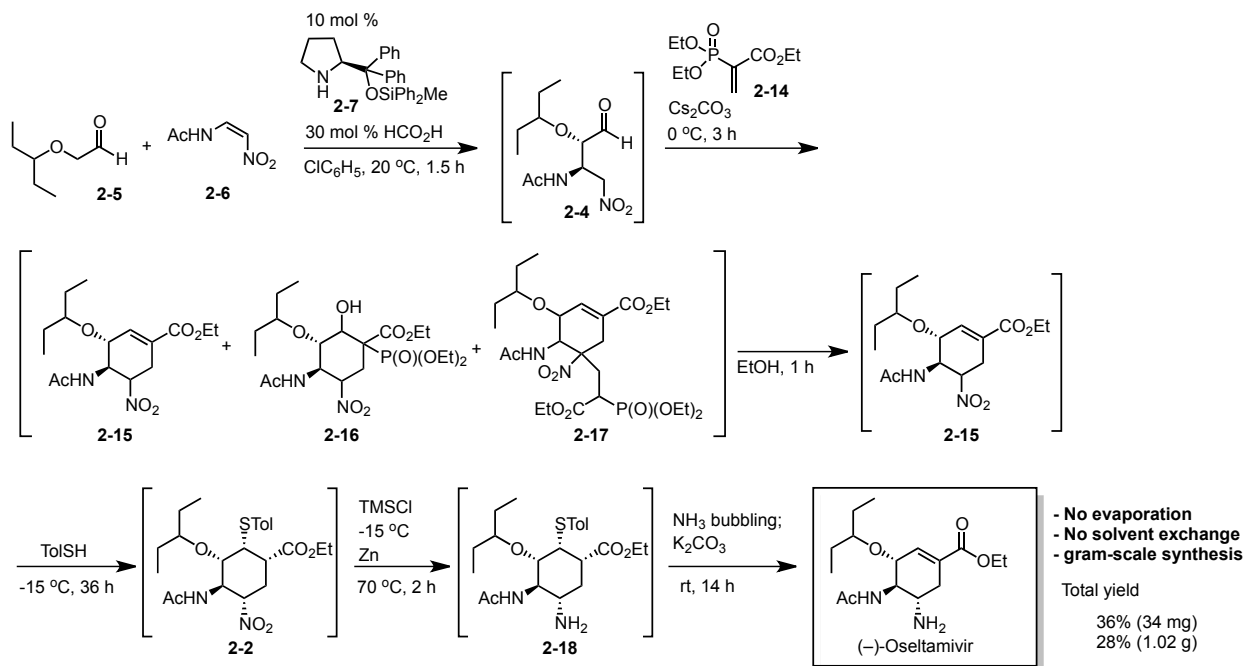
2-3 One-pot synthesis of (–)-Oseltamivir

As the best reaction conditions of the first Michael reaction were found, the complete “one-pot” sequential synthesis of (–)-Oseltamivir was examined next (Scheme 2). The Michael reaction of α -alkoxyaldehyde **2-5** and *cis*-nitroalkene **2-6**, catalyzed by (*S*)-diphenylprolinol silyl ether **2-7**, proceeded in the presence of HCO₂H in chlorobenzene to afford the Michael product **2-4** in good yield with excellent diastereo- and enantio-selectivities. In the same flask, the ethyl acrylate derivative **2-14** and Cs₂CO₃ were added. This generated multiple spots on TLC. Some compounds were identified as **2-15**, **2-16**, and **2-17**. The configuration of hydroxyl and diethylphosphonyl groups in **2-16** is assumed to be *anti* although the stereochemistry of **2-16** has not been determined.^[1] Therefore *syn* elimination does not occur. The compound **2-17** could be generated by further Michael reaction of the initially generated desired product **2-15** with acrylate derivative.^[1] The latter two compounds were successfully converted into **2-15** by the addition of EtOH. From **2-4** to **2-15**, several reactions proceed: 1) Michael reaction of nitroalkane **2-4** with **2-14** and intramolecular Horner-Wadsworth-Emmons reaction; 2) retro-aldol reaction of **2-16**, followed by intramolecular Horner-Wadsworth-Emmons reaction; and 3) retro-Michael reaction of **2-17**. The Michael reaction of toluenethiol, followed by epimerization of the α -position of nitro group, afforded the thiol-Michael adduct **2-2** with the desired stereochemical configuration. By addition of Zn and TMSCl into the same flask, reduction of the nitro group into the amine **2-18** occurred, from which a retro-Michael reaction of the thiol group proceeded by treatment with base to afford (–)-Oseltamivir in a single pot and without the need to exchange or evaporate solvents. The highest total yield of this “one-pot” procedure was 36% on forty milligram scale. The one-pot procedure was applicable for scale up synthesis. The gram-scale synthesis was demonstrated in 28% total yield, affording 1.02 g of (–)-Oseltamivir starting from 1.5 g of *cis*-nitroalkene **2-6** by one pot procedure. The procedure has a potential for scale up further to provide more amount of (–)-Oseltamivir.

It should be emphasized that removal of volatile materials in the reaction mixture, via evaporation or solvent exchange, which were found necessary in the previous two-pot syntheses,^[1] were not required in this one-pot process. Although strictly not the ideal solvent in each subsequent reaction, the choice of chlorobenzene did not interfere with the desired reaction course. This is key for the successful realization of a “one-pot” synthesis without solvent exchange. Here, we simply add each reagent and co-solvent successively, which is synthetically and operationally simple and ideal.

As we described in the previous work,^[1] the cyclohexane intermediate **2-2** is crystalline. Thus, diastereo- and enantiomerically pure highly substituted cyclohexane derivative **2-2** could be easily obtained by a single crystallization in 51% yield, when we quenched the reaction at this

stage. We believe this procedure to be one of the most efficient and practical methods for the preparation of (–)-Oseltamivir.



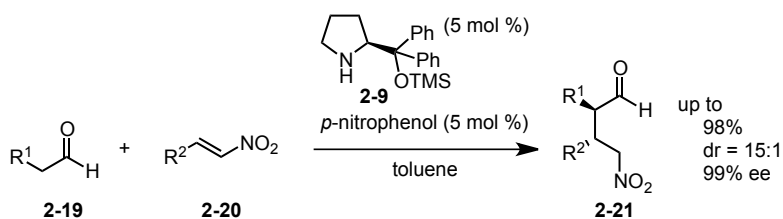
Scheme 2. One-pot synthesis of (–)-Oseltamivir

2-4 Mechanistic insights into organocatalyzed Michael reaction

Key reaction was the Michael reaction of α -alkoxyaldehyde **2-5** with *cis*-nitroalkene **2-6**, catalyzed by diphenylprolinol silyl ether **2-7**, in the “one-pot” synthesis of (–)-Oseltamivir. We noticed strange stereoselectivity in this Michael reaction. Before describing the strange stereoselectivity, background of the Michael reaction will be explained to understand the stereoselectivity.

2-4-1 Background of asymmetric organocatalyzed Michael reaction of aldehyde with nitroalkene

Our group previously reported asymmetric Michael reaction of aliphatic aldehyde **2-19** with *trans*-nitroalkene **2-20**, catalyzed by diphenylprolinol silyl ether **2-9**, to afford Michael product **2-21** in excellent yield and stereoselectivity (Scheme 3).^[8]



Scheme 3. Asymmetric Michael reaction of aliphatic aldehyde **2-19** with *trans*-nitroalkene **2-20**, catalyzed by diphenylprolinol silyl ether **2-9**

The postulated catalytic cycle of asymmetric Michael reaction of aliphatic aldehyde **2-19** with *trans*-nitroalkene **2-20**, catalyzed by diphenylprolinol silyl ether **2-9**, is described in figure 2.^[5,8,9] Diphenylprolinol silyl ether **2-9** and aliphatic aldehyde **2-19** generates *E*-enamine **2-22**. The *E*-enamine **2-22** attacks *trans*-nitroalkene **2-20** to afford cyclobutane **2-24** and 1,2-oxadine *N*-oxide **2-25**, which is in equilibrium with **2-22** and **2-20**.^[5] Zwitter ion **2-23** is assumed as an intermediate. Protonation of zwitter ion **2-23** generates iminium ion **2-26**, followed by hydrolysis affords the Michael product **2-21** with the recovery of the catalyst **2-9**. Deprotonation of iminium ion **2-26** generates γ -nitroenamine **2-27**. The reaction proceeds via formal [2+2] mechanism, not a normal Michael reaction mechanism.

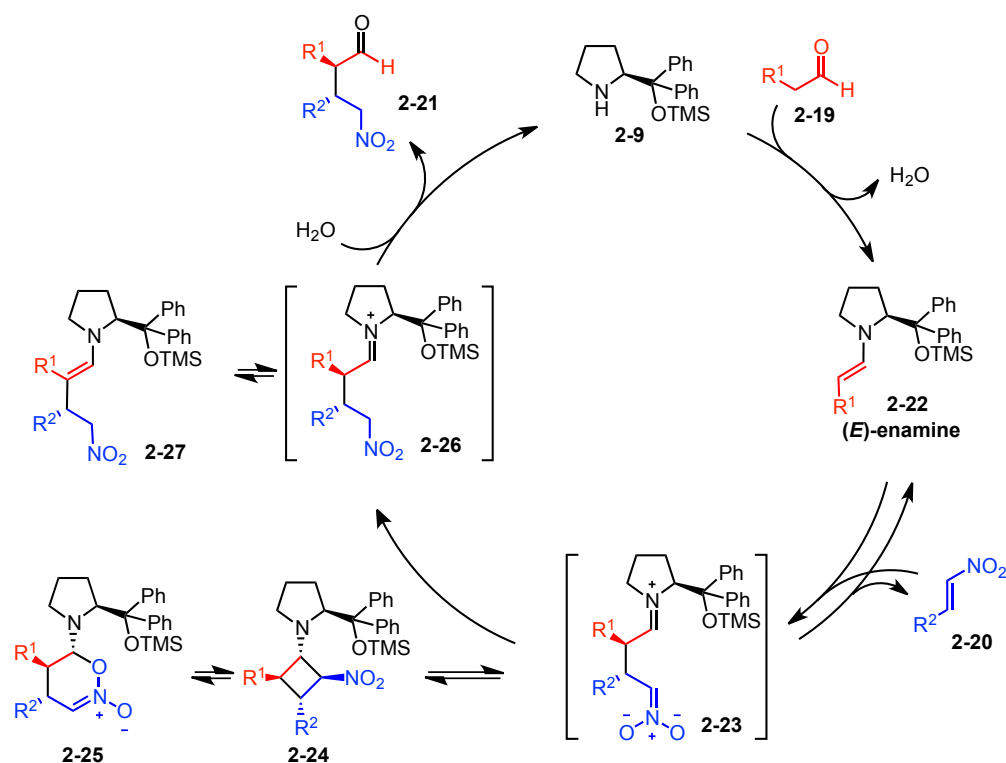


Figure 2. Postulated catalytic cycle of Michael reaction of aliphatic aldehydes **2-19** with *trans*-nitroalkenes **2-20**, catalyzed by diphenylprolinol silyl ether **2-9**

The excellent diastereo and enantioselectivity can be explained by considering a transition state model **TS-1** (Figure 3). *trans*-Nitroalkene approaches to *E*-enamine, avoiding bulky substituents on pyrrolidine, and reacts via acyclic synclinal transition state **TS-1** proposed by Seebach.^[10] As a result, Michael product **2-21** can be formed in excellent diastereo and enantioselectivity.

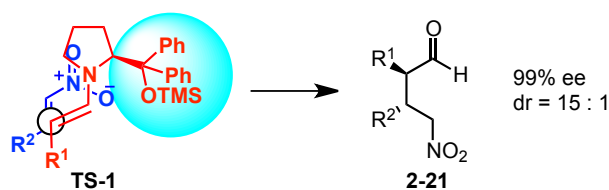


Figure 3. Transition state model

2-4-2 Strange stereoselectivity in the organocatalyzed Michael reaction

In the previous two “one-pot” sequential synthesis of (–)-Oseltamivir,^[1] Michael reaction of α -alkoxyaldehyde **2-5** with *trans*-nitroalkene **2-10**, catalyzed by (*R*)-diphenylprolinol silyl ether **2-28**, afforded (2*S*)-isomer **2-29** (Figure 4, eq. 1). On the other hand, Michael reaction of α -alkoxyaldehyde **2-5** with *cis*-nitroalkene **2-6**, catalyzed by (*S*)-diphenylprolinol silyl ether **2-7**, afforded (2*S*)-isomer **2-4** (Figure 4, eq. 2). By considering eq.1 and eq.2, Michael product with the same absolute stereochemistry at α -position of formyl group was obtained, although the same Michael donor and the opposite configuration of diphenylprolinol silyl ether were employed. We thought this phenomenon is very strange.

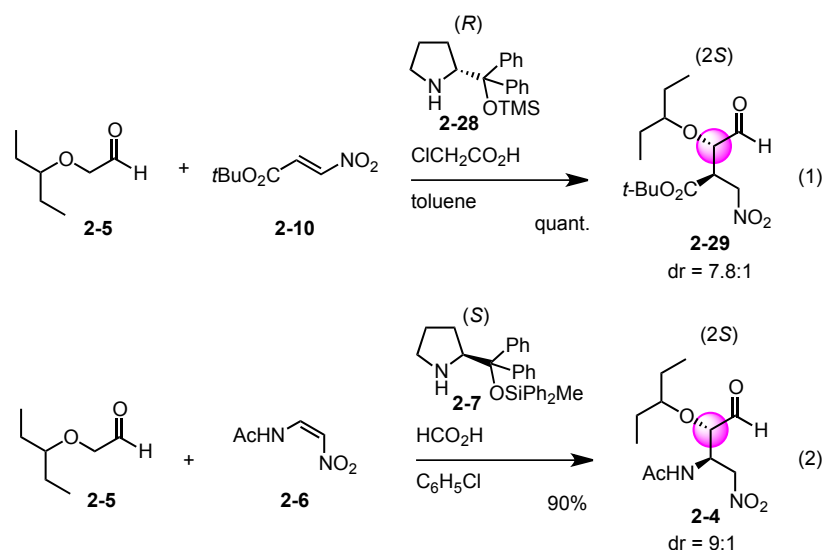


Figure 4. Strange stereoselectivity of organocatalyzed Michael reaction

The stereoselectivity of Michael reaction of α -alkoxyaldehyde **2-5** with nitroalkenes would be postulated as follows based on the established reaction mechanism of propanal and nitrostyrene, catalyzed by diphenylprolinol silyl ether **2-28**.^[5,7,8,9] The α -alkoxyaldehyde **2-5** and (*R*)-diphenylprolinol silyl ether **2-28** generates *E*-enamine (Figure 5, eq. 1). Then, *trans*-nitroalkene **2-10** approaches to the *E*-enamine, avoiding bulky substituents on pyrrolidine, and reacts via **TS-2** to afford (2*S*)-isomer **2-29**. Similarly, *E*-enamine would react with *cis*-nitroalkene **2-6** via **TS-3** to generate (2*R*)-isomer **2-8** (Figure 5, eq. 2). However, (2*S*)-isomer **2-4** was generated in the actual reaction (Figure 4, eq. 2). It was difficult to explain the stereoselectivity. We thought something strange occurred during the reaction and decided to investigate this reaction in detail.

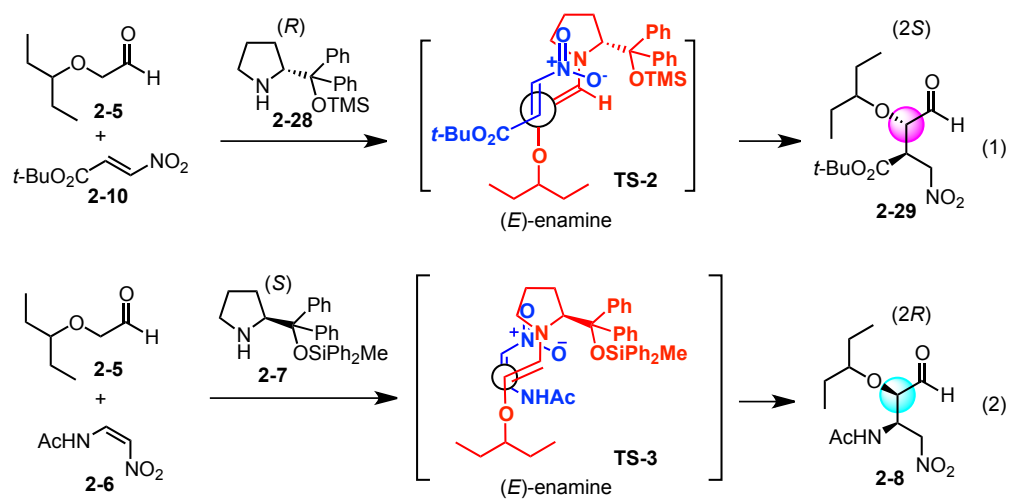
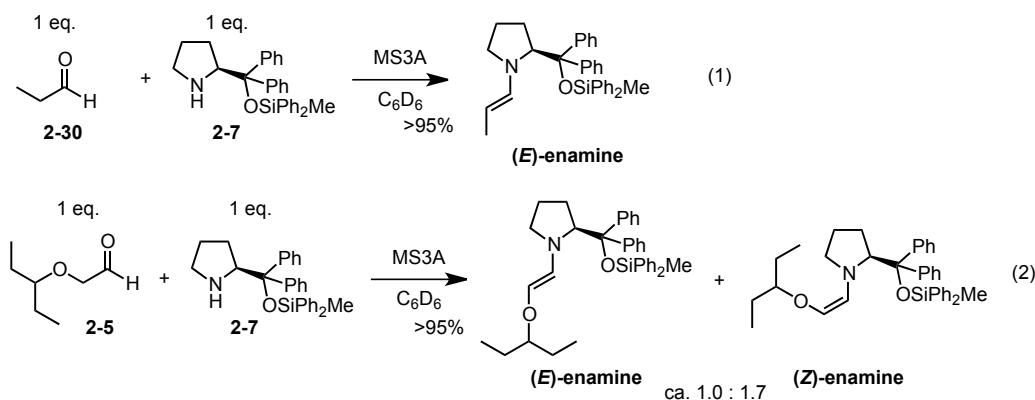


Figure 5. Transition state models and stereochemistry of Michael products

2-4-3 The geometry of enamine

As the first step of the Michael reaction is enamine formation from aldehyde with diphenylprolinol silyl ether, enamine formation was investigated. Previously we observed a selective formation of *E*-enamine by the reaction of aliphatic aldehyde such as propanal **2-30** and diphenylprolinol silyl ether **2-7** in the presence of molecular sieves in C₆D₆ (Scheme 5, eq. 1).^[5,9]

Equimolar amount of α -alkoxyaldehyde **2-5** and diphenylprolinol silyl ether **2-7** were mixed in the presence of molecular sieves in C₆D₆ (Scheme 5, eq. 2). The reaction was monitored by ¹H NMR spectroscopy. As a result, both *E*- and *Z*-enamines were generated over 95% yield. The ratio of *E*- and *Z*-enamine was approximately 1:1.7. In other solvents such as toluene-*d*₈ and CDCl₃, both *E*-enamine and *Z*-enamine were also generated over 95% yield. The ratio of *E*- and *Z*-enamine was approximately 1:1.7 in toluene-*d*₈ and 1:1 in CDCl₃. It was demonstrated that α -alkoxyaldehyde **2-5** generates both *E*- and *Z*-enamines while aliphatic aldehyde generates only *E*-enamine.



Scheme 5. Geometry of enamines from aliphatic aldehyde or α -alkoxyaldehyde

We were interested in the reason of the formation of *Z*-enamine in case of α -alkoxyaldehyde. First, we conducted calculation of relative energies of *E*- and *Z*-alkoxyenamines through a collaborative research with Prof. Seebach.^[7] Two calculation methods (BP86/TZVPP and BP86-D3/TZVPP) were employed, and results are shown in Figure 6. When silyl group is located at *sc-exo* position, the relative energy of **E-66** was higher than **Z-66**. When the silyl group is located at *ap* position, the relative energy of **E-67** was higher by BP86/TZVPP while **Z-67** was higher by BP86-D3/TZVPP. The opposite calculation results were obtained in case of enamine **67**. It seems that the bulky substitution on pyrrolidine ring affects the calculation and makes it more difficult to obtain reliable results. In addition, the obtained value of relative energy difference (1.9 – 2.6 kcal/mol) does not match with the experimental results (*E*:*Z* = ca. 1:1.7, scheme 5, eq. 2) since the energy difference of 1.4 kcal/mol corresponds to the ratio of 10:1 at room temperature.

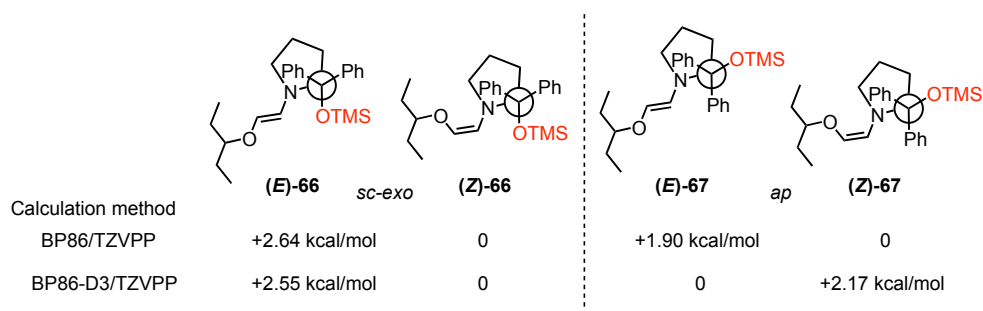
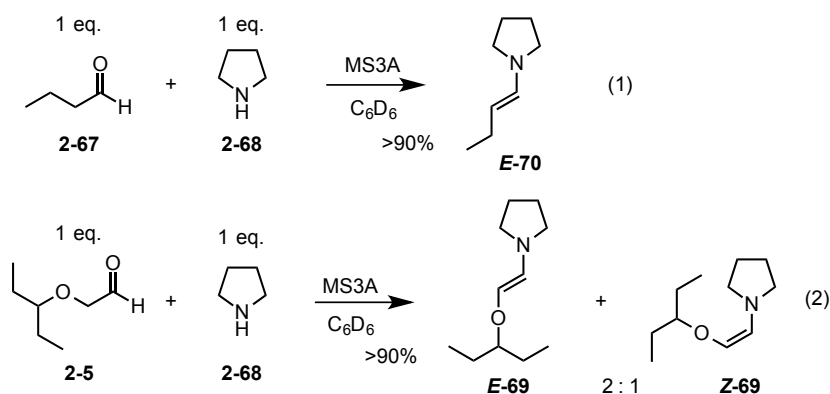


Figure 6. Relative energies of *E*- and *Z*-alkoxyenamines

To obtain more reliable calculation data, we decided to remove the bulky substituents on pyrrolidine ring. Before conducting the calculation, we investigated to see if enamine would be formed from pyrrolidine **2-68** with aliphatic aldehyde **2-67** or α -alkoxyaldehyde **2-5**. Pyrrolidine **2-68** was mixed with aliphatic aldehyde **2-67** in the presence of molecular sieves, which afforded *E*-**70** (Scheme 12, eq. 1). On the other hand, both *E*-**69** and *Z*-**69** were generated in the ratio 2:1 from pyrrolidine **2-68** and α -alkoxyaldehyde **2-5** (Scheme 12, eq. 2). These results are consistent with the enamine generation of diphenylprolinol silyl ether with aliphatic aldehyde or α -alkoxyaldehyde (Scheme 5).



Scheme 12. Enamine formation from pyrrolidine with aldehydes

As we confirmed the enamine generation from pyrrolidine with aldehydes, we conducted calculation for the relative energies of *E/Z*-alkylenamines and *E/Z*-alkoxyenamines. The pentyloxy group of alkoxyenamine was replaced to the methoxy group to simplify the structure for calculation. The most stable conformation was calculated and the conformation was used for the relative energy calculation (Figure 7). Five methods (B3LYP/6-31G(d), M062X/6-31G(d), wB97XD/6-31G(d), MP2/6-31G(d), and CBS-QB3) were employed for the gas phase energy calculation. As the enamines were formed in C₆D₆ shown in Scheme 12, the solution phase energy calculation was also conducted by B3LYP/6-31G(d) method with the consideration of solvent (benzene) effect. While relative energy of alkylenamine **Z-70** was greater (2.78 – 3.86 kcal/mol) than **E-70**, the relative energy difference of alkoxyenamine between **E-71** and **Z-71** was quite small (0.32 – 0.91 kcal/mol) in gas phase calculation. Almost similar results were obtained in solution phase calculation, in which alkylenamine **Z-70** has significantly higher energy (4.06 kcal/mol) than **E-70** while **Z-71** has slightly higher energy (0.57 kcal/mol) than **E-71**. The obtained calculation data is in agreement with the experimental results, in which aliphatic aldehyde **2-67** generates only *E*-enamine while α -alkoxyaldehyde **2-5** generates both *E*- and *Z*-enamine (Scheme 12).

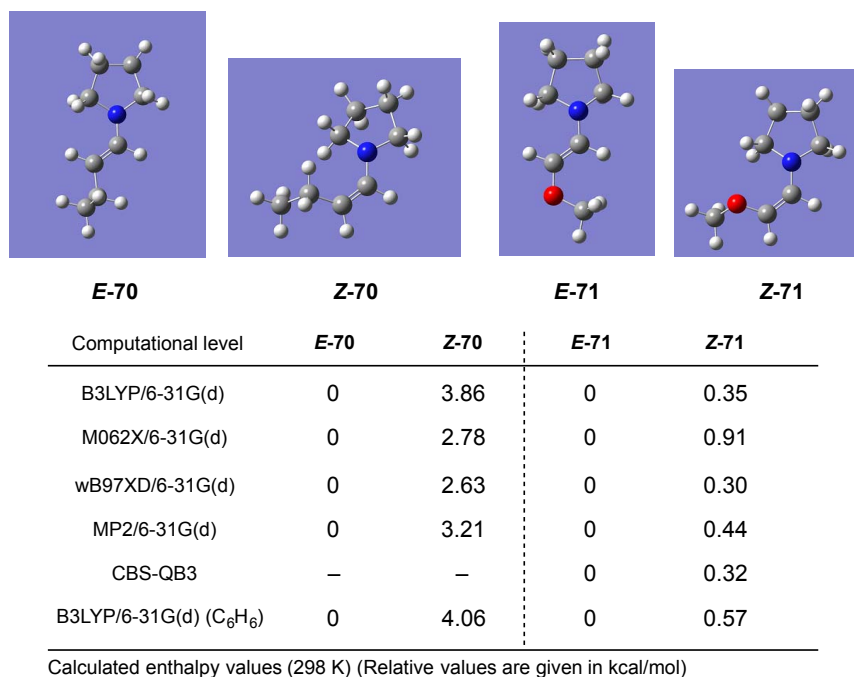
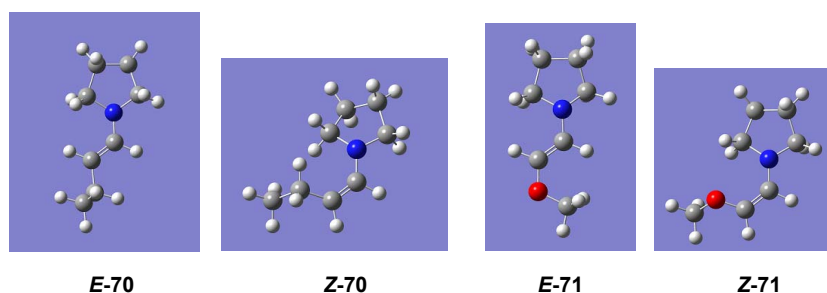


Figure 7. Relative energies of *E/Z*-alkylenamines and *E/Z*-alkoxyenamines

The Natural Bond Orbital (NBO) analysis was then carried out using most stable conformers, as the relative energy calculation results were consistent with the experimental data. The electric energy of alkylenamine **Z-70** is higher (3.68 kcal/mol) than **E-70**, indicating alkylenamine mostly exists as *E*-isomer (Table 2). The difference of electric energy of alkoxyenamine of **Z-71** and **E-71** is small (0.62 kcal/mol), indicating alkoxyenamine exists as a mixture of *E*- and *Z*-isomers. The energy of Lewis structure of **Z-70** and **Z-71** is greater (5.47 kcal/mol and 4.41 kcal/mol, respectively) than **E-70** and **E-71**, indicating *E*-isomer is energetically favored in both alkylenamine and alkoxyenamine if resonance is not considered. The resonance energy shows that alkylenamine **Z-70** is more stabilized (1.79 kcal/mol) than **E-70**, and alkoxyenamine **Z-71** is more stabilized (3.79 kcal/mol) than **E-71** by resonance, indicating alkoxyenamine **Z-71** is more stabilized than alkylenamine **Z-70** by resonance.



Results of NBO Calculations of Enamines (B3LYP/6-31G(d))

	Alkyl Enamine			Alkoxy Enamine		
	E-70	Z-70	Z - E	E-71	Z-71	Z - E
Electric Energy	-368.615403382	-368.609536749	3.68	-404.498663168	-404.497677538	0.62
Energy of Lewis Structure	-368.056257381	-368.047532606	5.47	-403.907491630	-403.900462245	4.41
Resonance Energy	-0.559146001	-0.562004143	-1.79	-0.591171538	-0.597215293	-3.79

Table 2. Results of NBO calculations of enamines

The 2nd order stabilization energy was calculated by NBO analysis to figure out which orbital interaction is stabilizing the *Z*-alkoxyenamine. The calculation indicated that antiperiplanar effect^[15] would be the reason for stabilizing *Z*-alkoxyenamine (Figure 21). There are four possible antiperiplanar effects, *E*-71a, *E*-71b, *E*-71c, *E*-71d, in *E*-enamine, and *Z*-71a, *Z*-71b, *Z*-71c, *Z*-71d, in *Z*-enamine respectively. The total 2nd order stabilization energy of *Z*-enamine is 18.07 kcal/mol and that of *E*-enamine is 13.85 kcal/mol. As the total 2nd order stabilization energy of *Z*-enamine is higher than *E*-enamine, *Z*-enamine would be stabilized by antiperiplanar effect, especially, *Z*-71a ($\sigma^*\text{CO} - \sigma\text{CH}$) and *Z*-71b ($\sigma\text{CH} - \sigma^*\text{CN}$).

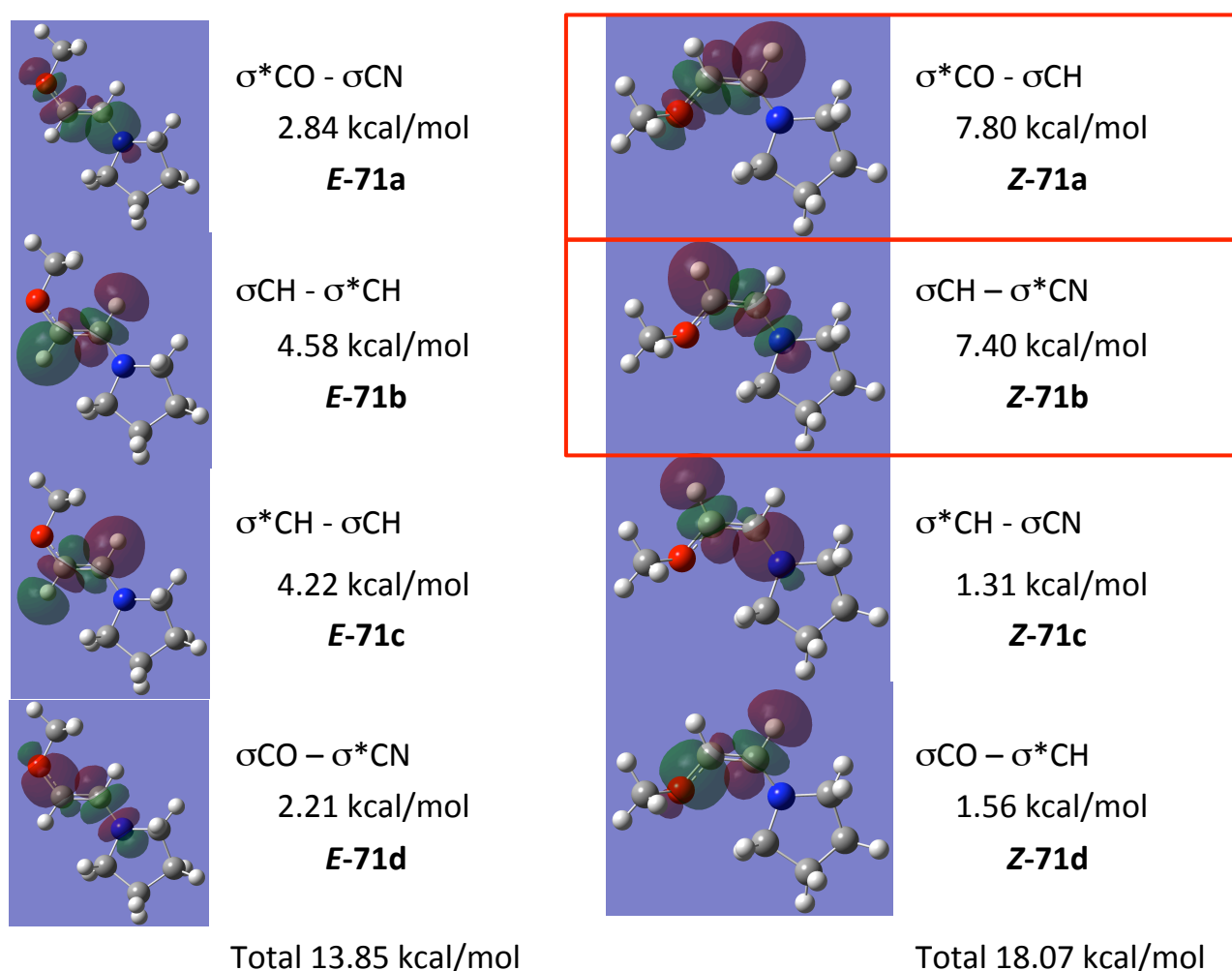


Figure 21. The 2nd order stabilization energy (kcal/mol) and orbital interaction of alkoxyenamines by NBO calculations.

2-4-4 The reactivity of enamine toward *trans*-nitroalkene

Both *E*- and *Z*-enamines were generated from α -alkoxyaldehyde **2-5**. We had the following question; “Why (2*S*)-isomer **2-29** was mainly formed even though both *E*- and *Z*-enamines were generated from α -alkoxyaldehyde with diphenylprolinol silyl ether?” (Figure 8). Nitroalkene **2-10** reacts with *E*-enamine, avoiding bulky substituents on pyrrolidine, to give (2*S*)-isomer **2-29**. In the same manner, *Z*-enamine provides (2*R*)-isomer **2-31**. Since both *E*- and *Z*-enamines were generated in the reaction mixture, (2*S*)- and (2*R*)-isomers should be formed in the same ratio with the *E*- and *Z*-enamines. However, (2*S*)-isomer **2-29** was formed as a major product. This phenomenon was difficult to explain considering our previous result of the organocatalyzed Michael reaction.^[5,8,9] Therefore, we investigated the reactivity of *E*- and *Z*-enamines toward nitroalkens.

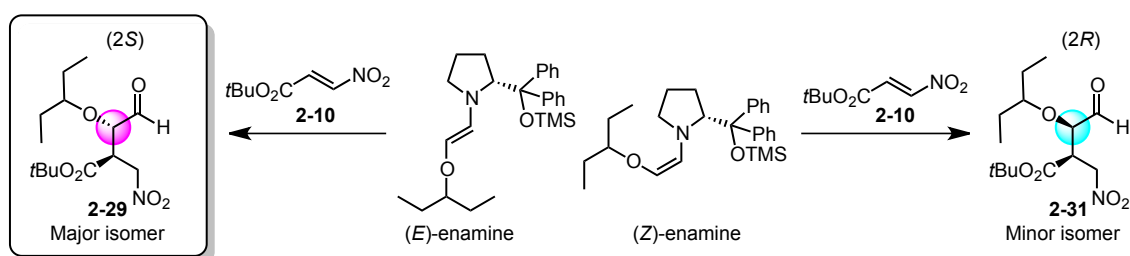


Figure 8. Formation of (2*S*)-isomer **2-29** as a major product

The reactivity of *E*- and *Z*-enamines toward *trans*-nitroalkene was investigated first. The following experiment was conducted to examine whether *E*- and *Z*-enamines possess different reactivity toward *trans*-nitroalkene **2-10**. The mixture of *E*- and *Z*-enamines was preformed from α -alkoxyaldehyde and diphenylprolinol silyl ether in the presence of molecular sieves in C_6D_6 . Then, *trans*-nitroalkene **2-10** was added to the mixture, followed by the mixture was transferred into a NMR tube without MS4A. The reaction progress was monitored by 1H NMR spectroscopy. The conversion of the reaction was calculated from 1H NMR, and plotted in Figure 9, 10 and 11.

When excess of *trans*-nitroalkene **2-10** (4.3 eq.) was added to the mixture of *E*- and *Z*-enamines (2.9 eq., 1:1.9 *E/Z*), both enamines were completely consumed within 5 minutes (Figure 9, red line for *E*-enamine, blue line for *Z*-enamine). Instead of disappearance of them, cyclobutane **2-31** and **2-32** were generated nearly 1:1 ratio as a major product (orange and green line). The cyclobutane **2-31** was stable, as the concentration did not change with time. The cyclobutane **2-32** disappeared and γ -nitro-enamine **2-33** appeared with time (light blue line). Before the addition of **2-10** to the mixture of *E*- and *Z*-enamines, the concentration of

E-enamine was 9 nM, and that of *Z*-enamine was 17 nM. If both *E*- and *Z*-enamines react with **2-10** in the same reaction rate, concentration of the newly formed cyclobutane would be around 9 nM and 17 nM. However, concentration of cyclobutane **2-31** was 13 nM, and that of **2-32** was 12 nM at 5 minutes. The concentration of *E*- and *Z*-enamines and cyclobutane **2-32** and **2-33** does not consistent. We thought that reactivity of *E*- and *Z*-enamines might be different.

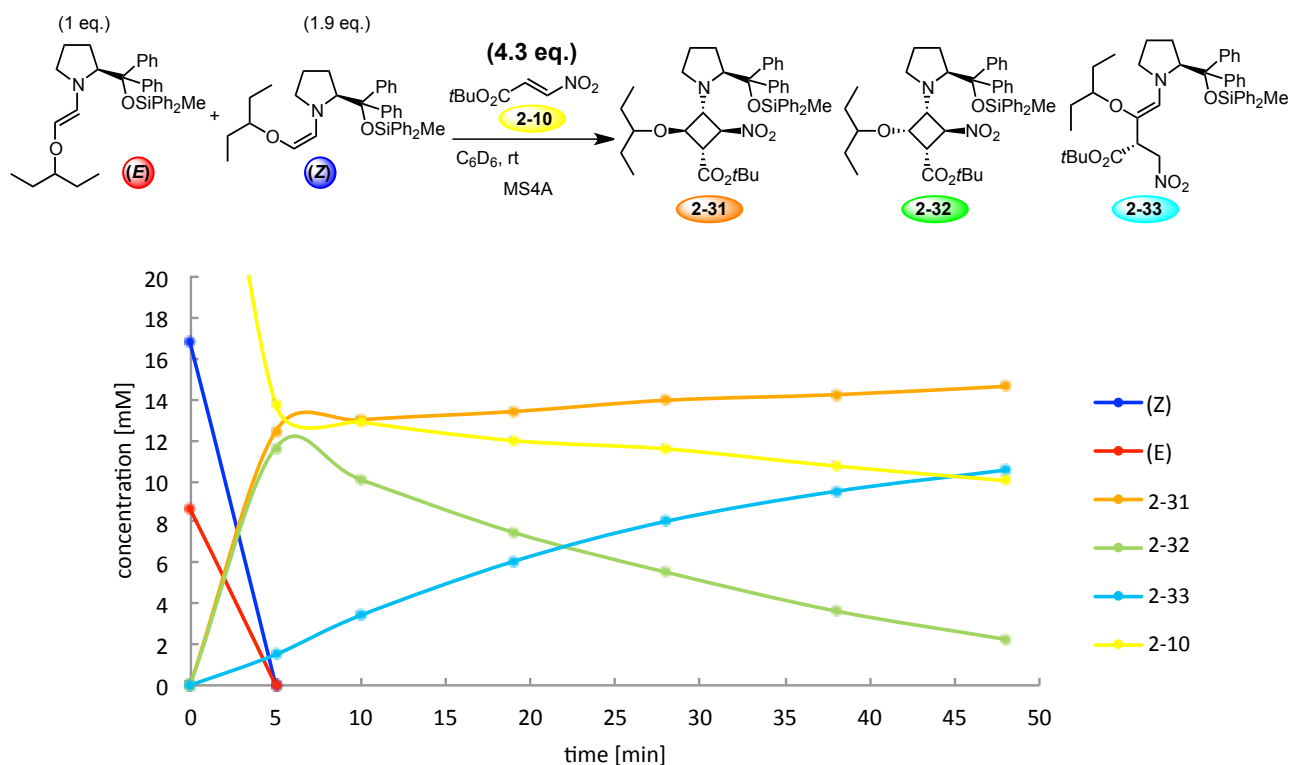


Figure 9. Reaction profile of *E*- and *Z*-enamines with *trans*-nitroalkene **2-10** (4.3 eq.)^[a,b]

[a] *trans*-Nitroalkene **2-10** (0.05 mmol, 0.5 ml, 0.1 M solution in C₆D₆) was added to the preformed C₆D₆ solution (0.73 ml) of *E*- and *Z*-enamine (0.0324 mmol: *E/Z* = 1/1.9) with toluene (internal standard: 0.02 mmol, 40 μ l, 0.5M solution in C₆D₆) in the presence of MS4A (200 mg). Without molecular sieves, an aliquot (0.6 ml) of this reaction mixture was transferred to a NMR tube. The reaction was monitored by ¹H NMR spectroscopy. The concentration of each product was calculated by integration of selected peaks in the ¹H NMR spectra and plotted on the graph. [b] The structure of **2-31**, **2-32**, and **2-33** was elucidated by 2D NMR spectroscopic analysis (COSY, HSQC, and HMBC). The relative stereochemistry of **2-31** and **2-32** was determined by NOESY.

We used less (1.2 eq.) of **2-10** than *E*- and *Z*-enamine (2.6 eq, *E/Z* = 1/1.6) to investigate which enamine reacts faster with **2-10**. When 1.2 equivalent of **2-10** was added to the preformed enamines solution, *E*-enamine was almost consumed immediately affording cyclobutane **2-31** (Fig. 10; red line for *E*-enamine, orange line for **2-31**) while *Z*-enamine was slightly consumed,

affording cyclobutane **2-32** (blue line for *Z*-enamine, green line for **2-32**). This indicates that *E*-enamine reacts faster than *Z*-enamine with *trans*-nitroalkene **2-10**. The concentration of cyclobutane **2-31** was almost constant after its generation, but cyclobutane **2-32** was decreased with time. And γ -nitro-enamine **2-33** was gradually increasing with time (light blue line). Presumably, γ -nitro-enamine **2-33** was generated from cyclobutane **2-32** through cyclobutane ring opening. The ratio of *E*-enamine and *Z*-enamine was about 1:7.5 at 5 minutes, and the ratio was slowly changing with time even nitroalkene **2** did not exist in the reaction mixture. This indicates that *E*- and *Z*-enamines is in equilibrium, and slow isomerization occurred between *E*- and *Z*-enamines. It was proved that *E*-enamine is more reactive than *Z*-enamine toward *trans*-nitroalkene **2-10**.

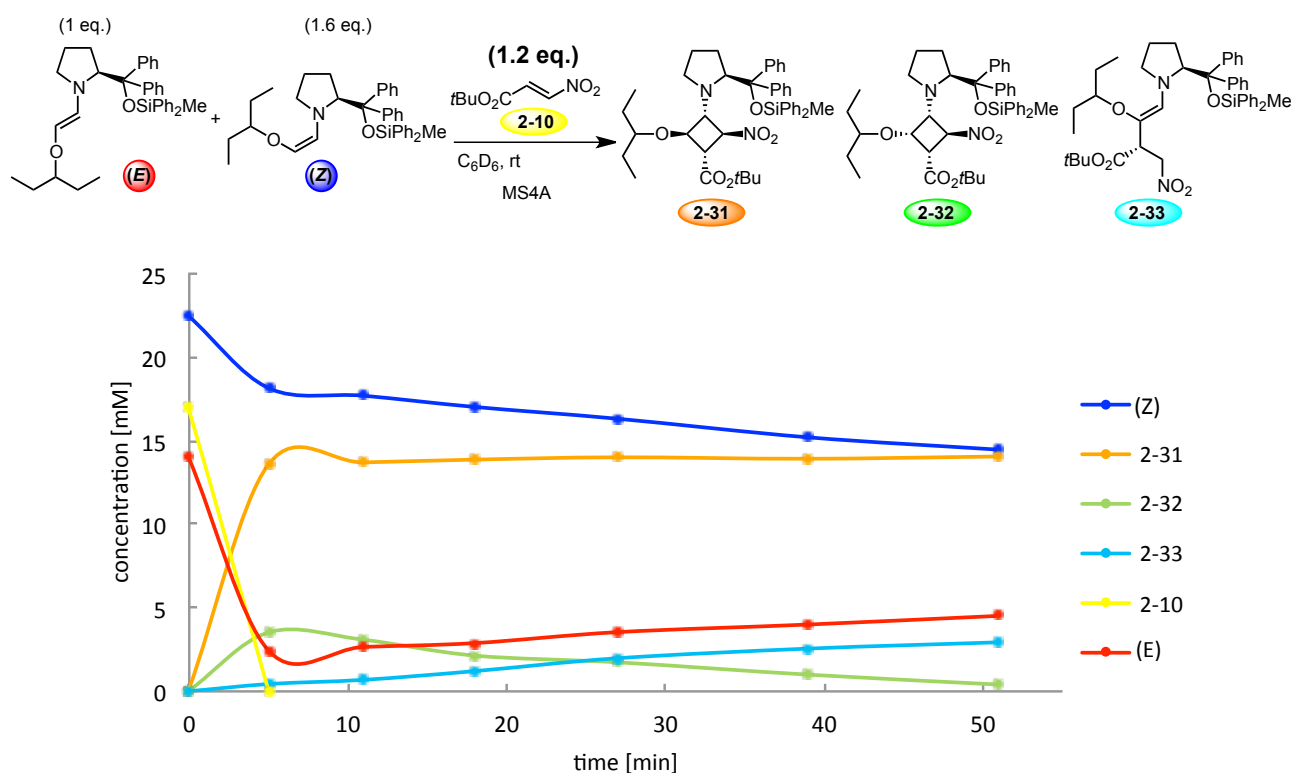


Figure 10. Reaction profile of *E*- and *Z*-enamines with *trans*-nitroalkene **2-10** (1.2 eq.)^[a]

[a] *trans*-Nitroalkene **2-10** (0.015 mmol, 0.15 ml, 0.1 M solution in C_6D_6) was added to the preformed C_6D_6 solution (0.73 ml) of *E*- and *Z*-enamine (0.0322 mmol, *E*/*Z* = 1/1.6) with toluene (internal standard: 0.02 mmol, 40 μ l, 0.5M solution in C_6D_6) in the presence of MS4A (200 mg). Without molecular sieves, an aliquot (0.6 ml) of this reaction mixture was transferred to a NMR tube. The reaction was monitored by 1H NMR spectroscopy. The concentration of each product was calculated by integration of selected peaks in the 1H NMR spectra and plotted on the graph.

When catalytic reaction was performed, acid additive was essential to realize high yield and stereoselectivity.^[1] Therefore, effect of acid was investigated next (Figure 11). When the *trans*-nitroalkene **2-10** (1.3 eq.) was added to a solution of the preformed enamine (2.9 eq., *E/Z* = 1/1.9), the *E*-enamine was consumed almost immediately to afford the cyclobutane **2-31**, whereas the *Z*-enamine was consumed more slowly to afford the cyclobutane **2-32**. A small amount of the nitro-enamine **2-33** was also observed. Next, acid was added to the mixture at 13 minutes; ClCH₂CO₂H was selected as the optimal acid additive for the catalytic Michael reaction due to our previous results between α -alkoxyaldehyde **2-5** and *trans*-nitroalkene **2-10**.^[1] The ratio of *E*- and *Z*-enamines dramatically changed from 7:1 to 2:1 immediately upon addition of ClCH₂CO₂H (blue line for *Z*-enamine, red line for *E*-enamine). This indicates that acid accelerates *E/Z*-enamine isomerization.

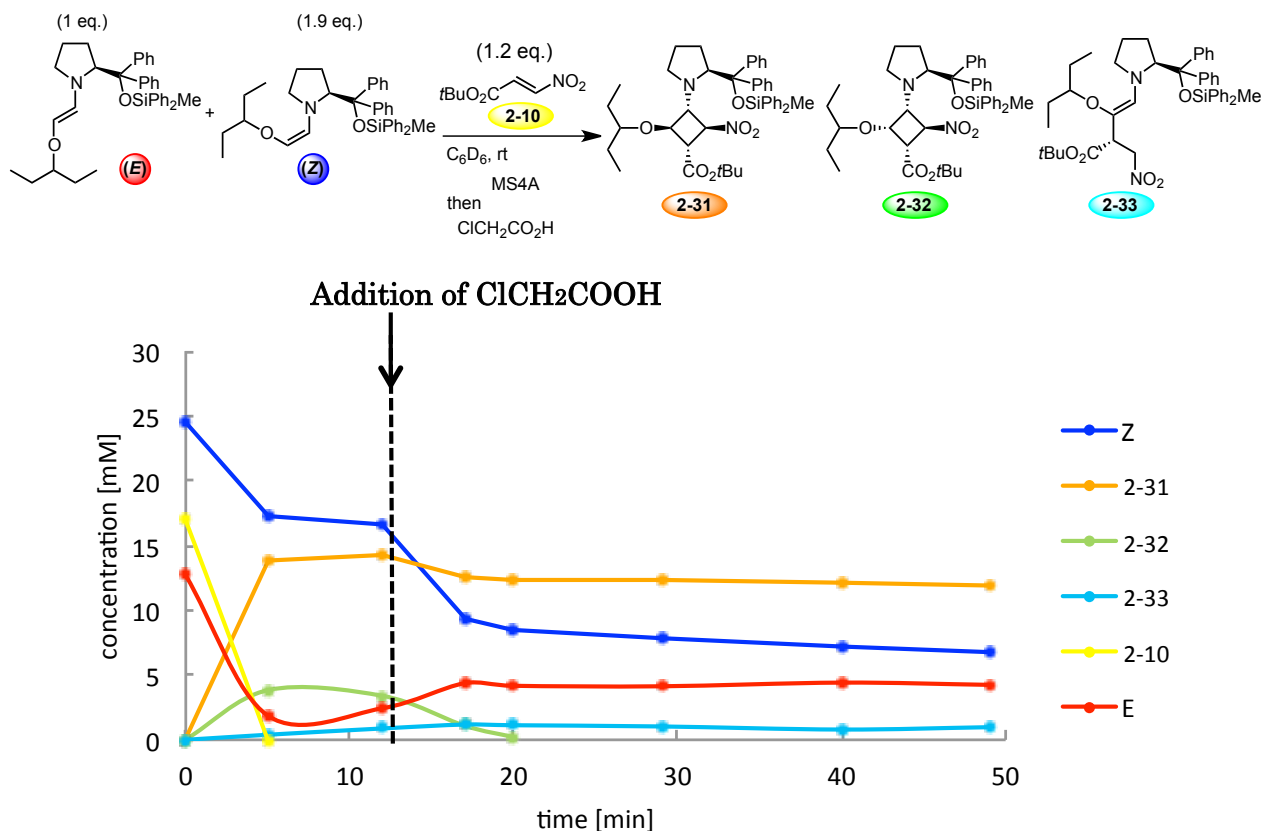


Figure 11. The effect of acid in the isomerization of *E*- and *Z*-enamine^[a]

[a] *trans*-Nitroalkene **2-10** (0.015 mmol, 0.15 ml, 0.1 M solution in C₆D₆) was added to the preformed C₆D₆ solution (0.73 ml) of *E*- and *Z*-enamine (0.033 mmol: *E/Z* = 1/1.9) with toluene (internal standard: 0.02 mmol, 40 μ l, 0.5M solution in C₆D₆) in the presence of MS4A (200 mg). Without molecular sieves, an aliquot (0.6 ml) of this reaction mixture was transferred to a NMR tube and ClCH₂COOH (0.015 mmol, 30 μ l, 0.5 M solution in C₆D₆) was subsequently added to the NMR tube after 13 minutes. The reaction was monitored by ¹H NMR spectroscopy. The concentration of each product was calculated by integration of

selected peaks in the ^1H NMR spectra and plotted on the graph.

These results indicate two main aspects of the reaction: 1) *E*-enamine reacts faster than *Z*-enamine toward *trans*-nitroalkene **2-10**, 2) acid accelerates *E/Z*-enamine isomerization.

2-4-5 The reactivity of enamine toward *cis*-nitroalkene

As we have examined the reaction of enamine with *trans*-nitroalkene, the reaction of enamine toward *cis*-nitroalkene **2-6** was investigated next. The reaction of *cis*-nitroalkene was investigated in the same manner with that of *trans*-nitroalkene.

When less (1.1 eq.) of *cis*-nitroalkene **2-6** was added to the preformed enamine solution (2.7 eq., *E/Z* = 1/1.7), *Z*-enamine was consumed to afford cyclobutane **2-34** while *E*-enamine remained unreacted (Figure 12, blue line for *Z*-enamine, green line for cyclobutane **2-34**, and red line for *E*-enamine). The result indicates that *Z*-enamine reacts faster than *E*-enamine toward *cis*-nitroalkene **2-6**. The γ -nitro-enamine **2-35** was also generated slightly (light blue). However, even in the presence of *E*- and *Z*-enamines, the reaction of *cis*-nitroalkene **2-6** did not progress further.

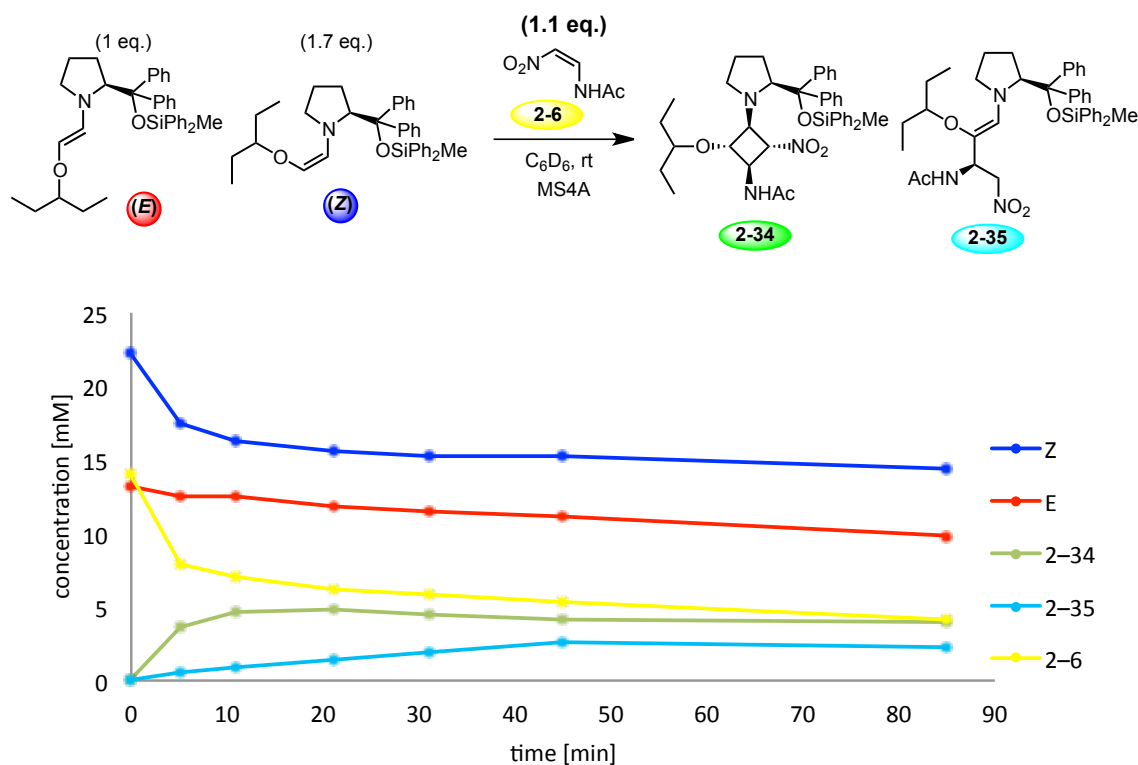
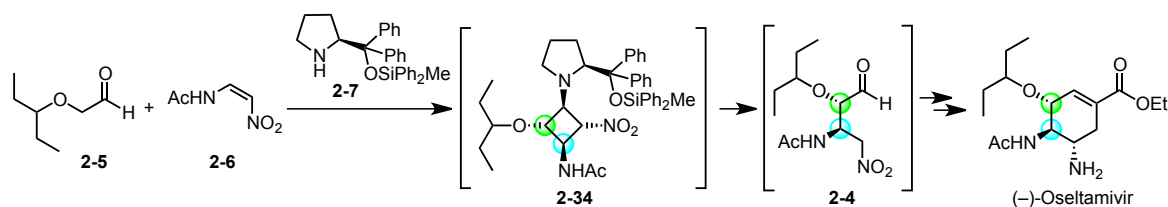


Figure 12. Reaction profile of *E*- and *Z*-enamines with *cis*-nitroalkene **2-6** (1.1 eq.)^[a,b]

[a] *cis*-Nitroalkene **2-6** (0.015 mmol, 0.3 ml, 0.05 M solution in C_6D_6) was added to the preformed C_6D_6 solution (0.73 ml) of *E*- and *Z*-enamine (0.0378 mmol: *E/Z* = 1/1.7) with toluene (internal standard: 0.02 mmol, 40 μ l, 0.5M solution in C_6D_6) in the presence of MS4A (200 mg). Without molecular sieves, an aliquot (0.6 ml) of this reaction mixture was transferred to a NMR tube. The reaction was monitored by 1H NMR spectroscopy. The concentration of each product was calculated by integration of selected peaks

in the ^1H NMR spectra and plotted on the graph. [b] The structure of **2-34** and **2-35** were elucidated by 2D NMR analysis; COSY, HSQC, and HMBC. The relative configuration of **2-34** was determined by NOESY. The Michael product **2-4** of α -alkoxyaldehyde **2-5** and *cis*-nitroalkene **2-6**, as catalyzed by **2-7**, was converted to (–)-Oseltamivir indicating the stated stereochemical configuration of **2-34** to be highly probable.



Similar tendency was observed when slightly excess (3.3 eq.) of **2-6** was employed (Figure 13). After the addition of **2-6** into the preformed enamines solution (2.7 eq, $E/Z = 1/1.7$), *Z*-enamine decreased, affording **2-34**, while *E*-enamine did not decrease (blue for *Z*-enamine, red for *E*-enamine). The results support that *Z*-enamine is more reactive than *E*-enamine toward *cis*-nitroalkene **2-6**. Again, the reaction stopped even in the presence of E/Z enamine and nitroalkene **2-6** after 5 minutes.

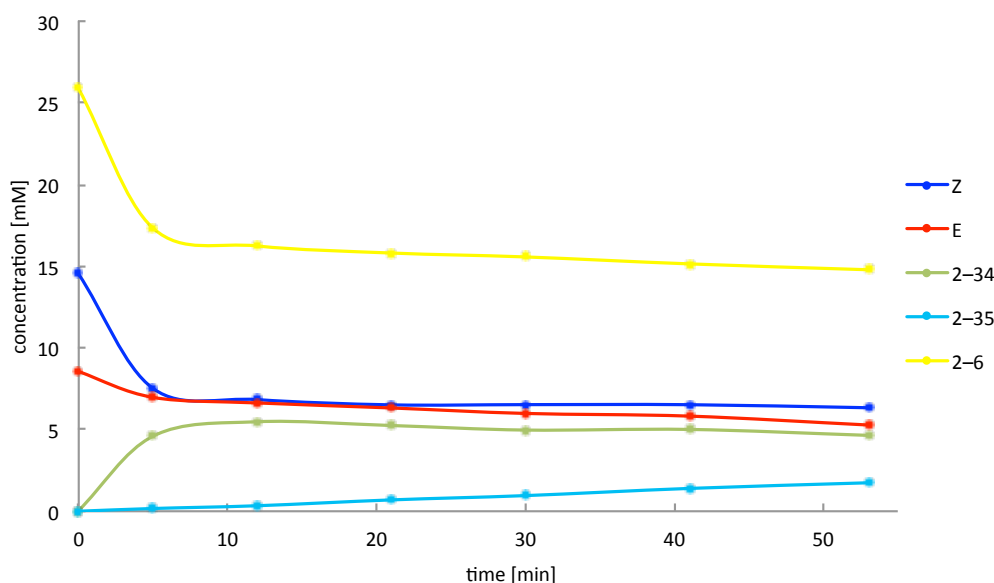
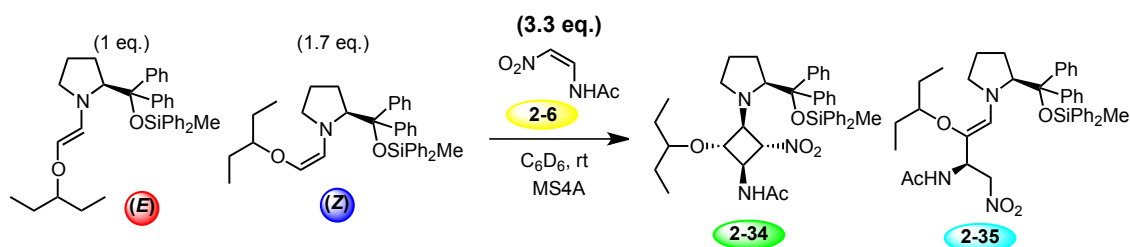


Figure 13. Reaction profile of *E*- and *Z*-enamines with *cis*-nitroalkene **2-6** (3.3 eq.)^[a]

[a] *cis*-Nitroalkene **2-6** (0.05 mmol, 1.0 ml, 0.05 M solution in C₆D₆) was added to the preformed C₆D₆ solution (0.73 ml) of *E*- and *Z*-enamine (0.041 mmol: *E/Z* = 1/1.7) with toluene (internal standard: 0.02 mmol, 40 ul, 0.5M solution in C₆D₆) in the presence of MS4A (200 mg). Without molecular sieves, an aliquot (0.6 ml) of this reaction mixture was transferred to a NMR tube. The reaction was monitored by ¹H NMR spectroscopy. The concentration of each product was calculated by integration of selected peaks in the ¹H NMR spectra and plotted on the graph.

When the catalytic reaction was performed, acid additive was essential in case of *cis*-nitroalkene **2-6** as well. Therefore, effect of acid was investigated. When *cis*-nitroalkene **2-6** (3.6 eq.) was added to the mixture of *E/Z*-enamine (2.7 eq., *E/Z* = 1/1.7), only *Z*-enamine reacted to afford cyclobutane **2-34**. The reaction did not progress further before the addition of acid. HCOOH (the best acid additive for the catalytic reaction of α -alkoxyaldehyde **2-5** and *cis*-nitroalkene **2-6**) was added after 21 min. Although the NMR spectra became rapidly complicated, few points are noteworthy. Not only *E* and *Z* enamines, but also cyclobutane **2-34**, were rapidly consumed within 10 min of the addition of HCO₂H. With their disappearance, the amount of Michael product **2-4** (black line) and γ -nitro-enamine **2-35** (light-blue line) increased. This infers two main roles for the acid (e.g. HCO₂H): 1) to facilitate cyclobutane ring opening, 2) to accelerate Michael addition of the enamine onto the *cis*-nitroalkene **2-6**.

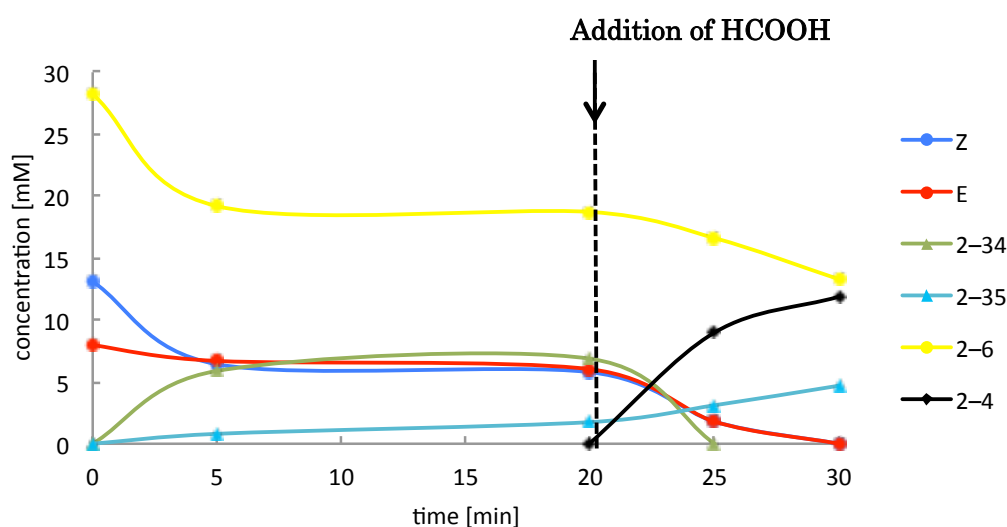
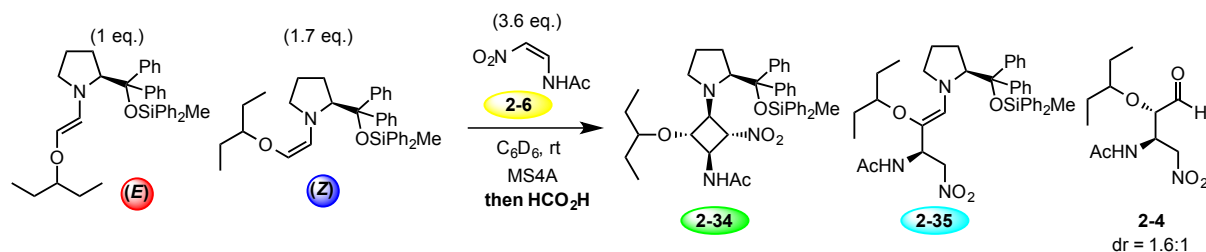


Figure 14. The effect of acid for acceleration of Michael reaction [a]

[a] *cis*-Nitroalkene **2-6** (0.05 mmol, 1.0 ml, 0.05 M solution in C₆D₆) was added to a preformed C₆D₆ solution (0.73 ml) of the *E*- and *Z*-enamines (0.0372 mmol: *E/Z* = 1/1.7) with toluene as internal standard (0.02 mmol, 40 ul, 0.5M solution in C₆D₆) in the presence of MS4A (200 mg). Without molecular sieves, an aliquot (0.6 ml) of this reaction mixture was transferred to a NMR tube and HCO₂H (62 ul, 0.5 M solution in C₆D₆) was subsequently added to the NMR tube after 21 minutes. The reaction was monitored by ¹H NMR spectroscopy. The concentration of each product was calculated by integration of selected peaks in the ¹H NMR spectra and plotted on the graph.

Thus, the mechanistic investigation of *E/Z*-enamines with *trans/cis*-nitroalkenes provides the following strong evidence: 1) *E*-enamine reacts faster toward *trans*-nitroalkene **2-10** while *Z*-enamine reacts faster toward *cis*-nitroalkene **2-6**, 2) acid accelerates isomerization of *E/Z*-enamines, 3) acid accelerates carbon-carbon bond forming addition of enamines to nitroalkenes. All of them contributes to the generation of 2*S*-isomer, that is to say excellent diastereo and enantioselectivity can be realized. Although the optimal acid additive differs according to the particular characteristics of the Michael acceptor, the stereoselectivity and yield in the Michael reaction of α -alkoxyaldehydes are generally improved by screening for an appropriate acid additive.

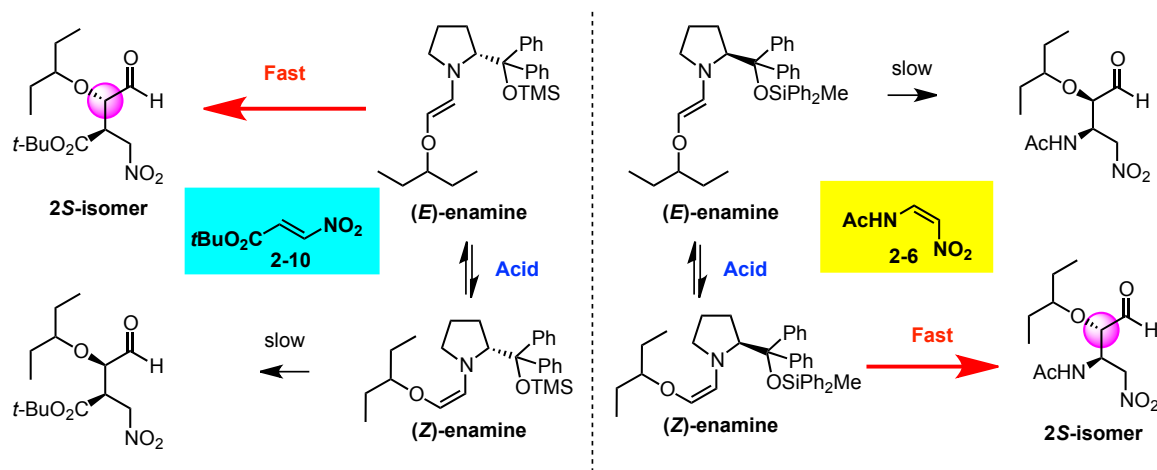
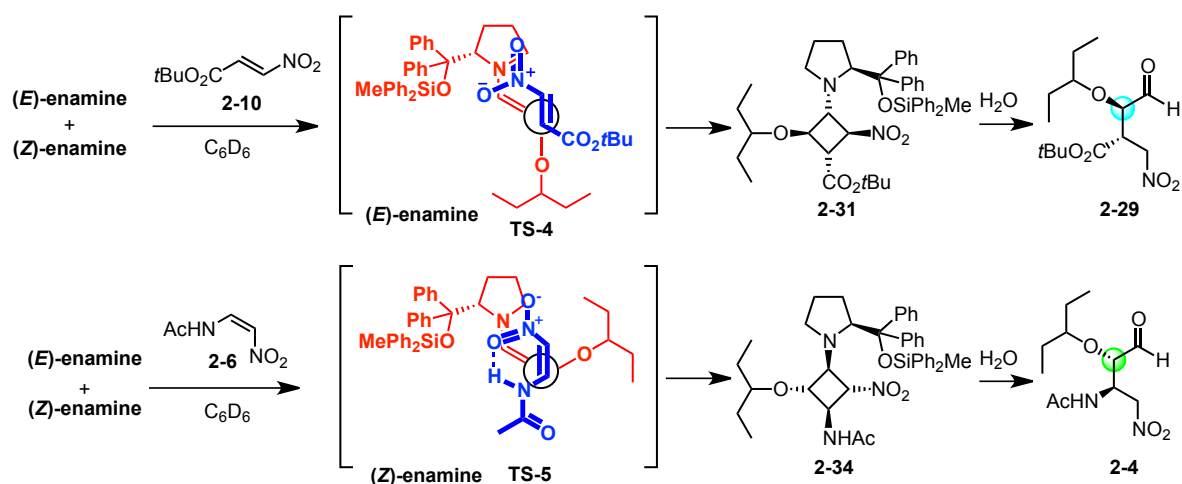


Figure 15. Summary of mechanistic investigation

2-4-6 Michael reaction of α -alkoxyaldehyde with other *cis*-Michael acceptor

The proposed transition state models for the Michael reaction of pentan-3-yloxyacetaldehyde (**2-5**) with (*E*)-*tert*-butyl-3-nitropropenoate (**2-10**) and (*Z*)-*N*-2-nitroethenylacetamide (**2-6**), when catalyzed by diphenylprolinol silyl ethers, are described in Scheme 6. When the *trans*-nitroalkene **2-10** was mixed with a mixture of *E*- and *Z*-enamines, the *E*-enamine reacts with **2-10** to generate the cyclobutane **2-31** through the proposed transition state model **TS-4**. The ring opening of **2-31** and hydrolysis subsequently generates the Michael product **2-29**. On the other hand, when the *cis*-alkene **2-6** was used as a Michael acceptor, the *Z*-enamine reacts with **2-6** to generate the cyclobutane **2-34**. In this case, ring opening of **2-34** and hydrolysis gives **2-4** possessing a (2*S*)-configuration, opposite to that of the (2*R*)-aldehyde **2-29**. The transition state model **TS-5**, which was independently proposed by Ma^[2] and Lu,^[4] is consistent with this absolute configurational outcome.

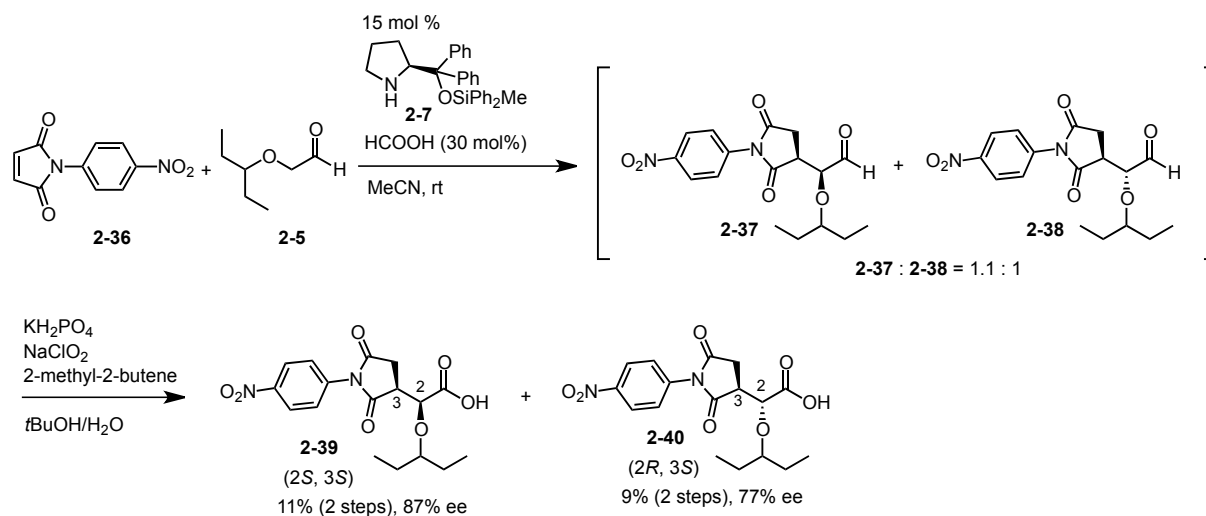


Scheme 6. Reactivity of *E*- and *Z*-enamines toward *trans*-nitroalkene **2-10** and *cis*-nitroalkene **2-6**. *E*-enamine reacts with **2-10** to give cyclobutane **2-31**, while the *Z*-enamine reacts with **2-6** to give cyclobutane **2-34**

Although the transition state model **TS-5** may explain the diastereo and enantioselectivities, a more complicated sequence might exist during the reaction course; for example, we found **2-6** exists as its *cis*-isomer in CDCl_3 (*cis:trans* = >99 : <1), while the *trans*-isomer prevails in DMSO (*cis:trans* = 7 : 93).^[7] The isomerization from *cis* to *trans* might need to be considered. Therefore, we selected to study a *cis*-alkene as the Michael acceptor that is known not to isomerize to its *trans*-form. This would allow for the unambiguous investigation of the transition state models of the Michael reaction between α -alkoxyaldehydes and *cis*-alkenes.

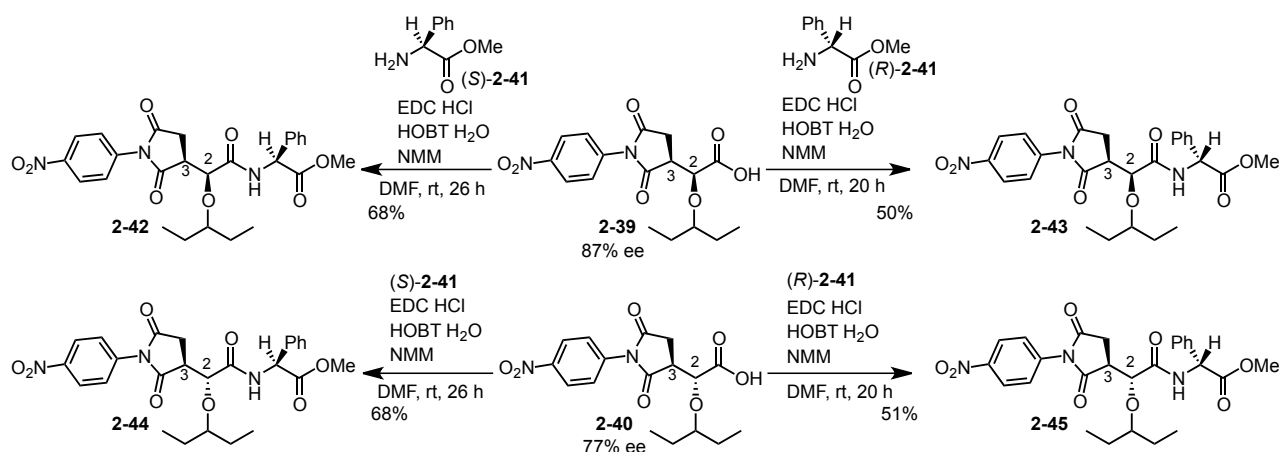
The first study we selected was the Michael reaction of α -alkoxyaldehyde **2-5** with phenylmaleimide **2-36** as the *cis*-alkenyl Michael acceptor. Cordova et al. reported that the

Michael reaction of maleimides and aliphatic aldehydes catalyzed by (*S*)-diphenylprolinol silyl ether gives (*2R*, *3S*)-isomer.^[11] We conducted the asymmetric Michael reaction of **2-5** and **2-36** catalyzed by **2-7**. This generated the Michael adducts as a mixture of diastereomers, **2-37**:**2-38** = 1.1:1 (Scheme 7). The reaction was not optimized. Since the generated Michael products were not stable enough for isolation, they were converted to their carboxylic acids without purification. The diastereomers were separated at this stage. The enantioselectivity of each isomer was determined by HPLC on chiral phase after conversion to the corresponding methyl ester. The enantiomeric excess of the (*2S*, *3S*)-isomer **2-39** was 87%, and that of the (*2R*, *3S*)-isomer **2-40** was 77%.



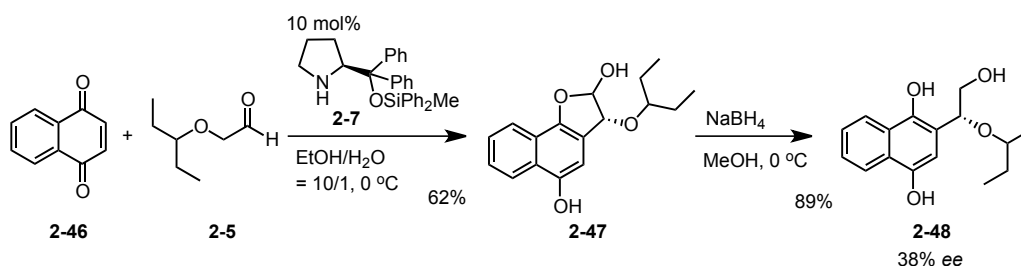
Scheme 7. Asymmetric Michael reaction of phenylmaleimide **2-36** and α -alkoxyaldehyde **2-5**

The relative and absolute configuration of carboxylic acids **2-39** and **2-40** were determined as follows (Scheme 8). The carboxylic acid **2-39** was condensed with (*S*)-phenylglycine methyl ester (PGME) (*S*)-**2-41** and (*R*)-**2-41** to give the (*S*)-PGME amide **2-42** and (*R*)-PGME amide **2-43**, respectively. The carboxylic acid **2-40** was also condensed with (*S*)-**2-41** and (*R*)-**2-41** to give the (*S*)-PGME amide **2-44** and (*R*)-PGME amide **2-45**, respectively. As key signals in the ¹H NMR spectra of compounds of **2-42** and **2-44** are readily resolved, as compared with those of **2-39** and **2-40**, the relative configuration was determined by an NMR study according to J-Based Configuration Analysis (JBCA method).^[12] In this way, **2-39** and **2-40** were found to possess (*2S*^{*}, *3S*^{*}) and (*2R*^{*}, *3S*^{*}) configurations, respectively. The absolute configuration at C₂ of **2-39** was then determined by the PGME method of Kusumi.^[13] The chemical shift difference between (*S*)-PGME amide **2-42** and (*R*)-PGME amide **2-43** was calculated and the absolute configuration at C₂ in **2-42** and **2-43** was determined to be (*2S*). Therefore, the absolute configuration of **2-39** was determined to be (*2S*, *3S*). The absolute configuration of **2-40** was similarly determined to be (*2R*, *3S*). The transition states of the reaction will be discussed later.



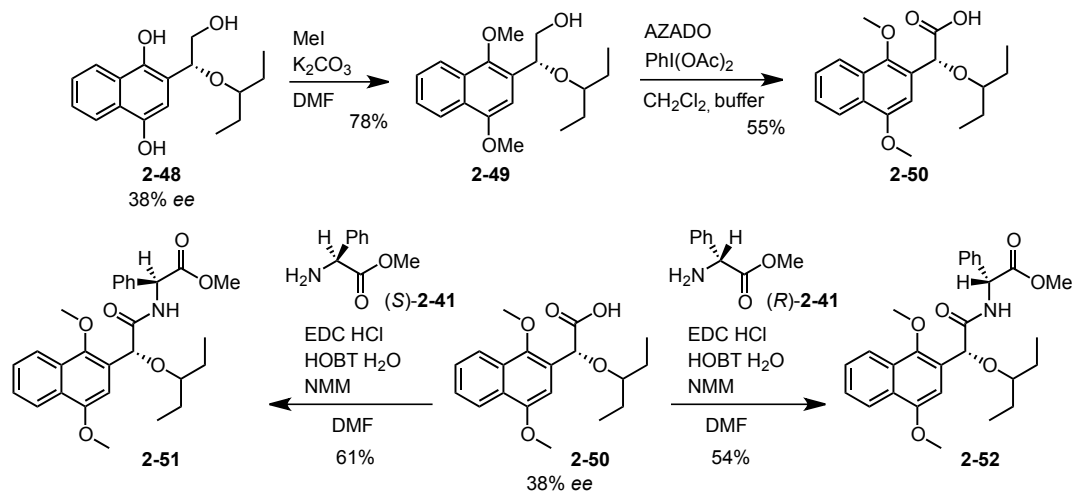
Scheme 8. Synthesis of *(S)*-amide **2-42**, **2-44** and *(R)*-amide **2-43**, **2-45**

As another *cis*-alkene to investigate, naphthoquinone (**2-46**) was selected. Jørgensen demonstrated the organocatalyzed Michael reaction of naphthoquinone (**2-46**) with several aliphatic aldehydes, which upon reduction generated primary alcohols in excellent enantiomeric excesses.^[14] We performed the Michael reaction of α -alkoxyaldehyde **2-5** and **2-46** to generate the hemiacetal **2-47** (Scheme 9). The enantiomeric excess was determined after reduction of the hemiacetal **2-47** to its corresponding alcohol **2-48**. The enantiomeric excess of **2-48** was determined to be 38%. This is low in contrast to the excellent value obtained in the reaction of aliphatic aldehydes as reported by Jørgensen.^[14]



Scheme 9. Asymmetric Michael reaction of naphthoquinone (**2-46**) and α -alkoxyaldehyde **2-5**

Compound **2-48** was converted to methyl ether **2-49**, followed by oxidation provided carboxylic acid **2-50** (Scheme 10). Acid **2-50** was condensed with *(S)*-**2-41** and *(R)*-**2-41** to afford *S*-amide **2-51** and *R*-amide **2-52**, respectively. The absolute configuration of **2-50** was determined to be *(R)* by the PGME method.^[13] The transition state models for these reactions will be discussed next.



Scheme 10. Synthesis of *S* amine **2-51** and *R* amide **2-52**

2-4-7 Transition state models

We propose the transition state models for phenylmaleimide **2-36** (Figure 15) and naphthoquinone (**2-46**) (Figure 16) as Michael acceptors. As mentioned previously, Cordova et al. reported the Michael reaction of aliphatic aldehydes and phenylmaleimides in the presence of (*S*)-diphenylprolinol silyl ether to give the Michael product **2-53** with a (2*R*, 3*S*) configuration in excellent diastereo- and enantio-selectivities.^[11] The Cordova group reasoned the observed selectivity by proposing the transition state model **TS-6** between the *E*-enamine and phenylmaleimide (eq. 1). In spite of the high enantioselectivity, the diastereoselectivity of the Michael reaction of pentan-3-yloxyacetaldehyde (**2-5**) and phenylmaleimide was low (Scheme 7). From our results, we propose the transition state models for Michael reaction of pentan-3-yloxyacetaldehyde (**2-5**) and phenylmaleimide as shown in Figure 15.

Three transition state models, i.e., **TS-7**, **TS-8** and **TS-9**, should be considered in the reaction of the *E*-enamine. **TS-7** is a similar model to that proposed by Cordova. **TS-7** is the least steric hindrance but it does not agree with the acyclic synclinal transition state as proposed by Seebach and Golinski.^[10] Although **TS-9**, which affords a wrong isomer, would provide better charge interactions than **TS-8**, **TS-9** is sterically encumbered. **TS-8** is preferable in terms of both steric hindrance and electrostatic interactions. Thus, the reaction of the *E*-enamine would likely proceed via **TS-8**. According to the same considerations of steric and electrostatic interactions, the reaction of the *Z*-enamine would proceed via **TS-10** to provide the observed (2*S*, 3*S*)-isomer.

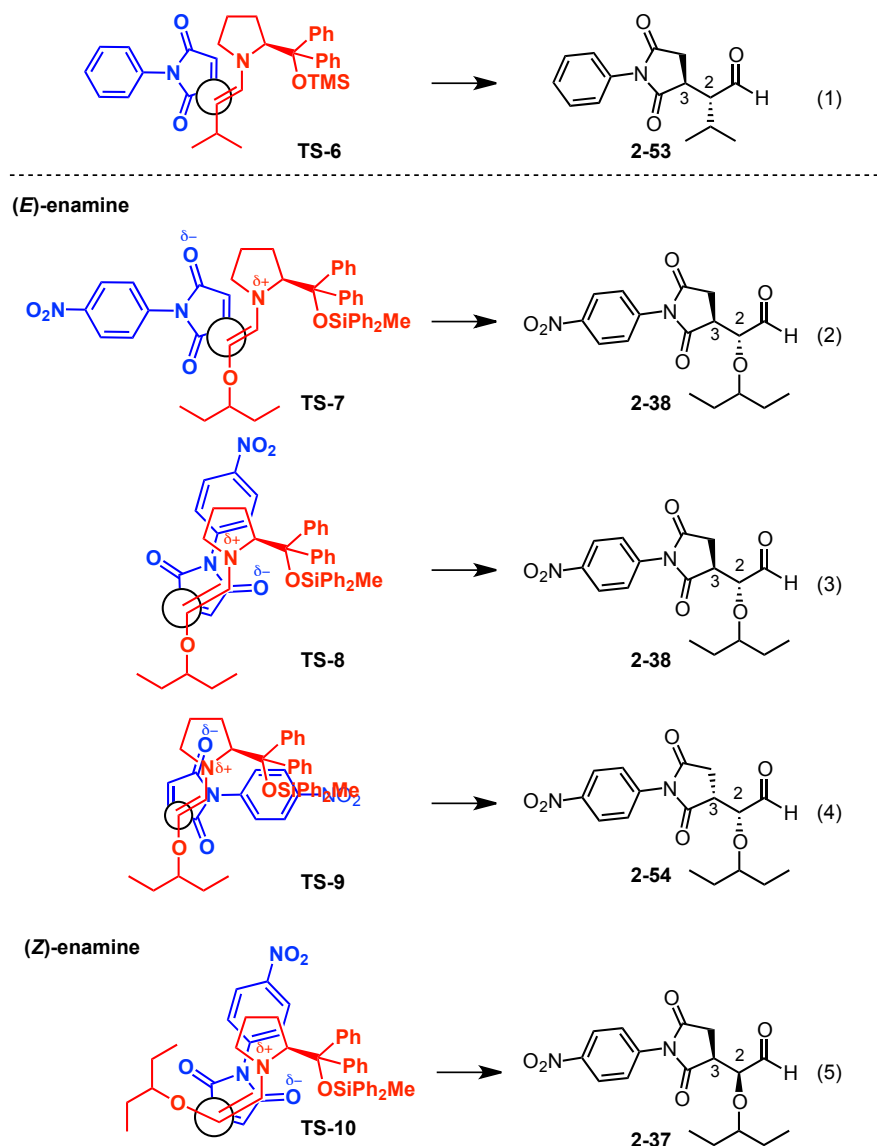


Figure 15. Transition state models of prolinol-derived enamines and phenylmaleimide

As mentioned previously, Jørgensen reported the Michael reaction of aliphatic aldehydes with naphthoquinone (**2-46**), as catalyzed by (*S*)-diphenylprolinol silyl ethers, to afford chiral adducts in excellent enantioselectivity.^[14] We propose herein a plausible transition state model as follows (Figure 16). The naphthoquinone approaches from the *Si* face of the *E*-enamine in alignment with optimal electrostatic interactions as described in Seebach's model^[17] (**TS-11**, eq. 1). This would generate the Michael product **2-55**, which would convert to **2-56** after aromatization. In contrast to the excellent enantioselectivity in the reaction of aliphatic aldehydes, the Michael reaction of α -alkoxyaldehydes gave low enantioselectivity (38% *ee*) (Scheme 9). This can be explained as follows (**TS-12**, eq. 2; **TS-13**, eq. 3). Both the *E* and *Z*-enamines would react with naphthoquinone. The *E*-enamine would generate **2-57** through **TS-12**, followed by aromatization to afford the (*R*)-isomer **2-47**. The *Z*-enamine would generate

the (*S*)-isomer **2-59**, the enantiomer of **2-47**, through **TS-13**. The resultant enantioselectivities are low because the *E*- and *Z*-enamines each afford the opposite enantiomer and the reaction proceeds through both *E*- and *Z*-enamine species.

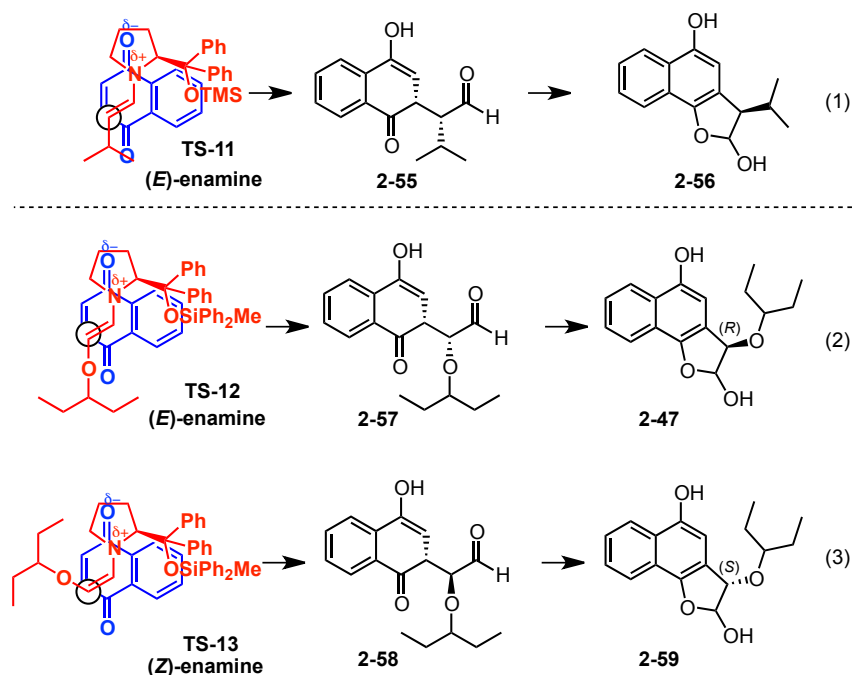


Figure 16. Transition state models of enamines and naphthoquinone

As mentioned earlier, the absolute configuration of the Michael product **2-8** was determined to be (*2R*, *3R*), and **2-4** as (*2S*, *3R*) (Figure 17). In both products, the absolute configuration next to the AcNH group in **2-4** and **2-8** is the same. The configuration at the α -position of the alkoxy group in **2-4** and **2-8** is opposite, which would be determined by geometry of the enamine. By analogy, these results are consistent with the transition state models proposed for the *cis*-Michael acceptors, phenylmaleimide **2-36** and naphthoquinone **2-46**. Specifically, the major isomer **2-4** would result from transition state model **TS-5** (eq. 1), while the minor isomer **2-8** would be derived from the reaction of the *E*-enamine via **TS-2** (eq. 2).

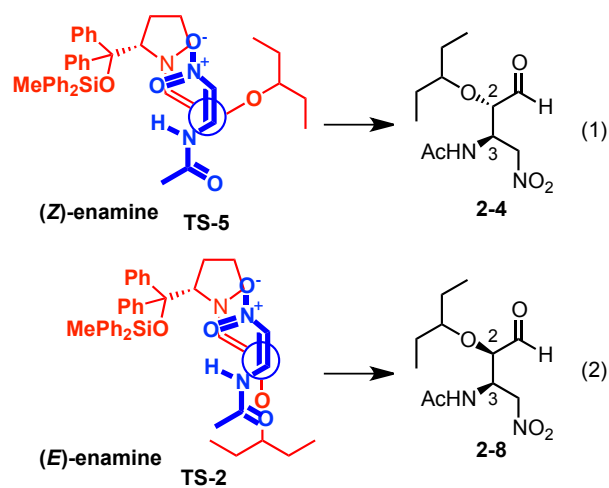


Figure 17. Transition state models of enamine with (*Z*)-*N*-2-nitroethenylacetamide

2-4-8 Isomerization and reactivity of *E*- and *Z*-enamine

In the case of phenylmaleimide **2-36**, both *E*- and *Z*- enamines that are generated from pentan-3-yloxyacetaldehyde (**2-5**) and diphenylprolinol silyl ether **2-7** react with **2-36** to furnish a 1:1.1 mixture of aldehyde **2-38** and **2-37** (Figure 18). Both the *E*- and *Z*- enamines also react with naphthoquinone (**2-46**), affording a 2.2:1 mixture of **2-47** and **2-59** (38% ee). These results indicate that both *E*- and *Z*- enamines react with each Michael acceptor.

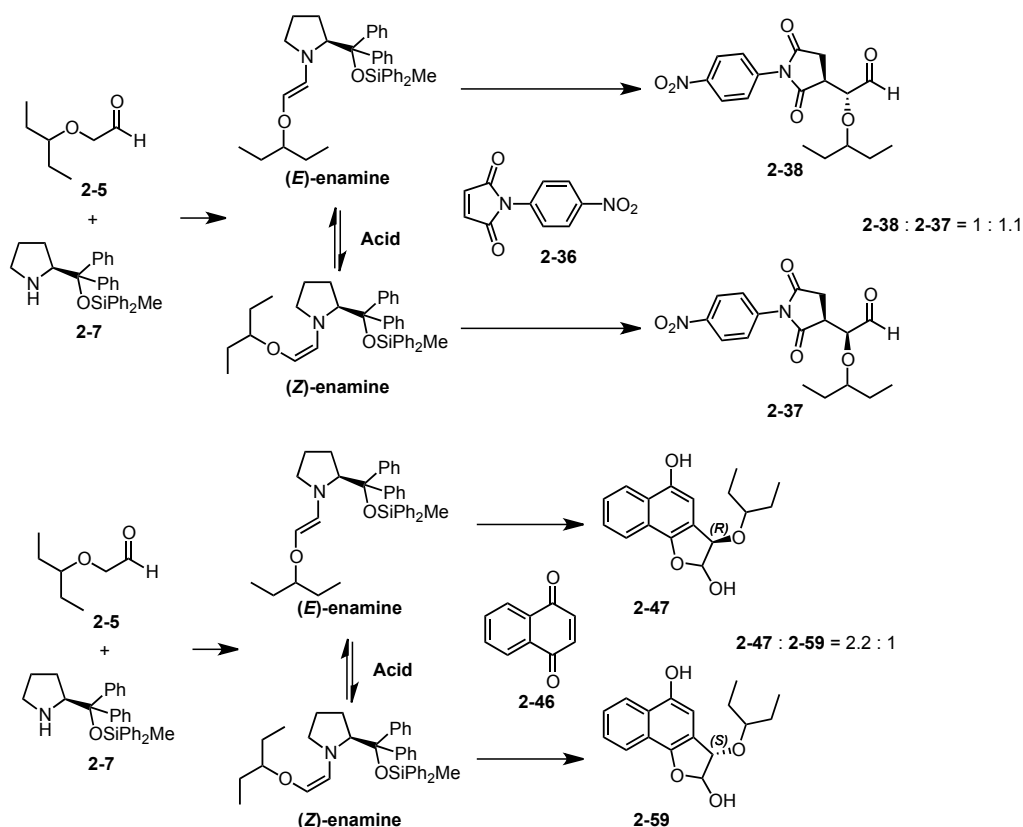


Figure 18. Reaction of both *E*- and *Z*- enamines with **2-36** and **2-46**

Contrary to the reactions with phenylmaleimide **2-36** and naphthoquinone (**2-46**), the reactions of (*Z*)-*N*-2-nitroethenylacetamide (**2-6**) and (*E*)-*tert*-butyl-3-nitropropenoate (**2-10**) exhibit a different profile. The reaction of (*Z*)-*N*-2-nitroethenylacetamide (**2-6**) and pentan-3-yloxyacetaldehyde (**2-5**), catalyzed by (*S*)-diphenylprolinol silyl ether **2-7**, afforded the Michael product **2-4** in good yield with excellent diastereo and enantioselectivities, even though both *E*- and *Z*- enamines are generated. A similar result is obtained with the reaction of (*E*)-*tert*-butyl-3-nitropropenoate (**2-10**) and pentan-3-yloxyacetaldehyde (**2-5**) when catalyzed by (*R*)-diphenylprolinol silyl ether **2-4**. The Michael product **2-29** is obtained in good yield with excellent diastereo and enantioselectivities, although both *E*- and *Z*- enamines are generated. These results can be explained as follows (Figure 19): the *Z*-enamine reacts with (*Z*)-*N*-2-nitroethenylacetamide (**2-6**) faster than the *E*-enamine, and the acid facilitates this

addition of *Z*-enamine. There is a fast equilibrium between the *E*- and *Z*-enamines in the presence of acid. Thus, the *Z*-enamine reacts preferentially and the remaining *E*-enamine isomerizes to its *Z*-form, which then reacts with Michael acceptor **2-6** to afford the product **2-4**. Similar phenomena are also observed with the (*E*)-*tert*-butyl-3-nitropropenoate (**2-10**), but the other *E*-enamine preferentially reacts with (*E*)-**2-10**, and the remaining *Z*-enamine readily isomerizes to its (*E*)-form before reacting with the Michael acceptor (*E*)-**2-10** to afford the product **2-29**. It is noteworthy that excellent diastereo and enantioselectivities are obtained with good yield in both reactions of (*Z*)-*N*-2-nitroethenylacetamide (**2-6**) and (*E*)-*tert*-butyl-3-nitropropenoate (**2-10**). This would be possible when the following three relative rates are orchestrated correctly: 1) the speed of generation of the *E*- and *Z*-enamines from pentan-3-yloxyacetaldehyde (**2-5**) and diphenylprolinol silyl ether, 2) the reaction speed of the *E*- and *Z*-enamines toward each Michael acceptor **2-6** and **2-10**, and 3) the isomerization speed between the *E*- and *Z*-enamines. As the reacting enantioface of *E*- and *Z*-enamine is opposite, we have to employ (*S*)-diphenylprolinol silyl ether **2-7** as a catalyst in the *Z*-enamine while (*R*)-diphenylprolinol silyl ether **2-4** is employed in the *E*-enamine.

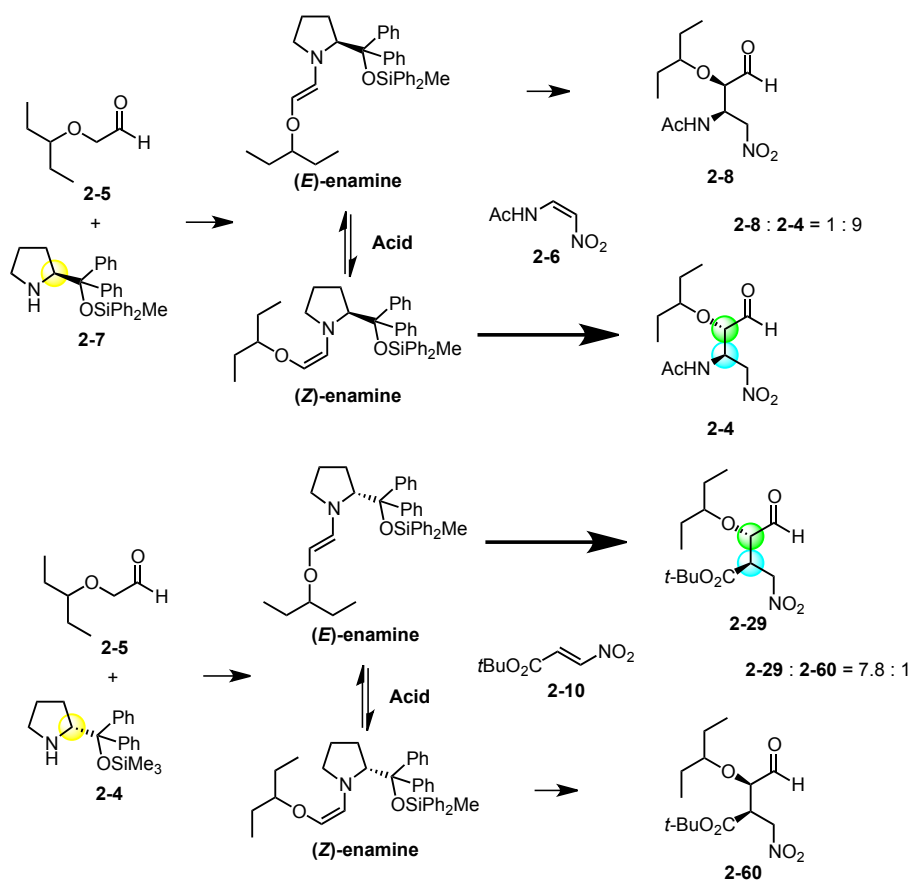
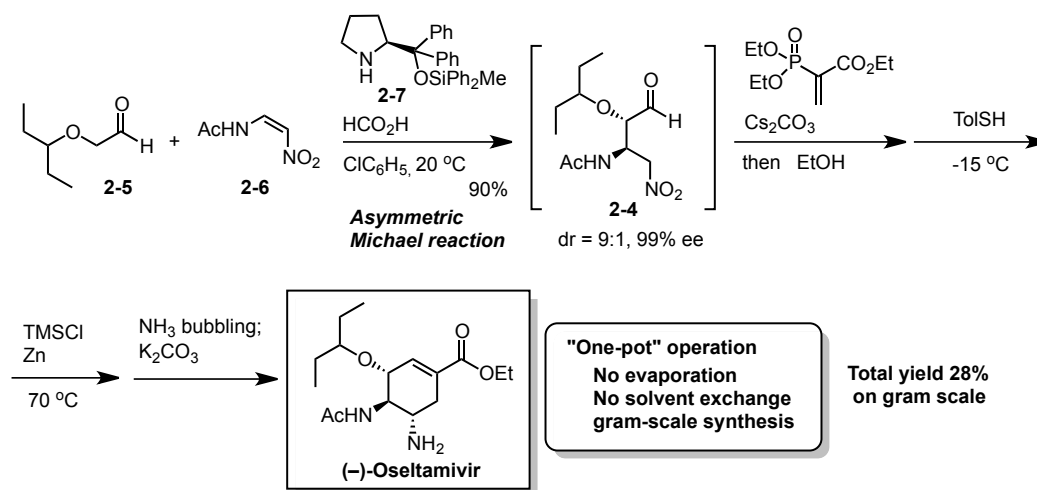


Figure 19. Isomerization and reaction of *E*- and *Z*-enamines with **2-6** and **2-10** in the presence of appropriate acid

2-5 Conclusion

We have achieved a completely “one-pot” sequential synthesis of (–)-Oseltamivir without solvent evaporations or exchange on gram-scale (Scheme 11). On the basis of our original route,^[1] and advancements by others,^[2,3,4] we have critically modified the first key asymmetric Michael reaction of pentan-3-yloxyacetaldehyde (**2-5**) with (*Z*)-*N*-2-nitroethenylacetamide (**2-6**) to proceed in good yield and with excellent diastereo and enantioselectivities. Key to the success of this transformation are five-fold: 1) the use of a bulky silyl substitution in the diphenylprolinol silyl ether organocatalyst **2-7**, 2) HCO₂H as an acid additive to accelerate the reaction course and to increase stereoselectivities, 3) the use of chlorobenzene as solvent to allow for all subsequent transformations and permit large scale production, 4) control of the internal reaction temperature at 20 °C to increase diastereoselectivity, and 5) slow addition of pentan-3-yloxyacetaldehyde (**2-5**) to suppress the self-condensation of **2-5**.



Scheme 11. Summary of “one-pot” synthesis of (–)-Oseltamivir

The mechanistic investigation of Michael reaction of α -alkoxyaldehyde **2-5** with *trans*-nitroalkene **2-10** and *cis*-nitroalkene **2-6**, catalyzed by diphenylprolinol silyl ether **2-7**, revealed the following things; 1) α -alkoxyaldehyde **2-5** generates both *E* and *Z*-enamines while aliphatic aldehyde generates only *E*-enamine, 2) *E* and *Z*-enamines are in equilibrium and acid accelerates isomerization, 3) *E*-enamine reacts faster with *trans*-nitroalkene **2-10** while *Z*-enamine reacts faster with *cis*-nitroalkene **2-6** (Figure 20). The transition state model for *cis*-nitroalkene **2-6** (**TS-2** and **TS-5**) was ultimately proposed by determining the absolute configuration of the minor isomer of Michael product **2-8** and by studying the Michael reaction of α -alkoxyaldehyde **2-5** with other *cis*-alkene Michael acceptors that cannot isomerize in geometry (i.e., with phenylmaleimide **2-36** and naphthoquinone **2-46**). The mechanistic study indicates that the Michael reaction can be effectively carried out by the correct orchestration of

three reaction processes: 1) the speed of generating the *E/Z*-enamines from pentan-3-yloxyacetaldehyde and diphenylprolinol silyl ether, 2) the relative reactivity of *E*- and *Z*-enamines toward the Michael acceptor **2-6** and **2-10**, and 3) the acid-promoted isomerization between the *E*- and *Z*-enamines.

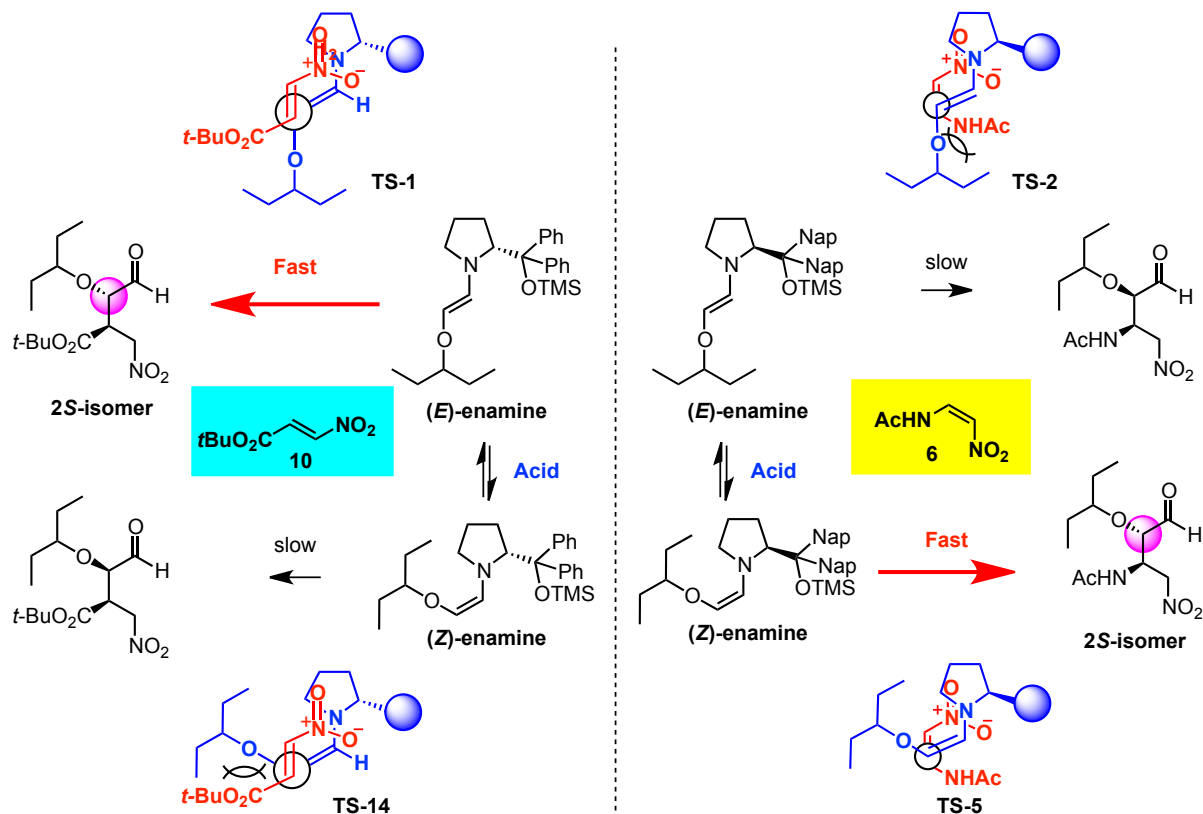


Figure 20. Summary of mechanistic investigation of Michael reaction of α-alkoxyaldehyde with *trans*-nitroalkene **2-10** and *cis*-nitroalkene **2-6**

Collectively, the synthesis presented herein is the first example of a drug of this stereochemical complexity to be synthesized in a single pot, in a significant yield, and without the need to evaporate or exchange solvents on gram-scale. We further believe the present synthesis of (–)-Oseltamivir to be not only environmentally benign, but also efficient enough for larger scale production.

References and notes

- [1] a) H. Ishikawa, T. Suzuki, Y. Hayashi, *Angew. Chem. Int. Ed.* **2009**, *48*, 1304. b) H. Ishikawa, T. Suzuki, H. Orita, T. Uchimar, Y. Hayashi, *Chem. Eur. J.* **2010**, *16*, 12616.
- [2] S. Zhu, S. Yu, Y. Wang, D. Ma, *Angew. Chem. Int. Ed.* **2010**, *49*, 4656.
- [3] J. Rehpuk, M. Hut'ka, A. Latika, H. Brath, A. Almassy, V. Hajzer, J. Durmis, S. Toma, R. Sebesta, *Synthesis* **2012**, *44*, 2424.
- [4] J. Weng, Y.-B. Li, R.-B. Wang, G. Lu, *ChemCatChem* **2012**, *4*, 1007.
- [5] K. Patora-Komisarska, M. Benohoud, H. Ishikawa, D. Seebach, Y. Hayashi, *Helv. Chim. Acta* **2011**, *94*, 719.
- [6] U. Grošelj, D. Seebach, D. M. Badine, W. B. Schweizer, A. K. Beck, I. Krossing, P. Klose, Y. Hayashi, T. Uchimar, *Helv. Chim. Acta* **2009**, *92*, 1225.
- [7] D. Seebach, S. Xiaoyu, M. O. Ebert, W. B. Schweizer, N. Purkayastha, A. K. Beck, J. Duschmalé, H. Wennemers, T. Mukaiyama, M. Benohoud, Y. Hayashi, M. Reiher, *Helv. Chim. Acta* **2013**, *96*, 799.
- [8] Y. Hayashi, H. Gotoh, T. Hayashi, M. Shoji, *Angew. Chem. Int. Ed.* **2005**, *44*, 4212.
- [9] D. Seebach, X. Sun, C. Sparr, M. O. Ebert, W. B. Schweizer, A. K. Beck, *Helv. Chim. Acta* **2012**, *95*, 1064.
- [10] D. Seebach, J. Golinski, *Helv. Chim. Acta* **1981**, *64*, 1413.
- [11] G.-L. Zhao, Y. Xu, H. Sunden, L. Eriksson, M. Sayah, A. Cordova, *Chem. Commun.* **2007**, 734.
- [12] G. Bifulco, P. Dambruoso, L. Gomez-Paloma, R. Riccio, *Chem. Rev.* **2007**, *107*, 3744.
- [13] a) Y. Nagai, T. Kusumi, *Tetrahedron Lett.* **1995**, *36*, 1853; b) T. Yabuuchi, T. Kusumi, *J. Org. Chem.* **2000**, *65*, 397.
- [14] J. Aleman, S. Cabrera. E. Maerten, J. Overgaard, K. A. Jørgensen, *Angew. Chem, Int. Ed.* **2007**, *46*, 5520.
- [15] a) T. Yamamoto, S. Tomoda, *Chem. Lett.* **1997**, 1069; b) T. Yamamoto, D. Kaneno, S. Tomoda, *Chem. Lett.* **2005**, *34*, 1190; c) T. Yamamoto, D. Kaneno, S. Tomoda, *Bull. Chem. Soc. Jpn.* **2008**, *81*, 1415.

Chapter 3. Asymmetric Michael addition of nitromethane to 2-oxoindoline-3-ylidene acetaldehyde and three “one-pot” sequential synthesis of (–)-Horsfiline and (–)-Coerulescine

We aimed to develop an efficient synthesis of both (–)-Horsfiline and (–)-Coerulescine, employing the “one-pot” reaction and organocatalyzed asymmetric reaction. The main challenge was to construct the all-carbon quaternary stereogenic centers in a catalytic enantioselective fashion.

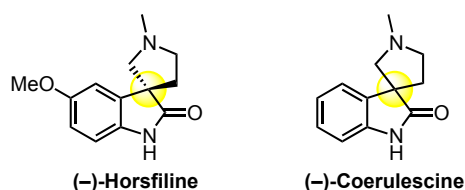


Figure 1. (–)-Horsfiline and (–)-Coerulescine

We planned to construct the all carbon quaternary stereogenic centers by organocatalyzed Michael addition of nitromethane to β,β -disubstituted- α,β -unsaturated aldehyde (Figure 2). There is a potential enantioselectivity issue to be solved. Since the α,β -unsaturated aldehyde possesses bis-substitution at β -position, the β,β -disubstituted- α,β -unsaturated aldehyde would generate both *E*- and *Z*-isomers. Both *E*- and *Z*-isomer would react with nitromethane and afford enantiomer, respectively. As a result, enantioselectivity would be decreased. Therefore, how to obtain the product in excellent enantioselectivity is the key to success for the synthesis of (–)-Horsfiline and (–)-Coerulescine.

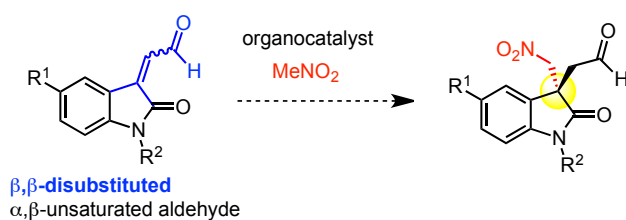


Figure 2. Construction of all-carbon quaternary stereogenic centers

3-1 Retrosynthesis

Our retrosynthesis is shown in Figure 3. The pyrrolidine in **3-1** and **3-2** would thus be constructed by reduction of the nitro group in **3-3** or **3-4** followed by intramolecular cyclization. We expected that the organocatalyzed Michael addition of nitromethane to 2-oxoindoline-3-ylidene acetaldehyde **3-5** or **3-6** would generate the aldehyde **3-3** or **3-4** with the necessary enantioselective construction of the quaternary carbon center. The enals **3-5**, **3-6** would be pre-generated from a commercially available isatin derivative **3-7** or **3-8** with acetaldehyde via aldol condensation.

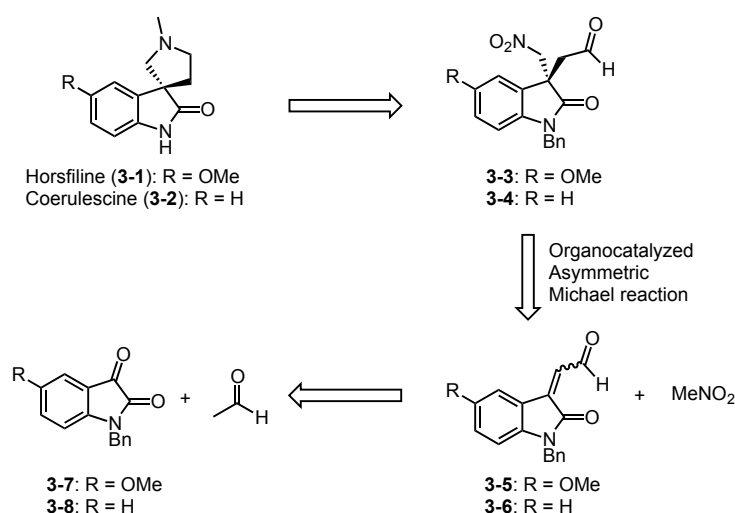


Figure 3. Retrosynthesis of Horsfiline (**3-1**) and Coerulescine (**3-2**)

3-2 Synthesis of 2-oxoindoline-3-ylidene acetaldehyde

The transformation of aldehyde **3-9** into α,β -unsaturated aldehyde **3-12** with two carbon homologation is often employed in the organic synthesis (Figure 4). The three steps synthesis is typically used for the synthesis of **3-12** from **3-9**. The conversion to the α,β -unsaturated ester **3-10** from **3-9** by Wittig or Horner-Wadsworth-Emmons reaction, followed by reduction to the alcohol **3-11**, then oxidation to **3-12**. Although this is good transformation, one of the most straightforward and practical methods would be the cross-aldol condensation reaction of acetaldehyde **3-13** with **3-9**. However, this is a difficult reaction, as the obtained product **3-12** possesses also formyl moiety, which reacts further with the other nucleophile.

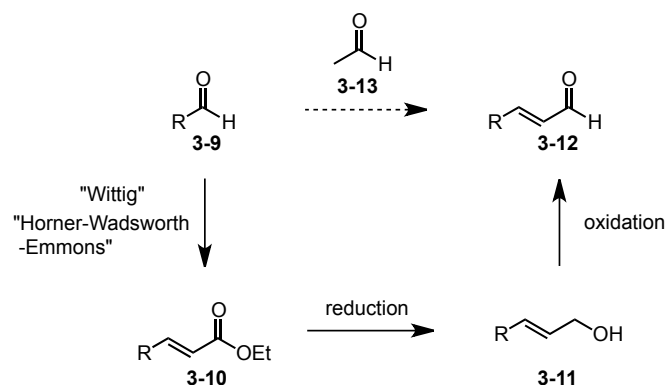


Figure 4. Synthesis of α,β -unsaturated aldehyde **3-12** from aldehyde **3-9**

Our group recently developed the straightforward synthesis of α,β -unsaturated aldehyde **3-15** from aryl aldehyde **3-14** and acetaldehyde **3-13** (Figure 5).^[1] The arylaldehyde **3-14** was mixed with acetaldehyde **3-13** in the presence of DBU to afford a mixture of α,β -unsaturated aldehyde **3-15** and acetal **3-16**. The mixture of **3-15** and **3-16** was evaporated at 50 °C to afford **3-15**. The yield is up to 85%.

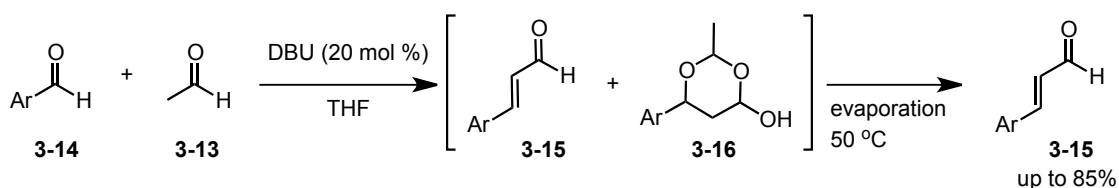
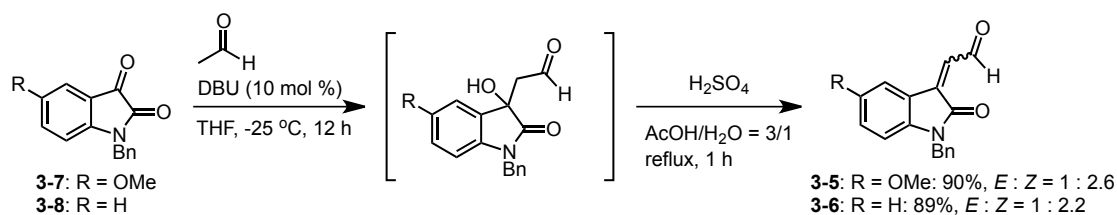


Figure 5. Synthesis of α,β -unsaturated aldehyde **3-15** from aryl aldehyde **3-14** and acetaldehyde **3-13**

This method was applied to the synthesis of 2-oxoindoline-3-ylidene acetaldehyde **3-5** and **3-6**. The aldol addition of isatin derivative **3-7** or **3-8** with acetaldehyde generated the β -hydroxyaldehyde and dehydration under acidic conditions provided **3-5** or **3-6** directly as a mixture of *E/Z* isomers (Scheme 1). The enals **3-5** and **3-6** were both obtained in a “one-pot” operation from isatin **3-7** or **3-8** in excellent yield. This method was found to be higher yielding and more convenient than reported methods, for example, enal **3-6** has been produced in 27%, over 3 steps by reduction of the 3-position on **3-8** to alcohol, alkylation with bromoacetaldehyde diethyl ether and acetal deprotection to afford **3-6**.^[2]



Scheme 1. Synthesis of 2-oxoindoline-3-ylidene acetaldehyde **3-5** and **3-6**

3-3 Construction of all-carbon quaternary stereogenic centers

Next, the conjugate addition of nitromethane to **3-6** was investigated (Table 1). As the generated aldehyde **3-4** was not stable enough for isolation, the yields and enantiomeric excesses were determined after reduction of **3-4** into alcohol **3-18**. Our group has already developed the asymmetric conjugate addition of nitromethane to β,β -disubstituted- α,β -unsaturated aldehydes under neat conditions.^[3] We, therefore, followed these neat conditions at first. The catalyst **3-17** gave better enantioselectivity than catalyst **3-16**, although the yield was low (entry 1, 2). As we reported MeOH as the best solvent for the conjugate addition of nitromethane to α,β -unsaturated aldehydes,^[4] MeOH was used; however, decomposition occurred (entry 3). When EtOH was used, both the yield and enantioselectivity improved (entry 4). The best enantioselectivity was observed when *i*PrOH was used (entry 5). Addition of water shortened the reaction time (entry 6). Water facilitates iminium ion hydrolysis and regeneration of the catalyst. Acid and base additives such as PhCO₂H and NaOAc did not improve the result (entry 7, 8). When the *Z*-isomer of **3-6** was used predominantly (*E:Z* = 1:6), almost the same yield and enantioselectivity was obtained starting from an *E:Z* = 1:2.2 mixture of **3-6** (entry 9).

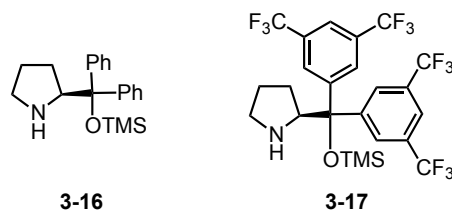
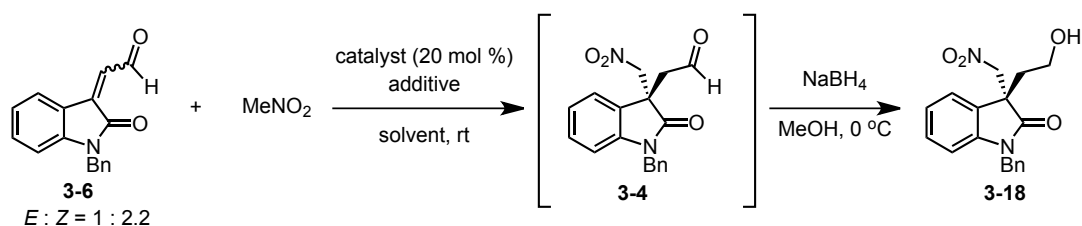


Figure 5. Organocatalysts used in the Michael addition of nitromethane

Table 1. Optimization of Michael addition of nitromethane to 2-oxoindoline-3-ylidene acetaldehyde **3-6**^[a]



Entry	Catalyst	Solvent	Additive	Temp /°C	Time /h	Yield of 13 /% ^[b]	Ee /% ^[c]
1 ^[d]	3-16	-	-	5	22	66	59
2 ^[d]	3-17	-	-	5	24	15	79
3	3-17	MeOH	-	rt	2	0	-
4	3-17	EtOH	-	rt	96	67	87
5	3-17	<i>i</i> PrOH	-	rt	120	68	94
6 ^[e]	3-17	<i>i</i> PrOH	H ₂ O	rt	42	72	94
7 ^{[e][f]}	3-17	<i>i</i> PrOH	H ₂ O	rt	46	59	90
8 ^{[e][g]}	3-17	<i>i</i> PrOH	PhCO ₂ H	rt	23	0	-
9 ^{[e][h]}	3-17	<i>i</i> PrOH	NaOAc	rt	38	72	93

[a] Unless stated otherwise, the reaction was performed by employing aldehyde **3-6** (0.1 mmol, $E:Z = 1:2$), nitromethane (0.5 mmol), catalyst (20 mol %), and additive (20 mol %) in solvent (1 ml) at room temperature for the indicated time. [b] Isolated yield. [c] The enantiomeric excess was determined by HPLC analysis on chiral phase. [d] Nitromethane (30 eq.) was used. [e] H₂O (10 eq.) was used. [f] PhCO₂H (20 mol %) was used. [g] NaOAc (20 mol %) was used. [h] $E:Z = 1:6$ for **3-6** was used.

It should be noted that excellent enantioselectivity was observed even though a mixture of *E/Z* isomers of **3-6** (*E:Z* = 1:2.2) was used (Figure 6, eq. 1). Both *Z* and *E* isomer would form iminium ion **3-19** and **3-20**, then nitromethane attacks to the iminium ion, avoiding bulky substituents on pyrrolidine, to afford **3-4** and **3-21**, respectively (Figure 6, eq. 2, 3). The ratio of **3-4**: **3-21** should be 2.2:1 (38 % ee) as the ratio of starting material was 2.2:1. However, the reaction provided the product in 94 % ee. We assumed that isomerization between the *E* and *Z* isomers of **3-6** occurred during the reaction.

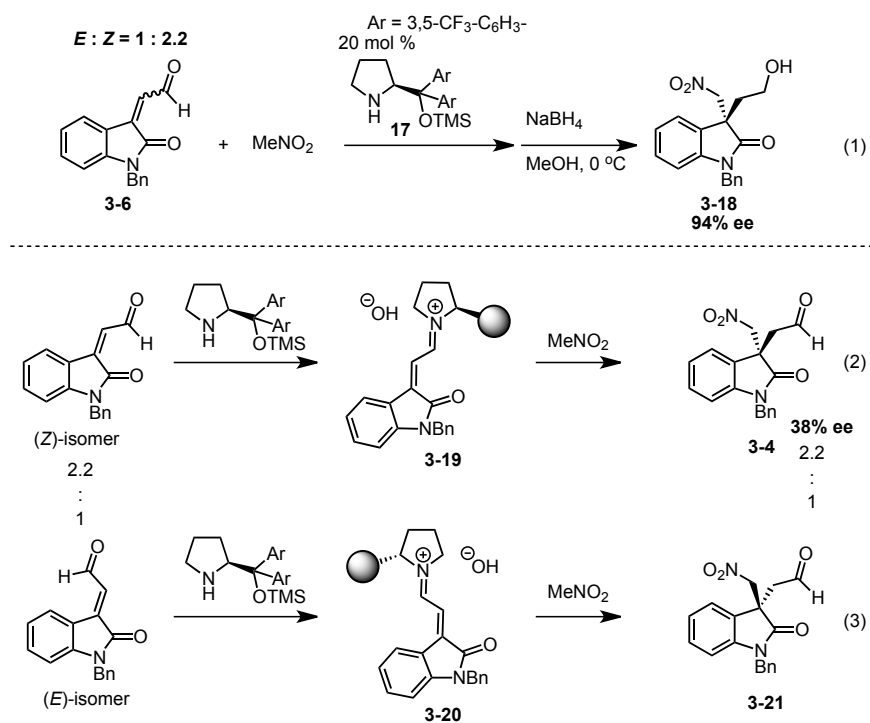


Figure 6. Unexpected enantioselectivity

In order to prove the hypothesis, isomerization was investigated. A mixture of *E/Z* isomer of **3-6** (*E:Z* = 1:9) was mixed with a catalyst **3-17** in the presence 2-nitropropane, which does not react with **3-6** due to steric reasons (Figure 7). The *E/Z* ratio of **3-6** was monitored by ^1H NMR spectroscopy, and the percentage of *Z*-isomer was plotted on a graph. The *Z*-isomer decreased in the absence of water with time (solid line), indicating isomerization between *E*- and *Z*-isomer occurred. Isomerization was slightly accelerated in the presence of water (dotted line).

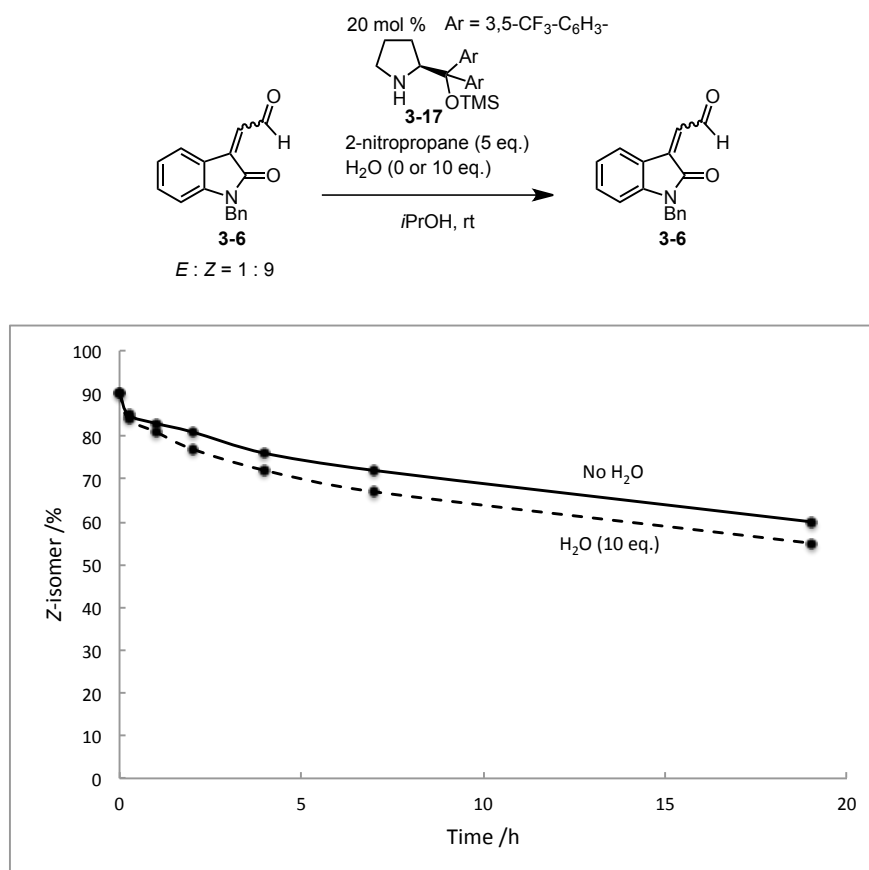


Figure 7. Isomerization between *E*- and *Z*-isomer of **3-6**

Here is a proposed isomerization mechanism and transition state models to explain the course of enantioselectivity in the Michael addition of nitromethane with 2-oxoindoline-3-ylidene acetaldehyde (Figure 8). Both *E* and *Z* isomer generates iminium ion. We assume that isomerization between *E* and *Z*-isomer would occur through the addition and elimination process of hydroxyl ion. Nitromethane forms nitronate, which reacts with the iminium ion via acyclic synclinal transition state proposed by Seebach,^[5] maximizing electrostatic interaction between nitro group and iminium ion. The **TS-1**, in which *Z*-isomer reacts, provides a major enantiomer. On the other hand, there is a steric repulsion between phenyl group and nitro group at synclinal position in **TS-2**. As a result, the addition of nitromethane proceeds via **TS-1** preferentially to form major enantiomer.

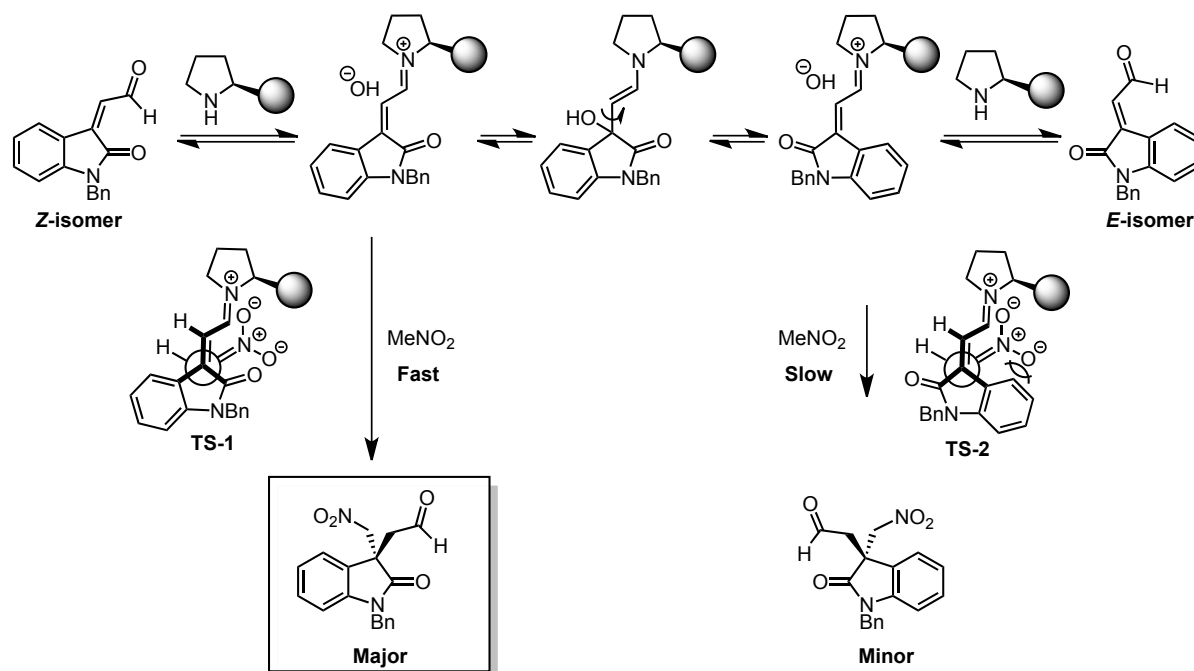
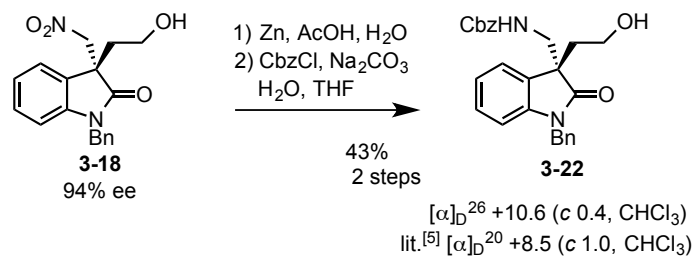


Figure 8. Proposed mechanism of isomerization between *E* and *Z*-isomer

3-4 Determination of absolute configuration of Michael product

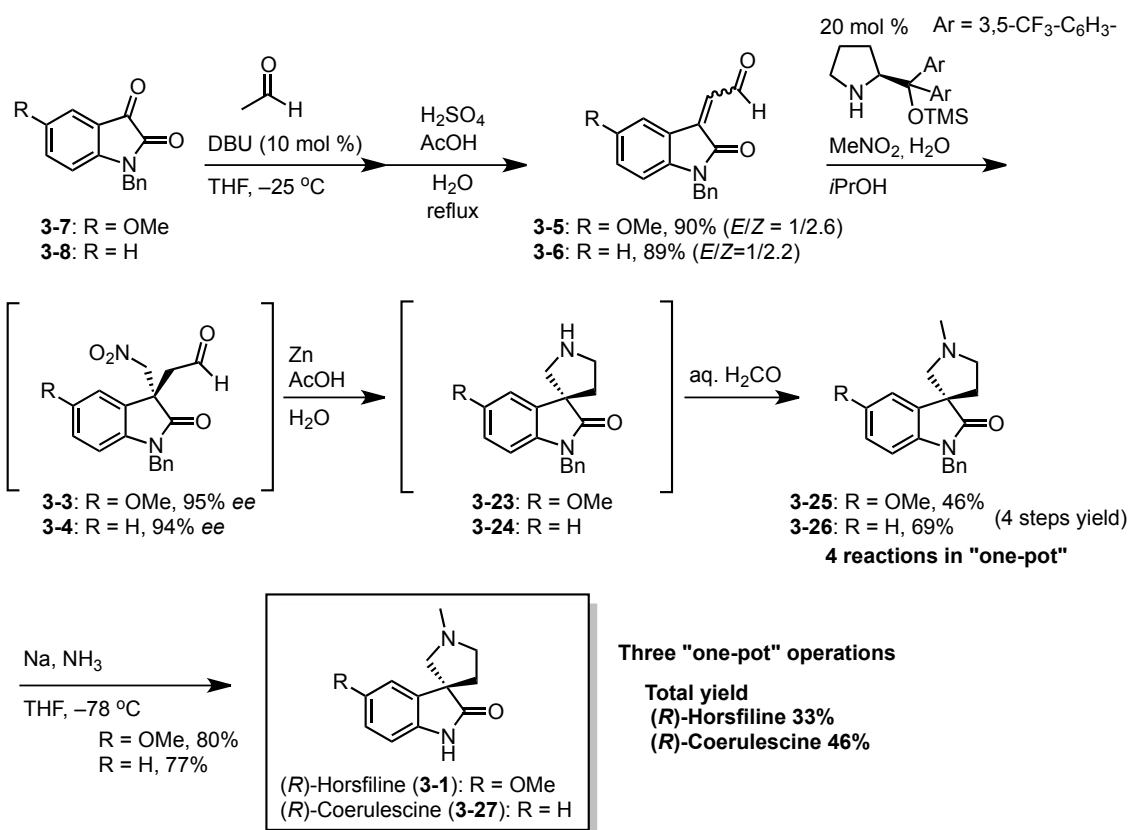
The absolute configuration was determined by converting the Michael product **3-18** into the known compound **3-22** (Scheme 2).^[6] The optical rotation indicates that **3-22** has an (*R*) configuration.



Scheme 2. Determination of absolute configuration

3-5 Three “one-pot” sequential synthesis of (*R*)-Horsfiline and (*R*)-Coerulescine

With the optimal reaction conditions for the Michael addition of nitromethane to the 2-oxoindoline-3-ylidene acetaldehyde secured, the three “one-pot” sequential synthesis of horsfiline and coerulescine was pursued (Scheme 3). Our synthesis started from an aldol reaction of commercially available isatin derivative **3-7** or **3-8** with acetaldehyde, followed by dehydration under acidic conditions, to give 2-oxoindoline-3-ylidene acetaldehyde **3-5** or **3-6** as *E/Z* mixtures in excellent yield. The enantioselective conjugate addition of nitromethane to **3-5** or **3-6** generated aldehyde **3-3** or **3-4** with excellent enantioselectivity in the construction of the all-carbon quaternary stereogenic centers. To the same reaction vessel, Zn, AcOH, and water were added to reduce the nitro group into an amine. At the same time, an intramolecular reductive amination proceeded to form the pyrrolidino-spirocycle. Formaldehyde was then added to the reaction mixture sequentially to install the *N*-methyl group by intermolecular reductive amination. This afforded **3-25** and **3-26** in 46% and 69% yields over 4 steps from aldehyde **3-5** and **3-6**, respectively. Four reactions from aldehyde **3-5** or **3-6** were performed in the same reaction vessel. Removal of the benzyl group under Birch conditions furnished (*R*)-horsfiline (**3-1**) and (*R*)-coerulescine (**3-27**) in good yield. The spirooxyindole tends to racemize under acidic condition,^[7,8] therefore the optical purity was checked by HPLC analysis over a chiral phase. This showed **3-1** to be 95% *ee* and **3-27** to be 94 % *ee* indicating that racemization did not occur during our synthesis. Hence, three “one-pot” sequential syntheses of (*R*)-horsfiline (**3-1**) and (*R*)-coerulescine (**3-27**) were developed in good total yield.



Scheme 3. Three "one-pot" sequential synthesis of (*R*)-horsfiline (**3-1**) and (*R*)-coerulescine (**3-27**)

3-6 Determination of absolute configuration of (–)-Coerulescine

The optical rotation of (*R*)-Horsfiline (95% ee) via our route was found to be -7.0 in MeOH, which is consistent with the reported data (Figure 9).^[9] As mentioned above (Scheme 2), the absolute configuration of the Michael product **3-4**, an intermediate to Coerulescine, was determined to be (*R*) by conversion to the known compound **3-22** and comparing the optical rotation. Synthetic (–)-Horsfiline via our route should thus have a (*R*)-configuration (95% ee). Similarly, synthetic Coerulescine should also have a (*R*)-configuration (94% ee). The optical rotation of (*R*)-Coerulescine via our route was -1.1 in MeOH. On the other hand, the optical rotation of Danishefsky's (*S*)-Coerulescine was -0.55 , although the solvent was not mentioned.^[10] The optical rotation of natural Coerulescine is -0.77 in MeOH. Although the solvent of optical rotation for Danishefsky's (*S*)-Coerulescine was not mentioned, synthetic (*R*)-Coerulescine via our route and Danishefsky's showed the same minus optical rotation, even though they were enantiomers. Due to the small optical rotations, we synthesized (*S*)-Coerulescine using Danishefsky's procedure to measure the optical rotation unambiguously in MeOH.

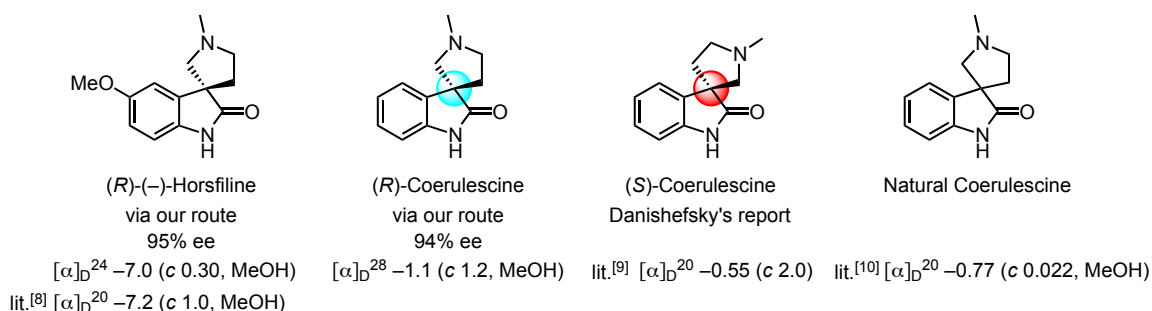
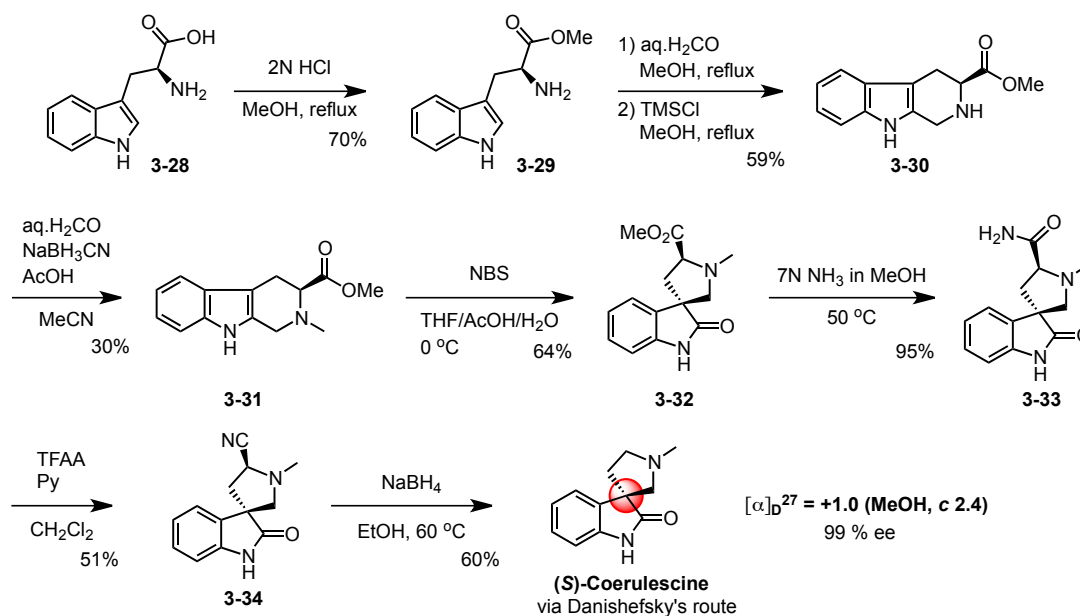


Figure 9. The structure of (*R*)-(-)-Horsfiline, (*R*)-Coerulescine, Danishefsky's (*S*)-Coerulescine, and natural (–)-Coerulescine

L-Tryptophan **3-28** was thus converted to amide **3-33** by following Danishefsky's procedure (Scheme 4).^[10] Compound **3-33** was treated with TFAA^[12] instead of TFA,^[10] and the nitrile **3-34** reductively removed to give (*S*)-Coerulescine. Chiral HPLC analysis and circular dichroism (CD) spectroscopy analysis showed that synthetic Coerulescine via our route and that of Danishefsky resulted in enantiomeric material.^[13] The optical rotation of (*S*)-Coerulescine via Danishefsky's route was found to be $+1.0$ in MeOH, the absolute but opposite value of the optical rotation of synthetic (*R*)-Coerulescine formed via our route (Scheme 3).



Scheme 4. Synthesis of (*S*)-Coerulescine via Danishefsky's route and its optical rotation

As the optical rotation of natural Coerulescine is -0.77 in MeOH and that of (*R*)-Coerulescine via our route is -1.1 in MeOH, we propose a (*R*)-configuration as the absolute configuration of (–)-Coerulescine (Figure 8).

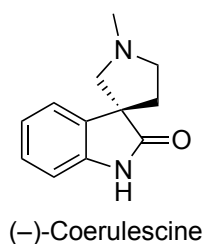
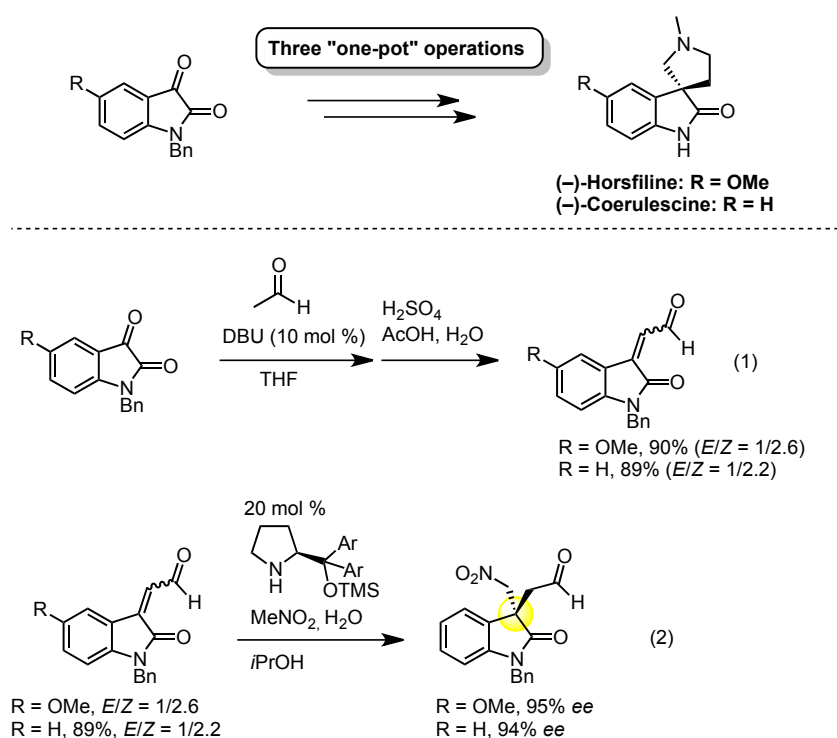


Figure 8. The absolute configuration of (–)-Coerulescine

3-7 Conclusion

In summary, we have achieved a three “one-pot” sequential synthesis of both (–)-Horsfiline and (–)-Coerulescine (Scheme 5). The first key reaction is the straightforward synthesis of 2-oxoindoline-3-ylidene acetaldehyde from an isatin derivative with acetaldehyde (Scheme 5, eq. 1). The aldol reaction of isatin with acetaldehyde, followed by dehydration under acidic conditions, provided the 2-oxoindoline-3-ylidene acetaldehyde in excellent overall yield. The second key reaction was the construction of the all-carbon quaternary stereogenic centers (Scheme 5, eq. 2). The Michael addition of nitromethane to 2-oxoindoline-3-ylidene acetaldehyde, by careful choice of diarylprolinol silyl ether catalyst and the reaction solvent, constructed the quaternary stereocenter in excellent enantioselectivity. The method allowed using the mixture of *E/Z*-isomer as a starting material to give the product in excellent enantioselectivity. This is synthetic advantage, as we do not need to prepare pure *Z*-isomer. In addition, we determined the absolute configuration of (–)-Coerulescine to be (*R*).



Scheme 5. Summary

References and notes

- [1] manuscript in preparation
- [2] R. L. Autrey, F. C. Tahk, *Tetrahedron* **1967**, *23*, 901.
- [3] Y. Hayashi, Y. Kawamoto, M. Honda, D. Okamura, S. Umemiya, Y. Noguchi, T. Mukaiyama, I. Sato, submitted
- [4] H. Gotoh, D. Okamura, H. Ishikawa, Y. Hayashi, *Org. Lett.* **2007**, *9*, 5307.
- [5] D. Seebach, J. Golinski, *Helv. Chim. Acta* **1981**, *64*, 1413.
- [6] G. Lakshmaiah, T. Kawabata, M. Shang, K. Fuji, *J. Org. Chem.* **1999**, *64*, 1699.
- [7] B. M. Trost, M. K. Brennan, *Org. Lett.* **2006**, *8*, 2027.
- [8] E. Wenkert, J. H. Udelhofen, N. K. Bhattacharyya, *J. Am. Chem. Soc.* **1959**, *81*, 3763.
- [9] A. Jossang, P. Jossang, H. A. Hadi, T. Sévenet, B. Bodo, *J. Org. Chem.* **1991**, *56*, 6527.
- [10] C. Li, C. Chan, A. C. Heimann, S. J. Danishefsky, *Angew. Chem. Int. Ed.* **2007**, *46*, 1444.
- [11] N. Anderton, P. A. Cockrum, S. M. Colegate, J. A. Edgar, K. Flower, I. Vit, R. I. Willing, *Phytochemistry* **1998**, *48*, 437.
- [12] C. Pellegrini, C. Strässler, M. Weber, H. J. Borschberg, *Tetrahedron Asymmetry* **1994**, *5*, 1979.
- [13] HPLC charts and Circular Dichroism (CD) spectra can be found in Supporting Information.

The “pot-economy” synthesis of (–)-Oseltamivir, (–)-Horsfiline, and (–)-Coerulescine was described in this doctoral thesis (Figure 1). I have developed a “one-pot” synthesis of (–)-Oseltamivir and three “one-pot” sequential synthesis of (–)-Horsfiline and (–)-Coerulescine.



4-1 + 4-2 $\xrightarrow[\text{C}_6\text{H}_5\text{Cl}, 20^\circ\text{C}]{\text{HCO}_2\text{H}}$ 4-3 (90%)

Asymmetric Michael reaction

4-3 $\xrightarrow[\text{then EtOH}]{\text{EtO}_2\text{P(O)CO}_2\text{Et}, \text{Cs}_2\text{CO}_3}$ 4-4 (99% ee)

4-4 $\xrightarrow[\text{NH}_3 \text{ bubbling}; \text{K}_2\text{CO}_3]{\text{TMSCl}, \text{Zn}}$ (-)-Oseltamivir (70 °C)

"One-pot" operation
 No evaporation
 No solvent exchange
 gram-scale synthesis

Total yield 28% on gram scale

Scheme 1. Summary of “one-pot” synthesis of (–)-Oseltamivir (Chapter 2)

The mechanistic investigation of Michael reaction of α -alkoxyaldehyde **4-1** with *trans*-nitroalkene **4-5** and *cis*-nitroalkene **4-2**, catalyzed by diphenylprolinol silyl ether **4-3**, demonstrated the following things; 1) α -alkoxyaldehyde **4-1** generates both *E* and *Z*-enamines while aliphatic aldehyde generates only *E*-enamine, 2) *E* and *Z*-enamines are in equilibrium and acid accelerates isomerization, 3) *E*-enamine reacts faster with *trans*-nitroalkene **4-5** while *Z*-enamine reacts faster with *cis*-nitroalkene **4-2** (Figure 2). The transition state model for *cis*-nitroalkene **4-2** (**TS-3** and **TS-4**) was ultimately proposed by determining the absolute configuration of the minor isomer of Michael product and by studying the Michael reaction of α -alkoxyaldehyde **4-1** with other *cis*-alkene Michael acceptors that cannot isomerize in geometry (i.e., with phenylmaleimide and naphthoquinone). The mechanistic study indicates that the Michael reaction can be effectively carried out by the correct orchestration of three reaction processes: 1) the speed of generating the *E/Z*-enamines from pentan-3-yloxyacetaldehyde and diphenylprolinol silyl ether, 2) the relative reactivity of *E*- and *Z*-enamines toward the Michael acceptor **4-5** and **4-2**, and 3) the acid-promoted isomerization between the *E*- and *Z*-enamines.

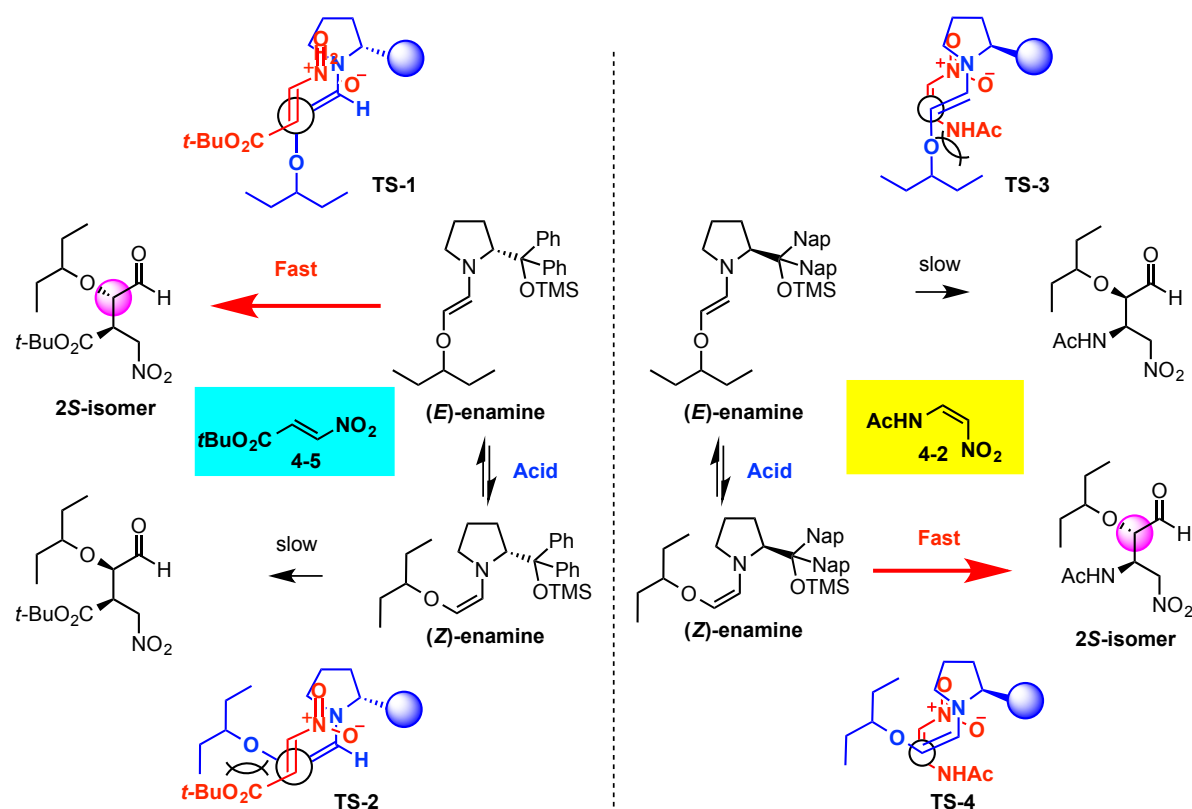
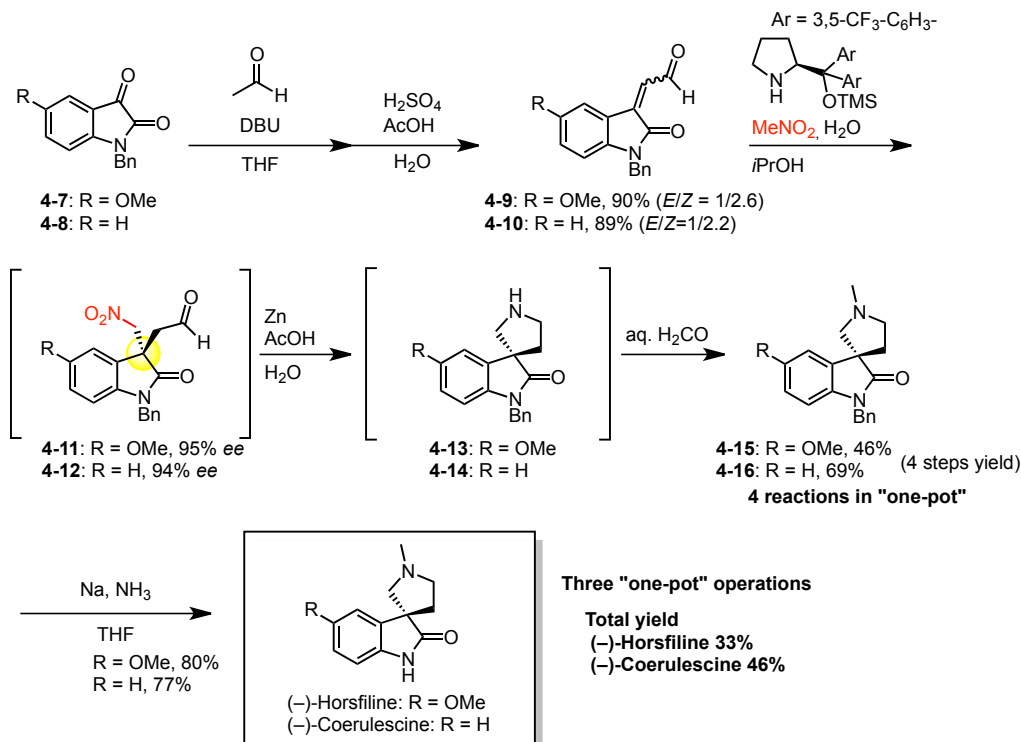


Figure 2. Summary of mechanistic investigation of Michael reaction of α -alkoxyaldehyde with *trans*-nitroalkene **4-5** and *cis*-nitroalkene **4-2** (Chapter 2)

The concept of “one-pot” reaction was extended to the synthesis of (–)-Horsfiline and (–)-Coerulescine. The three “one-pot” sequential synthesis of both (–)-Horsfiline and (–)-Coerulescine was described in chapter 3 (Scheme 2). The first key reaction is the straightforward synthesis of 2-oxoindoline-3-ylidene acetaldehyde **4-9** or **4-10** from an isatin derivative **4-7** or **4-8** with acetaldehyde. The aldol reaction of isatin derivative **4-7** or **4-8** with acetaldehyde, followed by dehydration under acidic conditions, provided the 2-oxoindoline-3-ylidene acetaldehyde **4-9** or **4-10** in excellent overall yield as a mixture of *E*- and *Z*-isomers. The second key reaction was the construction of the all-carbon quaternary stereogenic centers. The Michael addition of nitromethane to 2-oxoindoline-3-ylidene acetaldehyde **4-9** or **4-10**, by careful choice of diarylprolinol silyl ether catalyst and the reaction solvent, constructed the all-carbon quaternary stereogenic centers in excellent enantioselectivity. The method allowed using the mixture of *E/Z*-isomer **4-9** or **4-10** as a starting material to give the product in excellent enantioselectivity. This is synthetic advantage, as we do not need to prepare pure *Z*-isomer. Removal of the benzyl group under Birch conditions furnished (–)-Horsfiline and (–)-Coerulescine in good yield. Hence, three “one-pot” sequential syntheses of (–)-Horsfiline and (–)-Coerulescine were developed in good total yield. In addition, we determined the absolute configuration of (–)-Coerulescine to be (*R*).



Scheme 2. Summary of three “one-pot” sequential synthesis of (–)-Horsfiline and (–)-Coerulescine (Chapter 3)

References and notes

- [1] a) H. Ishikawa, T. Suzuki, Y. Hayashi, *Angew. Chem. Int. Ed.* **2009**, *48*, 1304. b) H. Ishikawa, T. Suzuki, H. Orita, T. Uchimaru, Y. Hayashi, *Chem. Eur. J.* **2010**, *16*, 12616.
- [2] S. Zhu, S. Yu, Y. Wang, D. Ma, *Angew. Chem. Int. Ed.* **2010**, *49*, 4656.
- [3] J. Rehak, M. Hut'ka, A. Latika, H. Brath, A. Almassy, V. Hajzer, J. Durmis, S. Toma, R. Sebesta, *Synthesis* **2012**, *44*, 2424.
- [4] J. Weng, Y.-B. Li, R.-B. Wang, G. Lu, *ChemCatChem* **2012**, *4*, 1007.

Experimental section

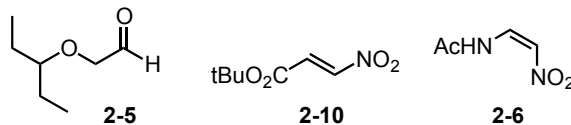
Chapter 2

One-pot synthesis of (–)-Oseltamivir and mechanistic insights into organocatalyzed Michael reaction

General Remarks: All reactions were monitored by thin-layer chromatography using Merck 60 F254 precoated silica gel plates (0.25 mm thickness). Specific optical rotations were measured using a JASCO P-1020 polarimeter. FT-IR spectra were recorded on a JASCO FT/IR-410 spectrometer. ^1H and ^{13}C NMR spectra were recorded on a Bruker AM-400 (400 MHz for ^1H NMR, 100 MHz for ^{13}C NMR), Bruker AMX-500 (500 MHz for ^1H NMR, 125 MHz for ^{13}C NMR), or Varian Gemini 300 (300 MHz for ^1H NMR, 75 MHz for ^{13}C NMR) instrument. Data for ^1H NMR are reported as chemical shift (d ppm), multiplicity (s = singlet, d = doublet, t = triplet, dd = doublet, dt = doublet, m = multiplet, br = broad), coupling constant (Hz), integration, and assignment. Data for ^{13}C NMR are reported as chemical shift. High-resolution mass spectral analyses (HRMS) were carried out using Bruker ESI-TOF MS. Preparative thin layer chromatography was performed using Wakogel B-5F purchased from Wako Pure Chemical Industries, Tokyo, Japan. Flash chromatography was performed using silica gel 60N of Kanto Chemical Co. Int., Tokyo, Japan. HPLC analysis was performed on a HITACHI Elite LaChrom Series HPLC, UV detection monitored at appropriate wavelength respectively, using Chiralcel Chiralpak IC (0.46 cm x 25 cm) and OD-H (0.46 cm x 25 cm).

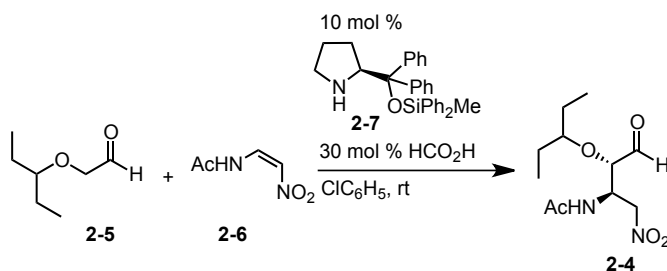
Experimental procedure and characterization of products

Pentan-3-yloxy-acetaldehyde (2-5), (*E*)-*tert*-butyl-1-nitropropenoate (2-10), and (*Z*)-*N*-2-nitroethenylacetamide (2-6)

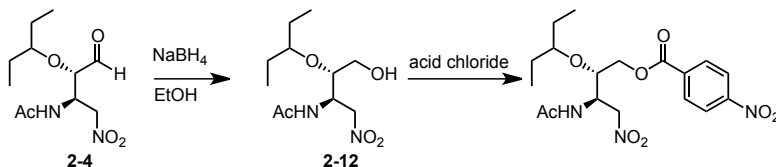


Pentan-3-yloxy-acetaldehyde (**2-5**) was prepared according to [S1]; (*E*)-*tert*-butyl-1-nitropropenoate (**2-10**) was prepared according to [S1]. (*Z*)-*N*-2-nitroethenylacetamide (**2-6**) was prepared according to [S2].

Procedure of asymmetric Michael reaction and chemical modification of 2-4 for the determination of enantiomeric excess



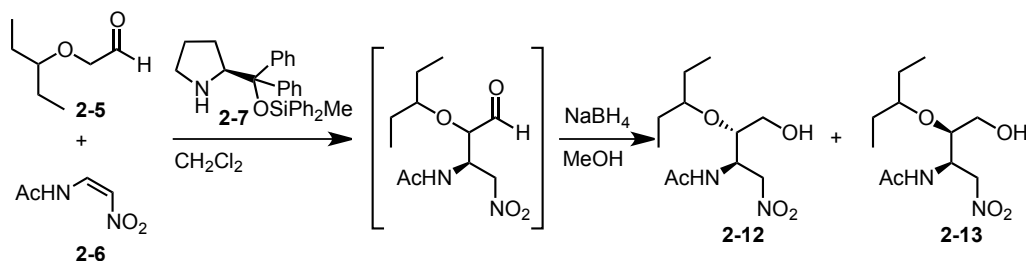
To a ClC₆H₅ suspension (1 mL) of (*Z*)-*N*-2-nitroethenylacetamide (**2-6**) (40 mg, 0.308 mmol) and (*S*)-2-(((methyl-diphenylsilyl)oxy)diphenylmethyl)pyrrolidine (**2-7**) (14 mg, 0.0308 mmol) was added pentan-3-yloxy-acetaldehyde (**2-5**) (60 mg, 0.0462 mmol) in ClC₆H₅ (1 mL) slowly by syringe pump for 45 min at room temperature. The aliquot was taken to ¹H NMR analysis to determine the diastereo selectivity and yield by comparison with the reported data.^[S2] The reaction mixture was taken to the next reaction without work up for HPLC analysis.



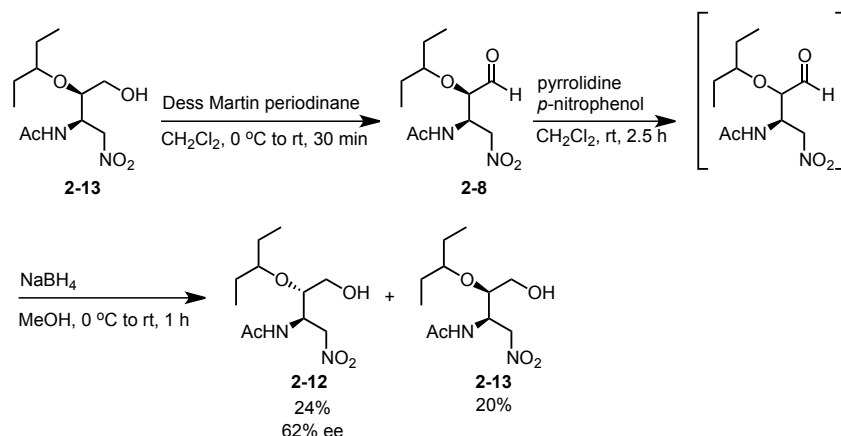
For HPLC analysis: The reaction mixture mentioned above was transferred to the EtOH solution (2 mL) of NaBH₄ (117 mg, 3.08 mmol) at −15 °C. After stirring the reaction mixture for 2 h at room temperature, the reaction was quenched with 28% NH₄OH in H₂O. The organic materials were extracted with CHCl₃ three times, and the combined extracts were washed with brine, dried over anhydrous magnesium sulphate, and concentrated in vacuo after filtration. Purification by thin-layer chromatography (ethyl acetate:hexane = 7:10) gave alcohol **2-12**. **2-12** was converted to the

corresponding ester with *p*-nitrobenzoyl chloride and enantiomeric excess was determined as 99% by HPLC with a Chiralpak OD-H column (1 : 10 = 2-propanol : *n*-hexane), 1 mL/min; *syn*-major enantiomer t_R = 22.23 min, *syn*-minor enantiomer t_R = 30.00 min.

Determination of absolute configuration of 2-13



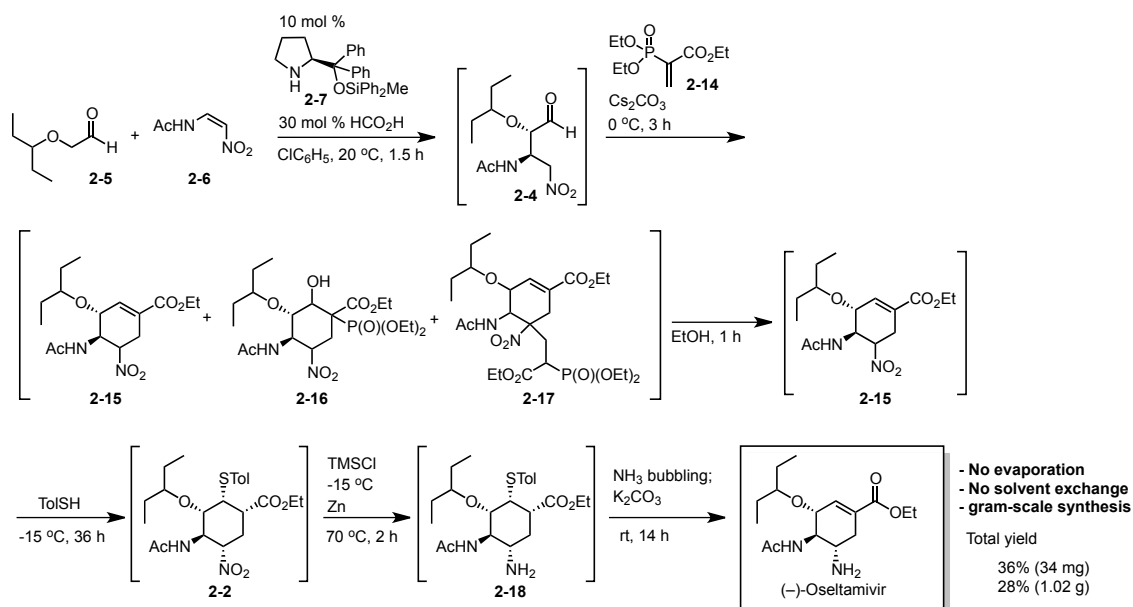
To a CH_2Cl_2 solution (2.5 mL) of pentan-3-yloxy-acetaldehyde (**2-5**) (98 mg, 0.750 mmol) was added *(Z)*-*N*-2-nitroethenylacetamide (**2-6**) (65 mg, 0.500 mmol) and *(S)*-2-(((methyl-diphenylsilyl)oxy)diphenylmethyl)pyrrolidine (**2-7**) (11 mg, 0.0250 mmol) at room temperature. After stirring the reaction mixture for 5 h, the mixture was transferred to the MeOH solution (2.5 mL) of NaBH_4 (113 mg, 3.00 mmol) at 0 °C. The mixture was stirred for 50 min at room temperature. The reaction was quenched with 28% NH_4OH in H_2O . The organic materials were extracted with CHCl_3 three times, and the combined extracts were washed with brine, dried over anhydrous magnesium sulphate, and concentrated in vacuo after filtration. Purification by thin-layer chromatography (ethyl acetate:hexane = 7:10) gave 43 mg (33%) of **2-12** and 11 mg (8%) of **2-13**. The enantiomeric excess of **2-13** was determined as 60% by HPLC with a Chiralpak OD-H column (1 : 10 = 2-propanol : *n*-hexane), 1 mL/min; *anti*-major enantiomer t_R = 15.01 min, *anti*-minor enantiomer t_R = 17.91 min.



To a CH_2Cl_2 solution (1.4 mL) of **2-13** (11 mg, 0.0419 mmol) was added Dess Martin Periodinane (28 mg, 0.067 mmol) at 0 °C. After stirring the reaction mixture for 30 min at room temperature, the reaction was quenched by addition of saturated aqueous solution of sodium bicarbonate. Organic

materials were extracted with ethyl acetate twice, and combined extracts were washed with brine, dried over anhydrous sodium sulfate, and concentrated in vacuo after filtration. The residue was dissolved in CH_2Cl_2 (1.4 mL). To the solution was added pyrrolidine (21 μL , 0.00419 mmol; 0.2M solution in CH_2Cl_2) and *p*-nitrophenol (21 μL , 0.00419 mmol; 0.2M solution in CH_2Cl_2) at room temperature. After stirring the reaction mixture for 2.5 h, the mixture was transferred to the MeOH solution (1.7 mL) of NaBH_4 (16 mg, 0.419 mmol) at 0 °C. The mixture was stirred for 1 h at room temperature. The reaction was quenched with 28% NH_4OH in H_2O . The organic materials were extracted with CHCl_3 three times, and the combined extracts were washed with brine, dried over anhydrous magnesium sulphate, and concentrated in vacuo after filtration. Purification by thin-layer chromatography (ethyl acetate:hexane = 7:10) gave 2.6 mg (24%) of **2-12** and 2.2 mg (20%) of **2-13**. The obtained **2-12** was converted to the corresponding *p*-nitrobenzoyl ester to determine the enantiomeric excess. The enantiomeric excess of **2-12** was determined as 62% by HPLC with a Chiralpak OD-H column (1 : 10 = 2-propanol : *n*-hexane), 1 mL/min; *syn*-major enantiomer t_R = 24.40 min, *syn*-minor enantiomer t_R = 33.50 min. The generated **2-12** after isomerization showed the same retention time with the (2*S*, 3*R*)-isomer **2-12** generated from **2-5** and **2-6**. Thus, the absolute configuration of **2-13** was determined to be (2*R*, 3*R*).

“One-pot” synthesis of (–)-Oseltamivir (**1**)



Gram-scale procedure

To a ClC_6H_5 suspension (42 mL) of (*Z*)-*N*-2-nitroethenylacetamide (**2-6**) (1.5 g, 11.5 mmol) was added (*S*)-2-(((methyl-diphenylsilyl)oxy)diphenylmethyl)pyrrolidine (**2-7**) (517 mg, 1.15 mmol),

HCO₂H (0.17 ml, 4.6 mmol) at room temperature. The flask was placed on a water bath, and the internal temperature was adjusted to 20 °C. The α -alkoxyaldehyde **2-5** (2.25 g, 17.3 mmol) in ClC₆H₅ (5.3 ml) was slowly added to the reaction mixture at 20 °C. The addition took 60 minutes (1 ml / 10 minutes). The reaction mixture was stirred for additional 30 minutes at 20 °C.

Note: The internal reaction temperature was carefully kept at 20 °C. If the reaction temperature exceeds 25 °C, the diastereoselectivity decreases. Nitroalkene 2-6 partially dissolves in ClC₆H₅, and the initial heterogeneous solution gradually becomes clear as the reaction proceeds to completion.

After confirming the completion of the reaction, ethyl acrylate derivative **2-14** (5.43g, 23 mmol) was added to the reaction mixture at 20 °C. The reaction mixture was cooled to 0 °C. To the reaction mixture was added Cs₂CO₃ (11.2 g, 34.5 mmol) at 0 °C, and the reaction mixture was stirred for 3 h at 0 °C. EtOH (190 ml) was slowly added to the reaction mixture at 0 °C, and the mixture was stirred for 1 h at 0 °C. The reaction mixture was cooled to -15 °C, and TolSH (7.1 g, 57.5 mmol) was added to the mixture at -15 °C. After stirring the reaction mixture for 36 h at -15 °C, TMSCl (43 mL, 345 mmol) was slowly added to the mixture, followed by activated Zn (37.6 g, 575 mmol) at -15 °C.

Note: Zinc powder was activated before use. 1N HCl was added to the zinc powder, and the supernatant solution was removed by decantation. This was repeated twice. To the residue was added distilled water, and the supernatant solution was removed by decantation. This was repeated three times. To the residue was added distilled EtOH, and the suspension was filtered, and washed with distilled EtOH, distilled Et₂O. The collected zinc powder was dried under the reduced pressure for 2 h.

The reaction temperature was slowly increased to room temperature, and the mixture was stirred for 1 h at room temperature. The reaction mixture was stirred for 2 h at 70 °C. The reaction mixture was cooled to -10 °C, and NH₃ gas was bubbled into the mixture for 20 minutes.

Note: Be careful monitoring the internal temperature. The internal temperature rapidly increased to 29 °C even though the flask was in the cool bath (-10 °C).

To the reaction mixture was added K₂CO₃ (31.8 g, 230 mmol), followed by EtOH (190 ml) at 0 °C. After stirring the reaction mixture for 14 h at room temperature, the mixture was filtered through a pad of celite, and washed with EtOH. The filtrate was concentrated in vacuo. The residue was dissolved in EtOAc, and 2N HCl was added to the solution at 0 °C. The mixture was stirred for 15 min at 0 °C. Ethyl acetate layer was removed. To the aqueous layer was added 28% NH₄OH at 0 °C to adjust the pH 11. The aqueous layer was extracted three times with 10% MeOH/CHCl₃. The combined organic layer was dried over MgSO₄ and concentrated under reduced pressure. Purification by silica gel column chromatography (MeOH:CHCl₃ = 1:10 to 1:4) gave 1.02 g (28% overall yield) of (-)-oseltamivir as a pale yellow oil.

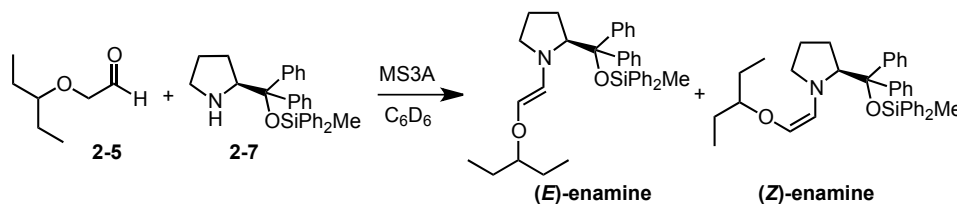
The obtained spectrum data is consistent with the reported data (S1).

40 mg scale procedure

To a ClC_6H_5 suspension (2 mL) of (*Z*)-*N*-2-nitroethenylacetamide (**2-6**) (40 mg, 0.308 mmol), (*S*)-2-(((methyldiphenylsilyl)oxy)diphenylmethyl)pyrrolidine (**2-7**) (14 mg, 0.0308 mmol), and HCO_2H (3.5 μL , 0.0915 mmol) was slowly added pentan-3-yloxy-acetaldehyde (**2-5**) (60 mg, 0.0462 mmol) in ClC_6H_5 (1 mL) at room temperature. The addition took 50 minutes (6 portion / 10 minutes). The reaction mixture became solution and stirred for additional 20 min. Ethyl acrylate derivative **2-14** (146 mg, 0.615 mmol) was added to the mixture, and the mixture was cooled to 0 °C. To the mixture was added Cs_2CO_3 (301 mg, 0.923 mmol) at 0 °C, and the mixture was stirred for 3 h at 0 °C. EtOH (2 mL) was added to the mixture at 0 °C, and the mixture was stirred for 30 min at 0 °C. The mixture was cooled to -15 °C, and TolSH (191 mg, 1.54 mmol) was added to the mixture at -15 °C. After stirring the reaction mixture for 48 h at -15 °C, TMSCl (1.2 mL, 9.23 mmol) was slowly added to the mixture, followed by activated Zn (1.0 g, 15.4 mmol) at -15 °C. The mixture was stirred for 30 min at room temperature, and additional 2 h at 70 °C. The mixture was cooled to 0 °C, and NH_3 gas was bubbled into the mixture for 10 minutes, followed by the addition of K_2CO_3 (848 mg, 6.15 mmol) at 0 °C. After stirring the reaction mixture for 14 h, the mixture was filtered through a pad of celite, and washed with EtOH. After being removed excess EtOH under reduced pressure, 2N HCl was added to the residue at 0 °C. The aqueous layer was washed with EtOAc followed by an adjustment to pH 11 with 28% NH_4OH . The aqueous layer was extracted three times with 10% MeOH/ CHCl_3 . The combined organic layer was washed with saturated aqueous NaCl, dried over MgSO_4 and concentrated under reduced pressure. Purification by silica gel column chromatography (MeOH: CHCl_3 = 1:10 to 1:4) gave 34.1 mg (36% overall yield) of (-)-oseltamivir as pale yellow oil.

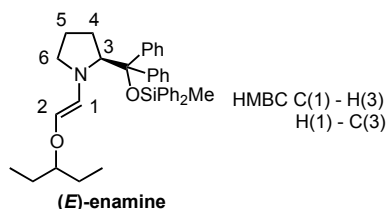
The obtained spectrum data is consistent with the reported data (S1).

Enamine formation



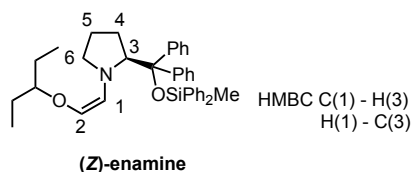
To a C₆D₆ solution (0.5 mL) of pentan-3-yloxy-acetaldehyde (**2-5**) (6.4 mg, 0.0492 mmol) in NMR tube was added (*S*)-2-(((methyldiphenylsilyl)oxy)diphenylmethyl)pyrrolidine (**2-7**) (22.1 mg, 0.0492 mmol), and MS3A at room temperature. The height of MS3A was about 3 mm from the bottom of NMR tube. The enamine formation was monitored by ¹H NMR spectroscopy.

E-enamine



¹H NMR (300 MHz, C₆D₆) δ 7.73-6.85 (20H, *m*), 6.41 (1H, *d*, *J* = 10.8 Hz, H(1)), 5.53 (1H, *d*, *J* = 10.8 Hz, H(2)), 4.32 (1H, *dd*, *J* = 9.0, 1.8 Hz, H(3)), 3.19-3.03 (1H, *m*), 2.60-2.36 (2H, *m*), 2.13-1.61 (2H, *m*), 1.54-1.10 (5H, *m*), 0.94-0.74 (7H, *m*), 0.17 (3H, *s*); ¹³C NMR (100 MHz, C₆D₆): δ 126.7 C(1), 125.4 C(2), 70.2 C(3).

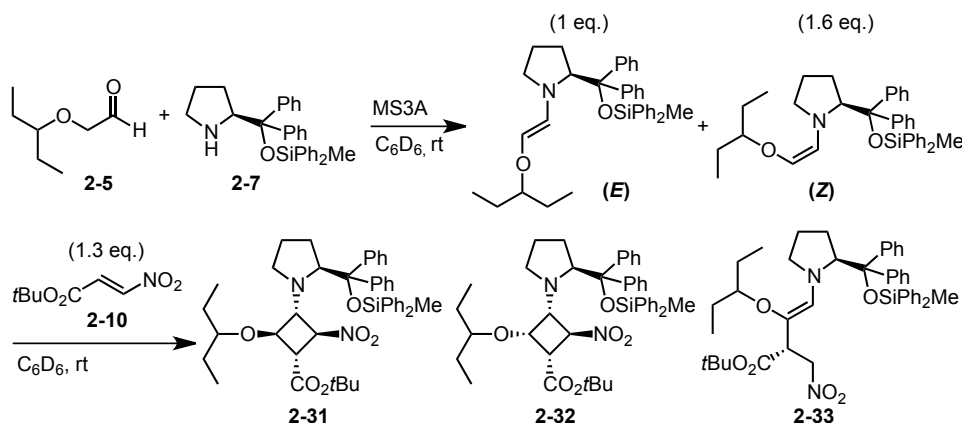
Z-enamine



¹H NMR (300 MHz, C₆D₆) δ 7.73-6.85 (20H, *m*), 5.09 (1H, *d*, *J* = 5.3 Hz, H(1)), 4.93 (1H, *d*, *J* = 5.3 Hz, H(2)), 4.26 (1H, *dd*, *J* = 8.7, 3.3 Hz, H(3)), 3.19-3.03 (1H, *m*), 2.60-2.36 (2H, *m*), 2.13-1.61 (2H, *m*), 1.54-1.10 (5H, *m*), 0.94-0.74 (7H, *m*), 0.21 (3H, *s*); ¹³C (100 MHz, C₆D₆) δ 125.4 C(2), 120.1 C(1), 71.9 C(3).

The effect of acid

Reaction of *E*- and *Z*-enamines (2.9 eq., *E/Z* = 1/1.6) with *trans*-nitroalkene **2-10** (1.3 eq.), followed by addition of ClCH_2COOH (1.3 eq.)



MS4A (200 mg, pellet) in 5 mL flask was heated by heatgun under the reduced pressure. After cooling to room temperature, the flask was backfilled with Argon. To the flask was added C_6D_6 (0.2 mL), (*S*)-2-(((methyldiphenylsilyl)oxy)diphenylmethyl)pyrrolidine **2-7** (0.25 mL, 0.05 mmol, 0.2M C_6D_6 solution), pentan-3-yloxy-acetaldehyde (**2-5**) (0.25 mL, 0.05 mmol, 0.2M C_6D_6 solution, purity is ca.80%), and toluene (40 μL , 0.02 mmol, 0.5M C_6D_6 solution) at room temperature. One more sample in other flask was prepared by exactly same procedure. The two flasks were left for 3 h. NMR sample was prepared from one flask to calculate how much *E*- and *Z*-enamines were generated.

E-enamine : *Z*-enamine : toluene = 1 : 1.92 : 1.77

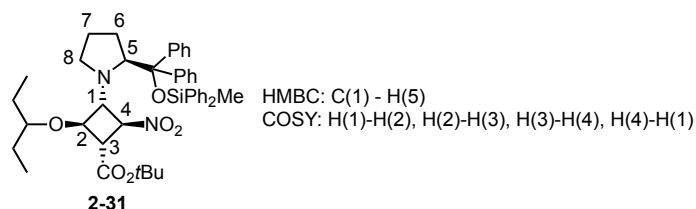
0.02 mmol of toluene was used for the experiment.

$(1+1.92) \times 0.02 / 1.77 = 0.033$ mmol of *E*- and *Z*-enamines were generated.

To the other flask was added (*E*)-*tert*-butyl 1-nitropropenoate (**2-10**) (0.15 mL, 0.015 mmol, 0.1M C_6D_6 solution) at room temperature. 0.6 mL of the sample was transferred to NMR tube without MS4A. The reaction was monitored by ^1H NMR spectroscopy. ClCH_2COOH (20 μL , 0.5M C_6D_6 solution) was added to the NMR tube. The reaction was monitored by ^1H NMR spectroscopy, and the progress was plotted on a graph.

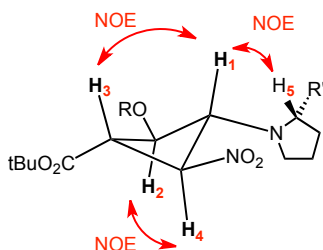
(1*S*,2*S*,3*R*,4*R*)-tert-butyl

3-(((*S*)-2-(((methyldiphenylsilyl)oxy)diphenylmethyl)pyrrolidin-1-yl)-2-nitro-4-(pentan-3-yloxy)cyclobutanecarboxylate (2-31)



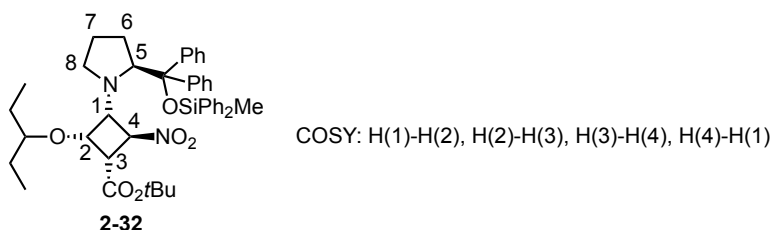
^1H NMR (300 MHz, C_6D_6) δ 7.75-6.95 (20H, *m*), 5.07 (1H, *t*, $J = 7.6$ Hz, H(4)), 4.61 (1H, *dd*, $J = 8.6$, 3.4 Hz, H(5)), 4.35-4.21 (1H, *br*, H(1)), 3.81 (1H, *t*, $J = 7.6$ Hz, H(2)), 3.27 (1H, *t*, $J = 7.6$ Hz, H(3)), 3.22-3.12 (1H, *m*), 2.45-2.34 (2H, *m*), 2.05-1.89 (2H, *m*), 1.46-1.34 (5H, *m*), 1.26 (9H, *s*), 0.92-0.78 (7H, *m*), 0.24 (3H, *s*); ^{13}C NMR (100 MHz, C_6D_6) δ 73.9 C(2), 73.9 C(4), 70.3 C(1), 68.4 C(5), 48.0 C(3).

NOESY(500 MHz, C_6D_6) at 7 $^\circ\text{C}$.



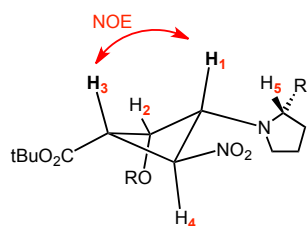
(1*S*,2*S*,3*R*,4*S*)-tert-butyl

3-(((*S*)-2-(((methyldiphenylsilyl)oxy)diphenylmethyl)pyrrolidin-1-yl)-2-nitro-4-(pentan-3-yloxy)cyclobutanecarboxylate (2-32)



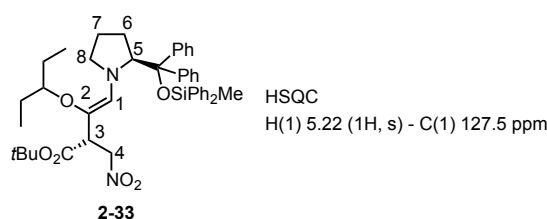
^1H NMR (300 MHz, C_6D_6) δ 7.73-6.98 (20H, *m*), 5.96 (1H, *t*, $J = 8.8$ Hz, H(4)), 4.35 (1H, *dd*, $J = 9.0$, 4.2 Hz, H(5)), 4.30-4.21 (1H, *br*, H(1)), 3.73 (1H, *t*, $J = 6.6$ Hz, H(2)), 3.19 (1H, *dd*, $J = 8.8$, 6.6 Hz, H(3)), 3.14-3.07 (1H, *m*), 2.62-2.48 (2H, *m*), 2.03-1.88 (2H, *m*), 1.57-1.38 (5H, *m*), 1.35 (9H, *s*), 0.92-0.75 (7H, *m*), 0.30 (3H, *s*).

NOESY (400 MHz, C₆D₆) at 7 °C



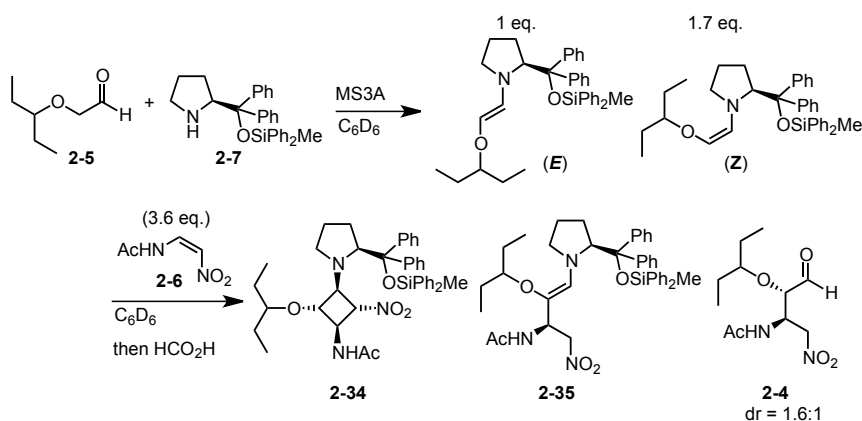
(*S,Z*)-tert-butyl

4-(((*S*)-2-(((methyldiphenylsilyl)oxy)diphenylmethyl)pyrrolidin-1-yl)-2-(nitromethyl)-3-(pentan-3-yloxy)but-3-enoate (26)



¹H NMR (300 MHz, C₆D₆) δ 7.74-6.98 (20H, *m*), 5.22 (1H, *s*, H(1)), 4.46-4.33 (1H, *m*, H(4)), 4.10 (1H, *dd*, *J* = 8.3, 3.2 Hz, H(5)), 3.75-3.60 (1H, *m*, H(4)), 3.23-3.10 (1H, *m*, C(3)), 3.03-2.91 (1H, *m*), 2.60-2.47 (2H, *m*), 2.04-1.90 (2H, *m*), 1.53-1.38 (5H, *m*), 1.36 (9H, *s*), 0.91-0.78 (7H, *m*), 0.20 (3H, *s*).

Reaction of *E*- and *Z*-enamines (2.7 eq., *E/Z* = 1/1.7) with *cis*-nitroalkene **2-6** (3.6 eq.), followed by addition of HCOOH



MS4A (250 mg, pellet) in 5 mL flask was heated by heatgun under the reduced pressure. After cooling to room temperature, the flask was backfilled with Argon. To the flask was added C₆D₆ (0.2 ml), (*S*)-2-(((methyldiphenylsilyl)oxy)diphenylmethyl)pyrrolidine (**2-7**) (0.25 mL, 0.05 mmol, 0.2M C₆D₆ solution), pentan-3-yloxy-acetaldehyde (**2-5**) (0.25 mL, 0.05 mmol, 0.2M C₆D₆ solution, purity

is ca. 80%), and toluene (40 uL, 0.02 mmol, 0.5M C₆D₆ solution) at room temperature. One more sample in other flask was prepared by exactly same procedure. The two flasks were left for 3 h. NMR sample was prepared from one flask to calculate how much *E*- and *Z*-enamines were generated.

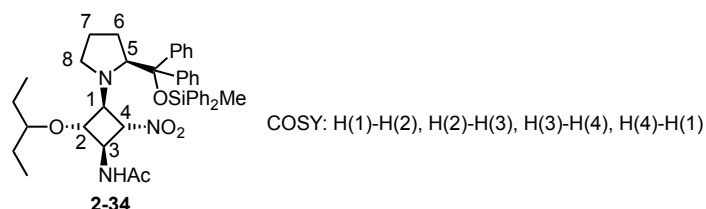
E-enamine : *Z*-enamine : toluene = 1 : 1.66 : 1.433

0.02 mmol of toluene was used for the experiment.

$(1+1.66) \times 0.02 / 1.433 = 0.0372$ mmol of *E*- and *Z*-enamines were generated.

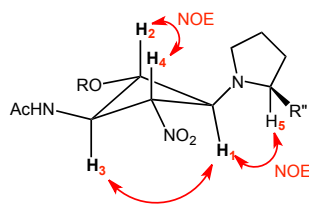
To the other flask was added (*Z*)-*N*-2-nitroethenylacetamide (**2-6**) (1 mL, 0.05 mmol, 0.05M C₆D₆ solution) at room temperature. 0.6 mL of the sample was transferred to NMR tube without MS4A. The reaction was monitored by ¹H NMR spectroscopy. After 20 min, HCOOH (62 uL, 0.5M C₆D₆ solution) was added to the NMR tube. The reaction was monitored by ¹H NMR spectroscopy, and the progress was plotted on a graph.

***N*-((1*R*,2*R*,3*S*,4*S*)-3-((*S*)-2-(((methyldiphenylsilyl)oxy)diphenylmethyl)pyrrolidin-1-yl)-2-nitro-4-(pentan-3-yloxy)cyclobutyl)acetamide (2-34)**

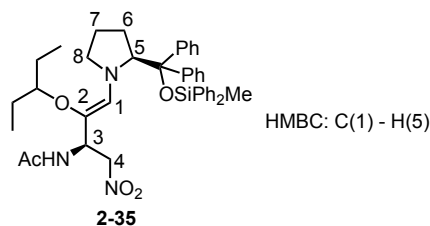


¹H NMR (300 MHz, C₆D₆) δ 7.74-6.88 (20H, *m*), 5.20 (1H, *t*, $J = 8.0$ Hz, H(4)), 4.73 (1H, *t*, $J = 7.2$ Hz, H(2)), 4.55 (1H, *dd*, $J = 8.8, 3.6$ Hz, H(5)), 4.38 (1H, *d*, $J = 6.8$ Hz, NH), 3.83 (1H, *br*, H(1)), 3.36 (1H, *ddd*, $J = 8.0, 7.2, 6.8$ Hz, H(3)), 3.05-2.96 (1H, *m*), 2.63-2.40 (2H, *m*), 2.04-1.75 (2H, *m*), 1.58-1.34 (5H, *m*), 1.28 (3H, *s*), 0.98-0.76 (7H, *m*), 0.30 (3H, *s*).

NOESY (500 MHz, C₆D₆) at 15 °C



N-((*R,Z*)-4-((*S*)-2-(((methyldiphenylsilyl)oxy)diphenylmethyl)pyrrolidin-1-yl)-1-nitro-3-(pentan-3-yloxy)but-3-en-2-yl)acetamide (2-35)

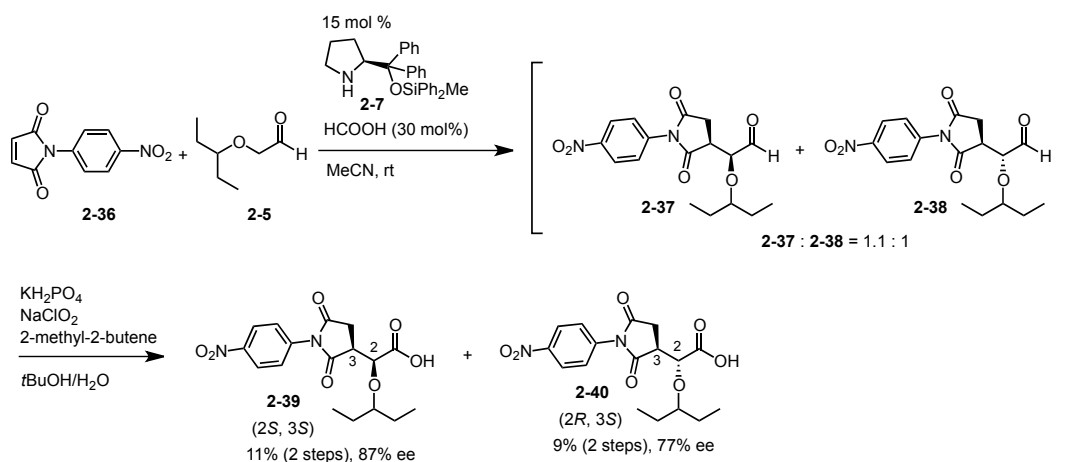


^1H NMR (400 MHz, C_6D_6) δ 7.74-6.97 (20H, *m*), 5.35 (1H, *s*, H(1)), 4.21 (1H, *dd*, $J = 12.0, 6.0$ Hz, H(4)), 4.08 (1H, *dd*, $J = 8.8, 4.0$ Hz, H(5)), 3.99-3.93 (1H, *m*, H(4)), 3.91-3.87 (1H, *m*, H(3)), 3.06-2.98 (1H, *m*), 2.55-2.40 (2H, *m*), 1.99-1.77 (2H, *m*), 1.60-1.46 (5H, *m*), 1.44 (3H, *s*), 0.94-0.72 (7H, *m*), 0.22 (3H, *s*); ^{13}C NMR (100 MHz, C_6D_6) δ 127.3 C(1), 78.9 C(3), 77.0 C(4), 74.3 C(5).

Michael reaction of α -alkoxyaldehyde with cyclic *cis*-Michael acceptor

(*S*)-2-((*S*)-1-(4-nitrophenyl)-2,5-dioxopyrrolidin-3-yl)-2-(pentan-3-yloxy)acetic acid (2-39)

(*R*)-2-((*S*)-1-(4-nitrophenyl)-2,5-dioxopyrrolidin-3-yl)-2-(pentan-3-yloxy)acetic acid (2-40)



To a MeCN solution (2.3 mL) of 1-(4-nitrophenyl)-1H-pyrrole-2,5-dione (**2-36**) (100 mg, 0.458 mmol) was added (*S*)-2-((methyldiphenylsilyloxy)diphenylmethyl)pyrrolidine (**2-7**) (31 mg, 0.0687 mmol), pentan-3-yloxy-acetaldehyde (**2-5**) (72 mg, 0.550 mmol), and HCOOH (6.3 mg, 0.137 mmol) at room temperature. After stirring the reaction mixture for 27 h, the mixture was concentrated in vacuo. To the residue was added *t*BuOH (1.8 mL), H₂O (0.36 mL), KH₂PO₄ (125 mg, 0.916 mmol), 2-methyl-2-butene (0.39 mL, 3.66 mmol), and NaClO₂ (166 mg, 1.83 mmol) at room temperature. After stirring the reaction mixture for 1 h, saturated aqueous solution of NaHCO₃ was added to the mixture. The mixture was washed with Et₂O. The water phase was acidified with 2N HCl, and organic materials were extracted with CHCl₃ three times, dried over anhydrous magnesium sulfate, and concentrated in vacuo after filtration to give crude material as brown oil. Purification by

thin layer chromatography (AcOEt with 1% AcOH) gave 18 mg (11%, 2steps) of (*S*)-2-((*S*)-1-(4-nitrophenyl)-2,5-dioxopyrrolidin-3-yl)-2-(pentan-3-yloxy)acetic acid (**2-39**) and 16 mg (9%, 2 steps) of (*R*)-2-((*S*)-1-(4-nitrophenyl)-2,5-dioxopyrrolidin-3-yl)-2-(pentan-3-yloxy)acetic acid (**2-40**) as a colorless oil.

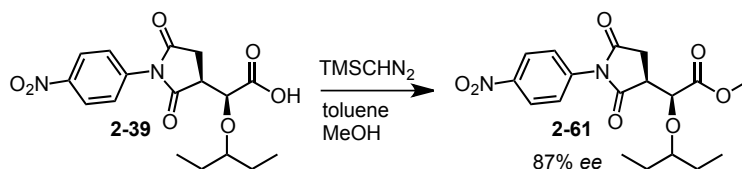
(*S*)-2-((*S*)-1-(4-nitrophenyl)-2,5-dioxopyrrolidin-3-yl)-2-(pentan-3-yloxy)acetic acid (2-39)

^1H NMR (400 MHz, CDCl_3) δ 0.74 (3H, *t*, $J = 7.4$ Hz), 0.91 (3H, *t*, $J = 7.4$ Hz), 1.38-1.61 (4H, *m*), 2.90 (1H, *dd*, $J = 9.6, 18.4$ Hz), 3.14 (1H, *dd*, $J = 5.2, 18.4$ Hz), 3.43 (1H, *q*, $J = 5.6$ Hz), 3.54 (1H, *ddd*, $J = 2.0, 5.2, 9.6$ Hz), 4.76 (1H, *d*, $J = 2.0$ Hz), 7.58 (2H, *d*, $J = 8.8$ Hz), 8.35 (2H, *d*, $J = 8.8$ Hz); ^{13}C NMR (100 MHz, CDCl_3) δ 175.2, 174.1, 173.9, 147.1, 137.3, 126.7, 124.4, 83.2, 73.3, 43.8, 29.1, 25.9, 24.6, 9.3, 9.0; IR (neat) ν 2966, 2935, 2875, 1725, 1714, 1597, 1527, 1498, 1387, 1345, 1173, 1129, 1109, 853, 751 cm^{-1} ; HRMS(ESI) $[\text{M}-\text{H}]^-$ calculated for $\text{C}_{17}\text{H}_{19}\text{N}_2\text{O}_7$: 363.1198, found: 363.1173; $[\alpha]_{\text{D}}^{17} +107$ (c 0.29, MeOH).

(*R*)-2-((*S*)-1-(4-nitrophenyl)-2,5-dioxopyrrolidin-3-yl)-2-(pentan-3-yloxy)acetic acid (2-40)

^1H NMR (400 MHz, CDCl_3) δ 0.84-0.95 (6H, *m*), 1.48-1.66 (4H, *m*), 2.78 (1H, *dd*, $J = 4.2, 18.4$ Hz), 3.06 (1H, *dd*, $J = 9.2, 18.4$ Hz), 3.46-3.58 (2H, *m*), 4.52 (1H, *bs*), 7.56 (2H, *d*, $J = 8.8$ Hz), 8.31 (2H, *d*, $J = 8.8$ Hz); ^{13}C NMR (100 MHz, CDCl_3) δ 174.8, 174.1, 174.1, 147.2, 137.3, 127.1, 124.4, 83.2, 76.1, 42.8, 31.9, 25.8, 25.1, 9.4, 9.2; IR (neat) ν 2968, 2831, 2878, 1725, 1718, 1609, 1597, 1528, 1498, 1458, 1387, 1345, 1177, 1114, 852, 751 cm^{-1} ; HRMS(ESI) $[\text{M}-\text{H}]^-$ calculated for $\text{C}_{17}\text{H}_{19}\text{N}_2\text{O}_7$: 363.1198, found: 363.1171; $[\alpha]_{\text{D}}^{16} +34$ (c 0.3, MeOH).

(*S*)-methyl 2-((*S*)-1-(4-nitrophenyl)-2,5-dioxopyrrolidin-3-yl)-2-(pentan-3-yloxy)acetate (2-61)



To a toluene (0.1 mL) and MeOH (0.08 mL) solution of (*S*)-2-((*S*)-1-(4-nitrophenyl)-2,5-dioxopyrrolidin-3-yl)-2-(pentan-3-yloxy)acetic acid (**2-39**) (1.5 mg, 0.00412 mmol) was added TMSCHN₂ (0.021 mL, 0.0412 mmol) at 0 °C. After stirring the reaction mixture for 5 min, the mixture was concentrated in vacuo. The residue was purified by preparative thin layer chromatography (ethyl acetate : hexane = 1 : 1) to give 1.4 mg (90%) of (*S*)-methyl 2-((*S*)-1-(4-nitrophenyl)-2,5-dioxopyrrolidin-3-yl)-2-(pentan-3-yloxy)acetate (**2-61**) as a colourless

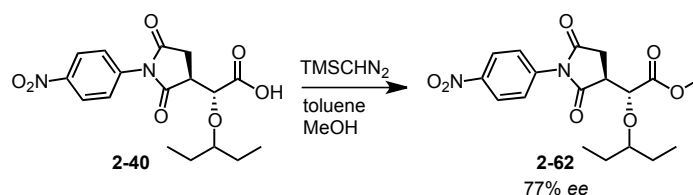
oil.

^1H NMR (400 MHz, CDCl_3) δ 0.76 (3H, *t*, J = 7.4 Hz), 0.90 (3H, *t*, J = 7.4 Hz), 1.30-1.60 (4H, *m*), 2.84 (1H, *dd*, J = 9.6, 18.4 Hz), 3.19 (1H, *dd*, J = 4.8, 18.4 Hz), 3.36 (1H, *q*, J = 5.7 Hz), 3.39-3.45 (1H, *m*), 3.81 (3H, *s*), 4.69 (1H, *d*, J = 2.4 Hz), 7.57 (2H, *d*, J = 8.8 Hz), 8.34 (2H, *d*, J = 9.2 Hz).

Enantiomeric excess = 87%

The enantiomeric excess was determined by HPLC using a Chiralpak AD-H (3/1 = hexane/*i*PrOH; flow rate 1 ml/min, $t_{\text{R}1}$ = 9.27 (minor), $t_{\text{R}2}$ = 20.26 (major) min).

(*R*)-methyl 2-((*S*)-1-(4-nitrophenyl)-2,5-dioxopyrrolidin-3-yl)-2-(pentan-3-yloxy)acetate (2-62)



To a toluene (0.1 mL) and MeOH (0.08 mL) solution of (*R*)-2-((*S*)-1-(4-nitrophenyl)-2,5-dioxopyrrolidin-3-yl)-2-(pentan-3-yloxy)acetic acid **2-40** (1.5 mg, 0.00412 mmol) was added TMSCHN₂ (0.021 mL, 0.0412 mmol) at 0 °C. After stirring the reaction mixture for 5 min at 0 °C, the mixture was concentrated in vacuo. The residue was purified by preparative thin layer chromatography (ethyl acetate : hexane = 1 : 1) to give 1.4 mg (90%) of (*R*)-methyl 2-((*S*)-1-(4-nitrophenyl)-2,5-dioxopyrrolidin-3-yl)-2-(pentan-3-yloxy)acetate (**2-62**) as a colourless oil.

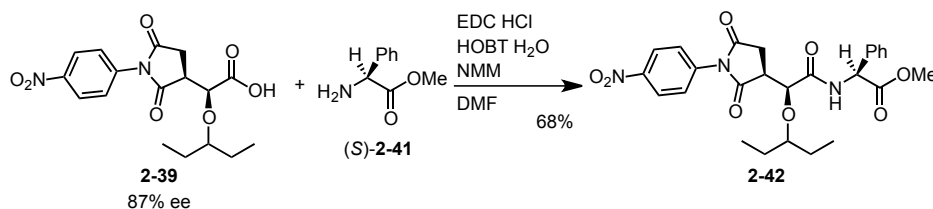
^1H NMR (400 MHz, CDCl_3) δ 1.13 (3H, *t*, J = 7.4 Hz), 1.16 (3H, *t*, J = 7.4 Hz), 1.70-1.90 (4H, *m*), 3.09 (1H, *dd*, J = 4.4, 18.4 Hz), 3.26 (1H, *dd*, J = 9.2, 18.4 Hz), 3.65-3.79 (2H, *m*), 4.03 (3H, *s*), 4.70 (1H, *d*, J = 3.6 Hz), 7.80 (2H, *d*, J = 8.8 Hz), 8.56 (2H, *d*, J = 8.8 Hz).

Enantiomeric excess = 77%

The enantiomeric excess was determined by HPLC using a Chiralpak AD-H (3/1 = hexane/*i*PrOH; flow rate 1 ml/min, $t_{\text{R}1}$ = 10.43 (minor), $t_{\text{R}2}$ = 17.01 (major) min).

(S)-methyl

2-((S)-2-((S)-1-(4-nitrophenyl)-2,5-dioxopyrrolidin-3-yl)-2-(pentan-3-yloxy)acetamido)-2-phenylacetate (2-42)

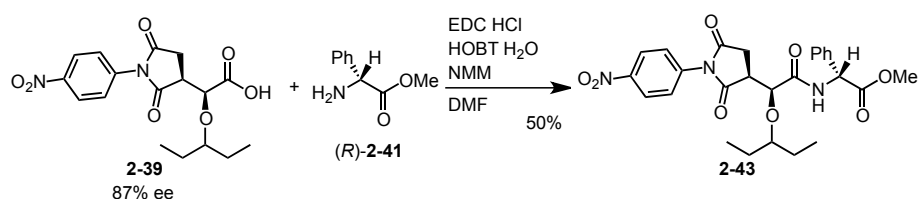


To a DMF solution (0.7 mL) of (S)-2-((S)-1-(4-nitrophenyl)-2,5-dioxopyrrolidin-3-yl)-2-(pentan-3-yloxy)acetic acid **2-39** (4.5 mg, 0.0123 mmol) was added EDC HCl (11 mg, 0.0615 mmol), HOBT H₂O (9.4 mg, 0.0615 mmol), N-methyl morpholine (13 μ L, 0.123 mmol), and (S)-methyl 2-amino-2-phenylacetate hydrochloride (S)-**2-41** (12 mg, 0.0615 mmol) at room temperature. After stirring the reaction mixture for 26 h, water was added to the mixture. Organic materials were extracted with ethyl acetate twice, and the combined extracts were washed with 10% aqueous solution of citric acid, saturated aqueous solution of sodium bicarbonate, and brine, dried over anhydrous sodium sulfate, and concentrated in vacuo after filtration. Purification by preparative thin layer chromatography (ethyl acetate : hexane = 1 : 2, three times) gave 4.4 mg (68%) of (S)-methyl 2-((S)-2-((S)-1-(4-nitrophenyl)-2,5-dioxopyrrolidin-3-yl)-2-(pentan-3-yloxy)acetamido)-2-phenylacetate (**2-42**) as a colorless oil.

¹H NMR (400 MHz, CDCl₃) δ 0.75 (3H, *t*, *J* = 7.4 Hz), 0.77 (3H, *t*, *J* = 7.4 Hz), 1.38-1.50 (4H, *m*), 2.93, 1H, *dd*, *J* = 9.6, 18.4 Hz), 3.09 (1H, *dd*, *J* = 5.6, 18.8 Hz), 3.31 (1H, *q*, *J* = 5.8 Hz), 3.67 (1H, *ddd*, *J* = 2.0, 5.6, 9.6 Hz), 3.76 (3H, *s*), 4.64 (1H, *d*, *J* = 2.0 Hz), 5.54 (1H, *d*, *J* = 7.2 Hz), 7.30-7.43 (5H, *m*), 7.58-7.63 (2H, *m*), 8.31-8.36 (2H, *m*); ¹³C NMR (100 MHz, CDCl₃) δ 9.4, 25.3, 25.9, 29.0, 29.7, 44.2, 53.0, 56.5, 75.5, 84.3, 124.4, 126.6, 127.2, 129.0, 129.2, 135.6, 137.4, 147.0, 169.9, 170.7, 174.4, 176.0; IR (neat) ν 3417, 2924, 1720, 1682, 1597, 1520, 1458, 1381, 1342, 1173, 1088, 856 cm⁻¹; HRMS(ESI) [M+Na]⁺ calculated for C₂₆H₂₉N₃O₈Na:534.1852, found: 534.1840; [α]_D²⁶ +75.3 (*c* 0.23, CHCl₃).

(R)-methyl

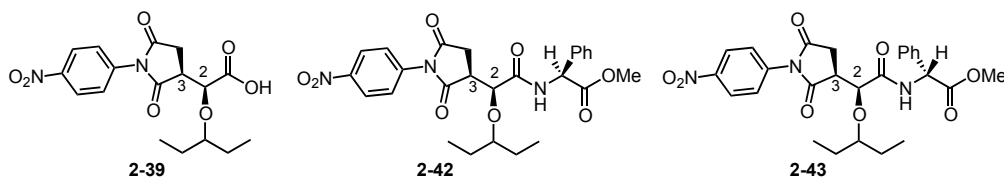
2-((S)-2-((S)-1-(4-nitrophenyl)-2,5-dioxopyrrolidin-3-yl)-2-(pentan-3-yloxy)acetamido)-2-phenylacetate (2-43)



To a DMF solution (0.7 mL) of (S)-2-((S)-1-(4-nitrophenyl)-2,5-dioxopyrrolidin-3-yl)-2-(pentan-3-yloxy)acetic acid (**2-39**) (4.3 mg, 0.0118 mmol) was added EDC HCl (20 mg, 0.103 mmol), HOBT H₂O (16 mg, 0.103 mmol), *N*-methyl morpholine (23 μ L, 0.206 mmol), and (R)-methyl 2-amino-2-phenylacetate hydrochloride (**(R)-2-41**) (21 mg, 0.103 mmol) at room temperature. After stirring the reaction mixture for 20 h, water was added to the mixture. Organic materials were extracted with ethyl acetate twice, and the combined extracts were washed with 10% aqueous solution of citric acid, saturated aqueous solution of sodium bicarbonate, and brine, dried over anhydrous sodium sulfate, and concentrated in vacuo after filtration. Purification by preparative thin layer chromatography (ethyl acetate : hexane = 1 : 2, four times) gave 3.0 mg (50%) of (R)-methyl 2-((S)-2-((S)-1-(4-nitrophenyl)-2,5-dioxopyrrolidin-3-yl)-2-(pentan-3-yloxy)acetamido)-2-phenylacetate (**2-43**) as a colorless oil.

¹H NMR (400 MHz, CDCl₃) δ 0.80 (3H, *t*, *J* = 7.4 Hz), 0.95 (3H, *t*, *J* = 7.4 Hz), 1.44-1.55 (2H, *m*), 1.57-1.77 (2H, *m*), 2.62 (1H, *dd*, *J* = 9.6, 18.4 Hz), 2.82 (1H, *dd*, *J* = 5.6, 18.4 Hz), 3.43 (1H, *q*, *J* = 5.9 Hz), 3.59 (1H, *ddd*, *J* = 2.0, 5.6, 9.6 Hz), 3.76 (3H, *s*), 4.67 (1H, *d*, *J* = 2.0 Hz), 5.59 (1H, *d*, *J* = 7.6 Hz), 7.30-7.44 (5H, *m*), 7.53-7.58 (2H, *m*), 7.78 (1H, *d*, *J* = 7.2 Hz), 8.30-8.35 (2H, *m*); ¹³C NMR (100 MHz, CDCl₃) δ 175.9, 174.2, 170.7, 169.8, 147.0, 137.3, 136.2, 129.2, 128.9, 127.0, 126.6, 124.4, 84.6, 75.5, 56.2, 53.0, 44.1, 28.8, 26.0, 25.3, 9.5, 9.4; IR (neat) ν 3332, 2924, 1778, 1746, 1722, 1713, 1660, 1529, 1348, 1172, 853, 697 cm⁻¹; HRMS(ESI) [M+Na]⁺ calculated for C₂₆H₂₉N₃O₈Na: 534.1852, found: 534.1861; [α]_D²⁷ +38 (*c* 0.22, CHCl₃).

Determination of absolute configuration of 2-39



As key protons in the compound **2-43** are well resolved compared with those of **2-39**, the relative configuration was determined as for the compound **2-43**. The relative configuration at C-2 and C-3 of the compound **2-43** was determined to be $2S^*$ and $3S^*$ by J -based configurational analysis, as shown in Fig. 1. A small homonuclear vicinal coupling constant between H-2 and H-3 ($^3J_{H2,H3} = 2.3$ Hz) indicated a *gauche* relationship between these protons. LSPD experiments were used to measure heteronuclear coupling constant values. In comparison of two heteronuclear coupling constants between H-2/C-4(CH₂) ($^3J_{H2,C4} = 4.2$ Hz) and H-2/C-6(CO) ($^3J_{H2,C6} = 2.9$ Hz), relatively large medium value of $^3J_{H2,C4} = 4.2$ Hz suggested an *anti* relationship between H-2 and C-4. This rotamer was supported by small coupling constants of $^2J_{H3,C2} = 2.6$ Hz and $^3J_{H3,C1} < 2$ Hz, suggesting an *anti* relationship between H-3 and the ether oxygen at C-2 and a *gauche* relationship of H-3 and C-1, respectively.

measured J values for 2-43	estimated magnitude for rotamers of ($2S$, $3S$)- 2-43		
$^3J_{H2,H3} = 2.3\text{Hz}$	small	small	large
$^3J_{H2,C4} = 4.2\text{Hz}$	large	small	small
$^3J_{H2,C6} = 2.9\text{Hz}$	small	large	small
$^2J_{H3,C2} = 2.6\text{Hz}$	small	large	large
$^3J_{H3,C1} < 2\text{Hz}$	small	large	small

Fig. 1. J -based configurational analysis

The absolute configuration at C-2 of **2-39** was determined by phenylglycine methyl ester method developed by Kusumi.^[S4] The chemical shift difference of (*S*)-amide **2-42** – (*R*)-amide **2-43** was calculated. The absolute configuration at C-2 in **2-42** and **2-43** was determined as ($2S$) by putting the obtained positive and negative value into the reported model by Kusumi. Therefore, the absolute configuration of **2-39** was determined as ($2S$, $3S$).

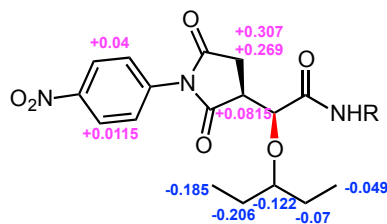
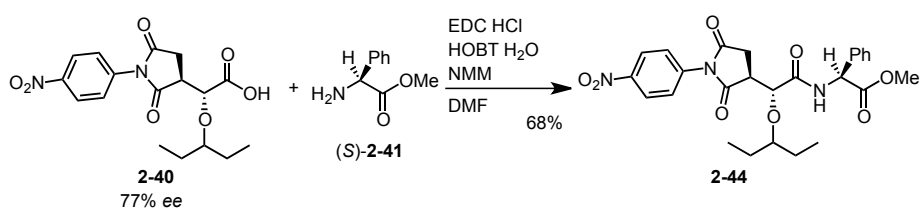


Fig.2. Determination of absolute configuration

(S)-methyl

2-((R)-2-((S)-1-(4-nitrophenyl)-2,5-dioxopyrrolidin-3-yl)-2-(pentan-3-yloxy)acetamido)-2-phenylacetate (2-44)



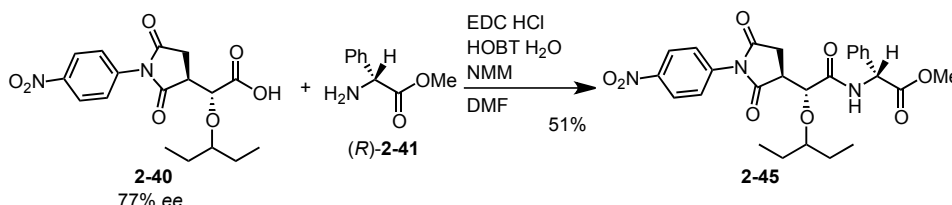
To a DMF solution (0.7 mL) of (R)-2-((S)-1-(4-nitrophenyl)-2,5-dioxopyrrolidin-3-yl)-2-(pentan-3-yloxy)acetic acid (**2-40**) (4.5 mg, 0.0123 mmol) was added EDC HCl (11 mg, 0.0615 mmol), HOBT H₂O (9.4 mg, 0.0615 mmol), *N*-methyl morpholine (13 μ L, 0.123 mmol), and (S)-methyl 2-amino-2-phenylacetate hydrochloride (**S-2-41**) (12 mg, 0.0615 mmol) at room temperature. After stirring the reaction mixture for 26 h, water was added to the mixture. Organic materials were extracted with ethyl acetate twice, and the combined extracts were washed with 10% aqueous solution of citric acid, saturated aqueous solution of sodium bicarbonate, and brine, dried over anhydrous sodium sulfate, and concentrated in vacuo after filtration. Purification by preparative thin layer chromatography (ethyl acetate : hexane = 1 : 2, twice) gave 4.4 mg (68%) of (S)-methyl 2-((R)-2-((S)-1-(4-nitrophenyl)-2,5-dioxopyrrolidin-3-yl)-2-(pentan-3-yloxy)acetamido)-2-phenylacetate (**2-44**) as a colorless oil.

¹H NMR (400 MHz, CDCl₃) δ 0.94 (3H, *t*, *J* = 7.2 Hz), 1.02 (3H, *t*, *J* = 7.2 Hz), 1.55-1.76 (4H, *m*), 2.44 (1H, *dd*, *J* = 4.4, 18.8 Hz), 2.86 (1H, *dd*, *J* = 9.6, 18.8 Hz), 3.35-3.39 (1H, *m*), 3.44-3.52 (1H, *m*), 3.74 (3H, *s*), 4.62 (1H, *d*, *J* = 3.6 Hz), 5.56 (1H, *d*, *J* = 7.6 Hz), 7.30-7.41 (5H, *m*), 7.50-7.57 (2H, *m*), 7.75 (1H, *d*, *J* = 7.2 Hz), 8.27-8.34 (2H, *m*); ¹³C NMR (100 MHz, CDCl₃) δ 174.8, 174.6, 170.7, 169.2, 147.1, 137.9, 135.8, 129.2, 128.8, 127.4, 127.2, 124.3, 83.4, 78.2, 56.3, 53.0, 42.6, 31.1, 26.0, 25.9, 9.9, 9.3; IR (neat) ν 3049, 2923, 1720, 1681, 1597, 1527, 1504, 1457, 1381, 1342, 1172, 1111, 856 cm⁻¹; HRMS(ESI) [M+Na]⁺ calculated for C₂₆H₂₉N₃O₈Na: 534.1852, found: 534.1838; [α]_D²⁶

+63.4 (*c* 0.20, CHCl₃).

(R)-methyl

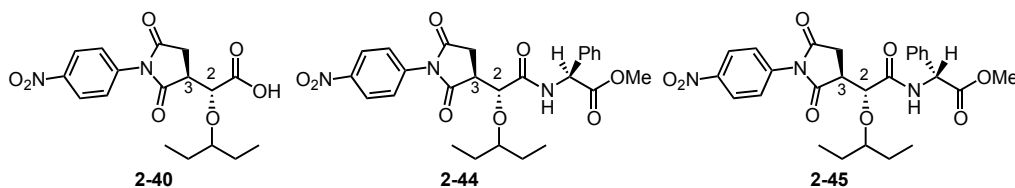
2-((R)-2-((S)-1-(4-nitrophenyl)-2,5-dioxopyrrolidin-3-yl)-2-(pentan-3-yloxy)acetamido)-2-phenylacetate (2-45)



To a DMF solution (0.7 mL) of *(R)*-2-((*S*)-1-(4-nitrophenyl)-2,5-dioxopyrrolidin-3-yl)-2-(pentan-3-yloxy)acetic acid (**2-40**) (4.2 mg, 0.0115 mmol) was added EDC HCl (18 mg, 0.0960 mmol), HOBT H₂O (15 mg, 0.0960 mmol), *N*-methyl morpholine (21 μ L, 0.192 mmol), and *(R)*-methyl 2-amino-2-phenylacetate hydrochloride (**(R)-2-41**) (19 mg, 0.0960 mmol) at room temperature. After stirring the reaction mixture for 20 h, water was added to the mixture. Organic materials were extracted with ethyl acetate twice, and the combined extracts were washed with 10% aqueous solution of citric acid, saturated aqueous solution of sodium bicarbonate, and brine, dried over anhydrous sodium sulfate, and concentrated in vacuo after filtration. Purification by preparative thin layer chromatography (ethyl acetate : hexane = 1 : 2, four times) gave 3.0 mg (51%) of *(R)*-methyl 2-((*R*)-2-((*S*)-1-(4-nitrophenyl)-2,5-dioxopyrrolidin-3-yl)-2-(pentan-3-yloxy)acetamido)-2-phenylacetate (**2-45**) as a colorless oil.

¹H NMR (400 MHz, CDCl₃) δ 0.91 (1H, *t*, *J* = 7.4 Hz), 0.95 (1H, *t*, *J* = 7.4 Hz), 1.54-1.67 (4H, *m*), 2.81 (1H, *dd*, *J* = 4.4, 18.8 Hz), 2.96 (1H, *dd*, *J* = 9.6, 18.8 Hz), 3.34-3.40 (1H, *m*), 3.43 (1H, *q*, *J* = 5.7 Hz), 3.72 (3H, *s*), 4.61 (1H, *d*, *J* = 3.2 Hz), 5.50 (1H, *d*, *J* = 7.2 Hz), 7.30-7.40 (5H, *m*), 7.58-7.65 (2H, *m*), 7.75 (1H, *d*, *J* = 7.2 Hz), 8.28-8.35 (2H, *m*); ¹³C NMR (100 MHz, CDCl₃) δ 9.3, 9.9, 25.9, 26.0, 31.1, 42.6, 52.9, 56.1, 78.1, 83.6, 124.3, 127.1, 127.3, 128.8, 129.1, 136.0, 137.8, 147.1, 169.0, 170.7, 174.2, 174.6; IR (neat) ν 3409, 2924, 1778, 1743, 1720, 1717, 1596, 1497, 1344, 1087, 853, 698 cm⁻¹; HRMS(ESI) [M+Na]⁺ calculated for C₂₆H₂₉N₃O₈Na: 534.1852, found: 534.1873; [α]_D²⁶ +7.8 (*c* 0.13, CHCl₃).

Determination of absolute configuration of 2-40



As key protons in the compound **2-44** are well resolved compared with those of **2-45**, the relative configuration was determined as for the compound **2-44**. The relative configuration at C-2 and C-3 of the compound **2-44** was determined to be $2R^*$ and $3S^*$ by J -based configurational analysis, as shown in Fig. 3. A small homonuclear vicinal coupling constant between H-2 and H-3 ($^3J_{H2,H3} = 3.2$ Hz) indicated a *gauche* relationship between these protons. LSPD experiments were used to measure heteronuclear coupling constant values. Large three bond heteronuclear coupling constant values of H-2/C-4(CH₂) ($^3J_{H2,C4} = 5.8$ Hz) and H-3/C-1 ($^3J_{H3,C1} = 5.8$ Hz) indicated that *anti* relationships of H-2 and C-4 and also H-3 and C-1. This rotamer with a *gauche* relationship between H-3 and the ether oxygen at C-2 was confirmed by large coupling constant of $^2J_{H3,C2} = 6.5$ Hz.

measured J values for 2-44	estimated magnitude for rotamers of ($2R$, $3S$)- 2-44		
$^3J_{H2,H3} = 3.2\text{Hz}$	small	small	large
$^3J_{H2,C4} = 5.8\text{Hz}$	large	small	small
$^3J_{H2,C6} = 2.2\text{Hz}$	small	large	small
$^2J_{H3,C2} = 6.5\text{Hz}$	large	small	large
$^3J_{H3,C1} = 5.8\text{Hz}$	large	small	small

Fig. 3. J -based configurational analysis

The absolute configuration at C₂ of **2-40** was determined by phenylglycine methyl ester method developed by Kusumi.^[S4] The chemical shift difference of (*S*)-amide **2-44** – (*R*)-amide **2-45** was calculated. The absolute configuration at C₂ in **2-44** and **2-45** was determined as ($2R$) by putting the obtained positive and negative value into the reported model by Kusumi. Therefore, the absolute configuration of **2-40** was determined as ($2R$, $3S$).

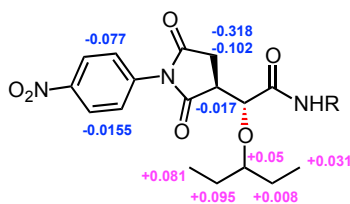
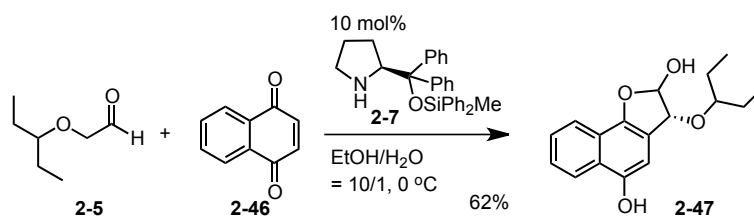


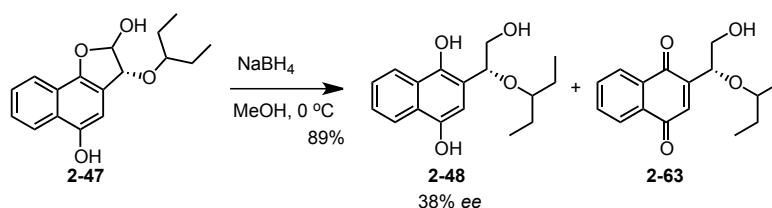
Fig.4. Determination of absolute configuration

(3R)-3-(pentan-3-yloxy)-2,3-dihydronaphtho[1,2-b]furan-2,5-diol (2-47)



To a EtOH (12 mL) solution of pentan-3-yloxy-acetaldehyde (**2-5**) (950 mg, 6.01 mmol) was added H₂O (1.2 mL), (*S*)-2-((methyl(diphenyl)silyloxy)diphenylmethyl)pyrrolidine (**2-7**) (270 mg, 0.60 mmol) and naphthalene-1,4-dione (**2-46**) at 0 °C. After stirring the reaction mixture for 22 h at 0 °C, buffer was added to the mixture. Organic materials were extracted with ethyl acetate twice, and the combined extracts were washed with brine, dried over anhydrous sodium sulfate, and concentrated in vacuo after filtration. Quick purification by silica gel column chromatography (ethyl acetate/hexane = 1/9 to 1/4) gave 910 mg (53%) of (*3R*)-3-(pentan-3-yloxy)-2,3-dihydronaphtho[1,2-b]furan-2,5-diol (**2-47**) as a brown oil, crude product. The obtained crude product was immediately used to the next reaction.

(R)-2-(2-hydroxy-1-(pentan-3-yloxy)ethyl)naphthalene-1,4-diol (2-48)



To a MeOH solution (13 mL) of (*3R*)-3-(pentan-3-yloxy)-2,3-dihydronaphtho[1,2-b]furan-2,5-diol (**2-47**) was added sodium borohydride (239 mg, 6.31 mmol) at 0 °C. After stirring the reaction mixture for 15 min, the reaction was quenched with saturated aqueous NH₄Cl. The pH of the mixture was adjusted to 4 by addition of 10% citric acid solution. Organic materials were extracted with ethyl acetate twice, and combined extracts were washed with brine, dried over anhydrous sodium sulfate, and concentrated in vacuo after filtration to afford 916 mg of brown oil (**2-48:2-63** = >20:1).

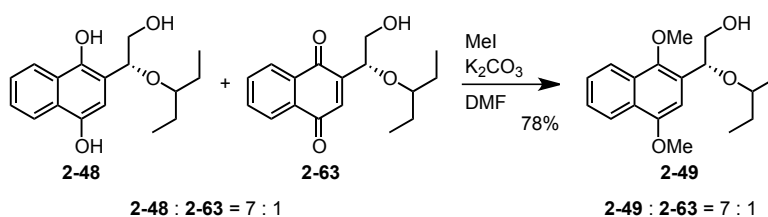
Note: Phenol (R)-2-(2-hydroxy-1-(pentan-3-yloxy)ethyl)naphthalene-1,4-diol (2-48) was easily oxidized to (R)-2-(2-hydroxy-1-(pentan-3-yloxy)ethyl)naphthalene-1,4-dione (2-63) under air. The work up was done under argon as much as possible. The obtained 2-48 was immediately used to next reaction without further purification.

^1H NMR (400 MHz, CDCl_3) δ 0.83 (3H, *t*, J = 7.4 Hz), 0.98 (3H, *t*, J = 7.4 Hz), 1.50-1.80 (4H, *m*), 3.53 (1H, *q*, J = 5.6 Hz), 3.73 (1H, *dd*, J = 4.4, 12.0 Hz), 3.93 (1H, *dd*, J = 8.0, 12.0 Hz), 4.63 (1H, *dd*, J = 4.4, 8.0 Hz), 6.46 (1H, *s*), 7.47-7.55 (2H, *m*), 8.04-8.09 (1H, *m*), 8.19-8.26 (1H, *m*), 8.35 (1H, *bs*); ^{13}C NMR (100 MHz, CDCl_3) δ 145.8, 144.4, 126.1, 126.0, 125.9, 124.9, 122.2, 121.2, 114.7, 108.2, 82.6, 82.5, 65.3, 25.8, 24.5, 9.2, 8.9; IR (neat) ν 3340, 2962, 2877, 1643, 1597, 1319, 1057, 964, 764, 679 cm^{-1} ; HRMS(ESI) $[\text{M}+\text{Na}]^+$ calculated for $\text{C}_{17}\text{H}_{22}\text{O}_4\text{Na}$: 313.1416, found: 313.1401.

Enantiomeric excess = 38%

The enantiomeric excess was determined by HPLC using a Chiralpak IC (10/1 = hexane/*i*PrOH; flow rate 1 mL/min, $t_{\text{R}1}$ = 10.39 (major), $t_{\text{R}2}$ = 13.09 (minor) min).

(R)-2-(1,4-dimethoxynaphthalen-2-yl)-2-(pentan-3-yloxy)ethanol (2-49)



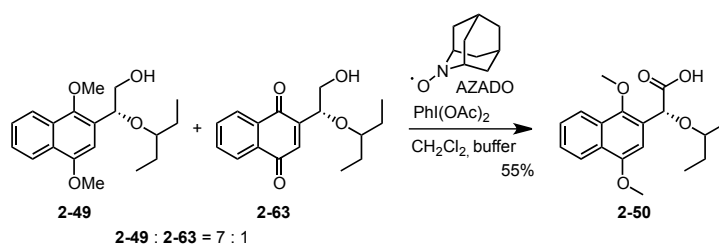
To a DMF solution (13 mL) of (R)-2-(2-hydroxy-1-(pentan-3-yloxy)ethyl)naphthalene-1,4-diol (**2-48**) (916 mg, 3.16 mmol, **2-48** : **2-63** = 7 : 1) was added K_2CO_3 (1.09 g, 7.90 mmol) and MeI (0.41 mL, 6.64 mmol) at 0 °C. After stirring the reaction mixture for 6 h at 0 °C, the reaction was quenched with buffer. Organic materials were extracted with ethyl acetate twice, and combined extracts were washed with water, dried over anhydrous sodium sulfate, and concentrated in vacuo after filtration. Purification by silica gel column chromatography (ethyl acetate/hexane = 1/4) gave 784 mg (78%) of (R)-2-(1,4-dimethoxynaphthalen-2-yl)-2-(pentan-3-yloxy)ethanol (**2-49**) as a brown oil.

Note: 2-49 and 2-63 was not separated at this stage. The obtained product was 7:1 mixture of 2-49 and 2-63.

^1H NMR (400 MHz, CDCl_3) δ 0.83 (3H, *t*, J = 7.4 Hz), 0.94 (3H, *t*, J = 7.6 Hz), 1.40-1.80 (4H, *m*),

3.24 (1H, *q*, *J* = 5.6 Hz), 3.69 (1H, *dd*, *J* = 4.0, 11.2 Hz), 3.80 (1H, *dd*, *J* = 8.8, 11.2 Hz), 3.92 (3H, *s*), 3.98 (3H, *s*), 5.20 (1H, *dd*, *J* = 4.0, 8.8 Hz), 6.86 (1H, *s*), 7.45-7.57 (2H, *m*), 8.02 (1H, *d*, *J* = 8.0 Hz), 8.24 (1H, *d*, *J* = 8.4 Hz); ^{13}C NMR (100 MHz, CDCl_3) δ 152.1, 147.5, 128.3, 127.4, 126.7, 126.4, 125.6, 122.4, 122.0, 102.3, 79.3, 73.5, 66.8, 62.8, 55.6, 26.5, 24.8, 10.2, 8.9; IR (neat) ν 3456, 2931, 2877, 1666, 1597, 1458, 1365, 1211, 1095, 771 cm^{-1} ; HRMS(ESI) $[\text{M}+\text{Na}]^+$ calculated for $\text{C}_{19}\text{H}_{26}\text{O}_4\text{Na}$:341.1729, found: 341.1740.

(*R*)-2-(1,4-dimethoxynaphthalen-2-yl)-2-(pentan-3-yloxy)acetic acid (2-50)



To a CH_2Cl_2 (1 mL) and buffer (1 mL) solution of (*R*)-2-(1,4-dimethoxynaphthalen-2-yl)-2-(pentan-3-yloxy)ethanol (**2-49**) (110 mg, 0.347 mmol, **2-49:2-63=7:1**) was added 2-Azaadamantane-*N*-oxyl (AZADO) (5.3 mg, 0.0347 mmol) and $\text{PhI}(\text{OAc})_2$ (335 mg, 1.04 mmol) at 0 °C. After stirring the reaction mixture for 2 h at room temperature, the reaction was quenched with saturated aqueous solution of $\text{Na}_2\text{S}_2\text{O}_3$. The mixture was stirred for 30 min. Organic materials were extracted with ethyl acetate twice, dried over anhydrous sodium sulfate, and concentrated in vacuo after filtration. Purification by silica gel column chromatography (ethyl acetate/hexane = 1/4 to $\text{CHCl}_3/\text{MeOH}$ =10/1) gave 63 mg (55%) of (*R*)-2-(1,4-dimethoxynaphthalen-2-yl)-2-(pentan-3-yloxy)acetic acid (**2-50**) as a brown oil.

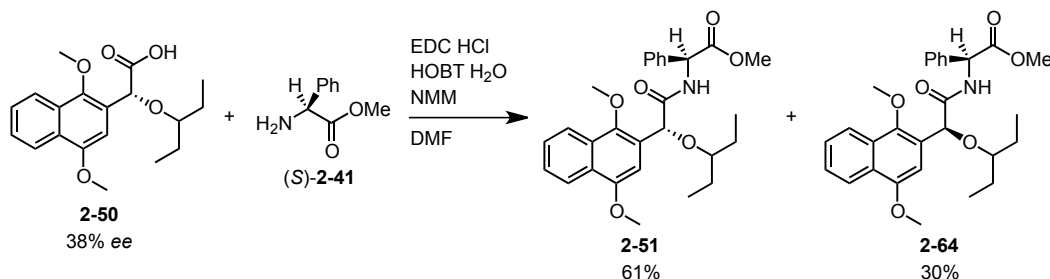
^1H NMR (400 MHz, CDCl_3) δ 0.76 (3H, *t*, *J* = 7.4 Hz), 0.95 (3H, *t*, *J* = 7.4 Hz), 1.40-1.53 (2H, *m*), 1.60-1.73 (2H, *m*), 3.36 (1H, *q*, *J* = 5.6 Hz), 3.96 (3H, *s*), 4.04 (3H, *s*), 5.64 (1H, *s*), 6.64 (1H, *s*), 7.48-7.61 (2H, *m*), 8.06 (1H, *d*, *J* = 8.0 Hz), 8.24 (1H, *d*, *J* = 7.6 Hz); ^{13}C NMR (100 MHz, CDCl_3) δ 173.0, 152.4, 148.6, 128.2, 127.2, 126.9, 126.2, 124.4, 122.6, 122.3, 101.7, 80.9, 72.4, 63.6, 55.7, 26.0, 25.1, 9.7, 9.0; IR (neat) ν 2962, 1728, 1597, 1458, 1365, 1219, 1088, 1003, 849, 771 cm^{-1} ; HRMS(ESI) $[\text{M}+\text{Na}]^+$ calculated for $\text{C}_{19}\text{H}_{24}\text{O}_5\text{Na}$:355.1521, found: 355.1504.

(S)-methyl

2-((R)-2-(1,4-dimethoxynaphthalen-2-yl)-2-(pentan-3-yloxy)acetamido)-2-phenylacetate (2-51);

(S)-methyl

2-((S)-2-(1,4-dimethoxynaphthalen-2-yl)-2-(pentan-3-yloxy)acetamido)-2-phenylacetate (2-64)



To a DMF solution (0.7 mL) of (*R*)-2-(1,4-dimethoxynaphthalen-2-yl)-2-(pentan-3-yloxy)acetic acid (**2-50**) (16.5 mg, 0.0498 mmol, 38% *ee*) was added EDC HCl (14 mg, 0.0747 mmol), HOBT H₂O (7.6 mg, 0.0498 mmol), *N*-methyl morpholine (22 μ L, 0.199 mmol), and (*S*)-methyl 2-amino-2-phenylacetate (**2-41**) (13 mg, 0.0647 mmol) at room temperature. After stirring the reaction mixture for 20 h, water was added to the mixture. Organic materials were extracted with ethyl acetate twice, and the combined extracts were washed with 10% aqueous solution of citric acid, saturated aqueous solution of sodium bicarbonate, and brine, dried over anhydrous sodium sulfate, and concentrated in vacuo after filtration. Purification by preparative thin layer chromatography (diethyl ether : hexane = 1 : 2) gave 14 mg (61%) of (*S*)-methyl 2-((*R*)-2-(1,4-dimethoxynaphthalen-2-yl)-2-(pentan-3-yloxy)acetamido)-2-phenylacetate (**2-51**) and 6.8 mg (30%) of (*S*)-methyl 2-((*S*)-2-(1,4-dimethoxynaphthalen-2-yl)-2-(pentan-3-yloxy)acetamido)-2-phenylacetate (**2-64**) as a yellow oil.

(S)-methyl

2-((R)-2-(1,4-dimethoxynaphthalen-2-yl)-2-(pentan-3-yloxy)acetamido)-2-phenylacetate (2-51)

¹H NMR (400 MHz, CDCl₃) δ 0.72 (3H, *t*, *J* = 7.4 Hz), 0.98 (3H, *t*, *J* = 7.4 Hz), 1.37-1.51 (2H, *m*), 1.60-1.75 (2H, *m*), 3.31 (1H, *q*, *J* = 5.7 Hz), 3.74 (3H, *s*), 3.77 (3H, *s*), 4.03 (3H, *s*), 5.56 (1H, *s*), 5.69 (1H, *d*, *J* = 8.0 Hz), 6.45 (1H, *s*), 7.29-7.55 (7H, *m*), 8.03 (1H, *d*, *J* = 8.0 Hz), 8.16 (1H, *d*, *J* = 8.0 Hz), 8.25 (1H, *d*, *J* = 8.0 Hz); ¹³C NMR (100 MHz, CDCl₃) δ 171.2, 171.0, 152.1, 148.7, 137.1, 129.0, 128.4, 128.3, 127.2, 126.8, 126.3, 125.8, 122.3, 122.3, 101.5, 80.5, 73.3, 63.9, 55.9, 55.3, 52.8, 26.1, 25.1, 9.7, 9.0; IR (neat) ν 3410, 2962, 1743, 1682, 1597, 1504, 1458, 1365, 1211, 1072, 995, 771, 702, 517 cm⁻¹; HRMS(ESI) [M+Na]⁺ calculated for C₂₈H₃₃NO₆Na:502.2206, found: 502.2186; [α]_D²⁹ +209 (*c* 1.5, CHCl₃).

(S)-methyl

2-((S)-2-(1,4-dimethoxynaphthalen-2-yl)-2-(pentan-3-yloxy)acetamido)-2-phenylacetate (2-64)

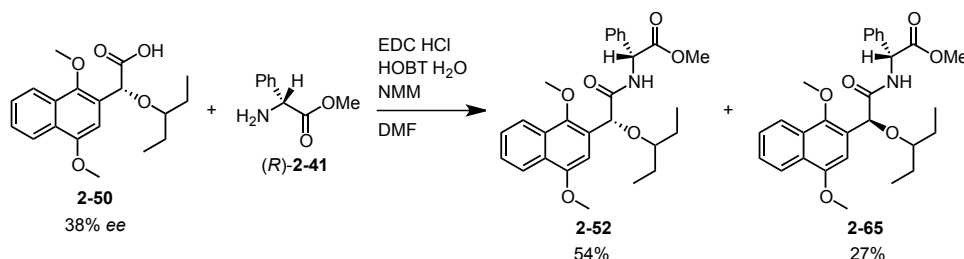
^1H NMR (400 MHz, CDCl_3) δ 0.74 (3H, *t*, J = 7.6 Hz), 0.86 (3H, *t*, J = 7.6 Hz), 1.36-1.48 (2H, *m*), 1.55-1.65 (2H, *m*), 3.25 (1H, *q*, J = 5.7 Hz), 3.73 (3H, *s*), 4.02 (3H, *s*), 4.05 (3H, *s*), 5.56 (1H, *s*), 5.65 (1H, *d*, J = 8.0 Hz), 6.84 (1H, *s*), 7.34-7.57 (7H, *m*), 8.05 (1H, *bd*, J = 7.6 Hz), 8.06 (1H, *d*, J = 7.6 Hz), 8.23 (1H, *d*, J = 7.6 Hz); ^{13}C NMR (100 MHz, CDCl_3) δ 171.3, 171.2, 152.3, 148.7, 136.4, 129.1, 128.6, 128.3, 127.3, 127.0, 126.6, 126.3, 125.8, 122.4, 122.3, 102.1, 80.0, 73.1, 63.9, 56.1, 55.7, 52.7, 26.1, 25.0, 9.8, 9.0; IR (neat) ν 3417, 2962, 1743, 1689, 1597, 1504, 1458, 1365, 1219, 1072, 995, 771, 702, 517 cm^{-1} ; HRMS(ESI) $[\text{M}+\text{Na}]^+$ calculated for $\text{C}_{28}\text{H}_{33}\text{NO}_6\text{Na}$:502.2206, found: 502.2184; $[\alpha]_D^{29}$ -40.4 (c 0.77, CHCl_3)

(R)-methyl

2-((R)-2-(1,4-dimethoxynaphthalen-2-yl)-2-(pentan-3-yloxy)acetamido)-2-phenylacetate (2-52);

(R)-methyl

2-((S)-2-(1,4-dimethoxynaphthalen-2-yl)-2-(pentan-3-yloxy)acetamido)-2-phenylacetate (2-65)



To a DMF solution (0.7 mL) of *(R)*-2-(1,4-dimethoxynaphthalen-2-yl)-2-(pentan-3-yloxy)acetic acid (**2-50**) (16 mg, 0.0483 mmol, 38 %ee) was added EDC HCl (14 mg, 0.0724 mmol), HOBT H₂O (7.4 mg, 0.0483 mmol), *N*-methyl morpholine (21 μL , 0.193 mmol), and *(R)*-methyl 2-amino-2-phenylacetate hydrochloride (**2-41**) (13 mg, 0.0628 mmol) at room temperature. After stirring the reaction mixture for 24 h, water was added to the mixture. Organic materials were extracted with ethyl acetate twice, and the combined extracts were washed with 10% aqueous solution of citric acid, saturated aqueous solution of sodium bicarbonate, and brine, dried over anhydrous sodium sulfate, and concentrated in vacuo after filtration. Purification by preparative thin layer chromatography (ether : hexane = 1 : 2) gave 12 mg (54%) of *(R)*-methyl 2-((*R*)-2-(1,4-dimethoxynaphthalen-2-yl)-2-(pentan-3-yloxy)acetamido)-2-phenylacetate (**2-52**) and 6.1 mg (27%) of *(R)*-methyl 2-((*S*)-2-(1,4-dimethoxynaphthalen-2-yl)-2-(pentan-3-yloxy)acetamido)-2-phenylacetate (**2-65**) as a colorless oil.

(R)-methyl

2-((R)-2-(1,4-dimethoxynaphthalen-2-yl)-2-(pentan-3-yloxy)acetamido)-2-phenylacetate (2-52)

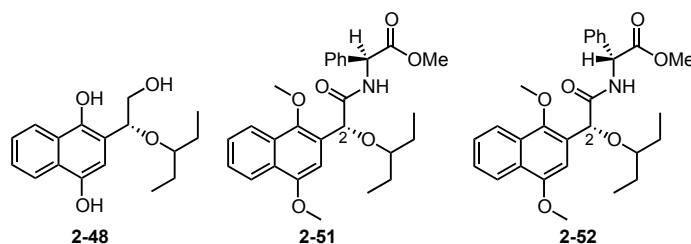
¹H NMR (400 MHz, CDCl₃) δ 0.74 (3H, *t*, *J* = 7.6 Hz), 0.86 (3H, *t*, *J* = 7.6 Hz), 1.36-1.48 (2H, *m*), 1.55-1.65 (2H, *m*), 3.25 (1H, *q*, *J* = 5.7 Hz), 3.73 (3H, *s*), 4.02 (3H, *s*), 4.05 (3H, *s*), 5.56 (1H, *s*), 5.65 (1H, *d*, *J* = 8.0 Hz), 6.84 (1H, *s*), 7.34-7.57 (7H, *m*), 8.05 (1H, *bd*, *J* = 7.6 Hz), 8.06 (1H, *d*, *J* = 7.6 Hz), 8.23 (1H, *d*, *J* = 7.6 Hz); ¹³C NMR (100 MHz, CDCl₃) δ 171.3, 171.2, 152.3, 148.7, 136.4, 129.1, 128.6, 128.3, 127.3, 127.0, 126.6, 126.3, 125.8, 122.4, 122.3, 102.1, 80.1, 73.1, 63.9, 56.1, 55.7, 52.7, 26.1, 25.1, 9.8, 9.0; IR (neat) ν 3417, 2962, 1743, 1689, 1597, 1504, 1458, 1365, 1219, 1072, 995, 771, 702, 517 cm⁻¹; [α]_D²⁹ +78 (*c* 1.73, CHCl₃); HRMS(ESI) [M+Na]⁺ calculated for C₂₈H₃₃NO₆Na:502.2206, found: 502.2191.

(R)-methyl

2-((S)-2-(1,4-dimethoxynaphthalen-2-yl)-2-(pentan-3-yloxy)acetamido)-2-phenylacetate (2-65)

¹H NMR (400 MHz, CDCl₃) δ 0.72 (3H, *t*, *J* = 7.4 Hz), 0.98 (3H, *t*, *J* = 7.4 Hz), 1.37-1.51 (2H, *m*), 1.60-1.75 (2H, *m*), 3.31 (1H, *q*, *J* = 5.7 Hz), 3.74 (3H, *s*), 3.77 (3H, *s*), 4.03 (3H, *s*), 5.56 (1H, *s*), 5.69 (1H, *d*, *J* = 8.0 Hz), 6.45 (1H, *s*), 7.29-7.55 (7H, *m*), 8.03 (1H, *d*, *J* = 8.0 Hz), 8.16 (1H, *d*, *J* = 8.0 Hz), 8.25 (1H, *d*, *J* = 8.0 Hz); ¹³C NMR (100 MHz, CDCl₃) δ 171.2, 171.0, 152.1, 148.7, 137.1, 129.0, 128.5, 128.3, 127.2, 126.8, 126.6, 126.3, 125.8, 122.3, 122.2, 101.5, 80.5, 73.3, 63.9, 55.9, 55.3, 52.8, 26.1, 25.1, 9.7, 9.0; IR (neat) ν 3409, 2962, 1743, 1689, 1597, 1504, 1458, 1365, 1265, 1211, 1072, 771, 702, 517 cm⁻¹; [α]_D²⁸ -210 (*c* 0.77, CHCl₃); HRMS(ESI) [M+Na]⁺ calculated for C₂₈H₃₃NO₆Na:502.2206, found: 502.2198.

Determination of absolute configuration of 2-48



The absolute configuration of **2-48** was determined by phenylglycine methyl ester method after converting **2-48** into the PGME amide **2-51** and **2-52**.^[S4] The chemical shift difference of (*S*)-amide **2-51** – (*R*)-amide **2-52**, was calculated. The absolute configuration at C₂ in **2-51** and **2-52** was determined as (*R*) by putting the obtained positive and negative value into the reported model by Kusumi.^[S4] Thus, the absolute configuration of **2-48** was determined as (*R*).

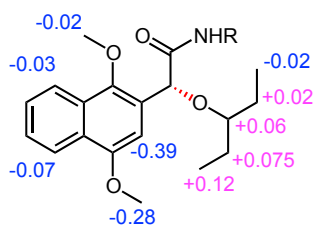
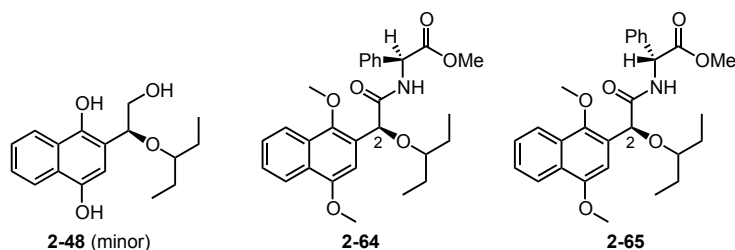


Fig. 3. Determination of the absolute configuration at C₂ of **2-48**

Determination of absolute configuration of minor isomer of 2-48



The absolute configuration of **2-48** (minor) was determined by phenylglycine methyl ester method after converting **2-48** (minor) into the PGME amide **2-64** and **2-65**.^[S4] The chemical shift difference of (*S*)-amide **2-64** – (*R*)-amide **2-65**, was calculated. The absolute configuration at C₂ in **2-64** and **2-65** was determined as (*S*) by putting the obtained positive and negative value into the reported model by Kusumi.^[S4] Thus, the absolute configuration of **2-48** (minor) was determined as (*2S*).

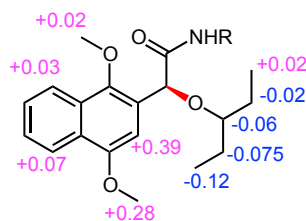
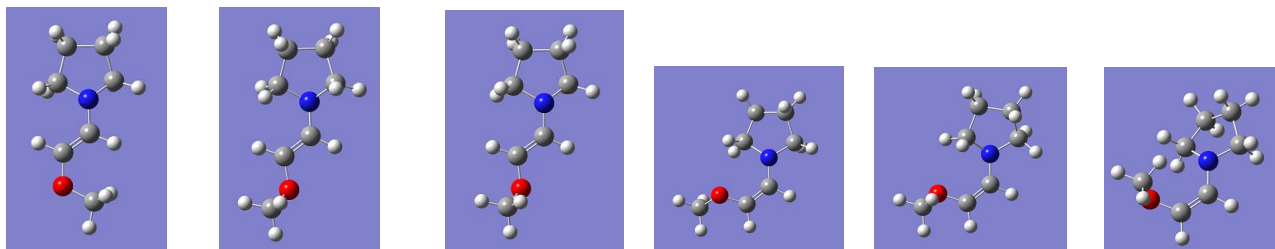


Fig. 4. Determination of the absolute configuration of minor isomer of **2-48**

Calculation study of *E*- and *Z*-enamines

Calculated enthalpy values for alkoxyenamine



E1

E2

E3

Z1

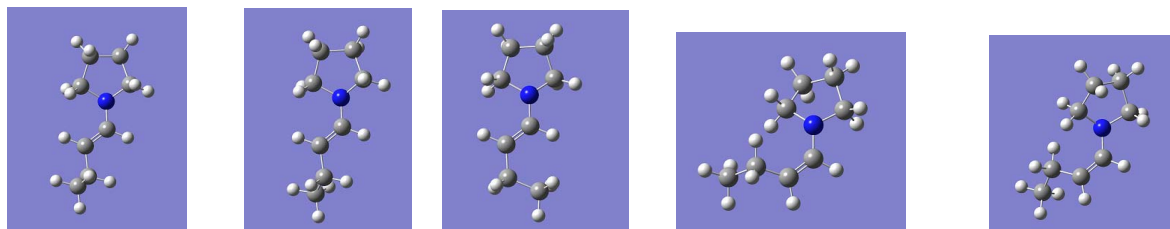
Z2

Z3

Table Calculated Enthalpy Values (298 K) (Relative Values are given in kcal/mol)

Enamine derived from alpha-alkoxy aldehyde						
computational level	<i>E</i> isomer			<i>Z</i> isomer		
	1	2	3	1	2	3
MMFF94s	21.0418	23.5103	23.5133	24.2982	24.3055	30.3164
	0.00	2.47	2.47	3.26	3.26	9.27
B3LYP/6-31G(d)	-404.291554	-404.291449	-404.291484	-404.290994	-404.291118	-404.291119
	0.00	0.07	0.04	0.35	0.27	0.27
M062X/6-31G(d)	-404.100228	-404.098553	-404.098653	-404.098773	-404.098721	-404.098110
	0.00	1.05	0.99	0.91	0.95	1.33
wB97XD/6-31G(d)	-404.164798	-404.164319	-404.164384	-404.164321	-404.164445	-404.164445
	0.00	0.30	0.26	0.30	0.22	0.22
MP2/6-31G(d)	-402.933596	-402.932883	-402.932808	-402.932888	-402.932768	-402.932105
	0.00	0.45	0.49	0.44	0.52	0.94
CBS-QB3	-403.741064			-403.740561		
	0.00			0.32		
B3LYP/6-31G(d) (C ₆ H ₆)	-404.300225	-404.300013	-404.300303	-404.299309	-404.299536	-404.299537
	0.00	0.13	-0.05	0.57	0.43	0.43

Calculated enthalpy values for alxylenamine



E1

E2

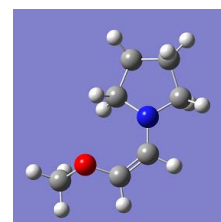
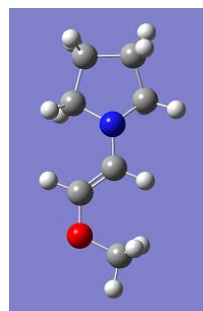
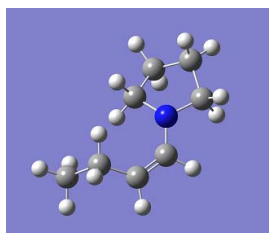
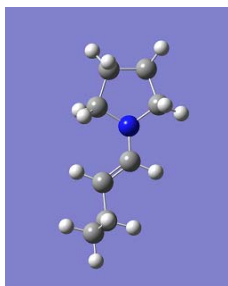
E3

Z1

Z2

Enamine derived from alkyl aldehyde						
computational level	<i>E</i> isomer			<i>Z</i> isomer		
	1	2	3	1	2	3
MMFF94s	3.2587	3.2611	3.6596	6.7140	6.8527	
	0.00	0.00	0.40	3.46	3.59	
B3LYP/6-31G(d)	-368.384480	-368.384470	-368.382645	-368.378324	-368.378185	
	0.00	0.01	1.15	3.86	3.95	
M062X/6-31G(d)	-368.194759	-368.194659	-368.194703	-368.190334	-368.190117	
	0.00	0.06	0.04	2.78	2.91	
wB97XD/6-31G(d)	-368.269573	-368.270577	-368.269463	-368.265389	-368.264813	
	0.00	-0.63	0.07	2.63	2.99	
MP2/6-31G(d)	-367.063776	-367.063780	-367.061842	-367.058653	-367.058933	
	0.00	0.00	1.21	3.21	3.04	
B3LYP/6-31G(d) (C ₆ H ₆)	-368.394967	-368.394934	-368.393002	-368.388492	-368.388325	
	0.00	0.02	1.23	4.06	4.17	

Results of NBO calculations of enamines (B3LYP/6-31G(d))



Results of NBO Calculations of Enamines (B3LYP/6-31G(d))

	Alkyl Enamine			Alkoxy Enamine		
	E	Z	Z - E	E	Z	Z - E
Electric Energy	-368.615403382	-368.609536749	3.68	-404.498663168	-404.497677538	0.62
Energy of Lewis Structure	-368.056257381	-368.047532606	5.47	-403.907491630	-403.900462245	4.41
Resonance Energy	-0.559146001	-0.562004143	-1.79	-0.591171538	-0.597215293	-3.79

Results of NBO calculations - 2 -

Table 3: Results of NBO calculations -2-

Z isomer						E isomer					
Orbital Interaction		2nd order Stabilization energy (kcal /mol)	E(j) - E(i)	F(i,j)		Orbital Interaction		2nd order Stabilization energy (kcal /mol)	E(j) - E(i)	F(i,j)	
n σ (O)	σ^* CC	—				n σ (O)	σ^* CC	6.59	1.17	0.079	
n σ (O)	π^* CC	1.74	0.70	0.032		n π (O)	π^* CC	27.54	0.36	0.091	
n π (O)	π^* CC	5.06	0.47	0.044		σ CN	σ^* CO	2.84	1.14	0.051	
n π (O)	σ^* CC	7.37	0.85	0.072		σ CO	σ^* CH	—			
σ CH	σ^* CO	7.80	0.89	0.074		n σ (N)	σ^* CC	—			
σ CO	σ^* CN	—				n π (N)	π^* CC	26.02	0.32	0.081	
nσ(N)	σ^* CC	—				n π (N)	σ^* CC	2.48	0.78	0.041	
n π (N)	π^* CC	24.39	0.40	0.089		σ CH	σ^* CN	7.40	1.01	0.077	
n π (N)	σ^* CC	2.48	0.78	0.041		σ CN	σ^* CO	—			
σ CH	σ^* CN	7.40	1.01	0.077		π^* CC	σ^* CC	22.67	0.39	0.236	
σ CN	σ^* CO	—				σ CN	σ^* CH	1.31	1.24	0.036	
π^* CC	σ^* CC	22.67	0.39	0.236		σ CO	σ^* CH	1.56	1.30	0.040	
σ CN	σ^* CH	1.31	1.24	0.036		σ CH	σ^* CH	—			
σ CO	σ^* CH	1.56	1.30	0.040		σ CH	σ^* CH	4.22	1.01	0.058	
σ CH	σ^* CH	—				σ CH	σ^* CH	4.58	0.99	0.060	
σ CH	σ^* CH	—				π^* CC	σ^* CC	2.95	0.57	0.102	
σ CH	σ^* CH	—				σ CH	σ^* CO	0.69	0.90	0.022	
σ CH	σ^* CH	—				σ CH	σ^* CN	—			

赤字: 二重結合のトランス位の軌道相互作用エネルギー

青字: 二重結合のシス位の軌道相互作用エネルギー

Referenes

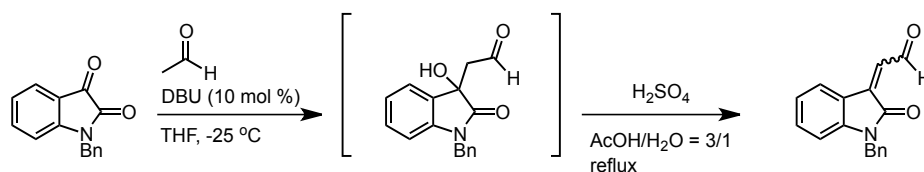
- [S1] H. Ishikawa, T. Suzuki, H. Orita, T. Uchimar, Y. Hayashi, *Chem. Eur. J.* **2010**, *16*, 12616.
[S2] S. Zhu, S. Yu, Y. Wang, D. Ma, *Angew. Chem., Int. Ed.* **2010**, *49*, 4656.
[S3] G. Bifulco, P. Dambruoso, L. Gomez-Paloma, R. Riccio, *Chem. Rev.* **2007**, *107*, 3744.
[S4] a) Y. Nagai, T. Kusumi, *Tetrahedron Lett.* **1995**, *36*, 1853; b) T. Yabuuchi, T. Kusumi, *J. Org. Chem.* **2000**, *65*, 397.

Chapter 3

Asymmetric Michael addition of nitromethane to 2-oxoindoline-3-ylidene acetaldehyde and three “one-pot” sequential synthesis of (–)-Horsfiline and (–)-Coerulescine

General Remarks: All reactions were monitored by thin-layer chromatography using Merck 60 F254 precoated silica gel plates (0.25 mm thickness). Specific optical rotations were measured using a JASCO DIP-370 polarimeter. FT-IR spectra were recorded on a Perkin Elmer spectrum BX FT-IP spectrometer. ^1H and ^{13}C NMR spectra were recorded on a Agilent-400 MR (400 MHz for ^1H NMR, 100 MHz for ^{13}C NMR) instrument. Data for ^1H NMR are reported as chemical shift (d ppm), multiplicity (s = singlet, d = doublet, t = triplet, dd = doubledoublet, dt = doubletriplet, m = multiplet, br = broad), coupling constant (Hz), integration, and assignment. Data for ^{13}C NMR are reported as chemical shift. High-resolution ESI-TOF mass spectral was measured Thermo Orbi-trap instrument. Preparative thin layer chromatography was performed using Wakogel B-5F purchased from Wako Pure Chemical Industries, Tokyo, Japan. Flash chromatography was performed using silica gel 60N of Kanto Chemical Co. Int., Tokyo, Japan. HPLC analysis was performed on a HITACHI Elite LaChrom Series HPLC, UV detection monitored at appropriate wavelength respectively, using Chiralcel Chiralpak IC (0.46 cm x 25 cm), AS-H (0.46 cm x 25 cm), and OB-H (0.46 cm x 25 cm).

2-(1-benzyl-2-oxoindolin-3-ylidene)acetaldehyde



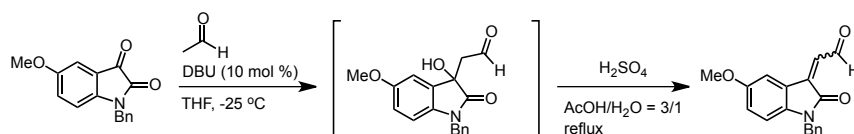
To a THF solution (8 ml) of isatin (1.0 g, 4.2 mmol) was added DBU (62 μ l, 0.42 mmol), then the flask was filled with Argon. Acetaldehyde (1.2 ml, 21 mmol; distilled just before the use) was added to the mixture, and the flask was sealed tightly and left for overnight at -25 °C. The mixture was concentrated in vacuo, and to the residue was added AcOH (3 ml), H₂O (1 ml), and H₂SO₄ (0.21 ml). The mixture was refluxed for 10 minutes, and diluted with H₂O. Organic materials were extracted with CHCl₃ three times, dried over anhydrous magnesium sulfate, and concentrated in vacuo after filtration. Purification by silica gel column chromatography (CHCl₃) gave 990 mg (89%) of product (*E*:*Z* = 1:2.2) as a red solid.

(*Z*)-isomer: ¹H NMR (400 MHz, CDCl₃) δ 11.1 (d, *J* = 7.6 Hz, 1H), 7.41 (d, *J* = 7.6 Hz, 1H), 7.29-7.19 (m, 6H, overlap with *E*), 6.99-6.94 (m, 1H, overlap with *E*), 6.65 (d, *J* = 7.6 Hz, 2H, overlap with *E*), 4.86 (s, 2H); ¹³C NMR (100 MHz, CDCl₃) δ 192.2, 166.1, 144.5, 139.5, 135.1, 133.0, 129.4, 128.9, 127.9, 127.3, 122.9, 122.5, 121.2, 109.8, 43.6.

(*E*)-isomer: ¹H NMR (400 MHz, CDCl₃) δ 10.5 (d, *J* = 6.4 Hz, 1H), 7.94 (d, *J* = 7.6 Hz, 1H), 7.29-7.19 (m, 5H, overlap with *E*), 6.99-6.94 (m, 2H, overlap with *E*), 6.69-6.65 (m, 2H, overlap with *E*), 4.88 (s, 2H); ¹³C NMR (100 MHz, CDCl₃) δ 190.0, 167.7, 145.4, 138.8, 135.1, 133.2, 129.4, 128.9, 127.9, 127.2, 123.0, 122.5, 120.0, 109.9, 43.9.

(*E*)-isomer/(*Z*)-isomer=1/2: IR (neat) ν 1701, 1664, 1608, 1495, 1479, 1468, 1438, 1375, 1349, 1163, 1123, 747, 702 cm⁻¹; HRMS(ESI) [M+Na]⁺ calculated for C₁₇H₁₃NO₂Na: 286.0844, found: 286.0844.

2-(1-benzyl-5-methoxy-2-oxoindolin-3-ylidene)acetaldehyde



To a THF solution (7 ml) of isatin (1.0 g, 3.7 mmol) was added DBU (55 μ l, 0.37 mmol), then the flask was filled with Argon. Acetaldehyde (1.0 ml, 18 mmol; distilled just before the use) was added to the mixture, and the flask was sealed tightly and left for overnight at -25 °C. The mixture was concentrated in vacuo, and to the residue was added AcOH (2.7 ml), H₂O (0.9 ml), and H₂SO₄ (0.18 ml). The mixture was refluxed for 1 h, and diluted with H₂O. Organic materials were extracted with

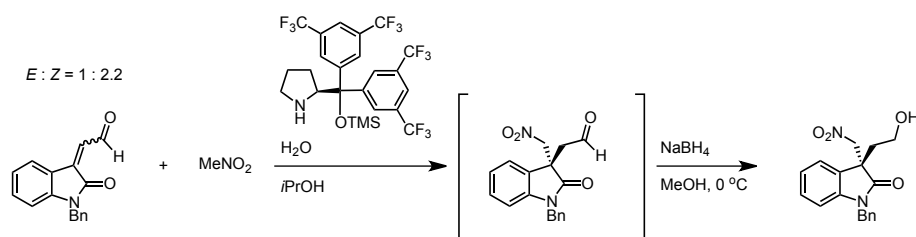
CHCl₃ three times, dried over anhydrous magnesium sulfate, and concentrated in vacuo after filtration. Purification by silica gel column chromatography (CHCl₃) gave 994 mg (91%) of product (*E*:*Z* = 1:2.6) as a dark-brown solid.

(*Z*)-isomer: ¹H NMR (400 MHz, CDCl₃) δ 11.1 (d, *J* = 8.0 Hz, 1H), 7.38-7.27 (m, 5H), 7.03 (d, *J* = 2.4 Hz, 1H), 6.83 (dd, *J* = 8.4, 2.4 Hz, 1H), 6.68 (d, *J* = 8.0 Hz, 1H), 6.60 (d, *J* = 8.4 Hz, 1H), 4.90 (s, 2H), 3.78 (s, 3H); ¹³C NMR (100 MHz, CDCl₃) δ 192.1, 165.9, 155.9, 139.9, 138.3, 135.2, 129.3, 128.8, 127.8, 127.2, 121.9, 118.3, 110.4, 108.5, 55.8, 43.6.

(*E*)-isomer: ¹H NMR (400 MHz, CDCl₃) δ 10.5 (d, *J* = 6.0 Hz, 1H), 7.68 (d, *J* = 2.4 Hz, 1H), 7.38-7.27 (m, 5H), 7.07 (d, *J* = 6.0 Hz, 1H), 6.86 (dd, *J* = 8.8, 2.4 Hz, 1H), 6.62 (d, *J* = 8.8 Hz, 1H), 4.92 (s, 2H), 3.80 (s, 3H); ¹³C NMR (100 MHz, CDCl₃) δ 189.9, 167.5, 155.7, 139.2, 139.0, 135.2, 128.8, 127.8, 127.7, 127.2, 120.6, 118.4, 113.5, 110.3, 55.8, 43.9.

(*E*)-isomer/(*Z*)-isomer=1/2.5: IR (neat) ν 2936, 1703, 1667, 1625, 1596, 1489, 1437, 1341, 1277, 1168, 1122, 1021, 698 cm⁻¹; HRMS(ESI) [M+Na]⁺ calculated for C₁₈H₁₅NO₃Na: 316.0950, found: 316.0951.

(*R*)-1-benzyl-3-(2-hydroxyethyl)-3-(nitromethyl)indolin-2-one



To a *i*PrOH solution (1 ml) of α,β -unsaturated aldehyde (26 mg, 0.099 mmol) was added diarylprolinol silyl ether (12 mg, 0.02 mmol), H₂O (18 μ l, 0.99 mmol), and nitromethane (27 μ l, 0.49 mmol) at room temperature. After stirring the reaction mixture for 42 h, the mixture was concentrated in vacuo. The residue was dissolved in MeOH (1 ml), and NaBH₄ (18 mg, 0.49 mmol) was added to the mixture at 0 °C. The mixture was stirred for 30 min, and the reaction was quenched by the addition of saturated aq.NH₄Cl. Organic materials were extracted with CHCl₃ three times, dried over anhydrous sodium sulfate, and concentrated in vacuo after filtration. Purification by silica gel column chromatography (ethyl acetate/hexane = 1/3 to 3/1) gave 23 mg (72%, 2 steps) of alcohol as colorless oil.

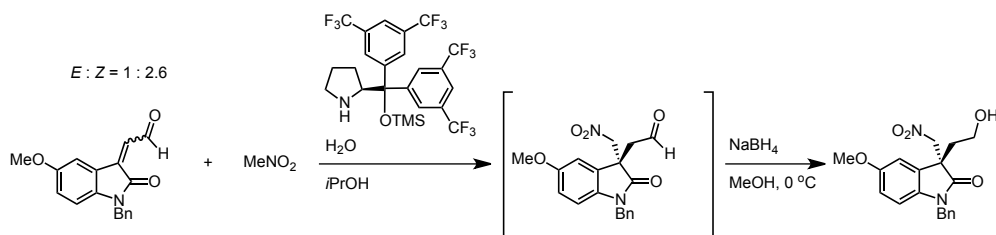
¹H NMR (400 MHz, CDCl₃) δ 7.40-7.19 (m, 7H), 7.05 (dt, *J* = 7.6, 0.8 Hz, 1H), 6.76 (d, *J* = 8.0 Hz, 1H), 5.08 (d, *J* = 13.6 Hz, 1H), 4.99 (d, *J* = 13.6 Hz, 1H), 4.97 (d, *J* = 2.0 Hz, 2H), 3.61 (dt, *J* = 6.0, 4.8 Hz, 2H), 2.20-2.02 (m, 2H); ¹³C NMR (100 MHz, CDCl₃) δ 177.3, 143.2, 135.3, 129.4, 128.8, 128.3, 127.7, 127.3, 127.1, 123.0, 110.0, 78.6, 58.1, 50.0, 44.4, 38.0; IR (neat) ν 3420, 2922, 1709,

1612, 1555, 1489, 1467, 1431, 1376, 1177, 1043, 910, 754, 697 cm^{-1} ; HRMS(ESI) $[\text{M}+\text{Na}]^+$ calculated for $\text{C}_{18}\text{H}_{18}\text{N}_2\text{O}_4\text{Na}$: 349.1164, found: 349.1169; $[\alpha]_D^{26} +28.7$ (c 1.6, CHCl_3).

Enantiomeric excess = 94%

The enantiomeric excess was determined by HPLC using a Chiralpak IC (3/1 = hexane/*i*PrOH; flow rate 1 ml/min, $t_{\text{R}1}$ = 9.01 (minor), $t_{\text{R}2}$ = 13.86 (major) min).

(R)-1-benzyl-3-(2-hydroxyethyl)-5-methoxy-3-(nitromethyl)indolin-2-one



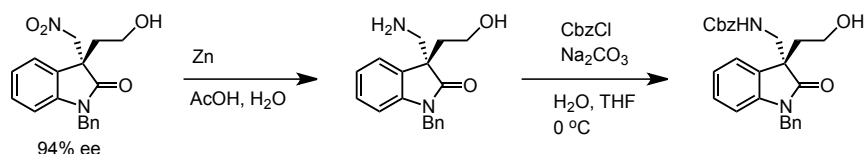
To a *i*PrOH solution (1.1 ml) of α,β -unsaturated aldehyde (32 mg, 0.11 mmol) was added diarylprolinol silyl ether (13 mg, 0.022 mmol), H_2O (20 μl , 1.1 mmol), and nitromethane (29 μl , 0.55 mmol) at room temperature. After stirring the reaction mixture for 71 h, the mixture was concentrated in vacuo. The residue was dissolved in MeOH (1 ml), and NaBH_4 (20 mg, 0.55 mmol) was added to the mixture at 0 $^\circ\text{C}$. The mixture was stirred for 30 min, and the reaction was quenched by the addition of saturated aq. NH_4Cl . Organic materials were extracted with CHCl_3 three times, dried over anhydrous sodium sulfate, and concentrated in vacuo after filtration. Purification by silica gel column chromatography (ethyl acetate/hexane = 1/3 to 2/1) gave 21 mg (54%, 2 steps) of alcohol as colorless oil.

^1H NMR (400 MHz, CDCl_3) δ 7.38-7.25 (m, 5H), 6.84 (d, J = 2.4 Hz, 1H), 6.72 (dd, J = 8.8, 2.4 Hz, 1H), 6.65 (d, J = 8.8 Hz, 1H), 5.08 (d, J = 13.2 Hz, 1H), 4.96 (d, J = 13.2 Hz, 1H), 4.95 (d, J = 5.2 Hz, 2H), 3.74 (s, 3H), 3.63 (q, J = 5.6 Hz, 2H), 2.14 (dt, J = 14.0, 6.0 Hz, 1H), 2.05 (dt, J = 14.0, 6.0 Hz, 1H); ^{13}C NMR (100 MHz, CDCl_3) δ 176.9, 156.2, 136.5, 135.4, 128.8, 128.3, 127.7, 127.3, 113.3, 110.7, 110.4, 78.6, 58.1, 55.7, 50.3, 44.5, 38.1; IR (neat) ν 3443, 2923, 1694, 1602, 1555, 1494, 1434, 1378, 1283, 1181, 1043, 808, 738, 696 cm^{-1} ; HRMS(ESI) $[\text{M}+\text{H}]^+$ calculated for $\text{C}_{19}\text{H}_{21}\text{N}_2\text{O}_5$: 357.1450, found: 357.1451; $[\alpha]_D^{26} +33.0$ (c 0.36, CHCl_3).

Enantiomeric excess = 95%

The enantiomeric excess was determined by HPLC using a Chiralpak IC (10/1 = hexane/*i*PrOH; flow rate 1 ml/min, $t_{\text{R}1}$ = 39.63 (minor), $t_{\text{R}2}$ = 67.59 (major) min).

Determination of absolute configuration

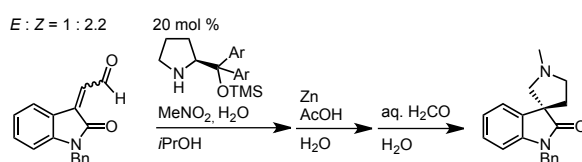


To a AcOH (0.1 ml) and H₂O (0.1 ml) solution of alcohol (7 mg, 0.021 mmol) was added Zn (35 mg, 0.54 mmol) at 0 °C. After stirring the reaction mixture for 2 h at room temperature, the reaction was quenched by the addition of 2N NaOH. Organic materials were extracted with CHCl₃/MeOH = 10/1 three times, dried over anhydrous sodium sulfate, and concentrated in vacuo after filtration. To the residue was added THF (0.1 ml), H₂O (0.2 ml), Na₂CO₃ (11 mg, 0.11 mmol), and cbzCl (5 ul, 0.34 mmol) at 0 °C. After stirring the reaction mixture for 30 min, the reaction was quenched by the addition of saturated aq. NaHCO₃. Organic materials were extracted with ethyl acetate three times, and the extracts were washed with brine, dried over anhydrous sodium sulfate, and concentrated in vacuo after filtration. Purification by preparative thin layer chromatography (ethyl acetate/hexane = 1/1.5) gave 4.0 mg (43%, 2 steps) of product as colorless oil.

$[\alpha]_D^{26} +10.2$ (c 0.4, CHCl₃)

The absolute configuration was determined by comparing the optical rotation with the reported data [S1]. lit. $[\alpha]_D^{20} +8.5$ (c 1.0, CHCl₃)

(R)-1-benzyl-1'-methylspiro[indoline-3,3'-pyrrolidin]-2-one

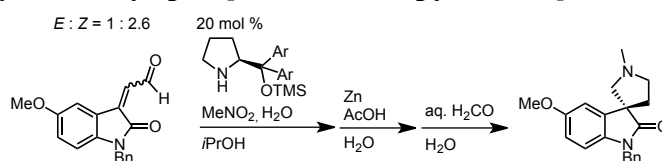


To a *i*PrOH solution (1.2 ml) of α,β -unsaturated aldehyde (33 mg, 0.13 mmol) was added diarylprolinol silyl ether (15 mg, 0.025 mmol), H₂O (23 ul, 1.3 mmol), and nitromethane (34 ul, 0.63 mmol) at room temperature. After stirring the reaction mixture for 42 h, AcOH (0.5 ml) and H₂O (0.5 ml) were added to the mixture. Zn (204 mg, 3.1 mmol) was added to the mixture at 0 °C, and the mixture was stirred for 1 h at room temperature. To the mixture was added 37% aqueous solution of formaldehyde (75 ul), and the mixture was stirred for 1 h. The mixture was diluted with 2N NaOH, and organic materials were extracted with CHCl₃/MeOH = 10/1 three times, dried over anhydrous sodium sulfate, and concentrated in vacuo after filtration. Purification by silica gel column chromatography (ethyl acetate/hexane = 1/1 to CHCl₃/MeOH = 10/1) gave 25 mg (69%, 4 steps) of product as yellow oil.

¹H NMR (400 MHz, CDCl₃) δ 7.42 (d, J = 7.6 Hz, 1H), 7.32-7.21 (m, 5H), 7.12 (dt, J = 7.6, 1.2 Hz,

1H), 7.01 (dt, $J = 7.6, 1.2$ Hz, 1H), 6.68 (d, $J = 7.6$ Hz, 1H), 4.89 (s, 2H), 3.11-3.01 (m, 1H), 2.91 (ABq, $J = 9.2$ Hz, 1H), 2.86 (ABq, $J = 9.2$ Hz, 1H), 2.46 (s, 3H), 2.44-2.38 (m, 1H), 2.11 (dt, $J = 12.8, 8.0$, 1H); ^{13}C NMR (100 MHz, CDCl_3) δ 180.4, 141.9, 136.0, 135.9, 128.7, 127.6, 127.5, 127.2, 123.0, 122.9, 108.7, 66.5, 56.8, 53.3, 43.8, 41.9, 38.1; IR (neat) ν 2941, 1713, 1611, 1487, 1466, 1360, 1182, 959, 752, 697 cm^{-1} ; HRMS(ESI) $[\text{M}+\text{H}]^+$ calculated for $\text{C}_{19}\text{H}_{21}\text{N}_2\text{O}$: 293.1654, found: 293.1653; $[\alpha]_{\text{D}}^{27} +4.7$ (c 0.26, MeOH).

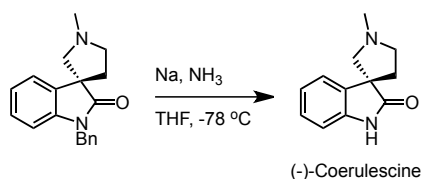
(R)-1-benzyl-5-methoxy-1'-methylspiro[indoline-3,3'-pyrrolidin]-2-one



To a *i*PrOH solution (1.1 ml) of α,β -unsaturated aldehyde (34 mg, 0.12 mmol) was added diarylprolinol silyl ether (14 mg, 0.023 mmol), H_2O (21 μl , 1.2 mmol), and nitromethane (31 μl , 0.58 mmol) at room temperature. After stirring the reaction mixture for 48 h, AcOH (0.5 ml) and H_2O (0.5 ml) were added to the mixture. Zn (190 mg, 2.9 mmol) was added to the mixture at 0 $^\circ\text{C}$, and the mixture was stirred for 1 h at room temperature. To the mixture was added 37% aqueous solution of formaldehyde (70 μl), and the mixture was stirred for 1 h. The mixture was diluted with 2N NaOH, and organic materials were extracted with $\text{CHCl}_3/\text{MeOH} = 10/1$ three times, dried over anhydrous sodium sulfate, and concentrated in vacuo after filtration. Purification by silica gel column chromatography (ethyl acetate/hexane = 1/1 - 1/0 to $\text{CHCl}_3/\text{MeOH} = 10/1$) gave 17 mg (46%, 4 steps) of product as yellow oil.

^1H NMR (400 MHz, CDCl_3) δ 7.34-7.22 (m, 5H), 7.08 (d, $J = 2.4$ Hz, 1H), 6.65 (dd, $J = 8.4, 2.4$ Hz, 1H), 6.57 (d, $J = 8.4$ Hz, 1H), 4.88 (s, 2H), 3.77 (s, 3H), 3.09 (dt, $J = 8.3, 3.6$ Hz, 1H), 2.94 (d, $J = 9.4$ Hz, 1H), 2.86 (d, $J = 9.4$ Hz, 1H), 2.75 (q, $J = 8.3$ Hz, 1H), 2.47 (s, 3H), 2.46-2.38 (m, 1H), 2.18-2.08 (m, 1H); ^{13}C NMR (100 MHz, CDCl_3) δ 180.1, 156.3, 137.2, 136.0, 135.3, 128.7, 127.5, 127.2, 112.0, 110.3, 109.1, 66.3, 56.7, 55.8, 53.7, 43.8, 41.8, 38.2; IR (neat) ν 2938, 2785, 1707, 1601, 1494, 1454, 1434, 1345, 1301, 1175, 1030, 805, 697 cm^{-1} ; HRMS(ESI) $[\text{M}+\text{H}]^+$ calculated for $\text{C}_{20}\text{H}_{23}\text{N}_2\text{O}_2$: 323.1760, found: 323.1760; $[\alpha]_{\text{D}}^{26} -0.99$ (c 0.70, CHCl_3).

(-)-Coerulescine



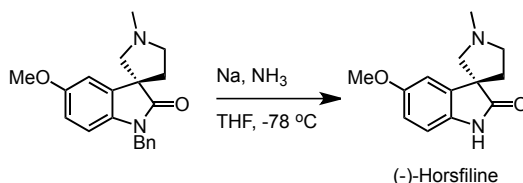
To a THF solution (1 ml) of (*R*)-1-benzyl-1'-methylspiro[indoline-3,3'-pyrrolidin]-2-one (25 mg, 0.086 mmol) was added liquid NH₃ (approximately 3 ml) at -78 °C. To the mixture was added sodium (approximately 50 mg), the color of the reaction mixture became dark blue. The mixture was stirred for 15 min after the reaction mixture became colorless. The reaction was quenched by the addition of solid ammonium chloride, and the mixture was stirred for 1 h to remove ammonia from the flask. Water was added to the mixture, and the mixture was saturated with potassium carbonate. Organic materials were extracted with CHCl₃/MeOH = 10/1 three times, dried over anhydrous magnesium sulfate, and concentrated in vacuo after filtration. Purification by silica gel column chromatography (ethyl acetate to CHCl₃/MeOH = 10/1) gave 13 mg (77%) of (-)-Coerulescine as colorless oil.

¹H NMR (400 MHz, CDCl₃) δ 8.83 (bs, 1H), 7.40 (d, *J* = 7.6 Hz, 1H), 7.19 (dt, *J* = 7.6, 1.2 Hz, 1H), 7.04 (t, *J* = 7.6 Hz), 6.86 (d, *J* = 7.6 Hz), 3.06-2.97 (m, 1H), 2.92-2.78 (m, 3H), 2.46 (s, 3H), 2.45-2.38 (m, 1H), 2.17-2.05 (m, 1H); ¹³C NMR (100 MHz, CDCl₃) δ 183.1, 140.1, 136.2, 127.7, 123.2, 122.8, 109.5, 66.4, 56.8, 53.7, 41.8, 37.9; IR (neat) ν 3208, 2943, 2789, 1709, 1618, 1600, 1471, 1336, 1196, 1152, 753, 676, 611 cm⁻¹; HRMS(ESI) [M+H]⁺ calculated for C₁₂H₁₅N₂O: 203.1184, found: 203.1184; [α]_D²⁸ -1.1 (*c* 1.2, MeOH).

Enantiomeric excess = 94%

The enantiomeric excess was determined by HPLC using a Chiralpak AS-H (10/1 = hexane/*i*PrOH; flow rate 1 ml/min, *t*_{R1} = 23.53 (major), *t*_{R2} = 53.18 (minor) min).

(-)-Horsfiline



To a THF solution (1 ml) of (*R*)-1-benzyl-5-methoxy-1'-methylspiro[indoline-3,3'-pyrrolidin]-2-one (17 mg, 0.053 mmol) was added liquid NH₃ (approximately 3 ml) at -78 °C. To the mixture was added sodium (approximately 50 mg), the color of the reaction mixture became dark blue. The mixture was stirred for 15 min after the reaction mixture became colorless. The reaction was quenched by the addition of solid ammonium chloride, and the mixture was stirred for 1 h to remove

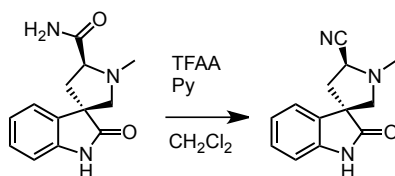
ammonia from the flask. Water was added to the mixture, and the mixture was saturated with potassium carbonate. Organic materials were extracted with $\text{CHCl}_3/\text{MeOH} = 10/1$ three times, dried over anhydrous magnesium sulfate, and concentrated in vacuo after filtration. Purification by silica gel column chromatography ($\text{CHCl}_3/\text{MeOH} = 10/1$) gave 10 mg (80%) of (–)-Horsfileline as colorless oil.

^1H NMR (400 MHz, CDCl_3) δ 7.95 (bs, 1H), 7.03 (d, $J = 2.4$ Hz, 1H), 6.77 (d, $J = 8.4$ Hz, 1H), 6.72 (dd, $J = 8.4, 2.4$ Hz, 1H), 3.79 (s, 3H), 3.06–2.98 (m, 1H), 2.88 (d, $J = 8.0$ Hz, 1H), 2.85 (d, $J = 8.0$, 1H), 2.75 (q, $J = 8.1$ Hz, 1H), 2.45 (s, 3H), 2.43–2.38 (m, 1H), 2.09 (dt, $J = 12.8, 7.6$ Hz, 1H); ^{13}C NMR (100 MHz, CDCl_3) δ 182.8, 156.2, 137.6, 133.4, 112.4, 110.3, 109.8, 66.3, 56.7, 55.9, 54.1, 41.8, 38.1; IR (neat) ν 3211, 2941, 2835, 2790, 1712, 1603, 1493, 1487, 1439, 1304, 1206, 1032, 810, 622 cm^{-1} ; HRMS(ESI) $[\text{M}+\text{H}]^+$ calculated for $\text{C}_{13}\text{H}_{17}\text{N}_2\text{O}_2$: 233.1290, found: 233.1290; $[\alpha]_D^{25} -7.0$ (c 0.30, MeOH).

Enantiomeric excess = 95%

The enantiomeric excess was determined by HPLC using a Chiralpak OB-H (10/1 = hexane/*i*PrOH; flow rate 1 ml/min, $t_{\text{R}1} = 6.97$ (major), $t_{\text{R}2} = 12.11$ (minor) min).

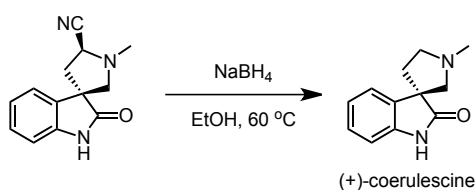
(3*S*,5'*S*)-1'-methyl-2-oxospiro[indoline-3,3'-pyrrolidine]-5'-carbonitrile



Amide was prepared following the reported procedure [S2]. To a CH_2Cl_2 solution (2 ml) of amide (100 mg, 0.408 mmol) was added pyridine (0.12 ml, 1.43 mmol) and TFAA (86 μl , 0.611 mmol) at room temperature. After stirring the reaction mixture for 4 h, the reaction was quenched with saturated aqueous sodium bicarbonate. Organic materials were extracted with $\text{CHCl}_3:\text{MeOH} = 10:1$ three times, and combined extracts were washed with saturated aqueous ammonium chloride, dried over anhydrous magnesium sulfate, and concentrated in vacuo after filtration. Purification by silica gel column chromatography (ethyl acetate/hexane = 1/2 to 1/1) gave 47 mg (51%) of nitrile as a colorless oil. ^1H NMR was consistent with the reported data [S2].

$[\alpha]_D^{19} -29.5$ (c 1.5, MeOH).

(+)-Coerulescine



To a EtOH solution (2 ml) of nitrile (45 mg, 0.198 mmol) was added NaBH₄ (37 mg, 0.99 mmol) at room temperature, and the reaction mixture was stirred for 3 h at 60 °C. The reaction was quenched with saturated aqueous potassium carbonate. Organic materials were extracted with CHCl₃:MeOH = 10:1 three times, dried over anhydrous magnesium sulfate, and concentrated in vacuo after filtration. Purification by silica gel column chromatography (ethyl acetate to CHCl₃:MeOH = 10:1) gave 24 mg (60%) of (+)-coerulescine as a colorless oil.

The spectra data (¹H NMR, ¹³C NMR, IR and HRMS) were consistent with (–)-coerulescine and those reported [S2].

[α]_D²⁷ +1.0 (*c* 2.4, MeOH).

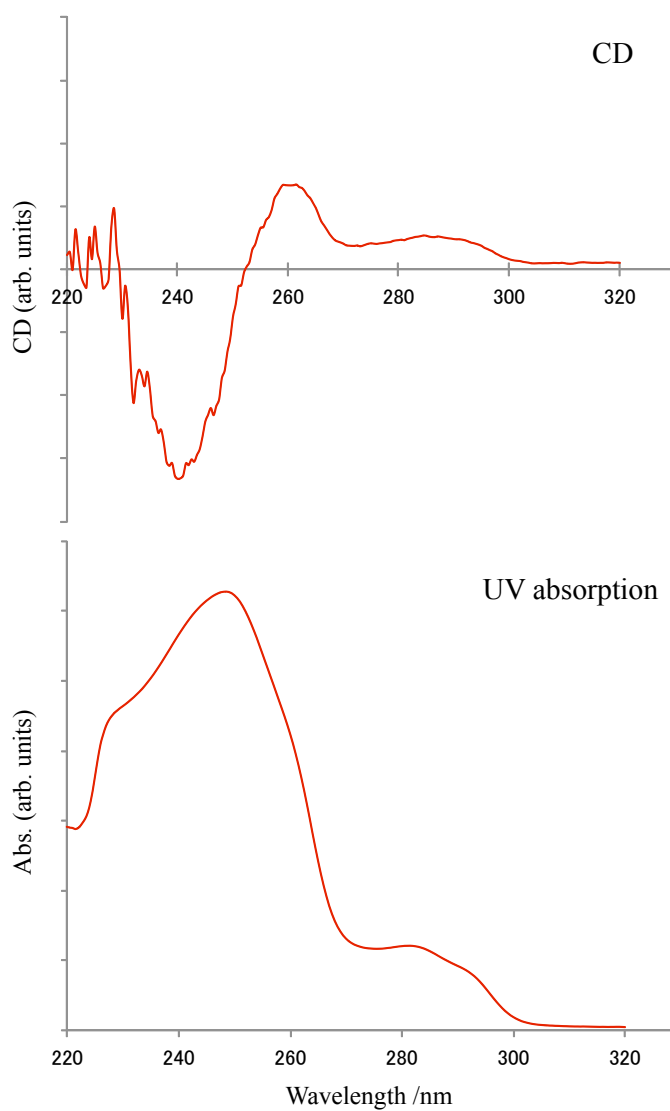
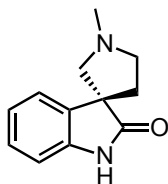
Enantiomeric excess = 99%

The enantiomeric excess was determined by HPLC using a Chiralpak AS-H (10/1 = hexane/*i*PrOH; flow rate 1 ml/min, *t*_{R1} = 25.44 (minor), *t*_{R2} = 40 to 58 (major, broad peak) min).

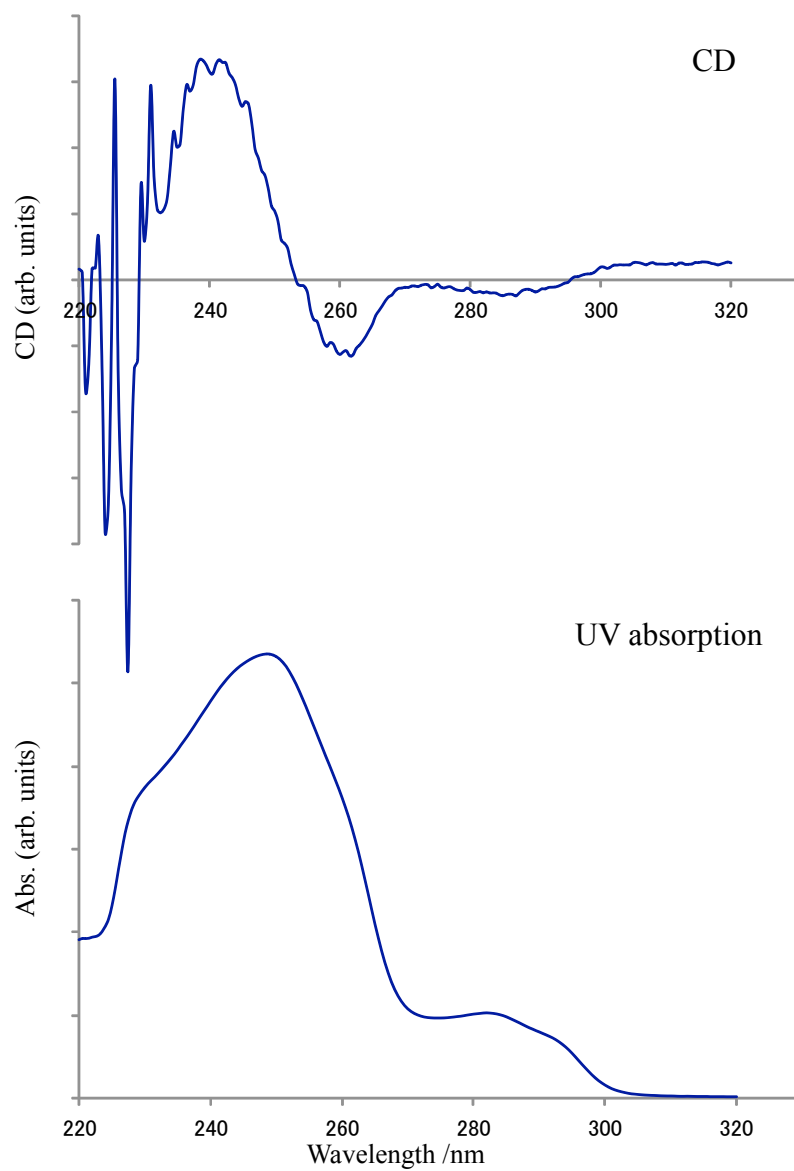
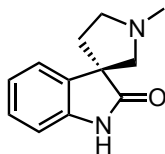
Magnetic circular dichroism (MCD) spectra

Electronic absorption spectra were recorded on a JASCO V-570 spectrophotometer. Circular dichroism (CD) spectra were recorded on a JASCO J-725 spectrodichrometer. CH₂Cl₂ was used as a solvent.

(-)-Coerulescine via our route



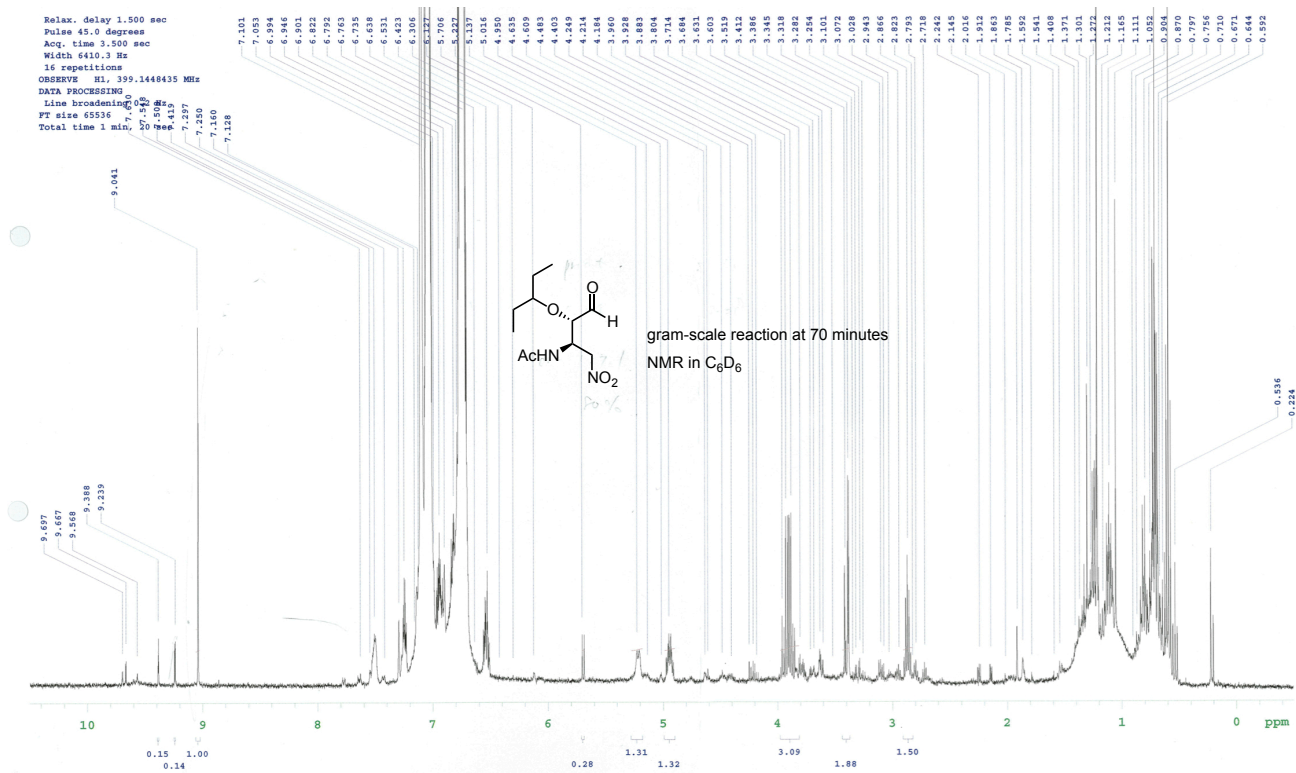
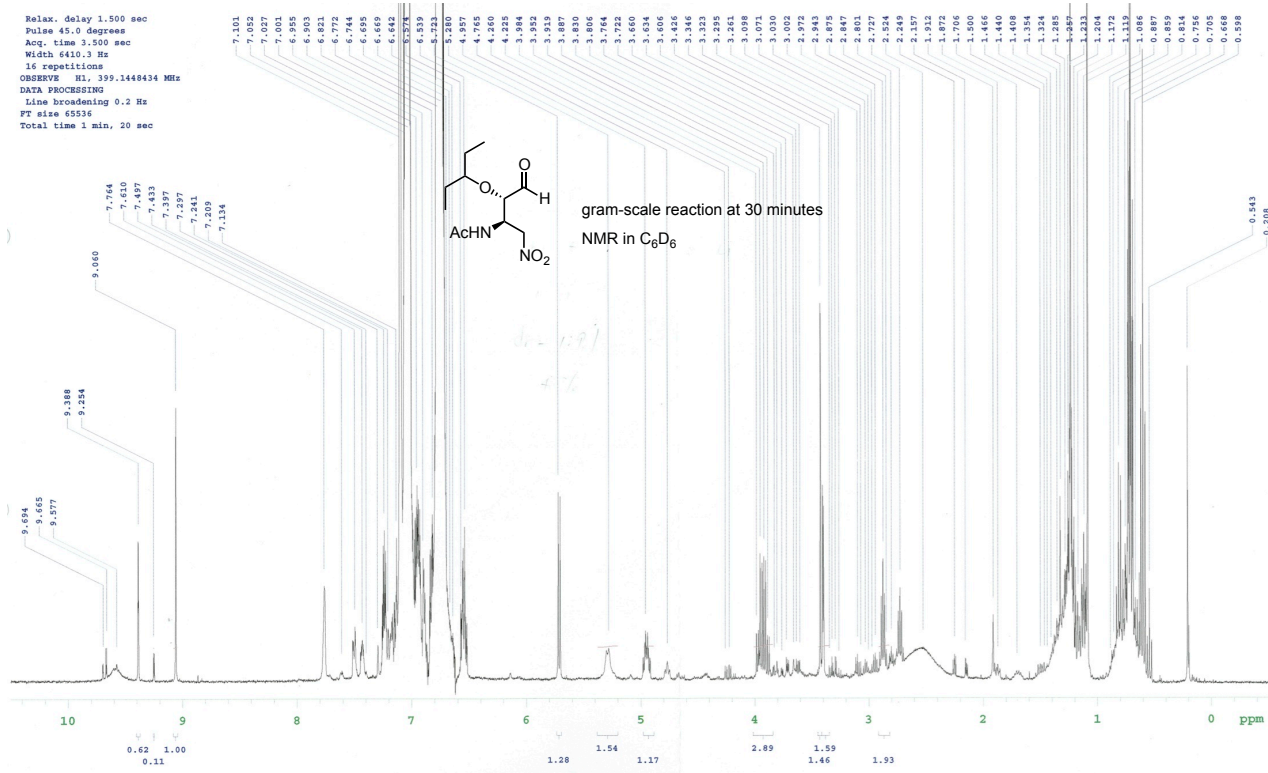
(+)-Coerulescine via Danishefsky's route

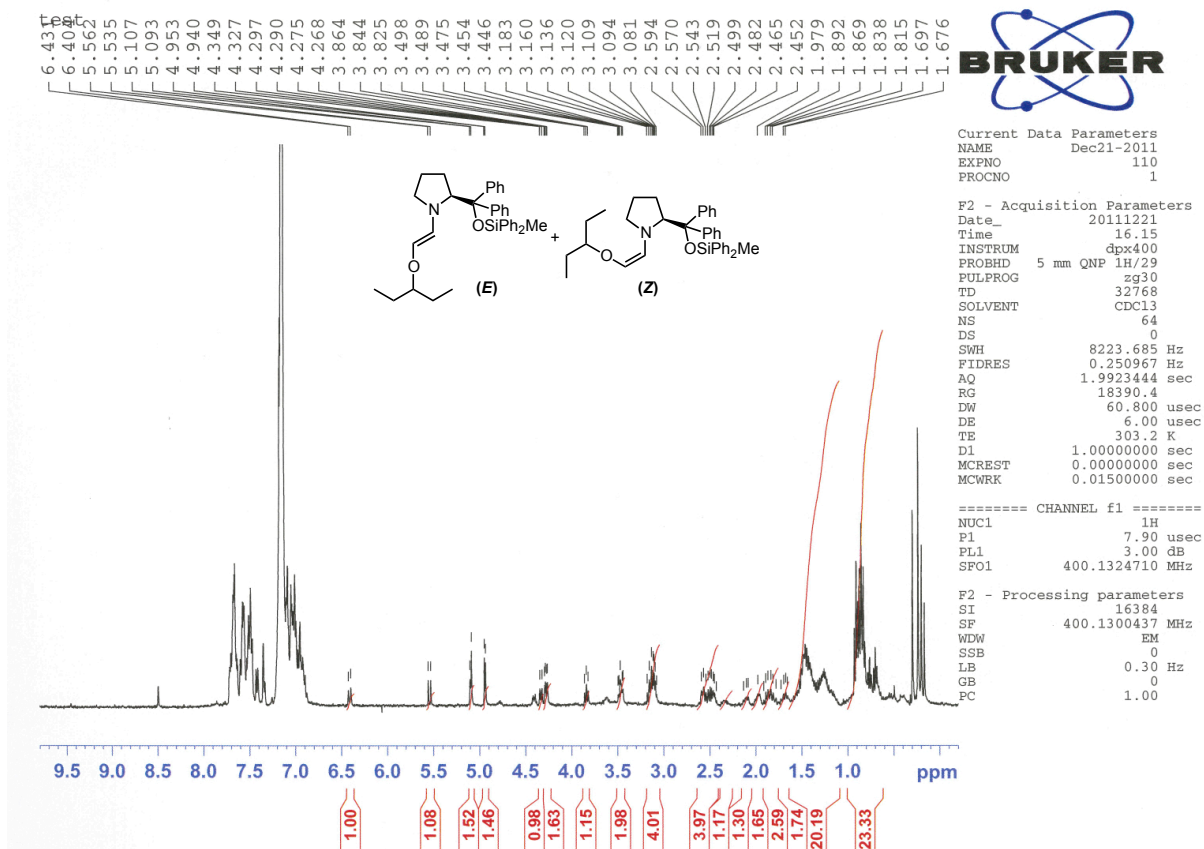
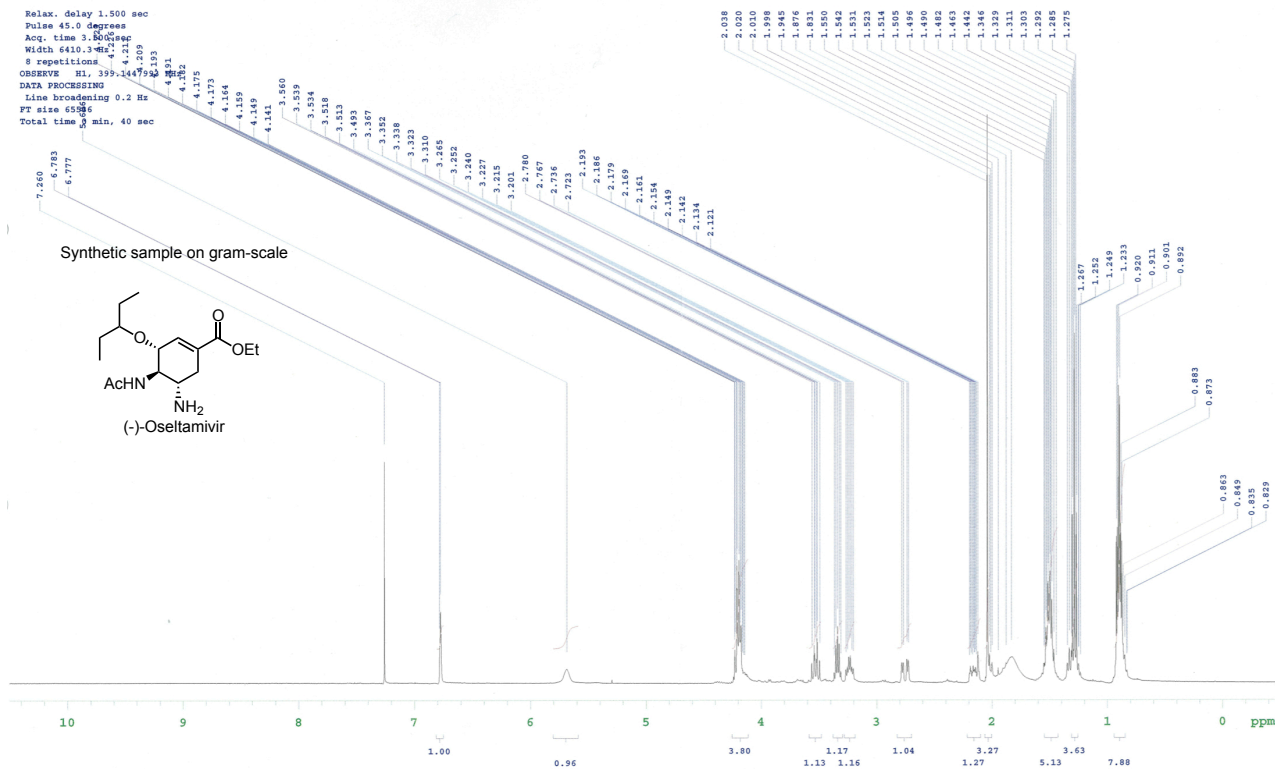


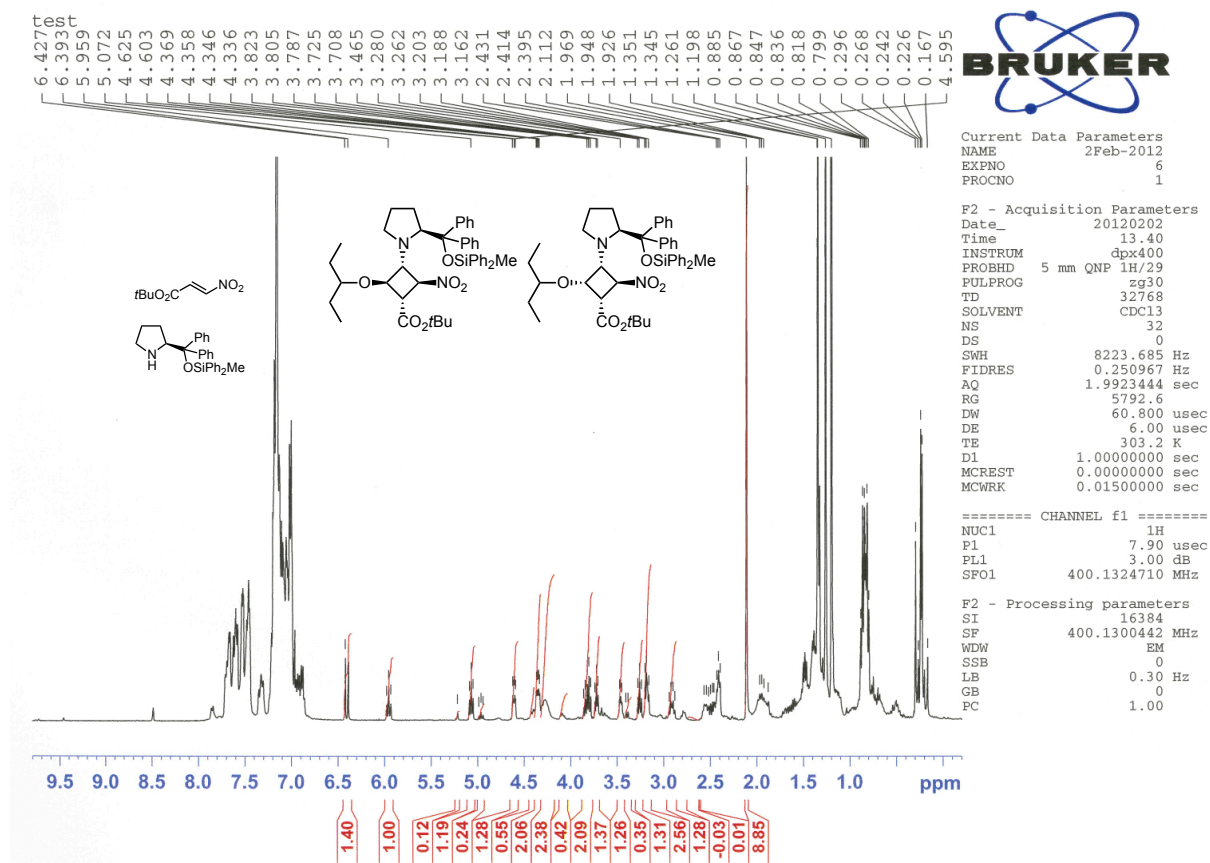
References

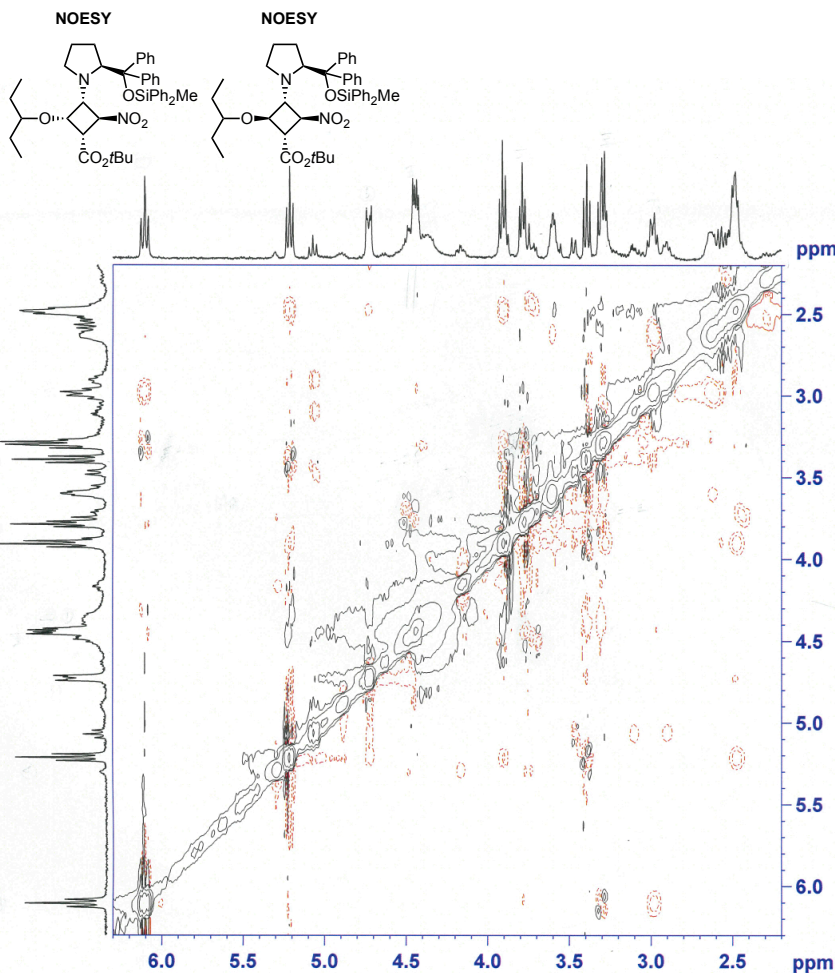
- [S1] G. Lakshmaiah, T. Kawabata, M. Shang, K. Fuji, *J. Org. Chem.* **1999**, *64*, 1699.
[S2] C. Li, C. Chan, A. C. Heimann, S. J. Danishefsky, *Angew. Chem. Int. Ed.* **2007**, *46*, 1444.

Spectra









Current Data Parameters
 NAME Feb03-2012-hayashi
 EXPNO 51
 PROCNO 1

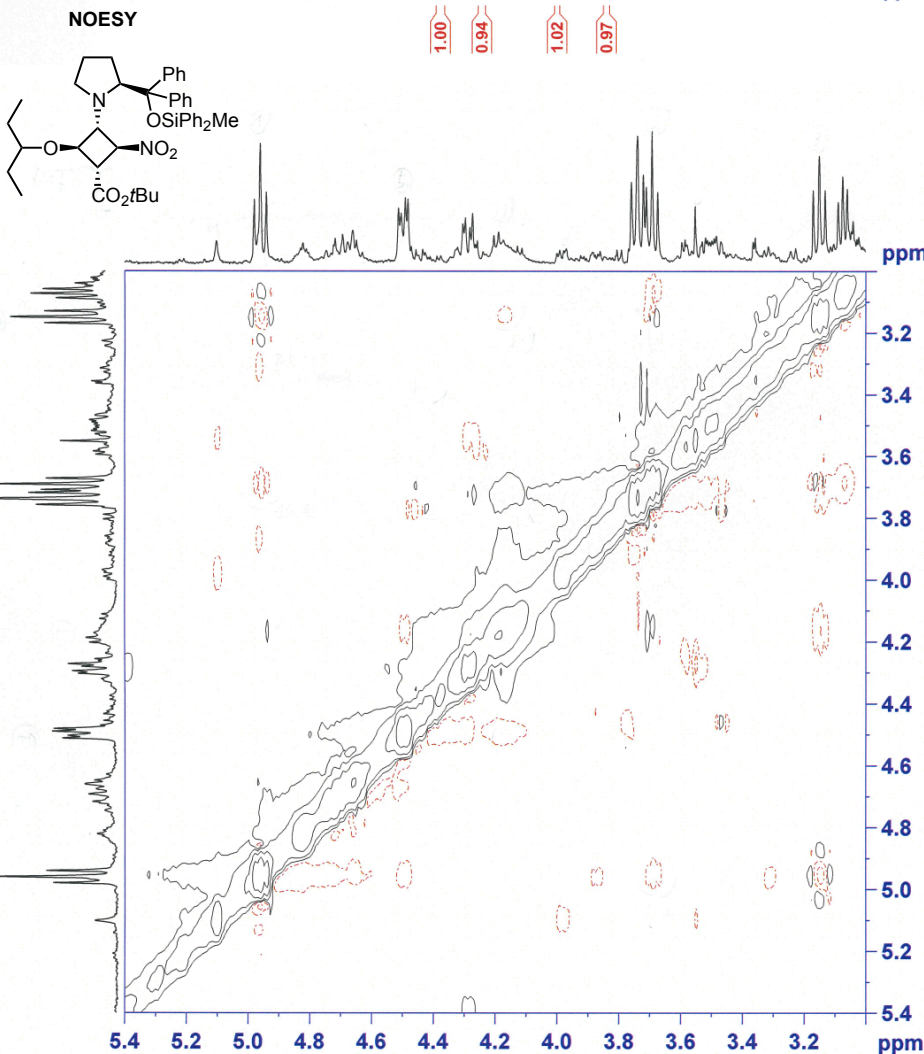
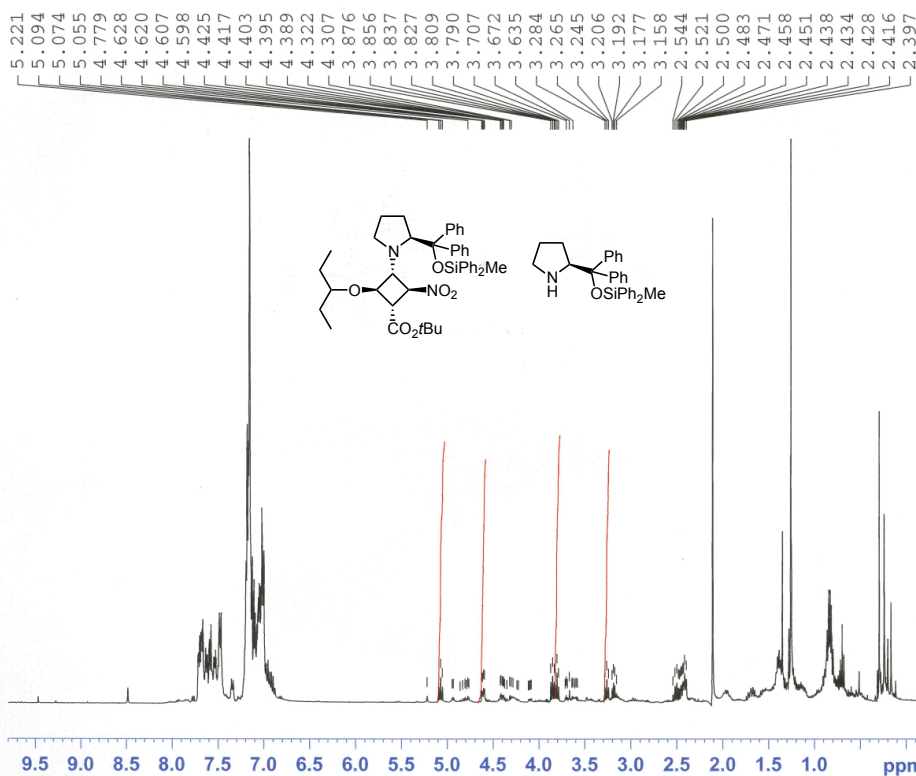
F2 - Acquisition Parameters
 Date_ 20120203
 Time 17.31
 INSTRUM spect
 PROBHD 5 mm PABBO BB-
 PULPROG noesyph
 TD 2048
 SOLVENT C6D6
 NS 16
 DS 4
 SWH 3787.879 Hz
 FIDRES 1.849550 Hz
 AQ 0.2703860 sec
 RG 114
 DW 132.000 usec
 DE 6.00 usec
 TE 280.5 K
 d0 0.00011545 sec
 D1 1.98033905 sec
 D8 0.30000001 sec
 INO 0.00026400 sec
 STICNT 128

===== CHANNEL f1 =====
 NUC1 1H
 P1 13.00 usec
 PL1 -3.40 dB
 SFO1 400.1815635 MHz

F1 - Acquisition parameters
 ND0 1
 TD 256
 SFO1 400.1816 MHz
 FIDRES 14.796402 Hz
 SW 9.465 ppm
 FMODE States-TPPI

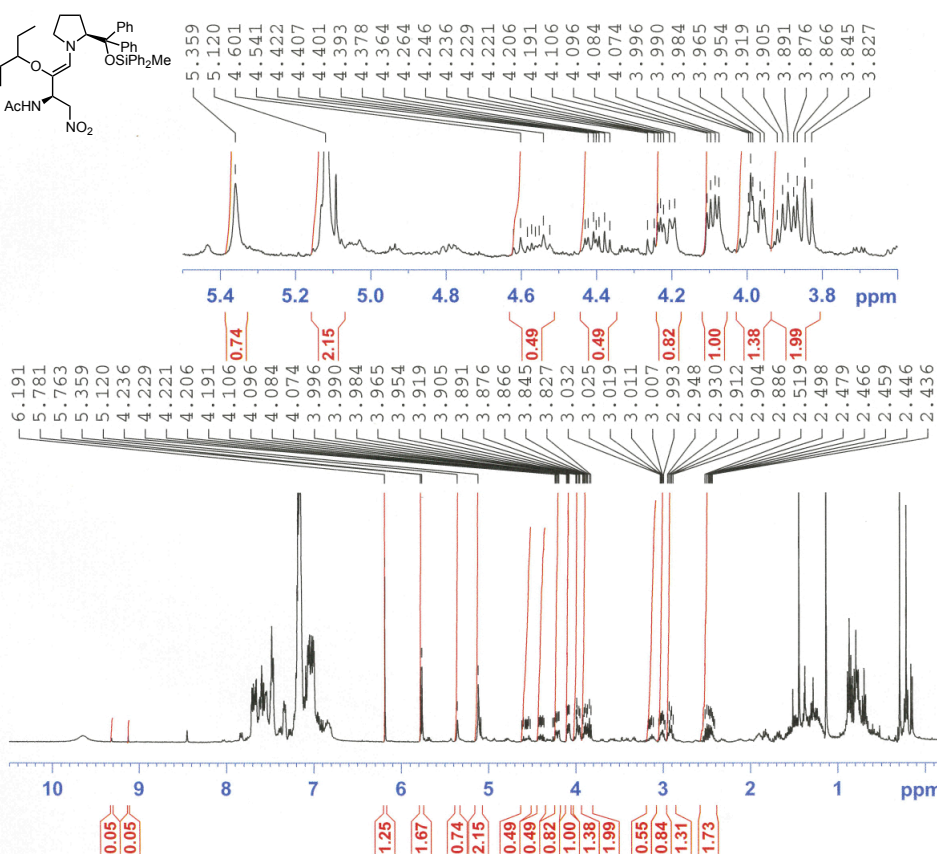
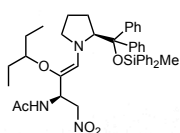
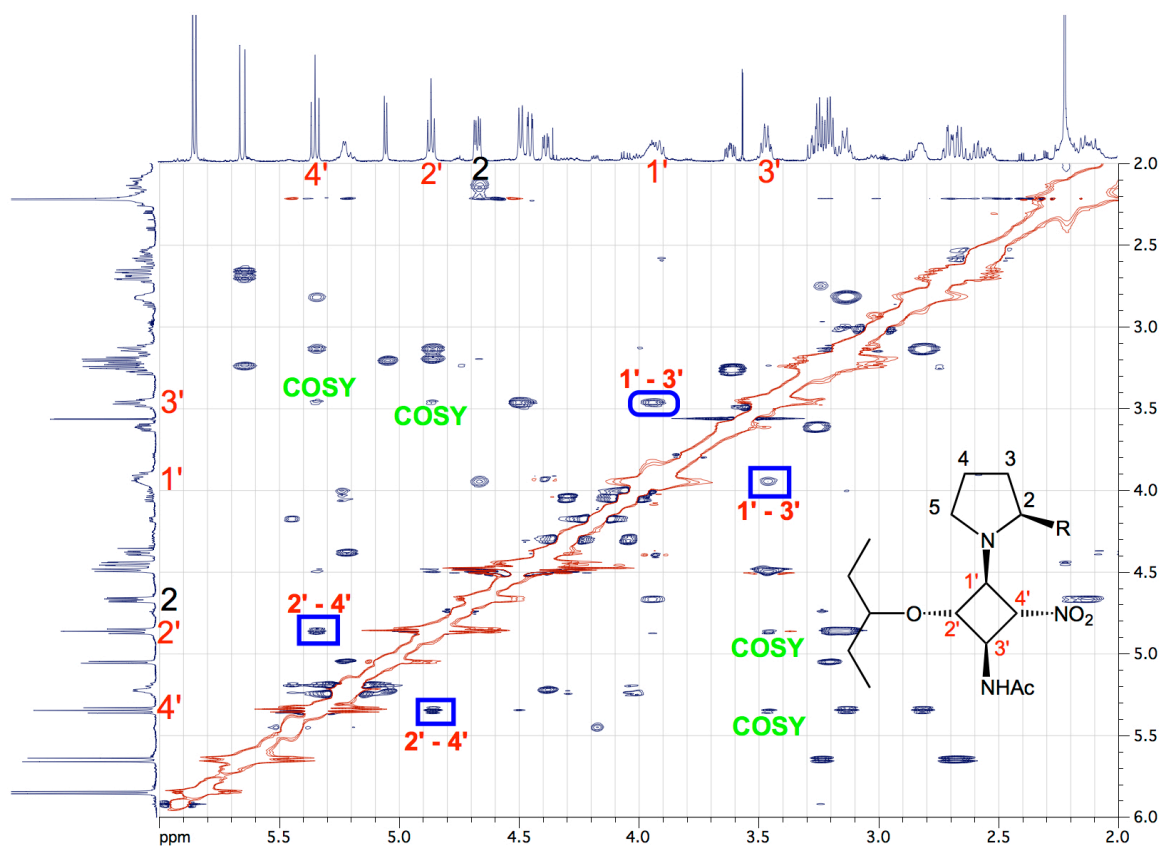
F2 - Processing parameters
 SI 1024
 SF 400.1800000 MHz
 WDW QSINE
 SSB 2
 LB 0.00 Hz
 GB 0
 PC 1.00

F1 - Processing parameters
 SI 1024
 MC2 States-TPPI
 SF 400.1800000 MHz
 WDW QSINE
 SSB 2
 LB 0.00 Hz
 GB 0





NOESY

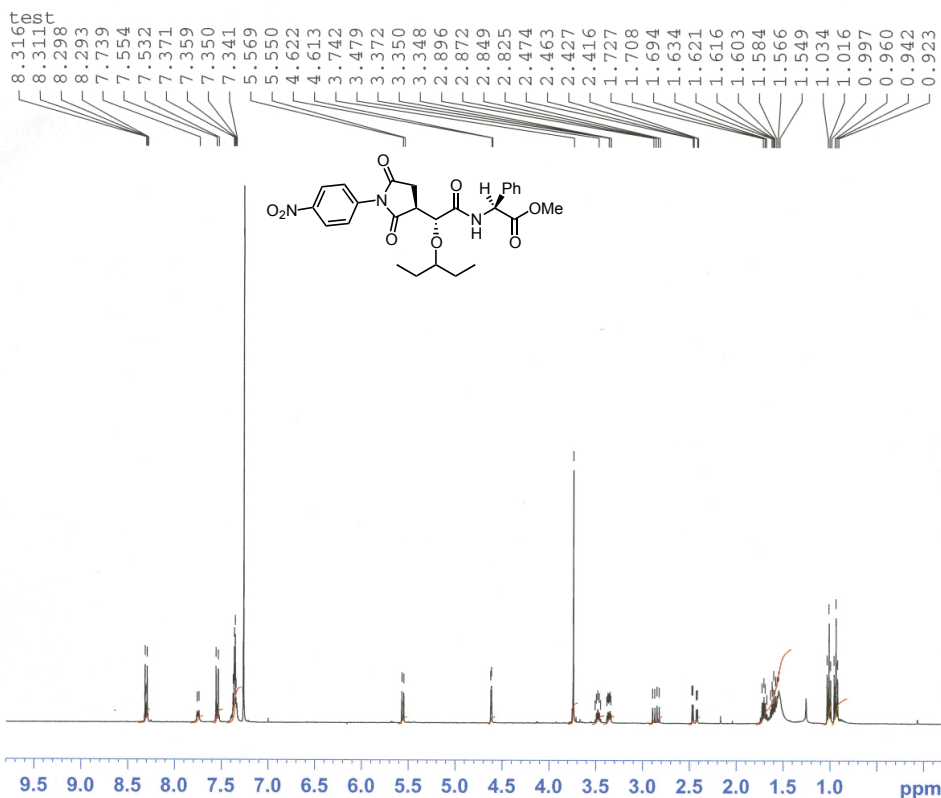


Current Data Parameters
NAME Jan12-2012-hayashi
EXPNO 270
PROCNO 1

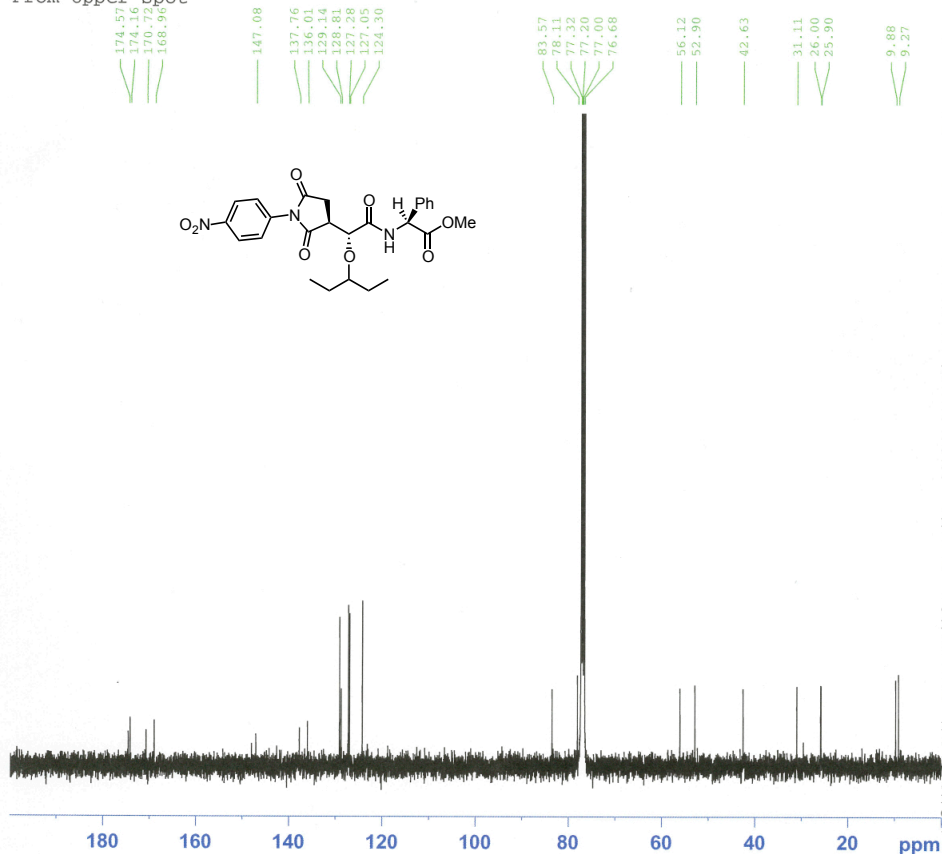
F2 - Acquisition Parameters
Date_ 20120112
Time 21.27
INSTRUM spect
PROBHD 5 mm PABBO BB-
PULPROG zg30
TD 65536
SOLVENT C6D6
NS 16
DS 2
SWH 8223.685 Hz
FIDRES 0.125483 Hz
AQ 3.9846387 sec
RG 287
DW 60.800 usec
DE 303.4 K
TE 1.00000000 sec
D1 1
TD0 1

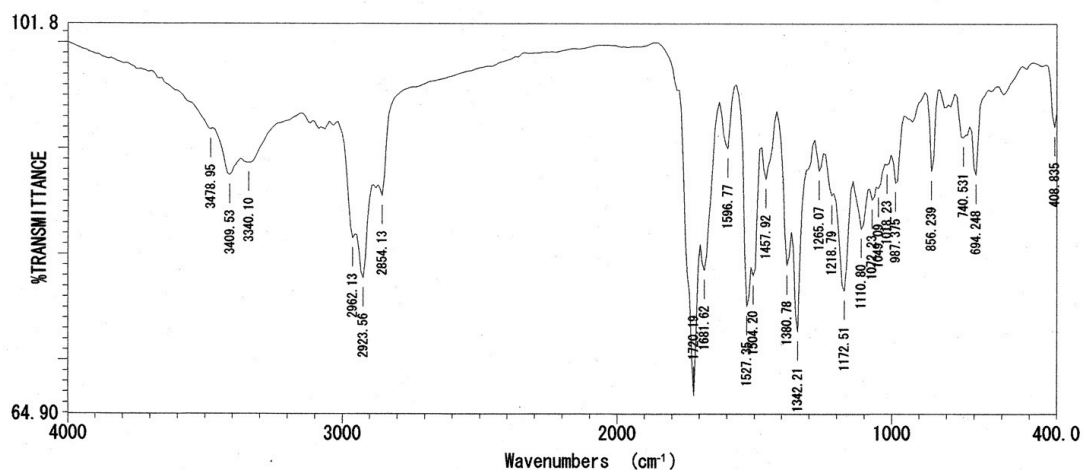
===== CHANNEL f1 =====
NUC1 1H
P1 13.00 usec
PL1 -3.40 dB
SFO1 400.1824713 MHz

F2 - Processing parameters
SI 32768
SF 400.1800427 MHz
WDW EM
SSB 0
LB 0.30 Hz
GB 0
PC 1.00

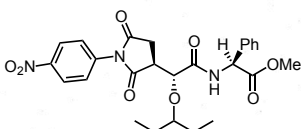


From Upper spot



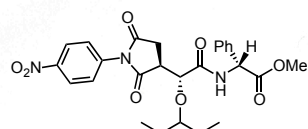
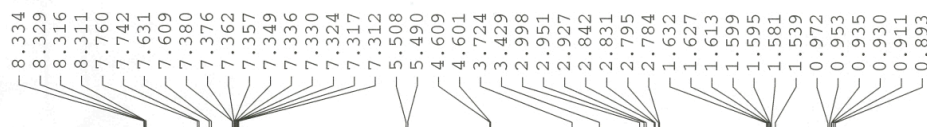


ファイル名 :
 タイトル :
 測定日時 : 2011年12月12日 19時41分08秒
 測定分解能 : 16 cm⁻¹
 スキャン回数 : 32 回
 測定ゲイン :
 コメント :



ピーク番号	波数 (cm⁻¹)	透過率 (%)	ピーク番号	波数 (cm⁻¹)	透過率 (%)
01	3478.95	91.7889	18	1110.80	82.4262
02	3409.53	87.4748	19	1072.23	85.1752
03	3340.10	88.6433	20	1049.09	86.2508
04	2962.13	81.5239	21	1018.23	88.4621
05	2923.56	77.7384	22	987.375	86.7574
06	2854.13	85.5284	23	987.373	87.8861
07	1720.19	66.6690	24	740.531	91.0551
08	1681.62	78.4884	25	694.248	87.5371
09	1596.77	89.9869	26	408.835	92.0595
10	1527.35	75.0664			
11	1504.20	78.0097			
12	1457.92	87.1023			
13	1380.78	78.9703			
14	1342.21	72.6828			
15	1265.07	87.9081			
16	1218.79	85.6081			
17	1172.51	76.5586			

test

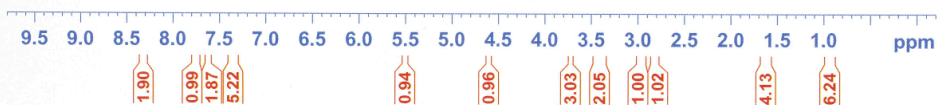


Current Data Parameters
 NAME Dec13-2011
 EXPNO 70
 PROCNO 1

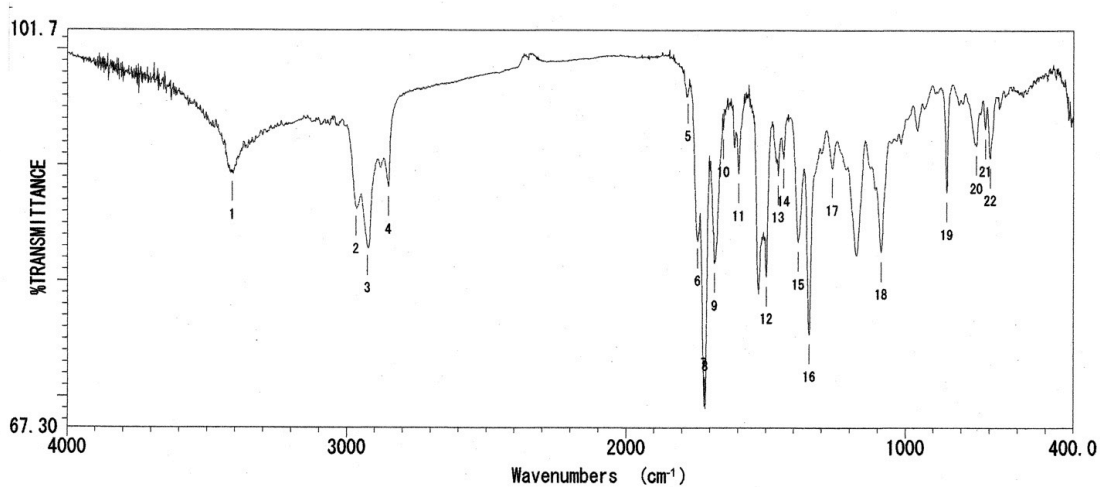
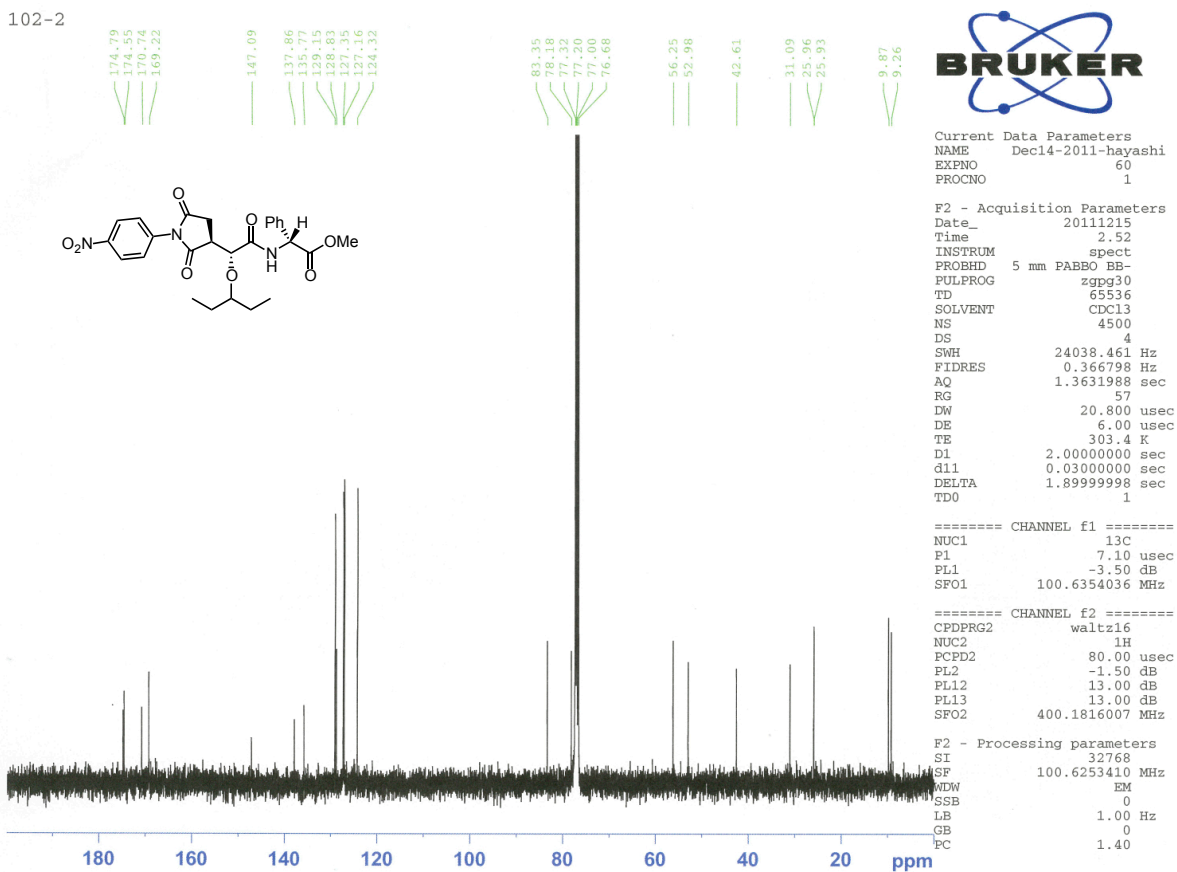
F2 - Acquisition Parameters
 Date_ 20111213
 Time 20.36
 INSTRUM dpx400
 PROBHD 5 mm QNP 1H/29
 PULPROG zg30
 TD 32768
 SOLVENT CDCl3
 NS 32
 DS 0
 SWH 8223.685 Hz
 FIDRES 0.250967 Hz
 AQ 1.9923444 sec
 RG 20642.5
 DW 60.800 usec
 DE 6.00 usec
 TE 303.2 K
 D1 1.00000000 sec
 MCREST 0.00000000 sec
 MCWRK 0.01500000 sec

===== CHANNEL f1 =====
 NUC1 1H
 P1 7.90 usec
 PL1 3.00 dB
 SFO1 400.1324710 MHz

F2 - Processing parameters
 SI 16384
 SF 400.1300087 MHz
 WDW EM
 SSB 0
 LB 0.30 Hz
 GB 0
 PC 1.00

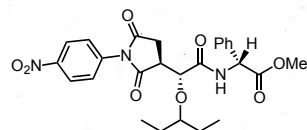


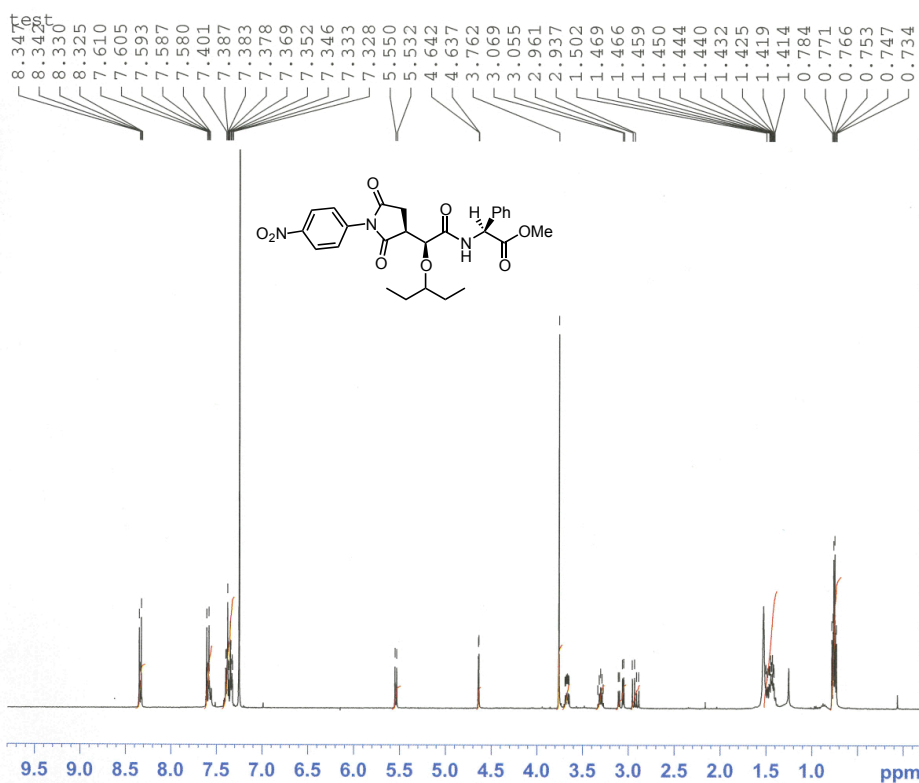
102-2



ファイル名 :
タイトル :
測定日時 : 2012年02月08日 15時28分56秒
測定分解能 : 2 cm⁻¹
スキャン回数 : 16 回
測定ゲイン :
コメント :

ピーク番号	波数 (cm ⁻¹)	透過率 (%)	ピーク番号	波数 (cm ⁻¹)	透過率 (%)
01	3409.53	89.3719	18	1087.66	82.5219
02	2965.98	86.4008	19	853.347	87.6453
03	2924.52	83.0184	20	747.281	91.6843
04	2849.31	88.0928	21	715.461	93.1670
05	1778.05	96.1772	22	698.105	90.6367
06	1743.33	83.6589			
07	1720.19	69.2243			
08	1717.30	68.9800			
09	1682.59	81.5059			
10	1651.73	93.0883			
11	1596.77	89.2648			
12	1497.45	80.3911			
13	1455.99	89.1798			
14	1435.74	90.5628			
15	1363.67	83.3434			
16	1344.14	75.3776			
17	1262.18	89.7624			





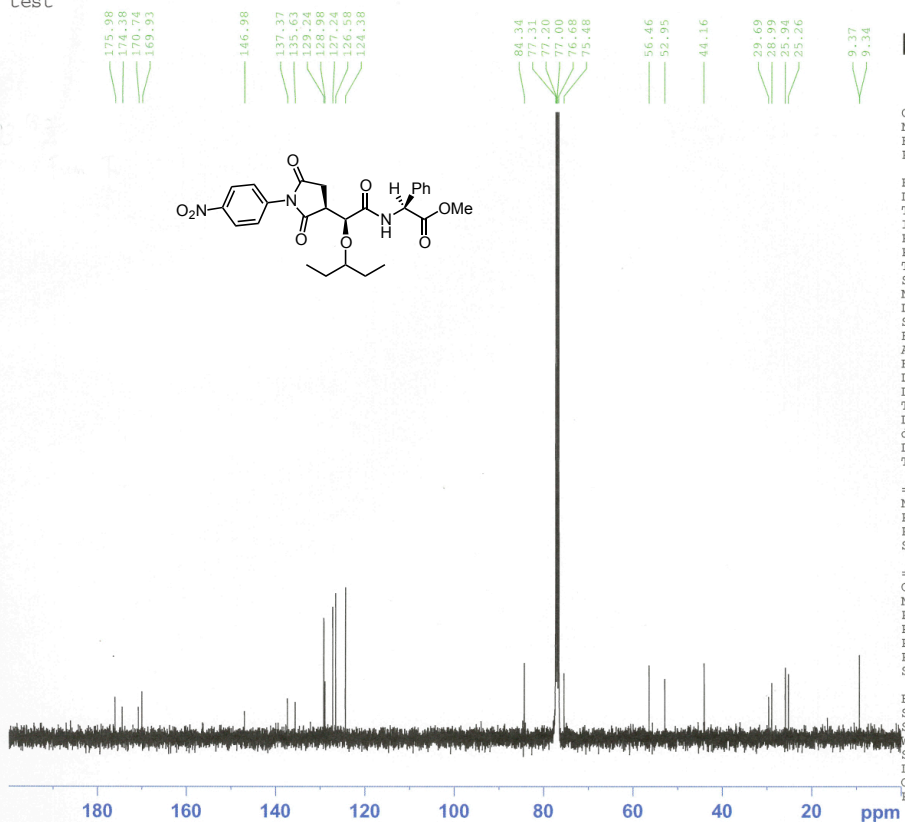
Current Data Parameters
NAME Dec07-2011
EXPNO 24
PROCNO 1

F2 - Acquisition Parameters
Date_ 20111207
Time 13.26
INSTRUM dpx400
PROBHD 5 mm QNP 1H/29
PULPROG zg30
TD 32768
SOLVENT CDCl3
NS 32
DS 0
SWH 8223.685 Hz
FIDRES 0.250967 Hz
AQ 1.9923444 sec
RG 18390.4
DW 60.800 usec
DE 6.00 usec
TE 303.2 K
D1 1.00000000 sec
MCREST 0.00000000 sec
MCWRK 0.01500000 sec

===== CHANNEL f1 =====
NUC1 1H
P1 7.90 usec
PL1 3.00 dB
SFO1 400.1324710 MHz

F2 - Processing parameters
SI 16384
SF 400.1300104 MHz
WDW EM
SSB 0
LB 0.30 Hz
GB 0
PC 1.00

test



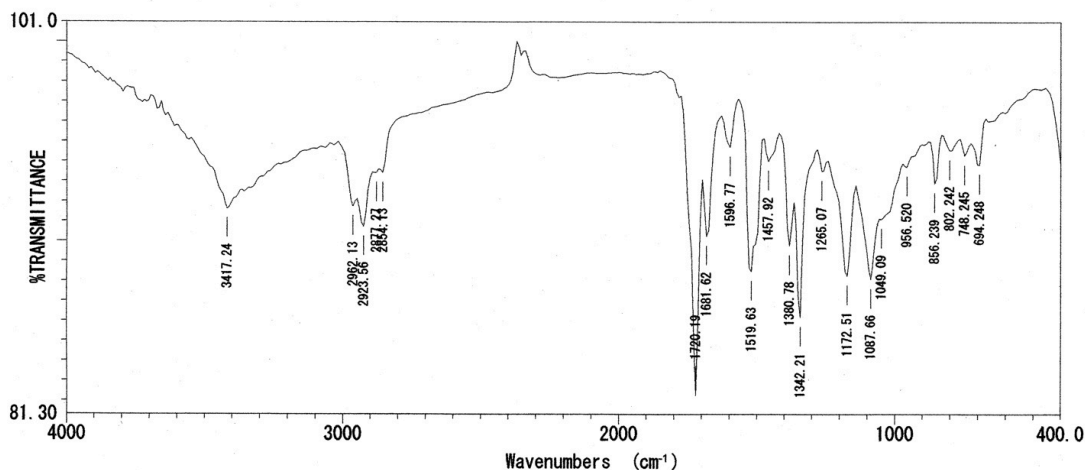
Current Data Parameters
NAME Dec10-2011-hayashi
EXPNO 100
PROCNO 1

F2 - Acquisition Parameters
Date_ 20111211
Time 1.20
INSTRUM spect
PROBHD 5 mm PABBO BB-
PULPROG zgpg30
TD 65536
SOLVENT CDCl3
NS 5000
DS 4
SWH 24038.461 Hz
FIDRES 0.366798 Hz
AQ 1.3631988 sec
RG 57
DW 20.800 usec
DE 6.00 usec
TE 303.4 K
D1 2.00000000 sec
d11 0.03000000 sec
DELTA 1.89999998 sec
TD0 1

===== CHANNEL f1 =====
NUC1 13C
P1 7.10 usec
PL1 -3.50 dB
SFO1 100.6354036 MHz

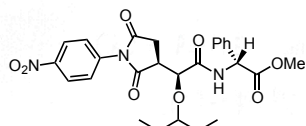
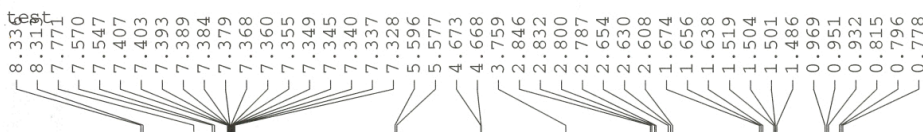
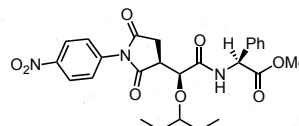
===== CHANNEL f2 =====
CPDPRG2 waltz16
NUC2 1H
PCPD2 80.00 usec
PL2 -1.50 dB
PL12 13.00 dB
PL13 13.00 dB
SFO2 400.1816007 MHz

F2 - Processing parameters
SI 32768
SF 100.6253421 MHz
WDW EM
SSB 0
LB 1.00 Hz
GB 0
PC 1.40



ファイル名 :
 タイトル :
 測定日時 : 2011年12月12日 19時50分15秒
 測定分解能 : 16 cm⁻¹
 スキャン回数 : 32 回
 測定ゲイン : 1
 コメント :

ピーク番号	波数 (cm⁻¹)	透過率 (%)	ピーク番号	波数 (cm⁻¹)	透過率 (%)
01	3417.24	91.6345	18	856.239	92.8929
02	2962.13	91.7475	19	802.242	94.5576
03	2923.56	90.7126	20	748.245	94.2991
04	2877.27	93.4228	21	694.248	93.8341
05	2854.13	93.4167			
06	1720.19	82.2694			
07	1681.62	90.2405			
08	1596.77	94.7170			
09	1519.63	88.4703			
10	1457.92	94.0182			
11	1380.78	89.7778			
12	1342.21	86.1706			
13	1285.07	93.5218			
14	1172.51	88.2603			
15	1087.66	88.0833			
16	1049.09	91.0998			
17	956.520	93.7225			

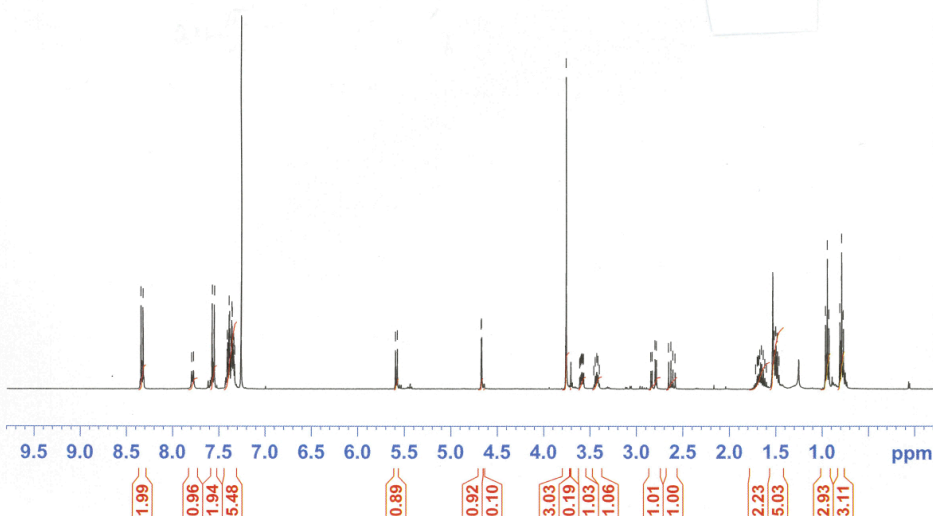


Current Data Parameters
 NAME Dec13-2011
 EXPNO 62
 PROCNO 1

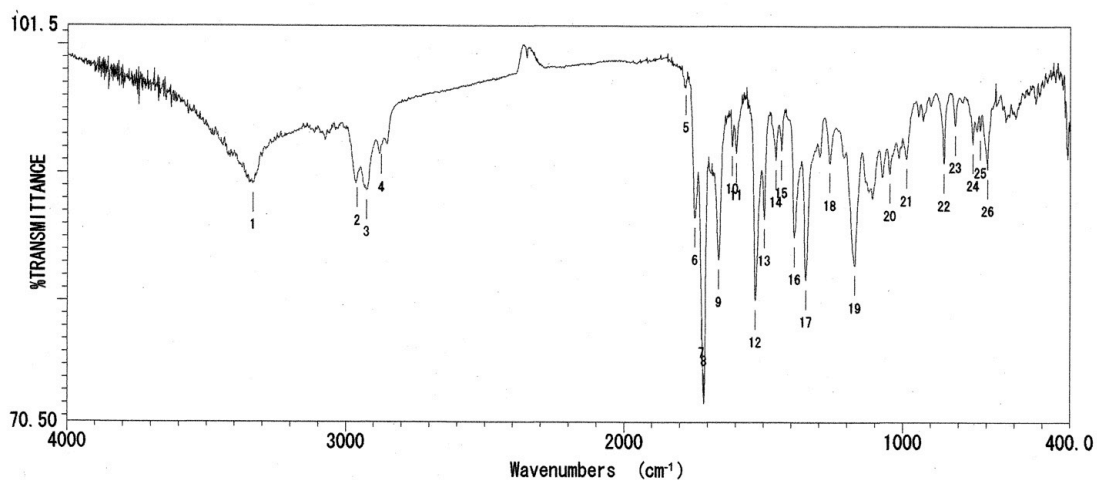
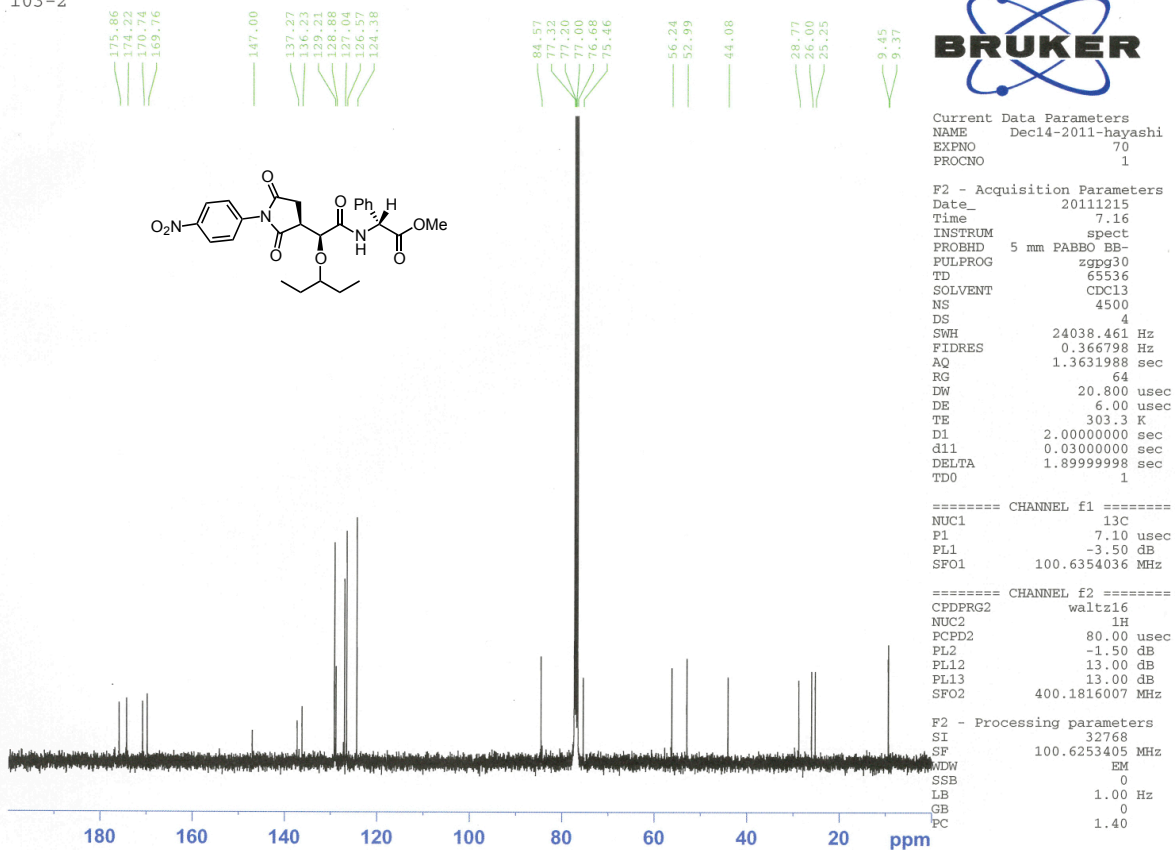
 F2 - Acquisition Parameters
 Date_ 20111213
 Time 22.27
 INSTRUM dpx400
 PROBHD 5 mm QNP 1H/29
 PULPROG zg30
 TD 32768
 SOLVENT CDCl3
 NS 32
 DS 0
 SWH 8223.685 Hz
 FIDRES 0.250967 Hz
 AQ 1.9923444 sec
 RG 23170.5
 DW 60.800 usec
 DE 6.00 usec
 TE 303.2 K
 D1 1.00000000 sec
 MCREST 0.00000000 sec
 MCWRK 0.01500000 sec

 ===== CHANNEL f1 =====
 NUC1 1H
 P1 7.90 usec
 PL1 3.00 dB
 SFO1 400.1324710 MHz

 F2 - Processing parameters
 SI 16384
 SF 400.1300092 MHz
 WDW EM
 SSB 0
 LB 0.30 Hz
 GB 0
 PC 1.00

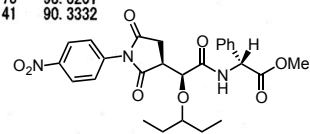


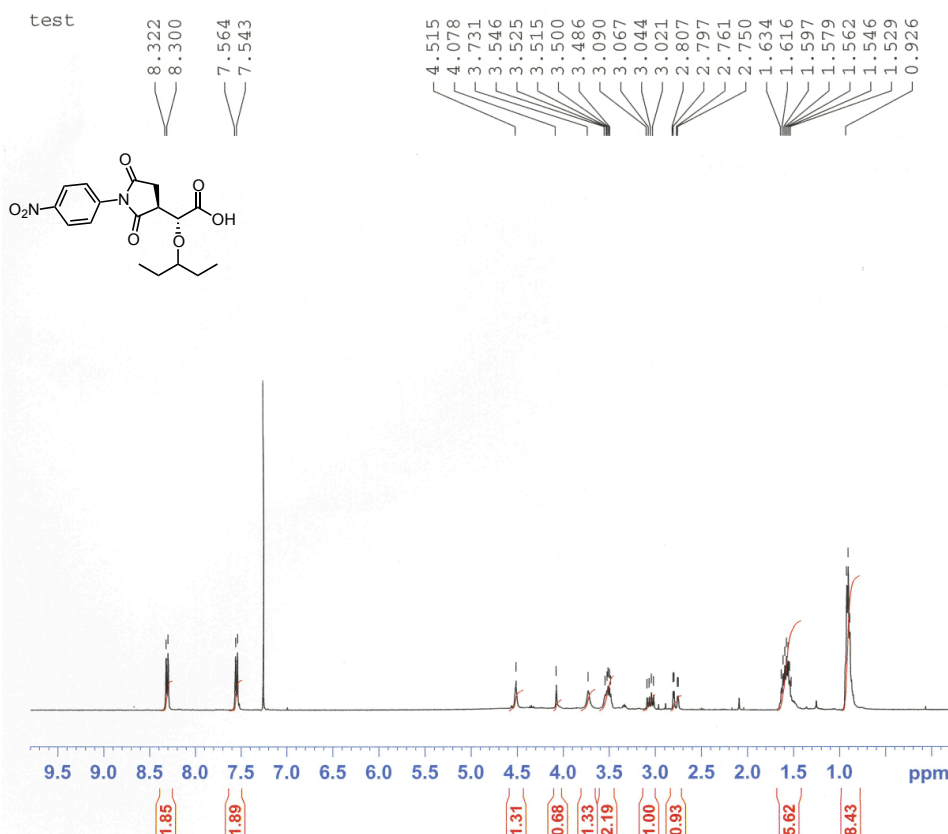
103-2



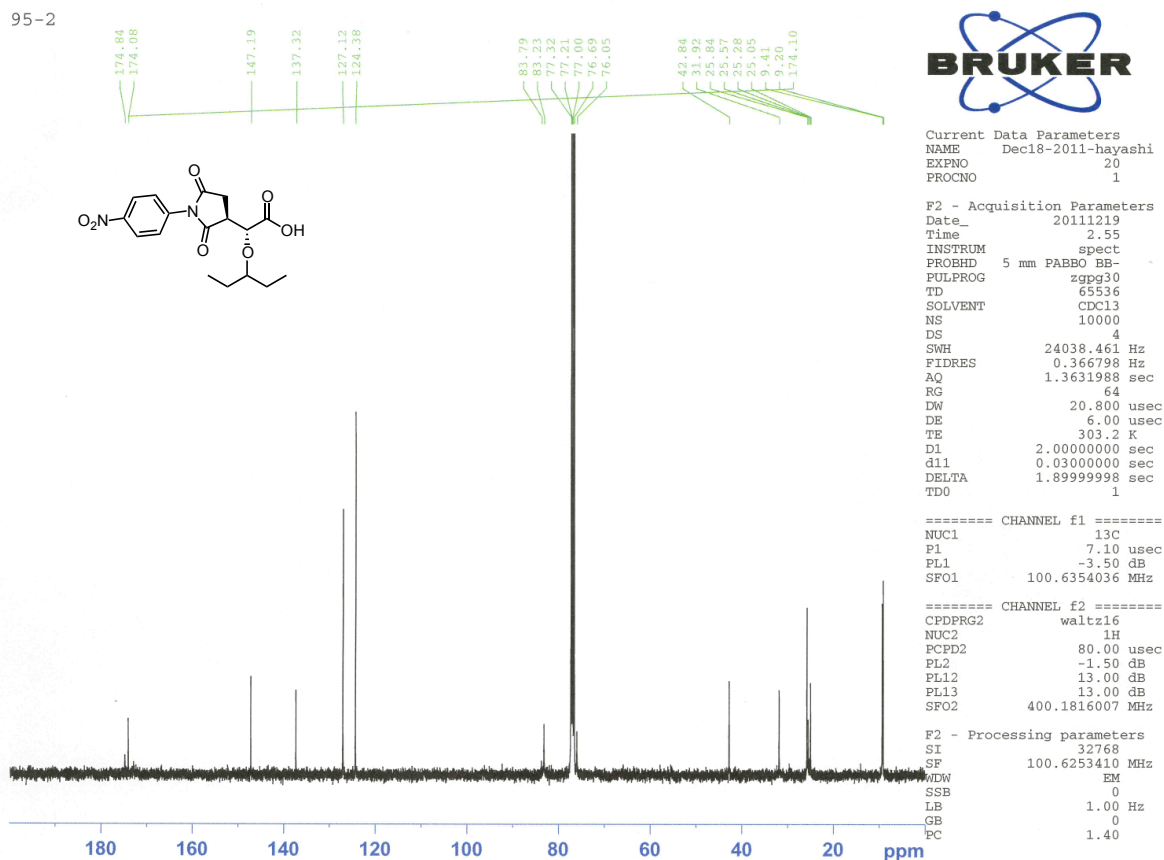
ファイル名 :
 タイトル :
 測定日時 : 2012年02月08日 15時38分48秒
 測定分解能 : 2 cm⁻¹
 スキャン回数 : 16 回
 測定ゲイン : 1
 コメント :

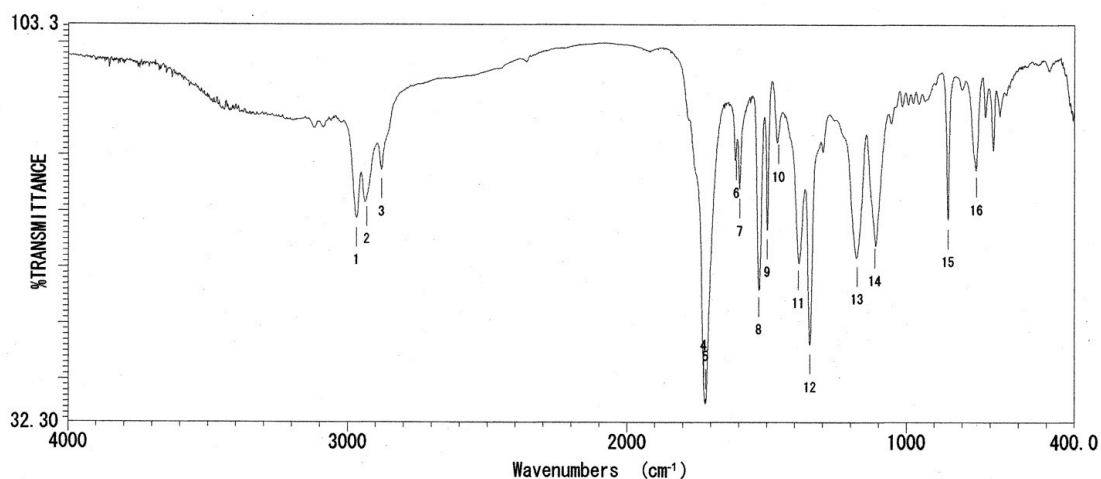
ピーク番号	波数 (cm⁻¹)	透過率 (%)	ピーク番号	波数 (cm⁻¹)	透過率 (%)
01	3332.39	89.2061	18	1262.18	90.7571
02	2959.23	89.5500	19	1172.51	82.7375
03	2924.52	88.6354	20	1047.16	89.9583
04	2871.49	92.1539	21	987.375	81.1010
05	1778.05	96.8607	22	853.347	90.7221
06	1746.23	86.4862	23	812.849	93.7428
07	1722.12	79.2553	24	750.174	92.3329
08	1713.44	71.9959	25	723.175	93.3201
09	1660.41	83.1964	26	697.141	90.3532
10	1612.20	92.0647			
11	1597.73	91.5964			
12	1529.27	80.0278			
13	1497.45	86.4400			
14	1455.99	91.0399			
15	1435.74	91.7480			
16	1389.46	84.9646			
17	1348.00	81.6461			





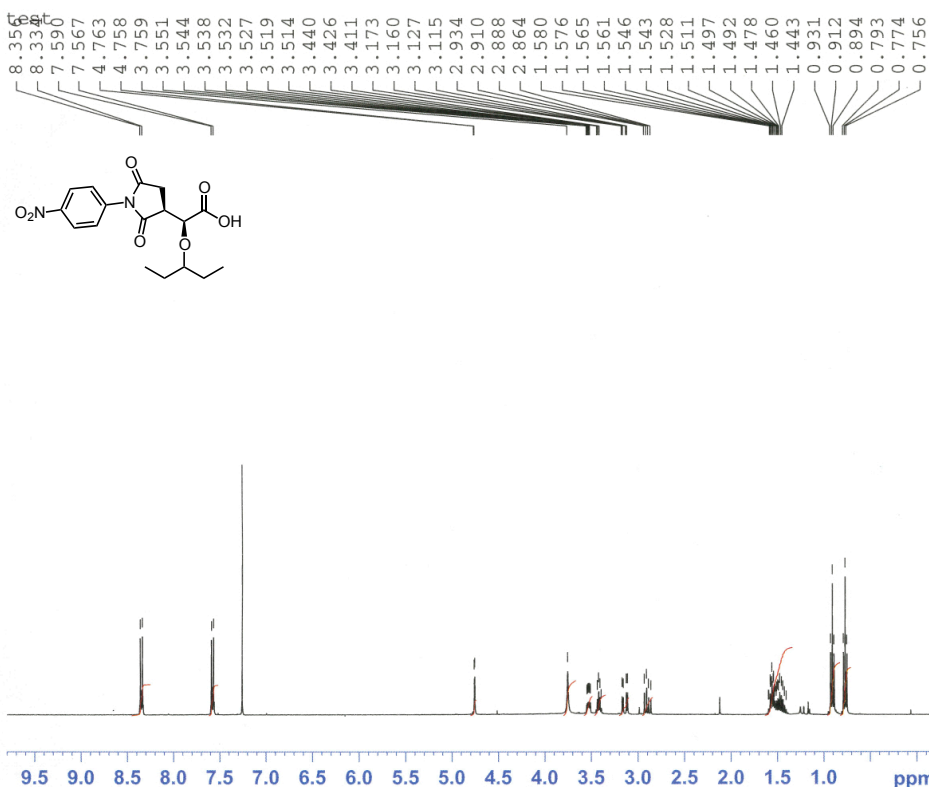
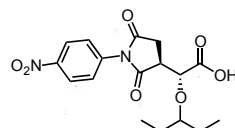
95-2





ファイル名 :
 タイトル :
 測定日時 : 2012年02月20日 15時47分25秒
 測定分解能 : 2 cm⁻¹
 スキャン回数 : 16 回
 測定ゲイン : 1
 コメント :

ピーク番号	波数 (cm⁻¹)	透過率 (%)
01	2967.91	68.7935
02	2931.27	72.5143
03	2878.24	77.4484
04	1725.01	38.5143
05	1718.26	36.5114
06	1609.31	80.7737
07	1596.77	73.9825
08	1528.31	56.4427
09	1498.42	66.7011
10	1457.92	83.6617
11	1386.57	61.1855
12	1345.11	46.1199
13	1177.33	61.8591
14	1113.69	65.1104
15	852.382	68.5022
16	751.138	77.8068



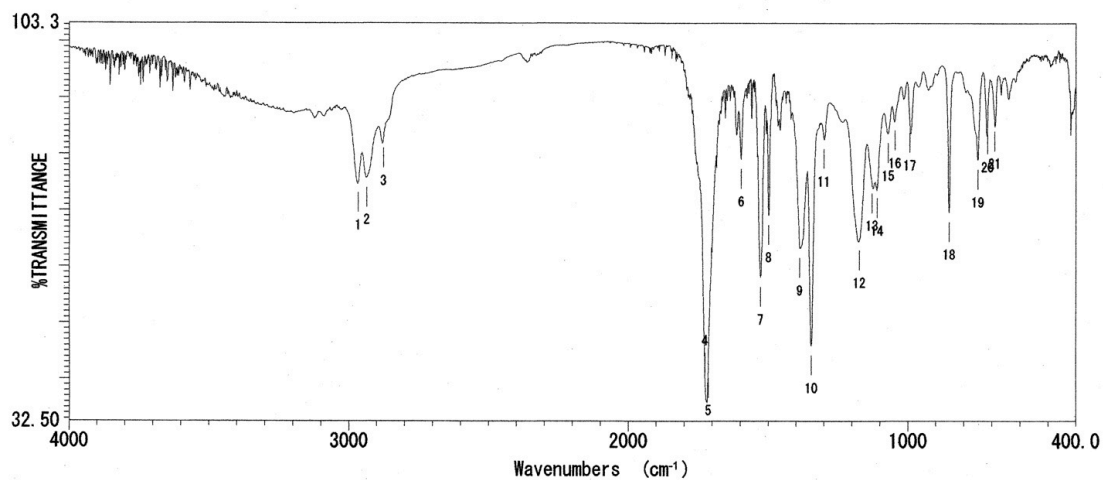
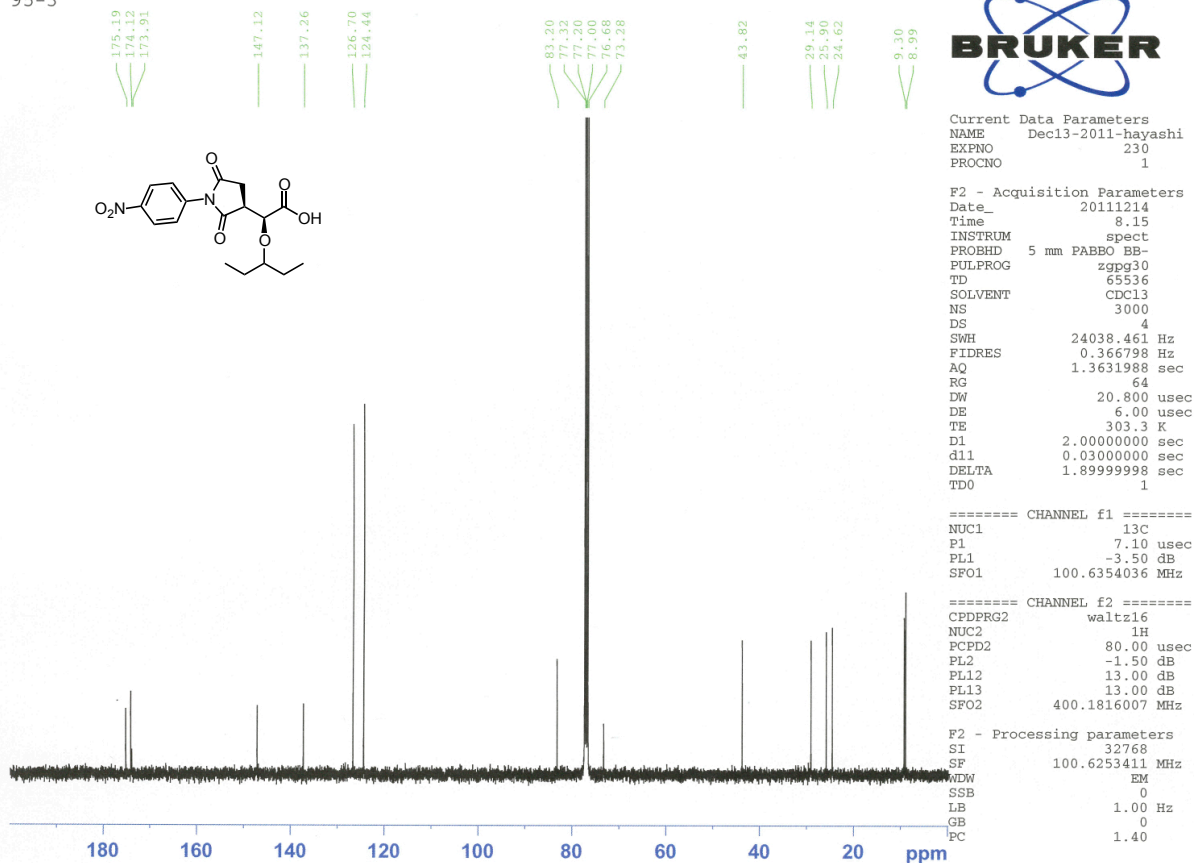
Current Data Parameters
 NAME : Dec06-2011
 EXPNO : 18
 PROCNO : 1

F2 - Acquisition Parameters
 Date_ : 20111206
 Time : 15.59
 INSTRUM : dpx400
 PROBHD : 5 mm QNP 1H/29
 PULPROG : zg30
 TD : 32768
 SOLVENT : CDC13
 NS : 16
 DS : 0
 SWH : 8223.685 Hz
 FIDRES : 0.250967 Hz
 AQ : 1.9923444 sec
 RG : 18390.4
 DW : 60.800 usec
 DE : 6.00 usec
 TE : 303.2 K
 D1 : 1.00000000 sec
 MCREST : 0.00000000 sec
 MCWPK : 0.01500000 sec

===== CHANNEL f1 =====
 NUC1 : 1H
 P1 : 7.90 usec
 PL1 : 3.00 dB
 SFO1 : 400.1324710 MHz

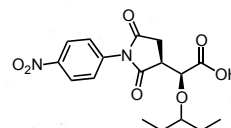
F2 - Processing parameters
 SI : 16384
 SF : 400.1300092 MHz
 WDW : EM
 SSB : 0
 LB : 0.30 Hz
 GB : 0
 PC : 1.00

95-3

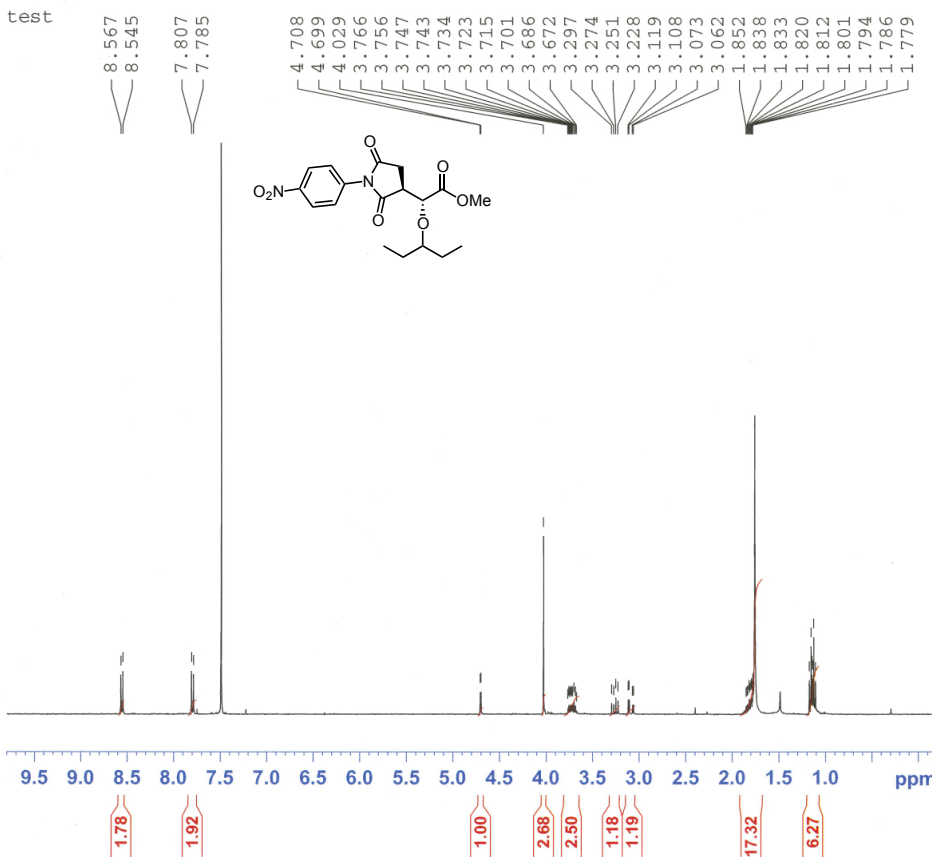


ファイル名 :
 タイトル :
 測定日時 : 2012年02月20日 16時02分31秒
 測定分解能 : 2 cm⁻¹
 スキャン回数 : 16 回
 測定ゲイン : 1
 コメント :

ピーク番号	波数 (cm⁻¹)	透過率 (%)	ピーク番号	波数 (cm⁻¹)	透過率 (%)
01	2965.98	74.8691	18	853.347	69.6264
02	2835.13	75.8144	19	751.138	78.9369
03	2875.34	82.7279	20	716.425	85.2178
04	1725.01	39.3154	21	691.355	85.8175
05	1714.41	41.9412			
06	1596.77	79.0294			
07	1527.35	58.0933			
08	1498.42	69.1042			
09	1386.57	63.2284			
10	1345.11	45.8953			
11	1299.79	82.6524			
12	1173.47	64.6252			
13	1129.12	74.7970			
14	1109.83	73.8710			
15	1071.26	83.6461			
16	1047.16	85.9119			
17	994.125	85.4727			



test



Current Data Parameters
NAME Dec08-2011
EXPNO 133
PROCNO 1

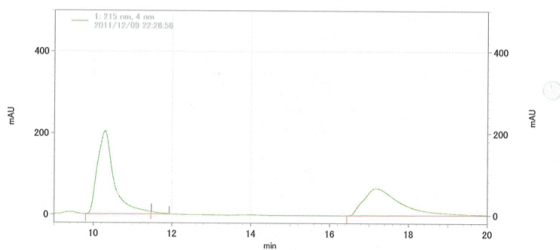
F2 - Acquisition Parameters
Date_ 20111208
Time 22.26
INSTRUM dpx400
PROBHD 5 mm QNP 1H/29
PULPROG zg30
TD 32768
SOLVENT CDC13
NS 16
DS 0
SWH 8223.685 Hz
FIDRES 0.250967 Hz
AQ 1.9923444 sec
RG 32768
DW 60.800 usec
DE 6.00 usec
TE 303.2 K
D1 1.00000000 sec
MCREST 0.00000000 sec
MCWRK 0.01500000 sec

===== CHANNEL f1 =====
NUC1 1H
P1 7.90 usec
PL1 3.00 dB
SFO1 400.1324710 MHz

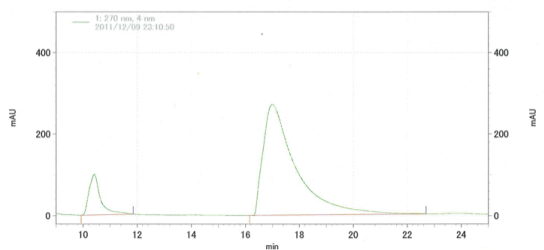
F2 - Processing parameters
SI 16384
SF 400.1299173 MHz
WDW EM
SSB 0
LB 0.30 Hz
GB 0
PC 1.00

ファイル名: W:\Server\Enterprise\Projects\Default\Data\2011-12-09 22-28-58 mukai
100-2 racemi AD-H 3vs1 1ml
ファイル名: W:\Server\Enterprise\Projects\Default\Method\10vs1. 1ml.met
システム名: System
分析日時: 2011/12/09 22:29:58
印刷日時: 2011/12/09 22:58:38

ファイル名: W:\Server\Enterprise\Projects\Default\Data\2011-12-09 23-10-50 mukai
99-2 AD-H 3vs1 1ml
ファイル名: W:\Server\Enterprise\Projects\Default\Method\10vs1. 1ml.met
システム名: System
分析日時: 2011/12/09 23:11:41
印刷日時: 2011/12/09 23:44:37

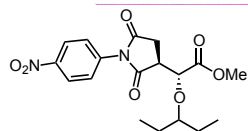


PK #	名前	保持時間	面積	面積%	ピークコメント
1		10.30	24175710	57.490 MM	
2		11.47	2	0.000 MM	
3		17.19	17875955	42.510 MM	
トータル			42051667	100.000	

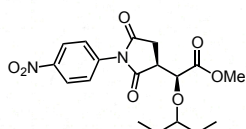


PK #	名前	保持時間	面積	面積%	ピークコメント
1		10.43	11783331	11.426 MM	
2		17.01	91344731	88.574 MM	
トータル			103128062	100.000	

racemi



test

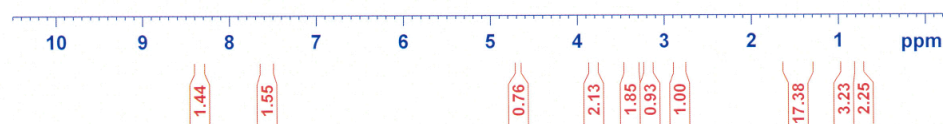


Current Data Parameters
NAME Dec07-2011
EXPNO 13
PROCNO 1

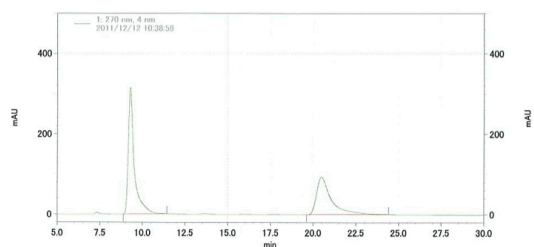
F2 - Acquisition Parameters
Date_ 20111207
Time_ 23.25
INSTRUM dpx400
PROBHD 5 mm QNP 1H/29
PULPROG zg30
TD 32768
SOLVENT CDC13
NS 32
DS 0
SWH 8223.685 Hz
FIDRES 0.250967 Hz
AQ 1.9923444 sec
RG 23170.5
DW 60.800 usec
DE 6.00 usec
TE 303.2 K
D1 1.00000000 sec
MCREST 0.00000000 sec
MCWRK 0.01500000 sec

===== CHANNEL f1 =====
NUC1 1H
P1 7.90 usec
PL1 3.00 dB
SFO1 400.1324710 MHz

F2 - Processing parameters
SI 16384
SF 400.1300087 MHz
WDW EM
SSB 0
LB 0.30 Hz
GB 0
PC 1.00

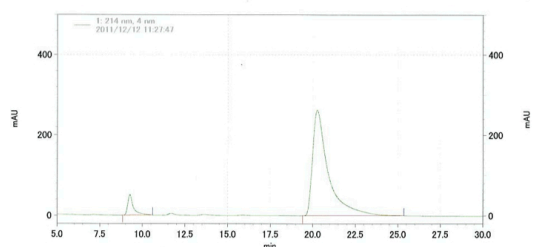


データファイル名: \\Server\Enterprise\Projects\Default\Data\2011-12-12 10-38-59 mukai
101-2 AD-Hi 3vs1 Im1 racemi
メソッド名: \\Server\Enterprise\Projects\Default\Method\10vs1. Im1.met
ユーザー名: System
分析日時: 2011/12/12 10:41:38
印刷日時: 2011/12/12 11:26:24



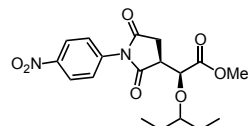
1: 270 nm, 4 nm結果	PK #	名前	保持時間	面積	面積%	ピークコード
	1		9.30	31087309	57.960 MM	
	2		20.50	22548572	42.040 MM	
				53635881	100.000	

データファイル名: \\Server\Enterprise\Projects\Default\Data\2011-12-12 11-27-47 mukai
97-2 AD-Hi 3vs1 Im1
メソッド名: \\Server\Enterprise\Projects\Default\Method\10vs1. Im1.met
ユーザー名: System
分析日時: 2011/12/12 11:29:02
印刷日時: 2011/12/12 12:37:27

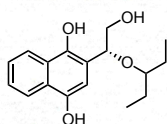


1: 214 nm, 4 nm結果	PK #	名前	保持時間	面積	面積%	ピークコード
	1		9.27	4731593	6.499 MM	
	2		20.26	68073492	93.501 MM	
				72805085	100.000	

racemi



test

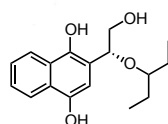
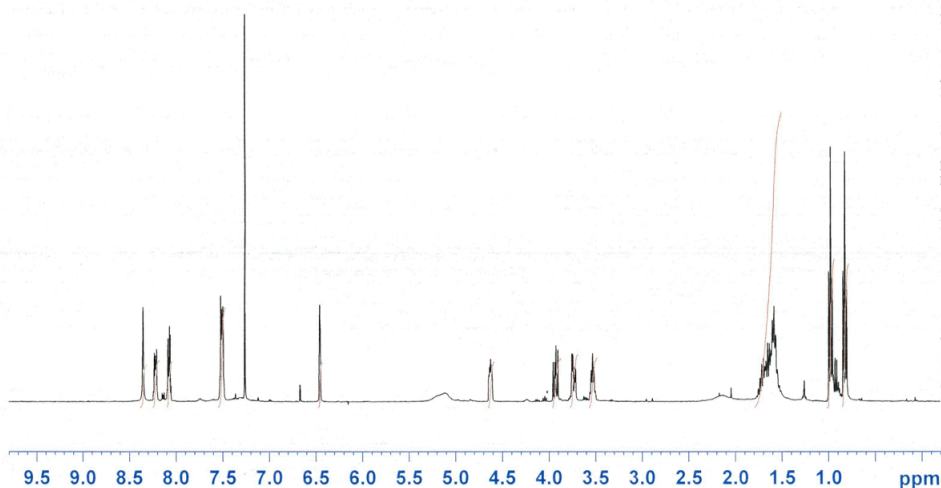


Current Data Parameters
NAME Mar24-2012
EXPNO 46
PROCNO 1

F2 - Acquisition Parameters
Date_ 20120324
Time 18.08
INSTRUM dpx400
PROBHD 5 mm QNP 1H/29
PULPROG zg30
TD 32768
SOLVENT CDCl3
NS 16
DS 0
SWH 8223.685 Hz
FIDRES 0.250967 Hz
AQ 1.9923444 sec
RG 18390.4
DW 60.800 usec
DE 6.00 usec
TE 303.2 K
D1 1.00000000 sec
MCREST 0.00000000 sec
MCWRK 0.01500000 sec

===== CHANNEL f1 =====
NUC1 1H
P1 7.90 usec
PL1 3.00 dB
SFO1 400.1324710 MHz

F2 - Processing parameters
SI 16384
SF 400.1300092 MHz
WDW EM
SSB 0
LB 0.30 Hz
GB 0
PC 1.00



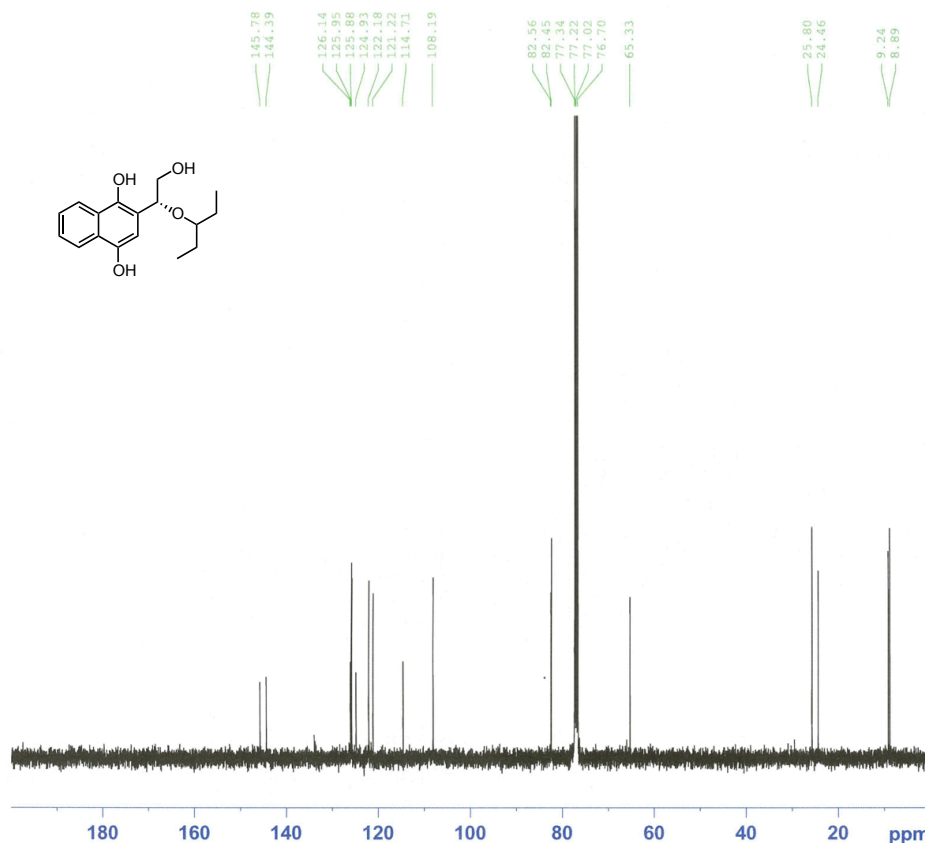
Current Data Parameters
NAME Mar24-2012-hayashi
EXPNO 90
PROCNO 1

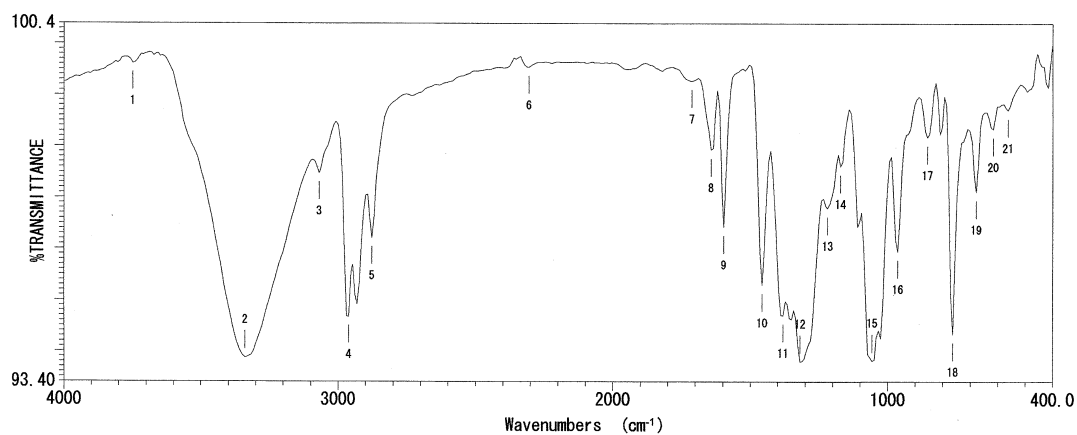
F2 - Acquisition Parameters
Date_ 20120324
Time 20.05
INSTRUM spect
PROBHD 5 mm PABBO BB-
PULPROG zgpg30
TD 65536
SOLVENT CDCl3
NS 2048
DS 4
SWH 24038.461 Hz
FIDRES 0.366798 Hz
AQ 1.3631988 sec
RG 57
DW 20.800 usec
DE 6.00 usec
TE 300.0 K
D1 2.00000000 sec
d11 0.03000000 sec
DELTA 1.89999998 sec
TD0 1

===== CHANNEL f1 =====
NUC1 13C
P1 7.10 usec
PL1 -3.50 dB
SFO1 100.6354036 MHz

===== CHANNEL f2 =====
CPDPRG2 waltz16
NUC2 1H
PCPD2 80.00 usec
PL2 -1.50 dB
PL12 13.00 dB
PL13 13.00 dB
SFO2 400.1816007 MHz

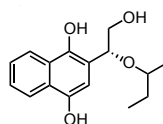
F2 - Processing parameters
SI 32768
SF 100.6253410 MHz
WDW EM
SSB 0
LB 1.00 Hz
GB 0
PC 1.40

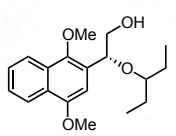
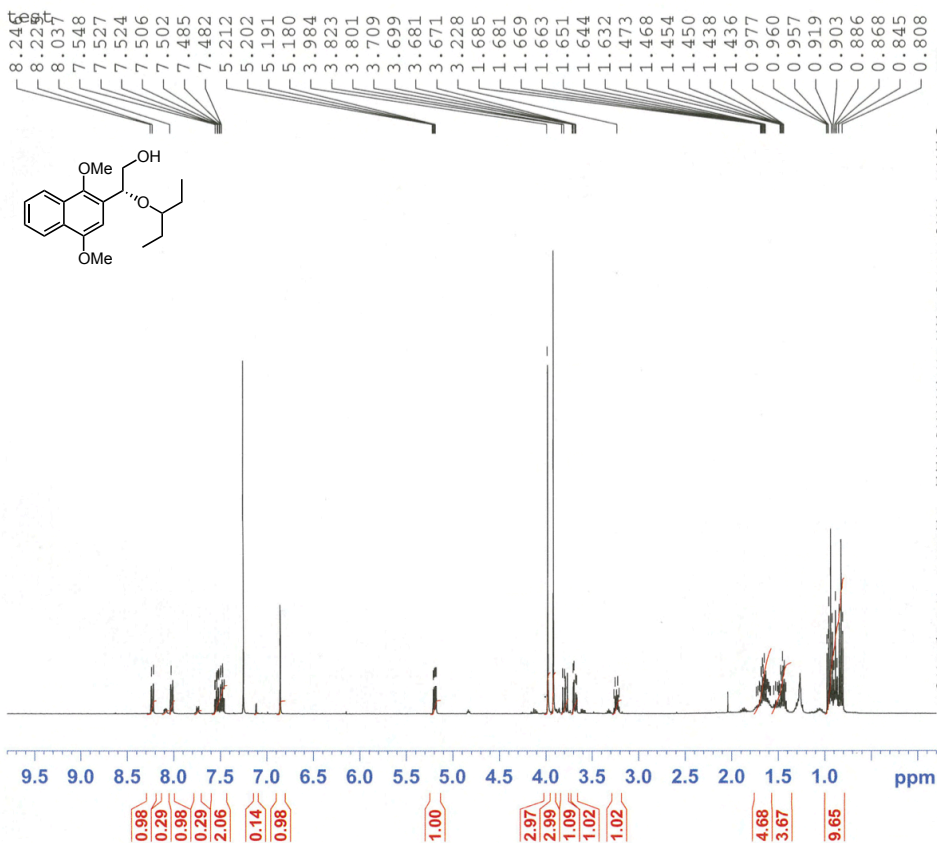




ファイル名 :
 タイトル :
 測定日時 : 2012年03月28日 17時31分12秒
 測定分解能 : 16 cm⁻¹
 スキャン回数 : 8 回
 測定ゲイン : 1
 コメント :

ピーク番号	波数 (cm⁻¹)	透過率 (%)
01	3748.94	99.6156
02	3340.10	93.8732
03	3070.12	97.4754
04	2962.13	94.6718
05	2877.27	96.2121
06	2306.45	99.5347
07	1712.48	99.2705
08	1643.05	97.9261
09	1596.77	96.4217
10	1457.92	95.2876
11	1380.78	94.6980
12	1319.07	93.7879
13	1218.79	96.7881
14	1172.51	97.6102
15	1056.80	93.8115
16	964.233	95.9484
17	856.239	98.1741
18	763.673	94.3335
19	678.820	97.1083
20	617.109	98.3317
21	563.112	98.7068





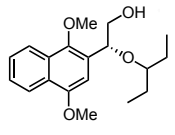
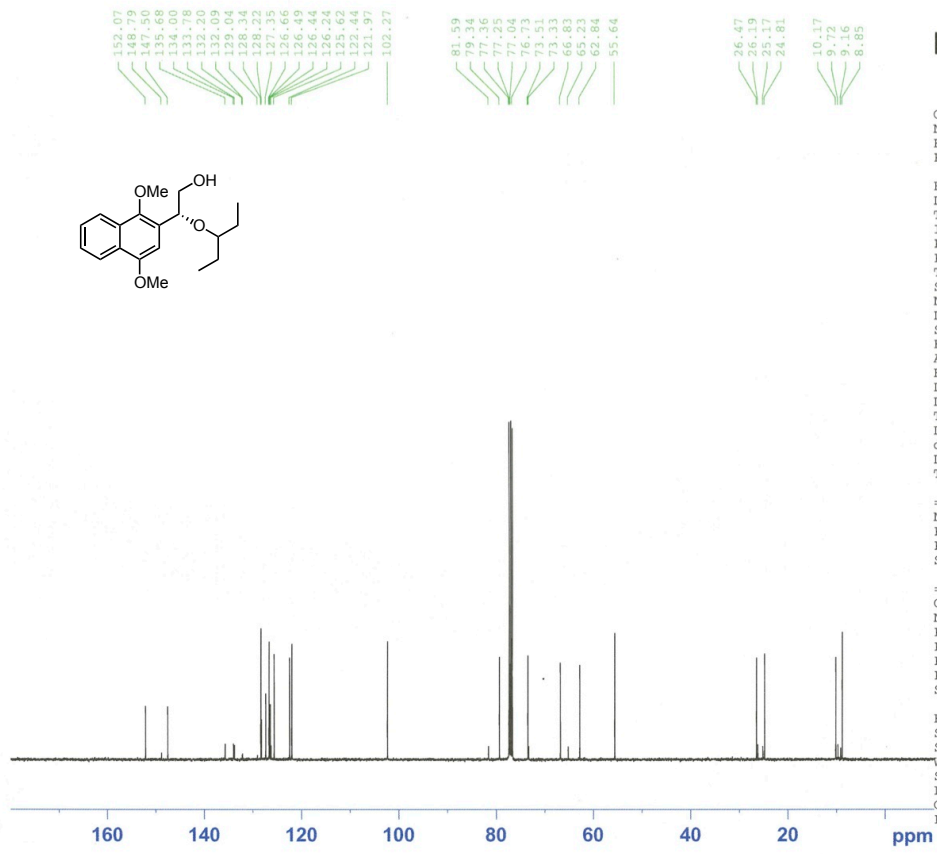
BRUKER

Current Data Parameters
 NAME Nov18-2011
 EXPNO 100
 PROCNO 1

F2 - Acquisition Parameters
 Date_ 20111118
 Time 13.16
 INSTRUM dpx400
 PROBHD 5 mm QNP 1H/29
 PULPROG zg30
 TD 32768
 SOLVENT CDCl3
 NS 16
 DS 0
 SWH 8223.685 Hz
 FIDRES 0.250967 Hz
 AQ 1.9923444 sec
 RG 14596.5
 DW 60.800 usec
 DE 6.00 usec
 TE 303.2 K
 D1 1.00000000 sec
 MCWREST 0.00000000 sec
 MCWRK 0.01500000 sec

===== CHANNEL f1 =====
 NUC1 1H
 P1 7.90 usec
 PL1 3.00 dB
 SFO1 400.1324710 MHz

F2 - Processing parameters
 SI 16384
 SF 400.130092 MHz
 WDW EM
 SSB 0
 LB 0.30 Hz
 GB 0
 PC 1.00



BRUKER

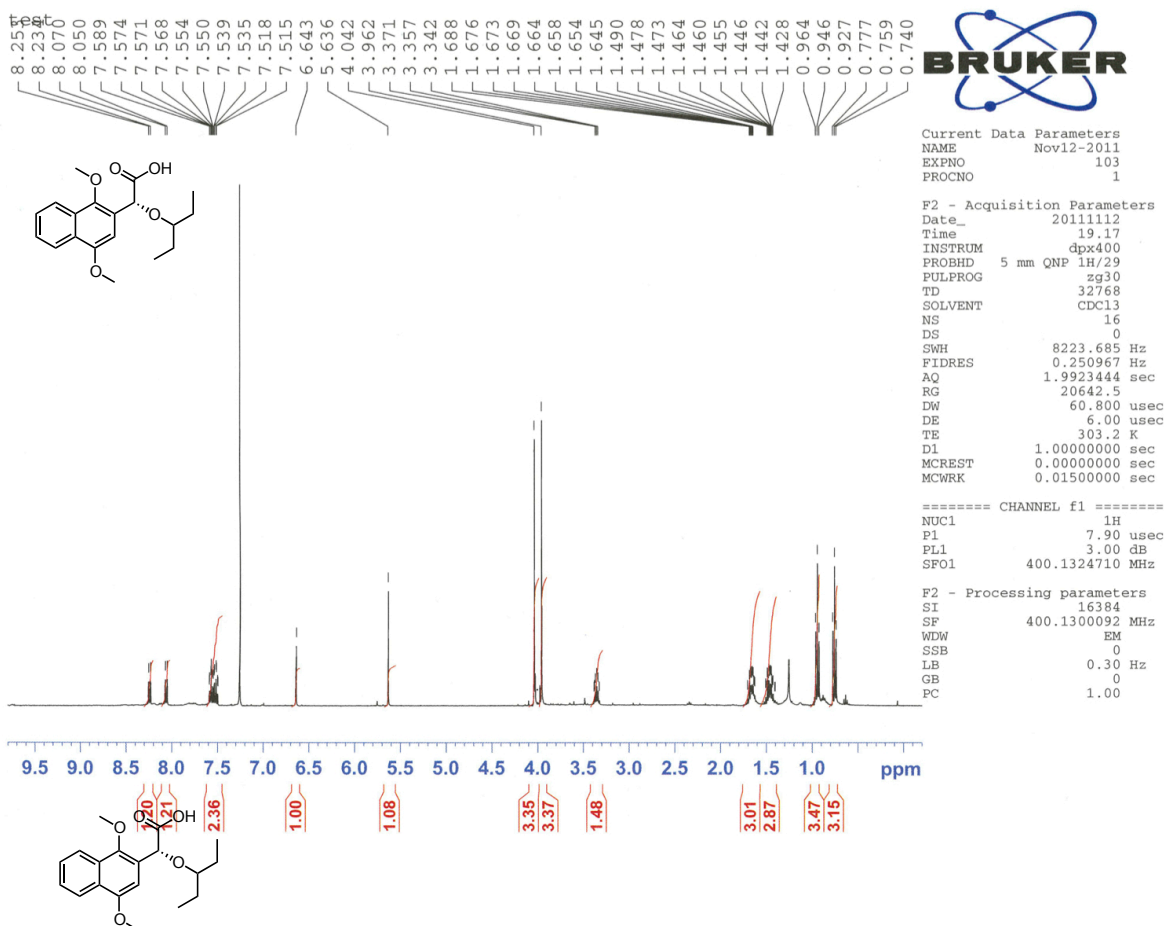
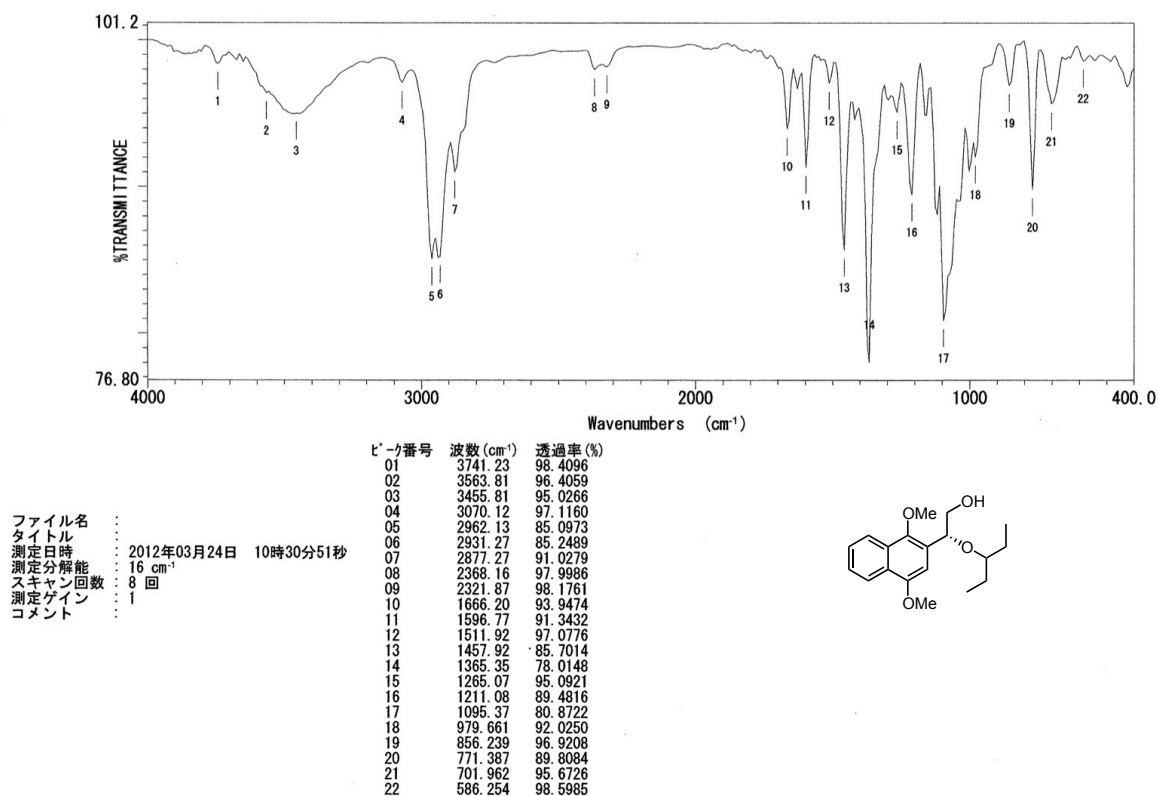
Current Data Parameters
 NAME Mar23-2012-hayashi
 EXPNO 180
 PROCNO 1

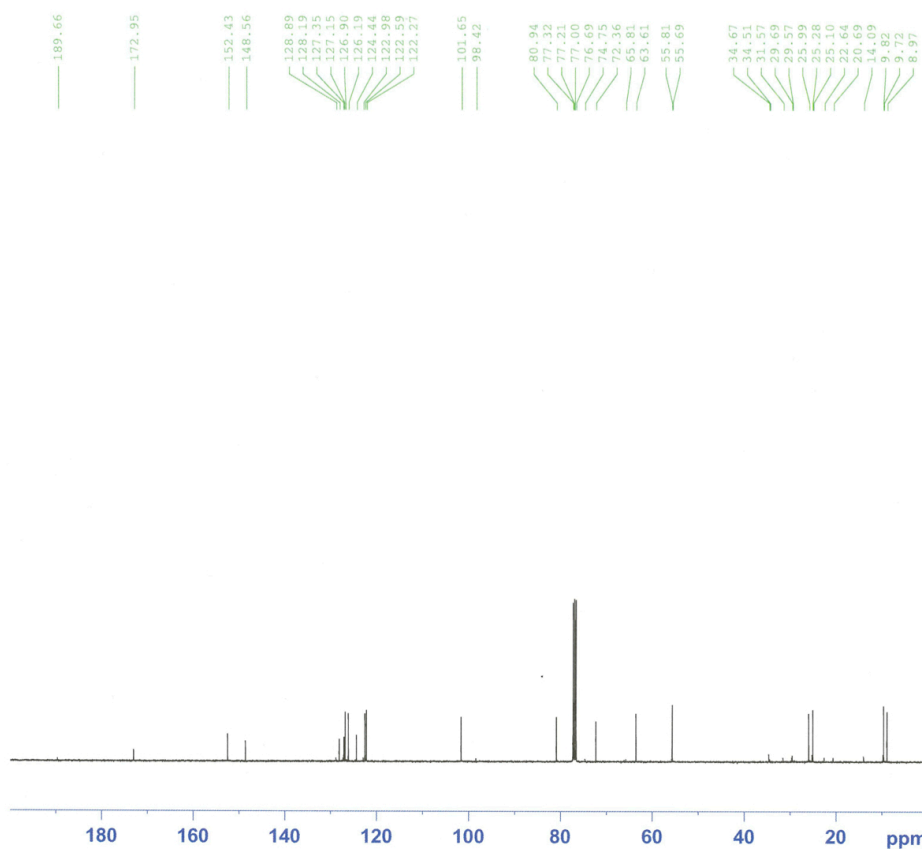
F2 - Acquisition Parameters
 Date_ 20120324
 Time 8.19
 INSTRUM spect
 PROBHD 5 mm PABBO BB-
 PULPROG zgpg30
 TD 65536
 SOLVENT CDCl3
 NS 1024
 DS 4
 SWH 24038.461 Hz
 FIDRES 0.366798 Hz
 AQ 1.3631988 sec
 RG 64
 DW 20.800 usec
 DE 6.00 usec
 TE 300.0 K
 D1 2.00000000 sec
 d11 0.03000000 sec
 DELTA 1.89999998 sec
 TDO 1

===== CHANNEL f1 =====
 NUC1 13C
 P1 7.10 usec
 PL1 -3.50 dB
 SFO1 100.6354036 MHz

===== CHANNEL f2 =====
 CPDPRG2 waltz16
 NUC2 1H
 PCPD2 80.00 usec
 PL2 -1.50 dB
 PL12 13.00 dB
 PL13 13.00 dB
 SFO2 400.1816007 MHz

F2 - Processing parameters
 SI 32768
 SF 100.6253410 MHz
 WDW EM
 SSB 0
 LB 1.00 Hz
 GB 0
 PC 1.40





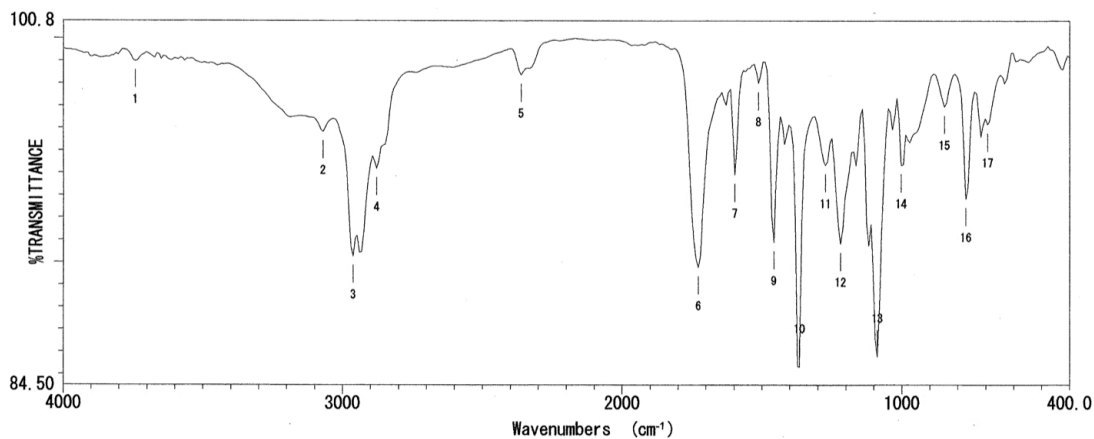
Current Data Parameters
NAME Mar14-2012-hayashi
EXPNO 360
PROCNO 1

F2 - Acquisition Parameters
Date_ 20120314
Time 23.56
INSTRUM spect
PROBHD 5 mm PABBO BB-
PULPROG zgpg30
TD 65536
SOLVENT CDCl3
NS 2048
DS 4
SWH 24038.461 Hz
FIDRES 0.366798 Hz
AQ 1.3631988 sec
RG 64
DW 20.800 usec
DE 6.00 usec
TE 303.5 K
D1 2.00000000 sec
d11 0.03000000 sec
DELTA 1.89999998 sec
TDO 1

===== CHANNEL f1 =====
NUC1 13C
P1 7.10 usec
PL1 -3.50 dB
SFO1 100.6354036 MHz

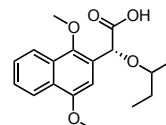
===== CHANNEL f2 =====
CPDPRG2 waltz16
NUC2 1H
PCPD2 80.00 usec
PL2 -1.50 dB
PL12 13.00 dB
PL13 13.00 dB
SFO2 400.1816007 MHz

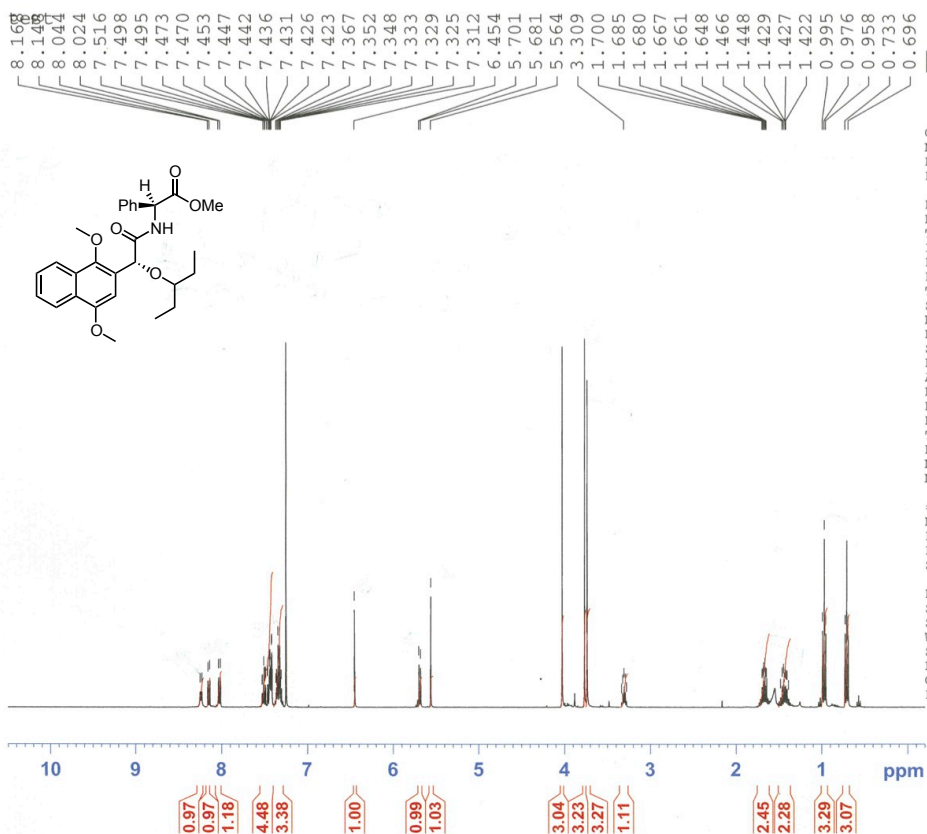
F2 - Processing parameters
SI 32768
SF 100.6253410 MHz
WDW EM
SSB 0
LB 1.00 Hz
GB 0
PC 1.40



ピーク番号	波数 (cm⁻¹)	透過率 (%)
01	3741.23	98.9828
02	3070.12	95.8295
03	2962.13	90.2631
04	2877.27	94.1773
05	2360.44	98.3723
06	1727.91	89.7667
07	1596.77	93.8966
08	1511.92	97.9938
09	1457.92	90.8814
10	1365.35	85.2998
11	1272.79	94.3212
12	1218.79	90.8170
13	1087.66	85.7681
14	1002.80	94.3294
15	848.525	96.9580
16	771.387	92.8187
17	694.248	96.1657

ファイル名 :
タイトル :
測定日時 : 2012年03月24日 10時16分22秒
測定分解能 : 16 cm⁻¹
スキャン回数 : 8 回
測定ゲイン : 1
コメント :



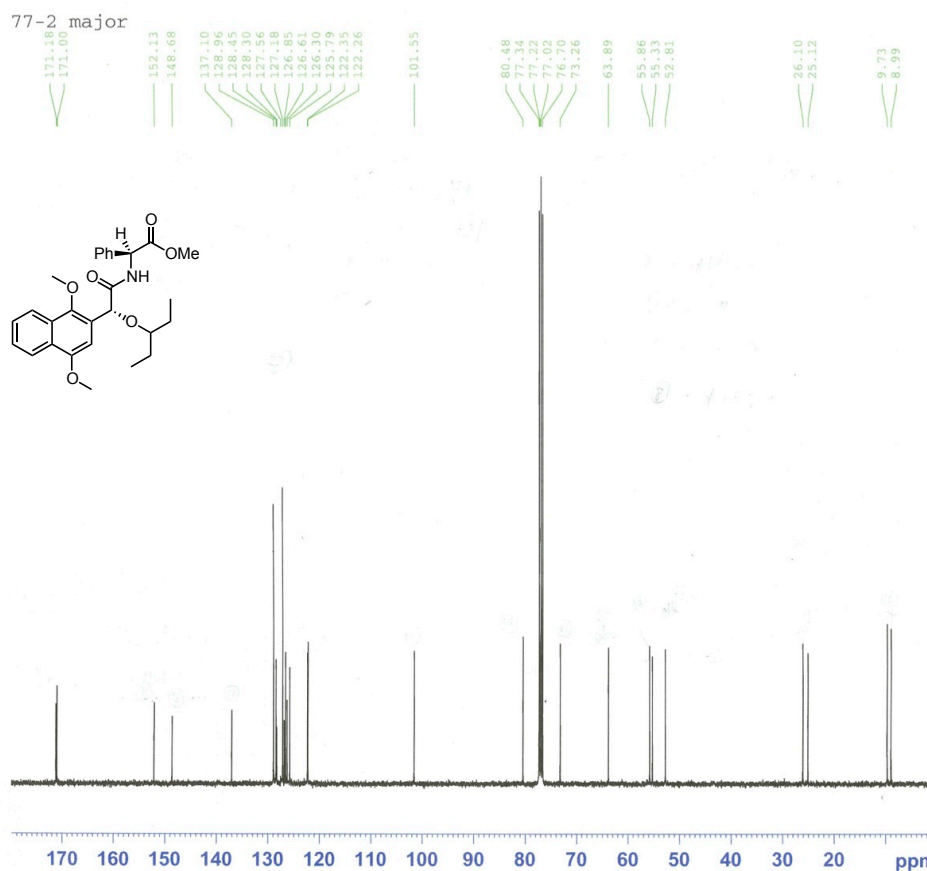


Current Data Parameters
NAME Nov21-2011
EXPNO 46
PROCNO 1

F2 - Acquisition Parameters
Date_ 20111121
Time 15.37
INSTRUM dpx400
PROBHD 5 mm QNP 1H/29
PULPROG zg30
TD 32768
SOLVENT CDCl3
NS 16
DS 0
SWH 8223.685 Hz
FIDRES 0.250967 Hz
AQ 1.9923444 sec
RG 18390.4
DW 60.800 usec
DE 6.00 usec
TE 303.2 K
D1 1.00000000 sec
MCREST 0.00000000 sec
MCWRK 0.01500000 sec

===== CHANNEL f1 =====
NUC1 1H
P1 7.90 usec
PL1 3.00 dB
SFO1 400.1324710 MHz

F2 - Processing parameters
SI 16384
SF 400.1300098 MHz
WDW EM
SSB 0
LB 0.30 Hz
GB 0
PC 1.00



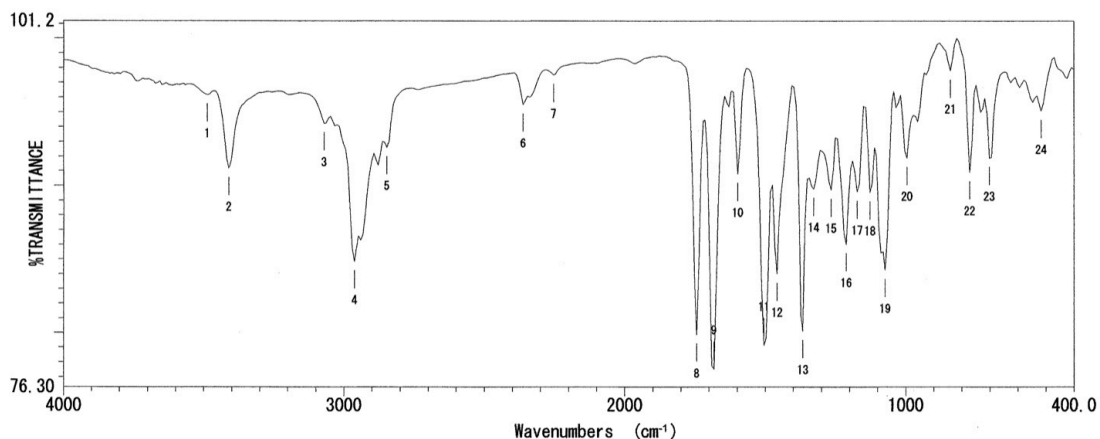
Current Data Parameters
NAME Mar12-2012-hayashi
EXPNO 170
PROCNO 1

F2 - Acquisition Parameters
Date_ 20120313
Time 2.11
INSTRUM spect
PROBHD 5 mm PABBO BB-
PULPROG zgpg30
TD 65536
SOLVENT CDCl3
NS 2000
DS 4
SWH 24038.461 Hz
FIDRES 0.366798 Hz
AQ 1.3631988 sec
RG 64
DW 20.800 usec
DE 6.00 usec
TE 303.3 K
D1 2.00000000 sec
d11 0.03000000 sec
DELTA 1.89999999 sec
TD0 1

===== CHANNEL f1 =====
NUC1 13C
P1 7.10 usec
PL1 -3.50 dB
SFO1 100.6354036 MHz

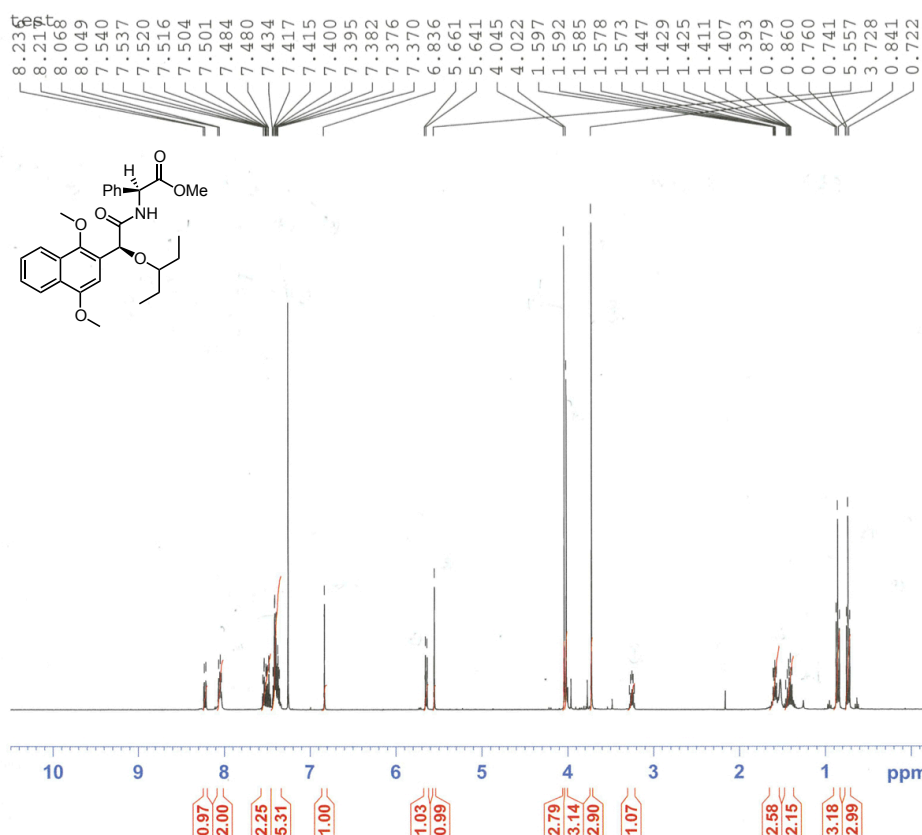
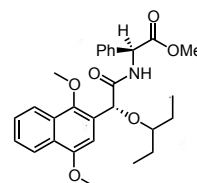
===== CHANNEL f2 =====
CPDPRG2 waltz16
NUC2 1H
PCPD2 80.00 usec
PL2 -1.50 dB
PL12 13.00 dB
PL13 13.00 dB
SFO2 400.1816007 MHz

F2 - Processing parameters
SI 32768
SF 100.6253410 MHz
WDW EM
SSB 0
LB 1.00 Hz
GB 0
PC 1.40



ピーク番号	波数 (cm⁻¹)	透過率 (%)	ピーク番号	波数 (cm⁻¹)	透過率 (%)
01	3486.67	96.1743	23	701.962	91.8854
02	3409.53	91.1794	24	516.829	95.0894
03	3070.12	94.2199			
04	2962.13	84.8608			
05	2846.42	92.6015			
06	2360.44	95.5093			
07	2252.45	97.5146			
08	1743.33	79.8571			
09	1681.62	77.5355			
10	1596.77	90.7763			
11	1504.20	79.1344			
12	1457.92	84.0025			
13	1365.35	80.0965			
14	1326.79	89.7745			
15	1265.07	89.7088			
16	1211.08	86.0191			
17	1172.51	89.5861			
18	1126.22	89.5353			
19	1072.23	84.2507			
20	995.089	91.8788			
21	840.812	97.8084			
22	771.387	90.8900			

ファイル名 :
 タイトル :
 測定日時 : 2012年03月24日 10時05分03秒
 測定分解能 : 16 cm⁻¹
 スキャン回数 : 8 回
 測定ゲイン : 1
 コメント :



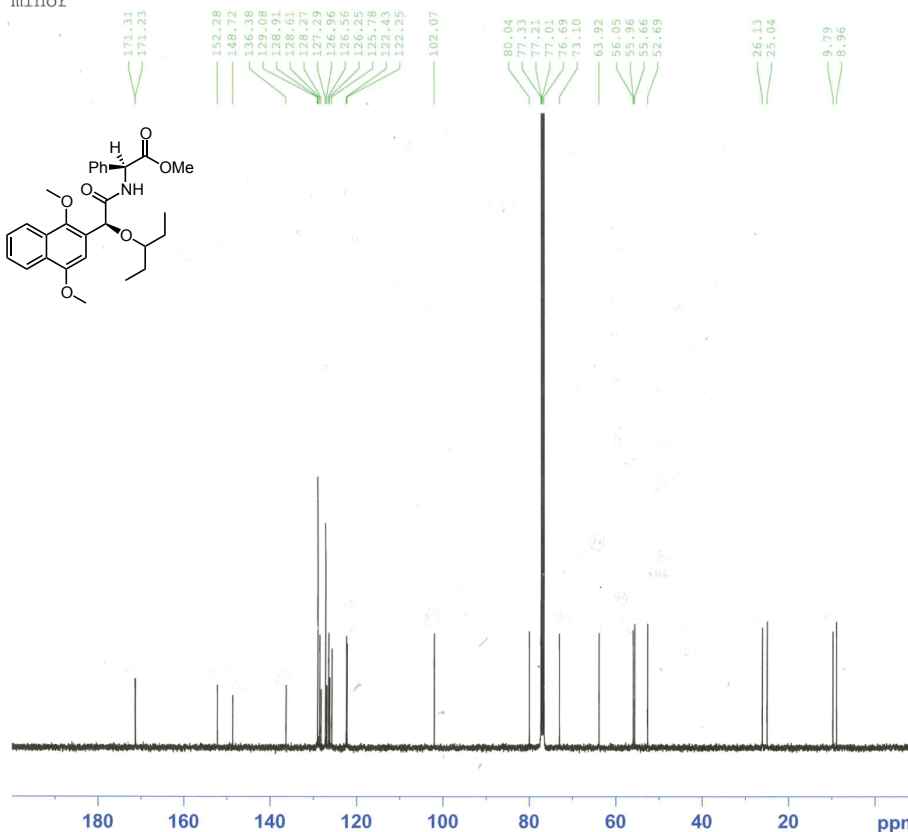
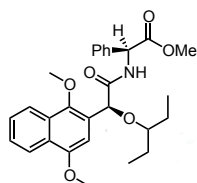
Current Data Parameters
 NAME Nov21-2011
 EXPNO 45
 PROCNO 1

 F2 - Acquisition Parameters
 Date_ 20111121
 Time 15.32
 INSTRUM dpx400
 PROBD 5 mm QNP 1H/29
 PULPROG zg30
 TD 32768
 SOLVENT CDC13
 NS 16
 DS 0
 SWH 8223.685 Hz
 FIDRES 0.250967 Hz
 AQ 1.9923444 sec
 RG 18390.4
 DW 60.800 usec
 DE 6.00 usec
 TE 303.2 K
 D1 1.00000000 sec
 MCREST 0.00000000 sec
 MCWRK 0.01500000 sec

 ===== CHANNEL f1 =====
 NUC1 1H
 P1 7.90 usec
 PL1 3.00 dB
 SFO1 400.1324710 MHz

 F2 - Processing parameters
 SI 16384
 SF 400.1300090 MHz
 WDW EM
 SSB 0
 LB 0.30 Hz
 GB 0
 PC 1.00

minor



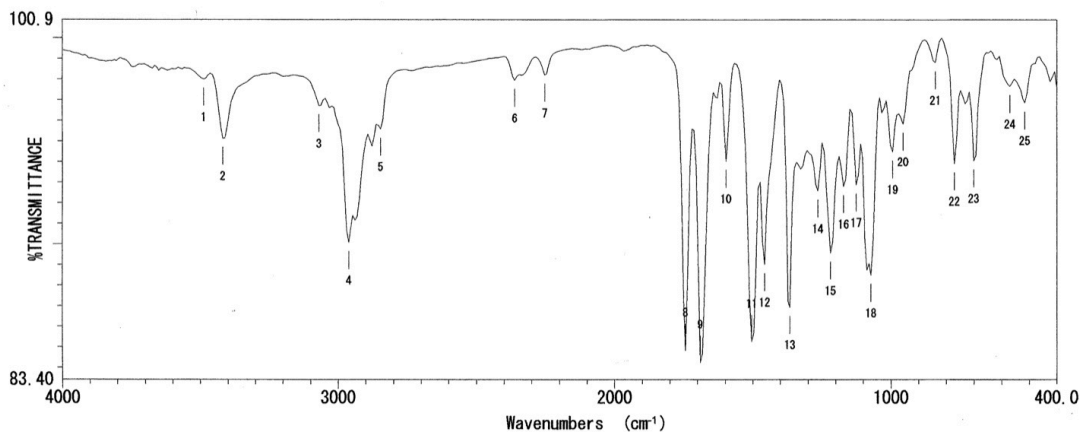
Current Data Parameters
NAME Mar04-2012-hayashi
EXPNO 20
PROCNO 1

F2 - Acquisition Parameters
Date_ 20120305
Time 0.22
INSTRUM spect
PROBHD 5 mm PABBO BB-
PULPROG zgpg30
TD 65536
SOLVENT CDCl3
NS 3000
DS 4
SWH 24038.461 Hz
FIDRES 0.366798 Hz
AQ 1.3631988 sec
RG 64
DW 20.800 usec
DE 6.00 usec
TE 303.5 K
D1 2.00000000 sec
d11 0.03000000 sec
DELTA 1.89999998 sec
TD0 1

===== CHANNEL f1 =====
NUC1 13C
P1 7.10 usec
PL1 -3.50 dB
SFO1 100.6254036 MHz

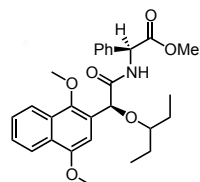
===== CHANNEL f2 =====
CPDPRG2 waltz16
NUC2 1H
PCPD2 80.00 usec
PL2 -1.50 dB
PL12 13.00 dB
PL13 13.00 dB
SFO2 400.1816007 MHz

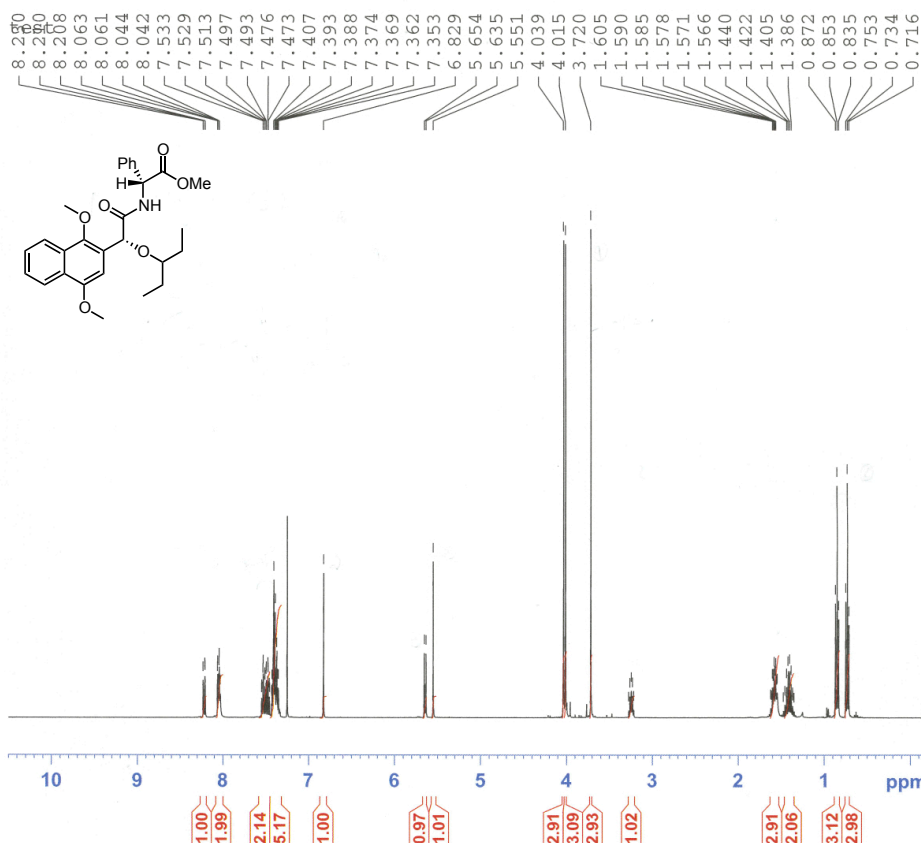
F2 - Processing parameters
SI 32768
SF 100.6253426 MHz
WDW EM
SSB 0
LB 1.00 Hz
GB 0
PC 1.40



ファイル名 :
タイトル :
測定日時 : 2012年03月24日 10時10分42秒
測定分解能 : 16 cm⁻¹
スキャン回数 : 8 回
測定ゲイン : 1
コメント :

ピーク番号	波数 (cm⁻¹)	透過率 (%)	ピーク番号	波数 (cm⁻¹)	透過率 (%)
01	3486.67	98.0034	23	701.962	94.0386
02	3417.24	95.1382	24	570.826	97.6599
03	3070.12	96.7149	25	516.829	96.8554
04	2962.13	90.0659			
05	2846.42	95.5895			
06	2360.44	97.9515			
07	2252.45	98.2044			
08	1743.33	84.8205			
09	1689.34	84.2411			
10	1596.77	94.0276			
11	1504.20	85.2530			
12	1457.92	89.0069			
13	1365.35	86.9386			
14	1265.07	92.5815			
15	1218.79	89.5567			
16	1172.51	92.7900			
17	1126.22	92.8705			
18	1072.23	88.4875			
19	995.089	94.4749			
20	956.520	95.8291			
21	840.812	98.8161			
22	771.387	93.9078			





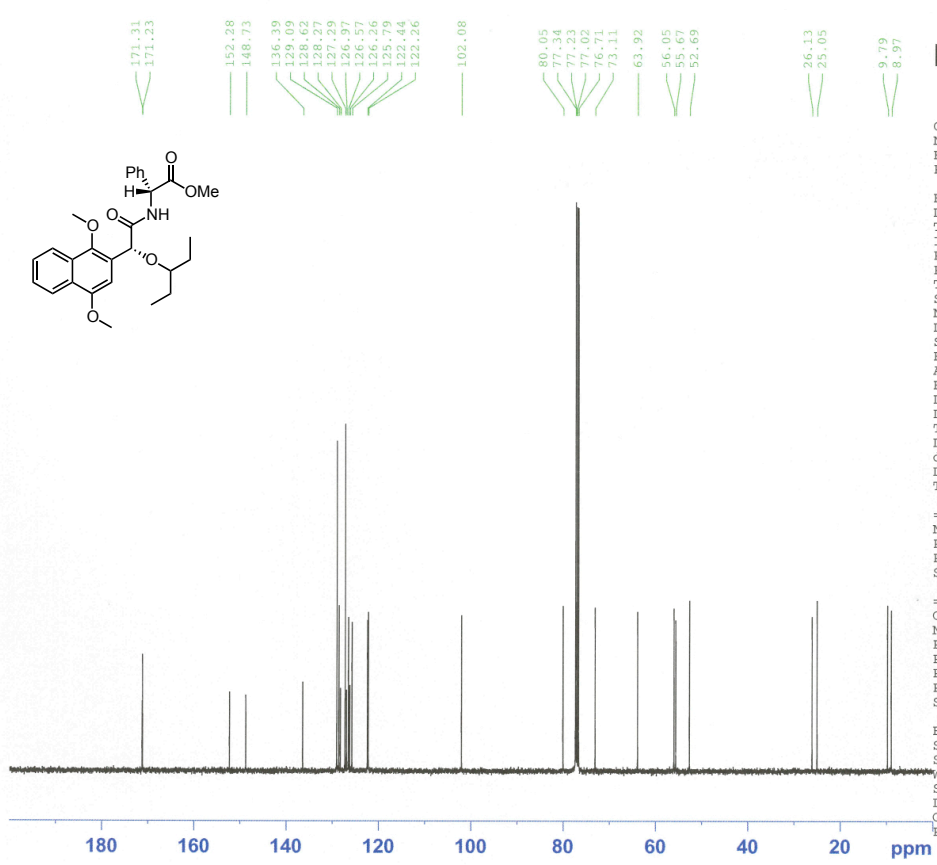
BRUKER

Current Data Parameters
 NAME Nov21-2011
 EXPNO 74
 PROCNO 1

F2 - Acquisition Parameters
 Date_ 20111121
 Time 19.02
 INSTRUM dpx400
 PROBHD 5 mm QNP 1H/29
 PULPROG zg30
 TD 32768
 SOLVENT CDCl3
 NS 16
 DS 0
 SWH 8223.685 Hz
 FIDRES 0.250967 Hz
 AQ 1.9923444 sec
 RG 11585.2
 DW 60.800 usec
 DE 6.00 usec
 TE 303.2 K
 D1 1.00000000 sec
 MCREST 0.00000000 sec
 MCWRK 0.01500000 sec

===== CHANNEL f1 =====
 NUC1 1H
 P1 7.90 usec
 PL1 3.00 dB
 SFO1 400.1324710 MHz

F2 - Processing parameters
 SI 16384
 SF 400.1300124 MHz
 WDW EM
 SSB 0
 LB 0.30 Hz
 GB 0
 PC 1.00



BRUKER

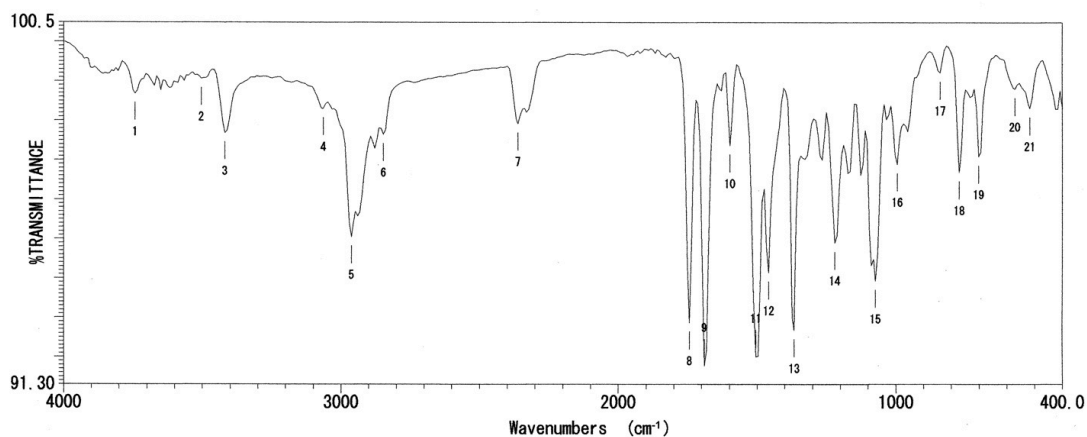
Current Data Parameters
 NAME Mar15-2012-hayashi
 EXPNO 190
 PROCNO 1

F2 - Acquisition Parameters
 Date_ 20120316
 Time 3.30
 INSTRUM spect
 PROBHD 5 mm PABBO BE-
 PULPROG zgpg30
 TD 65536
 SOLVENT CDCl3
 NS 1024
 DS 4
 SWH 24038.461 Hz
 FIDRES 0.366798 Hz
 AQ 1.3631988 sec
 RG 362
 DW 20.800 usec
 DE 6.00 usec
 TE 303.6 K
 D1 2.00000000 sec
 d11 0.03000000 sec
 DELTA 1.89999998 sec
 TD0 1

===== CHANNEL f1 =====
 NUC1 13C
 P1 7.10 usec
 PL1 -3.50 dB
 SFO1 100.6354036 MHz

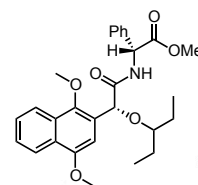
===== CHANNEL f2 =====
 CPDPRG2 waltz16
 NUC2 1H
 PCPD2 80.00 usec
 PL2 -1.50 dB
 PL12 13.00 dB
 PL13 13.00 dB
 SFO2 400.1816007 MHz

F2 - Processing parameters
 SI 32768
 SF 100.6253410 MHz
 WDW EM
 SSB 0
 LB 1.00 Hz
 GB 0
 PC 1.40

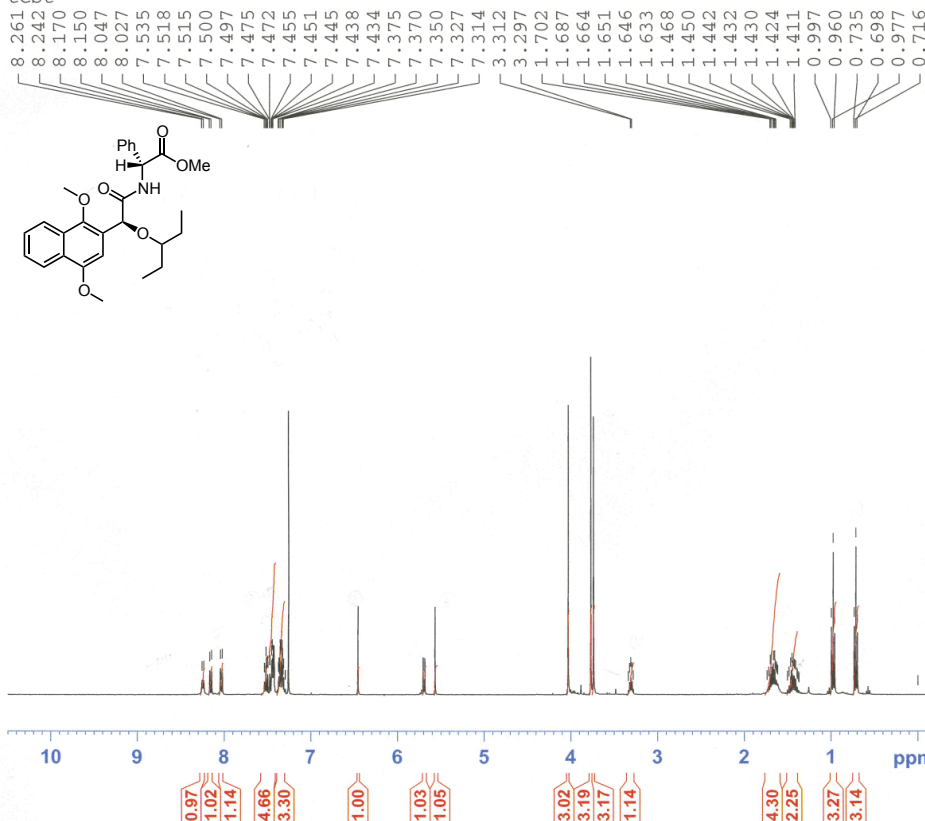


ピーク番号	波数 (cm⁻¹)	透過率 (%)
01	3741.23	98.6874
02	3502.10	99.0623
03	3417.24	97.6898
04	3062.41	98.3062
05	2962.13	95.0537
06	2846.42	97.6466
07	2360.44	97.9243
08	1743.33	92.8624
09	1689.34	91.7682
10	1596.77	97.3667
11	1504.20	92.0010
12	1457.92	94.1336
13	1365.35	92.6720
14	1218.79	94.8971
15	1072.23	93.9284
16	995.089	96.8978
17	840.812	99.2155
18	771.387	96.6819
19	701.962	97.0873
20	570.826	98.8052
21	516.829	98.3108

ファイル名
 タイトル
 測定日時 2012年03月24日 10時21分46秒
 測定分解能 16 cm⁻¹
 スキャン回数 8 回
 測定ゲイン 1
 コメント



test

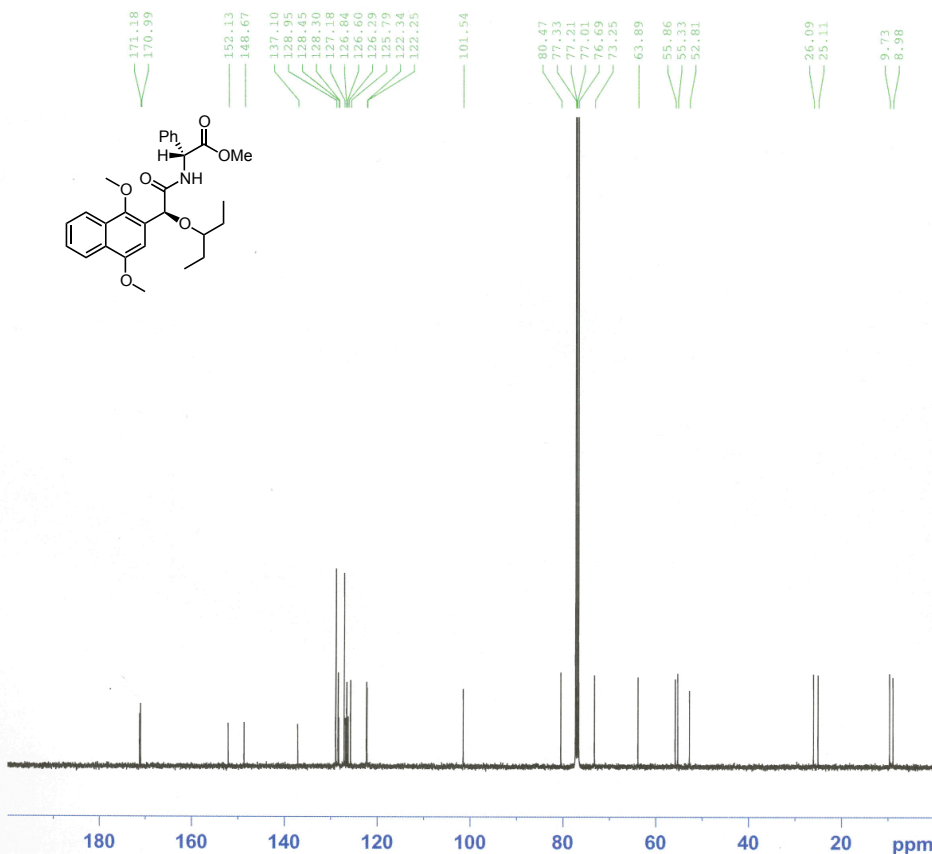
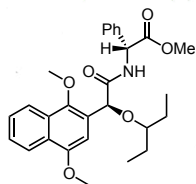


Current Data Parameters
 NAME Nov21-2011
 EXPNO 75
 PROCNO 1

F2 - Acquisition Parameters
 Date_ 20111121
 Time 19.06
 INSTRUM dpx400
 PROBHD 5 mm QNP 1H/29
 PULPROG zg30
 TD 32768
 SOLVENT DMSO
 NS 16
 DS 0
 SWH 8223.685 Hz
 FIDRES 0.250967 Hz
 AQ 1.9923444 sec
 RG 16384
 DW 60.800 usec
 DE 6.00 usec
 TE 303.2 K
 D1 1.00000000 sec
 MCREST 0.00000000 sec
 MCWRR 0.01500000 sec

===== CHANNEL f1 =====
 NUC1 1H
 P1 7.90 usec
 PL1 3.00 dB
 SFO1 400.1324710 MHz

F2 - Processing parameters
 SI 16384
 SF 400.1300089 MHz
 WDW EM
 SSB 0
 LB 0.30 Hz
 GB 0
 PC 1.00



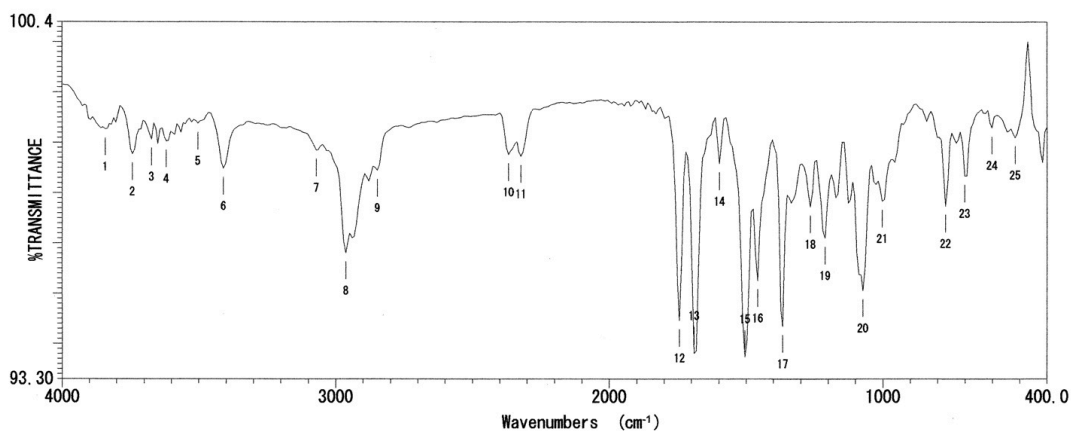
Current Data Parameters
NAME Mar15-2012-hayashi
EXPNO 200
PROCNO 1

F2 - Acquisition Parameters
Date_ 20120316
Time 5.31
INSTRUM spect
PROBHD 5 mm PABBO BB-
PULPROG zgpg30
TD 65536
SOLVENT CDCl3
NS 2000
DS 4
SWH 24038.461 Hz
FIDRES 0.366798 Hz
AQ 1.3631988 sec
RG 64
DW 20.800 usec
DE 6.00 usec
TE 303.4 K
D1 2.00000000 sec
d11 0.03000000 sec
DELTA 1.89999998 sec
TD0 1

===== CHANNEL f1 =====
NUC1 13C
P1 7.10 usec
PL1 -3.50 dB
SFO1 100.6354036 MHz

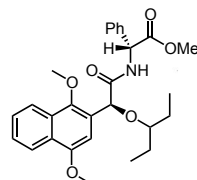
===== CHANNEL f2 =====
CPDPRG2 waltz16
NUC2 1H
PCPD2 80.00 usec
PL2 -1.50 dB
PL12 13.00 dB
PL13 13.00 dB
SFO2 400.1816007 MHz

F2 - Processing parameters
SI 32768
SF 100.6253410 MHz
WDW EM
SSB 0
LB 1.00 Hz
GB 0
PC 1.40

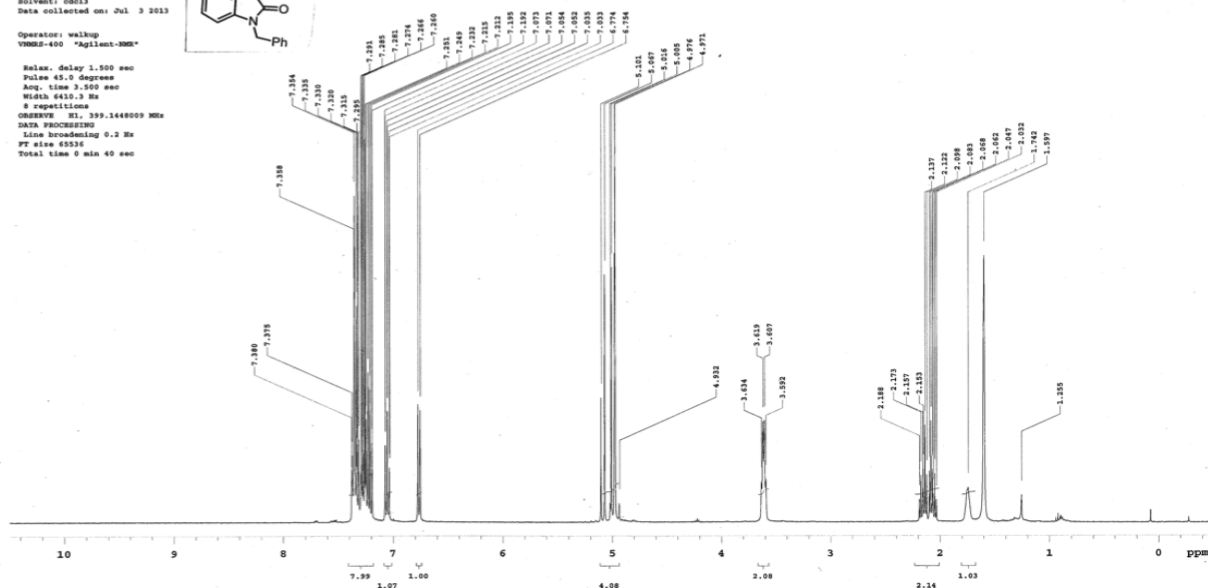
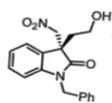


ピーク番号	波数 (cm⁻¹)	透過率 (%)	ピーク番号	波数 (cm⁻¹)	透過率 (%)
01	3841.51	98.2689	23	701.962	97.3377
02	3741.23	97.7739	24	601.682	98.2949
03	3671.80	98.0695	25	516.829	98.1003
04	3617.80	98.0273			
05	3502.10	98.3818			
06	3409.53	97.4897			
07	3070.12	97.8508			
08	2962.13	95.8099			
09	2846.42	97.4513			
10	2368.16	97.7608			
11	2321.87	97.7224			
12	1743.33	94.4657			
13	1689.34	93.8090			
14	1596.77	97.5796			
15	1504.20	93.7397			
16	1457.92	95.2553			
17	1365.35	94.3473			
18	1265.07	96.7261			
19	1211.08	96.1031			
20	1072.23	95.0595			
21	1002.80	96.8347			
22	771.387	96.7404			

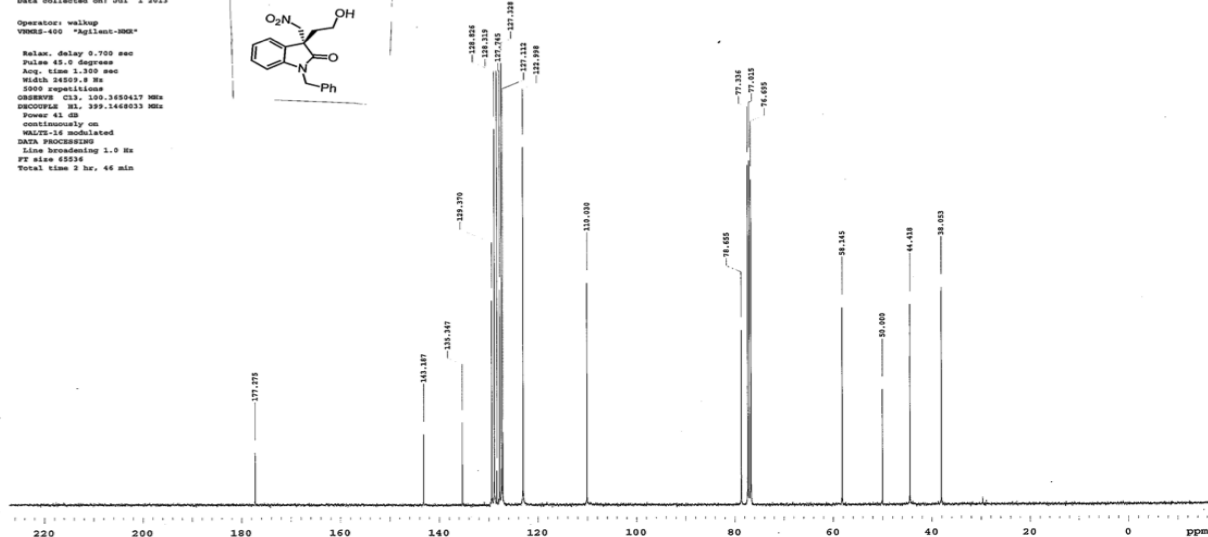
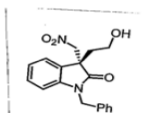
ファイル名 :
タイトル :
測定日時 : 2012年03月24日 10時26分33秒
測定分解能 : 16 cm⁻¹
スキャン回数 : 8 回
測定ゲイン : 1
コメント :

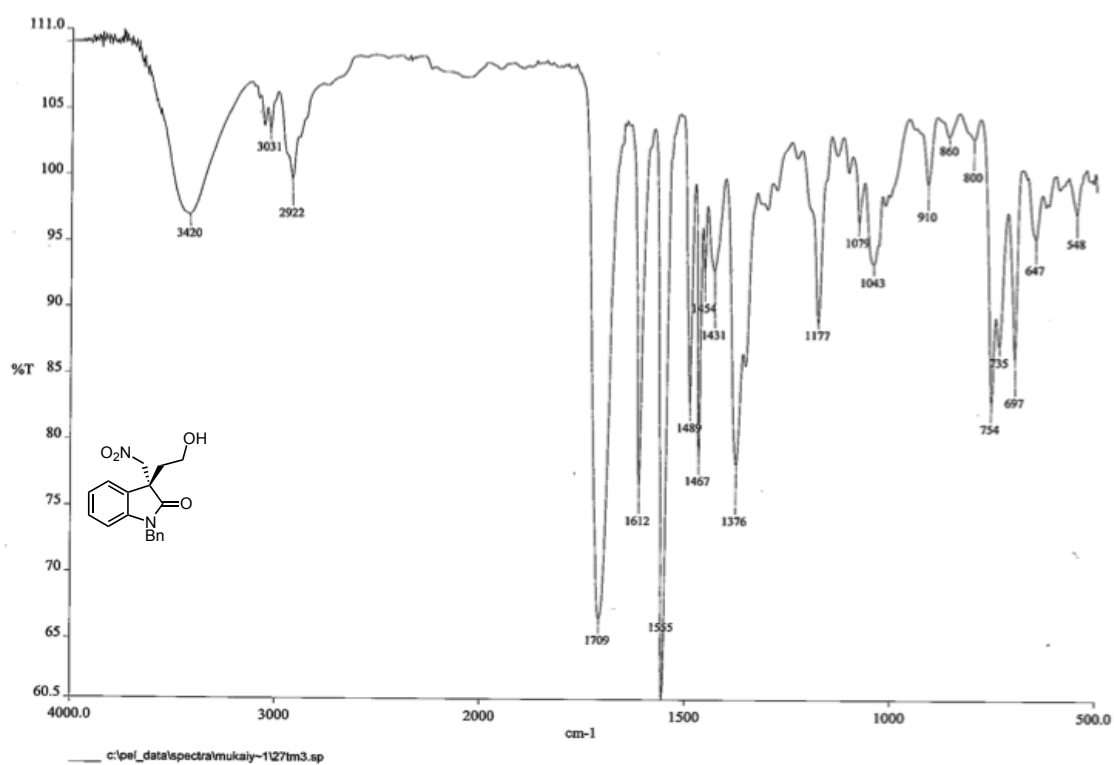


Sample Name:
 Archive directory:
 Sample directory:
 File: 27-3d4a
 Pulse Sequence: Proton (zgpg3)
 Solvent: cdcl3
 Data collected on: Jul 3 2013
 Operator: walkup
 VNMRS-400 "Agilent-VNMRS"
 Relax. delay: 1.500 sec
 Pulse: 45.0 degrees
 Acq. time: 1.500 sec
 Width: 6410.3 Hz
 9 repetitions
 OBSERVE: H1, 399.1448003 MHz
 DATA PROCESSING
 Line broadening: 0.2 Hz
 FT size: 65536
 Total time: 0 min 40 sec

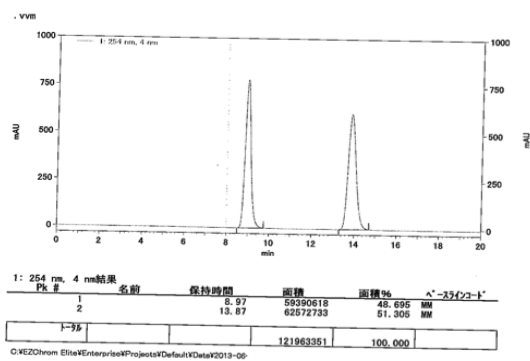


Sample Name:
 Archive directory:
 Sample directory:
 File: 27-3d4a
 Pulse Sequence: Carbon (zgpg3)
 Solvent: cdcl3
 Data collected on: Jul 3 2013
 Operator: walkup
 VNMRS-400 "Agilent-VNMRS"
 Relax. delay: 0.700 sec
 Pulse: 45.0 degrees
 Acq. time: 1.300 sec
 Width: 34507.8 Hz
 5000 repetitions
 OBSERVE: C13, 100.6250117 MHz
 DECOUPLE: H1, 399.1448033 MHz
 Power: 45.00
 continuously on
 MWD-16 modulated
 DATA PROCESSING
 Line broadening: 1.0 Hz
 FT size: 65536
 Total time: 2 hr, 46 min

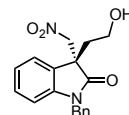
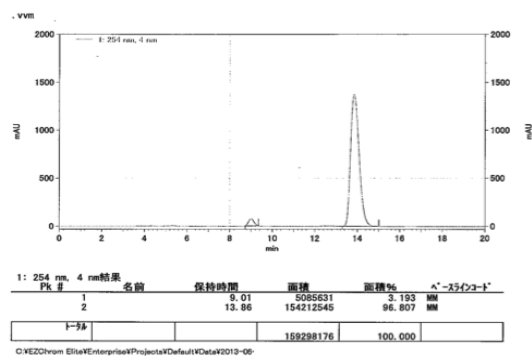




7-7776名: C:\VEZChrom Elite\Enterprise\Projects\Default\WData\2013-06-10 15-37-23
 mukaiyama IC 3vs1 1.0ml reami.dat
 77777776名: C:\VEZChrom Elite\Enterprise\Projects\Default\Method\10vs1. 1ml.met
 システム名: System
 分析日時: 2013/06/10 15:38:04
 印刷日時: 2013/06/12 19:44:56



7-7776名: C:\VEZChrom Elite\Enterprise\Projects\Default\WData\2013-06-10 15-59-06
 mukaiyama IC 3vs1 1.0ml 27-3.dat
 77777776名: C:\VEZChrom Elite\Enterprise\Projects\Default\Method\10vs1. 1ml.met
 システム名: System
 分析日時: 2013/06/10 15:59:46
 印刷日時: 2013/06/12 19:45:55



STANDARD IN OBSERVE - profile

Sample Name:

Archive directory:

Sample directory:

FidFile: 45-3

Pulse Sequence: Proton (zgpg3)

Solvent: cdcl3

Data collected on: Jun 18 2013

Operator: walkup

VNMRS-400 "Agilent-VNM"

Relax. delay 1.500 sec

Pulse 45.0 degrees

Aq. time 3.500 sec

Width 6410.3 Hz

repetitions

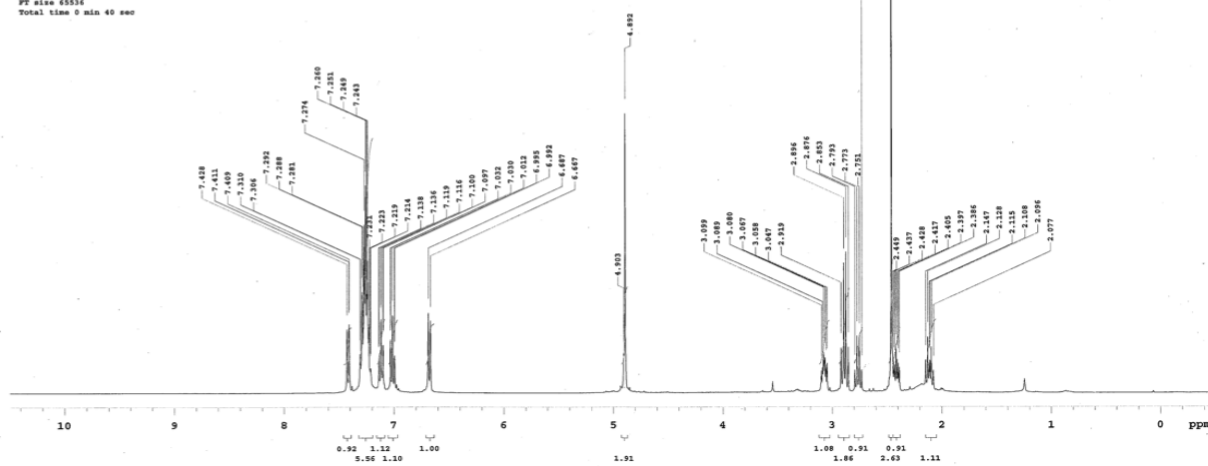
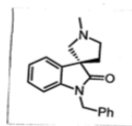
OBSERVE H1, 399.1448076 MHz

DATA PROCESSING

Line broadening 0.2 Hz

FT size 65536

Total time 0 min. 40 sec



STANDARD IN OBSERVE - profile

Sample Name:

Archive directory:

Sample directory:

FidFile: 45-3carbon

Pulse Sequence: Carbon (zgpg3)

Solvent: cdcl3

Data collected on: Jun 18 2013

Operator: walkup

VNMRS-400 "Agilent-VNM"

Relax. delay 0.700 sec

Pulse 45.0 degrees

Aq. time 1.300 sec

Width 24500.0 Hz

5000 repetitions

OBSERVE C13, 100.6250440 MHz

DECOUPLE H1, 399.1448076 MHz

Power 41.00

continuously on

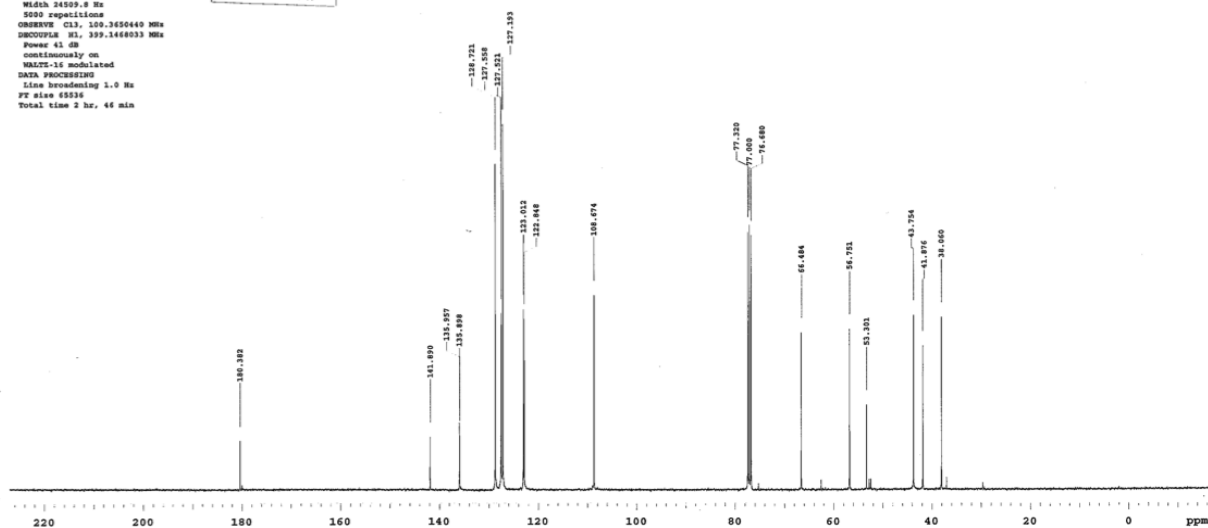
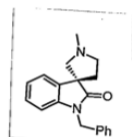
WALTZ-16 modulated

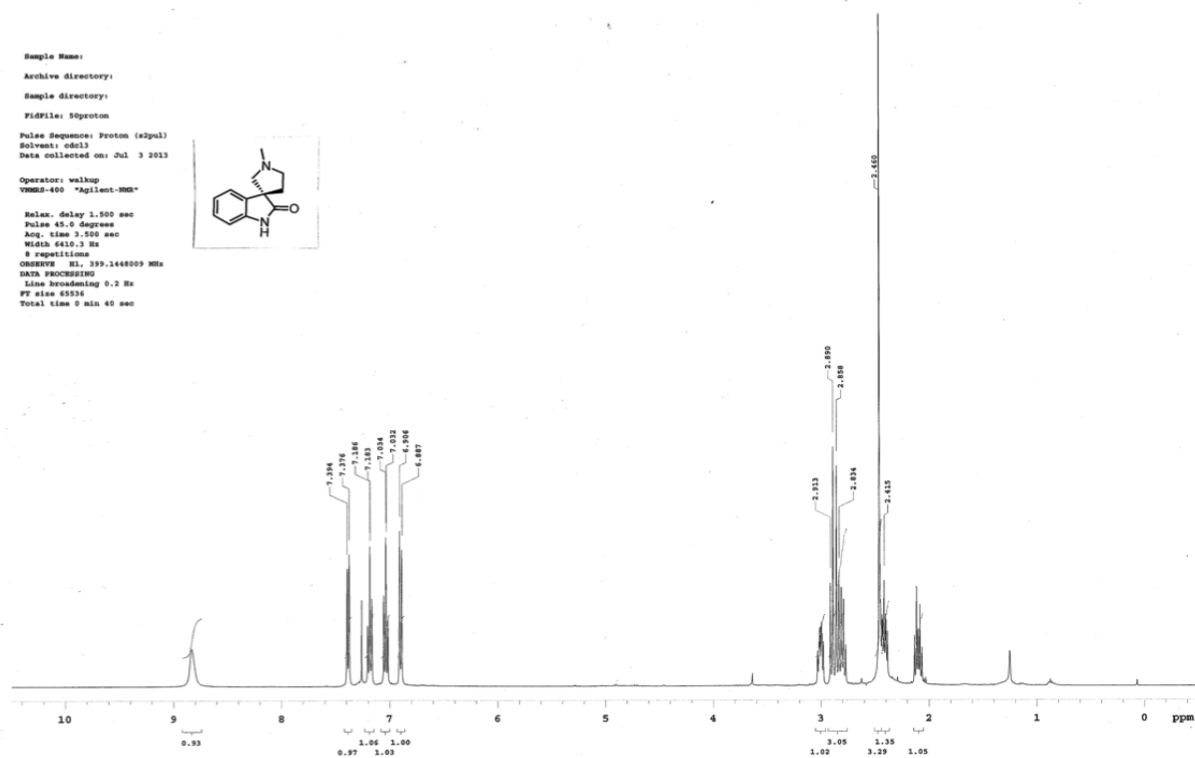
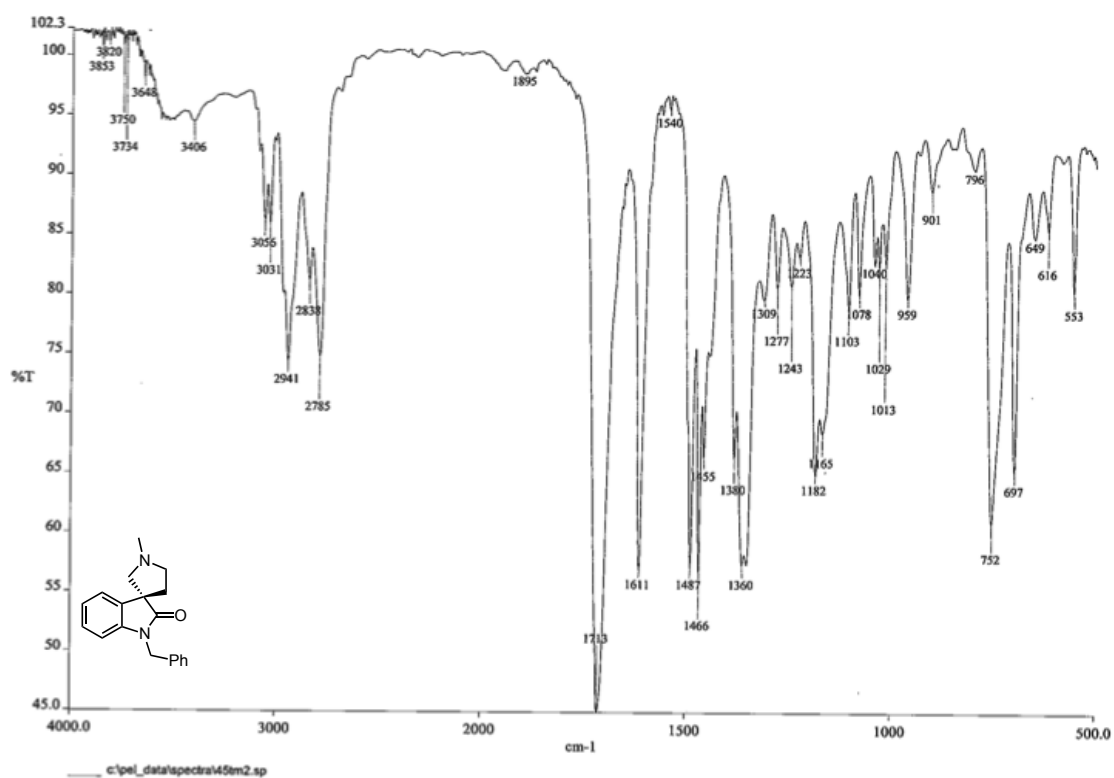
DATA PROCESSING

Line broadening 1.0 Hz

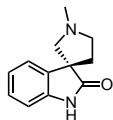
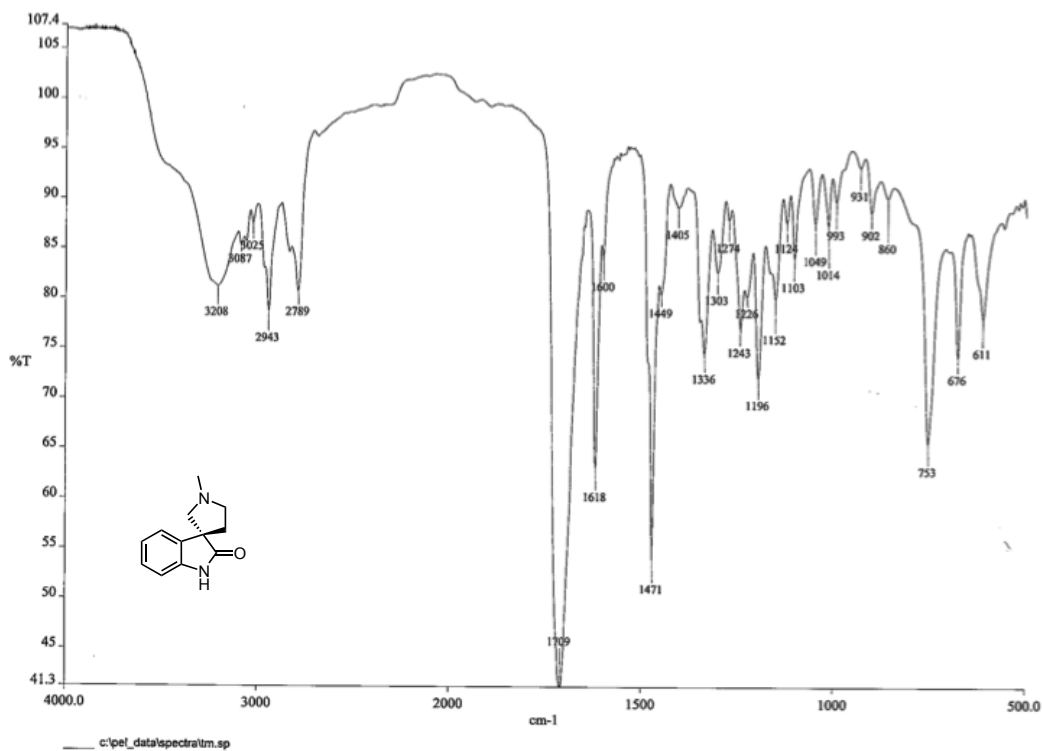
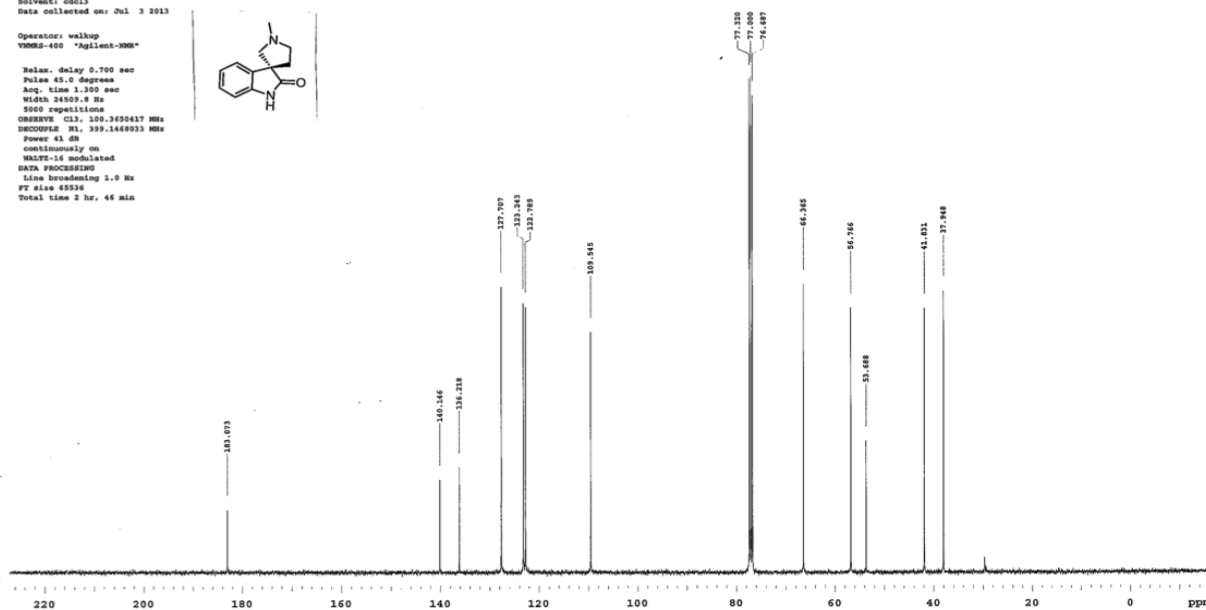
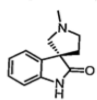
FT size 65536

Total time 2 hr, 46 min

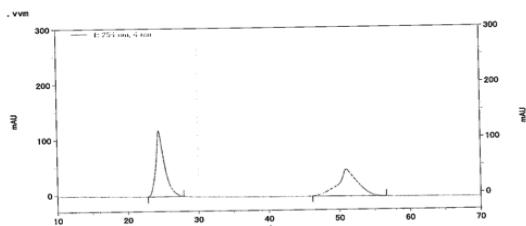




Sample Name:
 Archive directory:
 Sample directory:
 File: 504000
 Pulse Sequence: Carbon (zgpg30)
 Solvent: cdcl3
 Data collected on: Jul 3 2013
 Operator: walkup
 VENDOR: agilent-300m
 Relax. delay: 5.700 sec
 Pulse: zgpg30
 Acq. time: 1.300 sec
 Width: 24509.8 Hz
 5000 repetitions
 OBSERVE: C13, 100.6250417 MHz
 DECOUPLE: H1, 100.6250417 MHz
 Power: 41 dB
 continuously on
 WALTZ-16 modulated
 DATA PROCESSING
 Line broadening: 1.0 Hz
 FT size: 65536
 Total time: 2 hr, 46 min

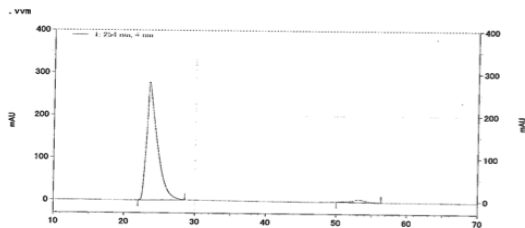


9'-97748名: C:\VEZChrom EliteEnterprise\Projects\Default\WData\2013-07-15 13-36-39
 mukaiyama AS-H 10vs1 1 ml racem 64-2.dat
 97747748名: C:\VEZChrom EliteEnterprise\Projects\Default\WMethod\10vs1. 1ml.met
 システム名: System
 分析日時: 2013/07/15 13:37:21
 印刷日時: 2013/07/15 16:17:38

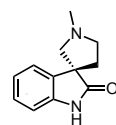


1: 254 nm, 4 nm結果	Peak #	名前	保持時間	面積	面積%	ピークタイプ
	1		24.45	40758317	52.252	MM
	2		50.96	37244547	47.748	MM
	トータル			78002864	100.000	

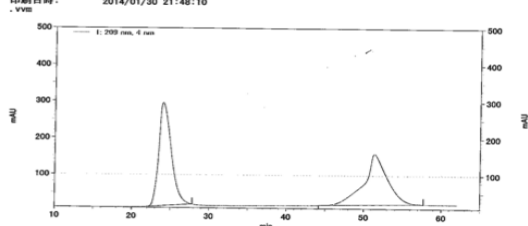
9'-97748名: C:\VEZChrom EliteEnterprise\Projects\Default\WData\2013-07-15 14-55-04
 mukaiyama AS-H 10vs1 1 ml 50-3.dat
 97747748名: C:\VEZChrom EliteEnterprise\Projects\Default\WMethod\10vs1. 1ml.met
 システム名: System
 分析日時: 2013/07/15 14:55:49
 印刷日時: 2013/07/15 16:16:47



1: 254 nm, 4 nm結果	Peak #	名前	保持時間	面積	面積%	ピークタイプ
	1		23.53	114491214	97.166	MM
	2		53.18	3339046	2.834	MM
	トータル			117830260	100.000	



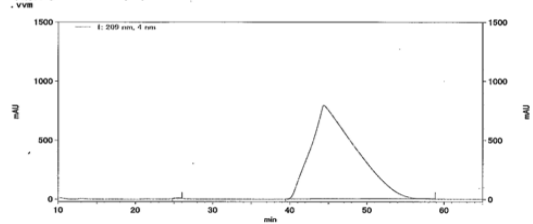
システム名: System
 分析日時: 2014/01/30 19:34:15
 印刷日時: 2014/01/30 21:48:10



1: 209 nm, 4 nm結果	Peak #	名前	保持時間	面積	面積%	ピークタイプ
	1		24.00	123756977	51.528	MM
	2		51.37	118790061	48.372	MM
	トータル			242547038	100.000	

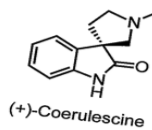
C:\VEZChrom EliteEnterprise\Projects\Default\WData\2014-01-

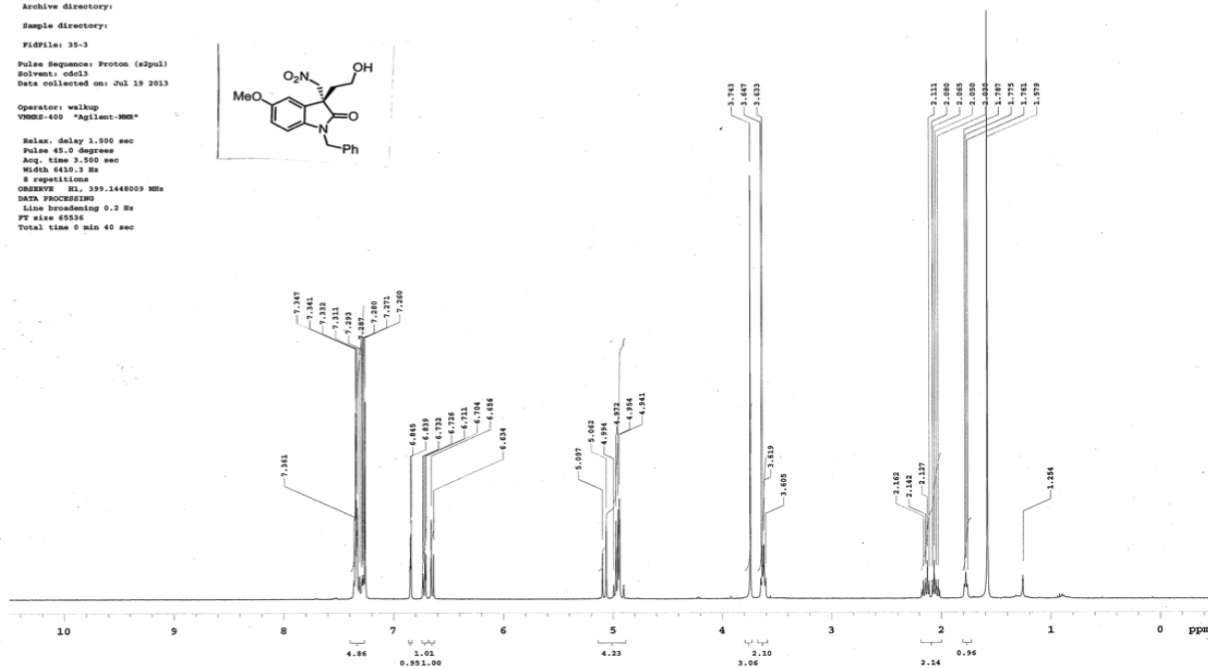
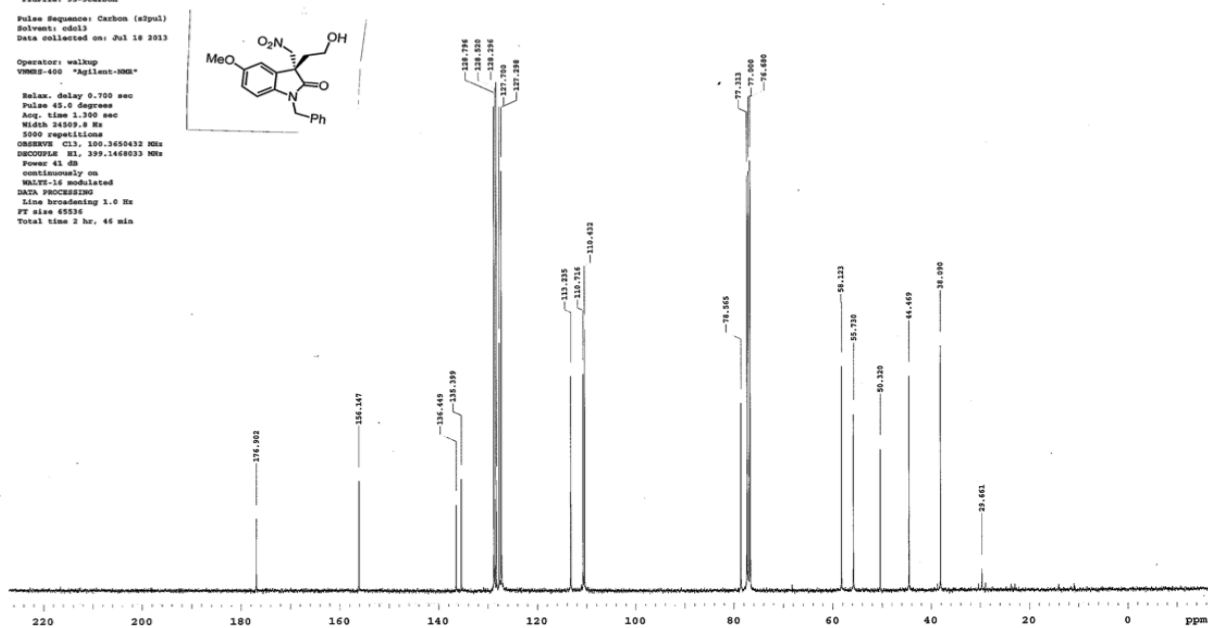
mukaiyama AS-H 10vs1 162-2.dat
 97747748名: C:\VEZChrom EliteEnterprise\Projects\Default\WMethod\10vs1. 1ml.met
 システム名: System
 分析日時: 2014/01/30 20:37:35
 印刷日時: 2014/01/30 22:04:01

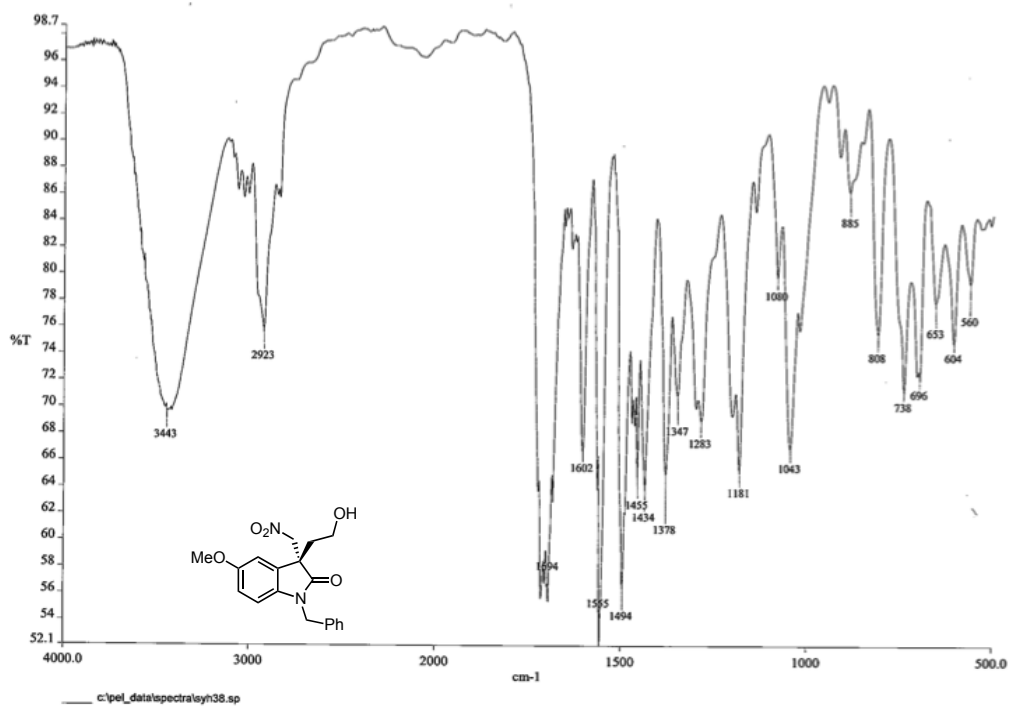


1: 209 nm, 4 nm結果	Peak #	名前	保持時間	面積	面積%	ピークタイプ
	1		25.44	884520	0.068	MM
	2		44.39	1284190431	99.932	MM
	トータル			1285074951	100.000	

C:\VEZChrom EliteEnterprise\Projects\Default\WData\2014-01-



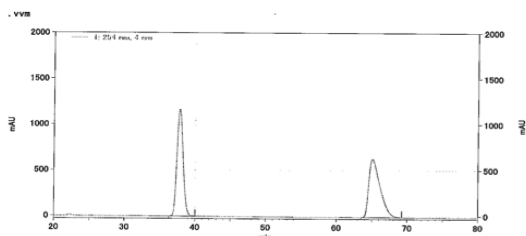
COc1ccc2c(c1)c(c[nH]2)C(=O)N(Cc3ccccc3)[C@H](CO)C(=O)NCOc1ccc2c(c1)c(c[nH]2)C(=O)N(Cc3ccccc3)[C@H](CO)[C@@H](O)N=[N+]([O-])=O



面積%レポート

ページ 1/1

データファイル名: C:\WEZChrom Elite\Enterprise\Projects\Default\Data\2013-06-27 10-25-36
 opata_1-119 IC 10vs1_1ml raceml.dat
 ファイル名: C:\WEZChrom Elite\Enterprise\Projects\Default\Method\10vs1_1ml.met
 システム名: System
 分析日時: 2013/06/27 10:26:19
 印刷日時: 2013/06/27 15:51:36

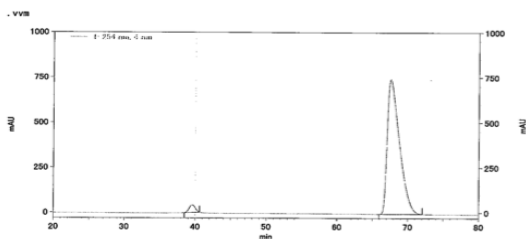


PK #	名前	保持時間	面積	面積%	ピーク番号
1		37.65	281878461	49.983	MM
2		65.10	282070873	50.017	MM
合計			563949334	100.000	

C:\WEZChrom Elite\Enterprise\Projects\Default\Data\2013-06

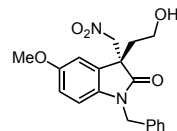
面積%レポート

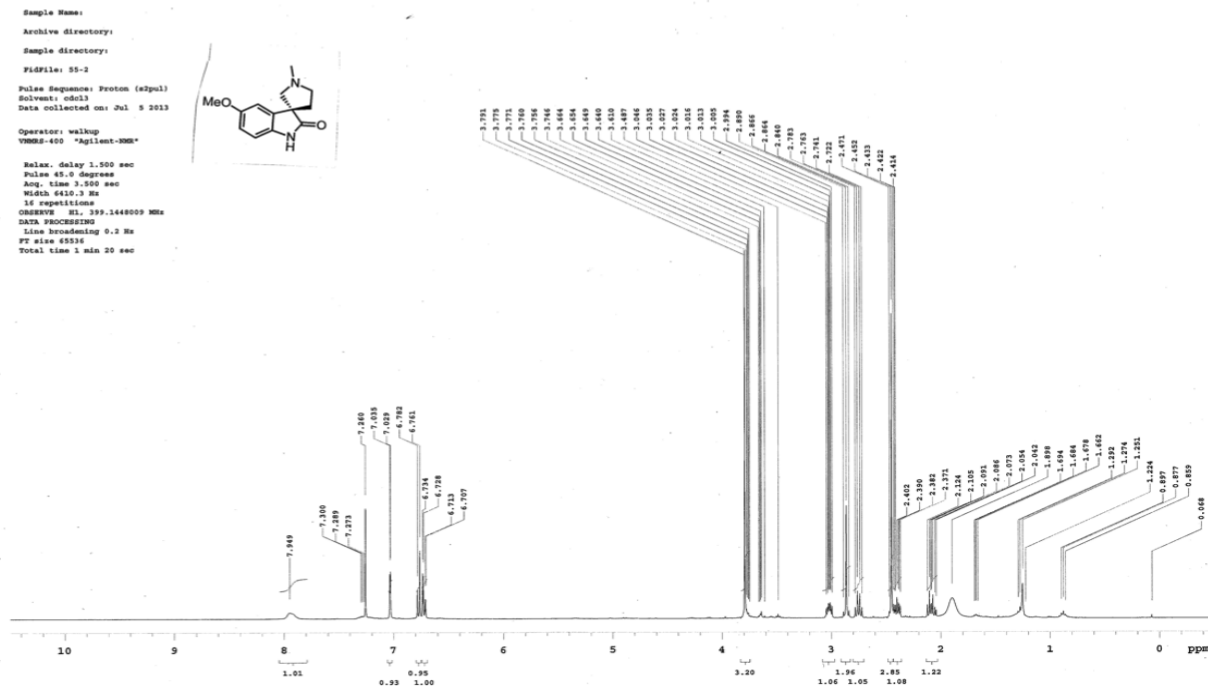
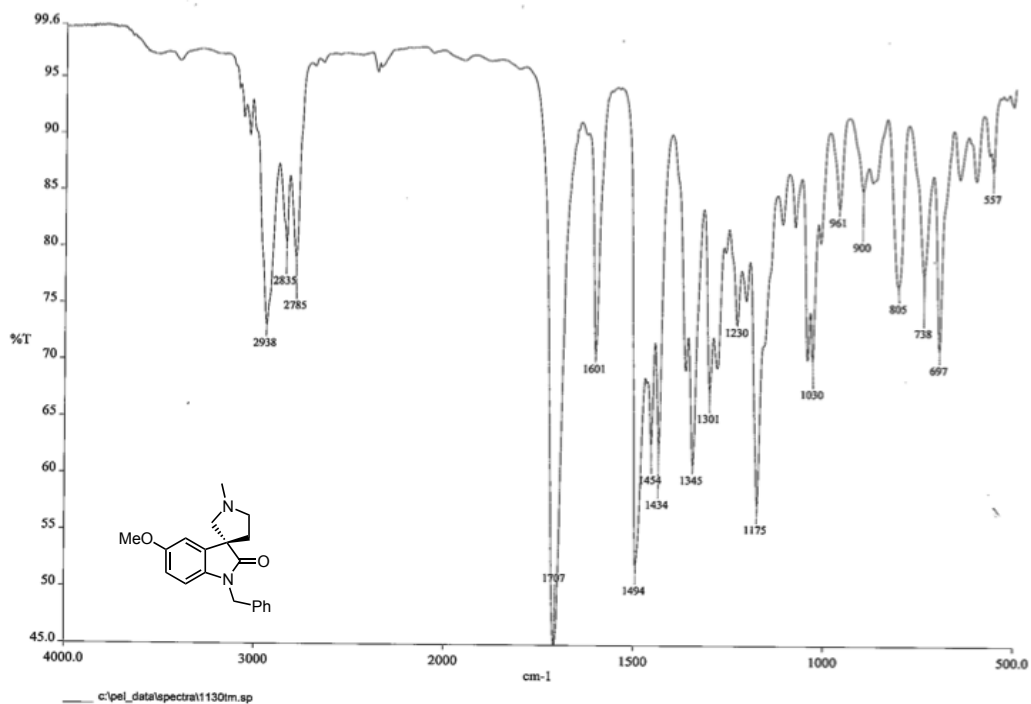
データファイル名: C:\WEZChrom Elite\Enterprise\Projects\Default\Data\2013-06-27 12-25-44
 mukaiyama IC 10vs1_1ml 35-3.dat
 ファイル名: C:\WEZChrom Elite\Enterprise\Projects\Default\Method\10vs1_1ml.met
 システム名: System
 分析日時: 2013/06/27 12:27:09
 印刷日時: 2013/06/27 15:52:27



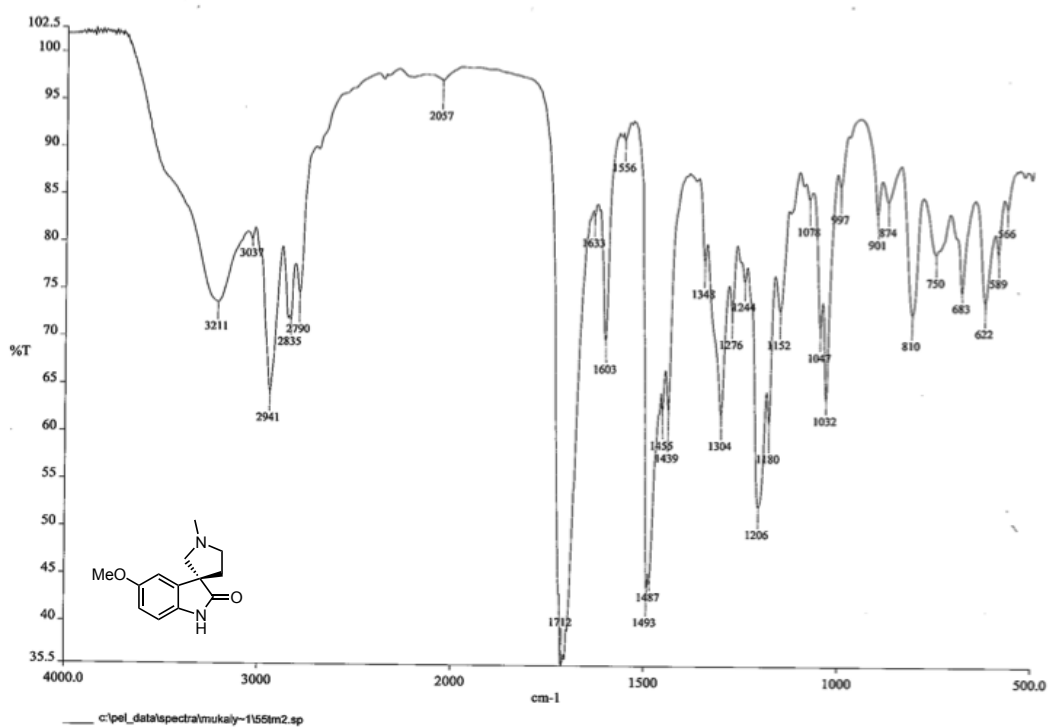
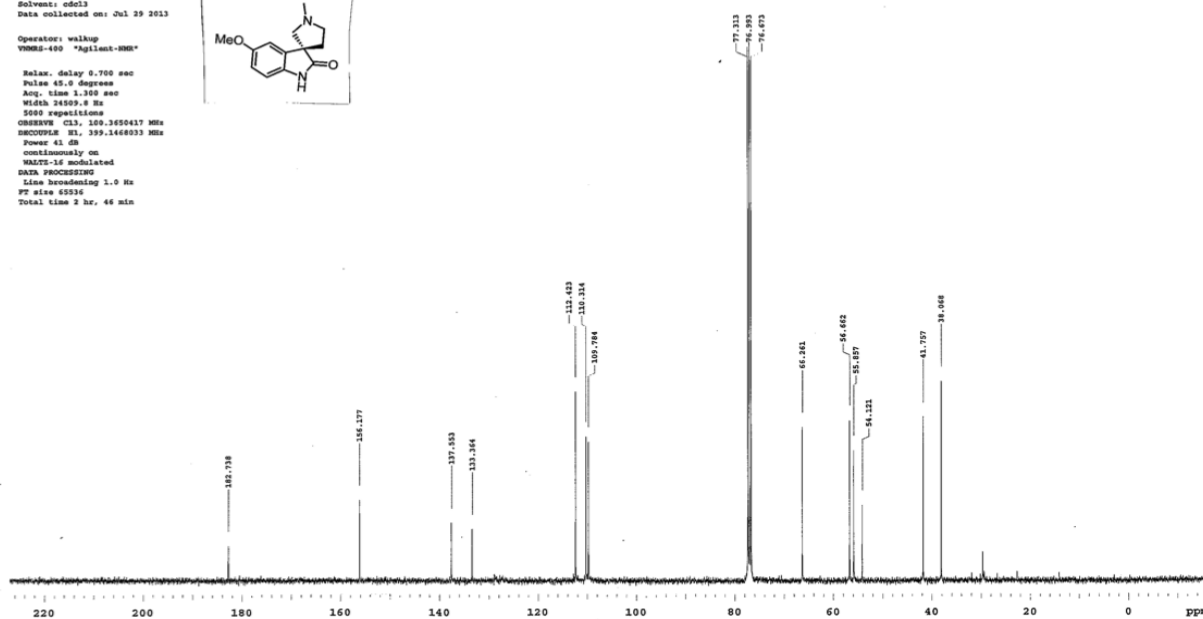
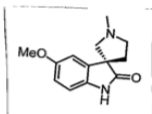
PK #	名前	保持時間	面積	面積%	ピーク番号
1		39.63	10071381	2.734	MM
2		67.59	358362469	97.266	MM
合計			368433850	100.000	

C:\WEZChrom Elite\Enterprise\Projects\Default\Data\2013-06



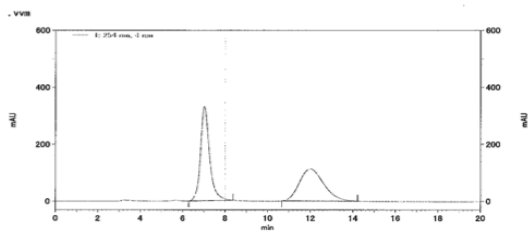


Sample Name:
 Archive directory:
 Sample directory:
 File: borefiline-carbon
 Pulse Sequence: Carbon (zgpg3)
 Solvent: cdcl3
 Data collected on: Jul 29 2012
 Operator: walkup
 VENDOR: Agilent-400
 Pulse: delay 0.700 sec
 Pulse: 45.0 degrees
 Acq. time 1.300 sec
 VSWH 24507.0 Hz
 5000 repetitions
 OBSERVE CL3, 100.625017 MHz
 DECUPLE 93, 199.1468033 MHz
 Power 41 dB
 continuously on
 WALTZ-16 modulated
 DATA PROCESSING
 Line broadening 1.0 Hz
 FT size 65536
 Total time 2 hr, 44 min



面積%レポート

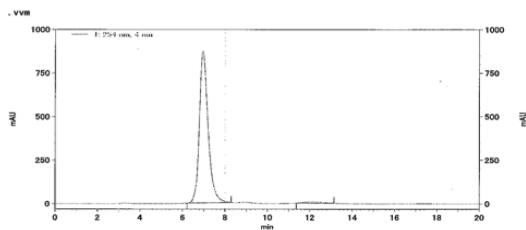
ファイル名: C:\VEZChrom\EliteEnterprise\Projects\Default\data\2013-07-18 22-17-28
 mukaiyama OB-H 10vol 1 ml 60-2 raceml.dat
 ファイル名: C:\VEZChrom\EliteEnterprise\Projects\Default\data\2013-07-18 22-17-28
 ユーザー名: System
 分析日時: 2013/07/18 22:18:08
 印刷日時: 2013/07/18 23:14:40



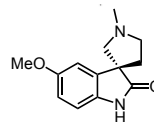
PK #	名前	保持時間	面積	面積%	ピークタイプ
1		7.03	35311873	52.386	MM
2		12.00	35731273	47.614	MM
トータル			75043146	100.000	

面積%レポート

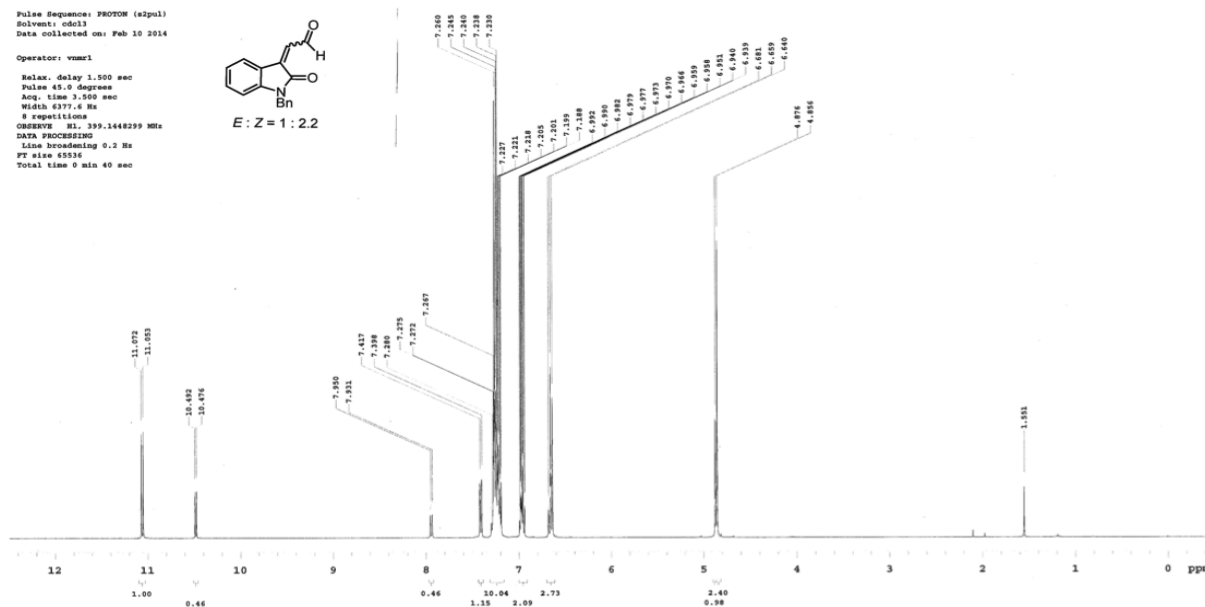
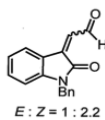
ファイル名: C:\VEZChrom\EliteEnterprise\Projects\Default\data\2013-07-18 22-47-05
 mukaiyama OB-H 10vol 1 ml 55-2 horafilline.dat
 ファイル名: C:\VEZChrom\EliteEnterprise\Projects\Default\data\2013-07-18 22-47-05
 ユーザー名: System
 分析日時: 2013/07/18 22:47:44
 印刷日時: 2013/07/18 23:13:55



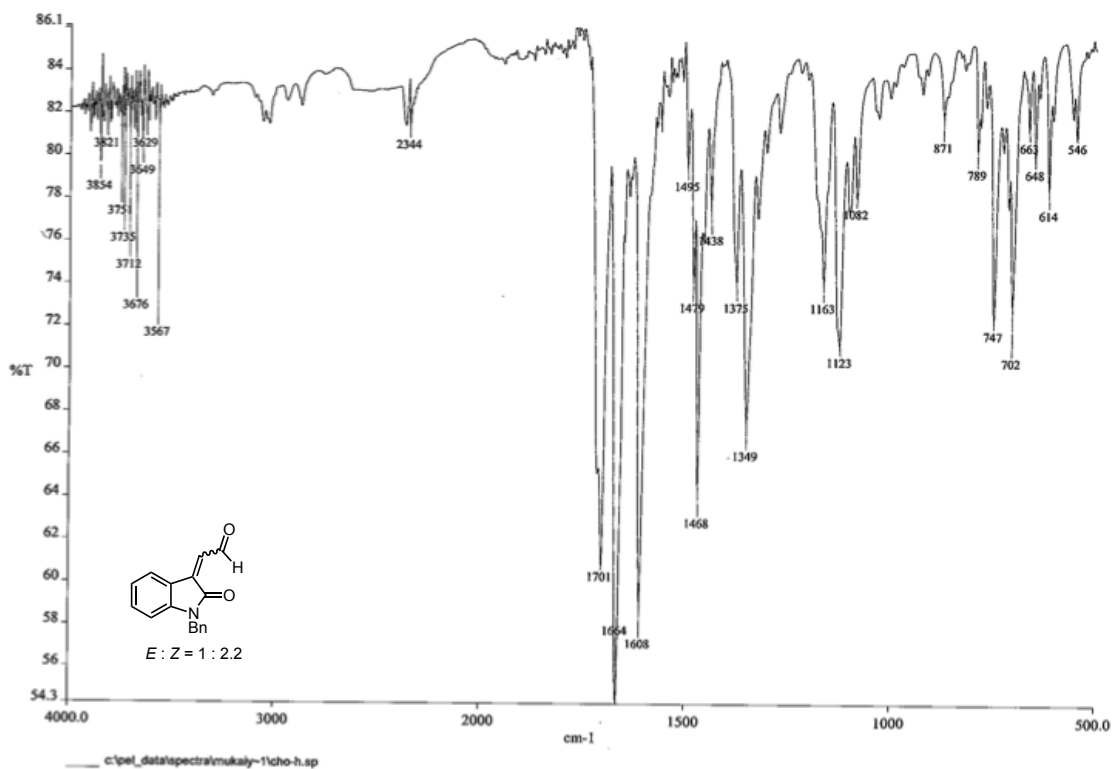
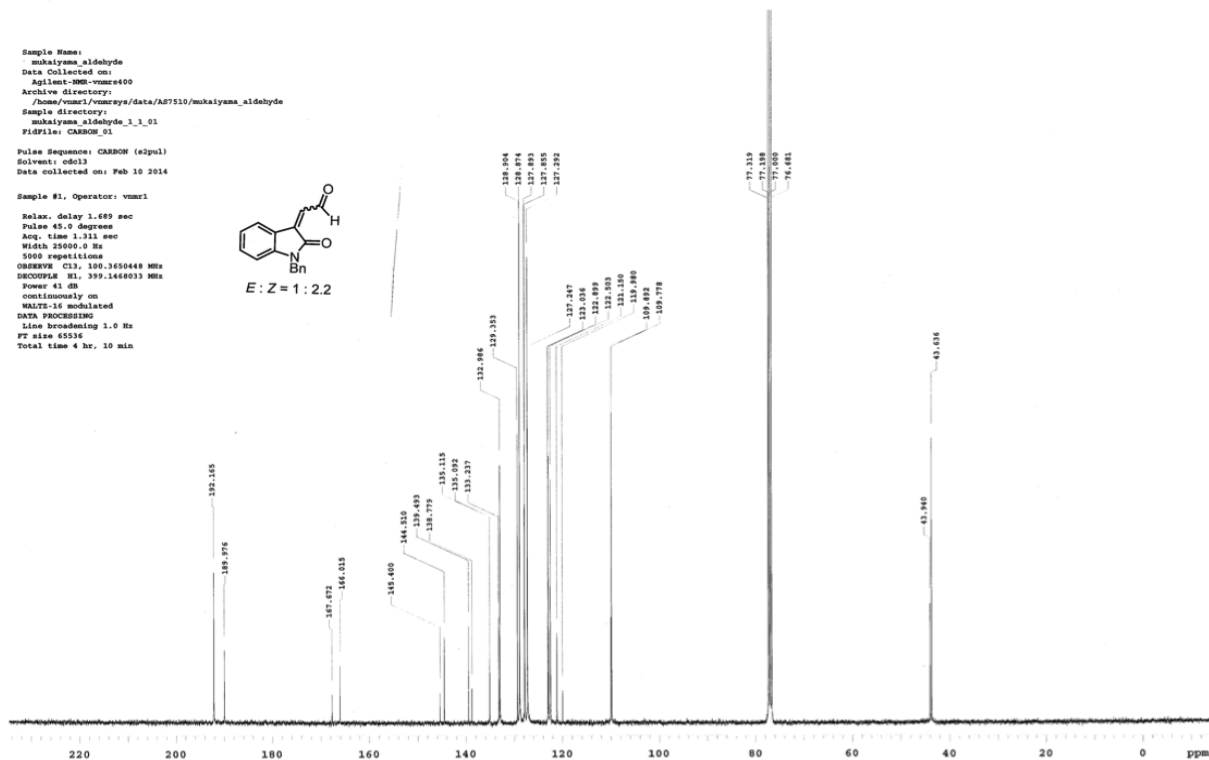
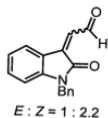
PK #	名前	保持時間	面積	面積%	ピークタイプ
1		6.97	95970211	98.262	MM
2		12.11	1768095	1.738	MM
トータル			101738306	100.000	



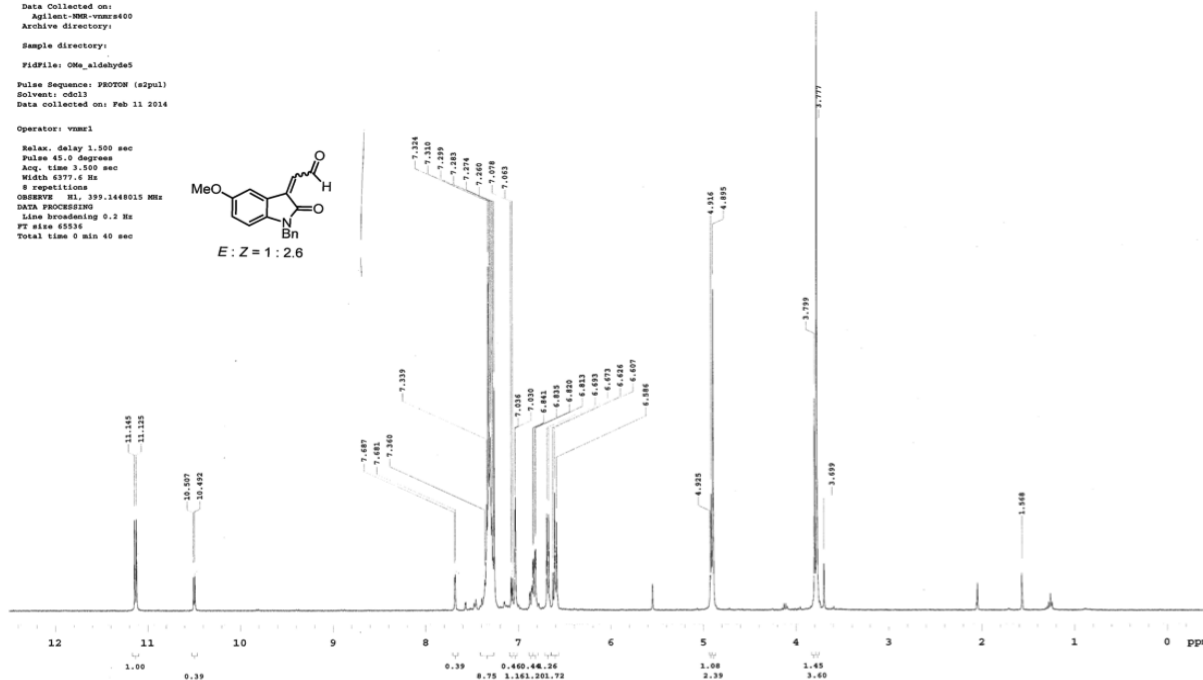
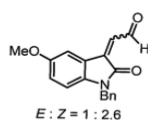
Sample Name:
 Data Collected on:
 Agilent-300-vnmr400
 Archive directory:
 Sample directory:
 File: PROTON
 Pulse Sequence: PROTON (zgpg3)
 Solvent: cdcl3
 Data collected on: Feb 10 2014
 Operator: vnmr1
 Relax. delay 1.500 sec
 Pulse 45.0 degree
 Acq. time 3.550 sec
 Width 6377.4 Hz
 8 repetitions
 OBSERVE M1, 399.1448299 MHz
 DATA PROCESSING
 Line broadening 0.2 Hz
 FT size 65536
 Total time 0 min 40 sec



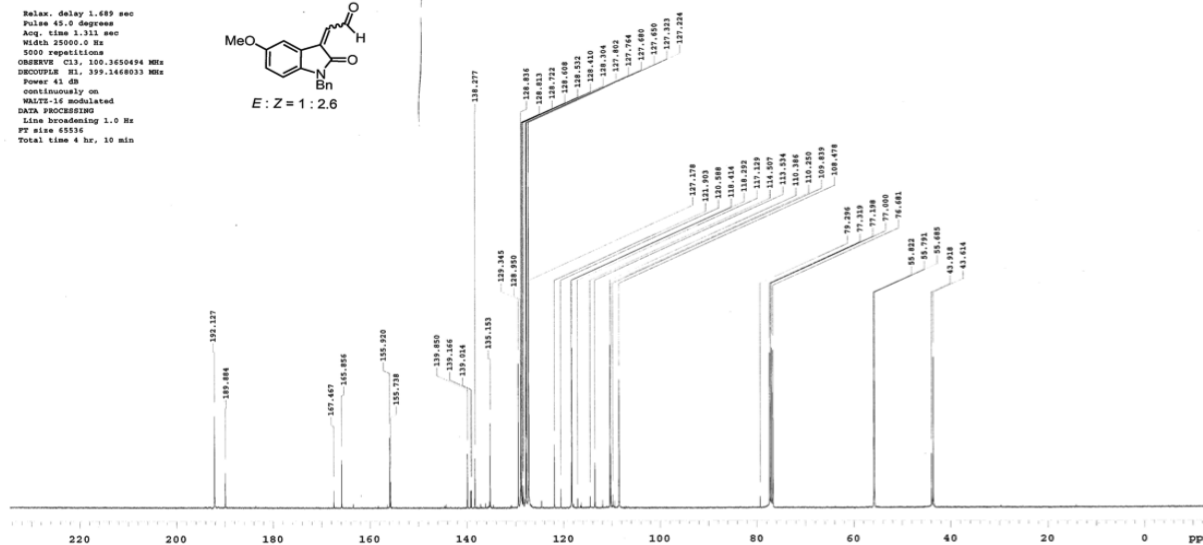
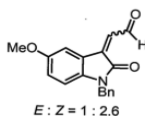
Sample Name: mukaiyama_aldehyde
 Data Collected on: Agilent-900-vnmr400
 Archive directory: /home/vnmr1/vnmr400/data/AS7510/mukaiyama_aldehyde
 Sample directory: mukaiyama_aldehyde_1_1_01
 FIDFile: CARBON_01
 Pulse Sequence: CARBON (e2pul)
 Solvent: cdcl3
 Data collected on: Feb 10 2014
 Sample #1, Operator: vnmr1
 Relax, delay 1.689 sec
 Pulse 45.0 degrees
 Acq. time 1.313 sec
 Width 25000.0 Hz
 5000 repetitions
 OBSERVE C13, 100.3650448 MHz
 DECOUPLE H1, 399.1460033 MHz
 Power 41 dB
 continuously on
 WALTZ-16 modulated
 DATA PROCESSING
 Line broadening 1.0 Hz
 FT size 45536
 Total time 4 hr, 10 min

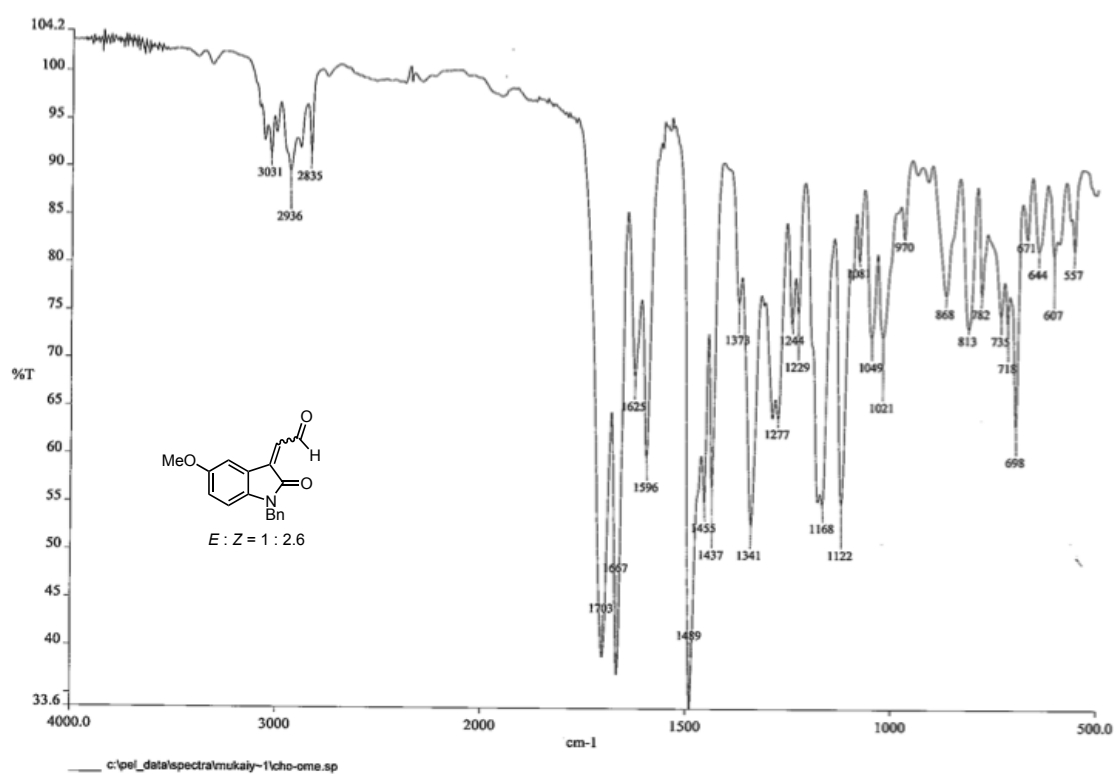


Sample Name:
 Date Collected on:
 Agilent-MMS-vmmr400
 Archive directory:
 Sample directory:
 Fidfile: CMO_aldehyde5
 Pulse Sequence: PROTON (s2pul)
 Solvent: cdcl3
 Data collected on: Feb 11 2014
 Operator: vmmr1
 Relax. delay 1.500 sec
 Pulse 45.0 degrees
 Acq. time 1.500 sec
 Width 6377.6 Hz
 8 repetitions
 OBSERVE H1, 399.1448015 MHz
 DATA PROCESSING
 Line broadening 0.2 Hz
 FT size 65536
 Total time 0 min 40 sec

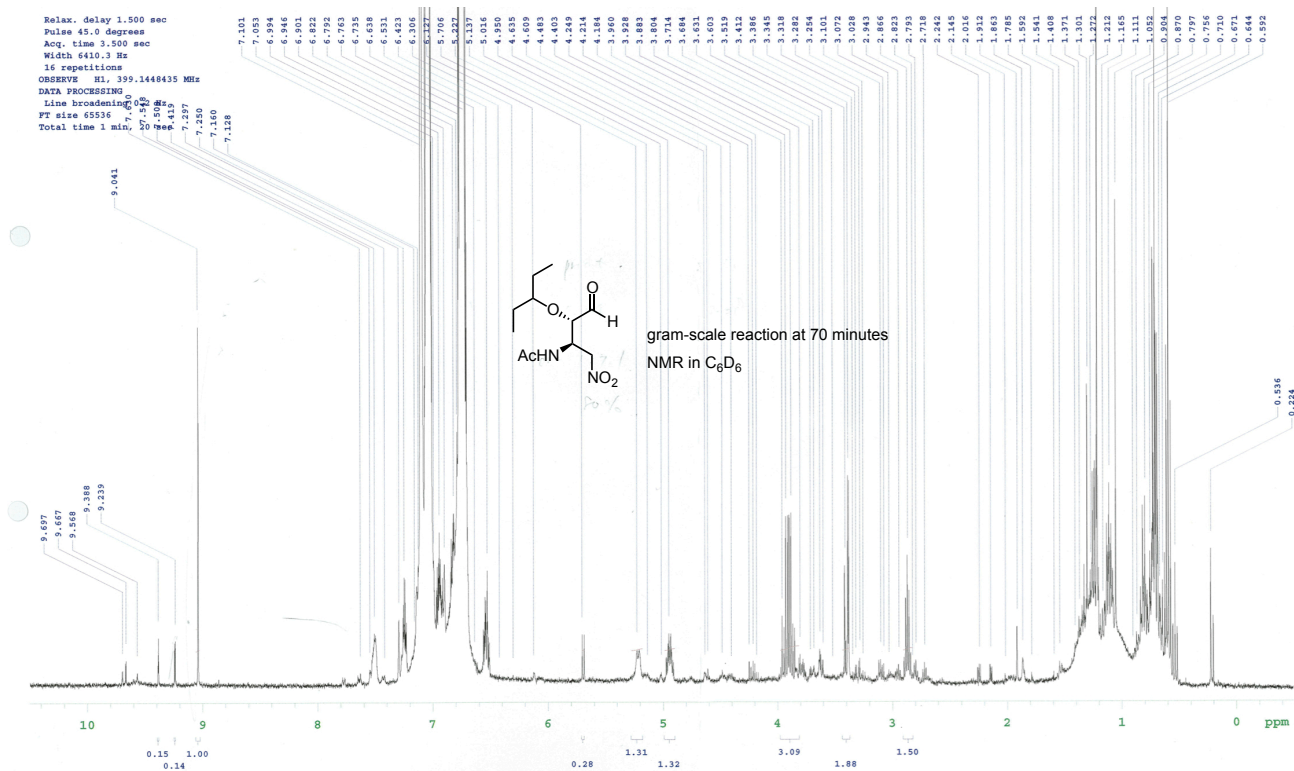
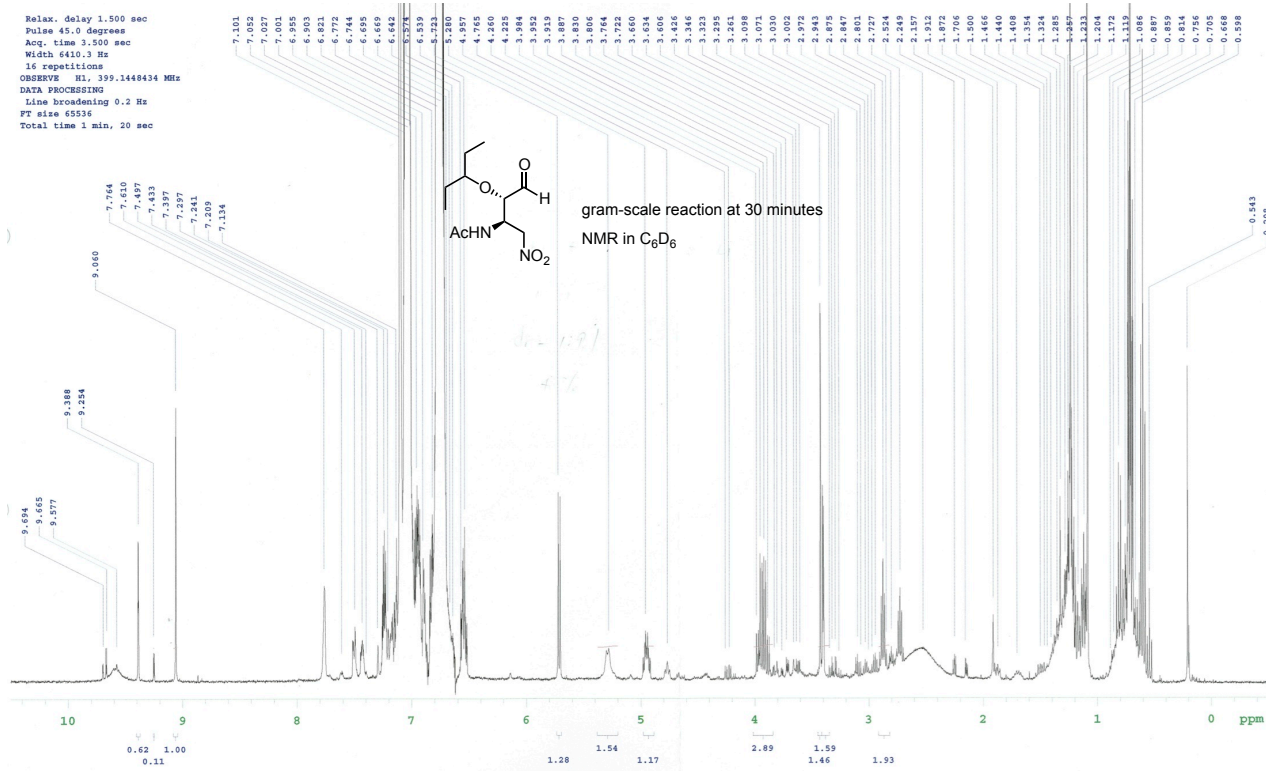


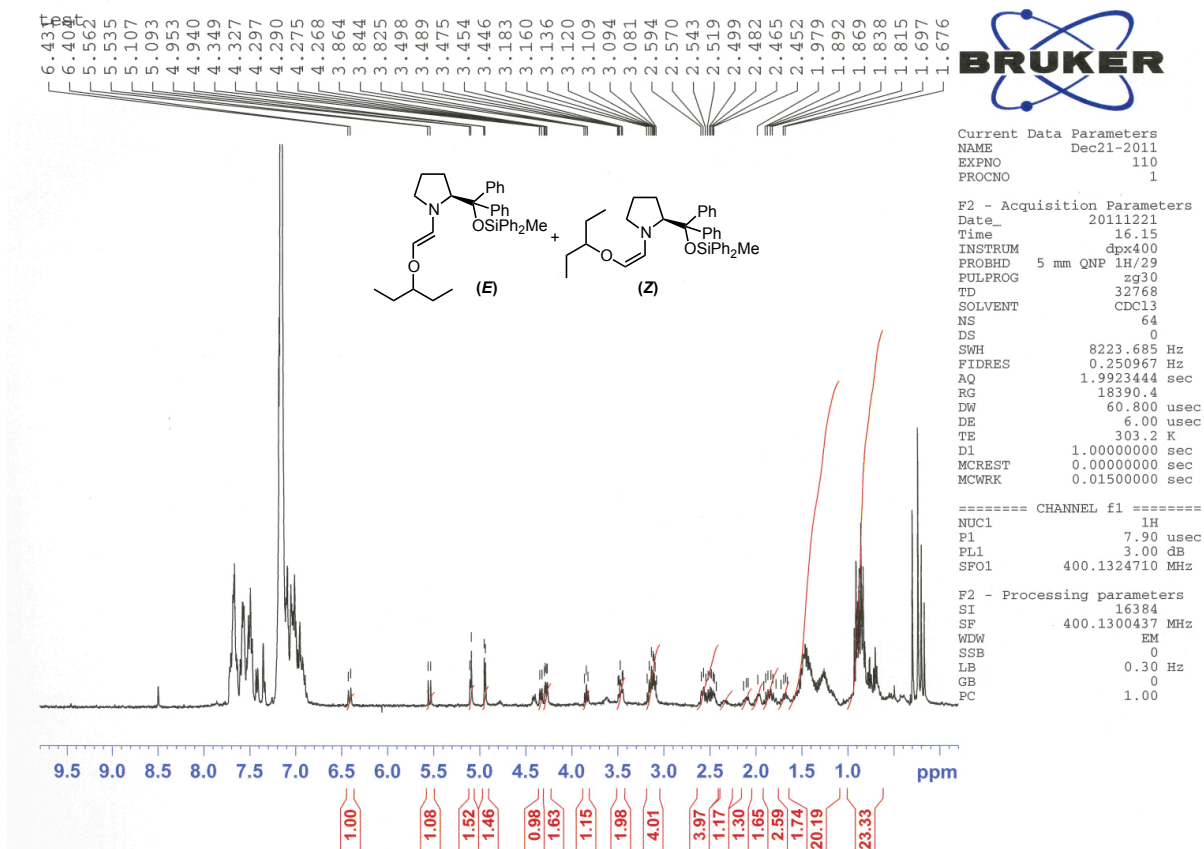
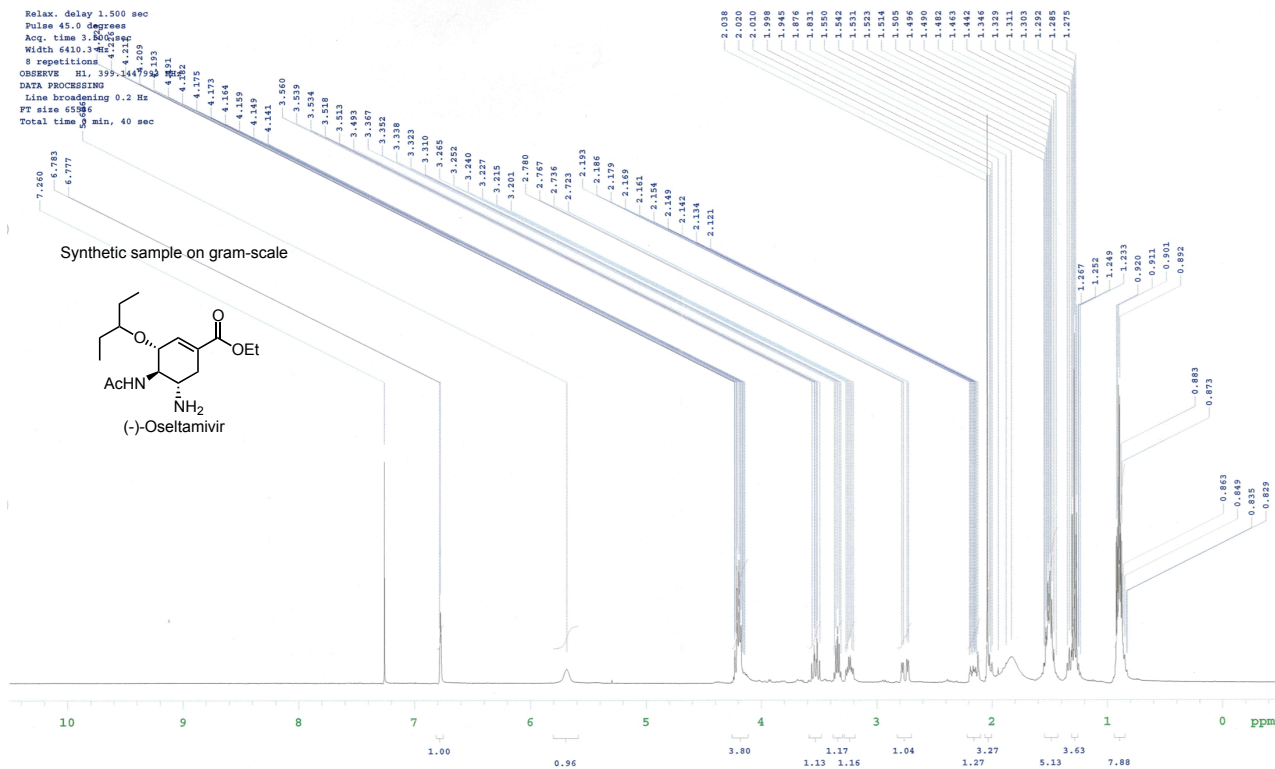
Sample Name:
 CMO_Ome
 Date Collected on:
 Agilent-MMS-vmmr400
 Archive directory:
 /home/vmmr1/vmmr400/Data/AG7510/CMO_Ome
 Sample directory:
 CMO_Ome_1_1_01
 Fidfile: CARBON_01
 Pulse Sequence: CARBON (s2pul)
 Solvent: cdcl3
 Data collected on: Feb 14 2014
 Sample #9, Operator: vmmr1
 Relax. delay 1.689 sec
 Pulse 45.0 degrees
 Acq. time 1.313 sec
 Width 25000.0 Hz
 5000 repetitions
 OBSERVE C13, 100.350494 MHz
 DECOUPLE H1, 399.1468033 MHz
 Power 41 dB
 continuously on
 WALTZ-16 modulated
 DATA PROCESSING
 Line broadening 1.0 Hz
 FT size 65536
 Total time 8 hr, 10 min

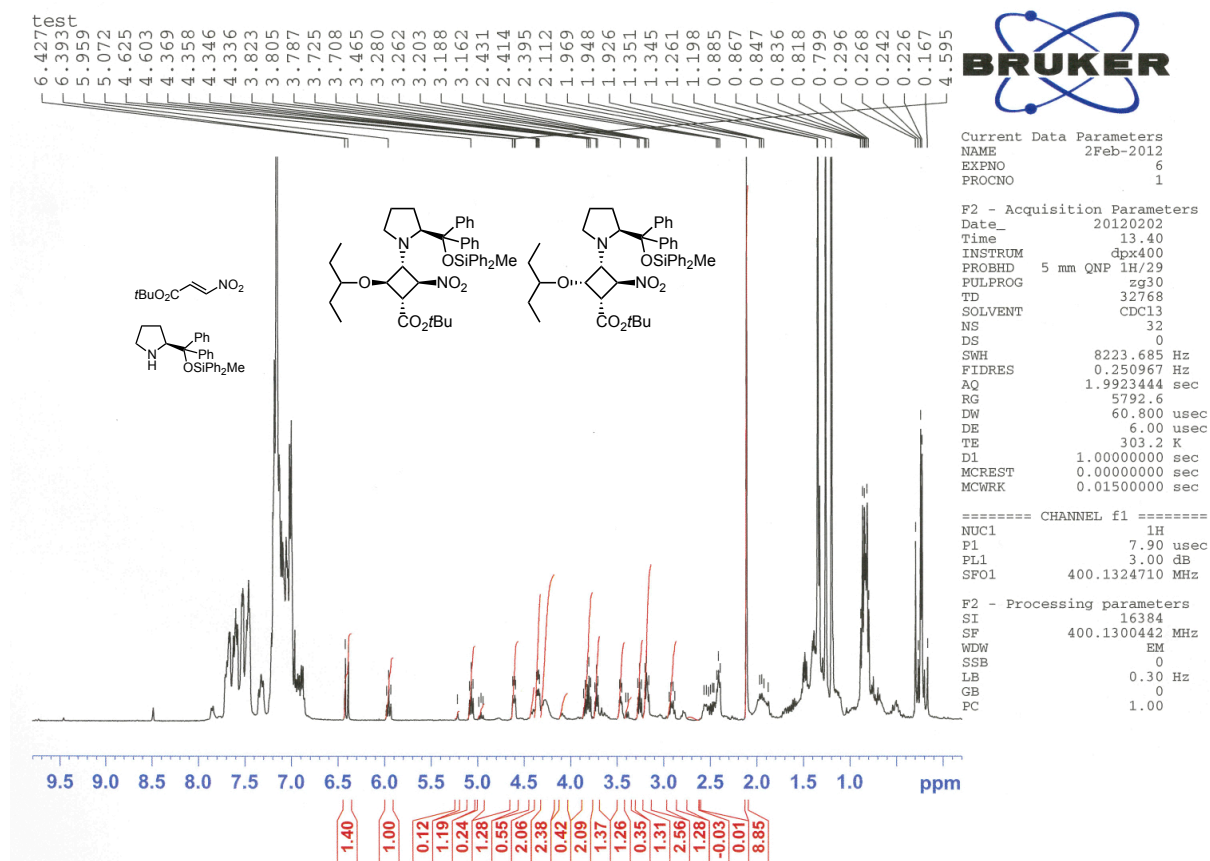


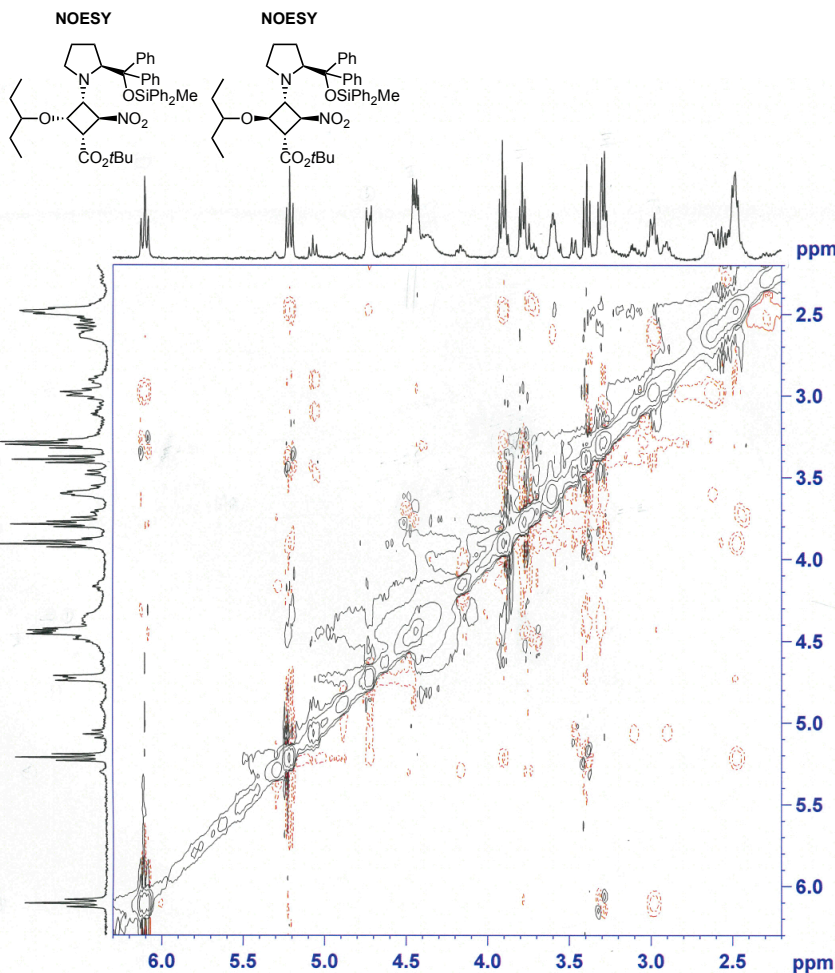


Spectra









Current Data Parameters
 NAME Feb03-2012-hayashi
 EXPNO 51
 PROCNO 1

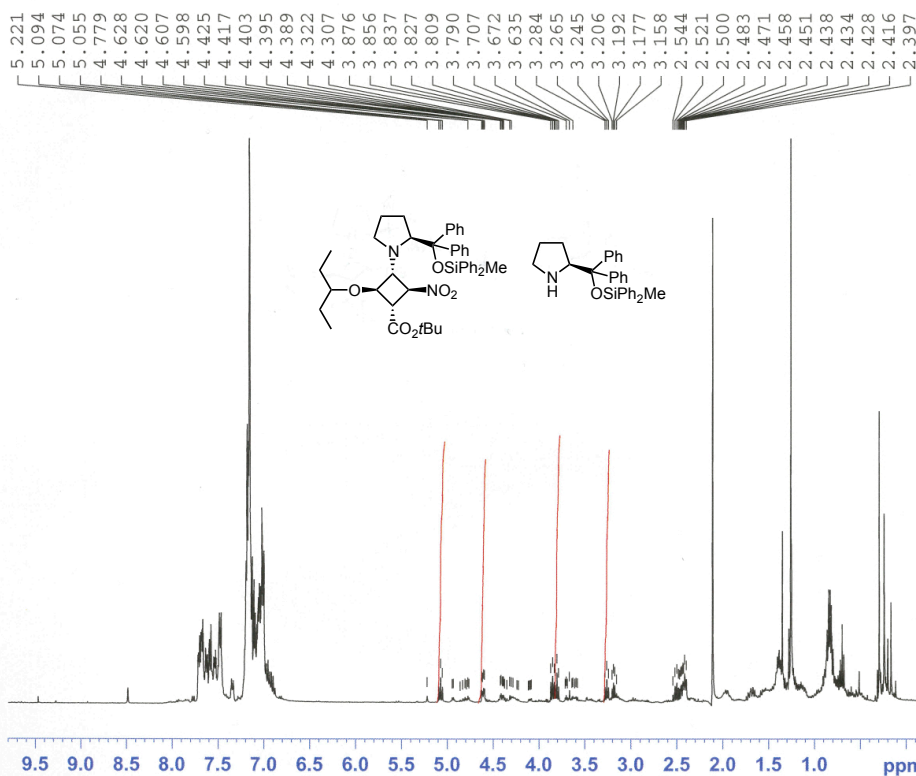
F2 - Acquisition Parameters
 Date_ 20120203
 Time 17.31
 INSTRUM spect
 PROBHD 5 mm PABBO BB-
 PULPROG noesyph
 TD 2048
 SOLVENT C6D6
 NS 16
 DS 4
 SWH 3787.879 Hz
 FIDRES 1.849550 Hz
 AQ 0.2703860 sec
 RG 114
 DW 132.000 usec
 DE 6.00 usec
 TE 280.5 K
 d0 0.00011545 sec
 D1 1.98033905 sec
 D8 0.30000001 sec
 INO 0.00026400 sec
 STICNT 128

===== CHANNEL f1 =====
 NUC1 1H
 P1 13.00 usec
 PL1 -3.40 dB
 SFO1 400.1815635 MHz

F1 - Acquisition parameters
 ND0 1
 TD 256
 SFO1 400.1816 MHz
 FIDRES 14.796402 Hz
 SW 9.465 ppm
 FMODE States-TPPI

F2 - Processing parameters
 SI 1024
 SF 400.1800000 MHz
 WDW QSINE
 SSB 2
 LB 0.00 Hz
 GB 0
 PC 1.00

F1 - Processing parameters
 SI 1024
 MC2 States-TPPI
 SF 400.1800000 MHz
 WDW QSINE
 SSB 2
 LB 0.00 Hz
 GB 0

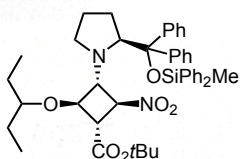


Current Data Parameters
NAME Feb01-2012
EXPNO 126
PROCNO 1

F2 - Acquisition Parameters
Date_ 20120201
Time 21.15
INSTRUM dpx400
PROBHD 5 mm QNP 1H/29
PULPROG zg30
TD 32768
SOLVENT CDC13
NS 32
DS 0
SWH 8223.685 Hz
FIDRES 0.250967 Hz
AQ 1.9923444 sec
RG 5792.6
DW 60.800 usec
DE 6.00 usec
TE 303.2 K
DL 1.00000000 sec
MCREST 0.00000000 sec
MCWRK 0.01500000 sec

===== CHANNEL f1 =====
NUC1 1H
P1 7.90 usec
PL1 3.00 dB
SFO1 400.1324710 MHz

F2 - Processing parameters
SI 16384
SF 400.1300442 MHz
WDW EM
SSB 0
LB 0.30 Hz
GB 0
PC 1.00



Current Data Parameters
NAME Feb01-2012-hayashi
EXPNO 221
PROCNO 1

F2 - Acquisition Parameters
Date_ 20120202
Time 6.46
INSTRUM spect
PROBHD 5 mm PABBO BB-
PULPROG noesyph
TD 2048
SOLVENT C6D6
NS 16
DS 4
SWH 4032.258 Hz
FIDRES 1.968876 Hz
AQ 0.2540020 sec
RG 64
DW 124.000 usec
DE 6.00 usec
TE 301.7 K
d0 0.00010745 sec
D1 1.99672306 sec
D8 0.30000001 sec
INO 0.00024800 sec
ST1CNT 128

===== CHANNEL f1 =====
NUC1 1H
P1 13.00 usec
PL1 -3.40 dB
SFO1 400.1814762 MHz

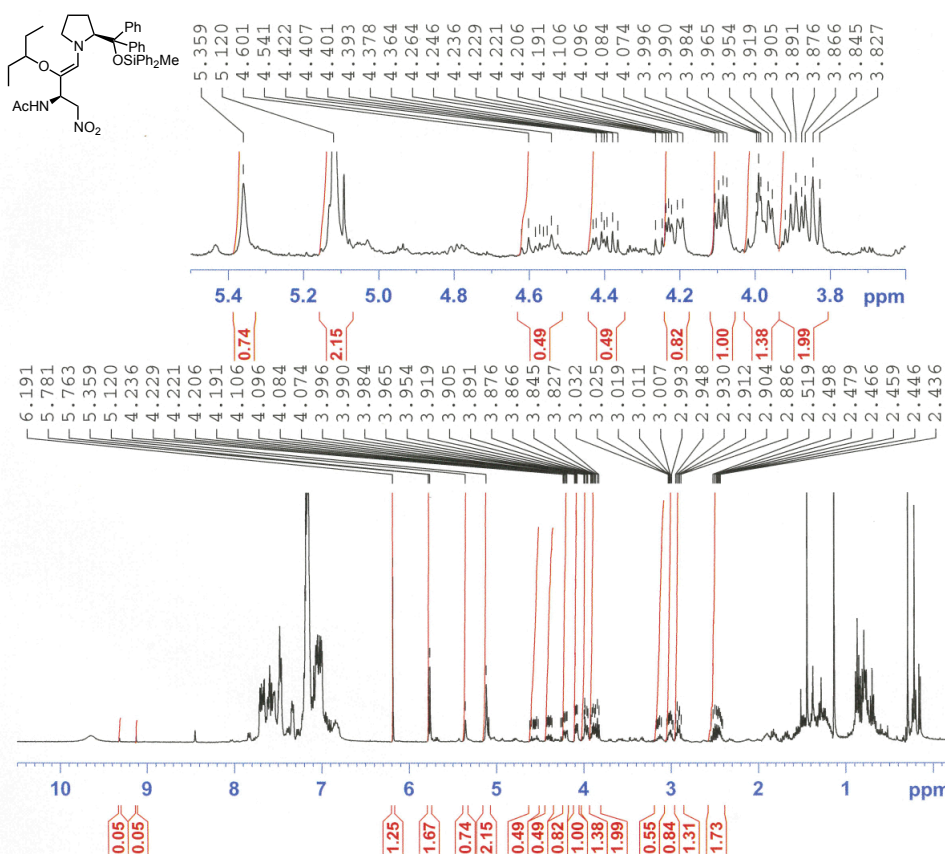
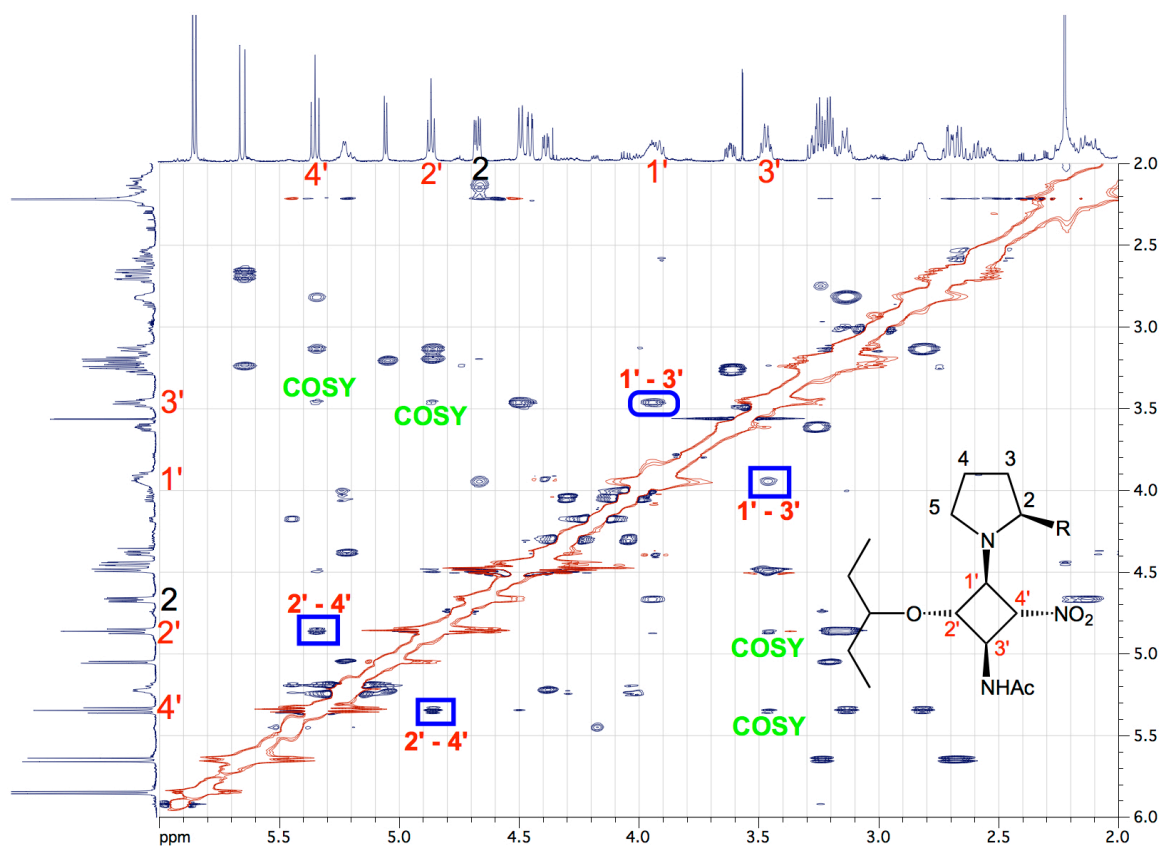
F1 - Acquisition parameters
ND0 1
TD 256
SFO1 400.1815 MHz
FIDRES 15.751008 Hz
SW 10.076 ppm
FnMODE States-TPPI

F2 - Processing parameters
SI 1024
SF 400.1800895 MHz
WDW QSINE
SSB 2
LB 0.00 Hz
GB 0
PC 1.00

F1 - Processing parameters
SI 1024
MC2 States-TPPI
SF 400.1800895 MHz
WDW QSINE
SSB 2
LB 0.00 Hz
GB 0



NOESY

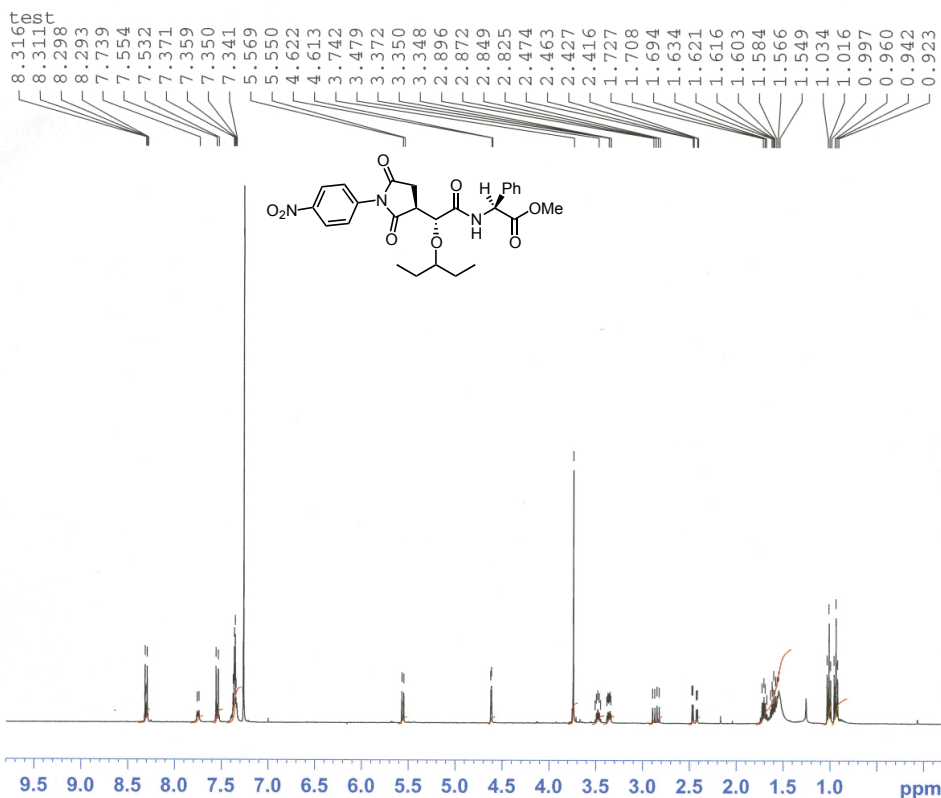


Current Data Parameters
 NAME Jan12-2012-hayashi
 EXPNO 270
 PROCNO 1

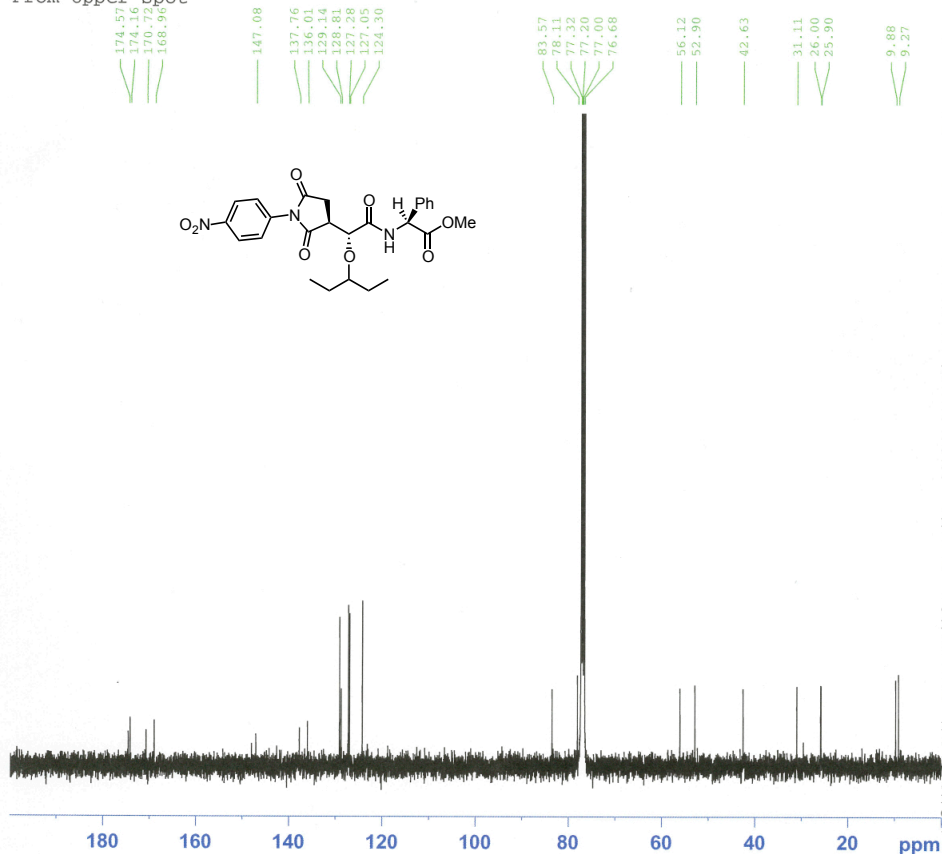
F2 - Acquisition Parameters
 Date_ 20120112
 Time 21.27
 INSTRUM spect
 PROBHD 5 mm PABBO BB-
 PULPROG zg30
 TD 65536
 SOLVENT C6D6
 NS 16
 DS 2
 SWH 8223.685 Hz
 FIDRES 0.125483 Hz
 AQ 3.9846387 sec
 RG 287
 DW 60.800 usec
 DE 303.4 K
 TE 1.00000000 sec
 D1 1
 TD0 1

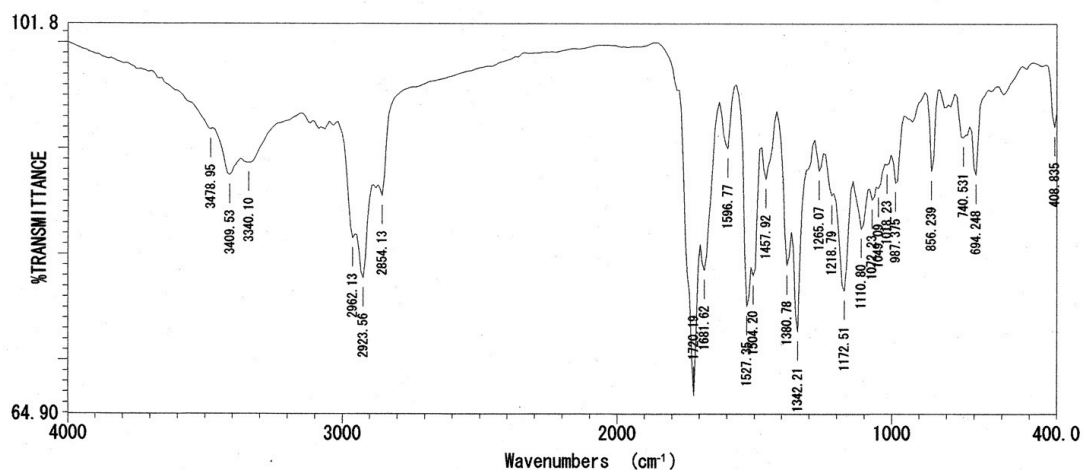
===== CHANNEL f1 =====
 NUC1 1H
 P1 13.00 usec
 PL1 -3.40 dB
 SFO1 400.1824713 MHz

F2 - Processing parameters
 SI 32768
 SF 400.1800427 MHz
 WDW EM
 SSB 0
 LB 0.30 Hz
 GB 0
 PC 1.00

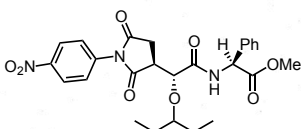


From Upper spot



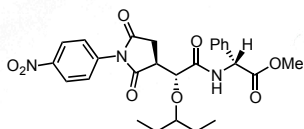
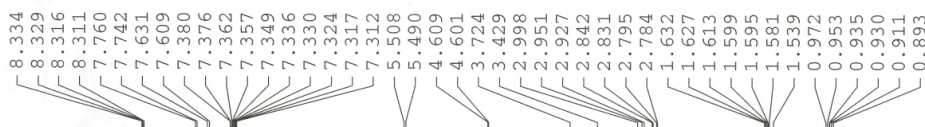


ファイル名 :
 タイトル :
 測定日時 : 2011年12月12日 19時41分08秒
 測定分解能 : 16 cm⁻¹
 スキャン回数 : 32 回
 測定ゲイン :
 コメント :



ピーク番号	波数 (cm⁻¹)	透過率 (%)	ピーク番号	波数 (cm⁻¹)	透過率 (%)
01	3478.95	91.7889	18	1110.80	82.4262
02	3409.53	87.4748	19	1072.23	85.1752
03	3340.10	88.6433	20	1049.09	86.2508
04	2962.13	81.5239	21	1018.23	88.4621
05	2923.56	77.7384	22	987.375	86.7574
06	2854.13	85.5284	23	987.373	87.8861
07	1720.19	66.6690	24	740.531	91.0551
08	1681.62	78.4884	25	694.248	87.5371
09	1596.77	89.9869	26	408.835	92.0595
10	1527.35	75.0664			
11	1504.20	78.0097			
12	1457.92	87.1023			
13	1380.78	78.9703			
14	1342.21	72.6828			
15	1265.07	87.9081			
16	1218.79	85.6081			
17	1172.51	76.5586			

test



Current Data Parameters
 NAME Dec13-2011
 EXPNO 70
 PROCNO 1

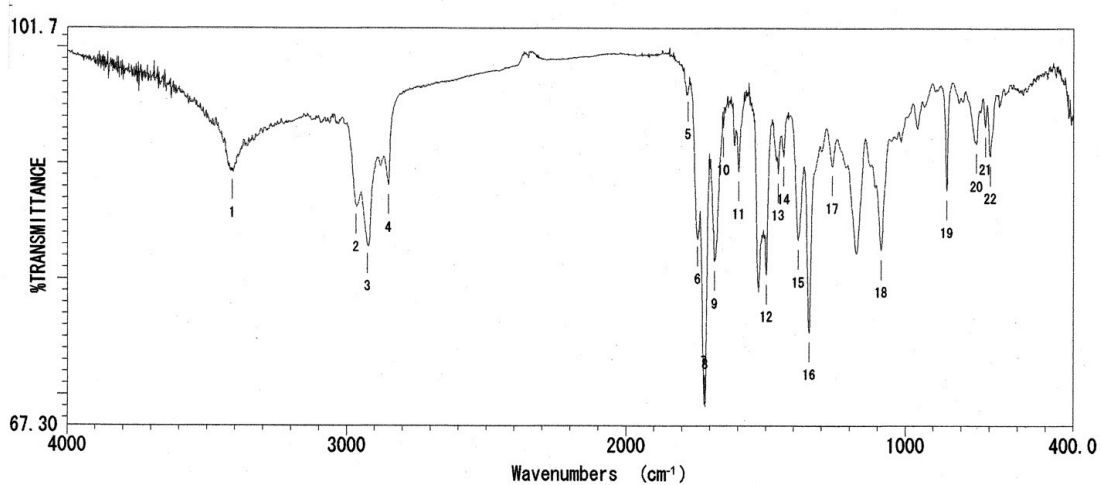
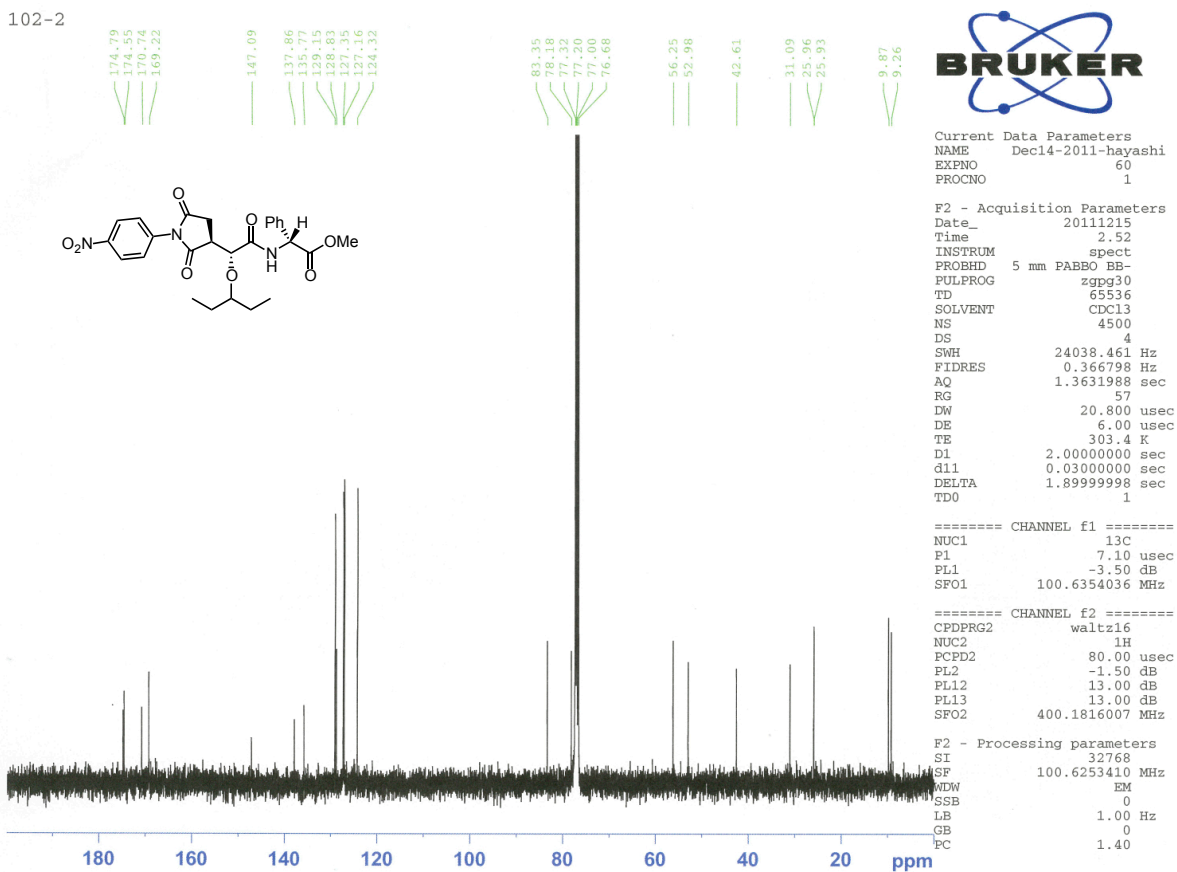
F2 - Acquisition Parameters
 Date_ 20111213
 Time 20.36
 INSTRUM dpx400
 PROBHD 5 mm QNP 1H/29
 PULPROG zg30
 TD 32768
 SOLVENT CDCl3
 NS 32
 DS 0
 SWH 8223.685 Hz
 FIDRES 0.250967 Hz
 AQ 1.9923444 sec
 RG 20642.5
 DW 60.800 usec
 DE 6.00 usec
 TE 303.2 K
 D1 1.00000000 sec
 MCREST 0.00000000 sec
 MCWRK 0.01500000 sec

===== CHANNEL f1 =====
 NUC1 1H
 P1 7.90 usec
 PL1 3.00 dB
 SFO1 400.1324710 MHz

F2 - Processing parameters
 SI 16384
 SF 400.1300087 MHz
 WDW EM
 SSB 0
 LB 0.30 Hz
 GB 0
 PC 1.00

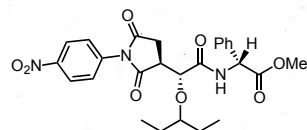


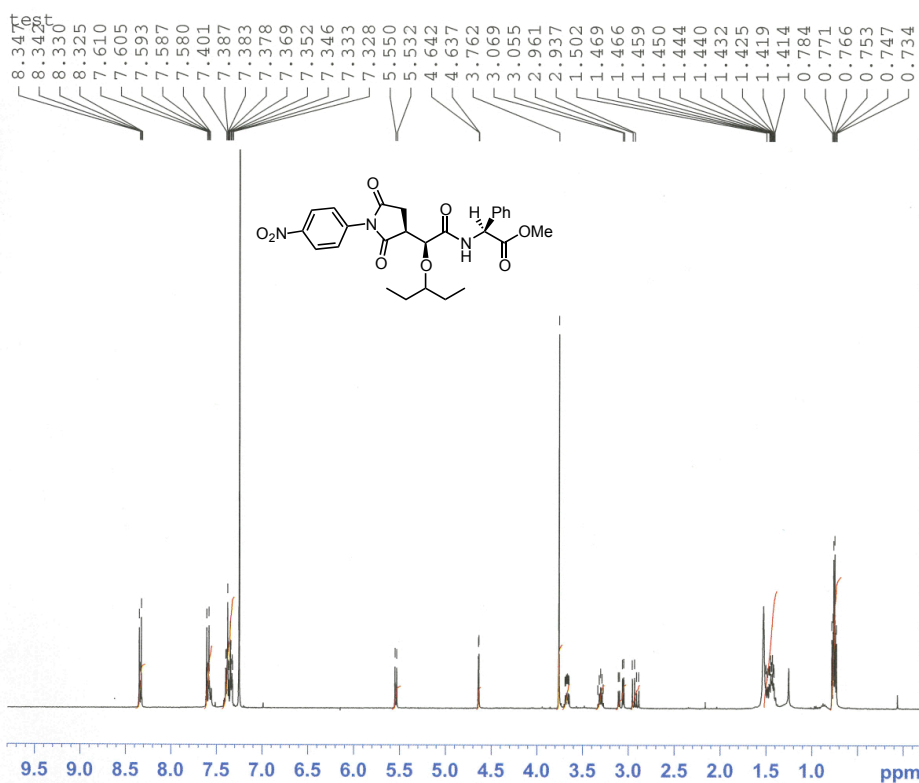
102-2



ファイル名 :
 タイトル :
 測定日時 : 2012年02月08日 15時28分56秒
 測定分解能 : 2 cm⁻¹
 スキャン回数 : 16 回
 測定ゲイン :
 コメント :

ピーク番号	波数 (cm⁻¹)	透過率 (%)	ピーク番号	波数 (cm⁻¹)	透過率 (%)
01	3409.53	89.3719	18	1087.66	82.5219
02	2965.98	86.4008	19	853.347	87.6453
03	2924.52	83.0184	20	747.281	91.6843
04	2849.31	88.0928	21	715.461	93.1670
05	1778.05	96.1772	22	698.105	90.6367
06	1743.33	83.6589			
07	1720.19	69.2243			
08	1717.30	68.9800			
09	1682.59	81.5059			
10	1651.73	93.0883			
11	1596.77	89.2648			
12	1497.45	80.3911			
13	1455.99	89.1798			
14	1435.74	90.5628			
15	1363.67	83.3434			
16	1344.14	75.3776			
17	1262.18	89.7624			





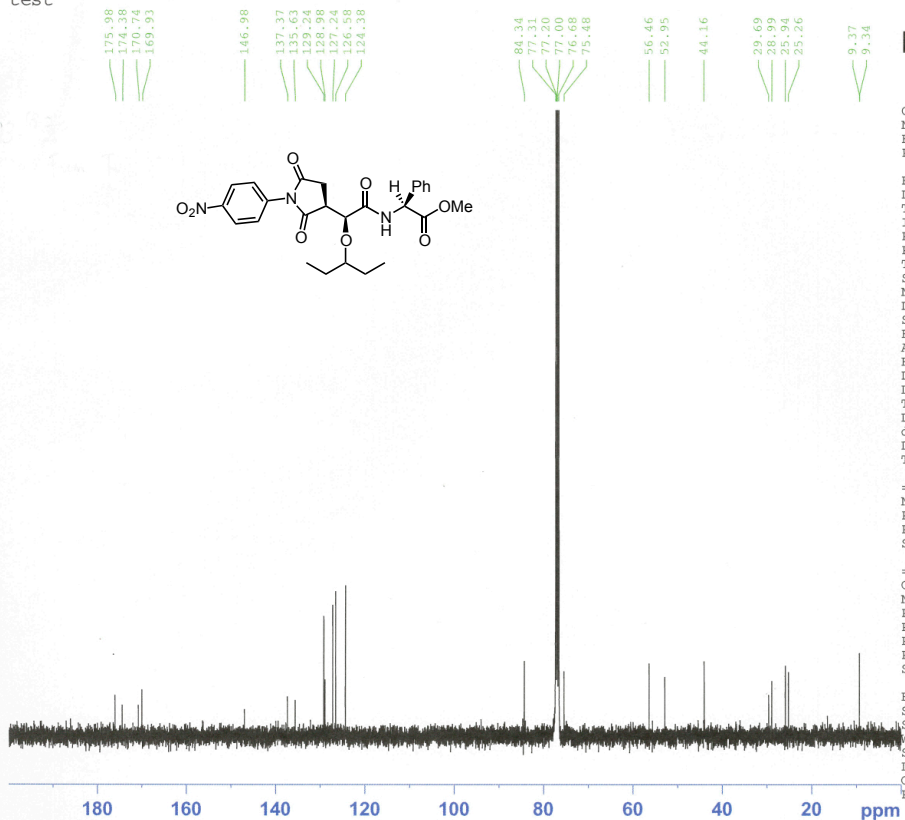
Current Data Parameters
NAME Dec07-2011
EXPNO 24
PROCNO 1

F2 - Acquisition Parameters
Date_ 20111207
Time 13.26
INSTRUM dpx400
PROBHD 5 mm QNP 1H/29
PULPROG zg30
TD 32768
SOLVENT CDCl3
NS 32
DS 0
SWH 8223.685 Hz
FIDRES 0.250967 Hz
AQ 1.9923444 sec
RG 18390.4
DW 60.800 usec
DE 6.00 usec
TE 303.2 K
D1 1.00000000 sec
MCREST 0.00000000 sec
MCWRK 0.01500000 sec

===== CHANNEL f1 =====
NUC1 1H
P1 7.90 usec
PL1 3.00 dB
SFO1 400.1324710 MHz

F2 - Processing parameters
SI 16384
SF 400.1300104 MHz
WDW EM
SSB 0
LB 0.30 Hz
GB 0
PC 1.00

test



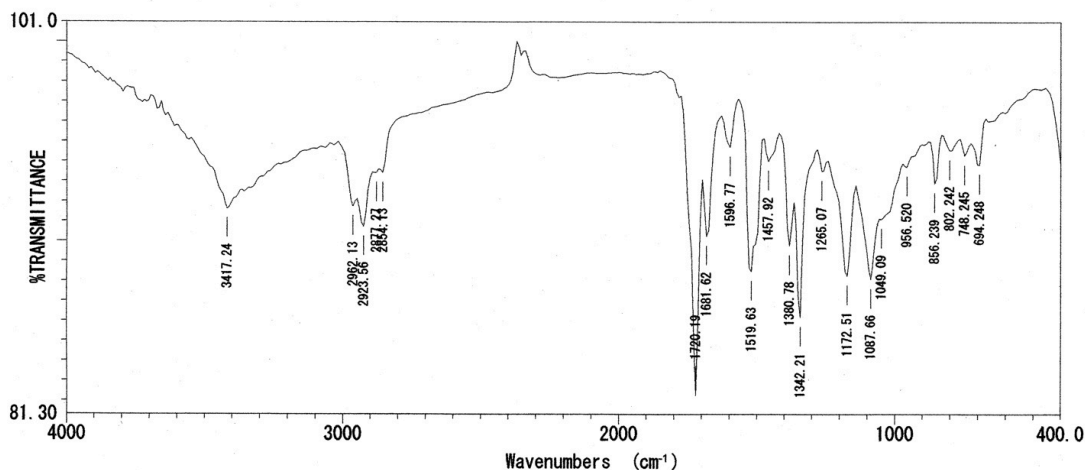
Current Data Parameters
NAME Dec10-2011-hayashi
EXPNO 100
PROCNO 1

F2 - Acquisition Parameters
Date_ 20111211
Time 1.20
INSTRUM spect
PROBHD 5 mm PABBO BB-4
PULPROG zgpg30
TD 65536
SOLVENT CDCl3
NS 5000
DS 4
SWH 24038.461 Hz
FIDRES 0.366798 Hz
AQ 1.3631988 sec
RG 57
DW 20.800 usec
DE 6.00 usec
TE 303.4 K
D1 2.00000000 sec
d11 0.03000000 sec
DELTA 1.89999998 sec
TD0 1

===== CHANNEL f1 =====
NUC1 13C
P1 7.10 usec
PL1 -3.50 dB
SFO1 100.6354036 MHz

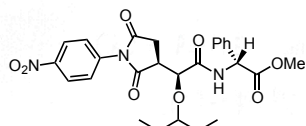
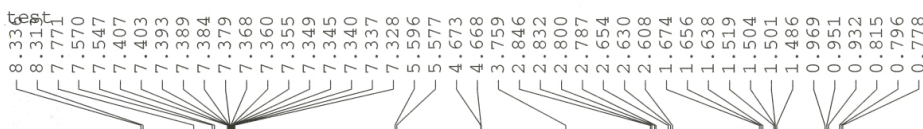
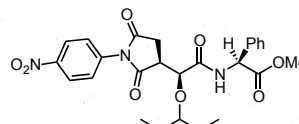
===== CHANNEL f2 =====
CPDPRG2 waltz16
NUC2 1H
PCPD2 80.00 usec
PL2 -1.50 dB
PL12 13.00 dB
PL13 13.00 dB
SFO2 400.1816007 MHz

F2 - Processing parameters
SI 32768
SF 100.6253421 MHz
WDW EM
SSB 0
LB 1.00 Hz
GB 0
PC 1.40



ファイル名 :
 タイトル :
 測定日時 : 2011年12月12日 19時50分15秒
 測定分解能 : 16 cm⁻¹
 スキャン回数 : 32 回
 測定ゲイン : 1
 コメント :

ピーク番号	波数 (cm⁻¹)	透過率 (%)	ピーク番号	波数 (cm⁻¹)	透過率 (%)
01	3417.24	91.6345	18	856.239	92.8929
02	2962.13	91.7475	19	802.242	94.5576
03	2923.56	90.7126	20	748.245	94.2991
04	2877.27	93.4228	21	694.248	93.8341
05	2854.13	93.4167			
06	1720.19	82.2694			
07	1681.62	90.2405			
08	1596.77	94.7170			
09	1519.63	88.4703			
10	1457.92	94.0182			
11	1380.78	89.7778			
12	1342.21	86.1706			
13	1285.07	93.5218			
14	1172.51	88.2603			
15	1087.66	88.0833			
16	1049.09	91.0998			
17	956.520	93.7225			

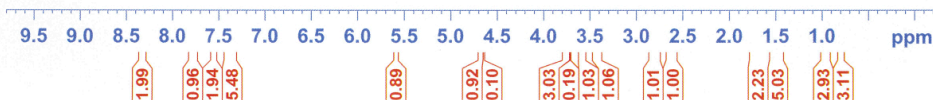


Current Data Parameters
 NAME Dec13-2011
 EXPNO 62
 PROCNO 1

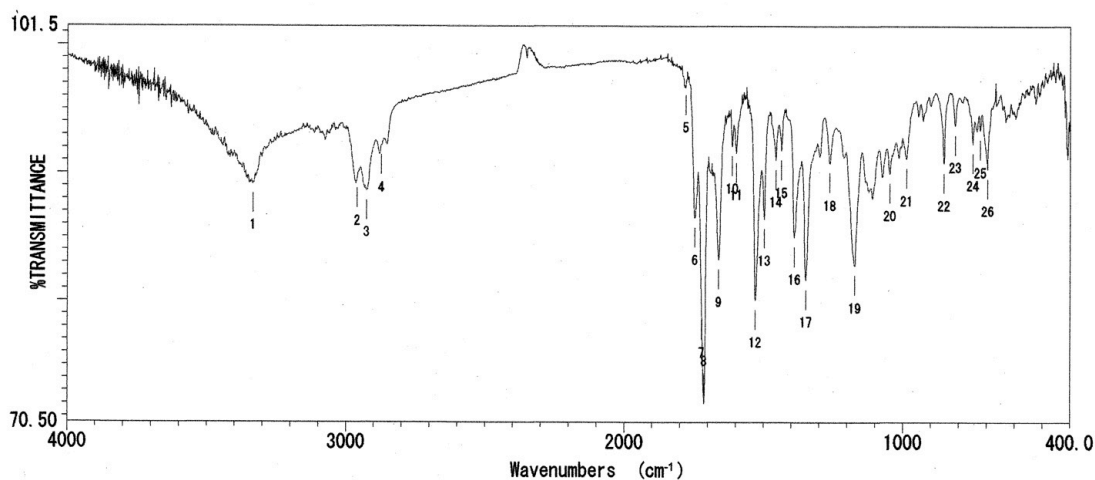
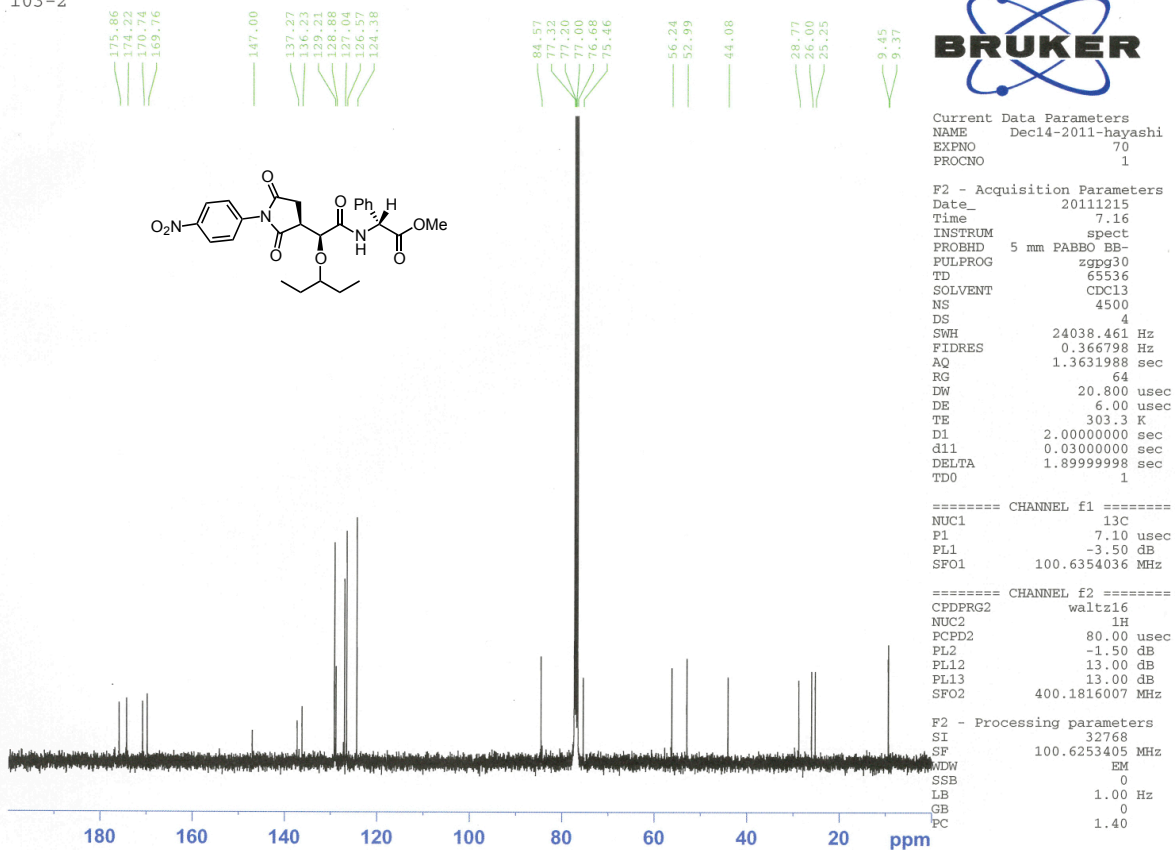
 F2 - Acquisition Parameters
 Date_ 20111213
 Time 22:27
 INSTRUM dpx400
 PROBHD 5 mm QNP 1H/29
 PULPROG zg30
 TD 32768
 SOLVENT CDCl3
 NS 32
 DS 0
 SWH 8223.685 Hz
 FIDRES 0.250967 Hz
 AQ 1.9923444 sec
 RG 23170.5
 DW 60.800 usec
 DE 6.00 usec
 TE 303.2 K
 D1 1.00000000 sec
 MCREST 0.00000000 sec
 MCWRK 0.01500000 sec

 ===== CHANNEL f1 =====
 NUC1 1H
 P1 7.90 usec
 PL1 3.00 dB
 SFO1 400.1324710 MHz

 F2 - Processing parameters
 SI 16384
 SF 400.1300092 MHz
 WDW EM
 SSB 0
 LB 0.30 Hz
 GB 0
 PC 1.00

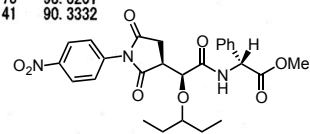


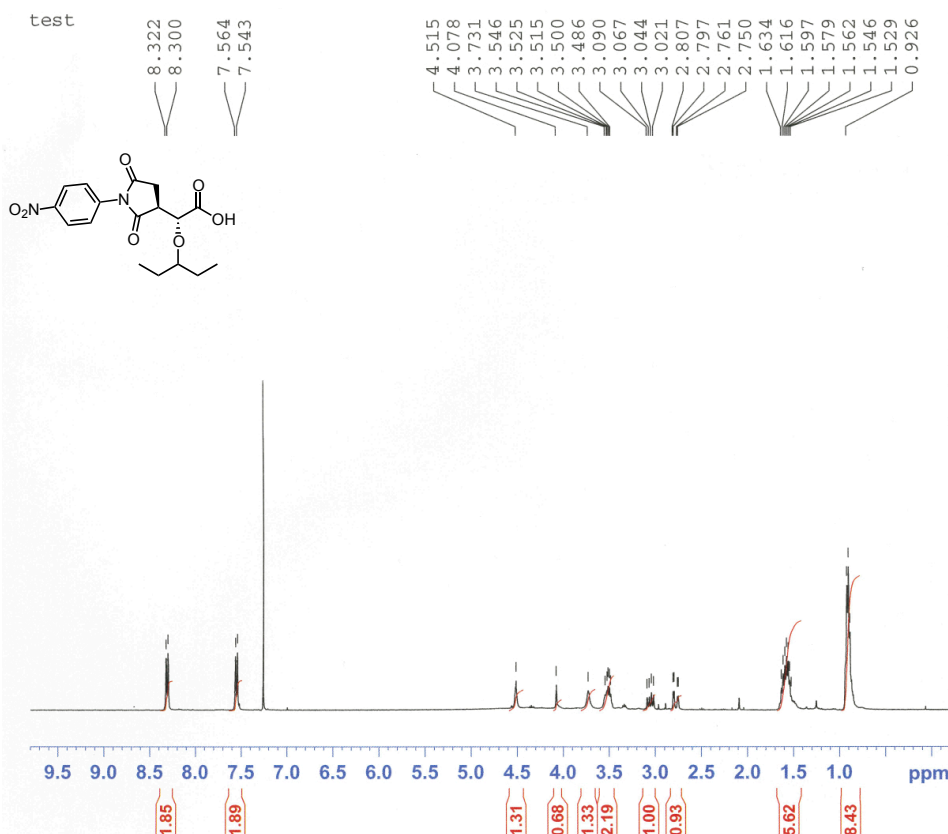
103-2



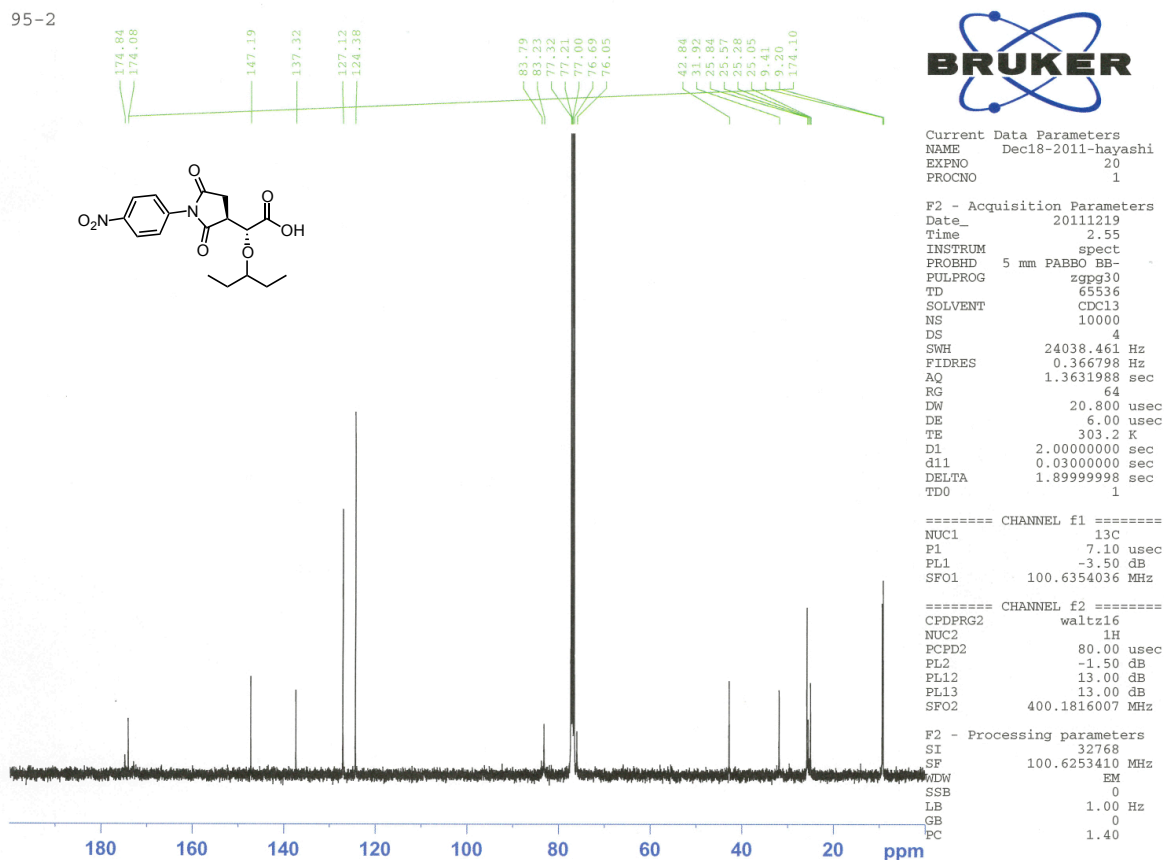
ファイル名 :
タイトル :
測定日時 : 2012年02月08日 15時38分48秒
測定分解能 : 2 cm⁻¹
スキャン回数 : 16 回
測定ゲイン : 1
コメント :

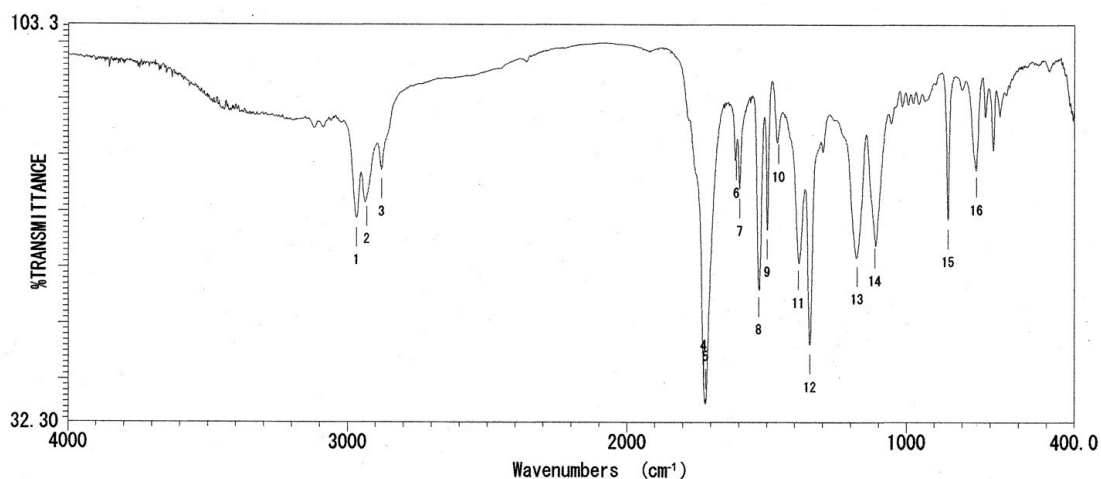
ピーク番号	波数 (cm⁻¹)	透過率 (%)	ピーク番号	波数 (cm⁻¹)	透過率 (%)
01	3332.39	89.2061	18	1262.18	90.7571
02	2959.23	89.5500	19	1172.51	82.7375
03	2924.52	88.6354	20	1047.16	89.9583
04	2871.49	92.1539	21	987.375	81.1010
05	1778.05	96.8607	22	853.347	90.7221
06	1746.23	86.4862	23	812.849	93.7428
07	1722.12	79.2553	24	750.174	92.3329
08	1713.44	71.9959	25	723.175	93.3201
09	1660.41	83.1964	26	697.141	90.3532
10	1612.20	92.0647			
11	1597.73	91.5964			
12	1529.27	80.0278			
13	1497.45	86.4400			
14	1455.99	91.0399			
15	1435.74	91.7480			
16	1389.46	84.9646			
17	1348.00	81.6461			





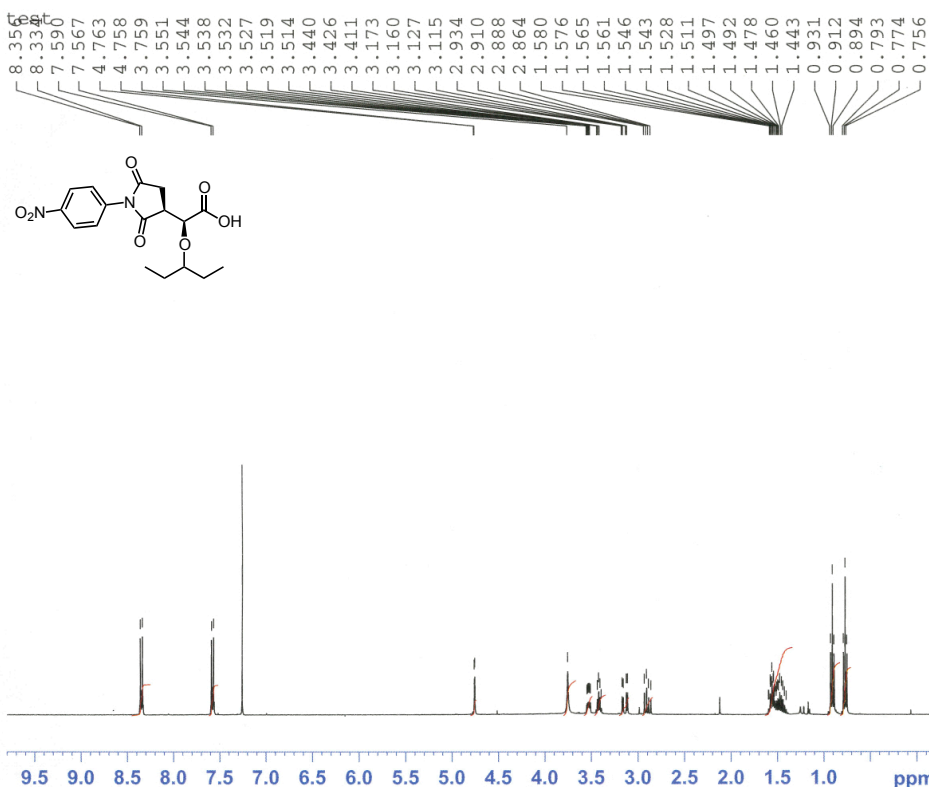
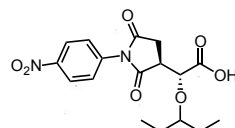
95-2





ファイル名 :
 タイトル :
 測定日時 : 2012年02月20日 15時47分25秒
 測定分解能 : 2 cm⁻¹
 スキャン回数 : 16 回
 測定ゲイン : 1
 コメント :

ピーク番号	波数 (cm⁻¹)	透過率 (%)
01	2967.91	68.7935
02	2931.27	72.5143
03	2878.24	77.4484
04	1725.01	38.5143
05	1718.26	36.5114
06	1609.31	80.7737
07	1596.77	73.9825
08	1528.31	56.4427
09	1498.42	66.7011
10	1457.92	83.6617
11	1386.57	61.1855
12	1345.11	46.1199
13	1177.33	61.8591
14	1113.69	65.1104
15	852.382	68.5022
16	751.138	77.8068



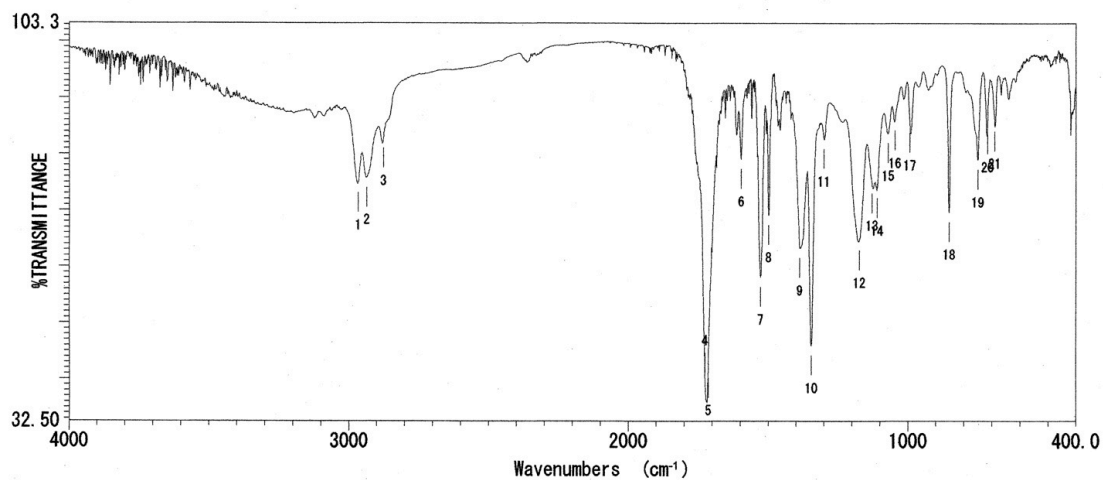
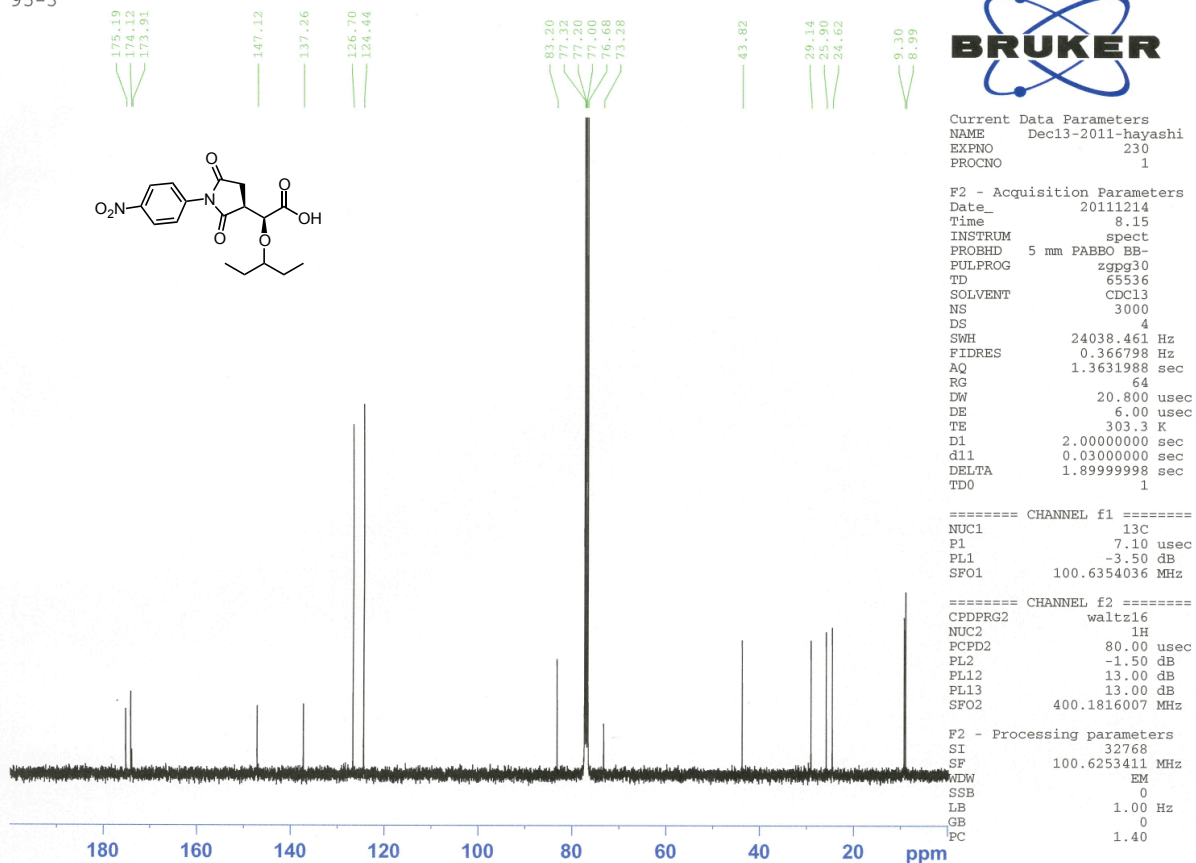
Current Data Parameters
 NAME : Dec06-2011
 EXPNO : 18
 PROCNO : 1

F2 - Acquisition Parameters
 Date_ : 20111206
 Time : 15.59
 INSTRUM : dpx400
 PROBHD : 5 mm QNP 1H/29
 PULPROG : zg30
 TD : 32768
 SOLVENT : CDC13
 NS : 16
 DS : 0
 SWH : 8223.685 Hz
 FIDRES : 0.250967 Hz
 AQ : 1.9923444 sec
 RG : 18390.4
 DW : 60.800 usec
 DE : 6.00 usec
 TE : 303.2 K
 D1 : 1.00000000 sec
 MCREST : 0.00000000 sec
 MCWPK : 0.01500000 sec

===== CHANNEL f1 =====
 NUC1 : 1H
 P1 : 7.90 usec
 PL1 : 3.00 dB
 SFO1 : 400.1324710 MHz

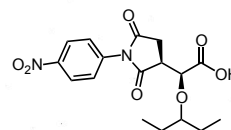
F2 - Processing parameters
 SI : 16384
 SF : 400.1300092 MHz
 WDW : EM
 SSB : 0
 LB : 0.30 Hz
 GB : 0
 PC : 1.00

95-3

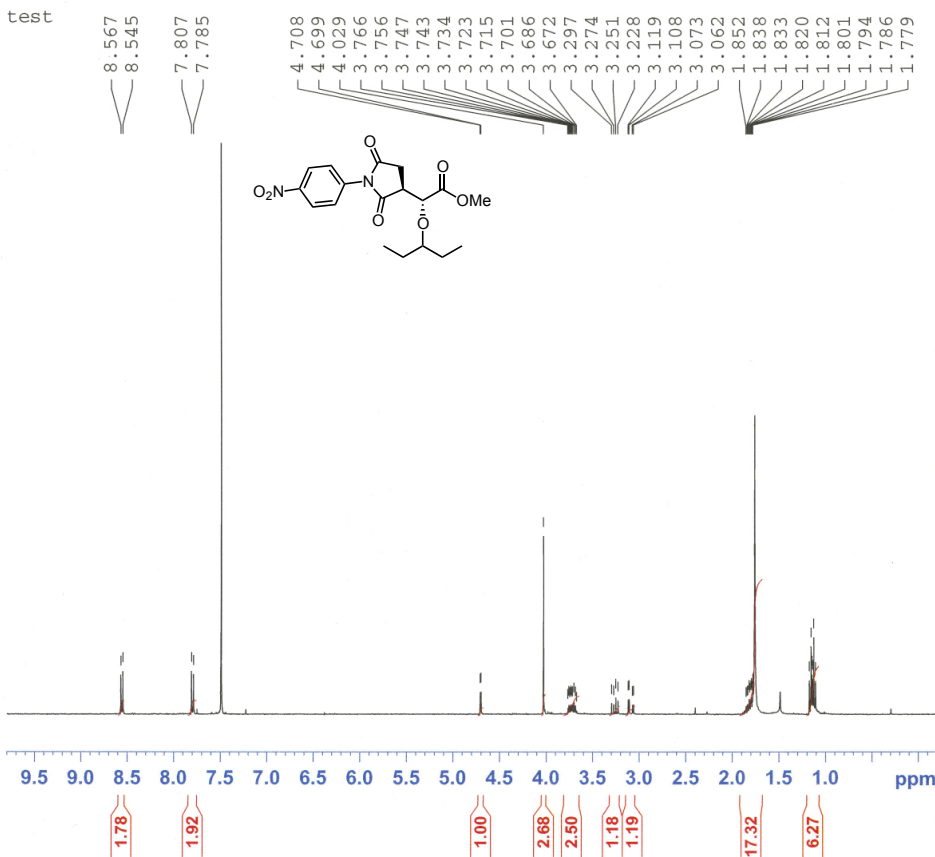


ファイル名 :
 タイトル :
 測定日時 : 2012年02月20日 16時02分31秒
 測定分解能 : 2 cm⁻¹
 スキャン回数 : 16 回
 測定ゲイン : 1
 コメント :

ピーク番号	波数 (cm⁻¹)	透過率 (%)	ピーク番号	波数 (cm⁻¹)	透過率 (%)
01	2965.98	74.8691	18	853.347	69.6264
02	2835.13	75.8144	19	751.138	78.9369
03	2875.34	82.7279	20	716.425	85.2178
04	1725.01	39.3154	21	691.355	85.8175
05	1714.41	41.9412			
06	1596.77	79.0294			
07	1527.35	58.0933			
08	1498.42	69.1042			
09	1386.57	63.2284			
10	1345.11	45.8953			
11	1299.79	82.6524			
12	1173.47	64.6252			
13	1129.12	74.7970			
14	1109.83	73.8710			
15	1071.26	83.6461			
16	1047.16	85.9119			
17	994.125	85.4727			



test



Current Data Parameters
 NAME Dec08-2011
 EXPNO 133
 PROCNO 1

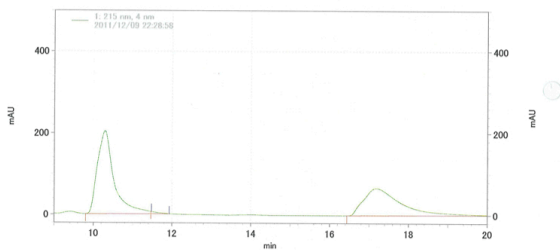
F2 - Acquisition Parameters
 Date_ 20111208
 Time 22.26
 INSTRUM dpx400
 PROBHD 5 mm QNP 1H/29
 PULPROG zg30
 TD 32768
 SOLVENT CDC13
 NS 16
 DS 0
 SWH 8223.685 Hz
 FIDRES 0.250967 Hz
 AQ 1.9923444 sec
 RG 32768
 DW 60.800 usec
 DE 6.00 usec
 TE 303.2 K
 D1 1.00000000 sec
 MCREST 0.00000000 sec
 MCWRK 0.01500000 sec

===== CHANNEL f1 =====
 NUC1 1H
 P1 7.90 usec
 PL1 3.00 dB
 SFO1 400.1324710 MHz

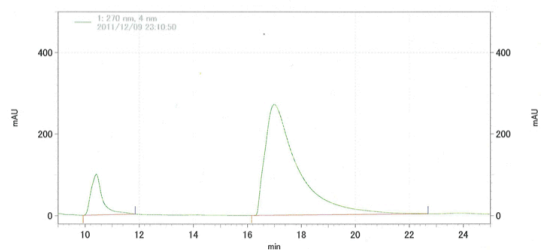
F2 - Processing parameters
 SI 16384
 SF 400.1299173 MHz
 WDW EM
 SSB 0
 LB 0.30 Hz
 GB 0
 PC 1.00

ファイル名: W:\Server\Enterprise\Projects\Default\Data\2011-12-09 22-28-58 mukai
 100-2 racemi AD-H 3vs1 1ml
 ファイル名: W:\Server\Enterprise\Projects\Default\Method\10vs1. 1ml.met
 システム名: System
 分析日時: 2011/12/09 22:29:58
 印刷日時: 2011/12/09 22:58:38

ファイル名: W:\Server\Enterprise\Projects\Default\Data\2011-12-09 23-10-50 mukai
 99-2 AD-H 3vs1 1ml
 ファイル名: W:\Server\Enterprise\Projects\Default\Method\10vs1. 1ml.met
 システム名: System
 分析日時: 2011/12/09 23:11:41
 印刷日時: 2011/12/09 23:44:37

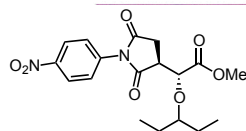


PK #	名前	保持時間	面積	面積%	ピークコメント
1		10.30	24175710	57.490 MM	
2		11.47	0.000	MM	
3		17.19	17875955	42.510 MM	
トータル			42051667	100.000	

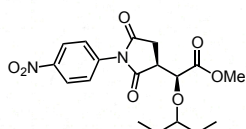


PK #	名前	保持時間	面積	面積%	ピークコメント
1		10.43	11783331	11.426 MM	
2		17.01	91344731	88.574 MM	
トータル			103128062	100.000	

racemi



test

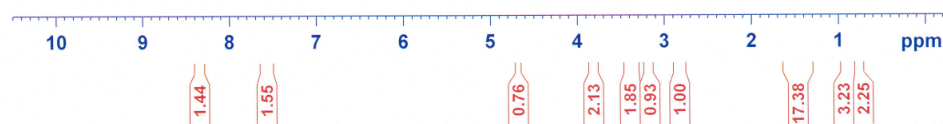


Current Data Parameters
NAME Dec07-2011
EXPNO 13
PROCNO 1

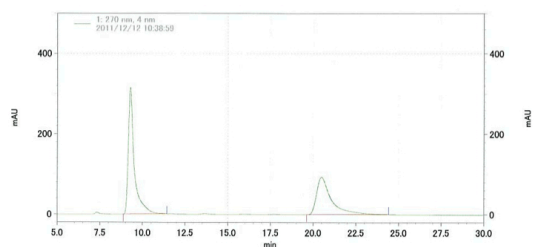
F2 - Acquisition Parameters
Date_ 20111207
Time_ 23.25
INSTRUM dpx400
PROBHD 5 mm QNP 1H/29
PULPROG zg30
TD 32768
SOLVENT CDC13
NS 32
DS 0
SWH 8223.685 Hz
FIDRES 0.250967 Hz
AQ 1.9923444 sec
RG 23170.5
DW 60.800 usec
DE 6.00 usec
TE 303.2 K
D1 1.00000000 sec
MCREST 0.00000000 sec
MCWRK 0.01500000 sec

===== CHANNEL f1 =====
NUC1 1H
P1 7.90 usec
PL1 3.00 dB
SFO1 400.1324710 MHz

F2 - Processing parameters
SI 16384
SF 400.1300087 MHz
WDW EM
SSB 0
LB 0.30 Hz
GB 0
PC 1.00

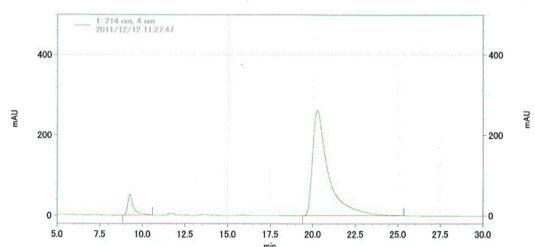


データファイル名: \\Server\Enterprise\Projects\Default\Data\2011-12-12 10-38-59 mukai
101-2 AD-Hi 3vs1 Im1 racemi
メソッド名: \\Server\Enterprise\Projects\Default\Method\10vs1. Im1.met
ユーザー名: System
分析日時: 2011/12/12 10:41:38
印刷日時: 2011/12/12 11:26:24



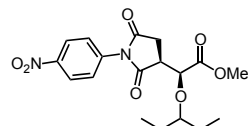
1: 270 nm, 4 nm結果	PK #	名前	保持時間	面積	面積%	ピークコード
	1		9.30	31087309	57.960	MM
	2		20.50	22548572	42.040	MM
				53635881	100.000	

データファイル名: \\Server\Enterprise\Projects\Default\Data\2011-12-12 11-27-47 mukai
97-2 AD-Hi 3vs1 Im1
メソッド名: \\Server\Enterprise\Projects\Default\Method\10vs1. Im1.met
ユーザー名: System
分析日時: 2011/12/12 11:29:02
印刷日時: 2011/12/12 12:37:27

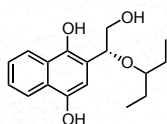


1: 214 nm, 4 nm結果	PK #	名前	保持時間	面積	面積%	ピークコード
	1		9.27	4731593	6.499	MM
	2		20.26	68073492	93.501	MM
				72805085	100.000	

racemi



test

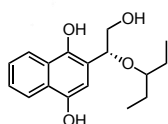
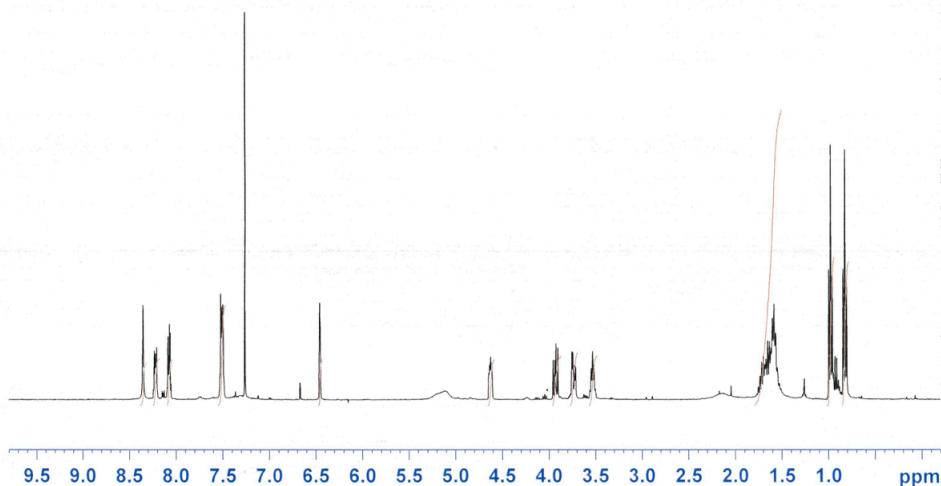


Current Data Parameters
NAME Mar24-2012
EXPNO 46
PROCNO 1

F2 - Acquisition Parameters
Date_ 20120324
Time 18.08
INSTRUM dpx400
PROBHD 5 mm QNP 1H/29
PULPROG zg30
TD 32768
SOLVENT CDCl3
NS 16
DS 0
SWH 8223.685 Hz
FIDRES 0.250967 Hz
AQ 1.9923444 sec
RG 18390.4
DW 60.800 usec
DE 6.00 usec
TE 303.2 K
D1 1.00000000 sec
MCREST 0.00000000 sec
MCWRK 0.01500000 sec

===== CHANNEL f1 =====
NUC1 1H
P1 7.90 usec
PL1 3.00 dB
SFO1 400.1324710 MHz

F2 - Processing parameters
SI 16384
SF 400.1300092 MHz
WDW EM
SSB 0
LB 0.30 Hz
GB 0
PC 1.00



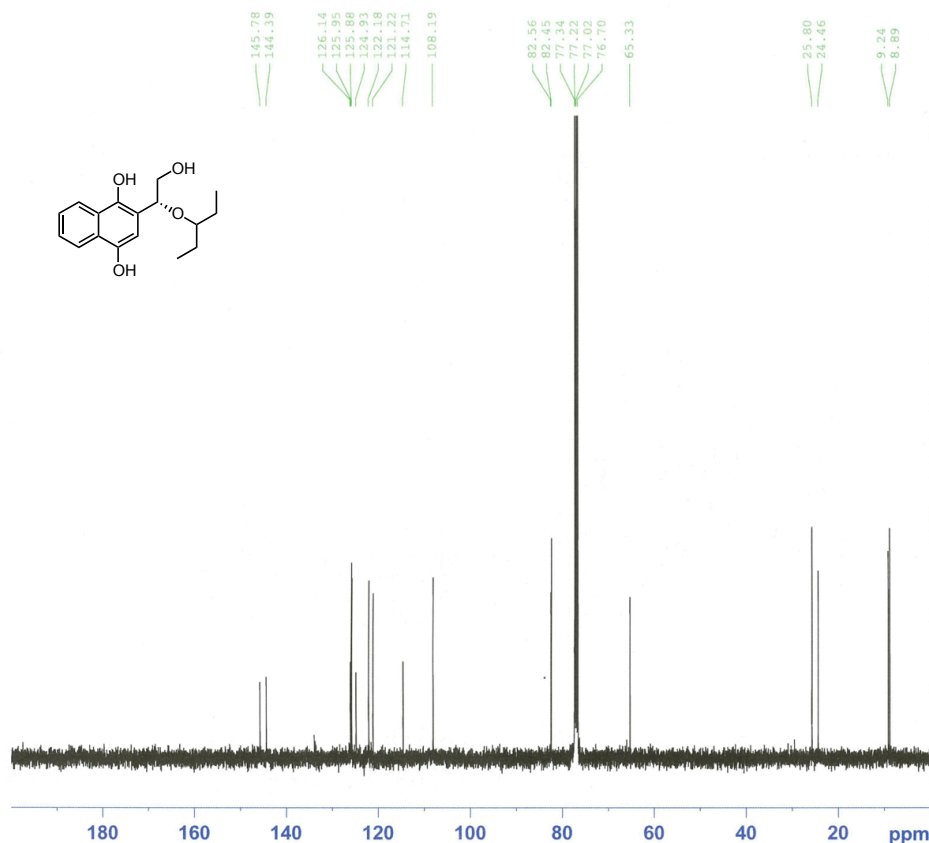
Current Data Parameters
NAME Mar24-2012-hayashi
EXPNO 90
PROCNO 1

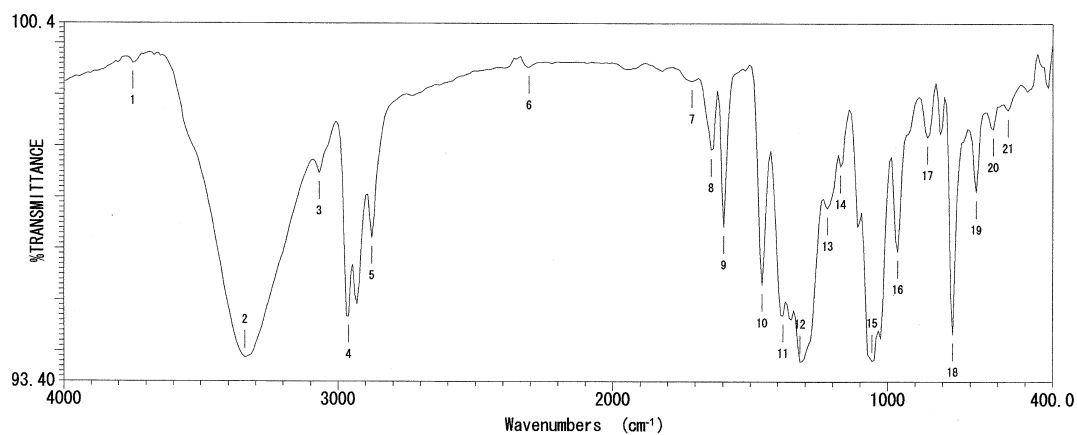
F2 - Acquisition Parameters
Date_ 20120324
Time 20.05
INSTRUM spect
PROBHD 5 mm PABBO BB-
PULPROG zgpg30
TD 65536
SOLVENT CDCl3
NS 2048
DS 4
SWH 24038.461 Hz
FIDRES 0.366798 Hz
AQ 1.3631988 sec
RG 57
DW 20.800 usec
DE 6.00 usec
TE 300.0 K
D1 2.00000000 sec
d11 0.03000000 sec
DELTA 1.89999998 sec
TD0 1

===== CHANNEL f1 =====
NUC1 13C
P1 7.10 usec
PL1 -3.50 dB
SFO1 100.6354036 MHz

===== CHANNEL f2 =====
CPDPRG2 waltz16
NUC2 1H
PCPD2 80.00 usec
PL2 -1.50 dB
PL12 13.00 dB
PL13 13.00 dB
SFO2 400.1816007 MHz

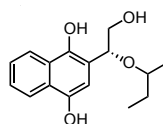
F2 - Processing parameters
SI 32768
SF 100.6253410 MHz
WDW EM
SSB 0
LB 1.00 Hz
GB 0
PC 1.40

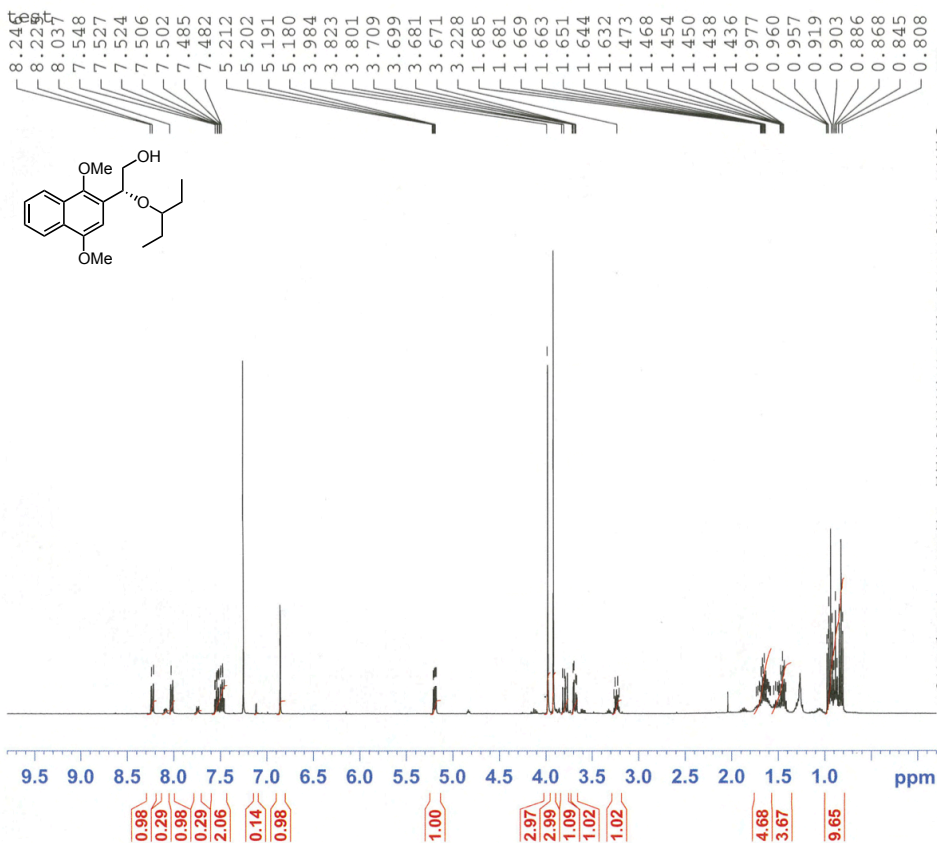




ピーク番号	波数 (cm⁻¹)	透過率 (%)
01	3748.94	99.6156
02	3340.10	93.8732
03	3070.12	97.4754
04	2962.13	94.6718
05	2877.27	96.2121
06	2306.45	99.5347
07	1712.48	99.2705
08	1643.05	97.9261
09	1596.77	96.4217
10	1457.92	95.2876
11	1380.78	94.6980
12	1319.07	93.7879
13	1218.79	96.7881
14	1172.51	97.6102
15	1056.80	93.8115
16	964.233	95.9484
17	856.239	98.1741
18	763.673	94.3335
19	678.820	97.1083
20	617.109	98.3317
21	563.112	98.7068

ファイル名 :
 タイトル :
 測定日時 : 2012年03月28日 17時31分12秒
 測定分解能 : 16 cm⁻¹
 スキャン回数 : 8 回
 測定ゲイン : 1
 コメント :



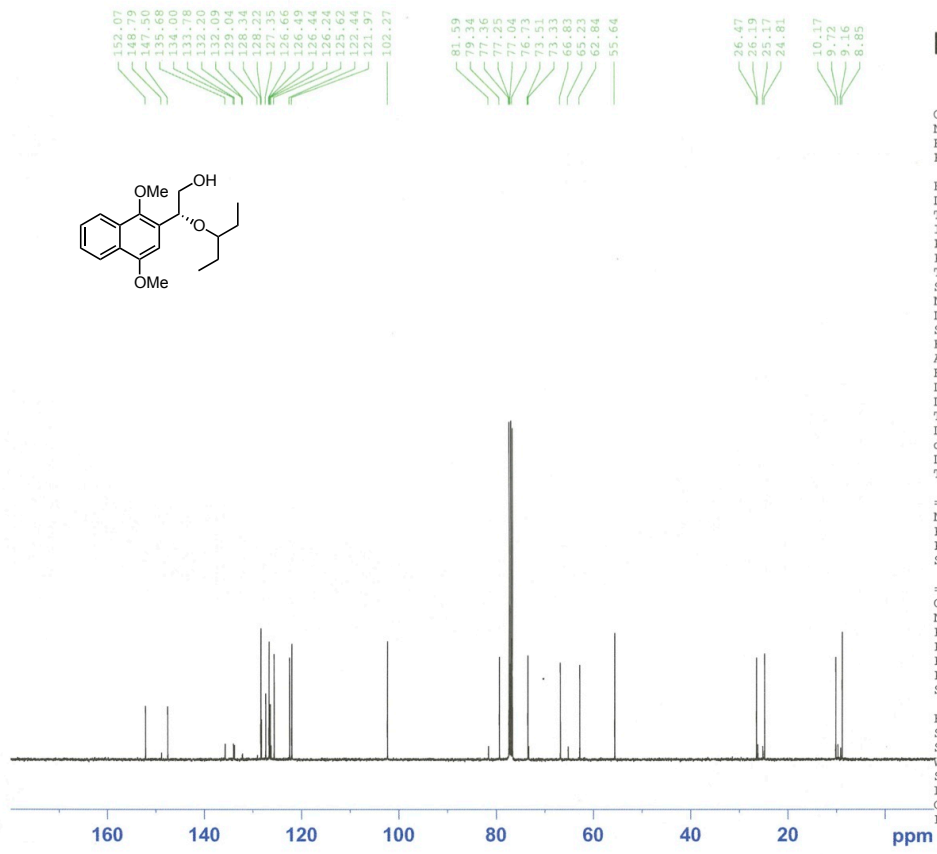


Current Data Parameters
 NAME Nov18-2011
 EXPNO 100
 PROCNO 1

F2 - Acquisition Parameters
 Date_ 20111118
 Time 13.16
 INSTRUM dpx400
 PROBHD 5 mm QNP 1H/29
 PULPROG zg30
 TD 32768
 SOLVENT CDCl3
 NS 16
 DS 0
 SWH 8223.685 Hz
 FIDRES 0.250967 Hz
 AQ 1.9923444 sec
 RG 14596.5
 DW 60.800 usec
 DE 6.00 usec
 TE 303.2 K
 D1 1.00000000 sec
 MCWREST 0.00000000 sec
 MCWRK 0.01500000 sec

===== CHANNEL f1 =====
 NUC1 1H
 P1 7.90 usec
 PL1 3.00 dB
 SFO1 400.1324710 MHz

F2 - Processing parameters
 SI 16384
 SF 400.130092 MHz
 WDW EM
 SSB 0
 LB 0.30 Hz
 GB 0
 PC 1.00



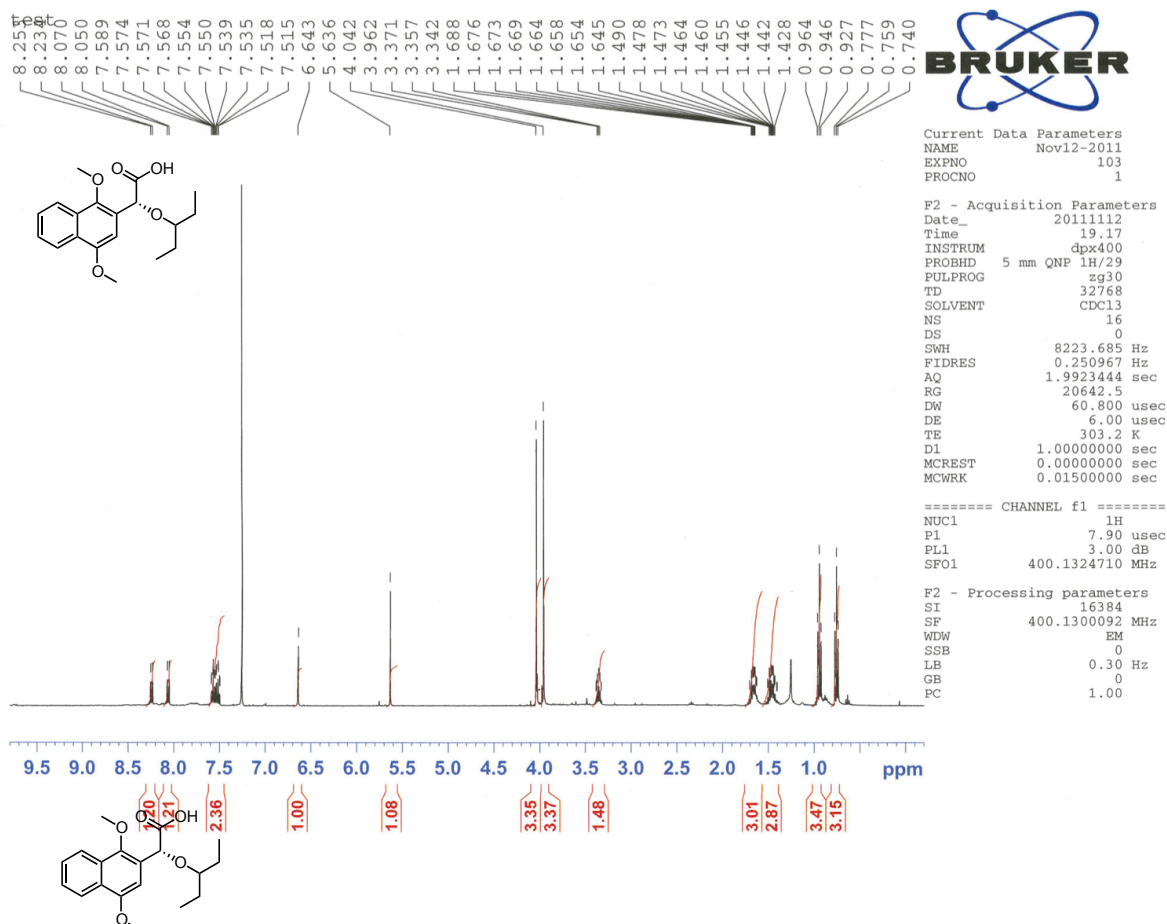
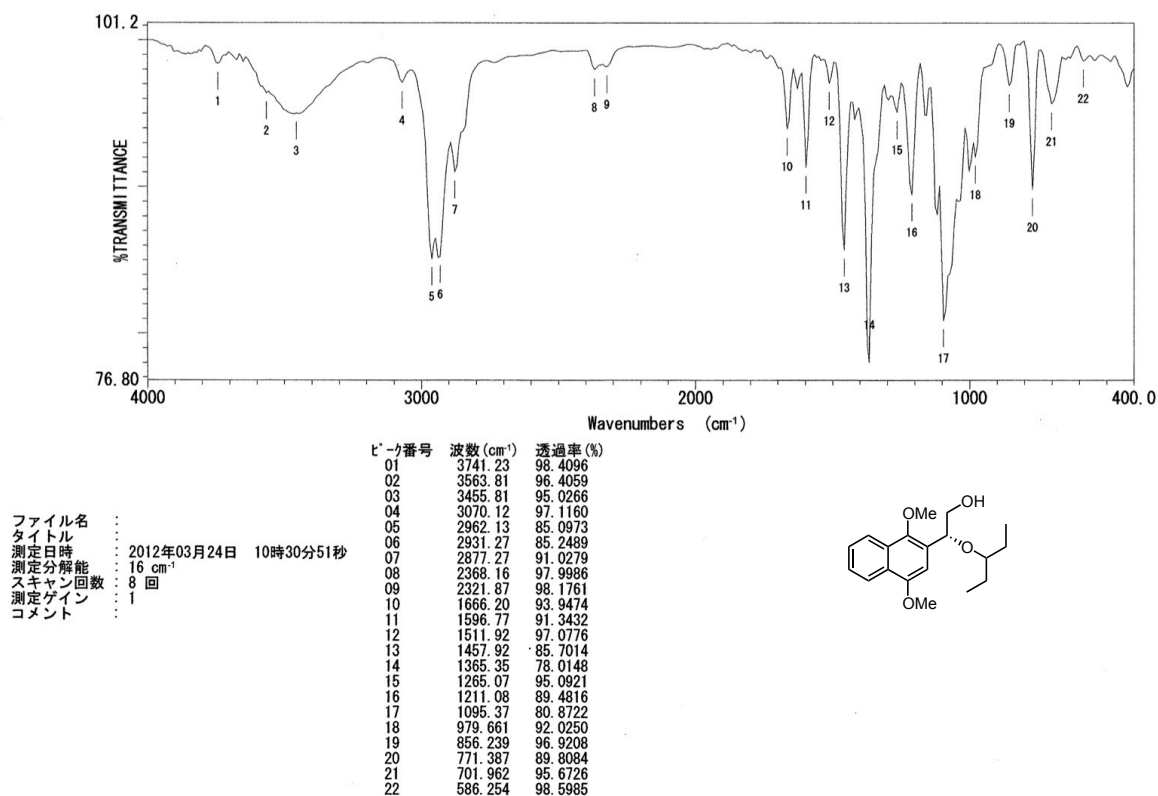
Current Data Parameters
 NAME Mar23-2012-hayashi
 EXPNO 180
 PROCNO 1

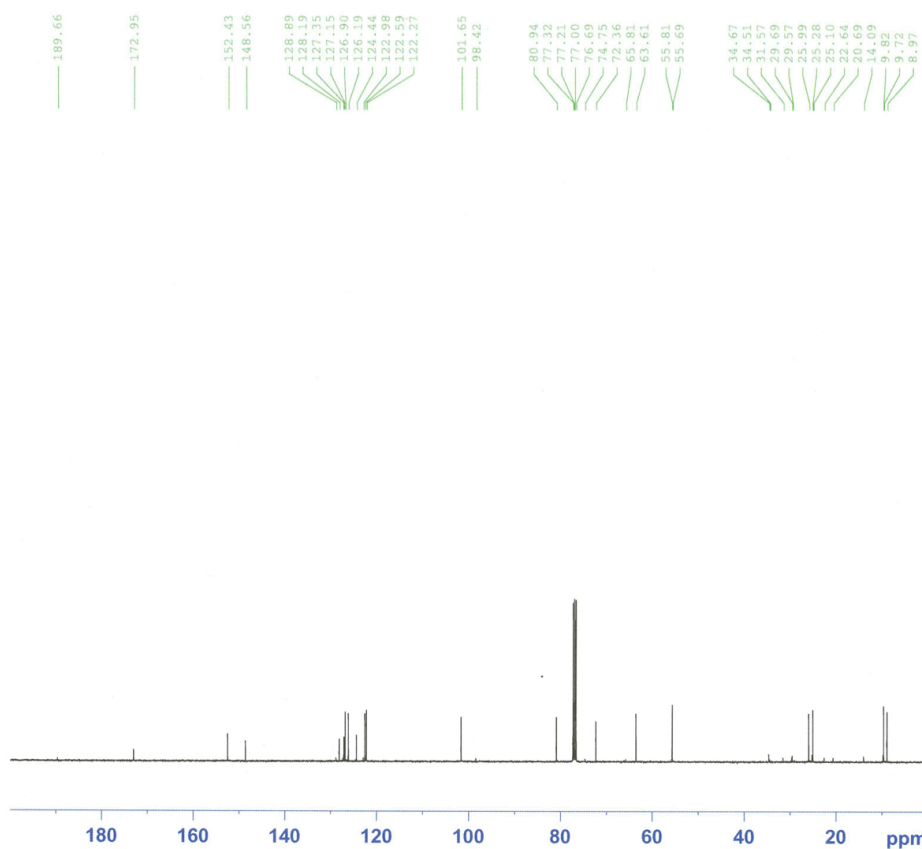
F2 - Acquisition Parameters
 Date_ 20120324
 Time 8.19
 INSTRUM spect
 PROBHD 5 mm PABBO BB-
 PULPROG zgpg30
 TD 65536
 SOLVENT CDCl3
 NS 1024
 DS 4
 SWH 24038.461 Hz
 FIDRES 0.366798 Hz
 AQ 1.3631988 sec
 RG 64
 DW 20.800 usec
 DE 6.00 usec
 TE 300.0 K
 D1 2.00000000 sec
 d11 0.03000000 sec
 DELTA 1.89999998 sec
 TDO 1

===== CHANNEL f1 =====
 NUC1 13C
 P1 7.10 usec
 PL1 -3.50 dB
 SFO1 100.6354036 MHz

===== CHANNEL f2 =====
 CPDPRG2 waltz16
 NUC2 1H
 PCPD2 80.00 usec
 PL2 -1.50 dB
 PL12 13.00 dB
 PL13 13.00 dB
 SFO2 400.1816007 MHz

F2 - Processing parameters
 SI 32768
 SF 100.6253410 MHz
 WDW EM
 SSB 0
 LB 1.00 Hz
 GB 0
 PC 1.40





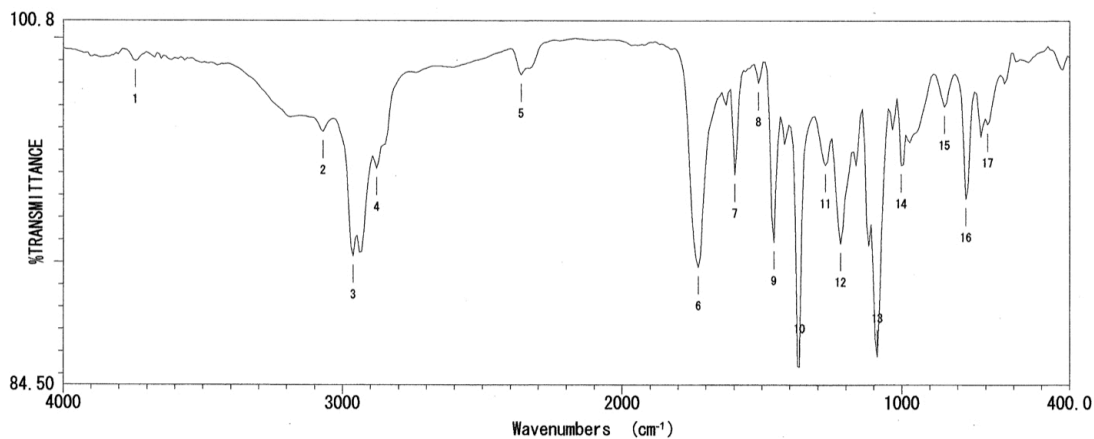
Current Data Parameters
NAME Mar14-2012-hayashi
EXPNO 360
PROCNO 1

F2 - Acquisition Parameters
Date_ 20120314
Time 23.56
INSTRUM spect
PROBHD 5 mm PABBO BB-
PULPROG zgpg30
TD 65536
SOLVENT CDCl3
NS 2048
DS 4
SWH 24038.461 Hz
FIDRES 0.366798 Hz
AQ 1.3631988 sec
RG 64
DW 20.800 usec
DE 6.00 usec
TE 303.5 K
D1 2.00000000 sec
d11 0.03000000 sec
DELTA 1.89999998 sec
TDO 1

===== CHANNEL f1 =====
NUC1 13C
P1 7.10 usec
PL1 -3.50 dB
SFO1 100.6354036 MHz

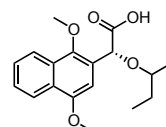
===== CHANNEL f2 =====
CPDPRG2 waltz16
NUC2 1H
PCPD2 80.00 usec
PL2 -1.50 dB
PL12 13.00 dB
PL13 13.00 dB
SFO2 400.1816007 MHz

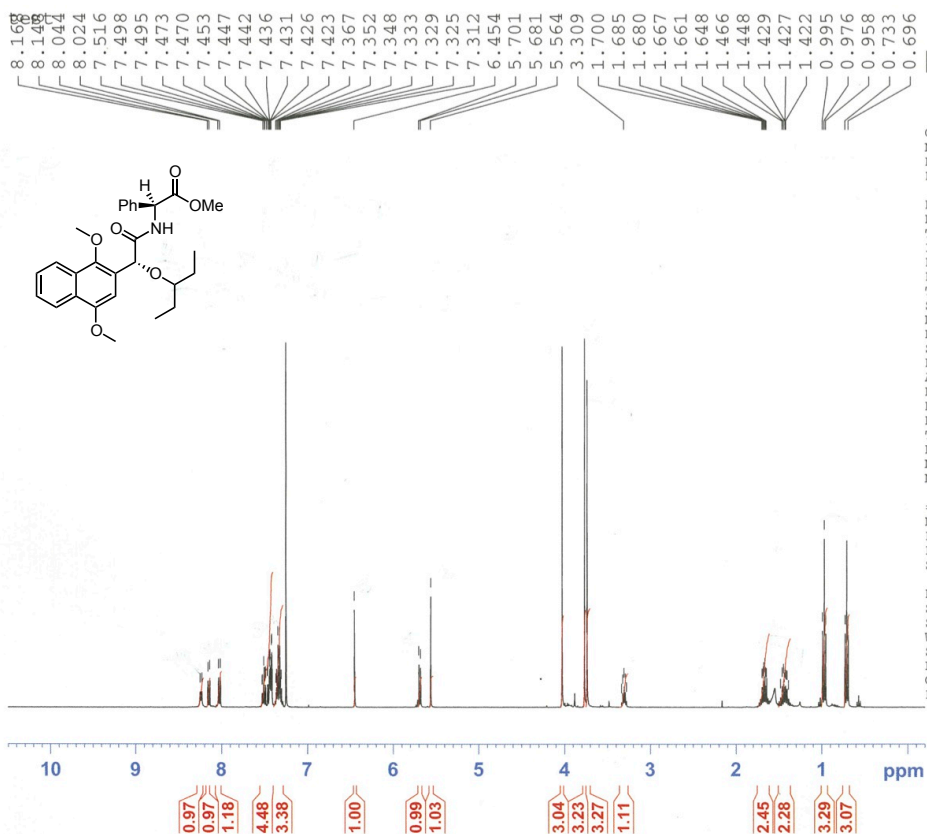
F2 - Processing parameters
SI 32768
SF 100.6253410 MHz
WDW EM
SSB 0
LB 1.00 Hz
GB 0
PC 1.40



ピーク番号	波数 (cm⁻¹)	透過率 (%)
01	3741.23	98.9828
02	3070.12	95.8295
03	2962.13	90.2631
04	2877.27	94.1773
05	2360.44	98.3723
06	1727.91	89.7667
07	1596.77	93.8966
08	1511.92	97.9938
09	1457.92	90.8814
10	1365.35	85.2998
11	1272.79	94.3212
12	1218.79	90.8170
13	1087.66	85.7681
14	1002.80	94.3294
15	848.525	96.9580
16	771.387	92.8187
17	694.248	96.1657

ファイル名 :
タイトル :
測定日時 : 2012年03月24日 10時16分22秒
測定分解能 : 16 cm⁻¹
スキャン回数 : 8 回
測定ゲイン : 1
コメント :



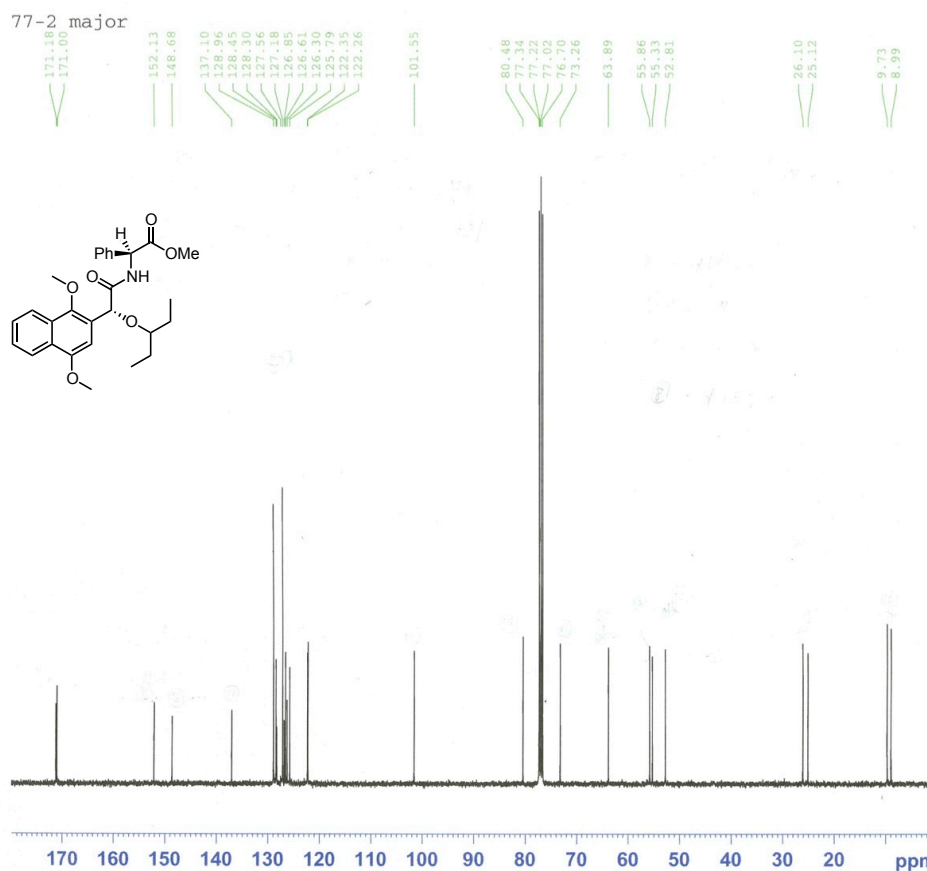


Current Data Parameters
 NAME Nov21-2011
 EXPNO 46
 PROCNO 1

F2 - Acquisition Parameters
 Date_ 20111121
 Time 15.37
 INSTRUM dpx400
 PROBHD 5 mm QNP 1H/29
 PULPROG zg30
 TD 32768
 SOLVENT CDCl3
 NS 16
 DS 0
 SWH 8223.685 Hz
 FIDRES 0.250967 Hz
 AQ 1.9923444 sec
 RG 18390.4
 DW 60.800 usec
 DE 6.00 usec
 TE 303.2 K
 D1 1.00000000 sec
 MCREST 0.00000000 sec
 MCWRK 0.01500000 sec

===== CHANNEL f1 =====
 NUC1 1H
 P1 7.90 usec
 PL1 3.00 dB
 SFO1 400.1324710 MHz

F2 - Processing parameters
 SI 16384
 SF 400.1300098 MHz
 WDW EM
 SSB 0
 LB 0.30 Hz
 GB 0
 FC 1.00



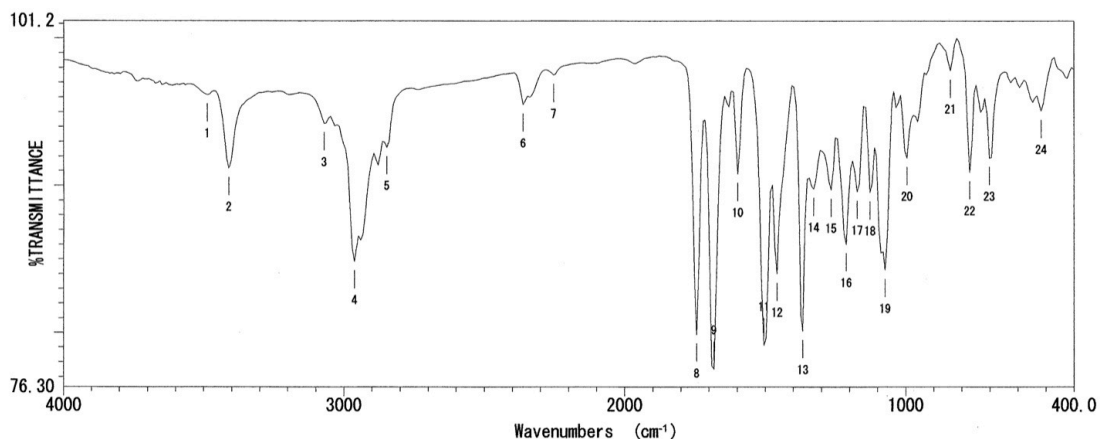
Current Data Parameters
 NAME Mar12-2012-hayashi
 EXPNO 170
 PROCNO 1

F2 - Acquisition Parameters
 Date_ 20120313
 Time 2.11
 INSTRUM spect
 PROBHD 5 mm PABBO BB-
 PULPROG zgpg30
 TD 65536
 SOLVENT CDCl3
 NS 2000
 DS 4
 SWH 24038.461 Hz
 FIDRES 0.366798 Hz
 AQ 1.3631988 sec
 RG 64
 DW 20.800 usec
 DE 6.00 usec
 TE 303.3 K
 D1 2.00000000 sec
 d11 0.03000000 sec
 DELTA 1.89999999 sec
 TD0 1

===== CHANNEL f1 =====
 NUC1 13C
 P1 7.10 usec
 PL1 -3.50 dB
 SFO1 100.6354036 MHz

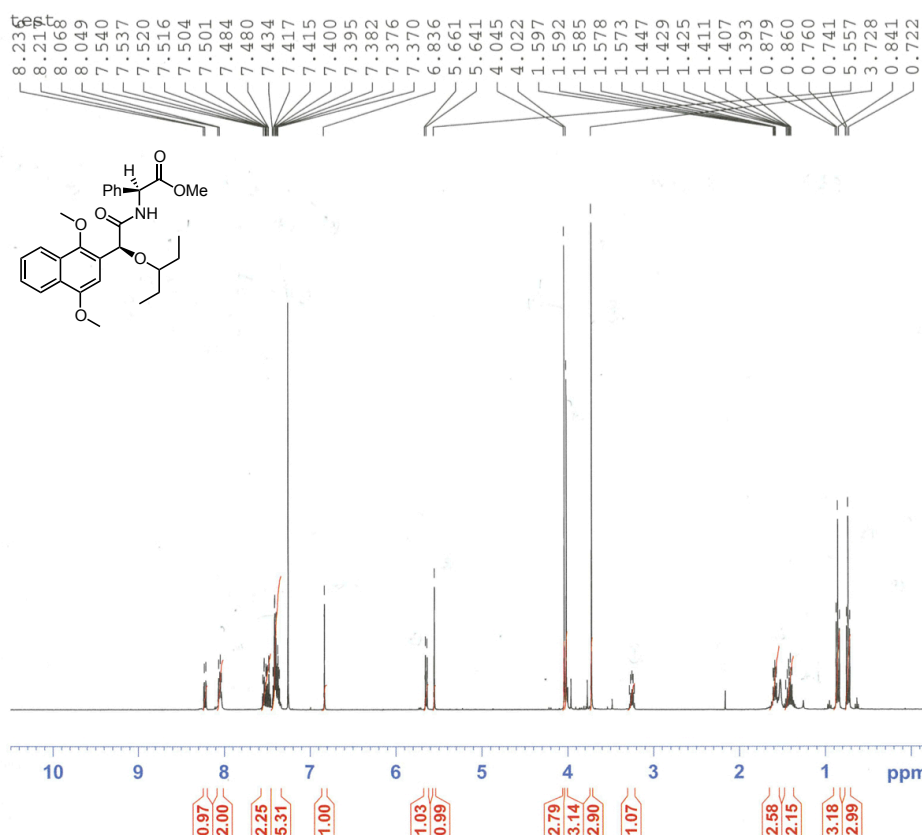
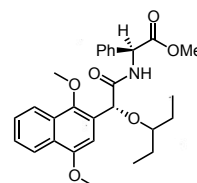
===== CHANNEL f2 =====
 CPDPRG2 waltz16
 NUC2 1H
 PCPD2 80.00 usec
 PL2 -1.50 dB
 PL12 13.00 dB
 PL13 13.00 dB
 SFO2 400.1816007 MHz

F2 - Processing parameters
 SI 32768
 SF 100.6253410 MHz
 WDW EM
 SSB 0
 LB 1.00 Hz
 GB 0
 FC 1.40



ピーク番号	波数 (cm⁻¹)	透過率 (%)	ピーク番号	波数 (cm⁻¹)	透過率 (%)
01	3486.67	96.1743	23	701.962	91.8854
02	3409.53	91.1794	24	516.829	95.0894
03	3070.12	94.2199			
04	2962.13	84.8608			
05	2846.42	92.6015			
06	2360.44	95.5093			
07	2252.45	97.5146			
08	1743.33	79.8571			
09	1681.62	77.5355			
10	1596.77	90.7763			
11	1504.20	79.1344			
12	1457.92	84.0025			
13	1365.35	80.0965			
14	1326.79	89.7745			
15	1265.07	89.7088			
16	1211.08	86.0191			
17	1172.51	89.5861			
18	1126.22	89.5353			
19	1072.23	84.2507			
20	995.089	91.8788			
21	840.812	97.8084			
22	771.387	90.8900			

ファイル名 :
 タイトル :
 測定日時 : 2012年03月24日 10時05分03秒
 測定分解能 : 16 cm⁻¹
 スキャン回数 : 8 回
 測定ゲイン : 1
 コメント :



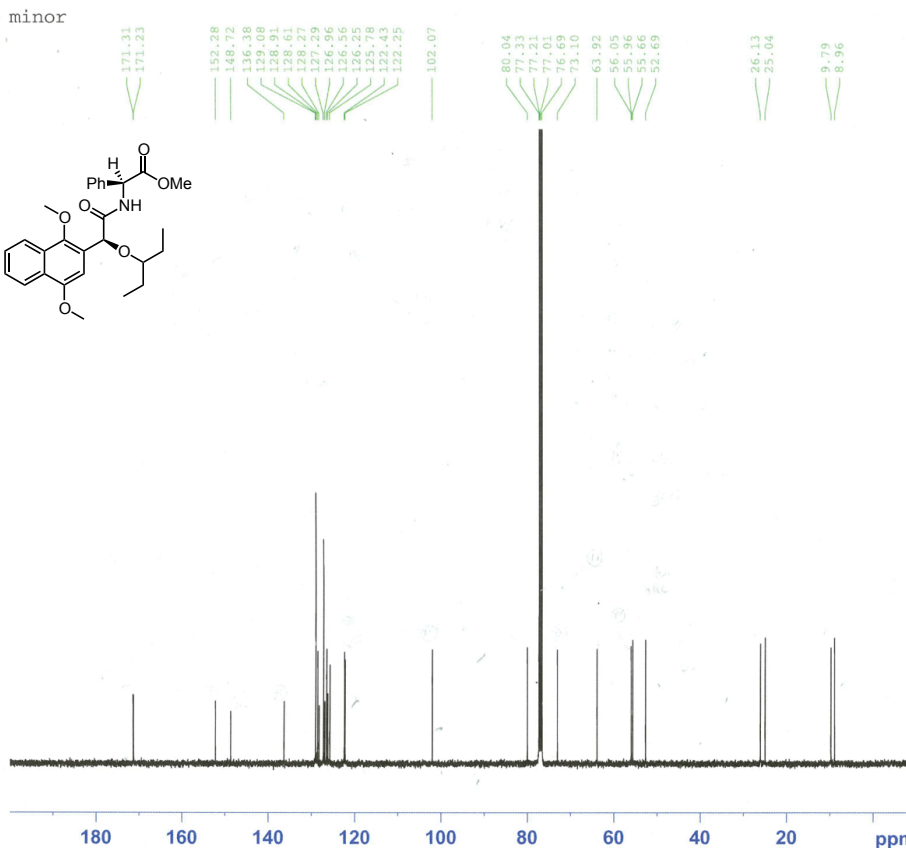
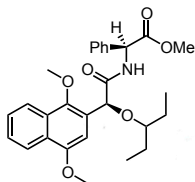
Current Data Parameters
 NAME Nov21-2011
 EXPNO 45
 PROCNO 1

 F2 - Acquisition Parameters
 Date_ 20111121
 Time 15.32
 INSTRUM dpx400
 PROBD 5 mm QNP 1H/29
 PULPROG zg30
 TD 32768
 SOLVENT CDC13
 NS 16
 DS 0
 SWH 8223.685 Hz
 FIDRES 0.250967 Hz
 AQ 1.9923444 sec
 RG 18390.4
 DW 60.800 usec
 DE 6.00 usec
 TE 303.2 K
 D1 1.00000000 sec
 MCREST 0.00000000 sec
 MCWRK 0.01500000 sec

 ===== CHANNEL f1 =====
 NUC1 1H
 P1 7.90 usec
 PL1 3.00 dB
 SFO1 400.1324710 MHz

 F2 - Processing parameters
 SI 16384
 SF 400.1300090 MHz
 WDW EM
 SSB 0
 LB 0.30 Hz
 GB 0
 PC 1.00

minor



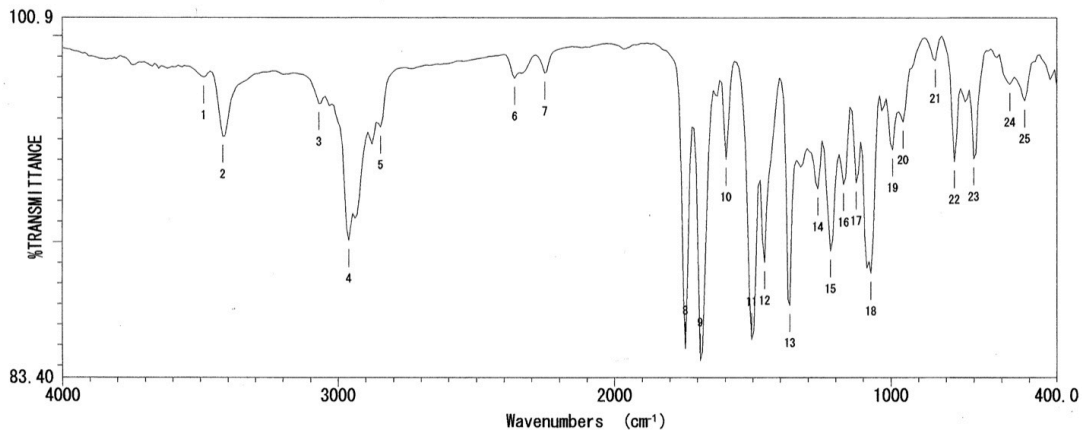
Current Data Parameters
NAME Mar04-2012-hayashi
EXPNO 20
PROCNO 1

F2 - Acquisition Parameters
Date_ 20120305
Time 0.22
INSTRUM spect
PROBHD 5 mm PABBO BB-
PULPROG zgpg30
TD 65536
SOLVENT CDCl3
NS 3000
DS 4
SWH 24038.461 Hz
FIDRES 0.366798 Hz
AQ 1.3631988 sec
RG 64
DW 20.800 usec
DE 6.00 usec
TE 303.5 K
D1 2.00000000 sec
d11 0.03000000 sec
DELTA 1.89999998 sec
TD0 1

===== CHANNEL f1 =====
NUC1 13C
P1 7.10 usec
PL1 -3.50 dB
SFO1 100.6354036 MHz

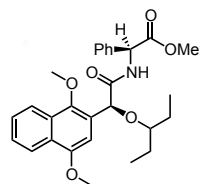
===== CHANNEL f2 =====
CPDPRG2 waltz16
NUC2 1H
PCPD2 80.00 usec
PL2 -1.50 dB
PL12 13.00 dB
PL13 13.00 dB
SFO2 400.1816007 MHz

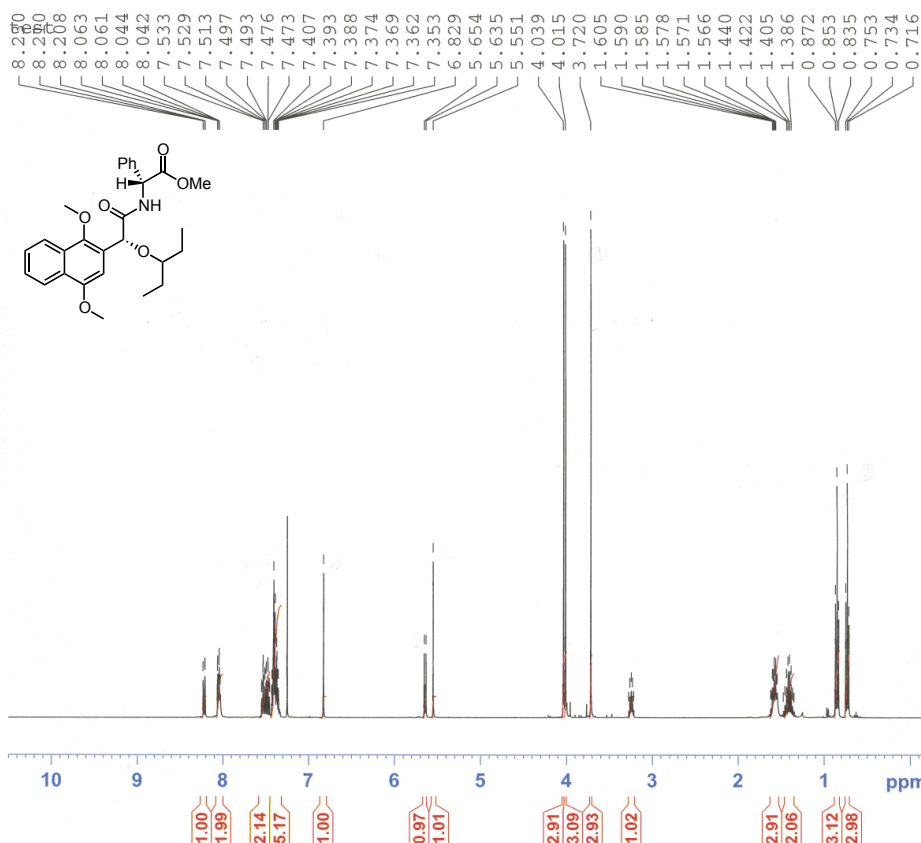
F2 - Processing parameters
SI 32768
SF 100.6253426 MHz
WDW EM
SSB 0
LB 1.00 Hz
GB 0
PC 1.40



ファイル名 :
タイトル :
測定日時 : 2012年03月24日 10時10分42秒
測定分解能 : 16 cm⁻¹
スキャン回数 : 8 回
測定ゲイン : 1
コメント :

ピーク番号	波数 (cm⁻¹)	透過率 (%)	ピーク番号	波数 (cm⁻¹)	透過率 (%)
01	3486.67	98.0034	23	701.962	94.0386
02	3417.24	95.1382	24	570.826	97.6599
03	3070.12	96.7149	25	516.829	96.8554
04	2962.13	90.0659			
05	2846.42	95.5895			
06	2360.44	97.9515			
07	2252.45	98.2044			
08	1743.33	84.8205			
09	1689.34	84.2411			
10	1596.77	94.0276			
11	1504.20	85.2530			
12	1457.92	89.0069			
13	1365.35	86.9386			
14	1265.07	92.5815			
15	1218.79	89.5567			
16	1172.51	92.7900			
17	1126.22	92.8705			
18	1072.23	88.4875			
19	995.089	94.4749			
20	956.520	95.8291			
21	840.812	98.8161			
22	771.387	93.9078			



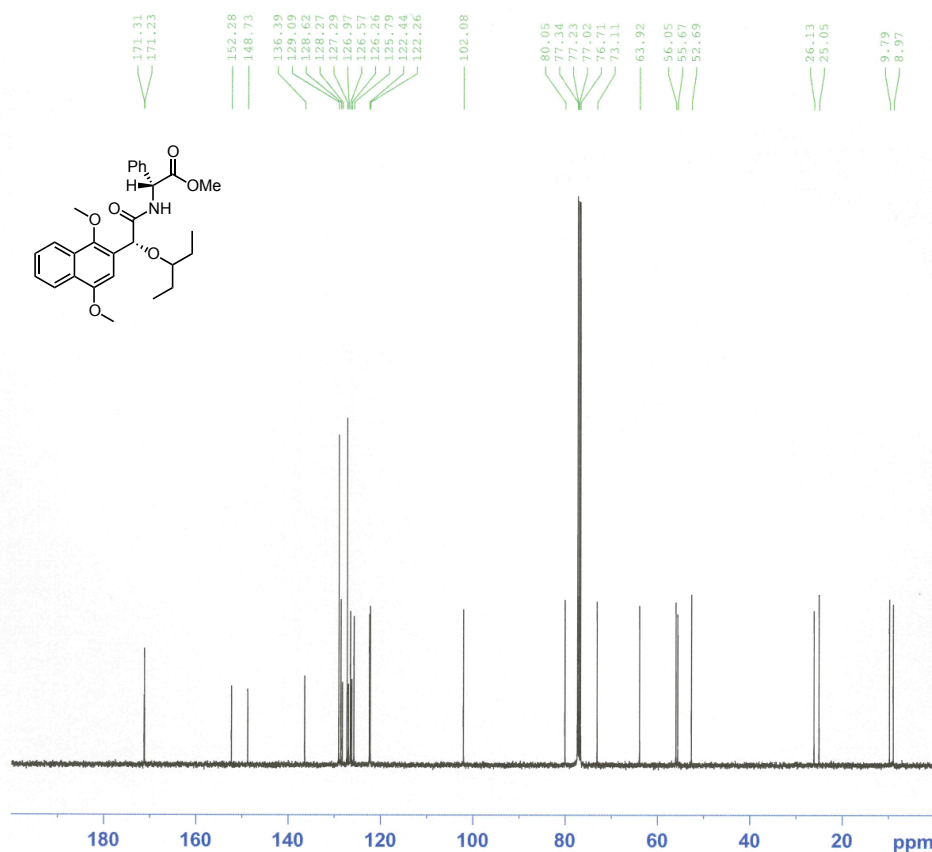


Current Data Parameters
 NAME Nov21-2011
 EXPNO 74
 PROCNO 1

F2 - Acquisition Parameters
 Date_ 20111121
 Time 19.02
 INSTRUM dpx400
 PROBHD 5 mm QNP 1H/29
 PULPROG zg30
 TD 32768
 SOLVENT CDCl3
 NS 16
 DS 0
 SWH 8223.685 Hz
 FIDRES 0.250967 Hz
 AQ 1.9923444 sec
 RG 11585.2
 DW 60.800 usec
 DE 6.00 usec
 TE 303.2 K
 D1 1.00000000 sec
 MCREST 0.00000000 sec
 MCWRK 0.01500000 sec

===== CHANNEL f1 =====
 NUC1 1H
 P1 7.90 usec
 PL1 3.00 dB
 SFO1 400.1324710 MHz

F2 - Processing parameters
 SI 16384
 SF 400.1300124 MHz
 WDW EM
 SSB 0
 LB 0.30 Hz
 GB 0
 PC 1.00



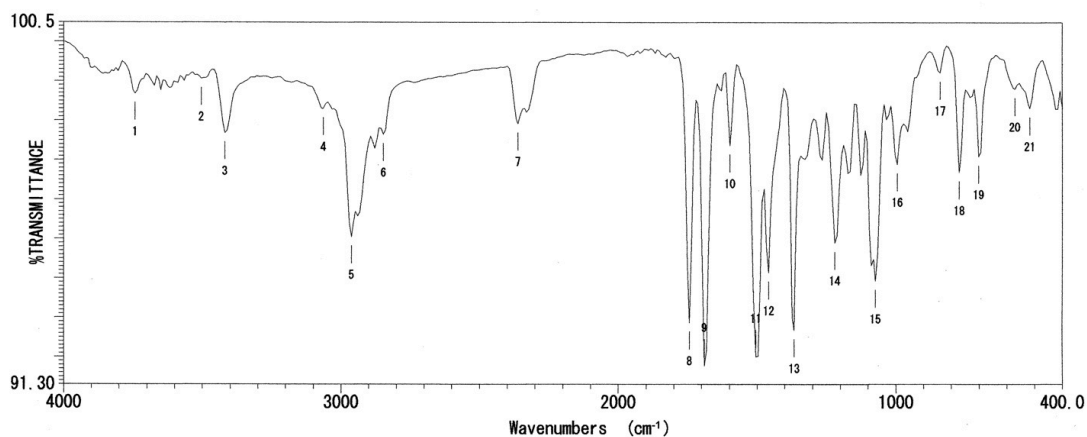
Current Data Parameters
 NAME Mar15-2012-hayashi
 EXPNO 190
 PROCNO 1

F2 - Acquisition Parameters
 Date_ 20120316
 Time 3.30
 INSTRUM spect
 PROBHD 5 mm PABBO BE-
 PULPROG zgpg30
 TD 65536
 SOLVENT CDCl3
 NS 1024
 DS 4
 SWH 24038.461 Hz
 FIDRES 0.366798 Hz
 AQ 1.3631988 sec
 RG 362
 DW 20.800 usec
 DE 6.00 usec
 TE 303.6 K
 D1 2.00000000 sec
 d11 0.03000000 sec
 DELTA 1.89999998 sec
 TD0 1

===== CHANNEL f1 =====
 NUC1 13C
 P1 7.10 usec
 PL1 -3.50 dB
 SFO1 100.6354036 MHz

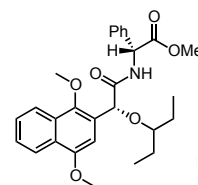
===== CHANNEL f2 =====
 CPDPRG2 waltz16
 NUC2 1H
 PCPD2 80.00 usec
 PL2 -1.50 dB
 PL12 13.00 dB
 PL13 13.00 dB
 SFO2 400.1816007 MHz

F2 - Processing parameters
 SI 32768
 SF 100.6253410 MHz
 WDW EM
 SSB 0
 LB 1.00 Hz
 GB 0
 PC 1.40

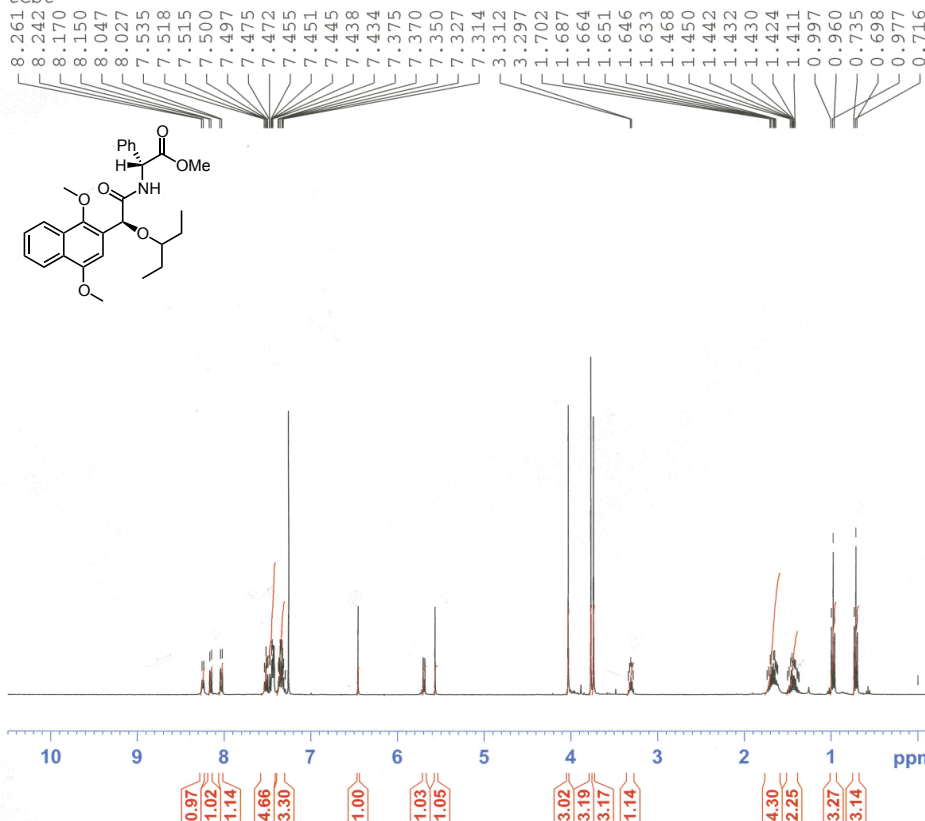


ピーク番号	波数 (cm⁻¹)	透過率 (%)
01	3741.23	98.6874
02	3502.10	99.0623
03	3417.24	97.6898
04	3062.41	98.3062
05	2962.13	95.0537
06	2846.42	97.6466
07	2360.44	97.9243
08	1743.33	92.8624
09	1689.34	91.7682
10	1596.77	97.3667
11	1504.20	92.0010
12	1457.92	94.1336
13	1365.35	92.6720
14	1218.79	94.8971
15	1072.23	93.9284
16	995.089	96.8978
17	840.812	99.2155
18	771.387	96.6819
19	701.962	97.0873
20	570.826	98.8052
21	516.829	98.3108

ファイル名
 タイトル
 測定日時 2012年03月24日 10時21分46秒
 測定分解能 16 cm⁻¹
 スキャン回数 8 回
 測定ゲイン 1
 コメント



test

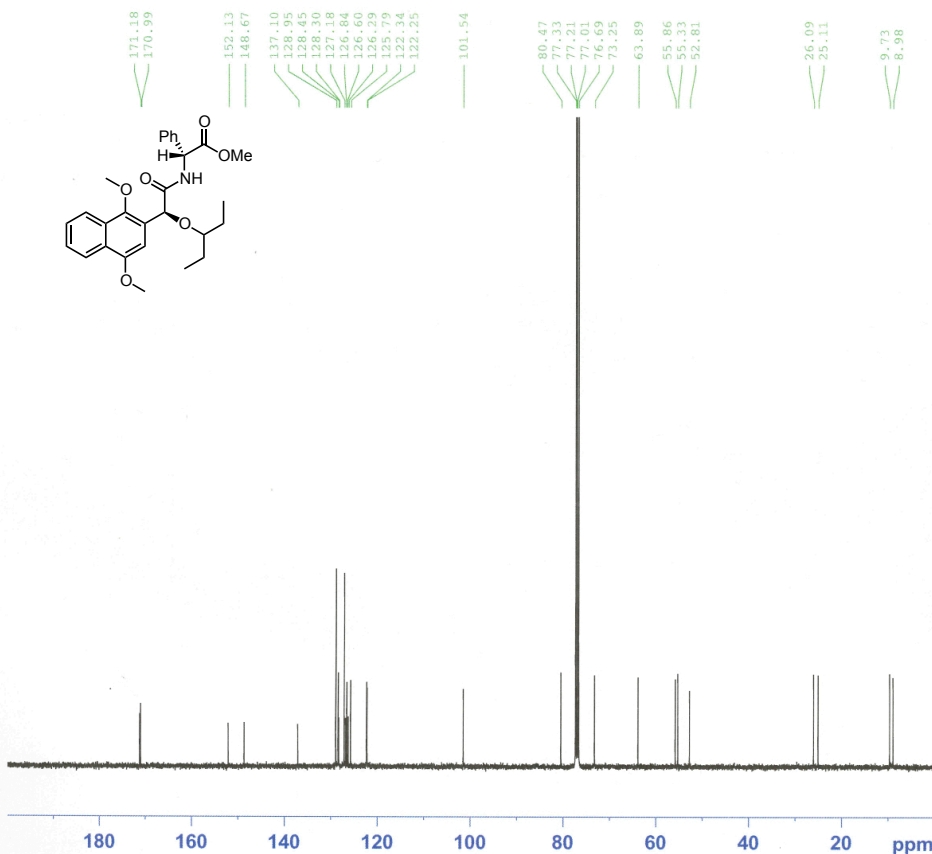
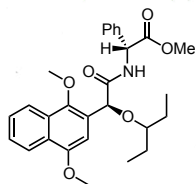


Current Data Parameters
 NAME Nov21-2011
 EXPNO 75
 PROCNO 1

F2 - Acquisition Parameters
 Date_ 20111121
 Time 19.06
 INSTRUM dpx400
 PROBHD 5 mm QNP 1H/29
 PULPROG zg30
 TD 32768
 SOLVENT DMSO
 NS 16
 DS 0
 SWH 8223.685 Hz
 FIDRES 0.250967 Hz
 AQ 1.9923444 sec
 RG 16384
 DW 60.800 usec
 DE 6.00 usec
 TE 303.2 K
 D1 1.00000000 sec
 MCREST 0.00000000 sec
 MCWRR 0.01500000 sec

===== CHANNEL f1 =====
 NUC1 1H
 P1 7.90 usec
 PL1 3.00 dB
 SFO1 400.1324710 MHz

F2 - Processing parameters
 SI 16384
 SF 400.1300089 MHz
 WDW EM
 SSB 0
 LB 0.30 Hz
 GB 0
 PC 1.00



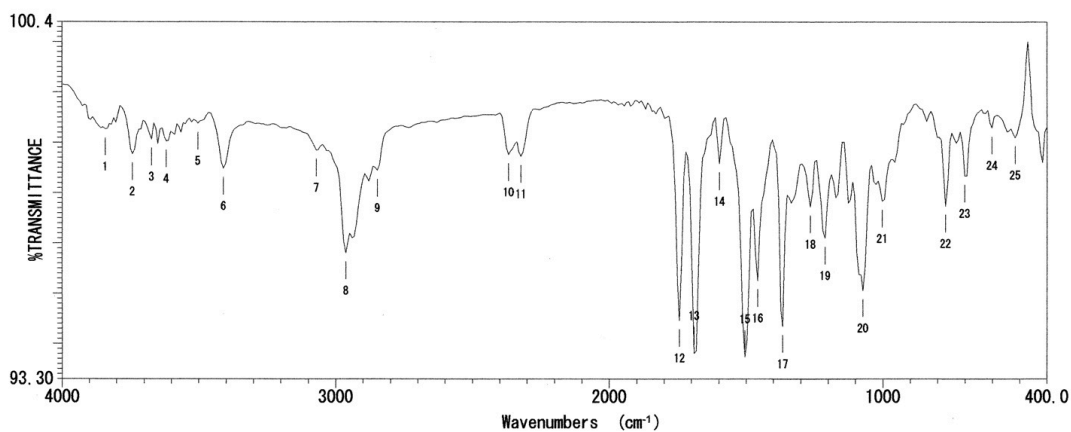
Current Data Parameters
NAME Mar15-2012-hayashi
EXPNO 200
PROCNO 1

F2 - Acquisition Parameters
Date_ 20120316
Time 5.31
INSTRUM spect
PROBHD 5 mm PABBO BB-
PULPROG zgpg30
TD 65536
SOLVENT CDCl3
NS 2000
DS 4
SWH 24038.461 Hz
FIDRES 0.366798 Hz
AQ 1.3631988 sec
RG 64
DW 20.800 usec
DE 6.00 usec
TE 303.4 K
D1 2.00000000 sec
d11 0.03000000 sec
DELTA 1.89999998 sec
TD0 1

===== CHANNEL f1 =====
NUC1 13C
P1 7.10 usec
PL1 -3.50 dB
SFO1 100.6354036 MHz

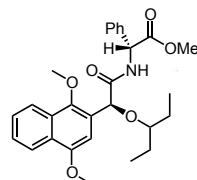
===== CHANNEL f2 =====
CPDPRG2 waltz16
NUC2 1H
PCPD2 80.00 usec
PL2 -1.50 dB
PL12 13.00 dB
PL13 13.00 dB
SFO2 400.1816007 MHz

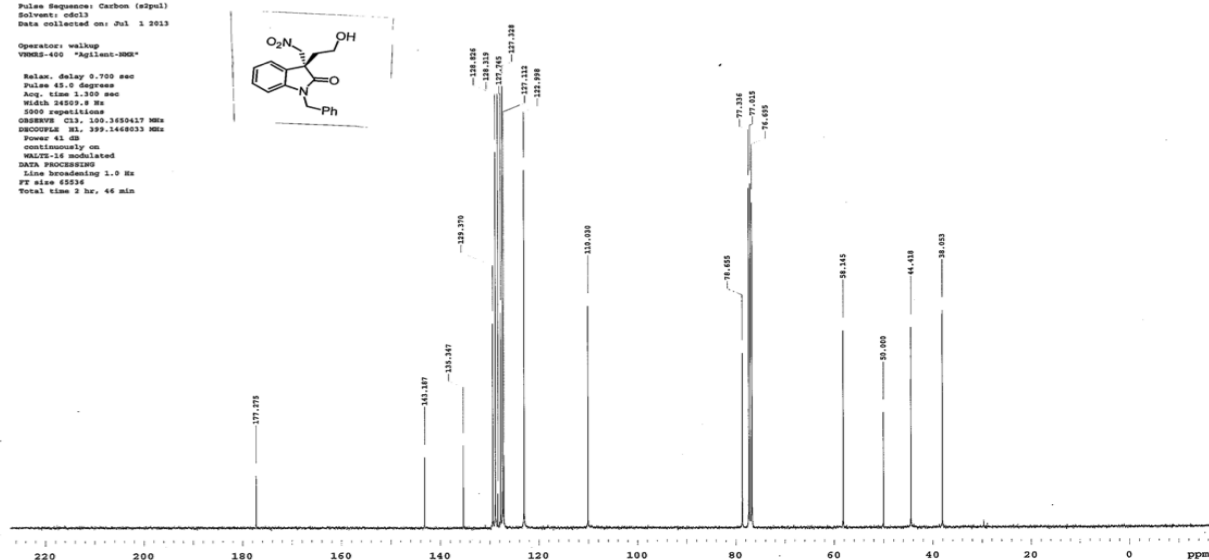
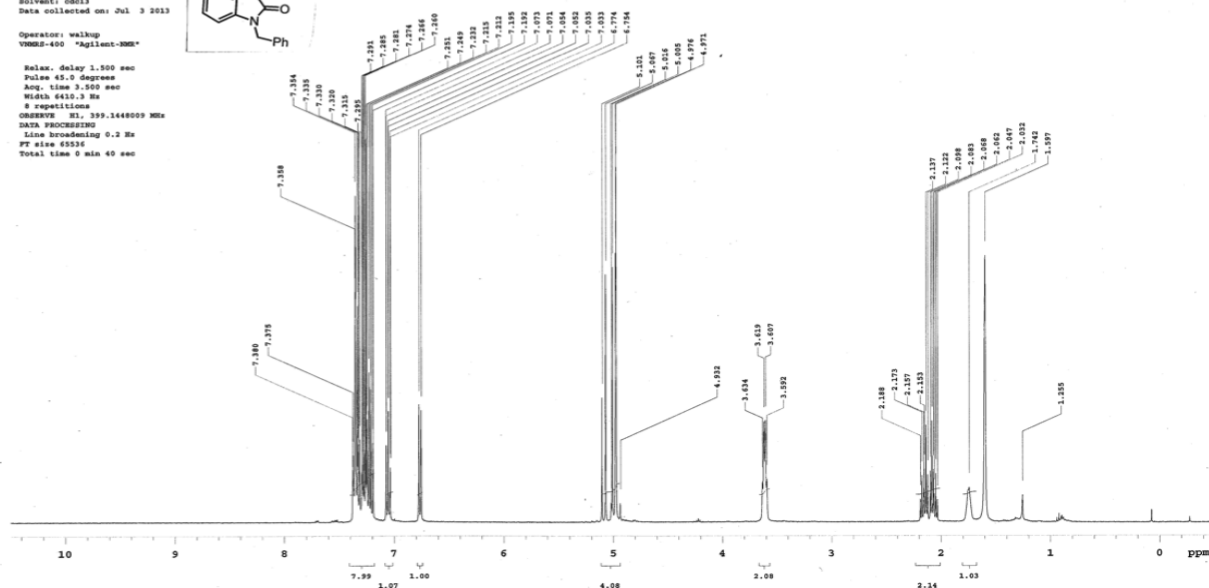
F2 - Processing parameters
SI 32768
SF 100.6253410 MHz
WDW EM
SSB 0
LB 1.00 Hz
GB 0
PC 1.40

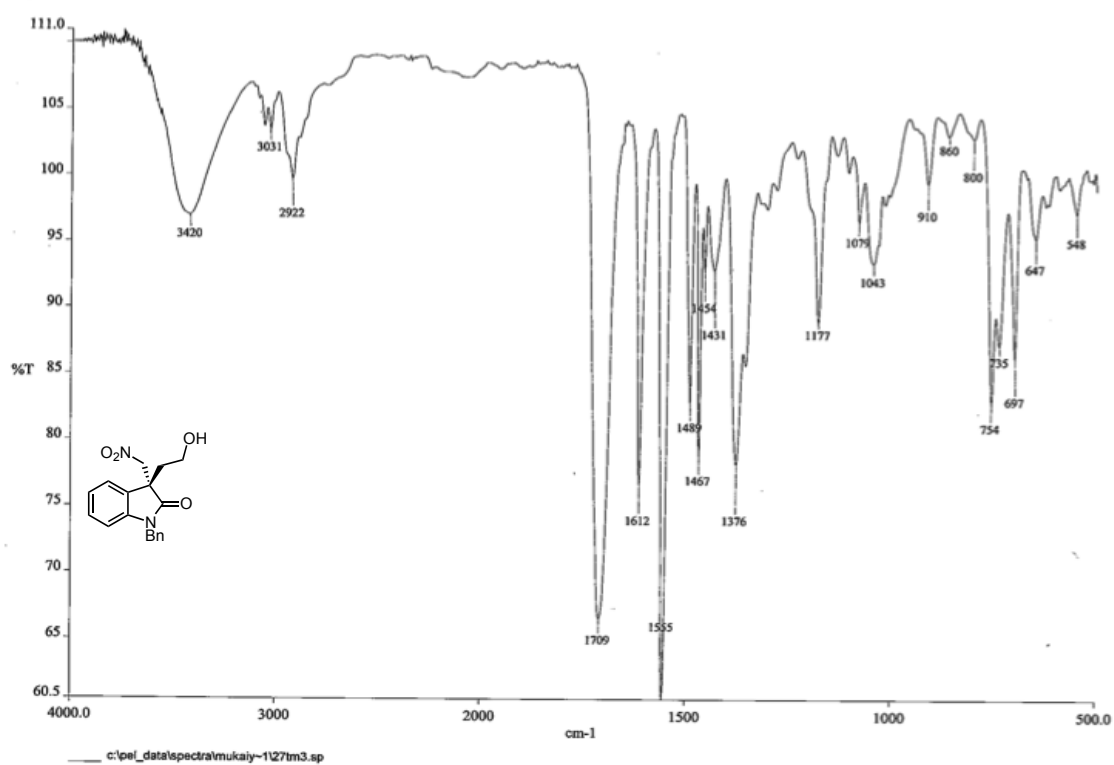


ピーク番号	波数 (cm ⁻¹)	透過率 (%)	ピーク番号	波数 (cm ⁻¹)	透過率 (%)
01	3841.51	98.2689	23	701.962	97.3377
02	3741.23	97.7739	24	601.682	98.2949
03	3671.80	98.0695	25	516.829	98.1003
04	3617.80	98.0273			
05	3502.10	98.3818			
06	3409.53	97.4897			
07	3070.12	97.8508			
08	2962.13	95.8099			
09	2846.42	97.4513			
10	2368.16	97.7608			
11	2321.87	97.7224			
12	1743.33	94.4657			
13	1689.34	93.8090			
14	1596.77	97.5796			
15	1504.20	93.7397			
16	1457.92	95.2553			
17	1365.35	94.3473			
18	1265.07	96.7261			
19	1211.08	96.1031			
20	1072.23	95.0595			
21	1002.80	96.8347			
22	771.387	96.7404			

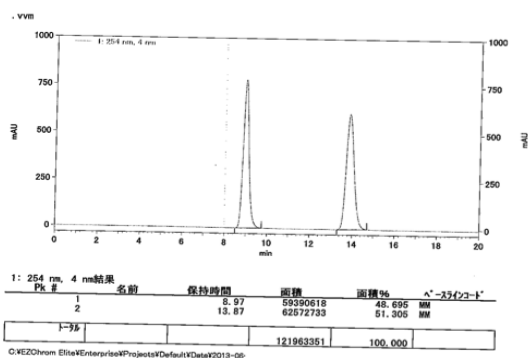
ファイル名 :
タイトル :
測定日時 : 2012年03月24日 10時26分33秒
測定分解能 : 16 cm⁻¹
スキャン回数 : 8 回
測定ゲイン : 1
コメント :



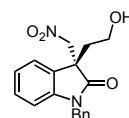
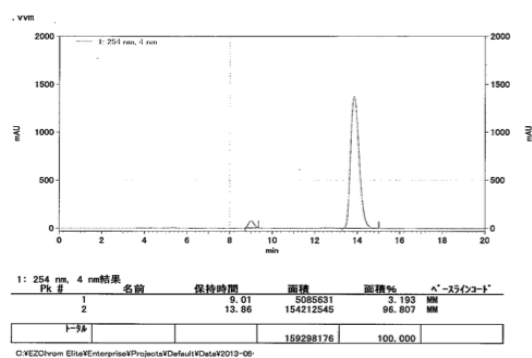
O=C1c2ccccc2N(C1)[C@H](CO)[C@@H](O)N1=CC=CC=C1



ファイル名: C:\VEZChrom Elite\Enterprise\Projects\Default\WData\2013-06-10 15-37-23
 mukaiyama IC 3vs1 1.0ml reami.dat
 ファイル名: C:\VEZChrom Elite\Enterprise\Projects\Default\Method\10vs1. 1ml.met
 システム名: System
 分析日時: 2013/06/10 15:38:04
 印刷日時: 2013/06/12 19:44:56



ファイル名: C:\VEZChrom Elite\Enterprise\Projects\Default\WData\2013-06-10 15-59-06
 mukaiyama IC 3vs1 1.0ml 27-3.dat
 ファイル名: C:\VEZChrom Elite\Enterprise\Projects\Default\Method\10vs1. 1ml.met
 システム名: System
 分析日時: 2013/06/10 15:59:46
 印刷日時: 2013/06/12 19:45:55



STANDARD IN OBSERVE - profile

Sample Name:

Archive directory:

Sample directory:

FidFile: 45-3

Pulse Sequence: Proton (zgpg3)

Solvent: cdcl3

Data collected on: Jun 18 2013

Operator: walkup

VNMRS-400 "Agilent-VNM"

Relax. delay 1.500 sec

Pulse 45.0 degrees

Acq. time 3.500 sec

Width 6410.3 Hz

repetitions

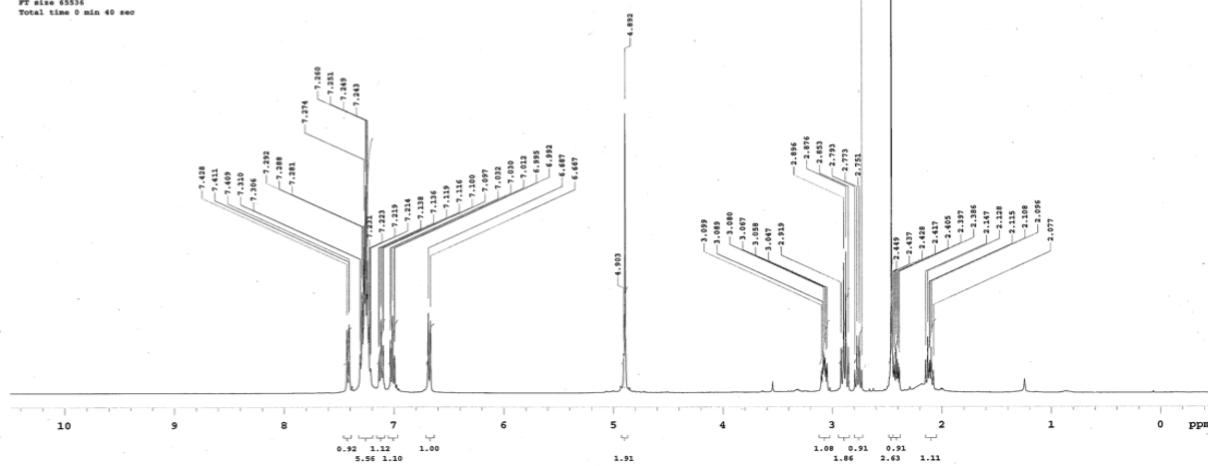
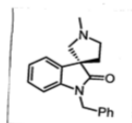
OBSERVE H1, 399.1448076 MHz

DATA PROCESSING

Line broadening 0.2 Hz

FT size 65536

Total time 0 min. 40 sec



STANDARD IN OBSERVE - profile

Sample Name:

Archive directory:

Sample directory:

FidFile: 45-3carbon

Pulse Sequence: Carbon (zgpg3)

Solvent: cdcl3

Data collected on: Jun 18 2013

Operator: walkup

VNMRS-400 "Agilent-VNM"

Relax. delay 0.700 sec

Pulse 45.0 degrees

Acq. time 1.300 sec

Width 24500.0 Hz

5000 repetitions

OBSERVE C13, 100.6250440 MHz

DECOUPLE H1, 399.1448076 MHz

Power 41.00

continuously on

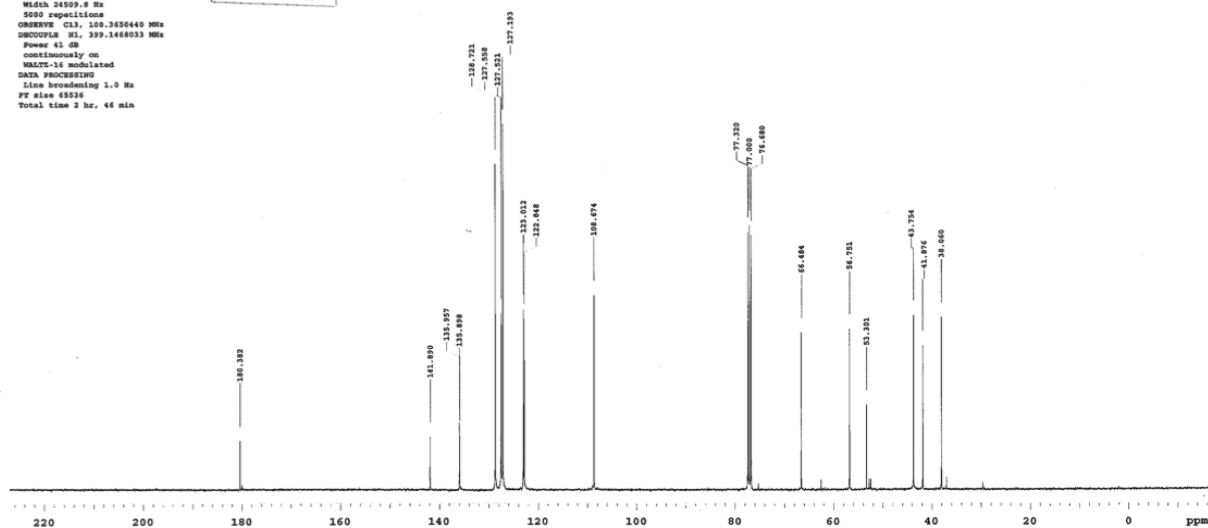
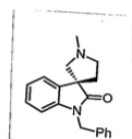
WALTZ-16 modulated

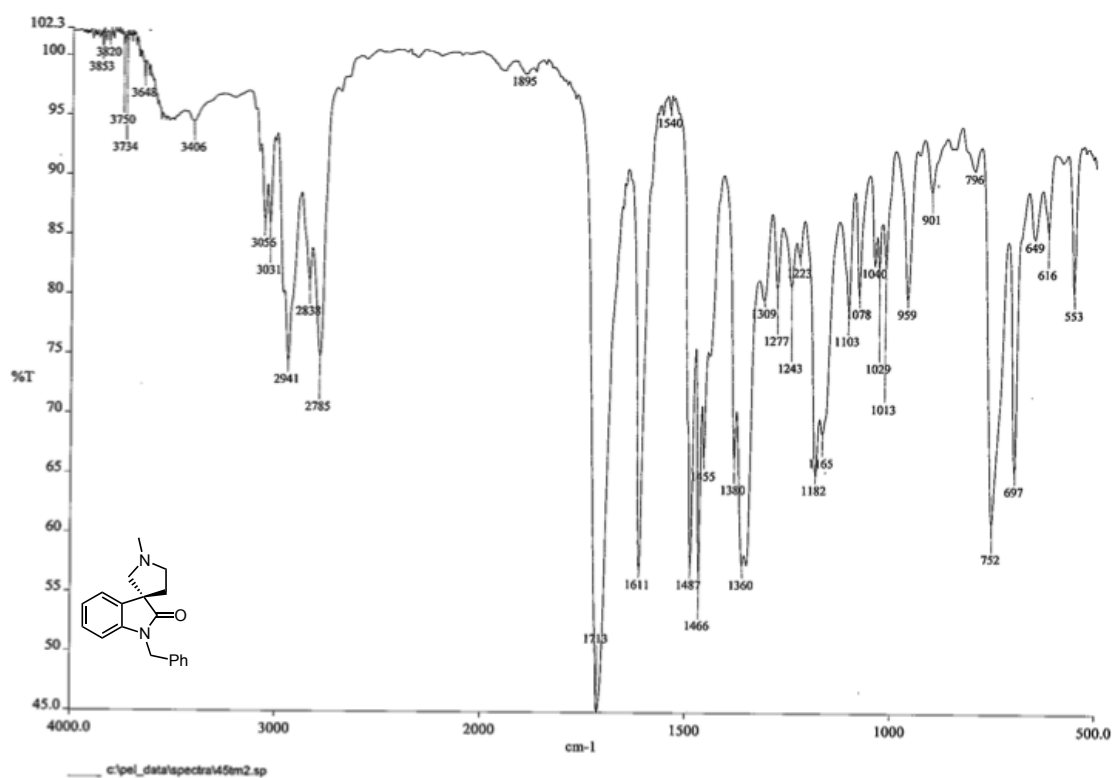
DATA PROCESSING

Line broadening 1.0 Hz

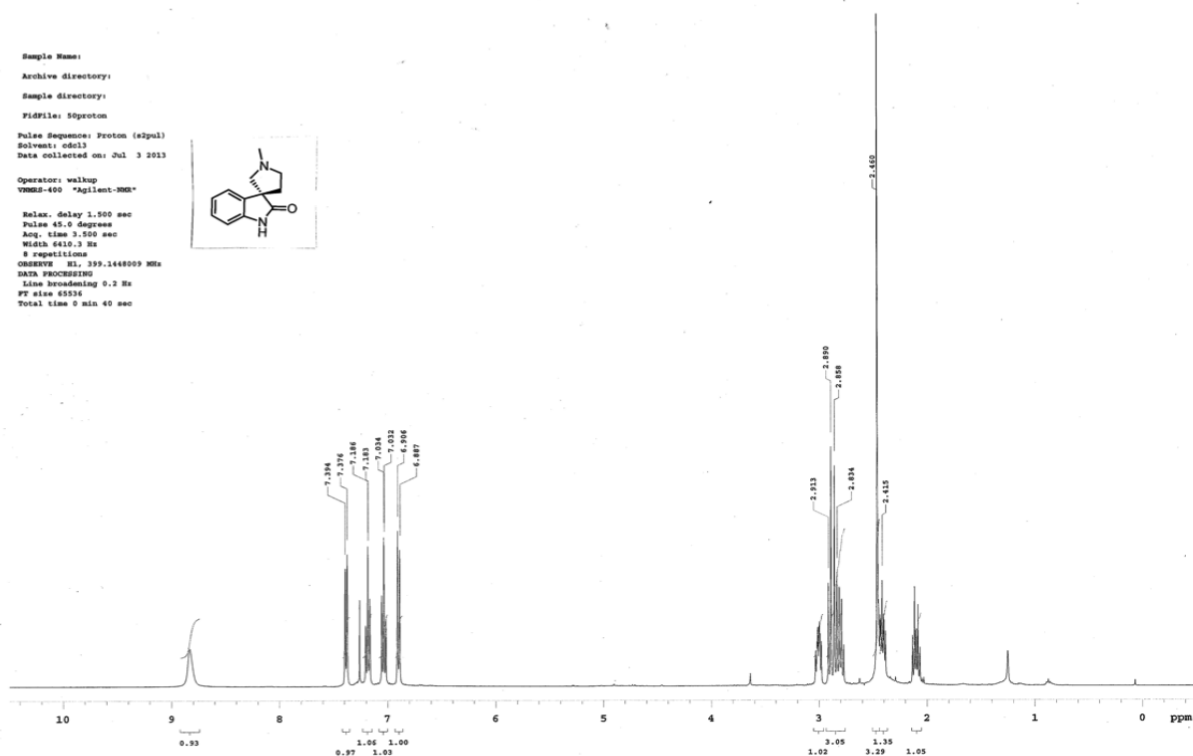
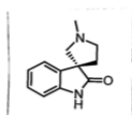
FT size 65536

Total time 2 hr, 46 min

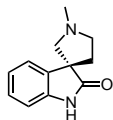
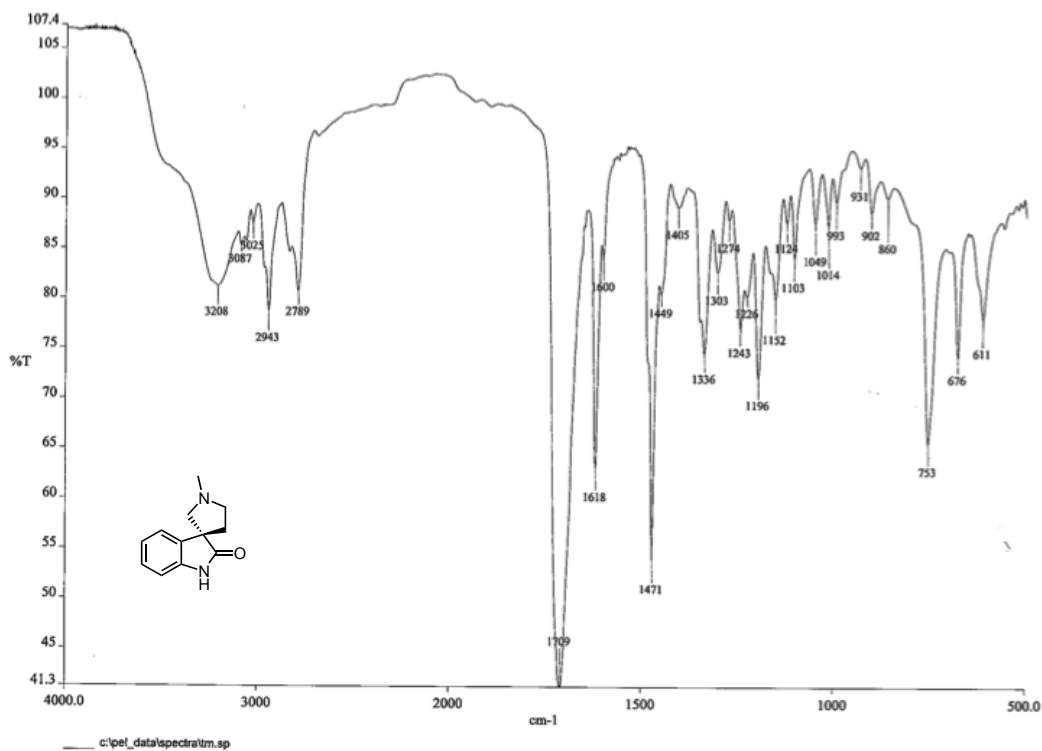
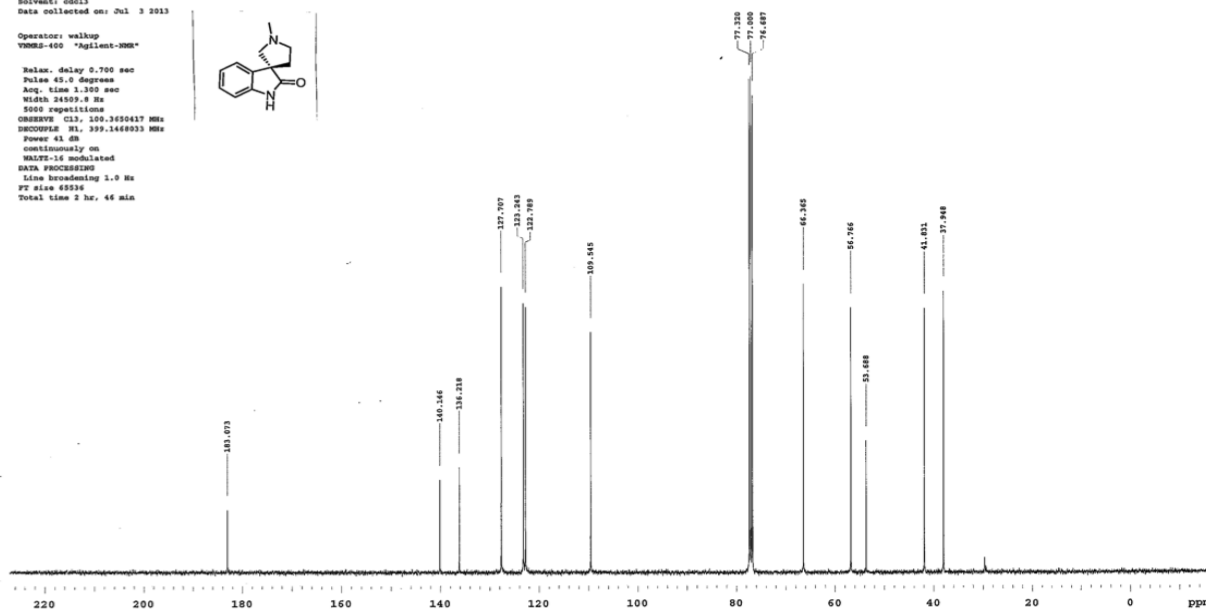
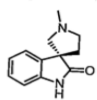




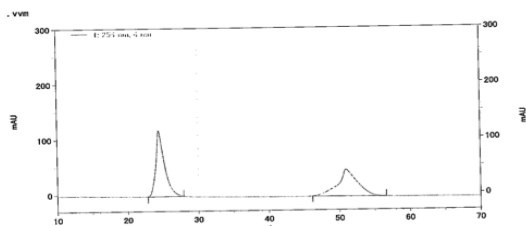
Sample Name:
 Archive directory:
 Sample directory:
 File: 50pcton
 Pulse Sequence: Proton (w2pall)
 Solvent: cdcl3
 Data collected on: Jul 3 2013
 Operator: walkup
 VENDOR: Agilent-9000
 Relax. delay 1.500 sec
 Pulse 45.0 degrees
 Acq. time 3.500 sec
 Width 6410.3 Hz
 8 repetitions
 OBSERVE: 90.139.1448009 MHz
 DATA PROCESSING
 Line broadening 0.2 Hz
 FT size 65536
 Total time 3 min 40 sec



Sample Name:
 Archive directory:
 Sample directory:
 File: 504000
 Pulse Sequence: Carbon (zgpg30)
 Solvent: cdcl3
 Data collected on: Jul 3 2013
 Operator: walkup
 VENDOR: agilent-300m
 Relax. delay: 5.700 sec
 Pulse: zgpg30
 Acq. time: 1.300 sec
 Width: 24509.8 Hz
 5000 repetitions
 OBSERVE: C13, 100.6250417 MHz
 DECOUPLE: H1, 100.6250417 MHz
 Power: 41 dB
 continuously on
 WALTZ-16 modulated
 DATA PROCESSING
 Line broadening: 1.0 Hz
 FT size: 65536
 Total time: 2 hr, 46 min

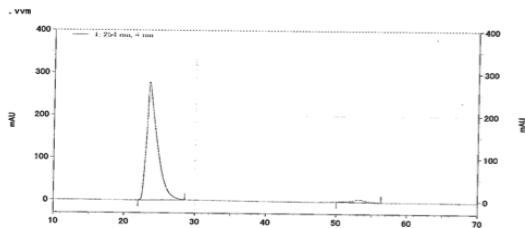


9'-97748名: C:\VEZChrom EliteEnterprise\Projects\Default\WData\2013-07-15 13-36-39
 mukaiyama AS-H 10vs1 1 ml racem 64-2.dat
 97747名: C:\VEZChrom EliteEnterprise\Projects\Default\WMethod\10vs1. 1ml.met
 97748名: System
 分析日時: 2013/07/15 13:37:21
 印刷日時: 2013/07/15 16:17:38

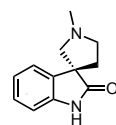


1: 254 nm, 4 nm結果	峰 #	名前	保持時間	面積	面積%	ピークタイプ
	1		24.45	40758317	52.252	MM
	2		50.96	37244547	47.748	MM
	トータル			78002864	100.000	

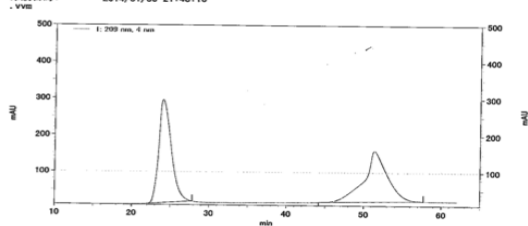
9'-97748名: C:\VEZChrom EliteEnterprise\Projects\Default\WData\2013-07-15 14-55-04
 mukaiyama AS-H 10vs1 1 ml 50-3.dat
 97747名: C:\VEZChrom EliteEnterprise\Projects\Default\WMethod\10vs1. 1ml.met
 97748名: System
 分析日時: 2013/07/15 14:55:49
 印刷日時: 2013/07/15 16:16:47



1: 254 nm, 4 nm結果	峰 #	名前	保持時間	面積	面積%	ピークタイプ
	1		23.53	114491214	97.166	MM
	2		53.18	3339046	2.834	MM
	トータル			117830260	100.000	



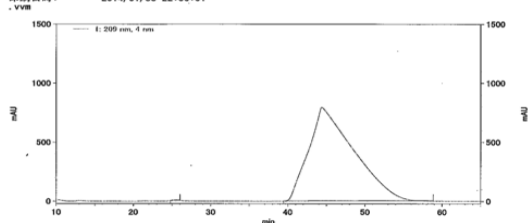
97748名: System
 分析日時: 2014/01/30 19:34:15
 印刷日時: 2014/01/30 21:48:10



1: 209 nm, 4 nm結果	峰 #	名前	保持時間	面積	面積%	ピークタイプ
	1		24.00	123756977	51.528	MM
	2		51.37	118790061	48.372	MM
	トータル			242547038	100.000	

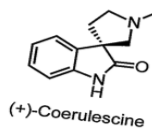
C:\VEZChrom EliteEnterprise\Projects\Default\WData\2014-01-

mukaiyama AS-H 10vs1 162-2.dat
 97747名: C:\VEZChrom EliteEnterprise\Projects\Default\WMethod\10vs1. 1ml.met
 97748名: System
 分析日時: 2014/01/30 20:37:35
 印刷日時: 2014/01/30 22:04:01

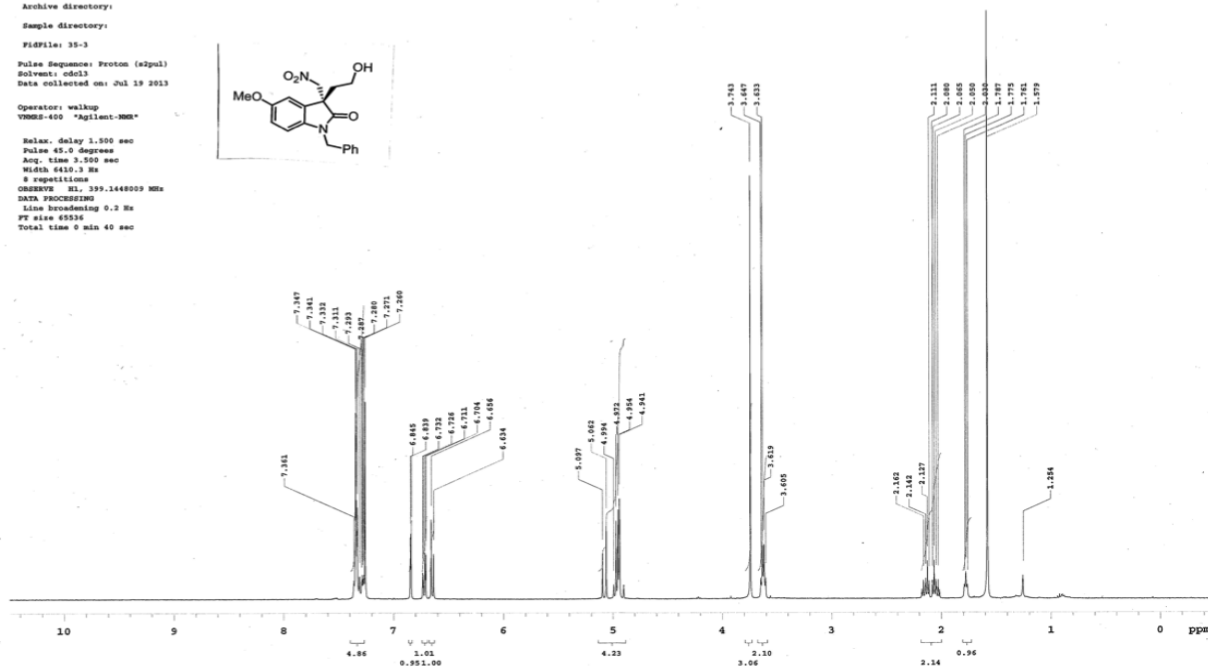
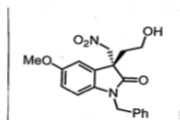


1: 209 nm, 4 nm結果	峰 #	名前	保持時間	面積	面積%	ピークタイプ
	1		25.44	884520	0.068	MM
	2		44.39	1284190431	99.932	MM
	トータル			1285074951	100.000	

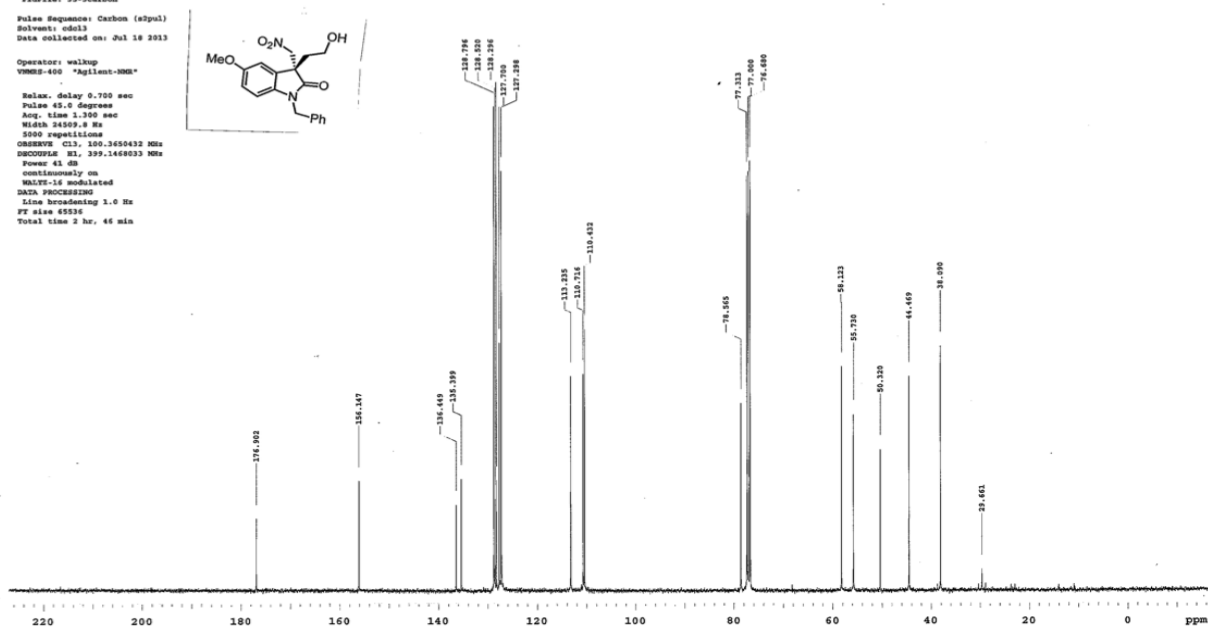
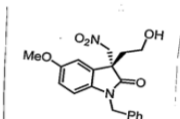
C:\VEZChrom EliteEnterprise\Projects\Default\WData\2014-01-

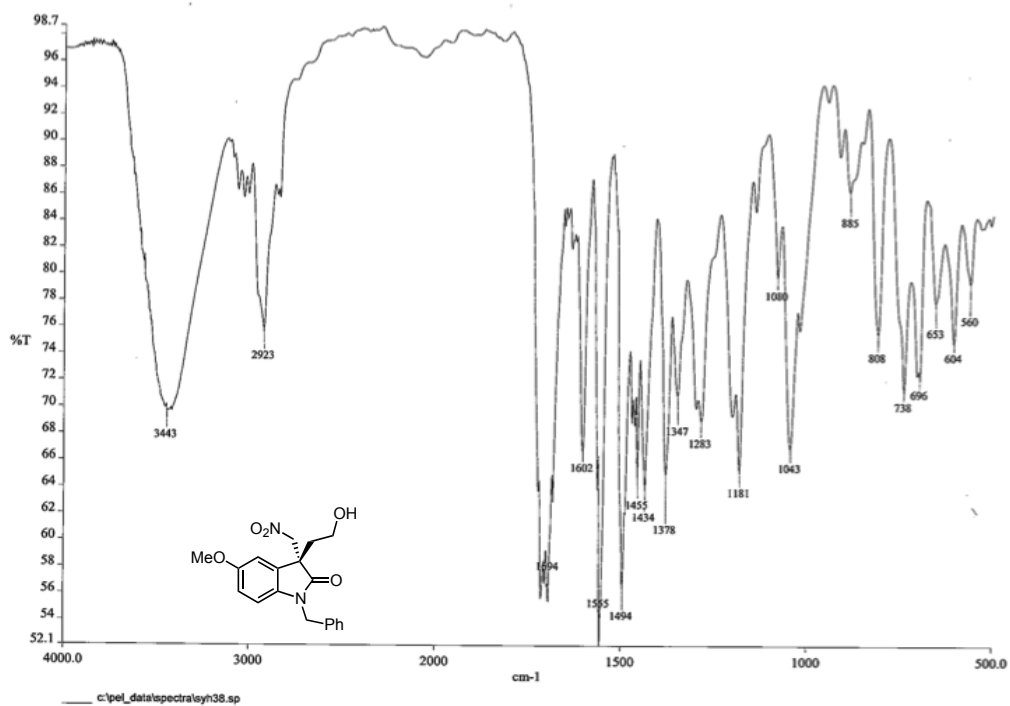


Sample Name:
 Archive directory:
 Sample directory:
 File: 35-3
 Pulse Sequence: Proton (zgpg3)
 Solvent: cdcl3
 Date collected on: Jul 19 2013
 Operator: walkup
 VNMRS-400 "Agilent-NMR"
 Relax. delay 1.500 sec
 Pulse 42.0 degrees
 Acq. time 1.500 sec
 Width 6410.3 Hz
 5 repetitions
 OBSERVE H1, 399.1448003 MHz
 DATA PROCESSING
 Line broadening 0.3 Hz
 FT size 65536
 Total time 0 min 40 sec



Sample Name:
 Archive directory:
 Sample directory:
 File: 35-3carbon
 Pulse Sequence: Carbon (zgpg3)
 Solvent: cdcl3
 Date collected on: Jul 19 2013
 Operator: walkup
 VNMRS-400 "Agilent-NMR"
 Relax. delay 0.700 sec
 Pulse 42.0 degrees
 Acq. time 1.300 sec
 Width 34509.8 Hz
 500 repetitions
 OBSERVE C13, 100.6250432 MHz
 DECOUPLE H1, 399.1448003 MHz
 Power 41.00
 continuously on
 WALTZ-16 modulated
 DATA PROCESSING
 Line broadening 1.0 Hz
 FT size 65536
 Total time 2 hr, 46 min

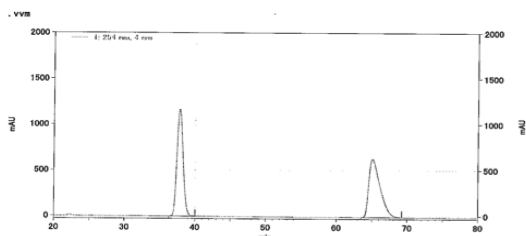




面積%レポート

ページ 1/1

データファイル名: C:\WEZChrom Elite\Enterprise\Projects\Default\Data\2013-06-27 10-25-36
 opata_1-119 IC 10vs1_1ml raceml.dat
 ファイル名: C:\WEZChrom Elite\Enterprise\Projects\Default\Method\10vs1_1ml.met
 システム名: System
 分析日時: 2013/06/27 10:26:19
 印刷日時: 2013/06/27 15:51:36

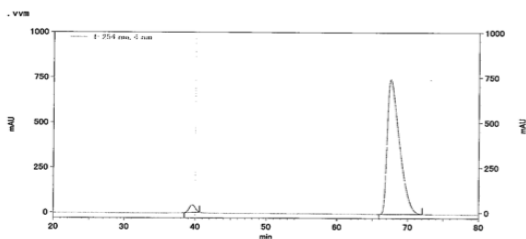


PK #	名前	保持時間	面積	面積%	ピーク番号
1		37.65	281878461	49.983	MM
2		65.10	282070873	50.017	MM
合計			563949334	100.000	

C:\WEZChrom Elite\Enterprise\Projects\Default\Data\2013-06

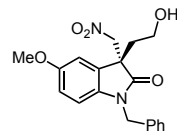
面積%レポート

データファイル名: C:\WEZChrom Elite\Enterprise\Projects\Default\Data\2013-06-27 12-25-44
 mukaiyama IC 10vs1_1ml 35-3.dat
 ファイル名: C:\WEZChrom Elite\Enterprise\Projects\Default\Method\10vs1_1ml.met
 システム名: System
 分析日時: 2013/06/27 12:27:09
 印刷日時: 2013/06/27 15:52:27

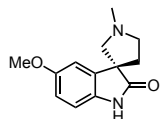
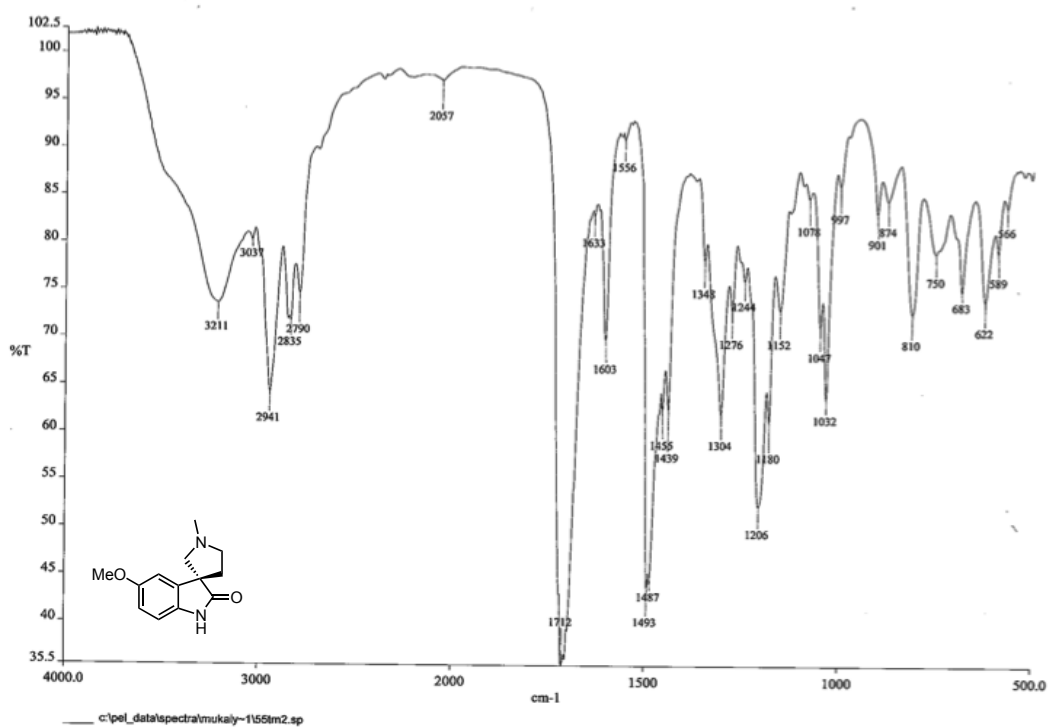
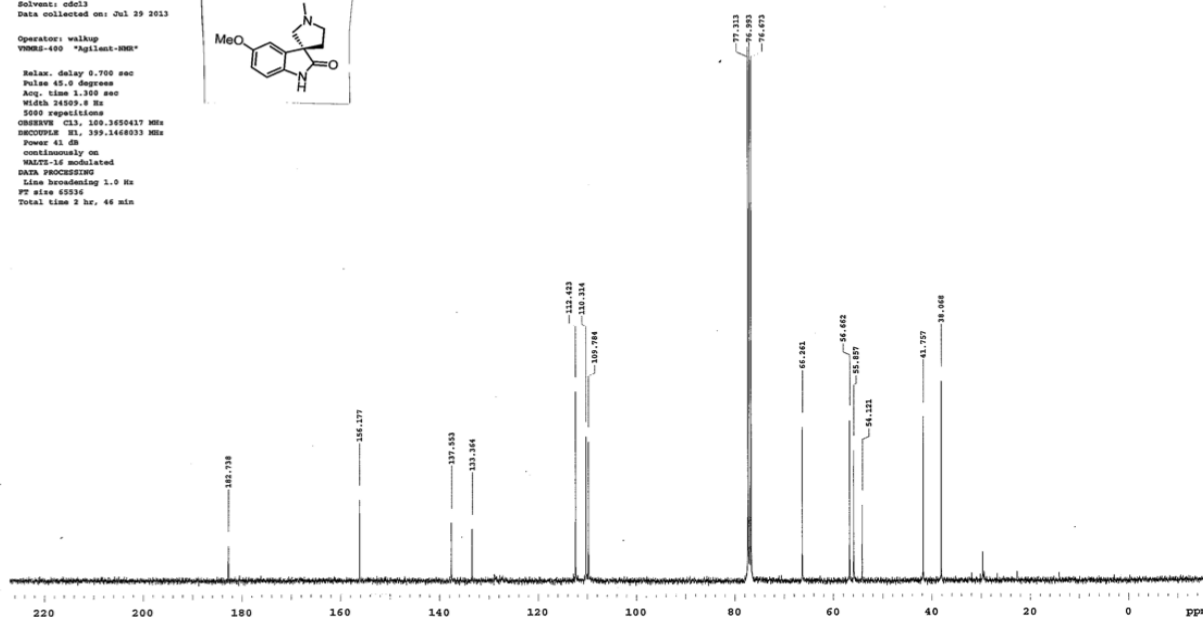
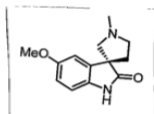


PK #	名前	保持時間	面積	面積%	ピーク番号
1		39.63	10071381	2.734	MM
2		67.59	358362469	97.266	MM
合計			368433850	100.000	

C:\WEZChrom Elite\Enterprise\Projects\Default\Data\2013-06

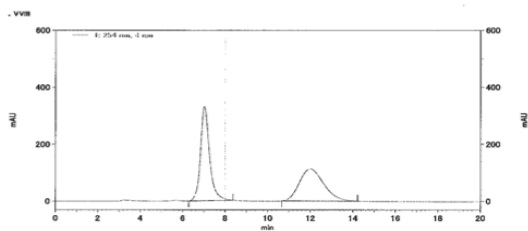


Sample Name:
 Archive directory:
 Sample directory:
 File: borefiline-carbon
 Pulse Sequence: Carbon (zgpg3)
 Solvent: cdcl3
 Data collected on: Jul 29 2012
 Operator: walkup
 VENDOR: Agilent-400
 Pulse: delay 0.700 sec
 Pulse: 45.0 degrees
 Acq. time 1.300 sec
 VSWH 24507.0 Hz
 5000 repetitions
 OBSERVE CL3, 100.625017 MHz
 DECUPLE 93, 199.1468033 MHz
 Power 41 dB
 continuously on
 WALTZ-16 modulated
 DATA PROCESSING
 Line broadening 1.0 Hz
 FT size 65536
 Total time 2 hr, 44 min



面積%レポート

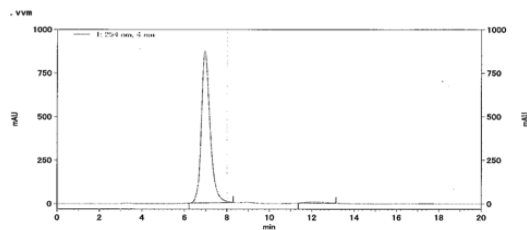
ファイル名: C:\VEZChrom\EliteEnterprise\Projects\Default\data\2013-07-18 22-17-28
 分析名: 10vsl 1 ml 60-2 raceml.dat
 ファイル名: C:\VEZChrom\EliteEnterprise\Projects\Default\data\2013-07-18 22-17-28
 システム: System
 分析日時: 2013/07/18 22:18:08
 印刷日時: 2013/07/18 23:14:40



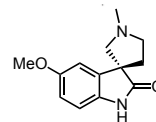
PK #	名前	保持時間	面積	面積%	ピークタイプ
1		7.03	35311873	52.386	MM
2		12.00	35731273	47.614	MM
トータル			75043146	100.000	

面積%レポート

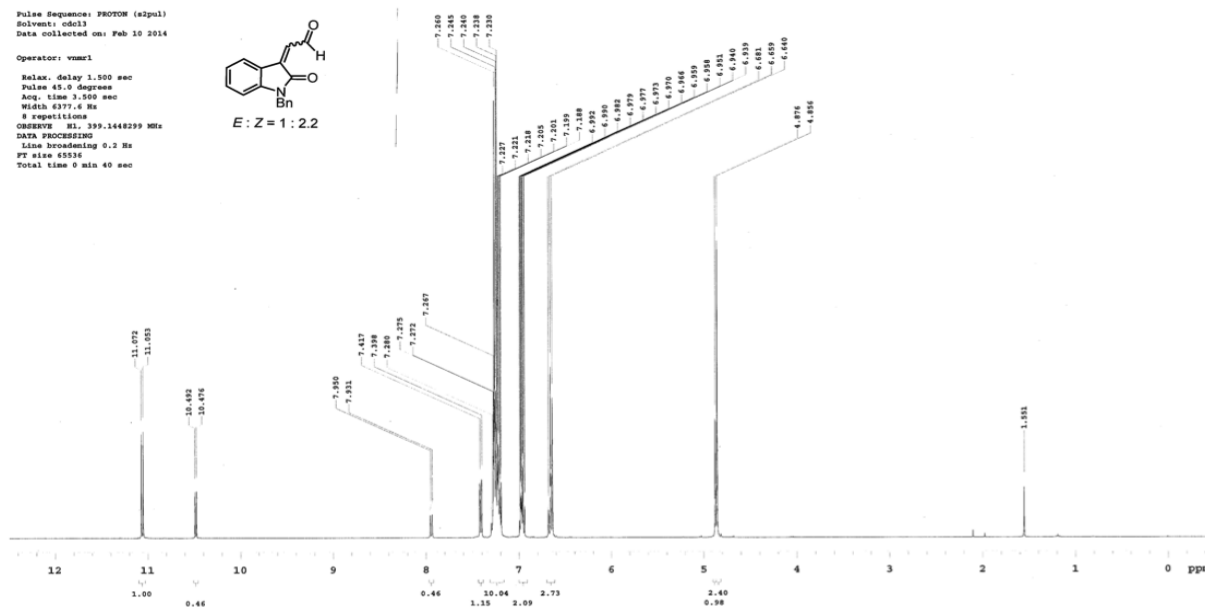
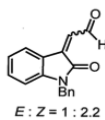
ファイル名: C:\VEZChrom\EliteEnterprise\Projects\Default\data\2013-07-18 22-47-05
 分析名: 10vsl 1 ml 55-2 horafiline.dat
 ファイル名: C:\VEZChrom\EliteEnterprise\Projects\Default\data\2013-07-18 22-47-05
 システム: System
 分析日時: 2013/07/18 22:47:44
 印刷日時: 2013/07/18 23:13:55



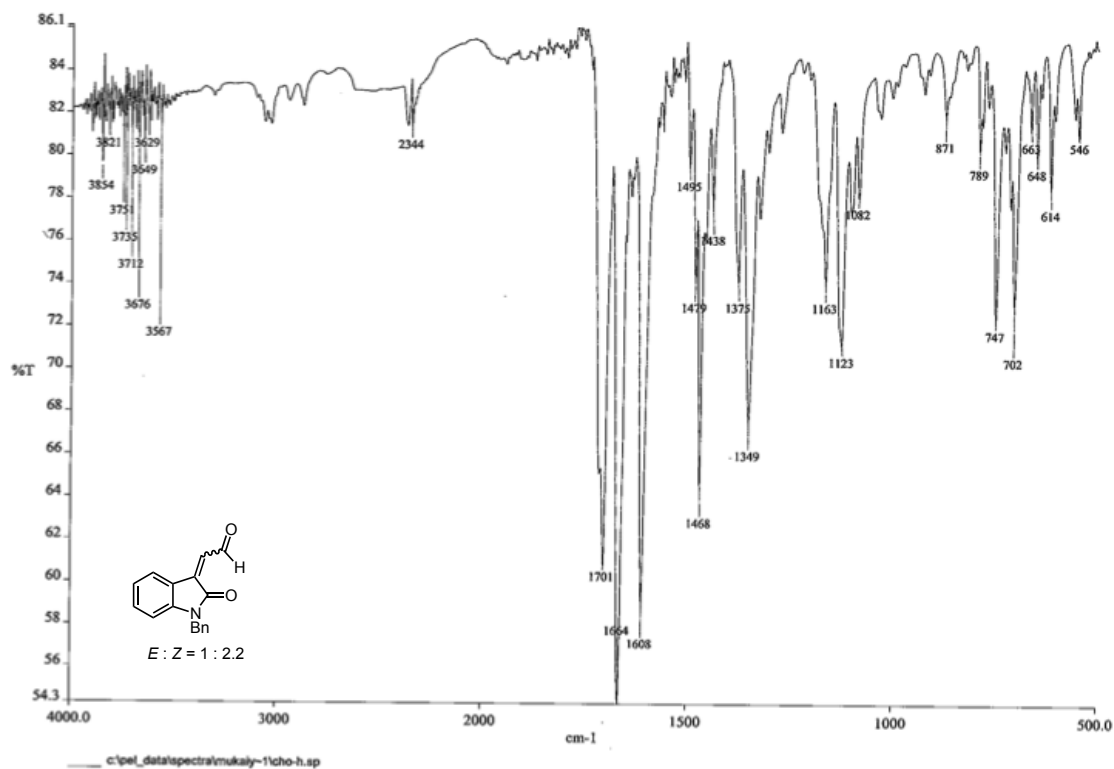
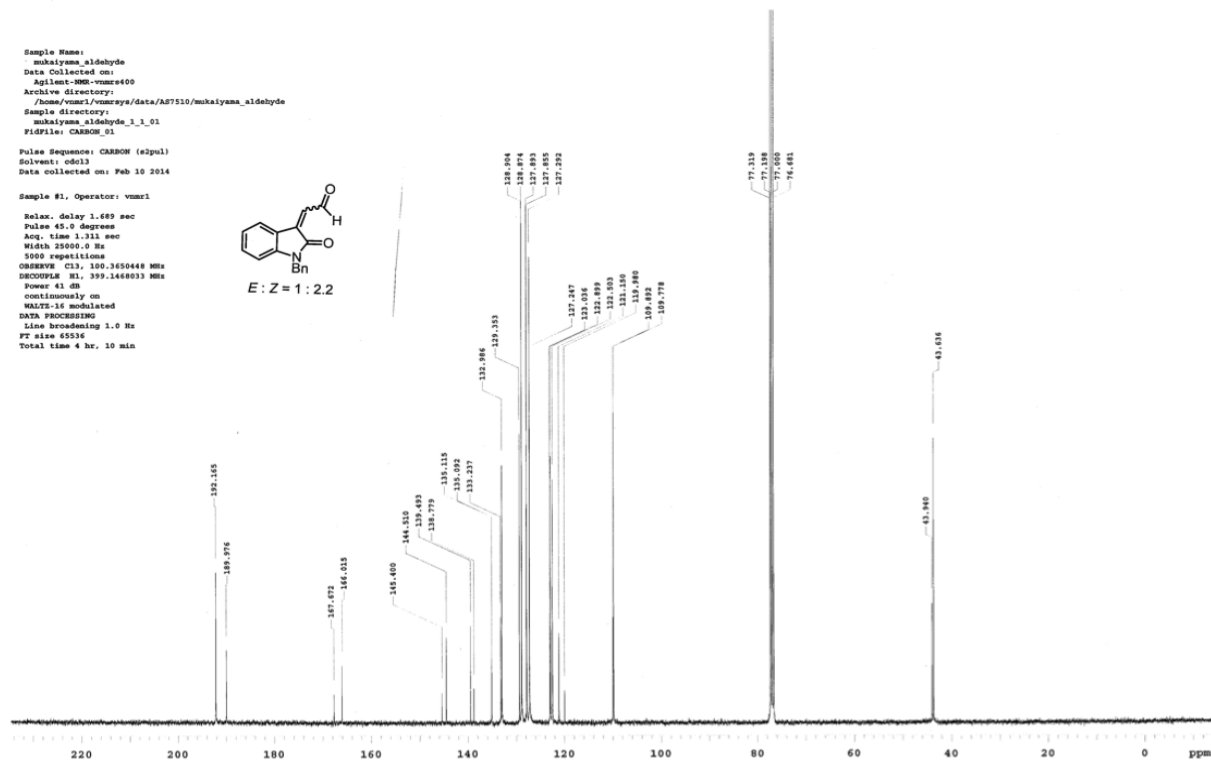
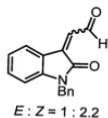
PK #	名前	保持時間	面積	面積%	ピークタイプ
1		6.97	95970211	98.262	MM
2		12.11	1768095	1.738	MM
トータル			101738306	100.000	




Sample Name:
 Data Collected on:
 Agilent-300-vnmr400
 Archive directory:
 Sample directory:
 File: PROTON
 Pulse Sequence: PROTON (zgpg3)
 Solvent: cdcl3
 Data collected on: Feb 10 2014
 Operator: vnmr1
 Relax. delay 1.500 sec
 Pulse 45.0 degree
 Acq. time 3.500 sec
 Width 6377.4 Hz
 8 repetitions
 OBSERVE M1, 399.1448299 MHz
 DATA PROCESSING
 Line broadening 0.2 Hz
 FT size 65536
 Total time 0 min 40 sec

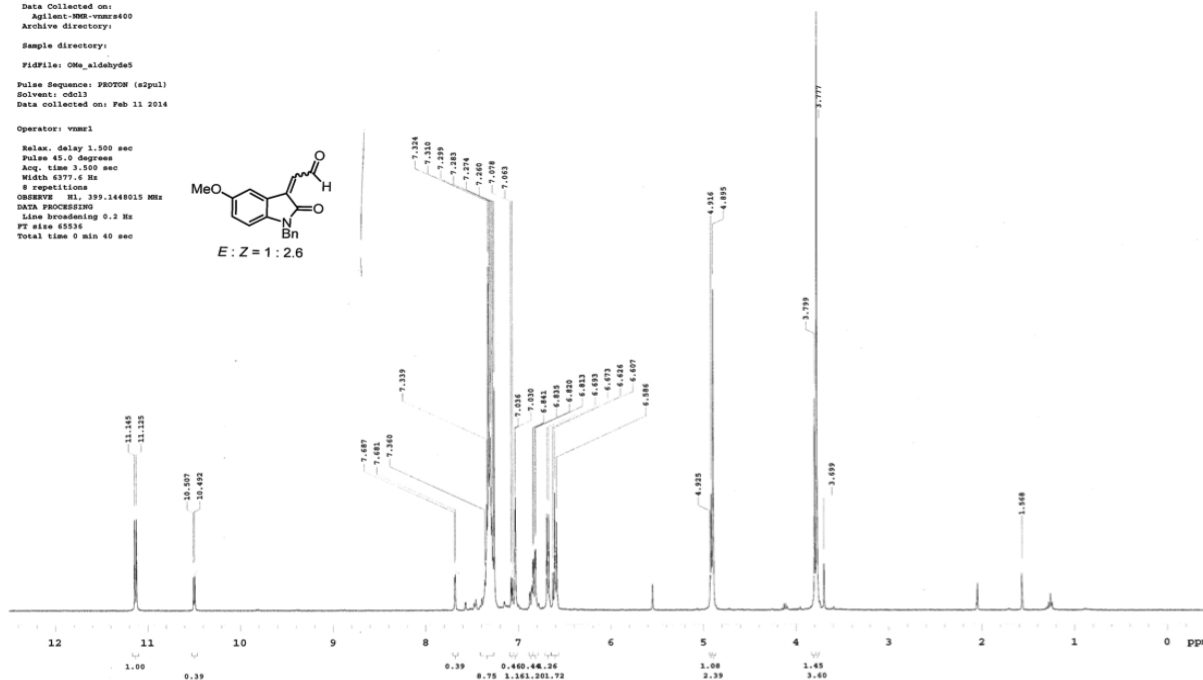



Sample Name: mukaiyama_aldehyde
 Data Collected on: Agilent-900-vnmr400
 Archive directory: /home/vnmr1/vnmr400/data/AS7510/mukaiyama_aldehyde
 Sample directory: mukaiyama_aldehyde_1_1_01
 FIDFile: CARBON_01
 Pulse Sequence: CARBON (e2pul)
 Solvent: cdcl3
 Data collected on: Feb 10 2014
 Sample #1, Operator: vnmr1
 Relax, delay 1.689 sec
 Pulse 45.0 degrees
 Acq. time 1.313 sec
 Width 25000.0 Hz
 5000 repetitions
 OBSERVE C13, 100.3650448 MHz
 DECOUPLE H1, 399.1460033 MHz
 Power 41 dB
 continuously on
 WALTZ-16 modulated
 DATA PROCESSING
 Line broadening 1.0 Hz
 FT size 45536
 Total time 4 hr, 10 min

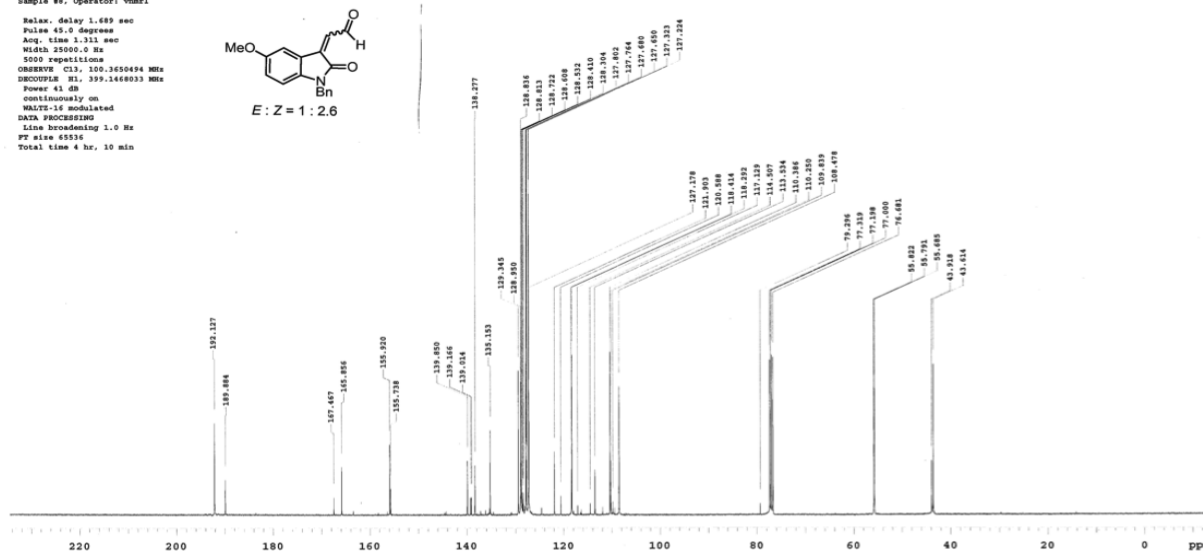


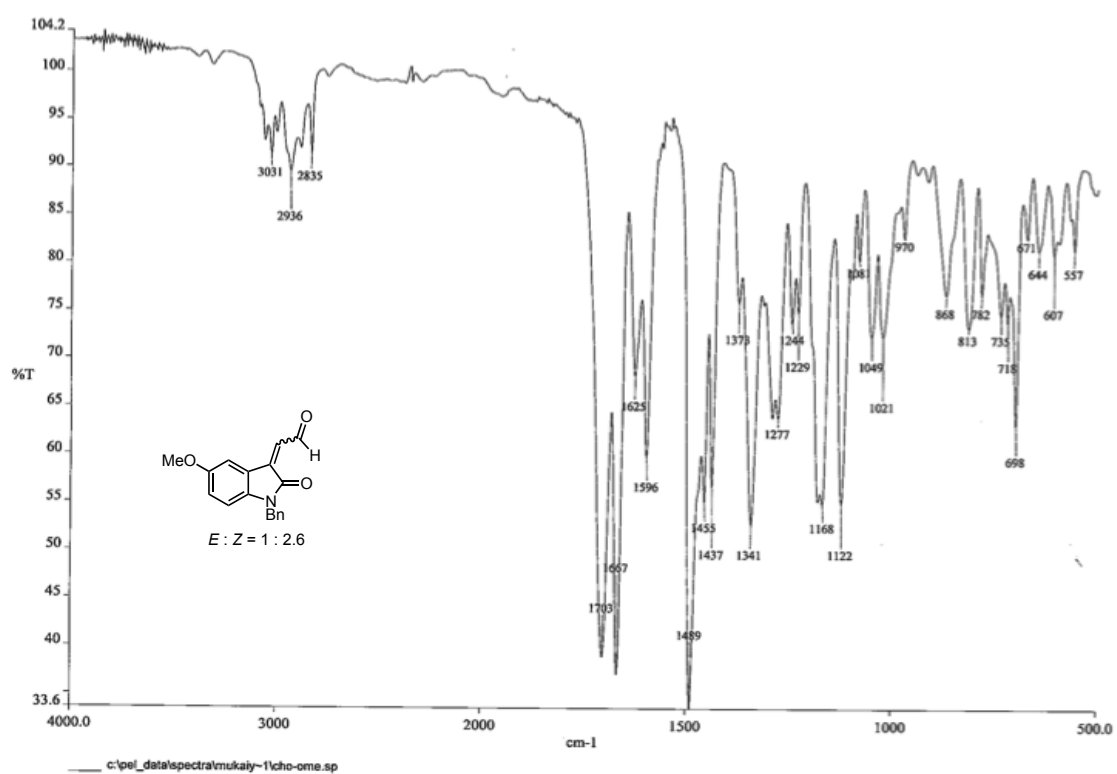
c:\pel_data\spectra\mukaiy-1\cho-h.sp


E : *Z* = 1 : 2.6




E : *Z* = 1 : 2.6





One-Pot Synthesis of (–)-Oseltamivir and Mechanistic Insights into the Organocatalyzed Michael Reaction

Takasuke Mukaiyama,^[a, b] Hayato Ishikawa,^[b, c] Hiroyuki Koshino,^[d] and Yujiro Hayashi^{*[a, b]}

Abstract: The one-pot sequential synthesis of (–)-oseltamivir has been achieved without evaporation or solvent exchange in 36 % yield over seven reactions. The key step was the asymmetric Michael reaction of pentan-3-yloxyacetaldehyde with (Z)-N-2-nitroethenylacetamide, catalyzed by a diphenylprolinol silyl ether. The use of a bulky O-silyl-substituted diphenylprolinol catalyst, chlorobenzene as a solvent, and HCO₂H as an acid additive, were key to produce the first Michael adduct

in both excellent yield and excellent diastereo- and enantioselectivity. Investigation into the effect of acid demonstrated that an acid additive accelerates not only the E–Z isomerization of the enamines derived from pentan-3-yloxyacetaldehyde with diphenylprolinol silyl ether, but also ring opening of the

cyclobutane intermediate and the addition reaction of the enamine to (Z)-N-2-nitroethenylacetamide. The transition-state model for the Michael reaction of pentan-3-yloxyacetaldehyde with (Z)-N-2-nitroethenylacetamide was proposed by consideration of the absolute configuration of the major and minor isomers of the Michael product with the results of the Michael reaction of pentan-3-yloxyacetaldehyde with phenylmaleimide and naphthoquinone.

Keywords: asymmetric synthesis • Michael addition • one-pot reaction • organocatalysis • Tamiflu

Introduction

(–)-Oseltamivir phosphate (**1**; Tamiflu), a neuraminidase inhibitor, is one of the most effective drugs for the treatment of influenza and has been used extensively. For this reason, many synthetic chemists have investigated its effective prepa-

ration and a large number of synthetic methods have been reported.^[1] However, a robust and efficient preparation method is still required to produce sufficient quantity of **1** for worldwide use.

On the other hand, the development of environmentally benign methods is a current key topic in chemistry and we have recently designated the importance of “pot-economy”^[2] in the multistep synthesis of molecules. A one-pot reaction is an effective method to conduct several transformations in a single vessel. Several transformations and bond formations can be achieved in a single vessel, which eliminates several purification operations and minimizes chemical waste to enable a shorter total production time. Over the last five years, we have applied the concept of pot-economy to the synthesis of several biologically active compounds. In 2009, we reported a sequential synthesis of **1** by three one-pot stages,^[3a] which was modified into two one-pot sequences in 2010.^[3b] We also reported the one-pot synthesis of ABT-341^[4] and the synthesis of prostaglandin E₁ methyl ester in three one-pot stages.^[2c]

In our reported synthesis of **1** by two one-pot sequences,^[3b] the first sequence starts with Michael reaction of pentan-3-yloxyacetaldehyde (**2**) and *trans*-nitroalkene **3**, catalyzed by (*R*)-diphenylprolinol silyl ether **4** (Scheme 1), a catalyst that has been developed independently by our group^[5] and that of Jørgensen.^[6] Without isolation, the Michael product **5** was treated with ethyl acrylate derivative **6**. After evaporation, the addition of toluenethiol afforded cyclohexane **7** with control of five consecutive chiral centers. The second one-pot sequence commenced with trifluoroacetic acid hydrolysis of the *tert*-butylester moiety. Subsequent-

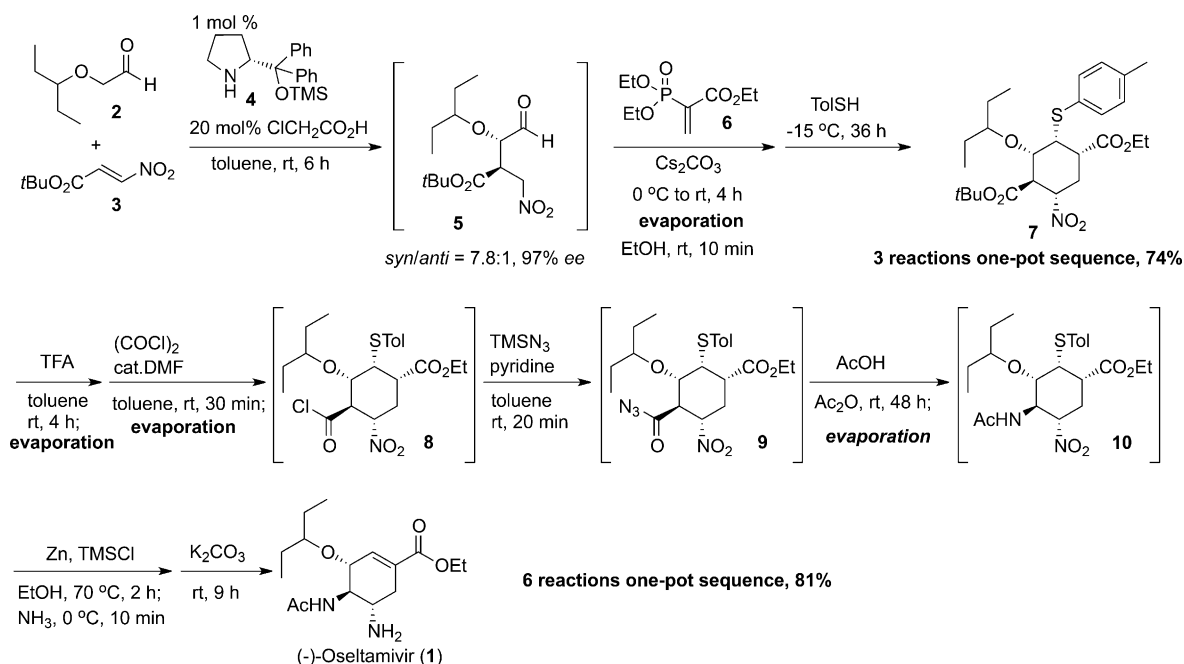
[a] T. Mukaiyama, Prof. Dr. Y. Hayashi
Department of Chemistry
Graduate School of Science
Tohoku University
6-3 Aramaki-Aza Aoba
Aoba-ku, Sendai 980-8578 (Japan)
Fax: (+81)22-795-6566
E-mail: yhayashi@m.tohoku.ac.jp

[b] T. Mukaiyama, Dr. H. Ishikawa, Prof. Dr. Y. Hayashi
Previous address (before 30th June 2012)
Department of Industrial Chemistry
Faculty of Engineering
Tokyo University of Science
Kagurazaka, Shinjuku-ku
Tokyo 162-8601 (Japan)

[c] Dr. H. Ishikawa
Department of Chemistry
Graduate School of Science and Technology
Kumamoto University
2-39-1, Kurokami, Chuo-ku
Kumamoto, 860-8555 (Japan)

[d] Dr. H. Koshino
Global Research Cluster, RIKEN
2-1 Hirosawa, Wako
Saitama, 351-0198 (Japan)

Supporting information for this article is available on the WWW under <http://dx.doi.org/10.1002/chem.201302371>.



Scheme 1. Previous synthesis of **1** by two one-pot sequences. TFA = trifluoroacetic acid, Tol = tolyl, Ac = acetyl.

ly, acid chloride **8** was generated, which was followed by Curtius rearrangement via acyl azide **9** to generate acetamide **10**. The nitro group was reduced to a primary amine, and retro-Michael reaction of the toluenethiol group furnished **1**. Solvent exchange was employed three times in the second one-pot sequence, even though the reaction sequences were carried out in the same vessel. Clearly, it would be more ideal, synthetically and operationally, if solvent exchange could be omitted in the one-pot operation. This would enable a reduction in solvent waste, production time, and cost.

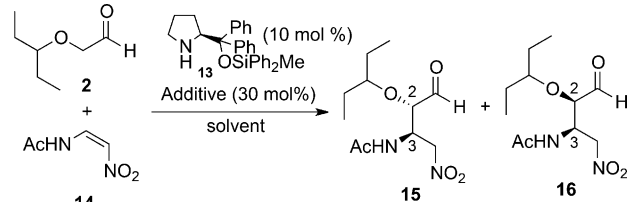
Recently, the groups of Ma,^[7] Sebesta,^[8a] and Lu^[9] have independently reported the synthesis of **1** in a short number of steps by similar routes to ours.^[3] The key change from our original route is that they all employed (*Z*)-*N*-2-nitroethenylacetamide (**14**) as a starting material instead of a (*E*)-*tert*-butyl-3-nitropropenoate (**3**). The former more conveniently possesses an aminoacetyl group and, importantly, avoids a potentially explosive Curtius rearrangement of acyl azide intermediate **9**. When we repeated the key Michael reaction between α -alkoxyaldehyde **2** and **14** in CHCl₃ in the presence of PhCO₂H, catalyzed by diphenylprolinol silyl ether **4**, the yield and diastereoselectivity was low. The solvents used were CHCl₃ and CH₂Cl₂. Given the unsatisfactory results, and to avoid the use of environmentally unfriendly chlorinated solvents for large-scale production, we set out to determine reliable conditions under which the desired aldehyde–nitroalkene Michael adduct should be obtained in good yield with excellent diastereo- and enantioselectivity. Moreover, we aimed to realize a one-pot sequential synthesis of **1** without any evaporation or solvent exchange by optimization of all subsequent reactions.^[3,7–9] During our investigation into organocatalyzed Michael reactions,^[10] including

those between α -alkoxyaldehydes and *cis*-nitroalkenes,^[11] we found that an acid additive is important to improve both selectivity and reactivity issues, which prompted us to investigate the effect of acid. In this paper, we disclose the successful realization of a complete one-pot synthesis of **1** without any solvent exchange, along with several new findings about the effect of acid and the course of the Michael reaction.

Results and Discussion

Michael reaction of α -alkoxyaldehyde with *cis*-nitroalkene:

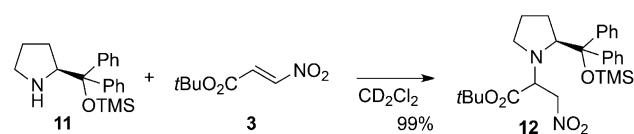
First, we examined the Michael reaction of **2** and **14** mediated by (*S*)-diphenylprolinol silyl ether **13** (Table 1), which is the key step in the synthesis of **1**. The reason for the use of the *Z* isomer as a Michael acceptor will be described later. Ma et al. obtained the products **15/16** in approximately 80 % yield with good diastereoselectivity (**15/16** = 5:1) by using PhCO₂H as an additive and CHCl₃ as the solvent.^[7] Sebesta et al. used CHCl₃/H₂O as the solvent system and chloroacetic acid as an additive to obtain good yield (88 %) and diastereoselectivity (**15/16** = 81:19).^[8a] Recently, the addition of *rac*-mandelic acid and 2,4-dinitrophenol was also found to be effective.^[8b] Lu et al. employed CH₂Cl₂ as the solvent and chloroacetic acid as an additive, which afforded good yield and selectivity (**15/16** = 4:1).^[9] When we performed the reaction in CHCl₃ in the presence of PhCO₂H, the NMR spectra of the crude mixture were not clean and the yield and diastereoselectivity were low. The first step of a one-pot multi-step reaction sequence needs to be supremely clean with high yield and selectivity. Halogenated solvents should be substituted with non-halogenated ones for scaleup. Although

Table 1. Asymmetric Michael reaction of **2** and **14** catalyzed by diphenylprolinol silyl ether **13**.^[a]


	Solvent	Acid	Time [h]	Yield [%] ^[b]	15/16 ^[c]	ee [%] ^[d]
1	CH ₃ CN	PhCO ₂ H	2	90	1.3:1	–
2	CH ₃ CN	ClCH ₂ CO ₂ H	16	90	3.6:1	–
3	C ₆ H ₅ Cl	PhCO ₂ H	0.5	80	2.7:1	–
4	C ₆ H ₅ Cl	ClCH ₂ CO ₂ H	2	80	9:1	–
5	C ₆ H ₅ Cl	HCO ₂ H	0.75	90	9:1	99
6 ^[e]	C ₆ H ₅ Cl	HCO ₂ H	4	85	9:1	–
7 ^[f]	C ₆ H ₅ Cl	HCO ₂ H	1.5	80	7.1:1	–

[a] Unless stated otherwise, reactions were performed as follows: **2** (0.60 mmol), **14** (0.30 mmol), acid additive (30 mol %), **13** (10 mol %), and solvent (1 mL) at rt for the indicated time. [b] Yield calculated from the ¹H NMR spectra of the reaction mixture. [c] Ratio determined by ¹H NMR spectroscopic analysis of reaction mixture. [d] The enantiomeric excess (*ee*) of the major isomer was determined by chiral HPLC analysis of the corresponding *p*-nitrobenzoyl ester derivative. The *p*-nitrobenzoyl ester was obtained by reduction of **15** to the alcohol, followed by formation of the ester. [e] Catalyst **13** (5 mol %) was employed. [f] α -Alkoxyaldehyde **2** (2.25 g, 17.3 mmol) in ClC₆H₅ (5 mL) was slowly added (60 min) to a mixture of nitroalkene **14** (1.5 g, 11.5 mmol), formic acid (0.17 mL, 4.6 mmol, 40 mol %), and **13** (517 mg, 1.15 mmol, 10 mol %) in ClC₆H₅ (42 mL) at 20 °C. The internal temperature of the reaction mixture was kept at 20 °C. The conversion was 46% and the ratio of **15/16** was 9:1 after 30 min.

a relatively dirty reaction was observed by crude NMR spectroscopy of the reaction mixture obtained when diphenylprolinol trimethylsilyl (TMS) ether **11** was used, the corresponding bulky silyl ether diphenylmethylsilyl (DPMS) ether **13**, developed by Seebach,^[12] proceeded in a clean manner, determined by NMR spectroscopy. The catalyst adduct **12** was observed in the stoichiometric reaction between the TMS catalyst **11** and **3** (Scheme 2),^[11] therefore

Scheme 2. Formation of catalyst adduct **12**

a similar addition reaction is possible between TMS catalyst **11** and *cis*-nitroalkene **14**. This unproductive side reaction could be responsible for the unfavorable results. By employing the bulky DPMS catalyst **13** instead of the TMS catalyst **11**, this side reaction would be suppressed to afford a clean reaction.

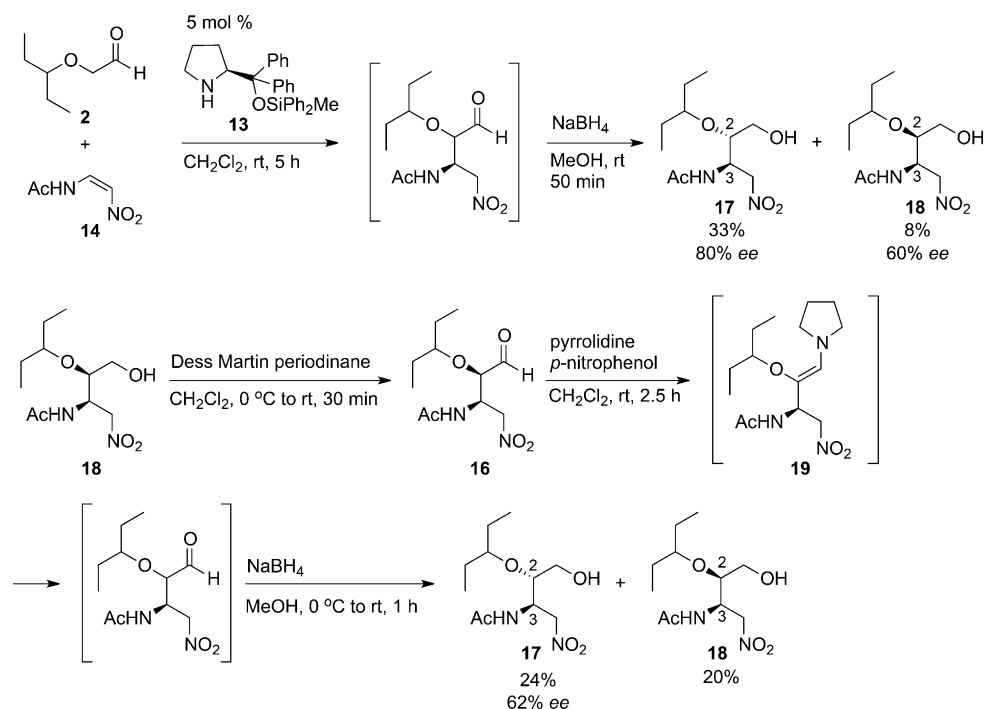
Next, an environmentally friendly solvent system was screened. In our first three one-pot synthesis of **1**^[3a] we employed a halogenated solvent system (CH₂Cl₂), which is unsuitable for process chemistry objectives. In our second de-

velopment with two one-pot synthesis^[3b] we found that toluene gave a good result for both yield and selectivity. Nitroalkenes were scarcely soluble in toluene, but chlorobenzene and CH₃CN were suitable solvent candidates and both are acceptable solvents for large-scale production. We know that acid is an effective additive in this type of Michael reaction,^[10] therefore we investigated the reaction in the presence of several acids in either CH₃CN or chlorobenzene (Table 1).

Although the reaction proceeds in CH₃CN, the reaction was slow, even in the presence of acid, and afforded the product with low diastereoselectivity (Table 1, entries 1 and 2). Contrary to CH₃CN, chlorobenzene was found to be the solvent of choice. In the presence of PhCO₂H the reaction was fast but resulted in low diastereoselectivity (Table 1, entry 3). The reaction was relatively slow in the presence of chloroacetic acid, the optimal acid in our previous synthesis of **1** in chlorinated solvents,^[3a,b] although excellent diastereoselectivity was obtained when chlorobenzene was used as the solvent (Table 1, entry 4). The best result was obtained with HCO₂H in chlorobenzene (Table 1, entry 5). The reaction was complete within 45 min, to afford the product in good yield with excellent diastereo- and enantioselectivity. The reaction also proceeded in the presence of 5 mol % of the organocatalyst (Table 1, entry 6). The gram-scale synthesis was realized with good yield and diastereoselectivity (Table 1, entry 7). The key points for scaleup are: 1) slow addition of α -alkoxyaldehyde **2** to suppress self-condensation, 2) control of the reaction temperature at 20 °C to maintain high diastereoselectivity. Better diastereoselectivity was observed at 0 and 10 °C, but the yield was lower. On the other hand, better yield was observed at 28 °C but the diastereoselectivity was 5:1 (**15/16**). It should be noted that nitroalkene **14** partially dissolves in chlorobenzene and the initial heterogeneous solution gradually becomes clear as the reaction proceeds to completion.

The stability of the Michael product **15** is noteworthy. Epimerization can readily occur because the α -alkoxyaldehyde Michael adduct possesses an acidic α -proton. For instance, the diastereomeric ratio was observed to decrease during evaporation and chromatographic (silica gel) operations. Thus, it is a great advantage to carry out the reaction in a one-pot process. Operations such as evaporation, solvent exchange, and isolation tend to reduce the overall diastereoselectivity.

The absolute configuration of the major stereoisomer **15** of the Michael reaction of **2** with **14** catalyzed by (*S*)-diphenylprolinol silyl ether was (2*S*, 3*R*), which was determined after conversion to **1** (see below). This is consistent with the observations of the groups of Ma,^[7] Sebesta,^[8a] and Lu.^[9] The absolute configuration of the minor isomer **16**, however, was not known. This identification would be important to understand the reaction mechanism. To obtain the minor isomer **16** in sufficient amounts, the reaction was performed without an acid additive to decrease the diastereoselectivity (Scheme 3). Compounds (2*S*, 3*R*)-**17** and **18** were obtained in 33 and 8% yield, respectively, after reduction with



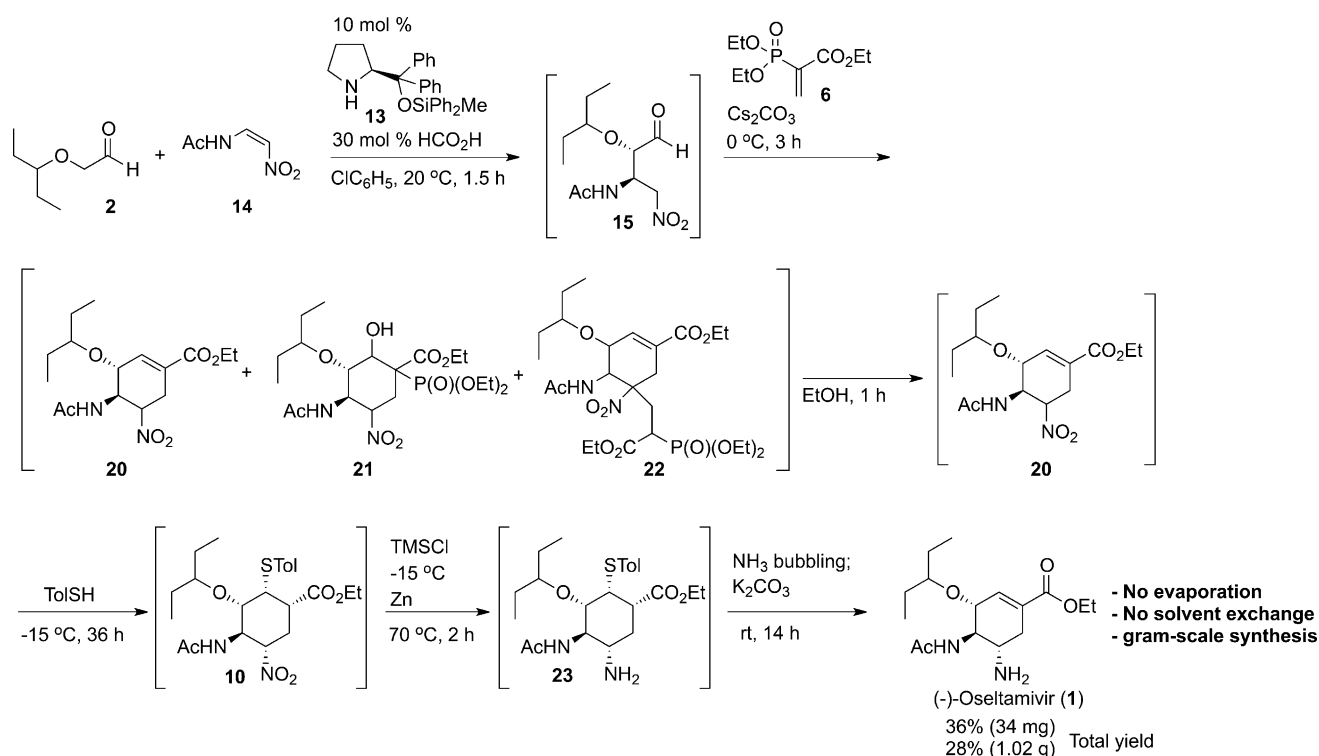
Scheme 3. Determination of the absolute configuration of the minor isomer **18** derived from Michael reaction of **2** and **14**.

NaBH_4 . The enantiomeric excess (*ee*) of these isomers was determined to be 80 and 60% *ee*, respectively. This result indicates that an acid additive increases not only the yield and diastereoselectivity, but also the enantioselectivity. Alcohol **18** was oxidized with Dess–Martin periodinane to give aldehyde **16**, which was isomerized with pyrrolidine in the presence of *p*-nitrophenol and reduced with NaBH_4 to afford **17** and **18** in 24 and 20% yield, respectively. Next, chiral HPLC analysis was performed. Compound **17**, generated after isomerization, showed the same retention time as (2*S*, 3*R*)-**17**, generated from **2** and **14**. Thus, the absolute configuration of **18** was determined to be (2*R*, 3*R*), therefore the absolute configuration of **16** was determined to be (2*R*, 3*R*). The (2*S*)-butanol derivative **17** was obtained, whereas the (2*R*) isomer **18** was generated. Transition-state models to rationalize the stereochemical results are discussed later.

One-pot sequential synthesis of 1: With the best reaction conditions for the first Michael reaction determined, the complete one-pot sequential synthesis of **1** was examined next (Scheme 4). The Michael reaction of α -alkoxyaldehyde **2** and *cis*-nitroalkene **14**, catalyzed by (*S*)-diphenylprolinol silyl ether **13**, proceeded in the presence of HCO_2H in chlorobenzene to afford the Michael product **15** in good yield with excellent diastereo- and enantioselectivity. Ethyl acrylate derivative **6** and Cs_2CO_3 were added to the same pot. This generated multiple spots upon TLC analysis. Some compounds present were identified as **20**, **21**, and **22**. The configuration of the hydroxyl and diethylphosphonyl groups in **21** is assumed to be *anti* although the stereochemistry of **21** has not been determined.^[3b] Therefore, *syn* elimination

does not occur. Compound **22** could be generated by further Michael reaction of the initially generated desired product **20** with acrylate derivative.^[3b] The latter two compounds were successfully converted into **20** by the addition of EtOH. Between **15** and **20**, several reactions proceed: 1) Michael reaction of nitroalkane **15** with **6** and intramolecular Horner–Wadsworth–Emmons reaction; 2) retro-aldol reaction of **21**, followed by intramolecular Horner–Wadsworth–Emmons reaction; 3) retro-Michael reaction of **22**. The Michael reaction of toluenethiol, followed by epimerization at the α -position of the nitro group, afforded the thiol Michael adduct **10** with the desired stereochemical configuration. By addition of Zn and TMSCl to the same vessel, reduction of the nitro group to give the amine **23** occurred, from which a retro-Michael reaction of the thiol group proceeded by treatment with base to afford **1** in a single pot and without the need to exchange or evaporate solvents. The highest total yield of this one-pot procedure was 36% on 40 mg scale. The one-pot procedure was applicable for scale-up synthesis. The gram-scale synthesis was demonstrated in 28% total yield, to afford **1** (1.02 g) from *cis*-nitroalkene **14** (1.5 g) in a one-pot procedure. The procedure has potential for further scale up to provide a greater amount of **1**.

It should be emphasized that removal of volatile materials from the reaction mixture, by evaporation or solvent exchange, which were necessary in our previous two- and three-pot syntheses,^[3a,b] were not required in this one-pot process. Although strictly not the ideal solvent for each subsequent reaction, chlorobenzene did not interfere with the desired reaction course. This is key for the successful realization of a one-pot synthesis without solvent exchange.

Scheme 4. One-pot synthesis of **1**.

Here, we simply add each reagent and co-solvent successively, which is synthetically and operationally simple and ideal.

As we described in our previous work,^[3a,b] the cyclohexane intermediate **10** is crystalline. Thus, the diastereo- and enantiomerically pure highly substituted cyclohexane derivative **10** could be easily obtained by a single crystallization in 51% yield when we quenched the reaction at this stage. We believe this procedure to be one of the most efficient and practical methods for the preparation of **1**.

The effect of acid additives: In our recent publication,^[11] we investigated the key Michael reaction of **2** with **3** or **14**, catalyzed by diphenylprolinol silyl ethers, in which the enamine generated from the α -alkoxyaldehyde reacts with the nitroalkene to generate cyclobutane intermediates. The *E/Z* ratio of the enamine was found to be 1.0:1.6 and the *E* enamine preferentially reacts with (*E*)-**3**, whereas the *Z* enamine reacts faster with (*Z*)-**14**. The effectiveness of acid additive in the Michael reaction of α -alkoxyaldehydes and nitroalkenes prompted us to investigate the effect of acid in this Michael reaction by comparison with the Michael reaction of **3**.

First, the effect of acid in the reaction of the *trans*-nitroalkene **3** was examined. We used less (1.3 equiv) of **3** than the *E* and *Z* enamine (2.9 equiv, 1:1.9 *E/Z*) to investigate which enamine reacts faster with **3**. When *trans*-nitroalkene **3** was added to a solution of preformed enamine, the *E* enamine was consumed almost immediately (Figure 1; red line) to afford cyclobutane **24** (Figure 1; orange line), whereas the *Z* enamine was consumed more slowly (Figure 1; blue

line) to afford cyclobutane **25** (Figure 1; green line). A small amount of nitro-enamine **26** was also observed (Figure 1; light-blue line). Next, acid was added to the mixture at *t* = 13 min; $\text{ClCH}_2\text{CO}_2\text{H}$ was selected as the optimal acid additive for the catalytic Michael reaction due to our previous results in the reaction between α -alkoxyaldehyde **2** and *trans*-nitroalkene **3**.^[3a,b] The *E/Z* enamine ratio dramatically changed from 7:1 to 2:1 immediately upon addition of $\text{ClCH}_2\text{CO}_2\text{H}$. These results indicate two main aspects of the reaction: 1) acid accelerates *E-Z* enamine isomerization, 2) the *E* enamine reacts faster than the *Z* enamine toward *trans*-nitroalkene **3**.

Next, the reaction of *E* and *Z* enamine with **14** was investigated in the same manner described above for the *trans*-nitroalkene **3**. When *cis*-nitroalkene **14** (1.3 equiv) was added to the preformed enamine solution only the *Z* enamine reacted to afford cyclobutane **27**. However, the reaction was slow. When **14** (3.3 equiv) was employed, the reaction was faster and the same phenomenon was observed (Figure 2). Therefore, *cis*-nitroalkene **14** (3.3 equiv) was used for this study. Only one stereoisomer of cyclobutane **27** was observed when *cis*-nitroalkene **14** was used. Also, the *Z* enamine reacted faster than the *E* enamine towards **14**. However, even in the presence of both *E* and *Z* enamines the reaction of *cis*-nitroalkene **14** did not progress further (or faster) before the addition of acid. HCO_2H (the best acid additive for the catalyzed reaction of α -alkoxyaldehyde **2** and *cis*-nitroalkene **14**) was added after 21 min. Although the NMR spectra became rapidly complicated, a few points are noteworthy. Not only the *E* and *Z* enamines, but also cyclobu-

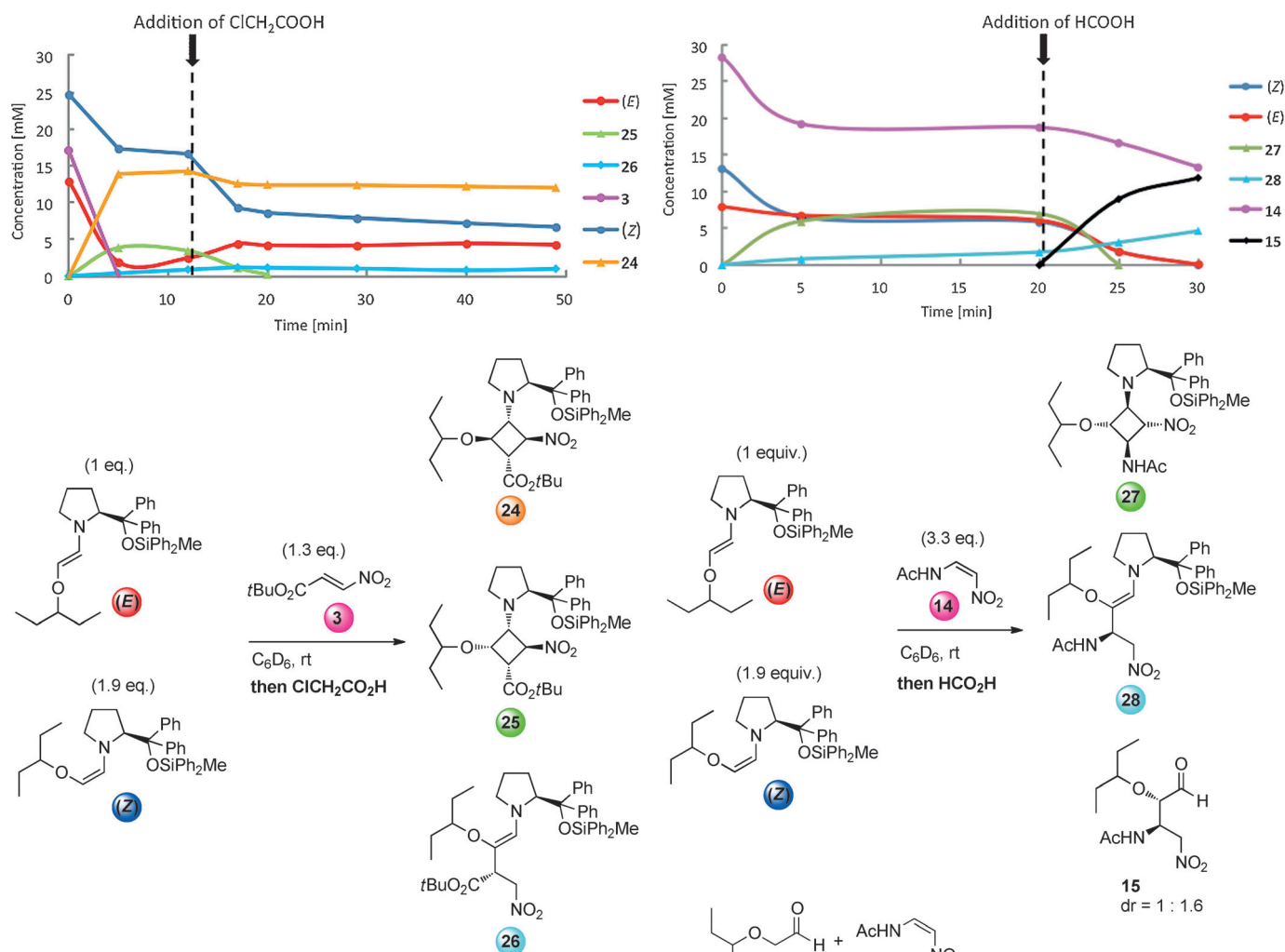


Figure 1. Reactivity of *E* and *Z* enamines with *trans*-nitroalkene **3** and the effect of acid to promote *E*–*Z* enamine isomerization.^[a,b] a) *Trans*-nitroalkene **3** (0.1 M solution in C_6D_6 , 0.015 mmol, 0.15 mL) was added to a preformed solution of *E* and *Z* enamine (0.033 mmol, *E*/*Z* = 1:1.9) in C_6D_6 (0.73 mL) with toluene as an internal standard (0.5 M solution in C_6D_6 , 0.02 mmol, 40 μL) in the presence of 4 Å molecular sieves (200 mg). Without molecular sieves, an aliquot (0.6 mL) of this reaction mixture was transferred to an NMR tube and $\text{ClCH}_2\text{CO}_2\text{H}$ (0.5 M solution in C_6D_6 , 0.015 mmol, 30 μL) was subsequently added to the NMR tube after 13 min. The reaction was monitored by ^1H NMR spectroscopy. The concentration of each product was calculated by integration of selected peaks in the ^1H NMR spectra and plotted on the graph. b) The structures of **24**, **25**, and **26** were elucidated by 2D NMR spectroscopic analysis (COSY, HSQC, and HMBC). The relative stereochemistry of **24** and **25** was determined by NOESY.

tane **27**, were rapidly consumed within 10 min of the addition of HCO_2H . With their disappearance, the amount of Michael product **15** (Figure 2; black line) and nitro-enamine **28** (Figure 2; light-blue line) increased. This infers two main roles for the acid (e.g. HCO_2H): 1) to facilitate cyclobutane ring opening, 2) to accelerate Michael addition of the enamine onto the *cis*-nitroalkene **14**.

Thus, this investigation provides strong evidence that acid additives accelerate three main aspects of the Michael reaction: 1) the *E*–*Z* enamine isomerization, 2) the ring opening

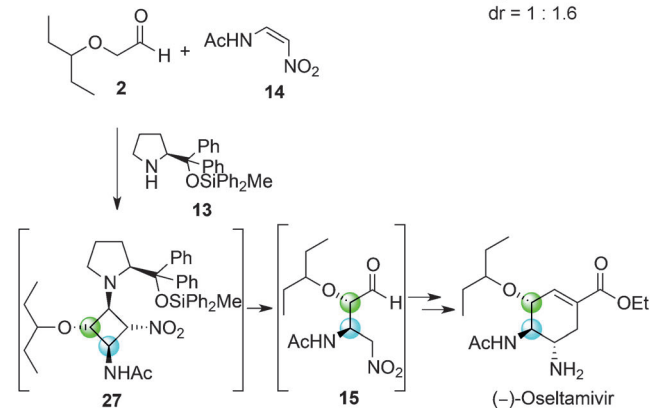


Figure 2. Reactivity of *E* and *Z* enamines with *cis*-nitroalkene **14** and effect of acid to accelerate Michael reaction.^[a,b] a) *Cis*-nitroalkene **14** (0.05 M solution in C_6D_6 , 0.05 mmol, 1.0 mL) was added to a preformed solution of the *E* and *Z* enamines (0.0372 mmol, *E*/*Z* = 1:1.7) in C_6D_6 (0.73 mL) with toluene (0.5 M solution in C_6D_6 , 0.02 mmol, 40 μL) as an internal standard in the presence of 4 Å molecular sieves (200 mg). Without molecular sieves, an aliquot (0.6 mL) of this reaction mixture was transferred to an NMR tube and HCO_2H (0.5 M solution in C_6D_6 , 62 μL) was added to the NMR tube after 21 min. The reaction was monitored by ^1H NMR spectroscopy. The concentration of each product was calculated by integration of suitable peaks in the ^1H NMR spectra and plotted on the graph. b) The structures of **27** and **28** were elucidated by 2D NMR analysis (COSY, HSQC, and HMBC). c) The relative configuration of **27** was determined by NOESY. The Michael product **15** of reaction between α -alkoxyaldehyde **2** and *cis*-nitroalkene **14**, catalyzed by **13**, was converted to (–)-Oseltamivir, which indicates the stated stereochemical configuration of **27** to be highly probable.

of cyclobutane intermediates, 3) the carbon–carbon bond-forming addition of enamines to nitroalkenes. Although the optimal acid additive differs according to the particular characteristics of the Michael acceptor, the stereoselectivity and yield in the Michael reactions of α -alkoxyaldehydes are generally improved by screening for an appropriate acid additive.

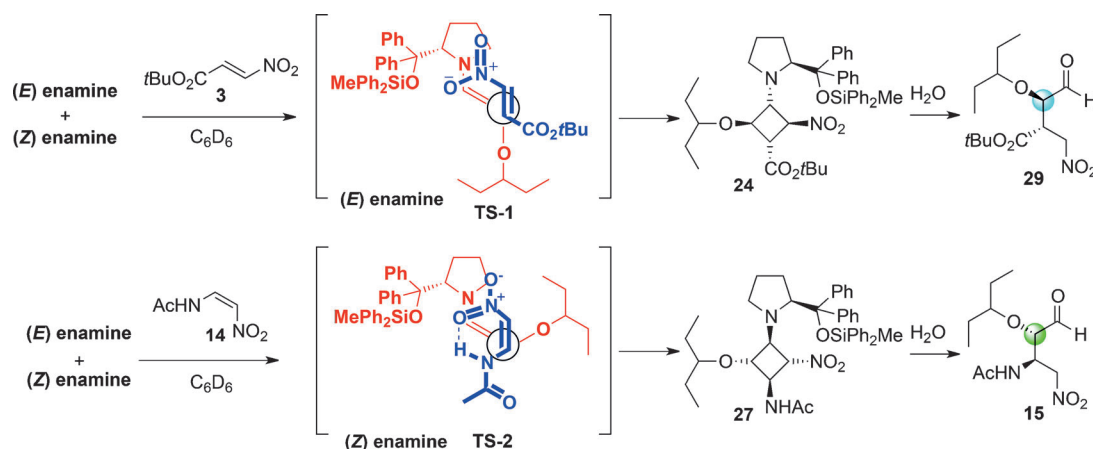
Michael reaction of α -alkoxyaldehyde with other *cis*-Michael acceptors: The proposed transition-state models for the Michael reaction of **2** with **3** and **14**, catalyzed by diphenylprolinol silyl ethers, are described in Scheme 5; these models have also been discussed in detail in our recent mechanistic studies.^[11] When the *trans*-nitroalkene **3** is combined with a mixture of *E* and *Z* enamine, the *E* enamine reacts with **3** to generate cyclobutane **24** through the proposed transition-state model **TS-1**. The ring opening of **24** and subsequent hydrolysis generates the Michael product **29**. On the other hand, when *cis* alkene **14** was used as a Michael acceptor, the *Z* enamine reacted with **14** to generate the cyclobutane **27**. In this case, ring opening of **27** and hydrolysis gives **15**, which has a (2*S*)-configuration, opposite to that of the (2*R*)-aldehyde **29**. The transition-state model **TS-2**, which was independently proposed by the group of Ma^[7] and Lu,^[9] is consistent with this absolute configuration.

Although the transition-state model **TS-2** may also explain the diastereo- and enantioselectivities achieved, a more complicated sequence might exist during the reaction course. For example, we found that **14** exists as its *cis* isomer in CDCl₃ (*cis/trans* = >99:1), whereas the *trans* isomer prevails in DMSO (*cis/trans* = 7:93).^[11] The isomerization from *cis* to *trans* isomer might need to be considered. Therefore, we selected to study a *cis* alkene Michael acceptor that is known not to isomerize to its *trans* form. This would allow for unambiguous investigation of the transition-state models of the Michael reaction between α -alkoxyaldehydes and *cis* alkenes.

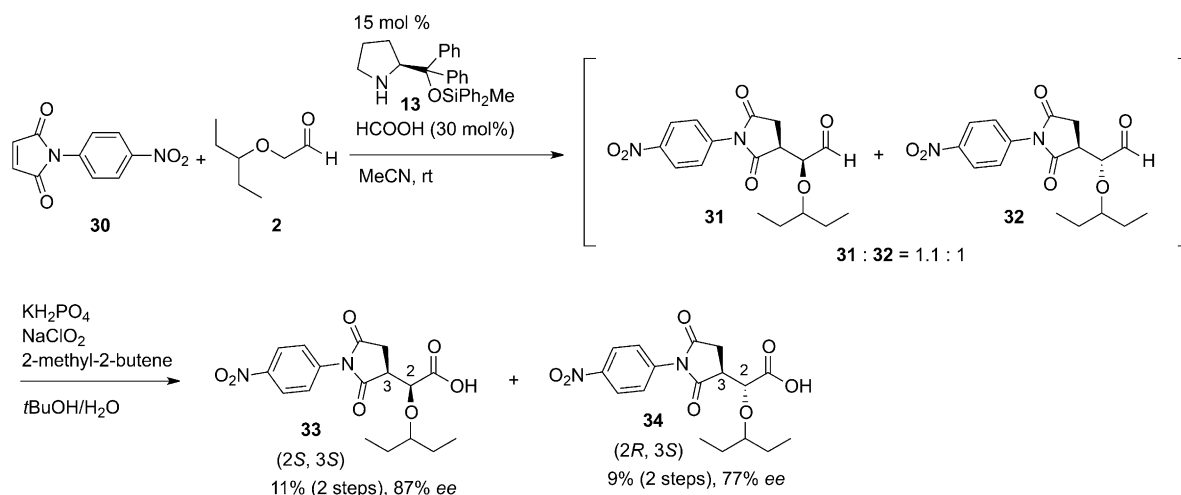
The first reaction we studied was the Michael addition of α -alkoxyaldehyde **2** to *cis*-alkenyl Michael acceptor phenyl-

maleimide **30**. Cordova et al. reported that the Michael reaction of maleimides and aliphatic aldehydes catalyzed by (*S*)-diphenylprolinol silyl ether gives the (2*R*, 3*S*)-isomer.^[13] We conducted the asymmetric Michael reaction of **2** and **30** catalyzed by **13**. This generated the Michael adducts as a mixture of diastereomers (**31/32** = 1.1:1; Scheme 6). The reaction was not optimized. The Michael products generated were not stable enough for isolation so they were converted to the respective carboxylic acids without purification. The diastereomers were separated at this stage. The enantioselectivity of each isomer was determined by chiral HPLC after conversion to the corresponding methyl ester. The enantiopurity of (2*S*, 3*S*)-**33** was 87% *ee*, and that of (2*R*, 3*S*)-**34** was 77% *ee*. These results indicate that the enantiofacial selectivity of the chiral enamine intermediate is relatively low.

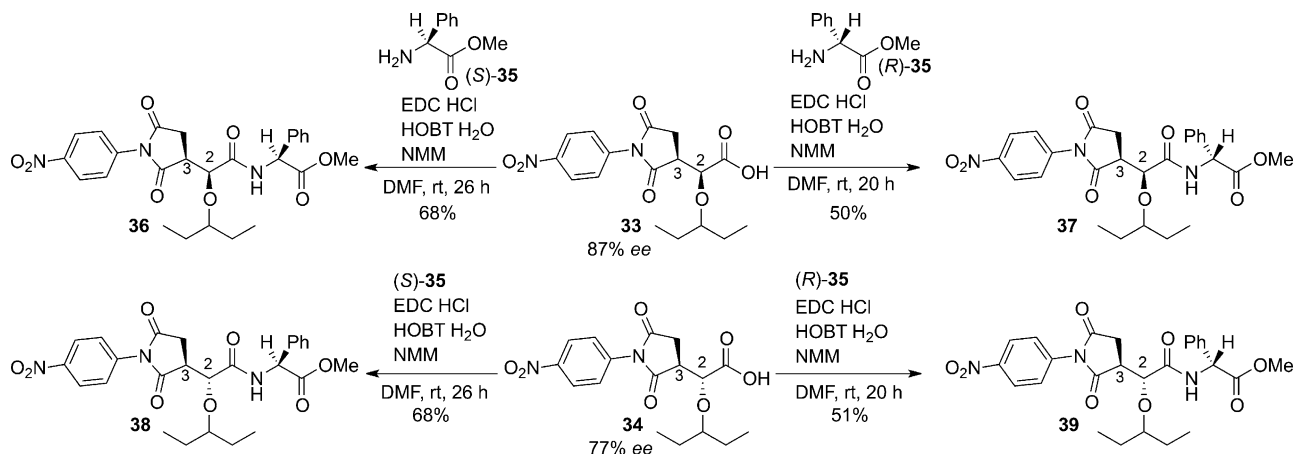
The relative and absolute configurations of carboxylic acids **33** and **34** were determined as follows (Scheme 7). The carboxylic acid **33** was condensed with phenylglycine methyl esters [PGME] (*S*)-**35** and (*R*)-**35** to give the (*S*)-PGME amide **36** and (*R*)-PGME amide **37**, respectively. The carboxylic acid **34** was also condensed with (*S*)-**35** and (*R*)-**35** to give the (*S*)-PGME amide **38** and (*R*)-PGME amide **39**, respectively. Key signals in the ¹H NMR spectra of compounds of **36** and **38** are more easily resolved than those of **33** and **34**, therefore the relative configuration was determined by a NMR spectroscopic study according to the J-based configuration analysis (JBCA) method.^[14] In this way, **33** and **34** were found to possess (2*S**, 3*S**) and (2*R**, 3*S**) configurations, respectively. The absolute configuration at C2 of **33** was then determined by the PGME method of Kusumi.^[15] The chemical shift difference between (*S*)-PGME amide **36** and (*R*)-PGME amide **37** was calculated and the absolute configuration at C2 in **36** and **37** was determined to be (2*S*). Therefore, the absolute configuration of **33** was determined to be (2*S*, 3*S*). The absolute configuration of **34** was similarly determined to be (2*R*, 3*S*). The transition states of the reaction will be discussed later.



Scheme 5. Reactivity of the *E* and *Z* enamines toward *trans*-nitroalkene **3** and *cis*-nitroalkene **14**. The *E* enamine reacts with **3** to give cyclobutane **24**, whereas the *Z* enamine reacts with **14** to give cyclobutane **27**.



Scheme 6. Asymmetric Michael reaction of **30** and α -alkoxyaldehyde **2**.

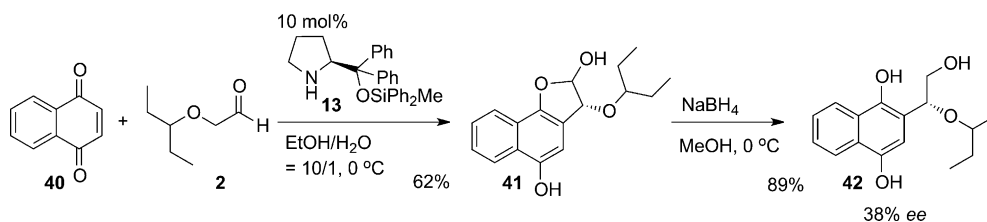


Scheme 7. Synthesis of *S* amides **36** and **38** and *R* amides **37** and **39**. EDC = *N*-(3-dimethylaminopropyl)-*N*-ethylcarbodiimide, HOBT = 1-hydroxybenzotriazole, NMM = *N*-methylmorpholine *N*-oxide.

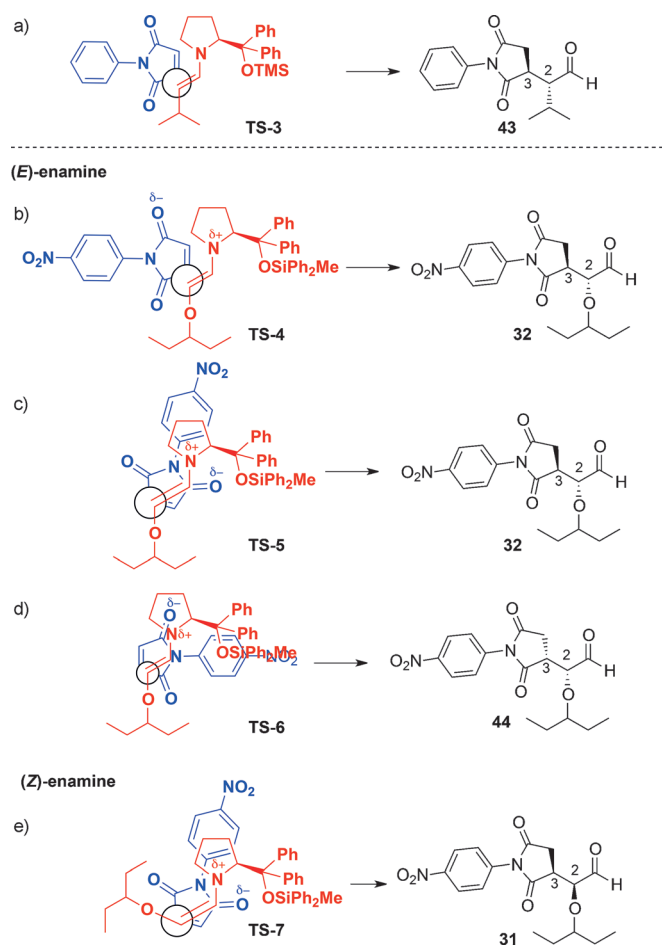
Naphthoquinone (**40**) was selected as another *cis* alkene for investigation (Scheme 8). Jørgensen et al demonstrated the organocatalyzed Michael reaction of **40** with several aliphatic aldehydes, which generated primary alcohols in excellent *ee* upon reduction.^[16] We performed the Michael reaction of α -alkoxyaldehyde **2** and **40** to generate the hemiacetal **41**. The *ee* was determined after reduction of the hemiacetal **41** to its corresponding alcohol **42**. The enantiomeric excess of **42** was determined to be 38%. This is low in con-

trast to the excellent values obtained in the reactions of aliphatic aldehydes reported by Jørgensen.^[16] The absolute configuration of **42** was determined to be *R* after conversion of **42** into the PGME amide.^[15] The transition-state models for these reactions will be discussed next.

Transition-state models: We have already reported that aldehyde **2** generates both *E* and *Z* enamines, whereas aliphatic aldehydes generate the *E* enamine preferentially,



Scheme 8. Asymmetric Michael reaction of **40** and α -alkoxyaldehyde **2**.

Scheme 9. Transition-state models of prolinol-derived enamines with **30**.

upon treatment with diphenylprolinol silyl ether organocatalysts.^[11] Herein, we propose transition-state models for **30** (Scheme 9) and **40** (Scheme 10) as Michael acceptors. As mentioned previously, Cordova et al. reported the Michael

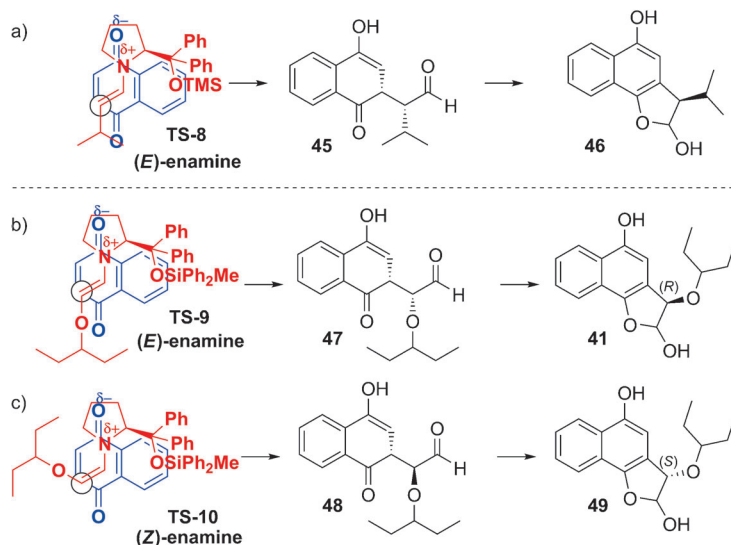
reaction of aliphatic aldehydes and phenylmaleimides in the presence of (*S*)-diphenylprolinol silyl ether to give the Michael product (**2R, 3S**)-**43** in excellent diastereo- and enantioselectivity.^[13] The Cordova group reasoned the observed selectivity by proposition of the transition-state model **TS-3** between the *E* enamine and phenylmaleimide (Scheme 9a). In spite of the high enantioselectivity, the diastereoselectivity of the Michael reaction of **2** and **30** was low (Scheme 6). From our results, we propose the transition-state models for the Michael reaction of **2** and **30** shown in Scheme 9b–e.

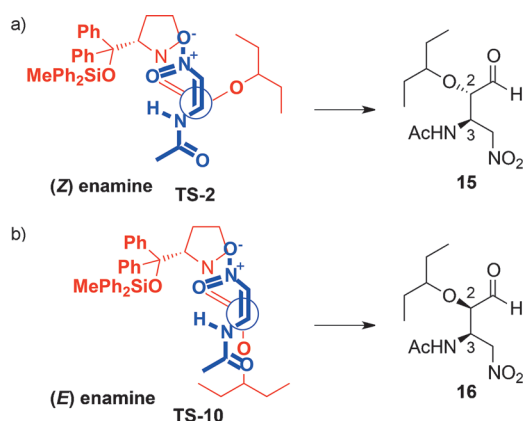
Three transition-state models, **TS-4**, **TS-5**, and **TS-6**, should be considered in the reaction of the *E* enamine. **TS-4** is a similar model to that proposed by Cordova. **TS-4** has the least steric hindrance but does not agree with the acyclic synclinal transition state proposed by Seebach and Golin-ski.^[17] Although **TS-6**, which affords a wrong isomer, would provide better charge interactions than **TS-5**, it is sterically encumbered. **TS-5** is preferable in terms of both steric hindrance and electrostatic interactions. Thus, the reaction of the *E* enamine would likely proceed via **TS-5** (Scheme 9c).

According to the same considerations of steric and electrostatic interactions, the reaction of the *Z* enamine would proceed via **TS-7** to provide the observed (**2S, 3S**) isomer **31** (Scheme 9e).

As mentioned previously, Jørgensen reported the Michael reaction of aliphatic aldehydes with **40**, catalyzed by (*S*)-diphenylprolinol silyl ethers, to afford chiral adducts in excellent enantioselectivity.^[16] Herein, we propose a plausible transition-state model (Scheme 10). The naphthoquinone approaches from the *Si* face of the *E* enamine in alignment with optimal electrostatic interactions, as described in Seebach's model^[17] (**TS-8**; Scheme 10a). This would generate the Michael product **45**, which converts to **46** after aromatization. In contrast to the excellent enantioselectivity in the reaction of aliphatic aldehydes, the Michael reaction of α -alkoxyaldehydes gave low enantioselectivity (38% *ee*; Scheme 8). This can be explained as follows: both the *E* and *Z* enamines would react with **40**. The *E* enamine would generate **47** through **TS-9** (Scheme 10b), followed by aromatization to afford the *R* isomer **41**. The *Z* enamine would generate the *S* isomer **49** through **TS-10** (Scheme 10c). The resultant enantioselectivities are low because the *E* and *Z* enamine each afford the opposite enantiomer and the reaction proceeds through both enamine species.

As mentioned earlier, the absolute configuration of the Michael product **16** was determined to be (**2R, 3R**) and that of **15** as (**2S, 3R**) [Scheme 11]. In both products, the absolute configuration of the α -position of the AcNH group in **15** and **16** is the same. The configuration at the α -position of the alkoxy group in **15** and **16** is opposite, which would be determined by geometry of the enamine. By analogy, these results are consistent with the transition-state models proposed for the *cis*-Michael acceptors **30** and **40**. Specifically, the major isomer **15** would result from transition-state model **TS-2** (Scheme 11a), whereas the minor isomer **16** would be derived from the reaction of the *E* enamine via **TS-10** (Scheme 11b).

Scheme 10. Transition-state models of enamines with **40**.



Scheme 11. Transition-state models of enamine with **14**.

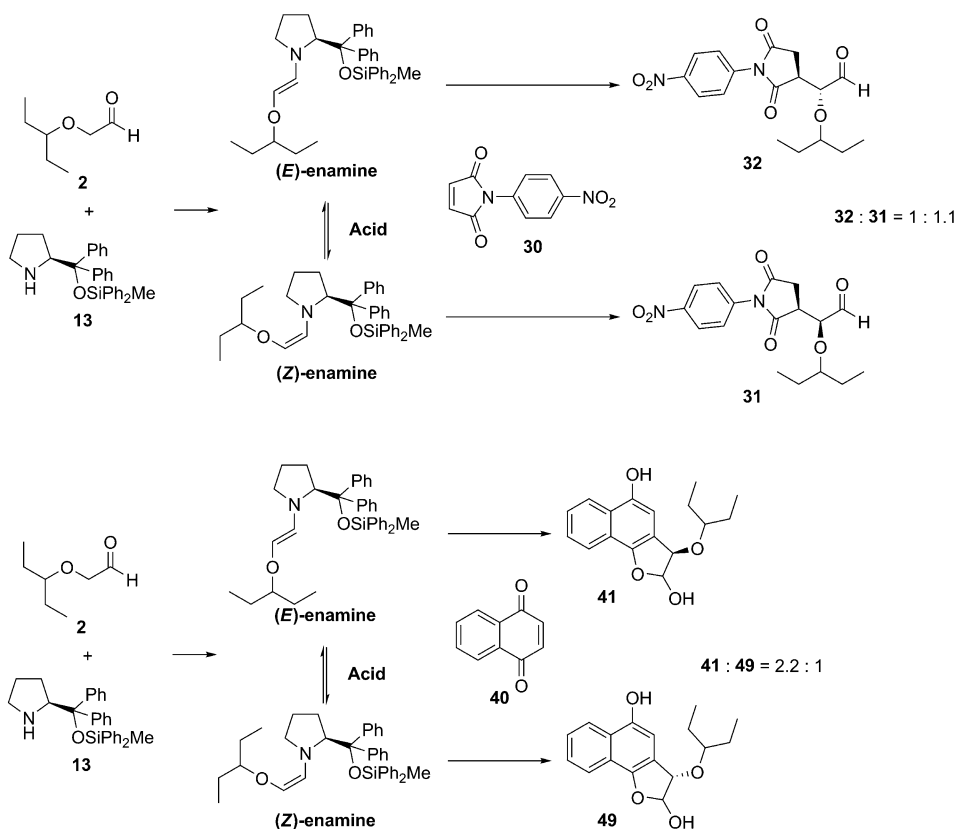
Isomerization and reactivity of the *E* and *Z* enamines: In the case of phenylmaleimide **30**, both the *E* and *Z* enamines generated from **2** and **13** react with **30** to furnish a 1:1.1 mixture of aldehydes **32** and **31** (Scheme 12). Both the *E* and *Z* enamine also react with **40** to afford a 2.2:1 mixture of hemiacetal **41** and **49**. These results indicate that both the *E* and *Z* enamine react with each Michael acceptor.

Contrary to substrates **30** and **40**, the reactions of **14** and **3** exhibit a different profile. The reaction of **14** and **2** catalyzed by (*S*)-diphenylprolinol silyl ether **13** afforded the Michael product **15** in good yield with excellent diastereo- and

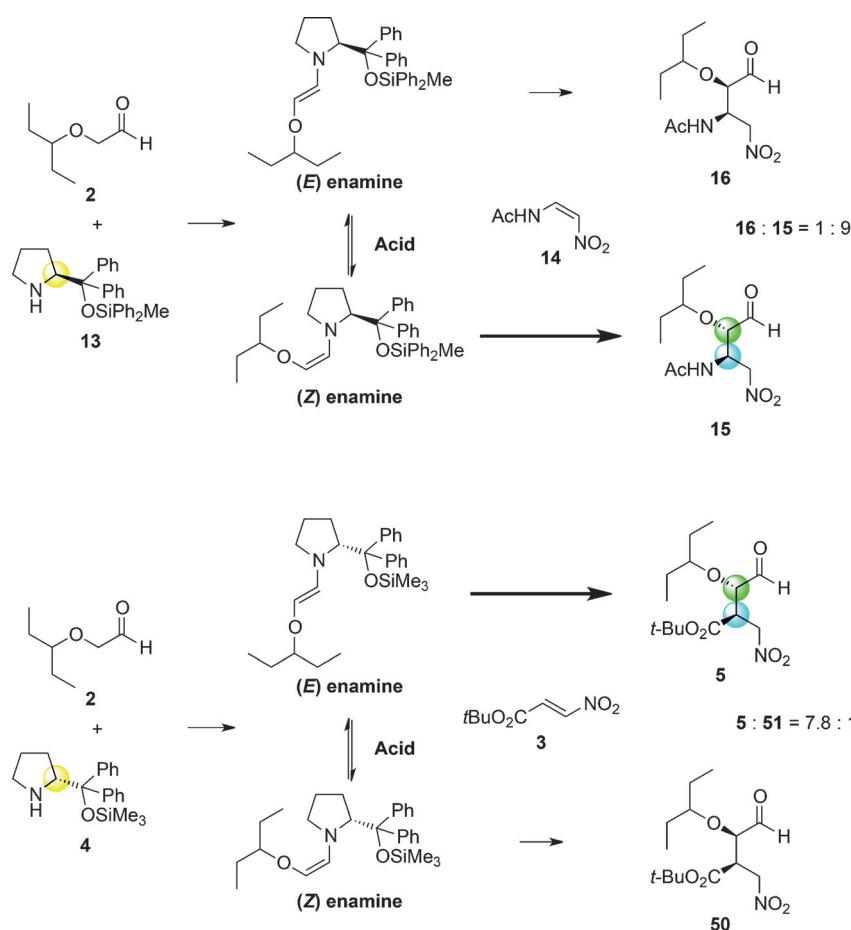
enantioselectivity, even though both the *E* and *Z* enamine were generated. A similar result was obtained for the reaction of **3** and **2** catalysed by (*R*)-diphenylprolinol silyl ether **4**: the Michael product **5** was obtained in good yield with excellent diastereo- and enantioselectivity, although both the *E* and *Z* enamine were generated. These results can be explained as follows (Scheme 13): the *Z* enamine reacts with **14** faster than the *E* enamine (Figure 2) and the addition reaction of the *Z* enamine is facilitated by the acid additive (Figure 2). There is a rapid equilibrium between the *E* and *Z* enamine in the presence of acid (Figure 1). Thus, the *Z* enamine reacts preferentially and the remaining *E* enamine isomerizes to the *Z* form, which then reacts with Michael acceptor **14** to afford the product **15**. Similar phenomena are also observed with **3**, but the *E* enamine preferentially reacts with (*E*)-**3** (Figure 1) and the remaining *Z* enamine readily isomerizes to its *E* form before reaction with the Michael acceptor (*E*)-**3** to afford the product **5**. It is noteworthy that excellent diastereo- and enantioselectivity are obtained with good yield in the reactions of both (*Z*)-**14** and (*E*)-**3**. This would be possible when the following three relative rates are orchestrated correctly: 1) the speed of generation of the *E* and *Z* enamines from **2** and the diphenylprolinol silyl ether, 2) the reaction rate of the *E* and *Z* enamines toward each Michael acceptor **3** and **14**, 3) the isomerization rate between the *E* and *Z* enamine. Because the reactive enantioface of the *E* and *Z* enamine is opposite we have to employ (*S*)-diphenylprolinol silyl ether **13** as a catalyst with the *Z* enamine, whereas (*R*)-diphenylprolinol silyl ether **4** is employed for the *E* enamine.

Conclusion

We have achieved a complete one-pot sequential synthesis of **1** without solvent evaporation or exchange on a gram-scale. On the basis of our original route^[3] and advancements by others^[7,8a,9] we have critically modified the first key asymmetric Michael reaction of **2** with **14** to proceed in good yield and with excellent diastereo- and enantioselectivity. Key to the success of this transformation are: 1) use of a bulky silyl substitution in the diphenylprolinol silyl ether organocatalyst, 2) use of HCO₂H as an acid additive to accelerate the reaction and increase stereoselectivities, 3) use of chlorobenzene as solvent to allow for all subsequent



Scheme 12. Reaction of *E* and *Z* enamines with **30** and **40**.



Scheme 13. Isomerization and reaction of *E* and *Z* enamines with **3** and **14** in the presence of acid.

transformations and permit large-scale production, 4) control of the internal reaction temperature at 20 °C to increase diastereoselectivity, 5) slow addition of **2** to suppress self-condensation.

The effects of the acid additive in the key Michael reaction were monitored by NMR spectroscopic analysis and demonstrated that acids not only accelerated isomerization of the *E* and *Z* enamines derived from **2** and organocatalyst **13**, but also facilitated the ring opening of the cyclobutane intermediates and the addition reaction of the enamine to **14**.

The transition-state model **TS-2** of the Michael reaction of **2** with **14** was ultimately proposed by determination of the absolute configuration of the Michael product **16** and by studying the Michael reaction of **2** with other *cis*-alkene Michael acceptors (**30** and **40**) that cannot isomerize. Insights into the relative reactivity of the enamine species and the resultant stereoselectivities of the reaction products were also rationalized. The mechanistic study indicated that the Michael reaction can be effectively carried out by the correct orchestration of three reaction processes: 1) the speed of generation of the *E* and *Z* enamines from **2** and diphenylprolinol silyl ether, 2) the relative reactivity of the *E* and *Z* enamines toward the Michael acceptors **3** and **14**, 3) the

ready acid-promoted isomerization between the *E* and *Z* enamine.

Collectively, the synthesis presented herein is the first example of a one-pot synthesis of a drug of this stereochemical complexity, in significant yield, without the need to evaporate or exchange solvents, on a gram scale. We believe the present synthesis of **1** to be not only efficient, but also applicable for larger preparative scales.

Acknowledgements

We would like to thank Prof. Dieter Seebach for significant discussions regarding the mechanistic study of the Michael reaction of α -alkoxyaldehydes with nitroalkenes. Some of the experiments discussed in the section “the effect of acid additives” were conducted by T.M. during a three-month stay at ETH Zurich (August–October 2012; financed by Tokyo University of Science) under the supervision of Prof. Seebach. This work was supported by a Grant-in-Aid for Scientific Research on Innovative Areas (Advanced Molecular Transformations by Organocatalysts) from The Ministry of Education, Culture, Sports, Science and Technology, Japan.

- [1] a) J. C. Rohloff, K. M. Kent, M. J. Postich, M. W. Becker, H. H. Chapman, D. E. Kelly, W. Lew, M. S. Louie, L. R. McGee, E. J. Prisbe, L. M. Schultze, R. H. Yu, L. J. Zhang, *J. Org. Chem.* **1998**, *63*, 4545; b) M. Federspiel, R. Fischer, M. Hennig, H.-J. Mair, T. Oberhauser, G. Rimmeler, T. Albiez, J. Bruhin, H. Estermann, C. Gandert, V. Göckel, S. Götzö, U. Hoffmann, G. Huber, G. Janatsch, S. Lauper, O. Röckel-Stäbler, R. Trussardi, A. G. Zwahlen, *Org. Process Res. Dev.* **1999**, *3*, 266; c) M. Karpf, R. Trussardi, *J. Org. Chem.* **2001**, *66*, 2044; d) S. Abrecht, M. Karpf, R. Trussardi, B. Wirz, EP 1127872 A1, **2001**; *Chem. Abstr.* **2001**, *135*, 195452; e) U. Zutter, H. Iding, B. Wirz, EP 1146036 A2, **2001**; *Chem. Abstr.* **2001**, *135*, 303728; f) P. J. Harrington, J. D. Brown, T. Foderaro, R. C. Hughes, *Org. Process Res. Dev.* **2004**, *8*, 86; g) S. Abrecht, P. Harrington, H. Iding, M. Karpf, R. Trussardi, B. Wirz, U. Zutter, *Chimia* **2004**, *58*, 621; h) Y.-Y. Yeung, S. Hong, E. J. Corey, *J. Am. Chem. Soc.* **2006**, *128*, 6310; i) Y. Fukuta, T. Mita, N. Fukuda, M. Kanai, M. Shibasaki, *J. Am. Chem. Soc.* **2006**, *128*, 6312; j) X. Cong, Z.-J. Yao, *J. Org. Chem.* **2006**, *71*, 5365; k) S. Abrecht, M. C. Federspiel, H. Estermann, R. Fischer, M. Karpf, H.-J. Mair, T. Oberhauser, G. Rimmeler, R. Trussardi, U. Zutter, *Chimia* **2007**, *61*, 93; l) N. Satoh, T. Akiba, S. Yokoshima, T. Fukuyama, *Angew. Chem.* **2007**, *119*, 5836; *Angew. Chem. Int. Ed.* **2007**, *46*, 5734; m) J.-J. Shie, J.-M. Fang, S.-Y. Wang, K.-C. Tsai, Y.-S. E. Cheng, A.-S. Yang, S.-C. Hsiao, C.-Y. Su, C.-H. Wong, *J. Am. Chem. Soc.* **2007**, *129*, 11892; n) T. Mita, N. Fukuda, F. X. Roca, M. Kanai, M. Shibasaki, *Org. Lett.* **2007**, *9*, 259; o) K. M. Bromfield, H. Gradén, D. P. Hagberg, T. Olsson, N. Kann, *Chem. Commun.* **2007**, 3183; p) K. Yamatsugu, S. Kamijo, Y. Suto,

- M. Kanai, M. Shaibasaki, *Tetrahedron Lett.* **2007**, *48*, 1403; q) U. Zutter, H. Iding, P. Spurr, B. Wirz, *J. Org. Chem.* **2008**, *73*, 4895; r) B. M. Trost, T. Zhang, *Angew. Chem.* **2008**, *120*, 3819; *Angew. Chem. Int. Ed.* **2008**, *47*, 3759; s) J.-J. Shie, J.-M. Fang, C.-H. Wong, *Angew. Chem.* **2008**, *120*, 5872; *Angew. Chem. Int. Ed.* **2008**, *47*, 5788; t) M. Matveenko, M. G. Banwell, A. C. Willis, *Tetrahedron Lett.* **2008**, *49*, 7018; u) N. T. Kipassa, H. Okamura, K. Kina, T. Hamada, T. Iwagawa, *Org. Lett.* **2008**, *10*, 815; v) L.-D. Nie, X.-X. Shi, K. H. Ko, W.-D. Lu, *J. Org. Chem.* **2009**, *74*, 3970; w) T. Mandai, T. Oshitari, *Synlett* **2009**, 783; x) T. Oshitari, T. Mandai, *Synlett* **2009**, 787; y) H. Sun, Y.-J. Lin, Y.-L. Wu, Y. Wu, *Synlett* **2009**, 2473; z) K. Yamatsugu, L. Yin, S. Kamijo, Y. Kimura, M. Kanai, M. Shibasaki, *Angew. Chem.* **2009**, *121*, 1090; *Angew. Chem. Int. Ed.* **2009**, *48*, 1070; aa) B. Sullivan, I. Carrera, M. Drouin, T. Hudlicky, *Angew. Chem.* **2009**, *121*, 4293; *Angew. Chem. Int. Ed.* **2009**, *48*, 4229; ab) M. Karpf, R. Trussardi, *Angew. Chem.* **2009**, *121*, 5871; *Angew. Chem. Int. Ed.* **2009**, *48*, 5760; ac) N. Satoh, T. Akiba, S. Yokoshima, T. Fukuyama, *Tetrahedron* **2009**, *65*, 3239; ad) L.-D. Nie, X.-X. Shi, *Tetrahedron: Asymmetry* **2009**, *20*, 124; ae) K. Yamatsugu, M. Kanai, M. Shibasaki, *Tetrahedron* **2009**, *65*, 6017; af) H. Osato, I. L. Jones, A. Chen, C. L. L. Chai, *Org. Lett.* **2010**, *12*, 60; ag) L. Werner, A. Machara, T. Hudlicky, *Adv. Synth. Catal.* **2010**, *352*, 195; ah) A. Kamimura, T. Nakano, *J. Org. Chem.* **2010**, *75*, 3133; ai) J. Weng, Y.-B. Li, R.-B. Wang, F.-Q. Li, C. Liu, A. S. C. Chan, G. Lu, *J. Org. Chem.* **2010**, *75*, 3125; aj) J. Ma, Y. Zhao, S. Ng, J. Zhang, J. Zeng, A. Than, P. Chen, X.-W. Liu, *Chem. Eur. J.* **2010**, *16*, 4533; ak) P. Wichienukul, S. Akkarasamiyo, N. Kongkathip, B. Kongkathip, *Tetrahedron Lett.* **2010**, *51*, 3208; al) J. S. Ko, J. E. Keum, S. Y. Ko, *J. Org. Chem.* **2010**, *75*, 7006; am) S. Raghavan, V. S. Babu, *Tetrahedron* **2011**, *67*, 2044; an) B. M. Trost, T. Zhang, *Chem. Eur. J.* **2011**, *17*, 3630; ao) T. Tanaka, Q. Tan, H. Kawakubo, M. Hayashi, *J. Org. Chem.* **2011**, *76*, 5477; ap) L.-D. Nie, X.-X. Shi, N. Quan, F.-F. Wang, X. Lu, *Tetrahedron: Asymmetry* **2011**, *22*, 1692; aq) L. Werner, A. Machara, B. Sullivan, I. Carrera, M. Moser, D. R. Adams, T. Hudlicky, *J. Org. Chem.* **2011**, *76*, 10050; ar) M. Trajkovic, Z. Ferjancic, R. N. Saicic, *Org. Biomol. Chem.* **2011**, *9*, 6927; as) N. Chuanopparat, N. Kongkathip, B. Kongkathip, *Tetrahedron Lett.* **2012**, *53*, 6209; at) T.-J. Cheng, S. Weinheimer, E. B. Tarbet, J.-T. Jan, Y.-S. Cheng, J.-J. Shie, C.-L. Chen, C.-A. Chen, W.-C. Hsieh, P.-W. Huang, *J. Med. Chem.* **2012**, *55*, 8657; au) H.-S. Oh, H.-Y. Kang, *J. Org. Chem.* **2012**, *77*, 8792; av) N. Chuanopparat, N. Kongkathip, B. Kongkathip, *Tetrahedron* **2012**, *68*, 6803; aw) L.-D. Nie, W. Ding, X.-X. Shi, N. Quan, X. Lu, *Tetrahedron: Asymmetry* **2012**, *23*, 742; ax) V. Rawat, S. Dey, A. Sudalai, *Org. Biomol. Chem.* **2012**, *10*, 3988; ay) D. S. Gunasekera, *Synlett* **2012**, 23, 573; az) H.-K. Kim, K.-J. J. Park, *Tetrahedron Lett.* **2012**, *53*, 1561; ba) M. Trajkovic, Z. Ferjancic, R. N. Saicic, *Synthesis* **2013**, *45*, 389; bb) K. Alagiri, M. Furutachi, K. Yamatsugu, N. Kumagai, T. Watanabe, M. Shibasaki, *J. Org. Chem.* **2013**, *78*, 4019; bc) L. D. Nie, F. F. Wang, W. Ding, X. X. Shi, X. Lu, *Tetrahedron: Asymmetry* **2013**, *24*, 638; Review, see: bd) V. Farina, J. D. Brown, *Angew. Chem.* **2006**, *118*, 7488; *Angew. Chem. Int. Ed.* **2006**, *45*, 7330; be) M. Shibasaki, M. Kanai, *Eur. J. Org. Chem.* **2008**, 1839; bf) J. Magano, *Chem. Rev.* **2009**, *109*, 4398; bg) J. Andraos, *Org. Process Res. Dev.* **2009**, *13*, 161; bi) J. Magano, *Tetrahedron* **2011**, *67*, 7875; bh) M. Shibasaki, M. Kanai, K. Yamatsugu, *Isr. J. Chem.* **2011**, *51*, 316.
- [2] a) P. A. Clarke, S. Santos, W. H. C. Martin, *Green Chem.* **2007**, *9*, 438; b) Review, see: C. Vaxelaire, P. Winter, M. Christmann, *Angew. Chem.* **2011**, *123*, 3685; *Angew. Chem. Int. Ed.* **2011**, *50*, 3605; c) Y. Hayashi, S. Umemiya, *Angew. Chem. Int. Ed.* **2013**, *52*, 3450.
 - [3] a) H. Ishikawa, T. Suzuki, Y. Hayashi, *Angew. Chem.* **2009**, *121*, 1330; *Angew. Chem. Int. Ed.* **2009**, *48*, 1304; b) H. Ishikawa, T. Suzuki, H. Orita, T. Uchimaru, Y. Hayashi, *Chem. Eur. J.* **2010**, *16*, 12616; c) H. Ishikawa, B. P. Bondzic, Y. Hayashi, *Eur. J. Org. Chem.* **2011**, *30*, 6020.
 - [4] H. Ishikawa, M. Honma, Y. Hayashi, *Angew. Chem.* **2011**, *123*, 2876; *Angew. Chem. Int. Ed.* **2011**, *50*, 2824.
 - [5] a) Y. Hayashi, H. Gotoh, T. Hayashi, M. Shoji, *Angew. Chem.* **2005**, *117*, 4284; *Angew. Chem. Int. Ed.* **2005**, *44*, 4212; b) H. Gotoh, Y. Hayashi, Diarylprolinol silyl ethers: Development and application as organic catalysis. In *Sustainable Catalysis: Challenges and Practices for the Pharmaceutical and Fine Chemical Industries*; P. J. Dunn, K. K. Hii, M. J. Krische, M. T. Williams, Eds.; John Wiley & Sons: Hoboken, NJ, **2013**; pp. 287–316.
 - [6] M. Marigo, T. C. Wabnitz, D. Fielenbach, K. A. Jørgensen, *Angew. Chem.* **2005**, *117*, 804; *Angew. Chem. Int. Ed.* **2005**, *44*, 794.
 - [7] S. Zhu, S. Yu, Y. Wang, D. Ma, *Angew. Chem.* **2010**, *122*, 4760; *Angew. Chem. Int. Ed.* **2010**, *49*, 4656.
 - [8] a) J. Reháček, M. Hut'ka, A. Latika, H. Brath, A. Almassy, V. Hajzer, J. Durmis, S. Toma, R. Sebesta, *Synthesis* **2012**, *44*, 2424; b) V. Hajzer, A. Latika, J. Durmis, R. Sebesta, *Helv. Chim. Acta* **2012**, *95*, 2421.
 - [9] J. Weng, Y.-B. Li, R.-B. Wang, G. Lu, *ChemCatChem* **2012**, *4*, 1007.
 - [10] K. Patora-Komisarska, M. Benohoud, H. Ishikawa, D. Seebach, Y. Hayashi, *Helv. Chim. Acta* **2011**, *94*, 719.
 - [11] D. Seebach, S. Xiaoyu, M. O. Ebert, W. B. Schweizer, N. Purkayastha, A. K. Beck, J. Duschmalé, H. Wennemers, T. Mukaiyama, M. Benohoud, Y. Hayashi, M. Reiher, *Helv. Chim. Acta* **2013**, *96*, 799.
 - [12] U. Grošelj, D. Seebach, D. M. Badine, W. B. Schweizer, A. K. Beck, I. Krossing, P. Klose, Y. Hayashi, T. Uchimaru, *Helv. Chim. Acta* **2009**, *92*, 1225.
 - [13] G.-L. Zhao, Y. Xu, H. Sunden, L. Eriksson, M. Sayah, A. Cordova, *Chem. Commun.* **2007**, 734.
 - [14] G. Bifulco, P. Dambruoso, L. Gomez-Paloma, R. Riccio, *Chem. Rev.* **2007**, *107*, 3744.
 - [15] a) Y. Nagai, T. Kusumi, *Tetrahedron Lett.* **1995**, *36*, 1853; b) T. Yabuuchi, T. Kusumi, *J. Org. Chem.* **2000**, *65*, 397.
 - [16] J. Alemán, S. Cabrera, E. Maerten, J. Overgaard, K. A. Jørgensen, *Angew. Chem.* **2007**, *119*, 5616; *Angew. Chem. Int. Ed.* **2007**, *46*, 5520.
 - [17] D. Seebach, J. Golinski, *Helv. Chim. Acta* **1981**, *64*, 1413.

Received: June 20, 2013

Published online: November 18, 2013

Stoichiometric Reactions of Enamines Derived from Diphenylprolinol Silyl Ethers with Nitro Olefins and Lessons for the Corresponding Organocatalytic Conversions – a Survey¹⁾

by **Dieter Seebach***, **Xiaoyu Sun^{2a)}**, **Marc-Olivier Ebert**, **W. Bernd Schweizer**, **Nirupam Purkayastha^{2b)}**, **Albert K. Beck**, **Jörg Duschmalé**, and **Helma Wennemers**

Laboratorium für Organische Chemie, Departement Chemie und Angewandte Biowissenschaften,
ETH-Zürich, Hönggerberg HCI, Wolfgang-Pauli-Strasse 10, CH-8093 Zürich
(phone: +41-44-632-2990; fax: +41-44-632-1144; e-mail: seebach@org.chem.ethz.ch)

and **Takasuke Mukaiyama^{2c)}**, **Meryem Benohoud^{2d)}**, and **Yujiro Hayashi***

Tokyo University of Science, Department of Industrial Chemistry, Faculty of Engineering, Kagurazaka,
Shinjuku-ku, Tokyo 162-8601, Japan
and Department of Chemistry, Tohoku University, 6-3 Aramaki-Aza, Aoba-ku, Sendai, Miyagi 980-8578,
Japan (phone: +81-22-795-3554; fax: +81-22-795-6566; e-mail: yhayashi@m.tohoku.ac.jp)

and **Markus Reiher***

Laboratorium für Physikalische Chemie, Departement Chemie und Angewandte Biowissenschaften,
ETH-Zürich, Hönggerberg HCI F 235, Wolfgang-Pauli-Strasse 10, CH-8093 Zürich
(phone: +41-44-633-4308; fax: +41-44-633-1595; e-mail: markus.reiher@phys.chem.ethz.ch)

Dedicated to *Jack D. Dunitz* – friend and ‘professor for the professors’ of LOC – on the occasion of his 90th birthday

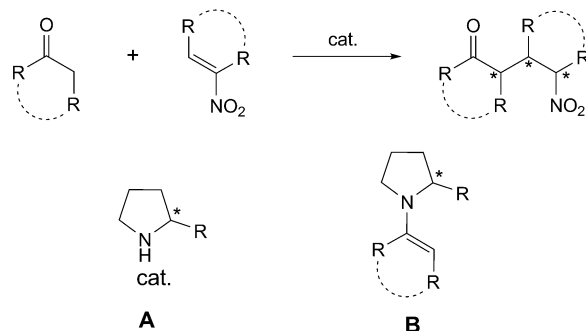
The stoichiometric reactions of enamines prepared from aldehydes and diphenyl-prolinol silyl ethers (intermediates of numerous organocatalytic processes) with nitro olefins have been investigated. As reported in the last century for simple achiral and chiral enamines, the products are cyclobutanes (**4** with monosubstituted nitro-ethenes), dihydro-oxazine *N*-oxide derivatives (**5** with disubstituted nitro-ethenes), and nitro enamines derived from γ -nitro aldehydes (**6**, often formed after longer reaction times). The same types of products were shown to be formed, when the reactions were carried out with peptides H-Pro-Pro-Xaa-OMe that lack an acidic H-atom. Functionalized components such as alkoxy enamines, nitro-acrylates, acetamido-nitro-ethylene, or hydroxylated nitro olefins also form products carrying the diphenyl-prolinol silyl ether as a substituent. All of these products must be considered intermediates in the corresponding catalytic reactions; the investigation of their chemical properties provided useful hints about the rates, the conditions, the catalyst resting states or irreversible traps, and/or the limitations of the corresponding organocatalytic processes. High-level DFT and MP2 computations of the structures of alkoxy enamines and thermodynamic data of a cyclobutane dissociation are also described. Some results obtained with the stoichiometrically prepared intermediates are not compatible with previous mechanistic proposals and assumptions.

¹⁾ Part of the results described herein had been reported in a preliminary communication [1].

²⁾ ^{a)} Postdoctoral fellow at ETH Zürich 2011/12, partially financed by *Swiss National Science Foundation* (SNF-No. 200020-126693). All the isolations of intermediates and preparations of single crystals, described herein, have been carried out by X. S. ^{b)} Postdoctoral fellow at ETH Zürich 2012/13. ^{c)} Some of the experiments were carried out by T. M. during a three-month stay at ETH Zürich (August–October 2012), financed by Tokyo University of Science. ^{d)} Postdoctoral fellow at Tokyo University of Science (2010–2012), financed by *JSPS* (PE10034; P10817).

1. Introduction. – Shortly after the renaissance [2] of organocatalysis [3] had started in the year 2000, the enantioselective *Michael* addition of aldehydes and ketones to nitro olefins, catalyzed by chiral *sec*-amines, was investigated [4–6]. This type of reaction, leading to γ -nitro carbonyl compounds with up to three new stereogenic centers, became a general test track for those organocatalysts that form enamines as nucleophilic reactive intermediates (*Scheme 1*). Most of the *sec*-amino derivatives used are of the pyrrolidine type **A**³⁾. The underlying reactions of chiral and achiral enamines (*cf.* **B**) with nitro olefins in stoichiometric applications have been studied in the years between 1964 and 2000 [8], and have led a rather shadowy existence. A careful study of this old literature provides the mechanistic manifold presented in *Scheme 2*. In these stoichiometric reactions, a mono- or disubstituted enamine and a nitro olefin are mixed under anhydrous conditions in an aprotic solvent such as MeCN, Et₂O, or hexanes, often with cooling, to give, after non-aqueous workup, either a cyclobutane **C** (preferentially with monosubstituted nitro olefins) or an oxazine derivative **D** (preferentially with disubstituted nitro olefins), or a nitro enamine, **E/E'**. All of these – isolable – primary products, **C–E**, are converted to the actual *Michael* adducts **F** upon hydrolysis under acidic conditions (*cf.* EtOH/H₂O/HCl). Possible routes for these hydrolytic conversions, mostly already proposed in the old literature [8], are included in *Scheme 2*. The elusive iminium-nitronate zwitterion **G** plays a central role in these proposals. For the reactions of the (*E*)- and (*Z*)-1-morpholinopropene (enamines from propanal and morpholine) with nitrostyrene, and of (*E*)- and (*Z*)-nitrostyrene with morpholino-cyclohexene (enamine from cyclohexanone and morpholine), the *Huisgen* test [9] for (2 + 2) cycloadditions *via* zwitterionic intermediates was positive: there is scrambling between the (*E*)- and (*Z*)-isomers, and the reaction is non-stereospecific (*Scheme 3*; see [10] and 1985 publication (with *Laube*) [8])⁴⁾. Trapping of the

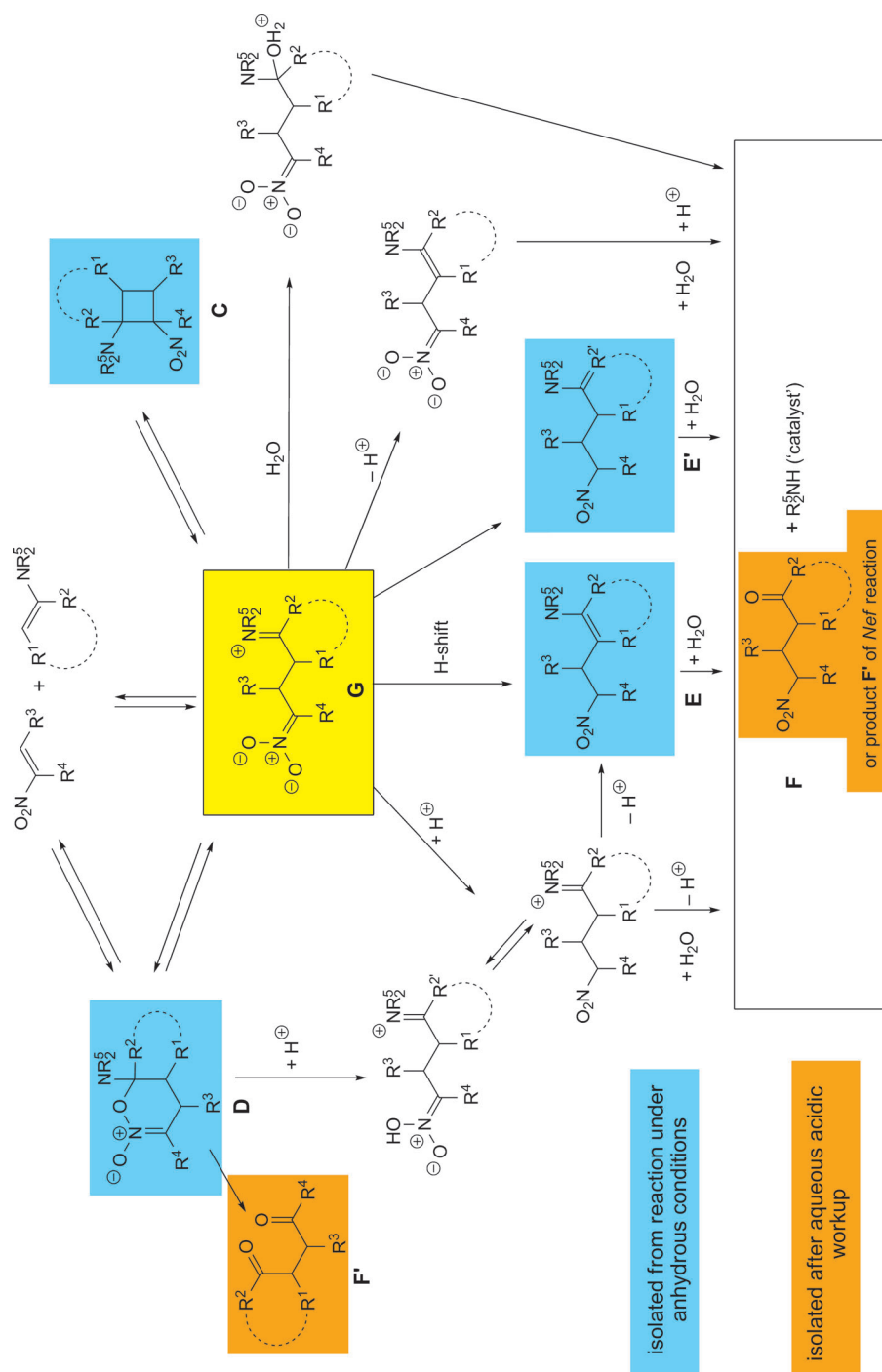
Scheme 1. *sec*-Amine (**A**)-Catalyzed *Michael* Additions of Aldehydes and Ketones to Nitro Olefins and Enamine Intermediate **B**



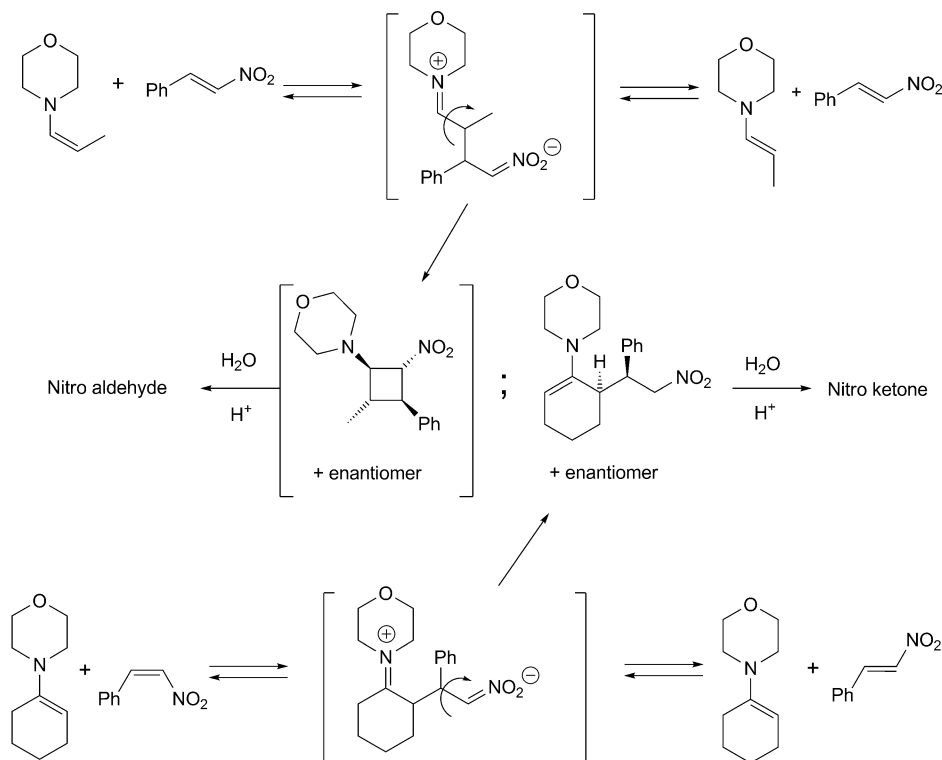
³⁾ The number of reports on this type of reactions is so large (many dozens!) that we can only refer to some selected reviews [7].

⁴⁾ In the case of the oxazine derivatives **D** (*Scheme 2*), a formally allowed [11], non-synchronous, concerted (4 + 2) cycloaddition, a so-called inverse-electron-demand *Diels–Alder* reaction, without a zwitterion intermediate, could be involved. In a recent *DFT calculation*, no zwitterion of type **G** was located as a low-lying energy minimum [12]. For synthetic applications and mechanistic discussions of oxazine derivatives resulting from (4 + 2) cycloadditions to nitro olefins of enes other than enamines (*e.g.*, enol ethers), see [13].

Scheme 2. Possible Routes from an Enamine and a Nitro Olefin to a γ -Nitro Carbonyl Compound **F**. Most of these routes have been proposed in the last century [8]. The formulae **D**, **C**, and **E**, colored blue, correspond to products isolated from stoichiometric reactions of enamines with nitro olefins under anhydrous aprotic conditions, and their acidic hydrolyses lead to nitro carbonyl compounds **F**. For the role of the zwitterionic iminium nitronate **G**, see also Scheme 3. Instead of the nitro carbonyl compounds **F**, i.e., nitro ketones or aldehydes, the products **F'** of Nef reactions have sometimes been isolated.



Scheme 3. Test for Zwitterionic Intermediates [9] in the (2+2) Cycloaddition of an (E)- and (Z)-Enamine, and an (E)- and (Z)-Nitro Olefin. The same results (yield, diastereoselectivity) were obtained with the (E)- and (Z)-starting materials (see 1985 paper with Laube in [8], and [10]).



zwitterion in the course of aqueous hydrolysis has been considered crucial for the cyclobutane **C** to be converted to the nitro carbonyl compound **F**, while the dihydro-oxazine *N*-oxide **D**, a cyclic nitronate ester, could also undergo acidic hydrolysis to an iminium-nitronic acid or nitro iminium ion⁵⁾ without the intermediacy of a zwitterion⁶⁾. Except on route **G** → **E** → **F**, the absolute (with chiral enamines) and relative configurations of the two stereogenic centers (bearing *R*¹ and *R*³) in *α*- and *β*-position

⁵⁾ This was suggested by us (Footnote 5 in [1]) as an alternative to other 'exits' from the cyclic intermediate **D** to open-chain precursors of the final nitro carbonyl compound **F**. *Computational* results by *Pihko* and co-workers [12] indicate that protonation of an oxazine derivative of type **D** in the 3-position of the heterocycle is 'clearly favored kinetically' (*vide infra* Footnote 38), generating a nitro-alkane moiety; we are unable to judge whether the alternative protonation on O[−], with subsequent formation of a nitronic acid group, has been probed in this computational analysis. Results of deuterolysis experiments are not compatible with *C*(3)-protonation (see Scheme 10.e).

⁶⁾ Rather than simple hydrolysis to the nitro carbonyl derivative of type **F**, *Nef* reactions have been observed to occur during acidic hydrolyses of the primary products (*cf.* *Valentin* and co-workers in [8], as well as *Yoshikoshi* and co-workers in [13]).

to C=O in **F** are set in the coupling step between the trigonal centers of the enamine and the nitro-olefin component⁷⁾.

All the products shown (in orange and blue) and all the processes outlined in *Schemes 2* and *3* for the stoichiometric reactions between enamines and nitro olefins must be considered for the *sec*-amine-catalyzed addition of aldehydes and ketones to nitro olefins presented in *Scheme 1*. At the beginning of the competitive run in enantioselective organocatalysis, there was no time for mechanistic investigations, so that no or only a simplistic catalytic cycle⁸⁾ was proposed, focusing on the relative topicity of the primary C,C-bond formation [4–7]⁷⁾⁸⁾.

Intrigued by the observation that the addition of aldehydes to nitro olefins, catalyzed by the diphenyl-prolinol silyl ethers **1a** and **1b** under standard conditions (5 mol-% **1**, 5 mol-% 4-nitrophenol, 24 h, room temperature) [14], appeared to be subject to steric hindrance, resulting from the size and the number of substituents on the two reactants (an effect which had not been noticed in the stoichiometric reactions)⁹⁾ two of our groups (*Y. H.* and *D. S.*) decided to study the addition of **1**-derived enamines to various nitro olefins under stoichiometric, anhydrous conditions¹⁰⁾¹¹⁾. In this work, we present hitherto unpublished (experimental) details and case studies, which show that, for the catalytic reaction to take place, and for identifying the best conditions, it is useful to know the chemical properties of the intermediates involved.

2. Stoichiometric Reactions of Enamines, Derived from the Diphenylprolinol Silyl Ethers 1 and Aldehydes, with Mono- and Disubstituted Nitro Olefins. – We prepared solutions, in dry (D₆)benzene or (D₈)toluene, of enamines **2** (formed immediately¹²⁾) from aldehydes and the pyrrolidines **1**, removing H₂O with molecular sieves¹³⁾ (*Scheme 4*). The solution of the enamines was then mixed with the nitro olefin, dissolved in the same solvent, and NMR spectra were recorded immediately and after certain periods of time. In fact, and as expected, the three types of products identified and reported in the old literature (*Scheme 2*) were detected by NMR analysis: the cyclobutanes **4** (*Fig. 1*; cf. **C**) the dihydro-oxazine *N*-oxides **5** (*Fig. 2*; cf. **D**), and the nitro enamines **6** (*Fig. 3*; cf. **E**). The ratio depended upon the particular pair of reactants **2** and **3**, upon the temperature, and upon the reaction time, with the

7) Following the general ‘*Topological Rule for C,C-Bond Forming Processes*’ involving coupling of two trigonal centers (see 1981 publication (with *Golinski*) in [8]).

8) See, e.g., *Scheme 1* in [14] and refs. cit. therein.

9) In fact, when mixing enamines with nitro olefins an exothermic reaction takes place, so that cooling or starting the reaction at dry-ice temp. is sometimes recommended [8].

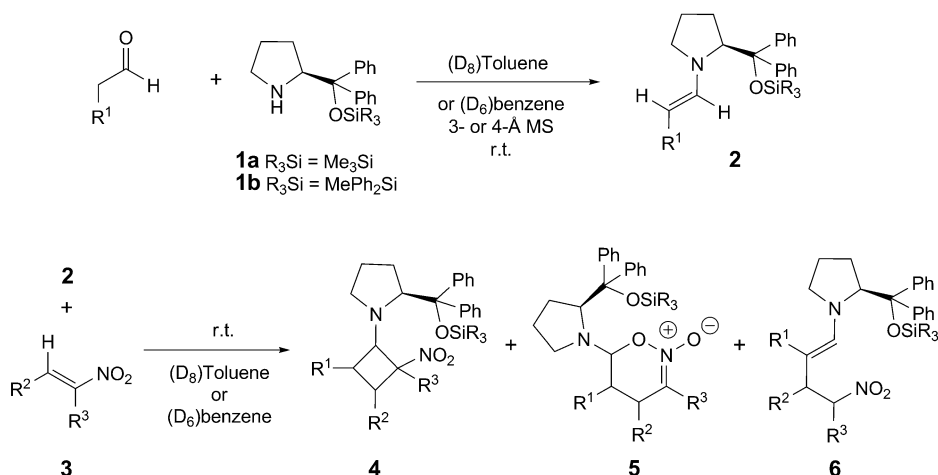
10) See [14] and the preliminary communication [1]. In the original work of *Hayashi et al.*, no acid additive was used, and the solvent was hexane [15].

11) For independent works along these lines, see [12][16][17]. For early mechanistic studies on the catalytic reaction, see *Sect. 3* and refs. cit. therein.

12) In all cases, the enamine had formed completely after a few minutes (‘before we arrived at the NMR machine for recording the spectrum’).

13) In the case of propanal, an excess aldehyde had to be employed to achieve complete conversion in the presence of 4-Å molecular sieves (MS), but not with 3-Å MS. We interpret this observation by assuming that propanal can enter the cavities of 4-Å but not of 3-Å MS.

Scheme 4. Preparation of Enamine **2** Solutions from Aldehydes and Pyrrolidines **1**, and Reactions with Nitro Olefins **3** with Formation of Mixtures of Cyclobutanes **4**, Dihydrooxazine N-Oxides **5**, and Nitro Enamines **6**. Cyclobutanes are preferred with monosubstituted nitro olefins, and oxazine derivatives are preferred with disubstituted nitro olefins, and nitro enamines are often the major products after longer periods of time.



cyclobutane **4** prevailing with monosubstituted nitro olefins, the heterocycle **5** being the only product detected with disubstituted nitro olefins, and the nitro enamine **6** often becoming the major product after extended periods of time. Equilibria between the four- and the six-membered rings, and between these cyclic compounds and the starting materials, enamine and nitro olefin, were observed. As will be discussed in the following *Sections* in detail, some of the four- and six-membered-ring compounds **4** and **5** are stable in solution at up to 50°, or even to 100°, and in five cases crystalline samples, suitable for single-crystal X-ray structure determination, could be prepared (*Fig. 4*)¹⁴. Most of the NMR data of compounds **4**, **5**, and **6**, presented in the *Exper. Part*, have been obtained by analysis of the complex spectra of mixtures of – sometimes equilibrating – compounds, using 2D-COSY, NOSY, HSQC, and EXSY techniques¹⁵)¹⁶).

2.1. *The Cyclobutanes 4*. As we had expected, cyclobutanes, **4a–4q**, are always formed from the enamines **2** and the monosubstituted nitro olefins **3** (R³ = H), not only in those cases, in which the corresponding catalytic reaction under our standard conditions (toluene, room temperature, 5 mol-% **1a**, 5 mol-% 4-nitrophenol, up to 48 h; *Scheme 1*) [14] takes place (*cf. 4a–4j* in *Fig. 1*), but also with the sterically more hindered reactants (*cf. 4k–4q* in *Fig. 1*). The reaction becomes slower with increasing

¹⁴) As can be seen from *Fig. 4* of the crystal structures, the virtual electron pair on the pyrrolidino N-atom is in all cases *antiperiplanar* to the most polar C–C–N (**4q**) and C–O–N (**5b–5d** and **5g**) bond within the ring, as if the molecules would be ready for opening up to zwitterions in a stereoelectronically assisted process.

¹⁵) See *Figs. 1–3* and *Scheme 6* in our preliminary communication [1].

¹⁶) The isolation and characterization of the cyclobutanes **4e** and **4q** have been described in our previous paper [14]; improved procedures are presented herein.

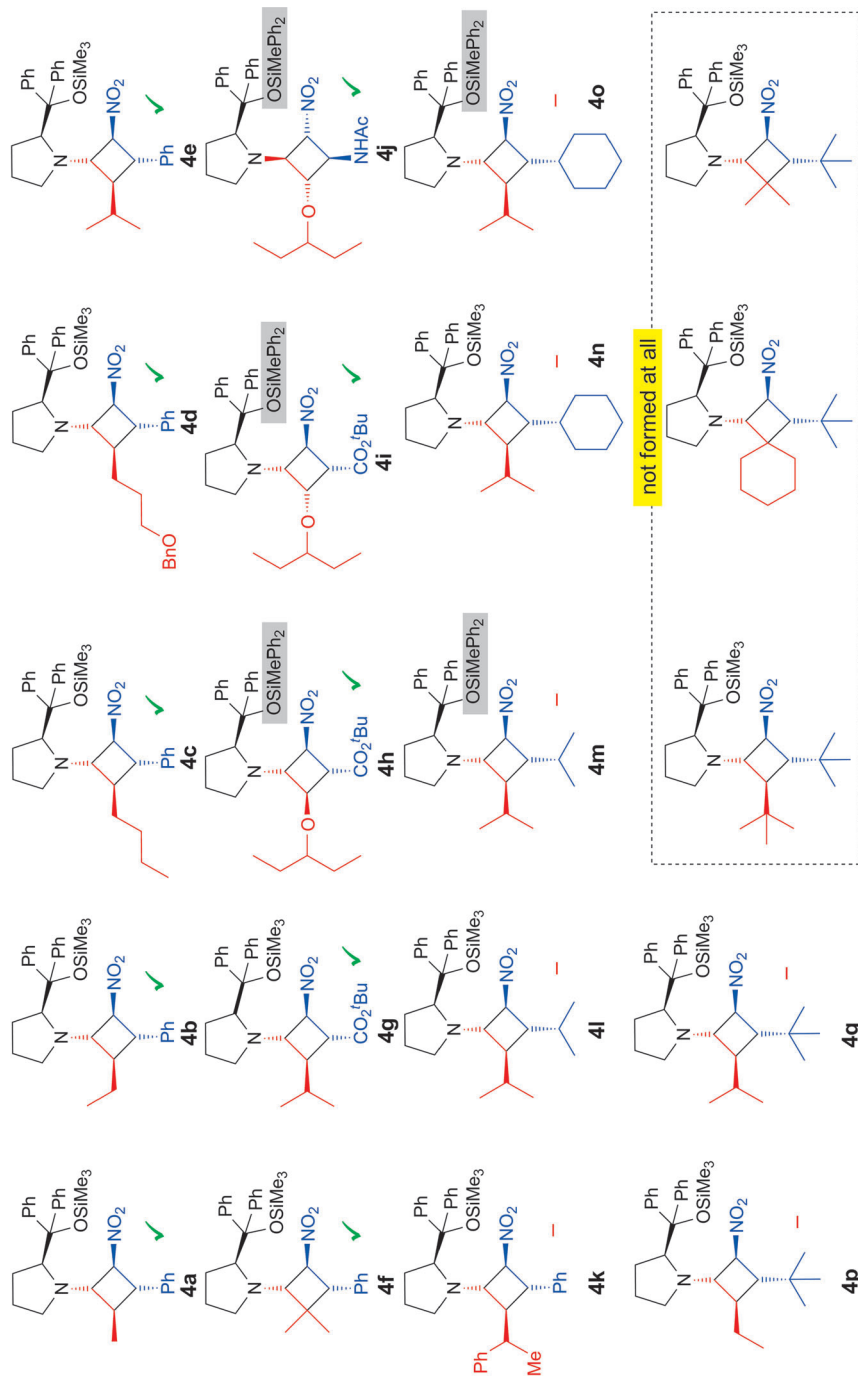


Fig. 1. Characterized (2 + 2) cycloadducts **4** obtained from pyrrolidino-enamines **2** and nitro olefins **3** ($R^3 = H$). The compounds were generated as outlined in Scheme 4 and identified by *in situ* NMR analysis, by isolation, and in one case, *i.e.*, **4q**, by X-ray analysis (see *Exper. Part*). ✓, Catalytic reaction under standard conditions (toluene, 5% **1**, 5% 4-NO₂-C₆H₄OH, 24 h, room temperature) [14] takes place with the corresponding aldehyde and nitro olefin. –, No catalytic nitro-aldehyde formation with the corresponding reactants. Box: These cyclobutanes are not formed at all under the conditions specified in Scheme 4. The NMR characterization of all compounds, *i.e.*, **4a–4e** and **4g–4q**, is reported in the *Exper. Part*; for **4f**, see [16] [17a].

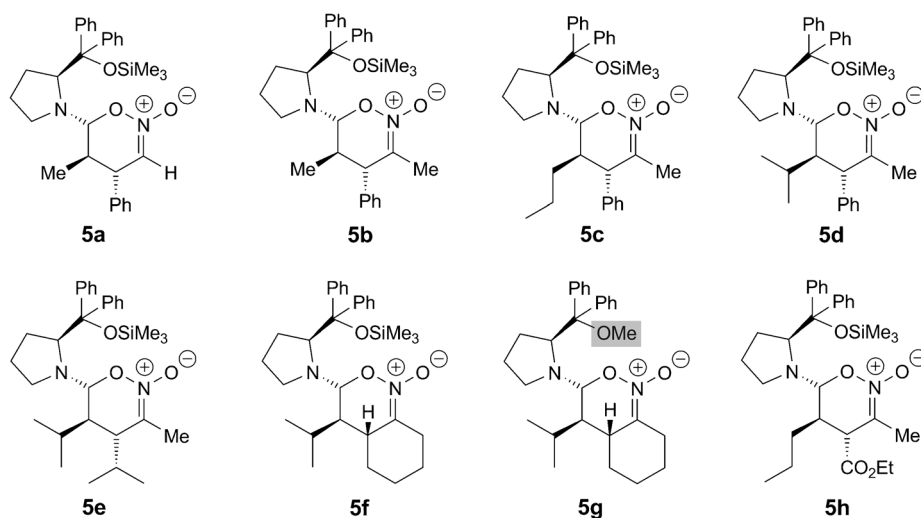


Fig. 2. Dihydro-oxazine N-oxides **5** formed under the conditions specified in Scheme 4. Identification by *in situ* NMR analysis, by isolation (chromatography, crystallization), and/or by X-ray crystal-structure determination (see *Exper. Part*).

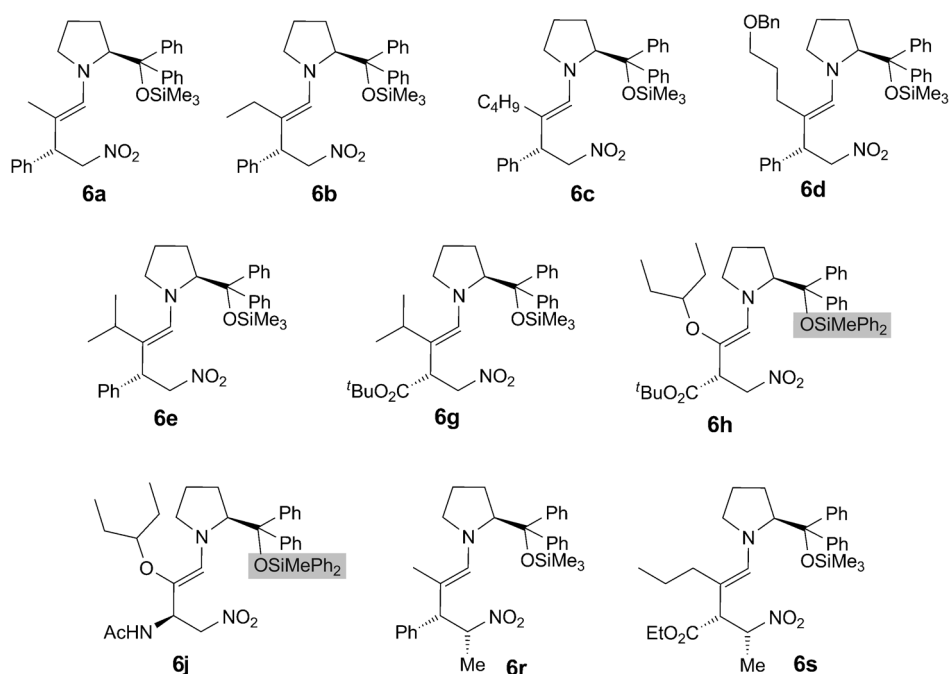


Fig. 3. Nitro Enamines **6** formed, especially after prolonged reaction times, from enamines **2** and nitro olefins **3** under anhydrous conditions (Scheme 4). Identification by *in situ* NMR analysis. Under carefully controlled conditions, solutions of 90% pure nitro enamine **6a** can be prepared. The letters in the compound numbering **6a–6j** correlate with those in Fig. 1.

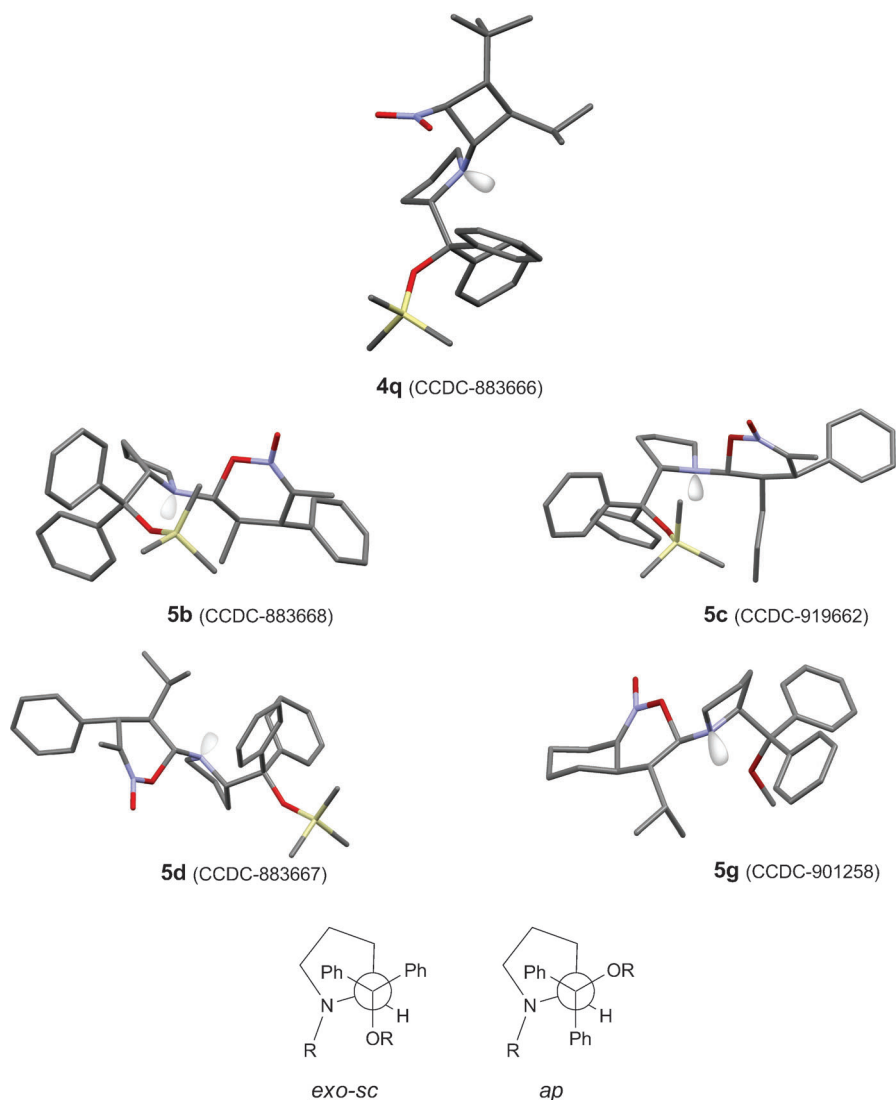


Fig. 4. *X-Ray crystal structures of the cyclobutane 4q, and of the dihydro-1,2-oxazine N-oxides 5b–5d and 5g.* The structures of **4q**, **5b**, and **5d** have been reported in our preliminary communication [1]. The structure of **5g** was determined by the *Gellman* group in 2009, but submitted to the *Cambridge Crystallographic Data Centre (CCDC)* only recently. In all structures, there is stereoelectronic $n_N \rightarrow \sigma^*_{C,C}$ or $n_N \rightarrow \sigma^*_{C,O}$ stabilization [18a] (see also *Footnote 14*). Note that the exocyclic bond of the pyrrolidine ring has the generally preferred [18b] *exo-synclinal* conformation only in **5b**, **5c**, and **5g**, while **4q** and **5d** have the *antiperiplanar* conformation of this bond (cf. results of calculations in Fig. 8 and structure of **21** in *Scheme 11*).

size of the substituents on the enamine and on the nitro olefin precursors, and only with too much bulk (cf. two *t*Bu groups) no cycloaddition product could be detected (see dotted-line box in Fig. 1). Thus, the lack of nitro-aldehyde formation under the

standard catalytic conditions with more bulky substituents is, in many cases, *not* due to lack of reactivity between the intermediate enamine and the nitro olefin.

2.1.1. Equilibrium between a Cyclobutane of Type 4 and Enamine + Nitro Olefin. A solution in C_6D_6 of the cyclobutane **4e**, prepared as shown in *Scheme 4*¹⁷⁾, containing no NMR-detectable amount of oxazine **5** or nitro enamine **6** derivative¹⁸⁾, but a few percent of nitrostyrene and of the enamine **2** (from 3-methylbutanal and **1a**), was stepwise heated to 66° and cooled back to r.t.; the ratio **4e**/enamine was determined by integration of suitable NMR signals after each change of temperature (for details, see *Exper. Part*). The results are presented in *Fig. 5* and show that there is a clean, fully reversible equilibrium between the (2 + 2) cycloadduct **4e** and its precursors; due to the ring strain of the cyclobutane and the necessarily large entropy factor, the cyclization is only weakly exergonic ($\Delta G = -4.3$ kcal/mol). We have not systematically looked for such equilibria with other cyclobutanes **4**, but it must be expected that they occur quite

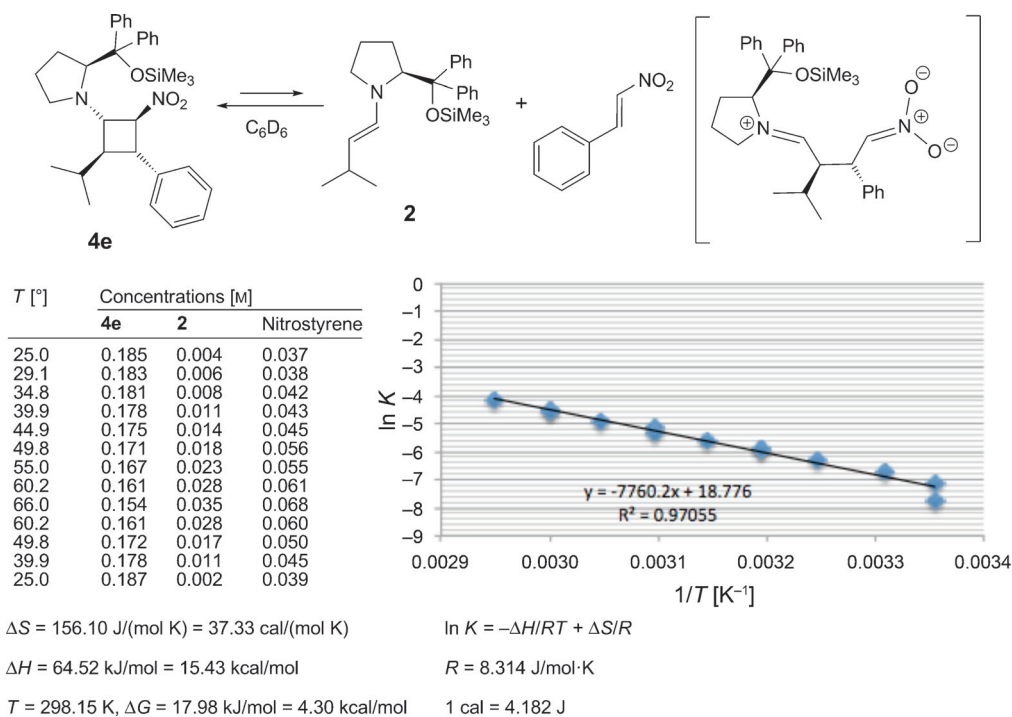


Fig. 5. Equilibrium between the amino-nitro-cyclobutane **4e**, and its precursors enamine and nitro olefin. There is an excess nitro olefin in the reaction mixture (for details, see *Table 5* in *Exper. Part*). According to the NMR analysis, the solution of the equilibrating species contains no oxazine derivative **5**, and no nitro enamine **6** is detected during this experiment. The iminium-nitronate zwitterion is assumed to be involved in this equilibration process (*cf. Scheme 3*).

¹⁷⁾ A similar experiment, conducted with a less pure sample of **4e**, has been described in our previous paper [14].

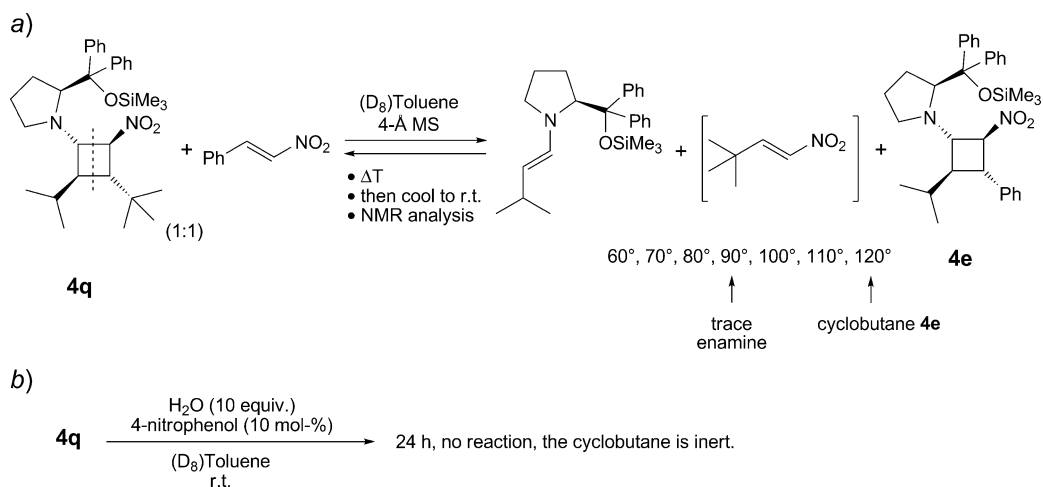
¹⁸⁾ ... at temperatures between 25 and 66°.

generally when there is not too much bulk of substituents on the four-membered ring (*cf.* **4q**).

The *conclusion for the corresponding catalytic reaction* (in toluene, Table 4 in [14]) would be that a *zwitterion* of type **G** is an intermediate *en route* from the cyclobutane to the open-chain nitro aldehyde of type **F**¹⁹).

2.1.2. *Stability of Cyclobutane 4q*. Our most stable *amino-nitro-cyclobutane 4q* (*Fig. 4* and *Footnote 16*) was prepared from the ^tBu-substituted nitro-ethene and the ⁱPr-substituted enamine as outlined in *Scheme 4*; formation of **4q** took 3 d in (D₆)benzene (85% yield after crystallization; m.p. 138–144° (dec.)) and 18 h in the presence of 1 equiv. 4-nitrophenol²⁰). To test the thermal stability of this cyclobutane, we heated its solution in (D₈)toluene in the presence of 1 equiv. of nitrostyrene (*i.e.*, (*E*)- β -nitrostyrene; sealed NMR tube). The result is outlined in *Scheme 5*: up to 80°, nothing happened; at 90°, we identified traces of the enamine precursor, and after heating to 120° the cyclobutane **4e** (product of scrambling) was detected. When the solution of **4q** was kept at room temperature in the presence of 4-nitrophenol and H₂O, there was no product of hydrolysis after 24 h; addition of acidic alumina (activity grade 1) or of ClCH₂CO₂H to the CHCl₃ solution, or chromatography of **4q** on silica gel did not lead to the corresponding nitro enamine or nitro aldehyde.

Scheme 5. *Thermal and Hydrolytic Stability of the Cyclobutane 4q in (D₈)Toluene.* a) The solution containing 1 equiv. of nitrostyrene was heated for 30 min at the indicated temperature in a sealed NMR tube, and, after cooling to ambient temperature, the spectra were recorded. The cyclobutane **4e** (with ‘exchanged’ nitro olefin-derived part of the molecule) is detected only after heating above 100°. b) The mixture containing 10 equiv. of H₂O and 4-nitrophenol was kept at r.t. (*cf.* the catalytic conditions [1][14]): no NMR-detectable trace of the corresponding nitro aldehyde was formed under these conditions. For other tested hydrolysis/decomposition conditions, see accompanying text.



¹⁹⁾ See the article by R. Huisgen entitled ‘Can Tetramethylene Intermediates Be Intercepted?’ [9b].

²⁰⁾ Acid additives are essential for effective catalysis of the *Michael* addition of carbonyl compounds to nitro olefins (*Scheme 1*); see discussions and references in [7][14] and in [19].

The *conclusion for the reaction under our standard catalytic conditions* would be that the (2 + 2) cycloadduct is slowly formed, but is not opening up to a linear intermediate to give the nitro aldehyde; in this case, the cyclobutane is a dead-end trap for the pyrrolidine catalyst.

2.1.3. *Equilibrium between Cyclobutane 4a and Oxazine Oxide Derivative 5a.* In an elaborate NMR analysis, we have found that the reaction between the propanal enamine and nitrostyrene in (D₆)benzene leads to an equilibrating mixture of the cyclobutane **4a** and the oxazine *N*-oxide **5a** (4 : 1 ratio at room temperature), which is converted to the nitro enamine **6a** within 15 h; in CH₂Cl₂ solution the open-chain compound is formed within 10 min (Scheme 6) [1]. This was recently confirmed by an independent investigation by Pihko and co-workers (propanal/nitrostyrene/**1a** 1 : 1 : 2, (D₈)toluene, room temperature, complete conversion in 24 h)²¹). A reasonable mechanism for the equilibration **4a** ⇌ **5a** and for the conversion **4a/5a** → **6a** would be formation of the zwitterion and an intra-²²) or intermolecular H-shift, which was confirmed by the D-labeling experiment outlined in Scheme 6, b.

2.1.4. *Acid Hydrolysis of the Nitro Enamine 6a to the Nitro Aldehyde 7a.* Under the conditions indicated in Scheme 6, a, we could prepare rather pure samples of the nitro enamine **6a** (84% on an 0.5-g scale), which we used to probe the diastereoselectivity of the acidic hydrolysis to the nitro aldehyde **7a** under two sets of conditions (Scheme 7): similar to the catalytic reaction [14], a 0.05M solution of **6a**, 1 equiv. 4-nitrophenol, and 1 equiv. H₂O in benzene was kept at room temperature for up to 40 h, and similar to the classical workup of stoichiometric reactions of enamines with nitro olefins [8], **6a** was dissolved in EtOH and treated with H₂O/HCl. As can be seen from the data in the table of Scheme 7, the selectivities determined by NMR analysis are poor (≤ 3 : 1), as compared to those of the corresponding catalytic reaction providing the diastereoisomer **7a** with a dr of 15 : 1 [14]. Burès *et al.* [17a] have performed a kinetic analysis of the reverse reactions (**7a** + **1a** ⇌ **6a** + H₂O and *epi-7a* + **1a** ⇌ **6a** + H₂O) from which they calculated a protonation selectivity of ≥ 39 : 1; they concluded that the configuration of the center bearing the Me group is not set in the coupling step of the trigonal centers of enamine and nitro olefin, but in the nitro enamine protonation step and modified the catalytic cycle accordingly. We are unable to interpret the discrepancies between these experimental results, *i.e.*, the diastereoselectivities of the catalytic reaction without added acid (14 : 1 [14]) or with 4-nitrophenol (15 : 1 [14]), the stoichiometric reaction with 4-nitrophenol (3 : 1) or with HCl (1.5 : 1) (Scheme 7), and the kinetics of equilibration between the diastereoisomers **7a** and *epi-7a* with **1a** (39 : 1 [17a]); an expert physical-chemical analysis is required²³).

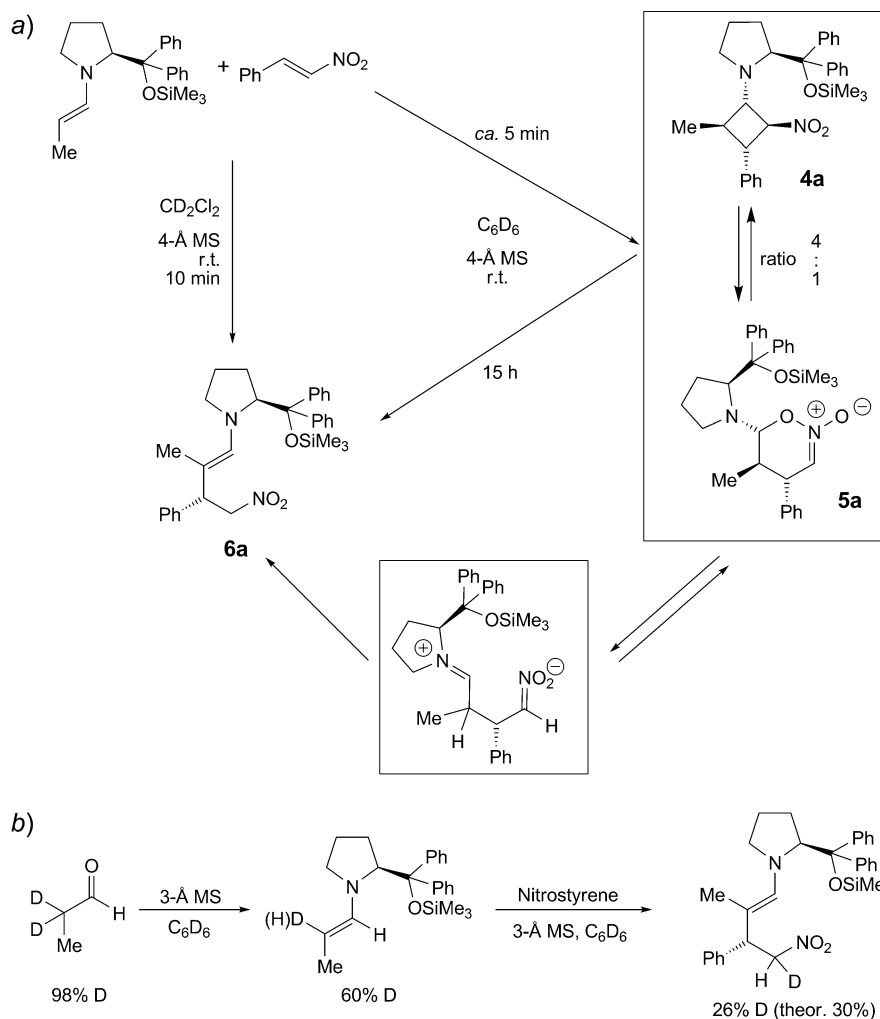
2.1.5. *Reactions of Enamines from 2-Alkoxyacetaldehyde with 3-Nitroacrylate (= (E)-3-Nitroprop-2-enoate) and 2-Acetamido-nitroethene.* These reactants have been used for syntheses of oseltamivir, the active agent of the antiviral drug *Tamiflu*® [21 –

²¹) See Fig. 2 in [12] (received June 20, revised October 10, and published online November 11, 2012); *cf.* also [17]; [1] was received May 31, and published online July 11, 2012.

²²) See also Scheme 1 in [1].

²³) Protonation, deprotonation, and iminium-ion formation are involved in the reaction between a *sec*-amine and an aldehyde, as well as in the reverse reaction, the hydrolysis of an enamine; in the reactions discussed here, the protonating species may be H₃O⁺, EtOH₂⁺, 4-nitrophenol, R₂⁺NH₂.

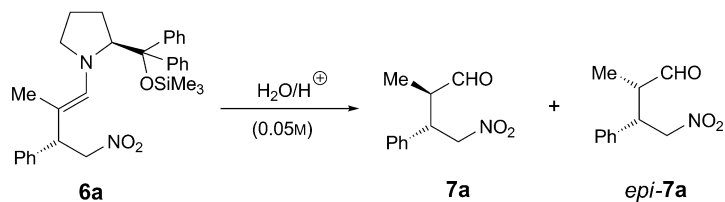
Scheme 6. *Equilibrium between the Nitrocyclobutane 4a and Its Six-Membered-Ring Isomer 5a, and Rearrangement to the Nitro Enamine 6a.* The NMR spectra for the detection of this process are shown and the detailed analysis is described in [1]. a) Slow ring opening in benzene, fast ring opening in CH_2Cl_2 with the corresponding zwitterion as presumed intermediate. b) With D-labeled enamine, the label ends up in the $\alpha\text{-NO}_2$ position. For a possible intramolecular H-shift converting the zwitterion to the nitro enamine, see Scheme 1 in [1]. For a preparation of the dideutero-propanal, see [20].



23]. Before turning to the stoichiometric reactions of the corresponding isopentyloxy enamine, a new type of resting state of the catalyst **1a** is discussed.

2.1.5.1. *The Michael Adduct of 1a to Nitroacrylate.* The nitroacrylate is a much more reactive *Michael* acceptor than nitrostyrenes or aliphatic nitro olefins. Indeed, when the ‘catalyst’ **1a** was added to a *tert*-butyl-3-nitroacrylate solution in C_6D_6 or CD_2Cl_2 , the

Scheme 7. *Poorly Stereoselective Hydrolysis of the Nitro Enamine 6a to the Nitro Aldehyde 7a.* Conditions *A* as for the catalytic reaction [14]; conditions *B* are typical for the workup of stoichiometric reactions of enamines with nitro olefins [8].

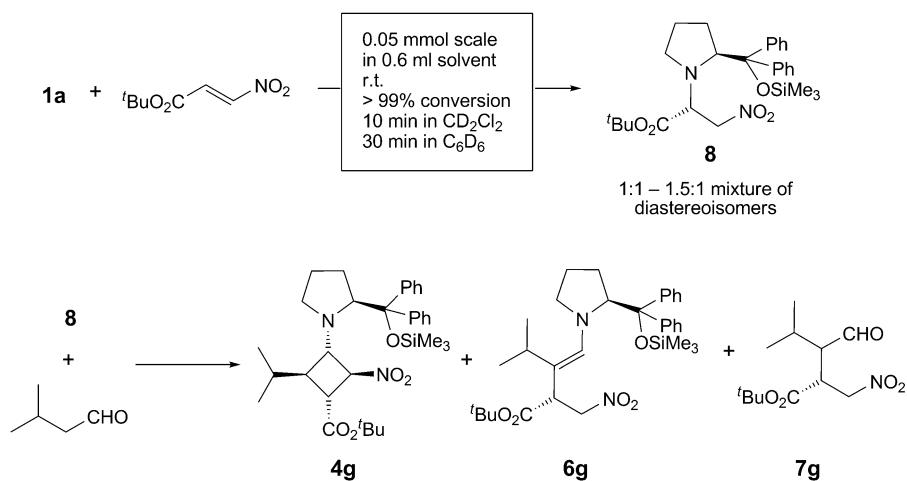


Conditions *A*: H_2O (1 equiv.), 4- $\text{NO}_2\text{-C}_6\text{H}_4\text{OH}$ (1 equiv.), C_6H_6 , r.t.
 Conditions *B*: H_2O (1 equiv.), 2N HCl (1 equiv.), EtOH , r.t.

Conditions	Time	7a / <i>epi-7a</i>	Conversion [%]
<i>A</i>	15 min	3.1: 1	83
<i>A</i>	30 min	2.7: 1	85
<i>A</i>	1.5 h	2.1: 1	86
<i>A</i>	16 h	1.5: 1	89
<i>A</i>	40 h	1.5: 1	89
<i>B</i>	10 min	1.5: 1	> 99
<i>B</i>	after workup	1: 1.1	

adduct **8** was formed (Scheme 8); in CH_2Cl_2 this took just a few minutes²⁴). The reaction was reversible, *i.e.*, the adduct **8** is a resting state of the catalyst: addition of 3-methylbutanal led to the cyclobutane **4g**, and then to the nitro enamine **6g**, and finally

Scheme 8. *Addition of ‘Catalyst’ 1a to Nitroacrylate and Reaction of the Adduct 8 with 3-Methylbutanal to Eventually Produce the Formyl Ester 7g (up to 72%; for details, see Table 7 in the Exper. Part)*

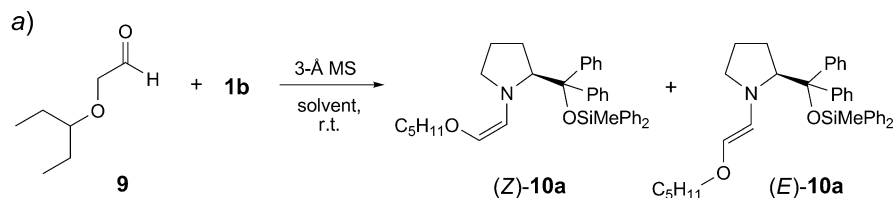


²⁴) With nitrostyrene, no reaction takes place (in C_6D_6) in 24 h; *Blackmond* and co-workers mention < 5% of adduct formation, without giving experimental evidence [16]. With ethyl (*E*)-3-nitrobut-2-enoate, there is 71% conversion to the corresponding adduct in 20 h (C_6D_6 , room temperature).

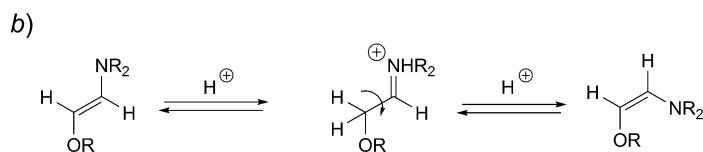
to the corresponding nitro aldehyde (**7g** in *Scheme 8*) over a period of hours and days (NMR analysis; for details see *Table 7* in *Exper. Part*). To consider the importance of this resting state **8** of the catalyst **1a**, we have to remember *a*) that there is a large excess of the nitro olefin *vs.* *sec*-amine under catalytic conditions (shifting an equilibrium towards adduct **8**), *b*) that there was always an acid co-catalyst necessary to render the catalytic reaction effective, and acid will catalyze the elimination **8** \rightarrow nitroacrylate + **1a**, and *c*) that this conjugate addition was much slower with the less reactive nitro olefins.

2.1.5.2. Reactions of (E)/(Z)-Pentyloxy enamines with Functionalized (E)- and (Z)-Nitro Olefins. When the pent-3-yloxy aldehyde **9**²⁵) shown in *Scheme 9* was mixed with the pyrrolidine **1b** in various dry solvents in the presence of 3-Å MS, a mixture (Z)/(E)-enamine **10a** was formed. The resulting solution in C₆D₆ of the two isomers contained an excess (up to 1.8 : 1) of the (Z)-form. For a theoretical analysis of this type

Scheme 9. Preparation of Solutions of (Z)/(E)-Mixtures of Enamine 10a from Aldehyde 9. *a*) Except in CDCl₃, the (Z)-isomer prevails slightly. There is essentially no temperature effect and only a small effect of 4-nitrophenol on the (Z)/(E)-ratio. In an EXSY-NMR spectrum, there is no cross-peak between the signals of the two isomers. We assume that the ratios are thermodynamical values, in agreement with some of the calculated energy differences between (E)- and (Z)-forms of alkoxy enamines (see the theoretical investigations of enamines of type **10** described in *Sect. 2.1.5.3* (*Fig. 8* and *Table 2*)). *b*) Under the typical catalytic conditions, there is always an acid co-catalyst present [21–23], which is expected to equilibrate the (E)- and (Z)-alkoxy enamines!



	(Z)/(E) Ratio in		
	C ₆ D ₆	C ₇ D ₈	CDCl ₃
after 30 min, r.t.	1.20	1.29	0.94
after 20 h, r.t.	1.61	1.76	0.92
at 70°	1.77		
with 5 mol-% 4-(NO ₂)C ₆ H ₄ OH after 5 min	1.70		
7 h	1.26		



²⁵) For organocatalytic *Michael* additions of 2-(trimethylsilyloxy)acetaldehyde to nitro olefins, see [24].

of an alkoxy enamine, which at the same time is an amino-enol ether, a highly electron-rich system [25a–c], see *Sect. 2.1.5.3*.

Upon addition of an equimolar amount of *t*-butyl 3-nitroacrylate to the solution in C₆D₆ of the alkoxy enamine **10a** ((*Z*)/(*E*) *ca.* 1.5:1), the highly electrophilic nitro compound disappeared completely and immediately (*Fig. 6*). The two stereoisomeric cyclobutanes **4i** (formally derived from (*Z*)-**10a**) and **4h** (from (*E*)-**10a**) were formed in a ratio of *ca.* 1:2, and very little nitro enamine **6h** was detected in the initial NMR analysis. Over a period of *ca.* 50 min, the fraction of the cyclobutane (**4i**), derived from (*Z*)-enamine, decreased, and the ratio of the five components of the mixture remained more or less constant (an equilibrium situation?), with the (*Z*)/(*E*)-enamine ratio still being close to 1.5:1, and the ratio all-*trans*/*cis,cis,trans,trans*-cyclobutane, *i.e.* **4h**/**4i**, being *ca.* 8:1; the nitro enamine (**6h**) concentration had somewhat increased at this point, more or less at the expense of the minor cyclobutane **4i**. Four points are worth emphasizing: *a*) in the instantaneous (≤ 5 min) reaction of the electron-rich alkoxy enamine with the electron-poor nitroacrylate, both enamines reacted, but there was twice as much product (*i.e.*, **4h**) derived from the minor enamine isomer ((*E*)-**10a**); *b*) the concentration of the all-*trans*-cyclobutane, **4h**, was constant after the first ‘flash’ reaction; *c*) the corresponding catalytic reaction gave best results when carried out in toluene and in the presence of ClCH₂CO₂H (yield of nitro aldehyde > 99%, *dr* 7.8:1, *er* 98.5:1.5) [14][21]; *d*) an epimerization on the RO-substituted center of **4i** to give **4h** would require dissociation back to the *cis*-enamine and *cis/trans*-isomerization thereof (*cf. Scheme 9*).

In any case, it looks as if *the success of the catalytic reaction* is the result of a complex series of steps involving various species, possibly including the resting state **8** (*Scheme 8*), and not just a simple preference of the transition state/zwitterion **H** (bottom part of *Fig. 6*)²⁶²⁷.

The stoichiometric reaction between the (*E*)/(*Z*)-enamines **10a** and acetamido-nitro-ethene took an even more surprising course (*Fig. 7*). The nitro compound is less reactive than nitroacrylate; (*Z*)-enamine **10a** reacts faster than the (*E*)-enamine. Besides the open-chain nitro enamine **6j** only one cyclobutane, the ‘all wrong’ all-*trans*-compound **4j** was formed, and not the *cis-trans-cis-trans*-isomer expected from the trajectory and zwitterion/transition state **I** (*Fig. 7*). Again, a more or less stable composition of the components resulted from this stoichiometric reaction after *ca.* 1 h. We wondered whether the acetamido-nitroethene really has the *cis*-configuration, stabilized by an intramolecular H-bond, as generally assumed, and recorded its NMR spectrum in carefully neutralized CDCl₃ and in a series of solvents containing H-bond acceptor groups, all the way to (D₆)DMSO (the solvent of choice for breaking intra- and intermolecular H-bonds, by being an excellent H-bond acceptor)²⁸. The results

²⁶) ... as seemed to be the case when 2-alkyl- and 2-aryloxy-acetaldehydes were added to nitro olefins (including ethyl nitroacrylate) in a less diastereoselective reaction (catalyst **1a**, toluene, room temperature, 55 or 96 h) [14][23b]; see, however, the reaction in DMSO and in CHCl₃/H₂O [23a].

²⁷) In the catalytic reaction, it is important to perform the workup at the right point in time to avoid erosion of the diastereoselectivity [21].

²⁸) This is why we have expressed doubt [25k] about the stereodirecting role of the carboxylic acid group by H-bonding in proline catalysis of reactions carried out in DMSO [6][26].

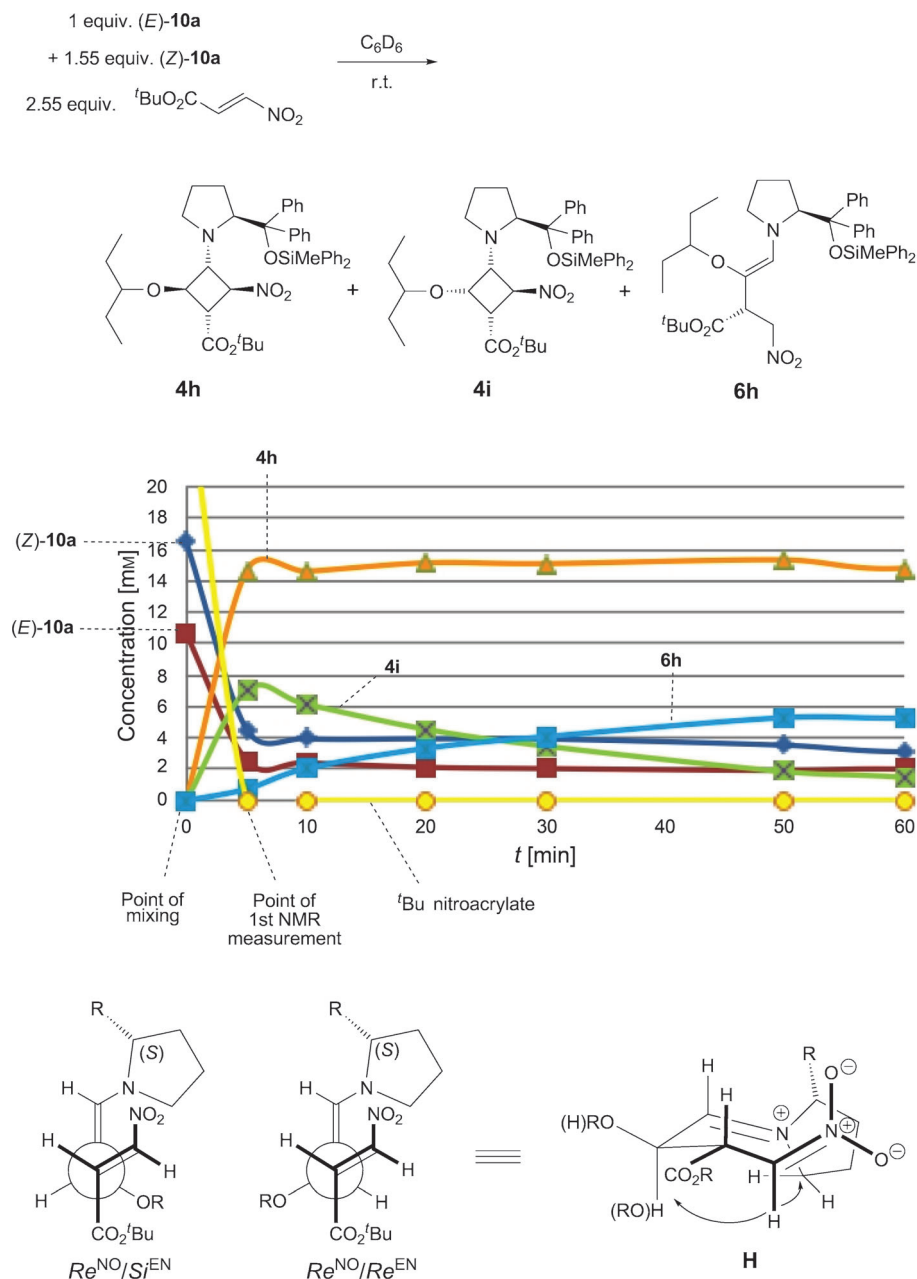


Fig. 6. Stoichiometric reaction of the (*Z/E*)-enamine **10a** with (*E*)-nitroacrylate in benzene, NMR analysis of the reaction mixture, and model for the transition state/zwitterion **H** with least steric hindrance between the substituents ((*E*)-enamine/(*E*)-nitroacrylate). The approach **H** would lead to the all-*trans*-cyclobutane **4h**. Epimerization **4i** \rightarrow **4h** would require dissociation to the starting materials (through a zwitterion) and (*Z/E*)-**10a** isomerization. From the concentration traces, it looks like **6h** is actually formed from **4i**, rather than from **4h** under these conditions. Note that in our (*Y. H.*) published [21] oseltamivir synthesis *ent*-**1a** was used as catalyst (solvent toluene, co-catalyst $\text{ClCH}_2\text{CO}_2\text{H}$).

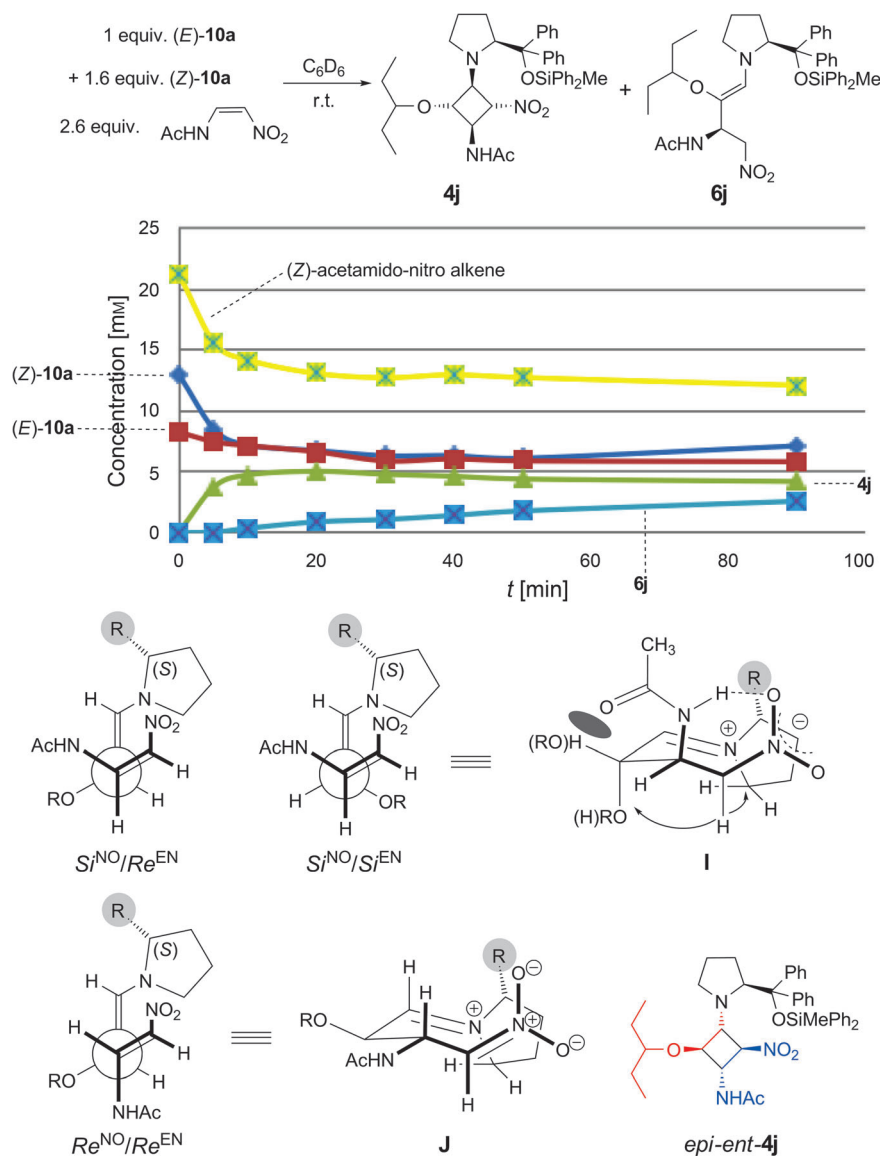
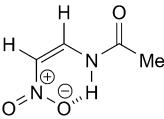
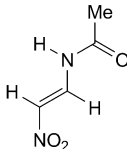


Fig. 7. Stoichiometric reaction of the (Z/E)-enamine **10a** with (Z)-acetamido-nitroethene in benzene, NMR analysis of the reaction mixture, and model for the transition state/zwitterion **I** with least steric hindrance between the substituents ((Z)-enamine/(Z)-nitro olefin). The approach **I** would lead to a *cis-trans-cis-trans*-cyclobutane, which is not detected. Note that the (*Re/Re*)-coupling (see **J**) of (*E*)-enamine with (*E*)-nitro olefin (cf. Table 1) would give a diastereoisomer of **4j**, in which the absolute configurations of all four stereogenic centers on the four-membered ring are reversed: *epi-ent-4j* (epimeric at C(2) of the pyrrolidine ring); by the NMR analysis, we could not reliably differentiate between **4j** and *epi-ent-4j*, for instance, from the NOE between the H-atom in α -position to NO₂ and the H-C(2) of the pyrrolidine ring (in some of the cyclobutanes **4**, this NOE is strong, in others it is absent). The *epi-ent-4j* cyclobutane would, of course, eventually lead to *ent*-oseltamivir! Note that, in the oseltamivir synthesis of Ma and co-workers [22], catalyst **1**, with R₃Si = Me₃Si and naphthalenyl instead of Ph groups on the prolinol ether unit, was used. In our (Y. H.) recent unpublished work, the catalyst **1b** turned out to be superior to **1a**.

are compiled in *Table 1*: in ‘neutral’ CHCl_3 ²⁹) the *cis*-isomer prevailed, in DMSO ³⁰) the *trans*-isomer was in excess. This means that the involvement of the *trans*-acetamido-nitroethene has to be considered in the oseltamivir syntheses using this nitro olefin derivative [21–23]³¹). However, as shown in *Fig. 7* (bottom part), coupling **J** of (*E*)-enamine **10a** with the (*E*)-acetamido-nitroethene would eventually lead to *ent*-oseltamivir.

Table 1. (*E*)/(*Z*) Ratio [%] of Acetamido-nitroethene in Different Solvents as Determined by NMR Spectroscopy

Solvents		
CDCl_3 washed with basic Al_2O_3	> 99	< 1
(D_8)THF	80	20
CD_3OD	18	82
(D_5)Pyridine	15	85
(D_7)DMF	11	89
(D_6)DMSO	7	93

Obviously, an even more complex, most puzzling sequence of events is likely to be involved in the case of the *successful catalytic application* of isopentyloxy-acetaldehyde addition to acetamido-nitroethene (see *Fig. 7*) than in the case of addition to the nitroacrylate.

2.1.5.3. *DFT- and MP2-Calculations of the Structures of Alkoxy enamines.* The experimental observation of a (*Z/E*)-ratio close to 1:1 of the enamine **10a** from diphenyl-prolinol Si ether **1a** and 2-(pentyloxy)acetaldehyde prompted us^{32a}) to carry out a computational investigation of alkoxy enamines, to evaluate whether the almost equal stability of these (*Z*)- and (*E*)-isomers is found for the isolated species^{32b}).

Computational Methodology. For all quantum-chemical calculations, we employed the Turbomole 6.4 suite of programs [25d]. All density-functional theory (DFT) calculations applied the BP86 density functional [25e,f]. To study the method dependence of the DFT results obtained, we compared with second-order *Møller-Plesset* perturbation theory (MP2) results for selected molecules. For large molecules, MP2 calculations became less and less feasible so that the empirical D3 corrections by

²⁹) We thank Dr. J. Durmis [23a,c] for a personal communication about a 10:1 *cis/trans* ratio of acetamido-nitroethene in CDCl_3 .

³⁰) In fact, the catalytic reaction used in a recent oseltamivir synthesis [23a] occurred with best diastereoselectivity in DMSO .

³¹) The acid co-catalyst present in all catalytic coupling reactions between 2-alkoxyacetaldehydes and acetamido-nitroethene will thus not only be able to catalyze (*Z*)/(*E*)-enamine (*cf. Scheme 9, b*) but might also cause (*Z*)/(*E*)-nitro olefin equilibration.

³²) ^a) Anti-intuitive ‘*cis*-effects’ have always been intriguing for organic chemists [25a–c]. ^b) For a comprehensive review (95 pages!) entitled ‘*Quantum Mechanical Investigations of Organocatalysis: Mechanisms, Reactivities, Selectivities*’, see [7] (Houk and co-workers).

Grimme et al. [25g] have been used to include dispersion effects in the DFT/BP86 calculations. All energies have been obtained after full structure optimization with the quantum-chemical method under consideration. *Ahlrichs'* basis sets of triple- (TZVPP) and quadruple-zeta (def2-QZVPP) quality, respectively, have been used as implemented in Turbomole 6.4. In these basis sets, polarization functions were taken from *Dunning's* correlation consistent basis sets. The resolution-of-the-identity density-fitting technique has been invoked for BP86 and MP2 with the corresponding auxiliary basis sets from Turbomole 6.4 in order to accelerate the calculations. The orbitals have been tightly converged until the change in relative electronic energy in the final self-consistent field iterations step was smaller than 10^{-8} Hartree. Moreover, the structure optimization was carried out until the length of the geometry gradient was on the order of 10^{-4} atomic units. In all DFT calculations, we employed a fine numerical integration grid ('m4' in Turbomole notation).

Conformational effects can blur the energetic ordering of different isomers if alkyl substituents are present. To avoid such effects, we made sure that corresponding (*Z*)- and (*E*)-isomers always feature similar conformations of the corresponding alkyl substituents (see also below for a more detailed discussion of such effects). The energies reported are differences of electronic energies. Hence, purely electronic effects have been considered rather than zero-point-energy and temperature corrections as well as entropy effects, which we have not taken into account.

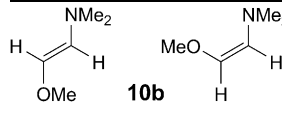
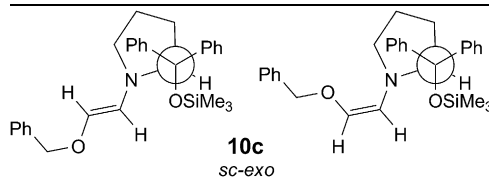
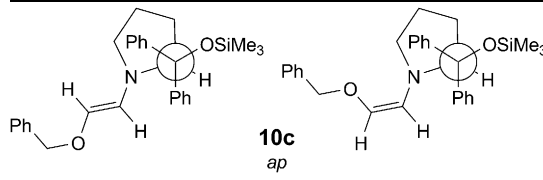
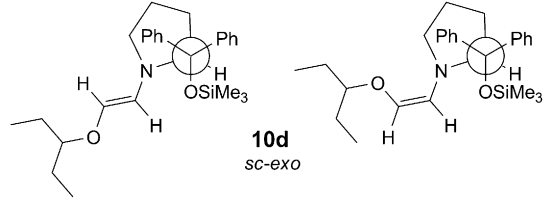
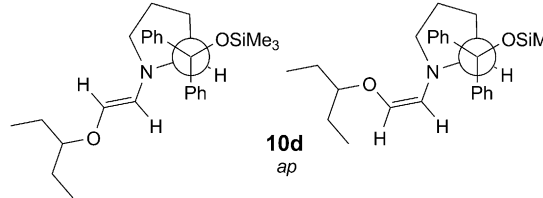
As molecules for the calculations, we chose the simple, prototypical 1-(dimethylamino)-2-methoxyethene (**10b**) and the diphenylprolinol trimethylsilyl ether-derived 1-(benzyloxy)-³³) and 1-(isopentyloxy)-2-pyrrolidinoethenes (**10c** and **10d**, resp.). The results are collected in Table 2 and Fig. 8.

Discussion. First of all, we find a more or less pronounced *pyramidalization of the N-atoms* in all calculated structures. We use *Dunitz's* definition for the degree of pyramidalization Δ [Å] as the distance of the N-atom from the plane spanned by its three bonding partners (here C-atoms) [25h]. The Δ values (Table 2, last two columns) are between 0.0 and 0.3 Å³⁴). For the generic small molecule **10b** that carries only Me groups as substituents, we found a BP86/TZVPP Δ value of 0.28 Å for the (*Z*)-isomer, whereas it was slightly larger (by 0.02 Å) for the (*E*)-isomer. While these Δ values increased in the MP2 calculations by 0.06 Å, the difference between the (*Z*)- and (*E*)-isomers remained the same, *i.e.*, 0.02 Å. For the isomers of **10c** and **10d** with bulky substituents, this difference increased to values between 0.03–0.04 Å (BP86/TZVPP). Also for the large molecules with benzyl and isopentyl substituents, the (*E*)-isomer was slightly more pyramidalized on N than the (*Z*)-isomer. It is interesting to note that the pyramidalization in **10c** and **10d** with bulky substituents is reduced when one considers attractive forces due to dispersion. As the BP86-D3/TZVPP results demonstrated, Δ was reduced by 0.10 to 0.13 Å in the *sc-exo* conformations (Table 2). This planarization affects the (*E*)- and (*Z*)-isomers to the same extent. However, the situation changed when the *ap*-conformations were investigated. Here, a reduced pyramidity of the N-atom was observed (because the two bulky substituents at the two ends of the molecule

³³) For a DFT calculation of this benzyloxy derivative, using B3LYP/6-311 + G**, see [23b] and Table 2.

³⁴) For an sp^2 -hybridized N, Δ is 0 Å; for an sp^3 -hybridized N, Δ is 0.48 Å (with C,N-bond lengths of 1.45 Å).

Table 2. *Relative Energies of (E)- and (Z)-Alkoxy-enamines Calculated by DFT and MP2. Method A: BP86/TZVPP; Method B: BP86-D3/TZVPP; Method C: MP2/def2-QZVPP; Method D: B3LYP/6-311 + G**. The value obtained with Method D is taken from [23b]. Besides the generic (dimethylamino)-methoxy-ethene, only the structures with the experimentally observed *sc-exo*- and *ap*-conformations (cf. [18b] and Fig. 4) of the exocyclic bond of the pyrrolidine ring have been optimized.*

Configuration (<i>E</i>)/(<i>Z</i>)	Method	Energy [kcal/mol]		Pyramidalization Δ [Å] on N	
		(<i>E</i>)	(<i>Z</i>)	(<i>E</i>)	(<i>Z</i>)
 10b	<i>A</i>	0	+0.26	0.30	0.28
	<i>C</i>	0	+0.25	0.36	0.34
 10c <i>sc-exo</i>	<i>A</i>	+0.77	0	0.27	0.24
	<i>B</i>	+2.79	0	0.18	0.11
 10c <i>ap</i>	<i>A</i>	0	+1.22	0.21	0.17
	<i>B</i>	0	+0.95	0.02	0.03
	<i>D</i>	0	+0.69		
 10d <i>sc-exo</i>	<i>A</i>	+2.64	0	0.28	0.25
	<i>B</i>	+2.55	0	0.16	0.15
 10d <i>ap</i>	<i>A</i>	+1.90	0	0.21	0.17
	<i>B</i>	0	+2.17	0.00	0.05

attract one another), which resulted in a significant structural distortion of each *ap*-isomer. This distortion is facilitated by a phenyl ring that, in the *ap*-conformation, can interact with the neighboring alkoxy substituent. However, because of the empirical character of the D3 dispersion correction, this observation should not be over-interpreted. In condensed phase, these interactions are likely to be reduced because of

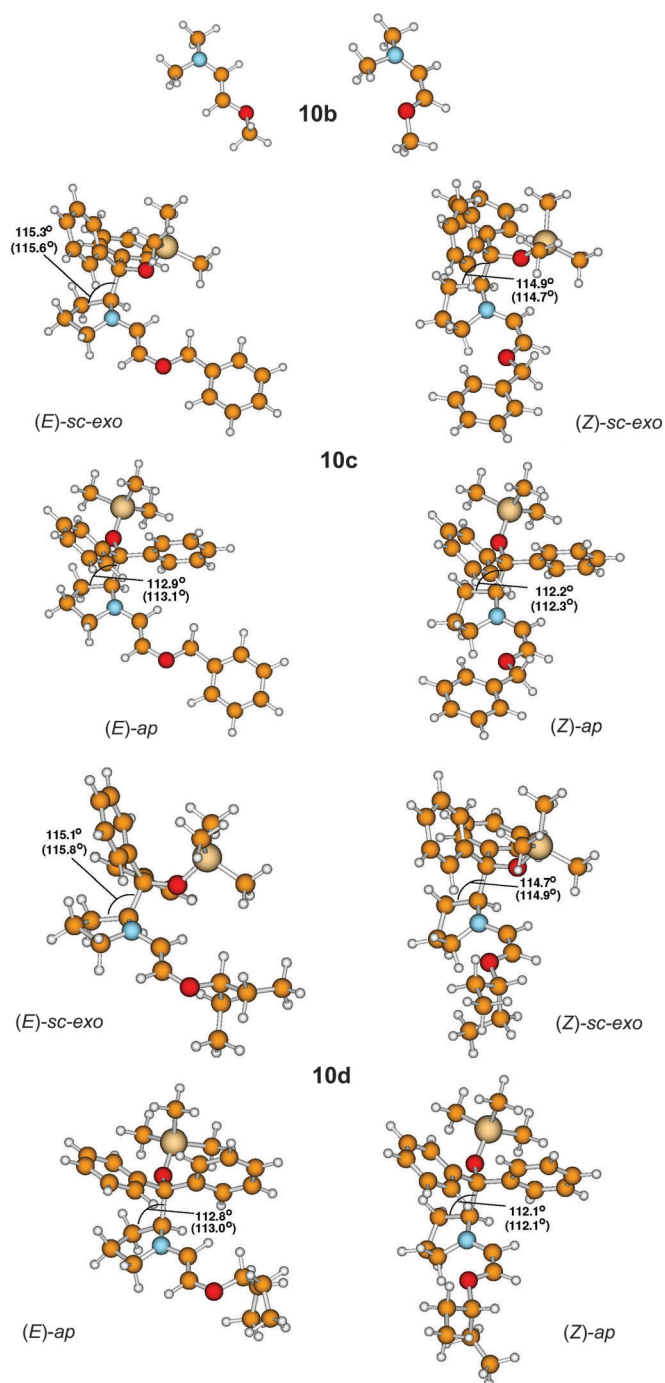


Fig. 8. BP86/TZVPP Structures of the (E)- and (Z)-alkoxy enamines **10b**, **10c**, and **10d** with the 'exocyclic' bond angles $C(3)-C(2)-C(\text{substituent})$. The angles in parentheses are those obtained with BP86-D3/TZVPP.

additional interactions that become possible with solvent molecules. Still, it clearly demonstrates that dispersion interactions of the bulky substituents can be more pronounced in the *ap*-conformer when compared to the *sc-exo* conformer.

In conclusion, the N-pyramidalization of enamines, found in X-ray crystal structures and discussed by *Eschenmoser*, *Dunitz*, and our groups [18b] [25h–l], was confirmed by the calculations. The direction of the pyramidalization was such that electrophilic attack from the face anti to the large substituent in **10a** would also be stereoelectronically favored.

Another interesting observation is evident from an inspection of the ‘*exocyclic*’ bond angles in *Fig. 8*: in all cases, the (diphenyl)(trimethylsilyloxy)methyl group is in a *quasi*-axial position on the puckered pyrrolidine ring, with a C(3)–C(2)–C(*exo*) bond angle, which is substantially larger than the tetrahedral angle of 109°, *i.e.* 114.7–115.8° in the *sc*-conformations and 112.1–113.1° in the *ap*-conformations of **10c** and **10d**. This leads to a closer proximity of the large substituent with the enamino double bond (increasing steric shielding for attack of an electrophile from the *cis*-face of the double bond?).

We next discuss the *relative energies of (Z)- and (E)-alkoxy-enamines 10* (see *Table 2*). When we compared the electronic energies of the generic Me-substituted compounds **10b**, for which MP2 calculations with a sufficiently large basis set are feasible, we found a rather small difference of 0.26 (BP86/TZVPP) and 0.25 kcal/mol (MP2/def2-QZVPP), respectively, with the (*E*)-isomer being more stable than the (*Z*)-isomer. Importantly, the BP86 result deviated only by 0.01 kcal/mol from the MP2 energy difference, which is an indication that the BP86 functional can be taken as a sufficiently accurate model for the description of the large derivatives.

However, two effects make the energetic comparison of the large derivatives more complicated. One is that dispersion interactions can play a significant role because of the bulky substituents. The other one is the multitude of stable conformers, which is difficult to sample in a standard quantum-chemical approach. While we have already considered the first issue above, we need to discuss the latter one in more detail, especially for the isopentyl derivative **10d**. All structure optimizations have been carried out starting from corresponding (*E*)- and (*Z*)-isomeric structures with the same conformation with respect to the isopentyl group. This procedure does hardly introduce an energetic bias owing to the conformations of the isopentyl group, although it might slightly affect the overall energy because of different long-range intramolecular interactions. Only a rigorous sampling approach would allow us to identify the lowest-energy structures of each conformer, which is beyond the scope of the present work. Still, we can extract all relevant information from the calculations carried out for the selected conformers under study. For example, in *Fig. 8* one can clearly see that the isopentyl conformation is different for the *ap*- and *sc-exo*-isomers. To investigate the relevance of these different conformations, we also considered an isopentyl conformation for the *ap*-conformers that resembles the one of the *sc-exo* conformers. The energy of the isomers was then reduced by *ca.* 2.4 kcal/mol so that all relative energies of corresponding (*E*)- and (*Z*)-isomers and especially their energetical ordering remain essentially the same. Hence, we use the energies of the structures depicted in *Fig. 8* in the following discussion, keeping in mind that lower-energy structures might be obtained in a rigorous sampling approach.

The relative electronic energies are collected in Table 2. Only for the *ap*-conformers, we found the same energetic ordering of (*E*)- and (*Z*)-isomers as for the Me-substituted generic structure **10b** (*vide supra*). For the *ap*-conformer of the benzyl derivative we found that the (*Z*)-isomer is higher in energy than the (*E*)-isomer by +1.22 kcal/mol (+0.95 kcal/mol). Here and in the following paragraph, the energy difference given first was obtained with BP86/TZVPP, while the number in parenthesis is the BP86-D3/TZVPP result. Surprisingly, the *ap*-(*Z*)-conformer of the isopentyl derivative **10d** was lower in energy by –1.90 kcal/mol (+2.17 kcal/mol), while the inclusion of dispersion interactions in the structure optimization reversed this order. For the *sc-exo*-isomers, the picture is without such ambiguity. The (*Z*)-isomers of **10c** and **10d** were lower in energy. For the benzyl derivative **10c**, we found the (*Z*)-isomer to be –0.77 kcal/mol (–2.79 kcal/mol) lower in energy than the (*E*)-isomer, while it was –2.64 kcal/mol (–2.55 kcal/mol) for the isopentyl derivative **10d**.

In general, we found a comparatively small energetic effect of dispersion interactions on the relative energies of (*E*)- and (*Z*)-isomers (with the sole exception of the isopentyl *ap*-structure), which can be taken as an indication that the dispersive attraction of the bulky substituents in both isomers is about the same, and hence does not affect their energy difference.

It is noteworthy that we found the *ap*-(*E*)-conformers to be lower in energy than the *sc-exo*-(*E*)-conformers of **10c** and **10d**, although the latter was usually found in X-ray structures. For the isopentyl (*E*)-isomers, *ap*-conformer was lower in energy by 0.56 kcal/mol (BP86/TZVPP) than *sc-exo*-conformer, while the difference was even larger in the case of the benzyl derivative, *i.e.*, by 3.04 kcal/mol (BP86/TZVPP).

The *general conclusion* from these calculations is that the energy differences between (*E*)- and (*Z*)-isomers of the isopentyloxy-diphenylprolinol-silyl ether derivative **10d** are quite larger (1.9–2.6 kcal/mol) than experimentally observed (*ca.* 1:1; remember that a 10:1 ratio corresponds to an energy difference of 1.4 kcal/mol at room temperature). To understand this discrepancy, two explanations can be offered. First of all, the accuracy of DFT could be limited, and a more accurate wave-function-based calculation is desirable. To investigate this issue, we are currently optimizing the structures with MP2/def2-QZVPP. Moreover, the bulky substituents will interact with solvent molecules in condensed phase, and this poses a rather complicated problem, in which the molecule's solvent environment and its conformations need to be rigorously sampled.

2.2. The Dihydro-1,2-oxazine N-Oxides 5. The organocatalytic addition of aldehydes to disubstituted nitro olefins, such as 1-phenyl-2-nitroprop-1-ene (**3**, R² = Ph, R³ = Me; 'methyl-nitrostyrene') or 1-nitrocyclopentene and 1-nitrocyclohexene, with the catalyst **1** or other pyrrolidine derivatives has been found to be sluggish; these reactions required a more acidic co-catalysts, CHCl₃ or CH₂Cl₂ instead of toluene as solvent, and long reaction times. Some typical conditions, under which this type of *Michael* addition can be carried out, are compiled in Table 3. Many authors considered the disubstituted nitro olefins sterically hindered or demanding substrates. This is in contrast to the results described in 1970 by Nielsen and Archibald (see ref. in [8]), who found that α -substituted nitro olefins add to cycloalkanone-derived, *i.e.*, disubstituted, enamines to form isolable 5,6-dihydro-4*H*-oxazine 1,2-

Table 3. Reported Additions of Aldehydes to Disubstituted Nitro Olefins **3**, Catalyzed by Pyrrolidine Derivatives

3

Conditions	Nitro olefin 3 Comments	Ref.
5 mol-% 1a , 5 mol-% 4NO ₂ -C ₆ H ₄ OH, toluene, r.t., up to 48 h	no reaction with , or with 3 R ² = ⁱ Pr, R ³ = Me	This work
20 mol-% <i>ent</i> - 1a , 60 mol-% PhCO ₂ H, H ₂ O, r.t.	no reaction with	[27]
10 mol-% 1a , 10 mol-% PhCO ₂ H, CH ₂ Cl ₂ , r.t., up to 48 h	reactions with	[28]
10 mol-% 1a , 40 mol-% 4-NO ₂ -C ₆ H ₄ OH, CHCl ₃ , r.t., up to 65 h	reactions with , not with R ¹ = ⁱ Pr	[12]
20 mol-% 1a , 10 mol-% 3-NO ₂ -C ₆ H ₄ CO ₂ H, CH ₂ Cl ₂ , r.t., up to 54 h	reactions with	[29a]
15 mol-% proline, Na ₂ SO ₄ , DMSO, r.t., 90 min	reaction with	[29b]
15 mol-% pyrrolidyl-pyrrolidine, CHCl ₃ , –10°, 7 d	reaction with	[30]
H-Pro-Pro-D-Gln-OH or -Asn-OH (5 mol-%), CHCl ₃ / ⁿ PrOH 1:9, r.t., up to 3 d	reaction with , and nitrocyclohexene, works with R ¹ = ⁱ Pr	[31]

oxides³⁵⁾ under conditions (hexane, 0–25°), which do not indicate that the reaction would be sluggish!

³⁵⁾ These authors also make the statement: ‘it has been found that α -substituted nitro olefins with enamines from cycloalkanones of less than eight ring members, in polar or nonpolar aprotic solvents (hexane, MeCN, ether), lead to a zwitterion which undergoes intramolecular O-alkylation to a cyclic nitro ester’. The intermediacy of a zwitterion in such reactions has been questioned by a recent calculation (see Footnote 4 and [12]), suggesting that oxazine derivatives, in contrast to cyclobutanes, may be formed by a concerted (4 + 2) cycloaddition of a nitro olefin to an enamine (see also Scheme 2).

2.2.1. Preparation and Identification of Oxazine Derivatives 5. We have now studied the stoichiometric reactions of various **1a**-derived enamines **2** ($R_3Si = Me_3Si$) with methyl-nitrostyrene (**3**, $R^2 = Ph$, $R^3 = Me$), 4-methyl-2-nitropent-2-ene (**3**, $R^2 = iPr$, $R^3 = Me$), ethyl 3-nitrobut-2-enoate, and nitrocyclohexene. The reactions were carried out as with the monosubstituted nitroethenes (*cf. Scheme 4*): to the enamine solution in C_6D_6 (NMR tube, in the presence of 4-Å MS, room temperature) was added an equimolar amount of the nitro olefin, and the first spectrum was recorded within *ca.* 10 min. The results are collected in *Table 4*. In all cases, the disubstituted nitro olefins gave (4 + 2) cycloadducts **5** (see formulae in *Fig. 2* and X-ray structures in *Fig. 4*). Compounds **5** were formed upon mixing of the components (*i.e.*, **5b**, **5c**, and **5h**), except when the *i*Pr-substituted enamine **2** ($R^1 = iPr$) was employed (**5d**, **5e**, and **5f** took hours or days for high degrees of conversions). To see whether the cycloadducts are in equilibrium with the precursors, we warmed the solutions to 50°, cooled them back down to ambient temperatures, and determined the ratios oxazine derivative **5**/corresponding enamine **2** by suitable NMR-peak integrations: equilibration could be detected with the *i*Pr/Ph/Me-substituted derivative **5d** and the bicyclic compound **5f** (derived from nitrocyclohexene).

Table 4. Cycloadditions of **1a**-Derived Enamines **2** to Disubstituted Nitro Olefins **3** with Formation of Oxazine Derivatives **5**

5	R^1	R^2	R^3	Yield [%]	Time	Comments	Ref. to corresp. catal. reaction
5b	Me	Ph	Me	> 90 (NMR), 72 (recryst.)	≤ 10 min	most stable of our compounds 5 ; no equilibration up to 50°	[12]
5c	<i>n</i> Pr	Ph	Me	> 90 (NMR), 63 (recryst.)	≤ 10 min	stable up to 50°; no equilibration	[28][31]
5d	<i>i</i> Pr	Ph	Me	> 85 (NMR), 68 (recryst.)	2 h	highly moisture-sensitive equilibrium 5d/2 ($R^1 = iPr$) 7 : 1 (r.t.), 1.5 : 1 (50°)	[31]
5e	<i>i</i> Pr	<i>i</i> Pr	Me	44 (after prep. TLC)	4 d	slowest reaction	–
5h	Pr	CO ₂ Et	Me	> 90 (NMR)	≤ 10 min	no equilibration; rearrange- ment to nitro enamine 6s within 3 d	[28]
5f	<i>i</i> Pr	–(CH ₂) ₄ –		50 (NMR)	16 h	equilibrium 5f/2 ($R^1 = iPr$) 1 : 1 (r.t.), 1 : 3 (50°)	[29a]

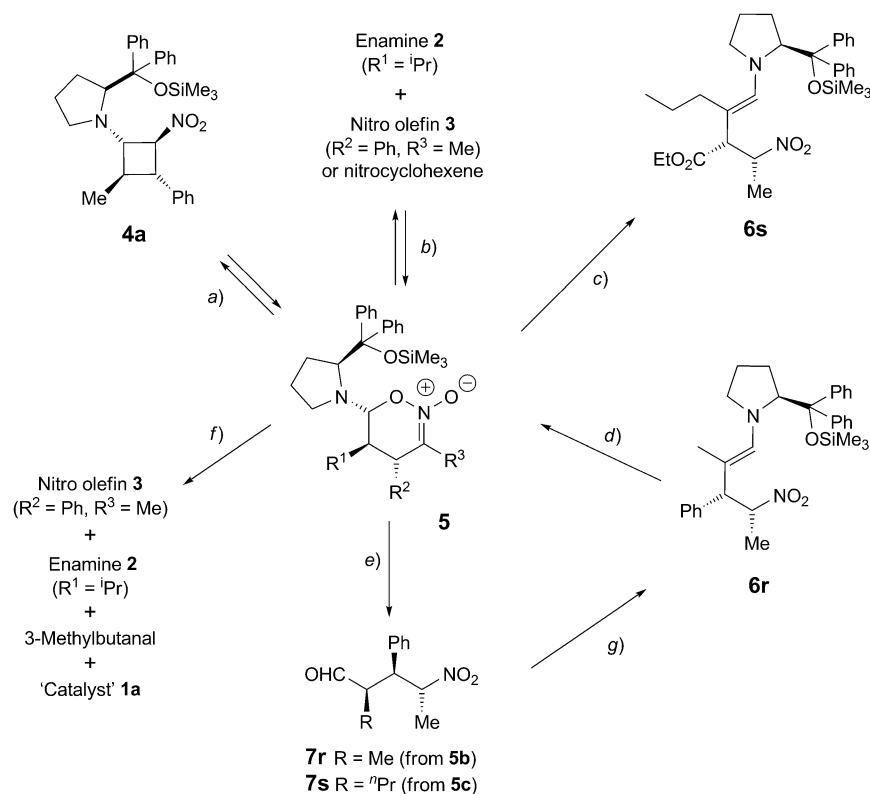
2.2.2. *Chemical Properties of the Oxazine Derivatives 5*. To learn about the role, which the (4 + 2) cycloadducts **5** might play in catalytic reactions, in comparison with the (2 + 2) cycloadducts **4**, we have investigated their properties, such as thermal stability (Table 4), hydrolytic stability, rearrangement, and formation from open-chain precursors (Scheme 10, a–f). As reported previously [1] (cf. Scheme 6), only the six-membered-ring compound **5a**, derived from a monosubstituted nitroethene, was shown to be in equilibrium with the corresponding cyclobutane **4a** (Scheme 10, a). In two cases, there was reversible dissociation of the oxazine derivative (**5d** and **5f**; b in Scheme 10). Non-hydrolytic ring opening to a linear nitro enamine, **6s**, and its reversal, **6r** → **5b**, as well as hydrolyses to nitro aldehydes were observed or studied with the ethyl-ester derivative **5h** and the heterocycles **5b/d**, as shown in Scheme 10, d and e, respectively. A most peculiar derivative was the oxazine *N*-oxide **5d** with 5-ⁱPr, 3-Me, and 4-Ph substitution: it was very sensitive to moisture, but could not be converted to a linear derivative (nitro enamine or aldehyde) under the conditions tested by us, rather it fell apart to the nitro olefin, aldehyde, and pyrrolidine **1a** (the catalyst molecule; see Scheme 10, f)³⁶).

As with the cyclobutanes, there is a discrepancy between the ease, in most cases, of cycloadduct formation and the failure of the catalytic reaction also with the oxazine derivatives (cf. Tables 3 and 4). The successful catalysis with disubstituted nitro olefins listed in Table 3 required stronger acidic conditions and, most remarkably, chlorinated solvents (CH₂Cl₂ and CHCl₃), which are known to be solvents of choice for many organic reactions involving cationic intermediates, notably iminium ions [32]³⁷).

Referring to the prototypical reaction of propanal with the methylated nitrostyrene (**3**; R² = Ph, R³ = Me), the experimental results presented in Tables 3 and 4, and Scheme 10 are as follows: *i*) there was no catalytic reaction under our standard conditions [14] (5 mol-% **1a**, 5 mol-% 4-nitrophenol, toluene, room temperature, 24 h); *ii*) ≥ 68% yield was obtained under the conditions of Pihko and co-workers for the catalytic reaction [12] (10 mol-% **1a**, 40 mol-% 4-nitrophenol, CHCl₃, room temperature, 30 h); *iii*) upon mixing the corresponding enamine **2** (R¹ = Me) with the disubstituted nitro olefin in toluene at room temperature, the oxazine derivative **5b** was formed in *ca.* 5 min; *iv*) the heterocycle **5b** was stable in C₆D₆ up to at least 50°; *v*) with 10 equiv. H₂O and 10 mol-% 4-nitrophenol, this compound was stable for 24 h in benzene; *vi*) switching to CH₂Cl₂ as solvent, 10 equiv. of H₂O and the stronger acid PhCO₂H (1.1 equiv.; conditions of Ma and co-workers for the catalytic reaction [28]) led to hydrolysis of **5b** to the nitro aldehyde with complete conversion in 24 h (Scheme 10, e); *vii*) deuterolysis of **5b** (4-NO₂C₆H₄OD, in CDCl₃) furnished *γ*-nitro aldehyde with > 50% D in the *α*- and < 10%

³⁶) As far as we know, there has been only one report on an organocatalytic *Michael* addition of 3-methylbutanal to disubstituted nitro olefins (by one of our groups (H. W. [31])).

³⁷) An example relevant to the discussion of this subject is the reaction of nitrostyrene with the **1a**-derived enamine **2**, R¹ = Me, R₃Si = Me₃Si, to give the nitro enamine **6a**: it took 15 h at room temperature in toluene and ≤ 5 min in CD₂Cl₂; see Scheme 6, and also Footnote 12 and Scheme 6 in [1].

Scheme 10. Conversions and Formations of Oxazin N-Oxide Derivatives **5**

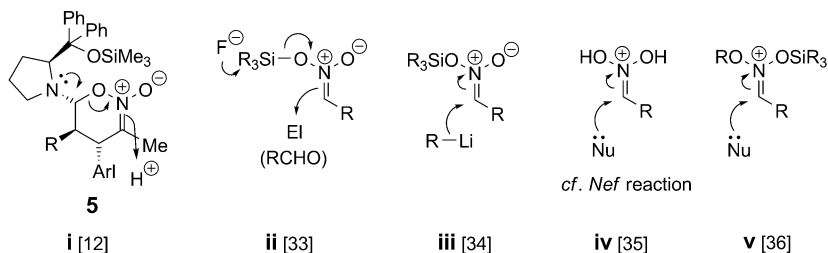
a) Equilibrium of **5a** with **4a** (C_6D_6 , room temperature; Scheme 6) [1][12][17]. *b*) Equilibrium of enamine and nitro olefin with **5** (see Table 3); for similar results with $R^2 = 4-F-C_6H_4$, see [12]. *c*) Ring opening of **5h** to nitro enamine **6s** (C_6D_6 , 3-Å MS, room temperature, 3 days, >99% conversion, 96% yield; dr 95 : 5) + 4% nitro aldehyde. *d*) Ring closure of nitro enamine **6r** to **5b** ((D_8) toluene, 40 mol-% 4- $NO_2-C_6H_4OH$, 3-Å MS, room temperature, 24 h; 30% conversion); for a similar experiment, see Supplementary Material in [12]. *e*) Hydrolysis of **5b** (10 equiv. H_2O , C_6D_6 , room temperature, 24 h: no reaction; after addition of 10 mol-% 4- $(NO_2)C_6H_4OH$, r.t., 24 h: no reaction; with 10 equiv. H_2O , 1.1 equiv. $PhCO_2H$, CD_2Cl_2 , room temperature, 24 h: >98% conversion to nitro aldehyde **7r** of dr 66:24:8:2); hydrolysis of **5c** (10 equiv. H_2O , 1.1 equiv. $PhCO_2H$, CH_2Cl_2 , room temperature, 24 h: 67% nitro aldehyde after chromatography); deuteroanalysis of **5b** (4 equiv. 4- $NO_2-C_6H_4OD$, 1.5 equiv. D_2O , $CDCl_3$, room temperature, 17 h) gives 41% γ -nitro aldehyde with >50% D in α - and <10% in γ -position. *f*) Products formed from moisture-sensitive **5d** in C_6D_6 at room temperature on contact with air: the oxazine derivative disassembled to its precursors; similarly, treatment of **5d** with 10 equiv. of H_2O , 1 equiv. of $PhCO_2H$, $CDCl_3$, room temperature, leads to total destruction; no nitro aldehyde detected in the product mixture. *g*) Conversion of a nitro aldehyde **7r** ($R = Me$) to nitro enamine **6r** (**7r/1a** 1 : 1; 3-Å MS, (D_8) toluene, room temperature, ≤ 10 min: >90% conversion to **6r** of high diastereoisomeric purity); for a similar experiment with the nitro aldehyde lacking the Me group next to NO_2 , see [17a].

D in the γ -position³⁸); viii) treatment of the Me/Ph/Me-substituted nitro enamine **6r** with 4-nitrophenol (anhydrous conditions in toluene) caused cyclization to the oxazine derivative **5b** (Scheme 10,d; in an equilibration?).

Thus, at least in this case, it must be *concluded for the catalytic reaction* that the plethora of conditions listed in Table 3 have, actually, not been elaborated to force the intermediate enamine to add to the disubstituted nitro olefin, but to hydrolyze the intermediate oxazine *N*-oxide derivative to the product nitro aldehyde. In general terms, the exact route of formation of the (4+2) cycloadducts **5** (zwitterion or concerted one-step reaction⁴) and of their hydrolysis to nitro aldehydes (site of protonation, direct acid-catalyzed hydrolysis⁵)³⁸, or zwitterion) still need to be discussed (see **D** \rightarrow **F** vs. **D** \rightarrow **G** \rightarrow **F** in Scheme 2).

3. Intermediates 13 and 14 in Tripeptide-Catalyzed Michael Additions. – One of our groups (H. W.) reported that tripeptides of the general type H-Pro-Pro-Xaa-X (with Xaa bearing a CO₂H group; e.g., **11a** in Fig. 9) are excellent catalysts (with loading of ≤ 1 mol-%) for enantioselective additions of aldehydes to monosubstituted nitro olefins [37]³⁹. Two such tripeptides have recently been found to catalyze aldehyde addition to disubstituted nitro olefins [31]; the reactions were much slower and required more catalyst (5 mol-%) than with monosubstituted nitro olefins. The important role of the intramolecularly available CO₂H group was demonstrated by employing corresponding methyl esters, which were much less active [19][37d]. Thus, trapping of short-lived species, such as zwitterions, or a kind of intramolecular acid-catalyzed hydrolysis of intermediates, such as cyclobutanes or oxazine derivatives, was proposed to explain the catalytic activity of these peptidic carboxylic acids.

³⁸) Pihko and co-workers have recently proposed [12], based on DFT calculations, that the heterocycle **5** was protonated at C(3) stereoselectively, as indicated in **i** (cf. **D** \rightarrow **F** in Scheme 2); compounds **5** are cyclic nitronic acid esters, and, at the same time *N*/O-acetal derivatives. The same type of reactivity, i.e., attack by electrophiles, was observed in the fluoride-catalyzed additions of silyl-nitronates to aldehydes (see **ii**). The opposite reactivity, i.e., attack by nucleophiles on nitronate C-atoms, was observed with organolithium compounds (cf. **iii**), in the *Nef* reaction (cf. **iv**), and with *O*-silylated nitronate esters (cf. **v**), which are kind of iminium ions. The result of the deuterolysis experiment (Scheme 10,e) is not compatible with protonation at C(3) of **5b**.



³⁹) Simple oligoprolines have also been tested for, e.g., H-(Pro)_{2,3,4}-OH, H-(Pro)₃-OBn, H-(Pro)₃NHBn, and H-(β^3 h-Pro)₂-OH. They are quite active catalysts (short reaction time, good-to-excellent diastereoselectivity), but the enantioselectivities, determined in some selected examples, were poor: hitherto unpublished results (N. P., ETH Zürich, 2012) and Universität Basel, 2009 [38].

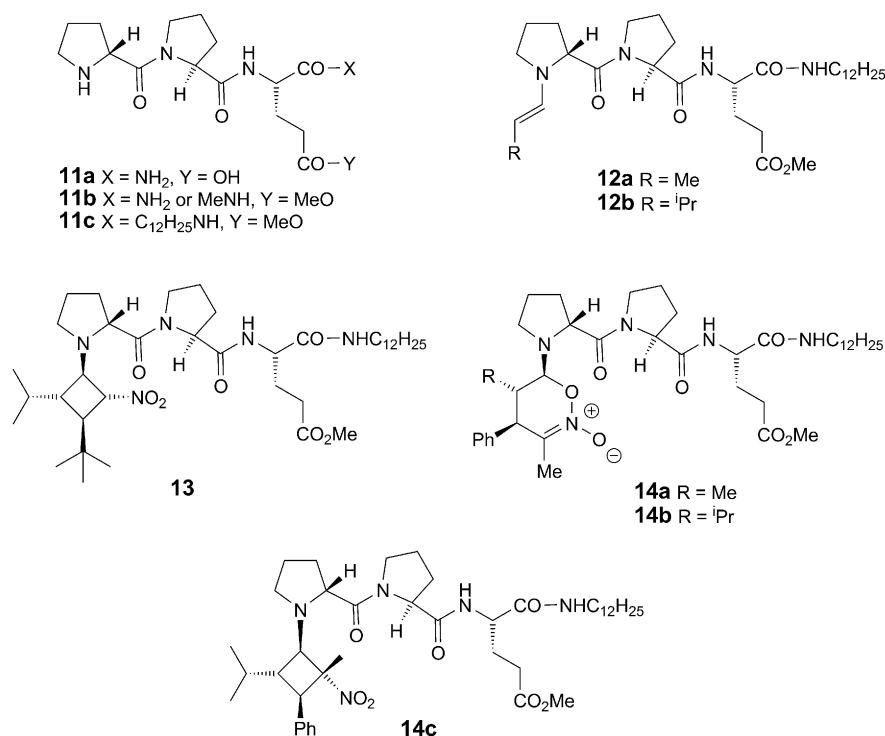


Fig. 9. Tripeptide derivatives **11**, used as organocatalysts for Michael additions to mono- and disubstituted nitro olefins [19][31][37][38], and/or identified or isolated enamines, as well as (2 + 2) and (4 + 2) adducts **12–14**, formed with **11c**. The configuration of the cyclobutane stereogenic center carrying NO₂ and Me in **14c** could not be safely deduced from the NMR spectra; it is tentatively assigned as (*R*), as expected from the collapse of the corresponding zwitterion. The amido-carboxylic acid derivatives of type **11a** and analogs containing Asp or Asn residues, as well as epimers with reversed configuration of one of the residues were also used or tested as catalysts. For disubstituted nitro olefins, H-Pro-Pro-D-Gln-OH and H-Pro-Pro-Asn-OH turned out to give best results in catalytic reactions [31].

We have now looked for stable intermediates in stoichiometric reactions. To prevent the action of CO₂H groups and to have better solubility in organic solvents, we used compounds **11b** and **11c** with a methyl ester group in the side chain and a terminal *N*-dodecylcarbamoyl group [19][37g]⁴⁰⁾ (Fig. 9). As aldehyde components, we chose propanal and 3-methylbutanal, from which the enamines **12** formed immediately with **11c** under our standard conditions (C₆D₆, 4-Å MS, room temperature). The solution of the ⁱPr-substituted enamine **12b** was combined with 4,4-dimethyl-1-nitrobut-1-ene, *i.e.*, the ^tBu-substituted nitroethene, which had led to the most stable cyclobutane, **4q**, with the **1a**-derived enamine. The corresponding cyclobutane **13** was indeed formed

⁴⁰⁾ Experiments with **11b**, which would have been better candidates for crystallizations of intermediates, were not successful.

(reaction time at room temperature, 20 h) and could be isolated in 52% yield after preparative TLC. In search for oxazine derivatives, we first chose enamine **12a** and 2-nitro-1-phenylpropene; product **14a** was formed with complete conversion within \leq 10 min; while the prolinol-derived analog **5b** was the most stable (4 + 2) cycloadduct (**5b**; *Scheme 10, e*), **14a** decomposed during attempts to crystallize it. The adduct **14b** with an ⁱPr group at C(5) of the heterocycle was formed much more slowly (2 h) and had the same peculiar properties as the **1a**-derived analog **5d** (*cf. Scheme 10, f*): it is in equilibrium with its precursors (**12b/14b** 1 : 7 at room temperature and 1 : 1.5 at 50°), and it falls apart to its components **11c**, aldehyde, and nitro olefin upon contact with moisture (without and with added PhCO₂H).

In the NMR spectrum of the reaction mixture obtained from the enamine **12b** and the disubstituted nitro olefin, we detected signals not only of the oxazine derivative **14b** (in equilibrium with the reactants) but also of an isomeric compound, likewise in equilibrium with **14b** (EXSY measurement). To our surprise, this isomer turned out to be the cyclobutane derivative **14c** (*Fig. 9*), which was identified on the basis of characteristic NMR signals and NOEs (*cf. compounds 4 and Exper. Part*). The cyclobutane **14c** was actually the main product: **14c/14b** at room temperature 1.5 : 1. Thus, the experiments with the tripeptide ester/amide **11c** have provided the first example of (2 + 2)-adduct formation with a disubstituted nitro olefin. As with the products from the monosubstituted nitro olefin (*cf. Scheme 6 and Fig. 5*), there was an equilibrium between starting materials (nitro olefin + enamine **12b**), four-membered ring (**14c**), and six-membered ring (**14b**). No signal characteristic of a nitro enamine was detected in these experiments.

The power of the intramolecular CO₂H group in catalyses with tripeptides Pro-Pro-D-Gln-OH and H-Pro-Pro-Asn-OH (epimers or lower homologs of **11a**) becomes evident by the fact that this is the only method, so far, by which 3-methylbutanal⁴¹⁾ has been added to 2-nitro-1-phenylprop-1-ene, to give 2-isopropyl-4-nitro-3-phenylpentanal⁴²⁾ 43). There may be a ‘connection’ between this successful catalytic reaction and the detection of a (2 + 2) cycloadduct with the 3-methylbutanal-derived enamine **12b**.

Thus, the same resting states/intermediates are formed when tripeptidic catalysts lacking a suitably positioned proton donor are used as those in the catalysis by the pyrrolidines **1** [19]. At which stage of the catalytic cycle the intramolecular CO₂H group of the peptidic catalyst plays a major role can, of course, not be deduced from our stoichiometric experiments. For reactions of monosubstituted nitro olefins, it is known that both, the cyclobutane (resting state) formation and ring opening, are acid-catalyzed [14]. In reactions of disubstituted nitro olefins, the oxazine *N*-oxides formed (as resting states or in-cycle intermediates) also require acid for the hydrolysis to the

⁴¹⁾ In only two publications cited in *Tables 3 and 4* did we find an example, in which this, otherwise common, β -branched aldehyde has been added to a disubstituted nitro olefin. Exception 1: catalysis with the tripeptide [31]; exception 2: addition to nitrocyclohexene [29a].

⁴²⁾ Of course, we cannot be sure whether the authors of one of the other reports actually tried – it is no more customary to mention unsuccessful experiments, *i.e.*, to give the *limitations* of a method [39].

⁴³⁾ The configuration of the NO₂-substituted stereogenic center is set in the protonation step from the (*Si*) diastereotopic face of an open-chain nitronate anion moiety (of a zwitterion?) [31][40][41] or of C(3) of an oxazine derivative (see **i**) in *Footnote 38* [12]).

desired open-chain nitro aldehydes. As an attractive common intermediate for all these reactions the elusive zwitterion (cf. **G** in *Scheme 2*) cannot be excluded, which would be efficiently trapped by the internal CO₂H group of the tripeptide acids ('how to hit a moving target') [19][31][37].

4. Addition of Aldehydes to Nitro Olefins Carrying an OH Group. – The ultimate 'catch' of a zwitterion may occur when the nitro olefin contains a nucleophilic substituent, so that, after coupling of the trigonal centers (cf. **K** in *Fig. 10*), there is intramolecular addition to the iminium end of the zwitterion (cf. **L** or **M** in *Fig. 10*). In fact, the 2-nitro-3-phenylprop-2-en-1-ol (**15**), the (benzyloxy)carbonyl (Cbz) analog **17**

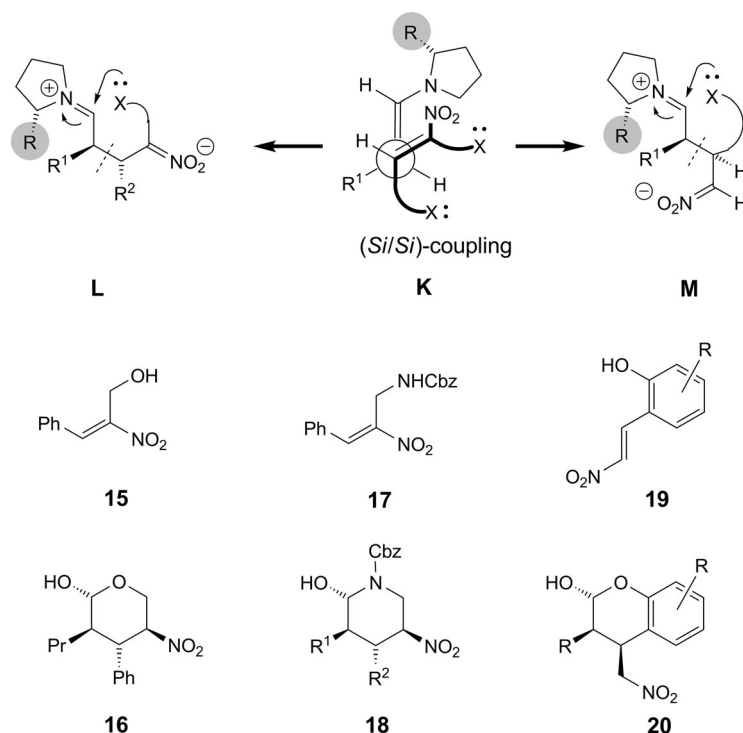
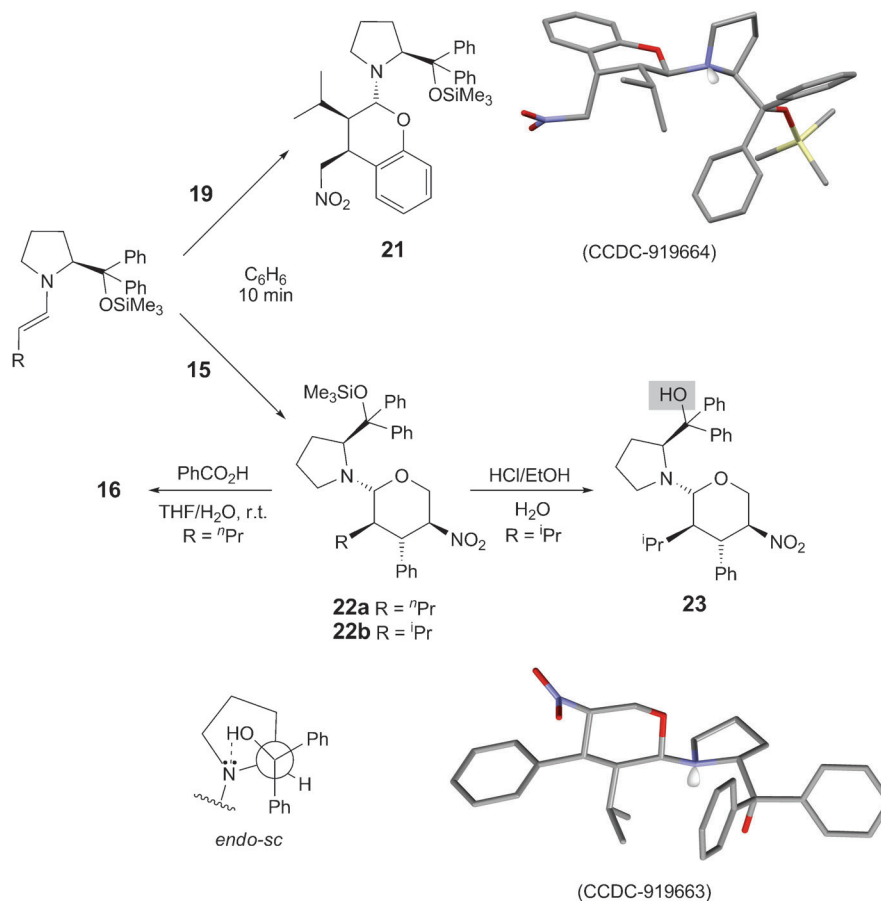


Fig. 10. Tetrahydropyran and piperidine derivatives, **16** and **20**, and **18**, respectively, are formed in **1a**-catalyzed additions of aldehydes to nitro olefins, i.e., **15**, **17**, and **19**, carrying nucleophilic substituents [27][42][43]. The observed product configurations can be derived from the trajectory **K**. Intramolecular trapping, i.e., **L** and **M**, of an intermediate zwitterion may be involved. Conditions: for **15** → **16**: 1 equiv. **15**, 2 equiv. aldehyde, 20 mol-% *ent*-**1a**, 60 mol-% PhCO₂H, H₂O, room temperature; for **17** → **18**: 1 equiv. **17**, 2 equiv. aldehyde, 10 mol-% *ent*-**1a**, 30 mol-% PhCO₂H, H₂O, room temperature; **19** → **20** (1 equiv. **19**, 3 equiv. aldehyde, 15 mol-% **1a**, 25 equiv. AcOH, r.t., 12–72 h) [27][42][43]. The compounds **15** and **17** are proposed to have a structure with intramolecular six-membered-ring H-bond (in H₂O, cf. Table 1), and thus be 'activated' [27]. Note that, in our experiments with **15** and **17**, the pyrrolidine **1a** was used (see *Scheme 11*), while *Ma* and co-workers [27] employed *ent*-**1a** in the reported catalytic reaction. For simplicity, we use the formulae of the (*S*)-prolinol-derived compounds and intermediates herein and in *Scheme 11*.

Scheme 11. Possible Intermediates, **21** and **22**, in the **1b**-Catalyzed Michael Additions of Pentanal and 3-Methylbutanal to *OH*-Substituted Nitro Olefins **15** and **19** (see Fig. 10), and Crystal Structures of **21** and **23**. While the *n*Pr-substituted **22a** can be hydrolyzed to the product, i.e., **16**, of the catalytic reaction [27], the *i*Pr derivative **22b** cannot; under forcing conditions, **22b** is desilylated (\rightarrow **23**). For a possible reason of the discrepancy between **22a** and **22b**, see Fig. 11 and accompanying text. Note that the conformation of the exocyclic bond on the pyrrolidine ring in **23** is *endo-synclinal* (O–C–C–N dihedral angle *ca.* -60°). This type of conformation has not been observed before (*cf.* Fig. 4 and [18b]) in structures of diphenylprolinol derivatives; it is due to a H-bond between the OH group and the N-atom in **23**.



(or NHAc and NHBoc derivatives) and *ortho*-hydroxy-nitrostyrenes **19** react with aldehydes, catalyzed by pyrrolidine **1a**, to give heterocyclic products **16**, **18**, and **20**, respectively (Fig. 10) [27][42][43]⁴⁴). Both groups, which have published these results,

⁴⁴) Similar reactions involving dienamine intermediates [44] or ketone-derived intermediates [45], and various co-catalysts have been reported. For dienamine intermediates adding to nitrostyrenes, see also [46].

assumed that the cyclic hemiacetal/aminal derivatives, **16**, **18**, and **20**, were actually formed by cyclization of the corresponding OH- and carbamoyl-substituted aldehydes, respectively, rather than by cyclization of a zwitterion (*cf.* **L** and **M**). To test this latter possible mode of reaction, we have, once more, carried out stoichiometric reactions (*Scheme 11*): to the (D_6)benzene solutions of the **1a**-derived enamines of pentanal or of 3-methylbutanal were added the hydroxy-nitro olefins **15** and **19** ($R = H$). In all cases there was instantaneous formation of the cyclic aminals **21** and **22**, respectively, which turned out to be stable enough to be isolated and purified (single diastereoisomers **22a** and **22b** in 77 and 66% yield, respectively, *Scheme 11*). With these two products, obtained with the HOCH₂-substituted nitrostyrene **15**, we performed hydrolysis experiments under conditions similar to those used in the reported catalytic reaction (PhCO₂H, H₂O). The ⁿPr-substituted heterocycle **22a** underwent replacement of the pyrrolidin-1-yl by a OH group, *i.e.*, the product **16** of the catalytic reaction was isolated. In contrast, the ⁱPr-substituted **22b** was stable under these conditions. After testing various other hydrolysis conditions, we found that a reaction with a 1:1 mixture HCl (10%)/EtOH occurred, which did, however, not lead to the cyclic hemiacetal but produced the OH compound **23**, *i.e.*, the product of desilylation (!), of which an X-ray structure was obtained (*Scheme 11*). No wonder, was there no catalytic reaction reported [27]⁴⁵⁾ or possible in our laboratory (*X. S.*) with 3-methylbutanal and nitro olefin **15**: the amino THP derivative **22**, $R = ^iPr$, is an irreversible trap, for the catalyst **1a**.

The stunning difference between the ⁿPr and the ⁱPr derivatives **22a** and **22b**, respectively, may be attributed to two fundamental steric effects: stereoelectronic interaction [18a] and 1,5-repulsion⁴⁶⁾. Inspection of the crystal structure of **23** (*Scheme 11*) shows that all four substituents on the THP ring are equatorial in a chair conformation of the six-membered ring (**N** in *Fig. 11*)⁴⁷⁾. For a stereoelectronically assisted, S_N1-type replacement of the pyrrolidin-1-yl by an OH group at the anomeric center of the THP ring, the leaving group has to be antiperiplanar (*ap*) to an electron pair at the O-atom [18a], to form an intermediate oxenium ion. This would require a ring inversion to an 'impossible', all-axially substituted chair conformation (*cf.* **O** in *Fig. 11*). A conformation, in which the stereoelectronic requirement is met, would be the boat form **P** with quasi-equatorial disposition of an ⁿPr group at C(3); replacement of the ⁿPr by ⁱPr in this position will generate 1,5-repulsion either between Me and O, or between Me and the benzene ring; this destabilizing effect (**Q** in *Fig. 11*) might be the reason why the ⁱPr group actually prevents hydrolysis of **22b** to the hemiacetal **16** (ⁱPr instead of ⁿPr), or slows it down to an extent that desilylation becomes the faster process. In the case of the piperidine derivatives **18**, $R^1 = ^iPr$, and of the chromanes **20**

⁴⁵⁾ *Cf. Footnote 42.*

⁴⁶⁾ The generic term 1,5-repulsion or *Newman* strain [47] includes the 1,3-diaxial effect in cyclohexane chair conformations, the double *gauche*-pentane effect, the A^{1,3} effect on double bonds, the *ortho/ortho'*-effect in biaryls, the *peri*-repulsion in 1,8-position of naphthalene, *etc.*

⁴⁷⁾ Comparison of the NMR spectra of **22b** and **23** leaves no doubt that the six-membered rings have the same conformation in both compounds.

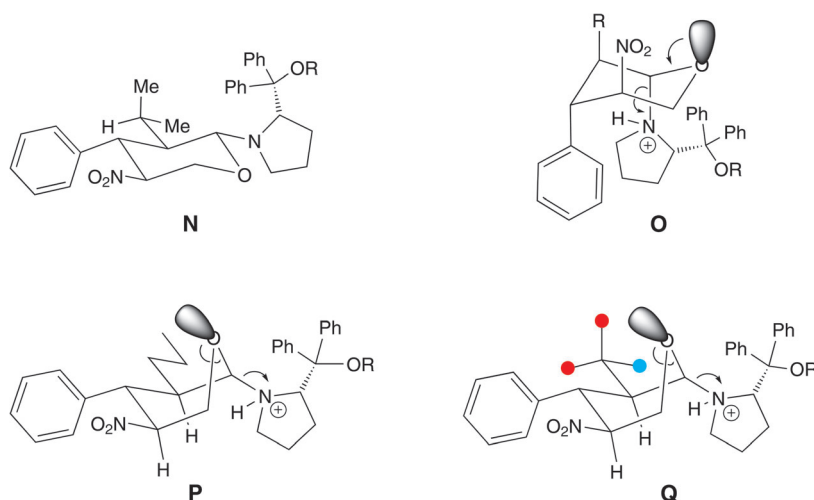
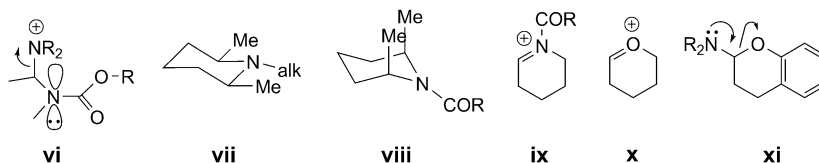


Fig. 11. Conformational analyses of the tetrahydropyran (THP) derivatives **22** and **23**. All-equatorially substituted conformation **N** (cf. X-ray structure of **23** in Scheme 11). Sterically 'impossible' all-axial conformation **O**. Boat conformation **P** of **22a**, from which lone-pair-assisted elimination of the R_2NH group could take place. Replacement of tPr by iPr in **P** leads to **Q**, of which all three conformations (● (blue) = Me, ●● (red) = Me/H or H/Me) around the exocyclic C–C bond are subject to 1,5-repulsion (Me/O or Me/Ph).

(see Fig. 10 and Scheme 11), the iPr group does apparently not prevent release of the catalyst [27][42][43]⁴⁸⁾.

5. Conclusions. – *In situ* NMR Investigations and isolations of products from 1:1 conversions of (diphenyl-silyloxy-methyl)-pyrrolidino enamines with nitro olefins have been used to study the chemical properties of intermediates in the catalytic *Michael* addition of aldehydes to mono- and disubstituted nitroethens. Some of the primary adducts (cyclobutane, oxazine, and THP derivatives) are thermally and/or hydrolytically so stable that they become traps for the catalyst moiety, and thus prevent successful catalysis. For alkoxy aldehydes, nitroacrylates, and acetamido-nitroethene,

⁴⁸⁾ The conformations of the corresponding intermediates are different: in *N*-acyl-piperidines, the $A^{1,3}$ strain pushes 2,6-substituents (cf. the pyrrolidino groups) into axial positions ('out' of the amide plane), see **vi**, the X-ray structures of **vii** and **viii** (CCDC: SUZBIY and BZOPIP), and the discussion in [48]; furthermore, an acyliminium ion, **ix**, is more stable than an oxenium ion, **x** [49]. Chromanes have a more flexible, cyclohexene-type conformation as compared to THPs, and the O-atom in a chromane is a better (phenolic) leaving group, so that ring opening to an iminium ion, **xi**, and hydrolysis thereof is more likely to occur.



components of the key steps in oseltamivir syntheses, a new possible resting state of the catalyst (its adduct to the acrylate) and *cis/trans*-equilibrations of the intermediate enamine and of the nitro olefin have been identified as complicating factors for establishing a catalytic cycle. Computational investigations show larger energy differences between (*Z*)- and (*E*)-alkoxy enamines than experimentally observed. With an ester of the H-D-Pro-Pro-Glu-tripeptide-derived organocatalyst we have shown that the same type of intermediates, *i.e.*, (2+2) and (4+2) cycloadducts, are involved as with the prolinol-derived catalysts; a unique cyclobutane derived from a disubstituted nitro olefin has been discovered with this peptide derivative. Results of hydrolysis and deuterolysis experiments with a product nitro enamine and with a dihydro-oxazine *N*-oxide are not compatible with previously reported experimental and calculational results. The numerous published optimizations of conditions for the catalytic processes, especially with disubstituted nitroethenes, have apparently not addressed the actual *Michael* addition step (of the enamines to the nitro-olefin acceptors) but the ‘recovery’ of the catalyst molecule from a primary product – in most cases. This is also suggested for reactions of 2-nitro-3-phenylprop-2-en-1-ol and of a nitrostyrene carrying a phenolic *ortho*-OH group. The crystal structures of seven intermediates/catalyst traps are shown.

Our experiments⁴⁹⁾ with stoichiometric conversions of enamines (derived from the pyrrolidine derivatives **1** and **11c**) and nitro olefins have provided evidence for equilibria at ambient temperatures, or slightly above, between

- (*E*)- and (*Z*)-enamine (**10a**; Schemes 3, 9)
- (*E*)- and (*Z*)-nitro olefin (Scheme 3 and Table 1)
- nitro olefin + catalyst and an amino-nitro ester (Scheme 8 and Table 7)
- enamine + nitro olefin and cyclobutanes (Figs. 5 and 9, and Scheme 5)
- enamine + nitro olefin and oxazine derivatives (Table 4, Fig. 9, and Scheme 10)
- cyclobutanes (Figs. 6 and 7)
- cyclobutanes and oxazine derivatives (Schemes 6, and 10, and Fig. 9)
- nitro enamine and oxazine derivative (Scheme 10)

Thus, there are surprisingly small energy (stability) differences between the (2+2) and the (4+2) cycloadduct, but also between these cycloadducts and their reactant precursors, as well as their products, setting the stage for a flat energy landscape of interconverting species⁴⁹⁾.

Finally, we should like to draw five *general conclusions*.

a) *There is not a single catalytic cycle* for the various reactants of the ‘simple’ catalytic *Michael* addition of aldehydes to nitro olefins shown in Scheme 1, and we speculate that this will also be true for other types of organocatalytic reactions.

⁴⁹⁾ For the three generic compounds with and without a Me group, **xii**–**xiv** and **xv**–**xvii**, respectively, in α -position to the NO₂ group, we have calculated the relative energies, using Spartan’08, PM3 for identifying reasonable conformations (*cf.* the crystal structures in Fig. 4), which were then subjected to a low-level DFT calculation (B3LYP/6-31G*). The energy differences between the isomers (numbers [kcal/mol] next to the formulae **xii**–**xvii**) are small and can be considered compatible with the equilibria observed experimentally. The measured ΔH value of –15.4 kcal/mol for nitrostyrene + enamine **2** \rightarrow cyclobutane **4e** also compares reasonably well with the result of the corresponding calculation (–18 kcal/mol). The – at first sight – surprisingly low energy differences

b) Stoichiometric model reactions and identifications of possible intermediates of organocatalyses may be useful tools for identifying key steps, optimizing conditions, and elucidating the stereochemical courses of the overall reactions. However, since the conditions (concentrations, solvent(s), acid additives, reaction times, presence of molecular sieves) of the catalytic and the stoichiometric reactions are different, ‘mutual’ mechanistic conclusions must be drawn with due care.

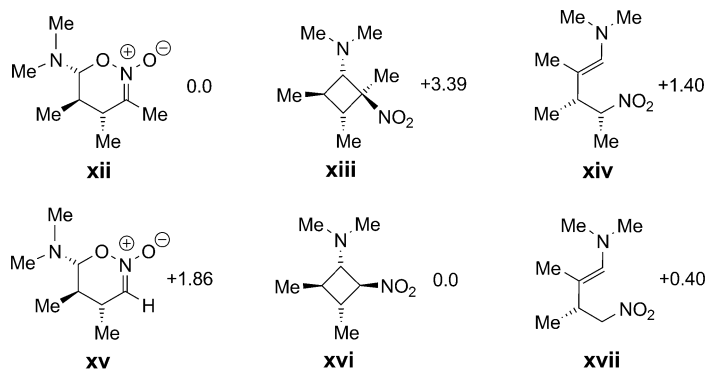
c) If an organocatalytic transformation is successful with certain reaction partners but fails with others, we recommend to carry out a traditional workup procedure and analyze for products that might be ‘slow’ intermediates or catalyst traps; after all, many organocatalytic transformations are carried out with 10–30 mol-% catalyst, so that substantial amounts of such catalyst derivatives may be present.

d) Thorough experimental analyses of the mechanisms of the present and of other organocatalytic conversions⁵⁰⁾ have all deepened our understanding, but, at the same time, increased complexity.

e) Thus, the pioneers in the field may have been right, not to look for details, but to just pragmatically optimize conditions to obtain the desired products with high yields and stereoselectivities (dr and er) to publish papers in high-impact-factor journals. After all, it is only worthwhile to study the mechanism of a synthetically valuable transformation that is of general utility.

We thank the NMR (*P. Zumbrennen*, *R. Arnold*, and *R. Frankenstein*), the MS (*R. Häfliger*, *O. Greter*, and *L. Bertschi*), the elementary-analyses (*P. Kälin* and *M. Schneider*), and the X-ray (*M. Solar*) services of the Laboratorium für Organische Chemie (ETH Zürich) for their assistance. We also acknowledge the financial support by the *Swiss National Science Foundation (SNF)*.

between species of type **4**, **5**, and **6** reveal that the statement made in [1]: ‘...we consider this proposal unlikely from a purely intuitive chemical point of view, since [...] it suggests an energetically uphill conversion of an open-chain enamino-nitronate to a cyclobutane upon protonation.’ did injustice to *Blackmond* and co-workers [17a].



⁵⁰⁾ For mechanistic work on *Michael* additions of aldehydes to nitro olefins, see [1][12][14][16][17][19][23b][37c]. For our contributions on the mechanisms of other organocatalytic reactions, see [18b][25k,l][50].

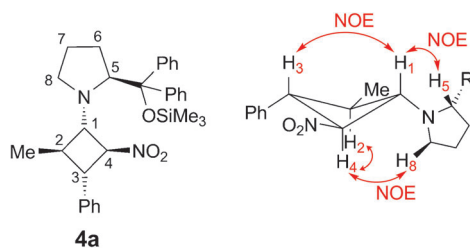
Experimental Part

General. All reactions were performed under Ar. The NMR solvents CDCl_3 , C_6D_6 , $(\text{D}_8)\text{toluene}$, and CD_2Cl_2 were purchased from *ARMAR Chemicals* (CH-Döttingen). Solvents for reactions and [2,2- D_2]propionaldehyde were purchased from *Sigma-Aldrich* and were used without purification and drying. The commercial aldehydes were of reagent grade and were carefully distilled prior to use. Aldehyde **9** was prepared according to [21]; its purity was 70–80%; the identity of the impurities (aldol products, trimer?) was not established; even upon storage at -78° , the amount of impurities increased slowly. Nitrostyrene (*Aldrich*), (*E*)- β -methyl- β -nitrostyrene (**3**, $\text{R}^2 = \text{Ph}$, $\text{R}^3 = \text{Me}$; *Acros*), and 1-nitrocyclohex-1-ene (*Aldrich*) are commercially available, all other nitro olefins [21][22][28][51] and the diphenylprolinol silyl ethers [52] were prepared according to literature procedures. TLC: *Merck* silica gel 60 F_{254} plates; visualization by UV fluorescence (254 nm) or by dipping into a soln. of phosphomolybdic acid (10 % in EtOH), followed by heating. FC: *Fluka* silica gel 60 (40–63 μm). M.p.: *Büchi* 510 melting-point apparatus (uncorrected). Optical rotations ($[\alpha]_D^{25}$): *Perkin-Elmer* 241 polarimeter (10 cm, 1-ml cell). IR Spectra: *Perkin-Elmer* 782 spectrophotometer; $\tilde{\nu}$ in cm^{-1} . NMR spectra: *Bruker AMX 600* (^1H : 600 and ^{13}C : 150.9 MHz), *AMX 500* (^1H : 500 and ^{13}C : 125 MHz), *AMX 400* (^1H : 400 and ^{13}C : 100 MHz), *AM 400* (^1H : 400 and ^{13}C : 100 MHz), *AV-400* (^1H : 400 and ^{13}C : 100 MHz), or *Varian Gemini 300* (^1H : 300 and ^{13}C : 75 MHz); chemical shifts δ in ppm and coupling constants J in Hz. Peak assignments were accomplished by a combination of 1D and 2D experiments (COSY, HSQC, HMBC, and NOESY). HR-MS: *IonSpec Ultima 4.7* (HR-ESI-MS) or *Bruker* ESI-TOF-MS; m/z . Elemental analyses: performed in the Microanalytical Laboratory of the Laboratorium für Organische Chemie, ETH Zürich. Activation of molecular sieves (MS; 3 Å or 4 Å) powder by heating under reduced pressure with a heat gun, after cooling to r.t., the flask was flushed with Ar.

1. **Standard Conditions for the Catalytic Michael Addition of Aldehydes to Nitro Olefins** [14]. To a mixture of nitro olefin (0.3 mmol) and aldehyde (0.45 mmol) in toluene (0.3 ml) was added (*S*)-diphenylprolinol trimethylsilyl ether (= (2*S*)-2-[diphenyl[(trimethylsilyl)oxy]methyl]pyrrolidine; **1a**; 0.015 mmol, 5 mol-%) and 4-nitrophenol (0.015 mmol, 5 mol-%). The mixture was stirred at r.t. (monitored by TLC), and the reaction was quenched after 24 h by addition of 1M HCl, and the mixture was extracted with AcOEt (3×15 ml). The combined org. layer was dried (MgSO_4), filtered, concentrated, and analyzed for nitro aldehyde (NMR).

2. **Reactions of Enamines with Nitro Olefins. General Procedure (GP).** To a soln. of **1a** or **1b** (0.1 mmol) in C_6D_6 (0.6 ml, with 3- or 4-Å MS) in an NMR tube, aldehyde (0.1 mmol) was added, and the reaction was monitored by ^1H -NMR. After complete conversion to the enamine, nitro olefin (1.0 equiv.) was added, and the mixture was agitated at r.t., and the reaction was monitored by ^1H -NMR.

3. **Characterization and Properties of the Cyclobutanes 4** 3.1. **Characterization.** (2*S*)-2-[Diphenyl[(trimethylsilyl)oxy]methyl]-1-[*(1S,2R,3S,4S)*-2-methyl-4-nitro-3-phenylcyclobutyl]pyrrolidine (**4a**) and (*4S,5R,6R*)-6-[*(2S)*-2-[Diphenyl[(trimethylsilyl)oxy]methyl]pyrrolidin-1-yl]-5-methyl-4-phenyl-5,6-dihydro-4*H*-1,2-oxazine 2-Oxide (**5a**). According to GP, from **1a** (32.6 mg, 0.1 mmol), propanal (7.2 μl , 0.1 mmol) and β -nitrostyrene (14.9 mg, 0.1 mmol), **4a** and **5a** formed immediately ($t < 10$ min; **4a/5a** 4:1). FC Purification failed due to decomposition. ^1H -NMR of **4a/5a** (400 MHz, C_6D_6): Data of **4a**: 7.59–7.55 (*m*, 4 H); 7.17–7.05 (*m*, 7 H); 7.00–6.99 (*m*, 2 H); 6.87 (*t*, $J = 7.6$, 1 H); 6.70 (*d*, $J = 7.2$, 1 H); 4.99 (*t*, $J = 8.0$, 1 H); 4.43 (*dd*, $J = 3.2, 9.6$, 1 H); 4.15 (*br. s*, 1 H); 3.28 (*t*, $J = 9.2$, 1 H); 2.34–2.24 (*m*, 2 H); 1.96–1.84 (*m*, 2 H); 1.80–1.73 (*m*, 1 H); 1.23–1.15 (*m*, 1 H); 1.03 (*d*, $J = 5.6$, 3 H); 0.66–0.56 (*m*, 1 H);



–0.03 (s, 9 H). Data of **5a**: 7.48–7.46 (m, 2 H); 7.42–7.37 (m, 2 H); 7.17–6.95 (m, 9 H); 6.83–6.79 (m, 2 H); 5.89 (d, $J = 2.8$, 1 H); 5.43 (br. s, 1 H); 4.72 (dd, $J = 2.8$, 9.2, 1 H); 2.95–2.89 (m, 2 H); 2.17–2.11 (m, 1 H); 1.96–1.81 (m, 2 H); 1.70–1.65 (m, 1 H); 1.42–1.29 (m, 1 H); 0.83 (d, $J = 5.2$, 3 H); 0.66–0.56 (m, 1 H); –0.05 (s, 9 H). Compounds **4a** and **5a** were identified and characterized by 1D- and 2D-NMR (COSY, HSQC, and NOESY). Equilibration between **4a** and **5a** was detected from an EXSY spectrum [1]. The data are in agreement with those in [12][16][17].

(2S)-2-[Diphenyl[(trimethylsilyl)oxy]methyl]-1-[(1S,2R,3S,4S)-2-ethyl-4-nitro-3-phenylcyclobutyl]pyrrolidine (**4b**). Prepared according to GP from **1a** (32.6 mg, 0.1 mmol), butanal (8.8 μ l, 0.1 mmol), and β -nitrostyrene (14.9 mg, 0.1 mmol). FC Purification failed due to decomposition. $^1\text{H-NMR}$ (400 MHz, C_6D_6): 7.62–6.93 (m, 11 H); 6.85 (t, $J = 7.6$, 2 H); 6.68 (d, $J = 7.6$, 2 H); 4.98 (t, $J = 7.6$, 1 H); 4.46 (dd, $J = 2.8$, 9.6, 1 H); 3.37 (t, $J = 9.2$, 1 H); 2.35 (dd, $J = 4.8$, 8.0, 2 H); 1.96–1.86 (m, 2 H); 1.84–1.74 (m, 2 H); 1.69–1.64 (m, 1 H); 1.21–1.12 (m, 2 H); 0.73 (t, $J = 7.2$, 3 H); 0.62–0.54 (m, 1 H); 0.02 (s, 9 H).

(2S)-1-[(1S,2R,3S,4S)-2-Butyl-4-nitro-3-phenylcyclobutyl]-2-[diphenyl[(trimethylsilyl)oxy]methyl]pyrrolidine (**4c**). Prepared according to GP from **1a** (32.6 mg, 0.1 mmol), hexanal (12.3 μ l, 0.1 mmol), and β -nitrostyrene (14.9 mg, 0.1 mmol). FC Purification failed due to decomposition. $^1\text{H-NMR}$ (400 MHz, C_6D_6): 7.63–7.58 (m, 4 H); 7.12–7.08 (m, 6 H); 7.05–7.03 (m, 4 H); 6.97–6.93 (m, 1 H); 5.00 (t, $J = 8.0$, 1 H); 4.47 (d, $J = 9.2$, 1 H); 3.39 (t, $J = 9.2$, 1 H); 2.39–2.36 (m, 2 H); 2.05–1.97 (m, 1 H); 1.84–1.77 (m, 1 H); 1.52–1.37 (m, 3 H); 1.20–1.15 (m, 4 H); 1.01–0.94 (m, 1 H); 0.87 (t, $J = 6.8$, 3 H); 0.78 (q, $J = 6.4$, 1 H); 0.62–0.51 (m, 1 H); –0.02 (s, 9 H). HR-ESI-TOF-MS: 579.3020 [$\text{C}_{34}\text{H}_{44}\text{N}_2\text{O}_5\text{Si} + \text{Na}$] $^+$; calc. 579.3014).

(2S)-1-[(1S,2R,3S,4S)-2-[3-(Benzyloxy)propyl]-4-nitro-3-phenylcyclobutyl]-2-[diphenyl[(trimethylsilyl)oxy]methyl]pyrrolidine (**4d**). Prepared according to GP from **1a** (32.6 mg, 0.1 mmol), 5-(benzyloxy)pentanal (19.2 mg, 0.1 mmol), and β -nitrostyrene (14.9 mg, 0.1 mmol). FC Purification failed due to decomposition. $^1\text{H-NMR}$ (400 MHz, C_6D_6): 7.62–7.59 (m, 4 H); 7.55–7.49 (m, 2 H); 7.45–7.40 (m, 2 H); 7.33–7.25 (m, 4 H); 7.12–7.10 (m, 3 H); 6.97–6.94 (m, 2 H); 6.87–6.83 (m, 2 H); 6.69–6.67 (m, 1 H); 5.00 (t, $J = 7.2$, 1 H); 4.47 (d, $J = 9.2$, 1 H); 4.32 (s, 2 H); 4.31–4.24 (m, 1 H); 3.24–3.22 (m, 2 H); 2.37–2.35 (m, 2 H); 2.06–2.04 (m, 1 H); 1.89–1.76 (m, 4 H); 1.75–1.60 (m, 2 H); 1.19–1.16 (m, 2 H); 0.63–0.57 (m, 1 H); –0.02 (s, 9 H).

(2S)-2-[Diphenyl[(trimethylsilyl)oxy]methyl]-1-[(1S,2R,3S,4S)-2-isopropyl-4-nitro-3-phenylcyclobutyl]pyrrolidine (**4e**). Prepared according to GP from **1a** (32.6 mg, 0.1 mmol), isovaleraldehyde (= 3-methylbutanal; 10.8 μ l, 0.1 mmol), and β -nitrostyrene (14.9 mg, 0.1 mmol) ($t < 10$ min). FC purification failed due to decomposition. $^1\text{H-NMR}$ (600 MHz, C_6D_6): 7.61 (d, $J = 7.2$, 2 H); 7.56 (dd, $J = 1.8$, 9.0, 2 H); 7.17–7.00 (m, 11 H); 4.91 (t, $J = 7.8$, 1 H); 4.45 (dd, $J = 3.0$, 9.0, 1 H); 4.24 (br. s, 1 H); 3.40 (t, $J = 9.0$, 1 H); 2.44–2.38 (m, 2 H); 1.91–1.78 (m, 3 H); 1.61–1.54 (m, 1 H); 1.17–1.14 (m, 1 H); 0.88–0.80 (m, 3 H); 0.60 (d, $J = 6.6$, 3 H); 0.54–0.46 (m, 1 H); –0.05 (s, 9 H). HR-ESI-TOF-MS: 565.2893 [$\text{C}_{33}\text{H}_{42}\text{N}_2\text{NaO}_5\text{Si}$] $^+$; calc. 565.2862).

tert-Butyl (1R,2R,3S,4S)-3-[(2S)-2-[Diphenyl[(trimethylsilyl)oxy]methyl]pyrrolidin-1-yl]-2-isopropyl-4-nitrocyclobutanecarboxylate (**4g**). Prepared according to GP from **1a** (32.6 mg, 0.1 mmol), isovaleraldehyde (10.8 μ l, 0.1 mmol), and tert-butyl (*E*)-3-nitroprop-2-enoate (17.3 mg, 0.1 mmol) ($t < 10$ min). FC purification failed due to decomposition. $^1\text{H-NMR}$ (300 MHz, C_6D_6): 7.59 (d, $J = 6.6$, 2 H); 7.54 (d, $J = 7.2$, 2 H); 7.16–7.06 (m, 6 H); 5.43 (t, $J = 7.6$, 1 H); 4.50 (dd, $J = 3.6$, 8.7, 1 H); 4.21 (br. s, 1 H); 3.13 (t, $J = 9.0$, 1 H); 2.56–2.50 (m, 1 H); 2.41–2.35 (m, 1 H); 2.00 (q, $J = 8.4$, 1 H); 1.83–1.75 (m, 2 H); 1.61–1.54 (m, 1 H); 1.29 (s, 9 H); 1.14–1.07 (m, 1 H); 0.88 (d, $J = 6.0$, 3 H); 0.77 (d, $J = 6.3$, 3 H); 0.56–0.43 (m, 1 H); –0.06 (s, 9 H).

(2S)-2-[Diphenyl[(trimethylsilyl)oxy]methyl]-1-[(1S,2S,3S,4R)-2-nitro-3-phenyl-4-(1-phenylethyl)cyclobutyl]pyrrolidine (**4k**). Prepared according to GP from **1a** (32.6 mg, 0.1 mmol), rac-3-phenylbutanal (14.9 μ l, 0.1 mmol), and β -nitrostyrene (14.9 mg, 0.1 mmol). FC Purification failed due to decomposition. The two diastereoisomers formed gave rise to the following NMR data (dr 1:1.3): $^1\text{H-NMR}$ (400 MHz, C_6D_6): Diastereoisomer A: 7.64–7.60 (m, 2 H); 7.52–7.48 (m, 2 H); 7.46–7.43 (m, 1 H); 7.26–7.19 (m, 5 H); 7.08–7.04 (m, 4 H); 6.96–6.92 (m, 4 H); 6.71–6.66 (m, 2 H); 5.06 (t, $J = 7.2$, 1 H); 4.54–4.51 (m, 1 H); 3.51–3.47 (m, 1 H); 2.73–2.66 (m, 2 H); 2.43–2.37 (m, 2 H); 2.32–2.25 (m, 2 H); 1.29 (d, $J = 4.4$, 3 H); 1.18–1.12 (m, 2 H); 0.59–0.49 (m, 1 H); 0.19 (s, 9 H); diastereoisomer B: 7.64–7.60 (m, 2 H); 7.52–7.48 (m, 2 H); 7.46–7.43 (m, 1 H); 7.26–7.19 (m, 5 H); 7.08–7.04 (m, 4 H);

6.96–6.92 (*m*, 4 H); 6.71–6.66 (*m*, 2 H); 4.89 (*t*, *J* = 7.6, 1 H); 4.41 (*d*, *J* = 8.8, 1 H); 3.44–3.39 (*m*, 1 H); 2.73–2.66 (*m*, 2 H); 2.43–2.37 (*m*, 2 H); 2.32–2.25 (*m*, 2 H); 1.03–0.96 (*m*, 2 H); 0.79 (*d*, *J* = 3.2, 3 H); 0.59–0.49 (*m*, 1 H); 0.19 (*s*, 9 H).

(2*S*)-1-[*(1S,2R,3R,4S)*-2,3-Diisopropyl-4-nitrocyclobutyl]-2-[*diphenyl*[(*trimethylsilyl*)oxy]methyl]pyrrolidine (**4l**). Prepared according to GP from **1a** (32.6 mg, 0.1 mmol), isovaleraldehyde (10.8 µl, 0.1 mmol), and (*E*)-3-methyl-1-nitrobut-1-ene (11.5 mg, 0.1 mmol; *t* 17 h). FC Purification failed due to decomposition. ¹H-NMR (300 MHz, C₆D₆): 7.67 (*d*, *J* = 6.6, 2 H); 7.61–7.58 (*m*, 2 H); 7.21–7.08 (*m*, 6 H); 4.75 (*t*, *J* = 7.5, 1 H); 4.40 (*m*, 1 H); 4.17 (*br. s*, 1 H); 2.43–2.29 (*m*, 2 H); 2.22–2.14 (*m*, 1 H); 1.91–1.79 (*m*, 2 H); 1.58–1.12 (*m*, 4 H); 0.90–0.82 (*m*, 4 H); 0.74 (*d*, *J* = 6.6, 3 H); 0.66 (*dd*, *J* = 3.0, 6.9, 6 H); –0.04 (*s*, 9 H). ¹³C-NMR (100 MHz, C₆D₆): 144.0; 143.5; 130.6; 130.4; 80.2; 76.8; 70.4; 69.4; 68.7; 65.5; 49.8; 45.7; 45.6; 45.3; 39.6; 38.0; 31.6; 29.7; 24.3; 21.2; 20.7; 19.2; 2.5. HR-ESI-TOF-MS: 531.3024 ([C₃₀H₄₄N₂O₃Si + Na]⁺; calc. 531.3014).

(2*S*)-1-[*(1S,2R,3R,4S)*-2,3-Diisopropyl-4-nitrocyclobutyl]-2-[*diphenyl*[(*trimethylsilyl*)oxy]methyl]pyrrolidine (**4m**). Prepared according to GP from **1b** (45.0 mg, 0.1 mmol), isovaleraldehyde (10.8 µl, 0.1 mmol), and (*E*)-3-methyl-1-nitrobut-1-ene (11.5 mg, 0.1 mmol; *t* 16 h). FC Purification failed due to decomposition. ¹H-NMR (300 MHz, C₆D₆): 7.50–7.42 (*m*, 4 H); 7.31–7.09 (*m*, 14 H); 7.05–7.01 (*m*, 2 H); 4.70 (*t*, *J* = 7.2, 1 H); 4.13–4.09 (*m*, 1 H); 3.40–3.35 (*m*, 1 H); 2.58–2.52 (*m*, 2 H); 1.97–1.89 (*m*, 3 H); 1.61–1.47 (*m*, 2 H); 1.37–1.20 (*m*, 2 H); 1.07 (*dd*, *J* = 0.9, 6.9, 1 H); 0.75 (*dd*, *J* = 4.5, 6.6, 6 H); 0.60 (*d*, *J* = 6.6, 3 H); 0.50 (*d*, *J* = 6.6, 3 H); 0.04 (*s*, 3 H).

(2*S*)-1-[*(1S,2R,3R,4S)*-3-Cyclohexyl-2-isopropyl-4-nitrocyclobutyl]-2-[*diphenyl*[(*trimethylsilyl*)oxy]methyl]pyrrolidine (**4n**). Prepared according to GP from **1a** (32.6 mg, 0.1 mmol), isovaleraldehyde (10.8 µl, 0.1 mmol), and (*E*)-(2-nitroethenyl)cyclohexane (15.5 mg, 0.1 mmol; *t* 18 h). FC Purification failed due to decomposition. ¹H-NMR (400 MHz, C₆D₆): 7.69 (*d*, *J* = 7.2, 2 H); 7.60 (*d*, *J* = 7.6, 2 H); 7.21–7.17 (*m*, 4 H); 7.13–7.07 (*m*, 2 H); 4.77 (*t*, *J* = 7.2, 1 H); 4.41 (*dd*, *J* = 4.0, 8.0, 1 H); 2.45–2.33 (*m*, 2 H); 2.22 (*q*, *J* = 8.0, 1 H); 1.96–1.87 (*m*, 2 H); 1.57–1.52 (*m*, 4 H); 1.50–1.48 (*m*, 3 H); 1.23–1.17 (*m*, 1 H); 1.12–1.08 (*m*, 1 H); 1.03–0.98 (*m*, 2 H); 0.85–0.80 (*m*, 2 H); 0.78 (*d*, *J* = 6.4, 6 H); 0.73–0.70 (*m*, 2 H); 0.54–0.42 (*m*, 1 H); –0.03 (*s*, 9 H). ¹³C-NMR (100 MHz, C₆D₆): 144.0; 143.5; 130.6; 130.5; 128.0; 127.8; 80.7; 69.4; 65.4; 49.8; 45.2; 44.2; 41.7; 31.5; 30.0; 29.8; 26.8; 26.7; 26.6; 24.3; 21.3; 19.5; 2.5. HR-ESI-TOF-MS: 571.3314 ([C₃₃H₄₈N₂O₄Si + Na]⁺; calc. 571.3327).

(2*S*)-1-[*(1S,2R,3R,4S)*-3-Cyclohexyl-2-isopropyl-4-nitrocyclobutyl]-2-[*diphenyl*[(*trimethylsilyl*)oxy]methyl]pyrrolidine (**4o**). Prepared according to GP from **1b** (45.0 mg, 0.1 mmol), isovaleraldehyde (10.8 µl, 0.1 mmol), and (*E*)-(2-nitroethenyl)cyclohexane (15.5 mg, 0.1 mmol; *t* 24 h). FC Purification failed due to decomposition. ¹H-NMR (300 MHz, C₆D₆): 7.79 (*br. s*, 2 H); 7.65–7.60 (*m*, 2 H); 7.54–7.48 (*m*, 2 H); 7.41–7.38 (*m*, 2 H); 7.22–7.06 (*m*, 10 H); 7.01–6.96 (*m*, 2 H); 4.68 (*t*, *J* = 7.5, 1 H); 4.50 (*dd*, *J* = 2.1, 8.7, 1 H); 3.71 (*br. s*, 1 H); 2.49–2.35 (*m*, 2 H); 2.07–2.01 (*m*, 3 H); 1.50–1.37 (*m*, 5 H); 1.27–1.21 (*m*, 2 H); 1.01–0.84 (*m*, 5 H); 0.66–0.55 (*m*, 9 H); 0.21 (*s*, 3 H).

(2*S*)-1-[*(1S,2R,3S,4S)*-3-(*tert*-Butyl)-2-ethyl-4-nitrocyclobutyl]-2-[*diphenyl*[(*trimethylsilyl*)oxy]methyl]pyrrolidine (**4p**). Prepared according to GP from **1a** (32.6 mg, 0.1 mmol), butanal (8.8 µl, 0.1 mmol), and (*E*)-3,3-dimethyl-1-nitrobut-1-ene (12.9 mg, 0.1 mmol; *t* 27 h). ¹H-NMR (600 MHz, C₆D₆): 7.61 (*d*, *J* = 5.4, 2 H); 7.57 (*d*, *J* = 7.8, 2 H); 7.19–7.08 (*m*, 6 H); 4.91 (*t*, *J* = 7.8, 1 H); 4.35 (*dd*, *J* = 2.4, 9.6, 1 H); 4.08 (*br. s*, 1 H); 2.42–2.39 (*m*, 2 H); 2.17 (*t*, *J* = 9.0, 1 H); 1.92–1.74 (*m*, 2 H); 1.62–1.58 (*m*, 1 H); 1.51–1.42 (*m*, 1 H); 1.32–1.22 (*m*, 1 H); 1.19–1.17 (*m*, 1 H); 0.84–0.79 (*m*, 3 H); 0.65 (*s*, 9 H); 0.52–0.46 (*m*, 1 H); –0.05 (*s*, 9 H).

3.2. Thermal Equilibration between **4e**, and Its Precursors Enamine **2** (R¹ = ⁱPr, R₃Si = Me₃Si) and β-Nitrostyrene. In an NMR tube, **1a** (48.83 mg, 0.15 mmol) and C₆D₆ (0.70 ml) were mixed; the concentration of **1a** was 0.214M. To this soln., isovaleraldehyde (16 µl, 0.15 mmol) and MS (4 Å) were added, the mixture was agitated, and its composition was monitored by ¹H-NMR. According to the recorded spectra, isovaleraldehyde had been completely converted to the enamine within 10 min, and only a trace of **1a** was detected. Then, β-nitrostyrene (23 mg, 0.15 mmol) was added to the soln. The mixture was agitated at r.t., and a ¹H-NMR spectrum was recorded immediately. By ¹H-NMR, immediate formation of the cyclobutane **4e** was detected, but there was still some enamine **2**, β-nitrostyrene, and **1a** present. The ratio of these components was determined by the NMR integrals. Based on the ratio and standard concentration [**1a**]₀ = 0.214M, the equilibrium concentrations of enamine **2**, β-nitrostyrene, and

cyclobutane **4e** at r.t. (25°) were determined: [enamine **2**] = 0.004M, [β -nitrostyrene] = 0.037M, [cyclobutane **4e**] = 0.185M. ¹H-NMR Spectra were recorded starting at 25°, heating up to 66°, followed by cooling back down to 25°. At various temp., the equilibrium concentrations of enamine **2**, β -nitrostyrene, and cyclobutane **4e** were determined (Fig. 5). From the equilibrium concentrations, the equilibrium constants ($K = ([\text{enamine}] \cdot [\beta\text{-nitrostyrene}]) / [\text{cyclobutane}]$), and the $\ln K$ values were calculated (see Table 5). By linear regression in Excel, the graph of $\ln K$ vs. $1/T$ was obtained; the data are presented in Table 5 and Fig. 5.

Table 5. Temperature-Dependent $\ln K$ Values for the Equilibrium between **4e**, and the Corresponding Enamine **2** and Nitrostyrene (see Fig. 5)

Entry	Temperature [K]	$\ln K$
1	298.15	− 7.1308
2	302.25	− 6.6879
3	307.95	− 6.2891
4	313.05	− 5.9304
5	318.05	− 5.6268
6	322.95	− 5.1337
7	328.15	− 4.9019
8	333.35	− 4.5461
9	339.15	− 4.1699
10	333.35	− 4.5626
11	322.95	− 5.3100
12	313.05	− 5.8850
13	298.15	− 7.7822

3.3. Preparation of Cyclobutane **4q** and Investigations of Its Chemical Properties. (2*S*)-1-[(1*S*,2*R*,3*S*,4*S*)-3-(tert-Butyl)-2-isopropyl-4-nitrocyclobutyl]-2-{diphenyl[(trimethylsilyl)oxy]methyl}pyrrolidine (**4q**). To a soln. of **1a** (97.5mg, 0.3 mmol) in benzene (0.3 ml; with 4-Å MS) was added isovaleraldehyde (33 μ l, 0.3 mmol), the mixture was stirred for 10 min, then (*E*)-3,3-dimethyl-1-nitrobut-1-ene (38.75 mg, 0.3 mmol) was added, and the mixture was stirred at r.t. for 3 d (monitored by TLC). Then, hexane was added, and the mixture was filtered. From the clear soln., crystallization took place to give **4q** (133 mg, 85%). Colorless crystals, suitable for X-ray analysis. M.p. 138–144° (dec). $[\alpha]_D^{25} = -10.1$ ($c = 0.80$, CHCl₃). ¹H-NMR (500 MHz, C₆D₆): 7.70 (br. s, 2 H); 7.61 (*d*, $J = 7.0$, 2 H); 7.21–7.13 (*m*, 5 H); 7.09 (*t*, $J = 7.5$, 1 H); 4.90 (*t*, $J = 7.5$, 1 H); 4.41 (*t*, $J = 5.5$, 1 H); 4.19 (br. s, 1 H); 2.45–2.41 (*m*, 2 H); 2.32 (*t*, $J = 9.5$, 1 H); 1.94–1.85 (*m*, 2 H); 1.73 (*td*, $J = 10.0$, 3, 5, 1 H); 1.57 (br. s, 1 H); 1.19–1.15 (*m*, 1 H); 0.82 (*d*, $J = 7.0$, 3 H); 0.87–0.73 (*m*, 3 H); 0.66 (s, 9 H); 0.38–0.49 (*m*, 1 H); − 0.04 (s, 9 H); ¹³C-NMR (75 MHz, C₆D₆): 143.5; 142.8; 130.2; 130.0; 127.3; 78.8; 69.4; 62.8; 49.5; 47.6; 42.4; 32.0; 29.4; 29.6; 29.2; 27.4; 24.0; 21.4; 18.0; 2.4. Anal. calc. for C₃₁H₄₆N₂O₃Si (522.80): C 71.22, H 8.87, N 5.36; found: C 71.16, H 8.77, N 5.36.

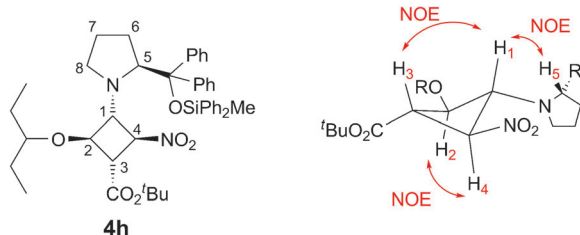
3.4. Thermal Stability of Cyclobutane **4q**. To the soln. of **4q** (18.3 mg, 0.035 mmol) in (D₈)toluene (0.6 ml) in an NMR tube in the presence of 4-Å MS, β -nitrostyrene (5.2 mg, 0.035 mmol) was added, and the NMR tube was sealed. The mixture was heated for 30 min each at 60°, 70°, 80°, 90°, 100°, 110°, 120°, followed by cooling to r.t., then ¹H-NMR was recorded. Up to 80° no change, at 90° traces of the enamine precursor, and after heating to 120° the cyclobutane **4e** were detected.

3.5. Hydrolytic Stability of the Cyclobutane **4q**. To the soln. of **4q** (26.1 mg, 0.05 mmol) in (D₈)toluene (0.6 ml) in an NMR tube in the presence of 10.0 equiv. H₂O, 4-nitrophenol (0.7 mg, 10 mol-%) was added, and the composition of the mixture was monitored by ¹H-NMR. After 24 h, no corresponding nitro aldehyde was detected, cyclobutane **4q** was stable under this conditions.

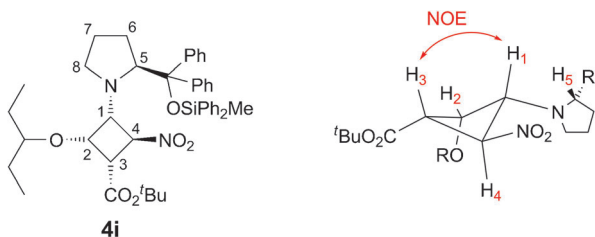
4. Reactions of Enamines from 2-(Isopentyloxy)acetaldehyde with 3-Nitroacrylate and 3-Acetamidonitroethene. 4.1. Formation of **4h**, **4i**, and **6h**. To a 5 ml flask with 4-Å MS (440 mg, pellets) were added

C_6D_6 (0.2 ml), a stock soln. of **1b** (0.05 mmol, 0.25 ml, 0.2M in C_6D_6), a stock soln. of 2-(pentan-3-yloxy)acetaldehyde (**9**; 0.05 mmol, 0.25 ml, 0.2M in C_6D_6), and a stock soln. of toluene (0.02 mmol, 40 μ l, 0.5M in C_6D_6) at r.t. In another flask, a further sample was prepared following exactly the same procedure. The two flasks were kept for 4 h at r.t. for the enamine formation. An NMR sample was prepared from one of the solns. to determine the (*E*)/(*Z*)-enamine ratio: (*E*)-**10a**/(*Z*)-**10a**/toluene 1:1.55:1.84. Calculation of the generated enamine **10a**: enamine $(1 + 1.55) \times$ toluene $(0.02 \text{ mmol})/1.84 = 0.028 \text{ mmol}$. To the other sample was added a stock soln. of *tert*-butyl (*E*)-3-nitroacrylate (0.028 mmol, 0.28 ml, 0.1M in C_6D_6) at r.t. Then, 0.55 ml of this sample was transferred to an NMR tube. The formation of **4h**, **4i**, and **6h** was monitored by 1H -NMR spectroscopy, and the progress (concentration vs. time) was plotted (Fig. 6).

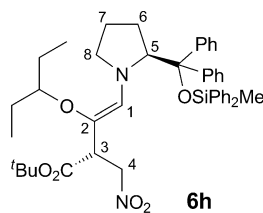
tert-Butyl (1*S*,2*S*,3*R*,4*R*)-3-[(2*S*)-2-[[Methyl(diphenyl)silyl]oxy](diphenyl)methyl]pyrrolidin-1-yl]-2-nitro-4-(pentan-3-yloxy)cyclobutanecarboxylate (**4h**). 1H -NMR (300 MHz, C_6D_6): 7.75–6.95 (*m*, 20 H); 5.07 (*t*, $J = 7.6$, H(4)); 4.61 (*dd*, $J = 8.6$, 3.4, H(5)); 4.35–4.21 (*br.*, H(1)); 3.81 (*t*, $J = 7.6$, H(2)); 3.27 (*t*, $J = 7.6$, H(3)); 3.22–3.12 (*m*, 1 H); 2.45–2.34 (*m*, 2 H); 2.05–1.89 (*m*, 2 H); 1.46–1.34 (*m*, 5 H); 1.26 (*s*, 9 H); 0.92–0.78 (*m*, 7 H); 0.24 (*s*, 3 H). ^{13}C -NMR (100 MHz, C_6D_6): 73.9 (C(2)); 73.9 (C(4)); 70.3 (C(1)); 68.4 (C(5)); 48.0 (C(3)). NOESY (400 MHz, C_6D_6 , 7°). COSY: H(1)/H(2), H(2)/H(3), H(3)/H(4), H(4)/H(1). HMBC: C(1)/H(5).



tert-Butyl (1*S*,2*S*,3*R*,4*S*)-3-[(2*S*)-2-[[Methyl(diphenyl)silyl]oxy](diphenyl)methyl]pyrrolidin-1-yl]-2-nitro-4-(pentan-3-yloxy)cyclobutanecarboxylate (**4i**). 1H -NMR (300 MHz, C_6D_6): 7.73–6.98 (*m*, 20 H); 5.96 (*t*, $J = 8.8$, H(4)); 4.35 (*dd*, $J = 9.0$, 4.2, H(5)); 4.30–4.21 (*br.*, 1 H, H(1)); 3.73 (*t*, $J = 6.6$, H(2)); 3.19 (*dd*, $J = 8.8$, 6.6, H(3)); 3.14–3.07 (*m*, 1 H); 2.62–2.48 (*m*, 2 H); 2.03–1.88 (*m*, 2 H); 1.57–1.38 (*m*, 5 H); 1.35 (*s*, 9 H); 0.92–0.75 (*m*, 7 H); 0.30 (*s*, 3 H). NOESY (500 MHz, D_8 toluene, 0°). COSY: H(1)/H(2), H(2)/H(3), H(3)/H(4), H(4)/H(1).

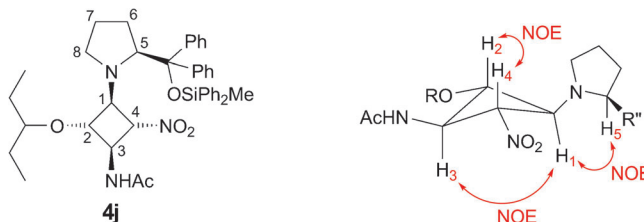


tert-Butyl (2*S*,3*Z*)-4-[(2*S*)-2-[[Methyl(diphenyl)silyl]oxy](diphenyl)methyl]pyrrolidin-1-yl]-2-(nitromethyl)-3-(pentan-3-yloxy)but-3-enoate (**6h**). 1H -NMR (300 MHz, C_6D_6): 7.74–6.98 (*m*, 20 H); 5.22 (*s*, H(1)); 4.46–4.33 (*m*, H(4)); 4.10 (*dd*, $J = 8.3$, 3.2, H(5)); 3.75–3.60 (*m*, H(4)); 3.23–3.10 (*m*, H(3)); 3.03–2.91 (*m*, 1 H); 2.60–2.47 (*m*, 2 H); 2.04–1.90 (*m*, 2 H); 1.53–1.38 (*m*, 5 H); 1.36 (*s*, 9 H); 0.91–0.78 (*m*, 7 H); 0.20 (*s*, 3 H). HSQC: H(1) (δ 5.22)/C(1) (δ 127.5).

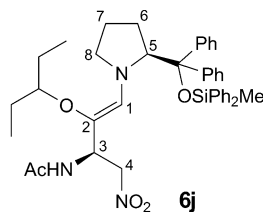


4.2. Formation of **4j and **6j**.** To a 5 ml flask with 4-Å MS (440 mg, pellets) were added at r.t. C_6D_6 (0.2 ml), a stock soln. of **1b** (0.04 mmol, 0.20 ml, 0.2M in C_6D_6), a stock soln. of 2-(pent-3-yloxy)acetaldehyde (**9**; 0.04 mmol, 0.20 ml, 0.2M in C_6D_6), and a stock soln. of toluene (0.016 mmol, 32 μ l, 0.5M in C_6D_6). In another flask, a further sample was prepared following exactly the same procedure. The two flasks were kept for 4 h at r.t. for the enamine formation. An NMR sample was prepared from one of the solns. to determine the (*E*)/(*Z*)-enamine ratio; (*E*)-**10a**/(*Z*)-**10a**/toluene 1 : 1.58 : 1.76. Calculation of the generated enamine **10a**: enamine $(1 + 1.58) \times$ toluene $(0.016 \text{ mmol})/1.76 = 0.024 \text{ mmol}$. To the other sample was added a stock soln. of *N*-[(*Z*)-2-nitroethenyl]acetamide (0.024 mmol, 0.47 ml, 0.05M in C_6D_6) at r.t.. Then 0.60 ml of this sample was transferred to an NMR tube. The formation of **4j** and **6j** was monitored by 1H -NMR spectroscopy, and the progress (concentration vs. time) was plotted (Fig. 7).

N-[(1*R*,2*R*,3*S*,4*S*)-3-[(2*S*)-2-[[[Methyl(diphenyl)silyl]oxy](diphenyl)methyl]pyrrolidin-1-yl]-2-nitro-4-(pentan-3-yloxy)cyclobutyl]acetamide (**4j**). 1H -NMR (300 MHz, C_6D_6): 7.74–6.88 (*m*, 20 H); 5.20 (*t*, $J = 8.0$, H(4)); 4.73 (*t*, $J = 7.2$, H(2)); 4.55 (*dd*, $J = 8.8$, 3.6, H(5)); 4.38 (*d*, $J = 6.8$, NH); 3.83 (*br.*, H(1)); 3.36 (*ddd*, $J = 8.0$, 7.2, 6.8, H(3)); 3.05–2.96 (*m*, 1 H); 2.63–2.40 (*m*, 2 H); 2.04–1.75 (*m*, 2 H); 1.58–1.34 (*m*, 5 H); 1.28 (*s*, 3 H); 0.98–0.76 (*m*, 7 H), 0.30 (*s*, 3 H). NOESY (500 MHz, C_6D_6 , 15°). COSY: H(1)/H(2), H(2)/H(3), H(3)/H(4), H(4)/H(1).



N-[(2*R*,3*Z*)-4-{(2*S*)-2-[[[Methyl(diphenyl)silyl]oxy](diphenyl)methyl]pyrrolidin-1-yl]-1-nitro-3-(pentan-3-yloxy)but-3-en-2-yl]acetamide (**6j**). 1H -NMR (400 MHz, C_6D_6): 7.74–6.97 (*m*, 20 H); 5.35 (*s*, H(1)); 4.21 (*dd*, $J = 12.0$, 6.0, H(4)); 4.08 (*dd*, $J = 8.8$, 4.0, H(5)); 3.99–3.93 (*m*, H(4)); 3.91–3.87 (*m*, H(3)); 3.06–2.98 (*m*, 1 H); 2.55–2.40 (*m*, 2 H); 1.99–1.77 (*m*, 2 H); 1.60–1.46 (*m*, 5 H); 1.44 (*s*, 3 H); 0.94–0.72 (*m*, 7 H); 0.22 (*s*, 3 H). ^{13}C -NMR (100 MHz, C_6D_6): 127.3 (C(1)); 78.9 (C(3)); 77.0 (C(4)); 74.3 (C(5)). HMBC: C(1)/H(5).



5. Preparation, Identification, and Reactivity of Oxazine Derivatives **5.** 5.1. Preparation of **5b–5f** and **5h**. (4*S*,5*R*,6*R*)-6-[(2*S*)-2-{Diphenyl[(trimethylsilyl)oxy]methyl]pyrrolidin-1-yl]-5,6-dihydro-3,5-dimethyl-4-phenyl-4*H*-1,2-oxazine 2-Oxide (**5b**). Prepared according to GP from **1a** (32.6 mg, 0.1 mmol),

propanal (7.2 μ l, 0.1 mmol), and (*E*)- β -methyl- β -nitrostyrene (16.3 mg, 0.1 mmol; $t \leq 10$ min). After complete reaction, the soln. was filtered and concentrated to afford the crude product. Crystallization from hexane yielded **5b** (38 mg, 72%). Colorless crystals, suitable for X-ray analysis. M.p. 120–121° (dec). $[\alpha]_D^{25} = -13.4$ ($c = 0.83$, CHCl_3). IR (neat): 2965*m*, 1611*m*, 1493*w*, 1447*w*, 1374*w*, 1249*m*, 1138*w*, 1089*w*, 1056*m*, 878*m*, 833*s*, 787*m*, 771*m*, 747*m*, 699*s*. $^1\text{H-NMR}$ (400 MHz, C_6D_6): 7.51–7.49 (*m*, 2 H); 7.42–7.40 (*m*, 2 H); 7.16 (*s*, 5 H); 7.12–7.09 (*m*, 2 H); 7.05–7.01 (*m*, 2 H); 6.83 (*dd*, $J = 2.0, 8.0$, 2 H); 5.38 (*d*, $J = 6.8$, 1 H); 4.80 (*dd*, $J = 3.2, 9.6$, 1 H); 2.96–2.89 (*m*, 2 H); 2.19–2.15 (*m*, 1 H); 2.09–1.97 (*m*, 2 H); 1.75 (*d*, $J = 1.2$, 3 H); 1.71–1.65 (*m*, 1 H); 1.35–1.29 (*m*, 1 H); 0.88 (*d*, $J = 6.4$, 3 H); 0.64–0.59 (*m*, 1 H); –0.04 (*s*, 9 H). $^1\text{H-NMR}$ (300 MHz, C_6D_6) of **5b** at 50° in the presence of 4-Å MS was recorded, and compared to that recorded at r.t., there were no changes (cf. Table 4). $^{13}\text{C-NMR}$ (100 MHz, C_6D_6): 144.0; 141.3; 130.2; 130.2; 129.2; 128.6; 128.2; 127.9; 127.7; 127.6; 127.4; 127.1; 119.3; 100.4; 85.4; 67.7; 54.4; 45.4; 41.9; 29.1; 24.5; 17.1; 15.2; 2.2. HR-ESI-MS: 529.2881 ($[M + \text{H}]^+$, $\text{C}_{32}\text{H}_{41}\text{N}_2\text{O}_3\text{Si}^+$; calc. 529.2881 (err., 0.0 ppm)). Anal. calc. for $\text{C}_{32}\text{H}_{40}\text{N}_2\text{O}_3\text{Si}$ (528.77): C 72.69, H 7.62, N 5.30; found: C 72.85, H 7.59, N 5.24.

(4*S*,5*R*,6*R*)-6-[2*S*]-2-[Diphenyl(trimethylsilyl)oxy]methylpyrrolidin-1-yl]-5,6-dihydro-3-methyl-4-phenyl-5-propyl-4*H*-1,2-oxazine 2-Oxide (**5c**). Prepared according to GP from **1a** (32.6 mg, 0.1 mmol), valeraldehyde (10.6 μ l, 0.1 mmol), and (*E*)- β -methyl- β -nitrostyrene (16.3 mg, 0.1 mmol) ($t \leq 10$ min). After completion of the reaction, the soln. was filtered and concentrated to afford the crude product. Crystallization from hexane yielded **5c** (35 mg, 63%). Colorless crystals, suitable for X-ray analysis. M.p. 130–131° (dec). $^1\text{H-NMR}$ (400 MHz, C_6D_6): 7.50 (*dd*, $J = 2.0, 8.4$, 2 H); 7.44–7.42 (*m*, 2 H); 7.15 (*s*, 5 H); 7.11–7.07 (*m*, 2 H); 7.03–7.00 (*m*, 2 H); 6.93–6.90 (*m*, 2 H); 5.39 (*d*, $J = 7.6$, 1 H); 4.86 (*dd*, $J = 3.2, 9.6$, 1 H); 3.06 (*d*, $J = 8.0$, 1 H); 2.96 (*q*, $J = 8.8$, 1 H); 2.25–2.15 (*m*, 2 H); 2.10–1.99 (*m*, 1 H); 1.80–1.72 (*m*, 1 H); 1.75 (*d*, $J = 1.2$, 3 H); 1.53–1.43 (*m*, 1 H); 1.39–1.31 (*m*, 1 H); 1.29–1.20 (*m*, 1 H); 1.11–0.88 (*m*, 2 H); 0.75 (*t*, $J = 7.2$, 3 H); 0.65–0.55 (*m*, 1 H); –0.05 (*s*, 9 H). $^1\text{H-NMR}$ (300 MHz, C_6D_6) of **5c** at 50° in the presence of 4-Å MS was recorded, and compared to that recorded at r.t., there were no changes (cf. Table 4). $^{13}\text{C-NMR}$ (100 MHz, C_6D_6): 144.1; 143.8; 142.2; 130.2; 129.2; 128.6; 127.9; 127.7; 127.7; 127.5; 127.3; 120.1; 100.4; 85.2; 68.4; 51.9; 46.5; 46.3; 32.8; 29.2; 24.7; 19.5; 17.0; 14.6; 2.3. HR-ESI-MS: 557.3189 ($[M + \text{H}]^+$, $\text{C}_{34}\text{H}_{45}\text{N}_2\text{O}_3\text{Si}^+$; calc. 557.3194 (err., 0.9 ppm)).

(4*S*,5*R*,6*R*)-6-[2*S*]-2-[Diphenyl(trimethylsilyl)oxy]methylpyrrolidin-1-yl]-5,6-dihydro-5-isopropyl-3-methyl-4-phenyl-4*H*-1,2-oxazine 2-Oxide (**5d**). Prepared according to GP from **1a** (32.6 mg, 0.1 mmol), isovaleraldehyde (10.8 μ l, 0.1 mmol), and (*E*)- β -methyl- β -nitrostyrene (16.3 mg, 0.1 mmol; t 2 h, > 85% conversion). After completed reaction, the soln. was filtered and concentrated to afford the crude product. Crystallization from hexane yielded **5d** (38 mg, 68%). Colorless crystals (moisture-sensitive), suitable for X-ray analysis. IR (neat): 2956*w*, 1614*m*, 1493*w*, 1447*w*, 1406*w*, 1341*w*, 1248*m*, 1218*w*, 1090*w*, 1056*m*, 1032*w*, 939*w*, 909*w*, 882*m*, 836*s*, 702*s*. $^1\text{H-NMR}$ (600 MHz, C_6D_6): 7.63–7.50 (*m*, 5 H); 7.13 – 7.03 (*m*, 9 H); 7.00–6.97 (*m*, 1 H); 5.45 (*br. s*, 1 H); 5.01 (*dd*, $J = 3, 9.6$, 1 H); 3.19 (*s*, 1 H); 2.92 (*m*, 1 H); 2.43 (*m*, 1 H); 2.29–2.24 (*m*, 1 H); 2.10–2.07 (*m*, 1 H); 1.95–1.84 (*m*, 2 H); 1.80 (*s*, 3 H); 1.30–1.23 (*m*, 1 H); 0.71 (*br. s*, 3 H); 0.65 (*d*, $J = 6.6$, 3 H); 0.55–0.46 (*m*, 1 H); –0.05 (*s*, 9 H). HR-ESI-MS: 557.3209 ($[M + \text{H}]^+$, $\text{C}_{34}\text{H}_{45}\text{N}_2\text{O}_3\text{Si}^+$; calc. 557.3194 (err., –2.7 ppm)). Measurement of the temp.-dependent equilibrium of **5d** with the corresponding enamine **2** and nitro olefin **3**: $^1\text{H-NMR}$ (300 MHz, C_6D_6) of **5d** in the presence of 4-Å MS was recorded at r.t., **5d**/enamine **2** 7:1; at 50°, **5d**/enamine **2** 1.5:1; cooling the sample to r.t., after further 2 h, **5d**/enamine **2** 7:1 (cf. Table 4).

(4*R*,5*R*,6*R*)-6-[2*S*]-2-[Diphenyl(trimethylsilyl)oxy]methylpyrrolidin-1-yl]-5,6-dihydro-4,5-diisopropyl-3-methyl-4*H*-1,2-oxazine 2-Oxide (**5e**). To a soln. of **1a** (65.1 mg, 0.2 mmol) in benzene (0.1 ml, with 4-Å MS) was added isovaleraldehyde (21.6 μ l, 0.2 mmol), the mixture was stirred for 10 min, then (*E*)-3-methyl-1-nitrobut-1-ene (23.0 mg, 0.2 mmol) was added, and stirring at r.t. was continued for 90 h. Purification by prep. TLC (hexane/AcOEt, 3:1) afforded **5e** (46 mg, 44%). $[\alpha]_D^{25} = -47.7$ ($c = 1.0$, CHCl_3). IR (neat): 2958*m*, 2873*w*, 1724*w*, 1608*m*, 1493*w*, 1463*w*, 1410*w*, 1249*m*, 1091*m*, 1063*m*, 879*m*, 837*s*, 749*m*, 702*s*. $^1\text{H-NMR}$ (300 MHz, C_6D_6): 7.69–7.62 (*m*, 4 H); 7.04–7.23 (*m*, 6 H); 5.08 (*d*, $J = 10.5$, 1 H); 4.95 (*dd*, $J = 3.0, 9.0$, 1 H); 3.10–2.94 (*m*, 1 H); 2.55–2.48 (*m*, 1 H); 2.15–2.10 (*m*, 3 H); 1.94 (*s*, 3 H); 1.86–1.80 (*m*, 1 H); 1.54 – 1.47 (*m*, 1 H); 1.36–1.31 (*m*, 1 H); 0.98–0.90 (*m*, 1 H); 0.75–0.70 (*m*, 9 H); 0.65–0.56 (*m*, 1 H); 0.44 (*d*, $J = 5.7$, 3 H); –0.04 (*s*, 9 H). $^{13}\text{C-NMR}$ (100 MHz, C_6D_6): 144.1; 143.4; 130.5; 130.0; 128.2; 127.9; 127.7; 127.4; 127.3; 124.7; 102.6; 84.8; 69.2; 49.5; 47.4; 47.3; 33.5; 28.1; 25.1; 24.6;

21.5; 21.4; 20.6; 19.2; 17.2; 2.3. HR-ESI-MS: 523.3368 ($[M+H]^+$, $C_{31}H_{47}N_2O_3Si^+$; calc. 523.3350 (err., – 3.3 ppm)).

(3R,4R,4aR)-3-[(2S)-2-{Diphenyl[(trimethylsilyl)oxy]methyl}pyrrolidin-1-yl]-4,4a,5,6,7,8-hexahydro-4-isopropyl-3H-2,1-benzoxazine 1-Oxide (**5f**). Prepared according to GP from **1a** (32.6 mg, 0.1 mmol), isovaleraldehyde (10.8 μ l, 0.1 mmol), and 1-nitrocyclohexene (12.7 mg, 0.1 mmol; *t* 16 h, 50% conversion). 1H -NMR (400 MHz, C_6D_6): 7.57–7.44 (*m*, 4 H); 7.15–7.04 (*m*, 6 H); 5.24 (br. *s*, 1 H); 4.91 (*dd*, *J* = 2.8, 9.2, 1 H); 3.40 (*d*, *J* = 14.0, 1 H); 2.90 (*q*, *J* = 8.4, 1 H); 2.25–2.18 (*m*, 1 H); 2.10–2.04 (*m*, 1 H); 2.04–1.94 (*m*, 2 H); 1.90–1.82 (*m*, 1 H); 1.80–1.75 (*m*, 1 H); 1.73–1.65 (*m*, 2 H); 1.61–1.57 (*m*, 1 H); 1.46–1.51 (*m*, 2 H); 1.33–1.24 (*m*, 3 H); 0.98–0.96 (*m*, 3 H); 0.77 (*d*, *J* = 6.8, 3 H); 0.58–0.48 (*m*, 1 H); – 0.10 (*s*, 9 H). Measurement of the temp.-dependent equilibrium of **5f** with the corresponding enamine **2** and nitro olefin **3**: 1H -NMR (300 MHz, C_6D_6) of **5f** in the presence of 4-Å MS was recorded at r.t., **5f**/enamine **2** 1:1; at 50°, **5f**/enamine **2** 1:3; cooling the sample back to r.t., after further 2 h, **5f**/enamine **2** 1:1 (cf. Table 4).

Ethyl (4R,5R,6R)-6-[(2S)-2-{Diphenyl[(trimethylsilyl)oxy]methyl}pyrrolidin-1-yl]-5,6-dihydro-3-methyl-5-propyl-4H-1,2-oxazine-4-carboxylate 2-Oxide (**5h**). Prepared according to GP from **1a** (32.6 mg, 0.1 mmol), valeraldehyde (10.6 μ l, 0.1 mmol), and ethyl (*E*)-3-nitrobut-2-enoate (15.9 mg, 0.1 mmol) in the presence of 3-Å MS (*t* \leq 10 min, > 90%). 1H -NMR (600 MHz, C_6D_6): 7.48 (*d*, *J* = 7.2, 2 H); 7.40–7.39 (*m*, 2 H); 7.12–7.05 (*m*, 6 H); 5.23 (br. *s*, 1 H); 4.74 (*dd*, *J* = 2.4, 9.0, 1 H); 3.86–3.82 (*m*, 2 H); 3.05 (*q*, *J* = 7.8, 1 H); 2.91 (*s*, 2 H); 2.37 (br. *s*, 1 H); 2.02 (*s*, 3 H); 1.97–1.91 (*m*, 1 H); 1.74–1.66 (*m*, 1 H); 1.57–1.52 (*m*, 1 H); 1.29–1.12 (*m*, 4 H); 0.90 (*t*, *J* = 6.0, 3 H); 0.84 (*t*, *J* = 7.2, 3 H); 0.63–0.58 (*m*, 1 H); – 0.10 (*s*, 9 H). 1H -NMR (300 MHz, C_6D_6) of **5h** at 50° in the presence of 3-Å MS was recorded, and compared to that recorded at r.t., there were no changes (cf. Table 4). ^{13}C -NMR (100 MHz, C_6D_6): 170.6; 144.0; 143.8; 130.1; 128.5; 127.7; 127.4; 127.2; 116.8; 102.3; 85.3; 68.5; 61.6; 51.3; 46.5; 41.7; 34.2; 29.2; 24.6; 19.8; 17.1; 14.5; 2.2.

5.2. Deuterolysis of Oxazine Derivative **5b**. To a $CDCl_3$ soln. (0.3 ml) of **1a** (19 mg, 0.058 mmol) in an NMR tube, propanal (4.2 μ l, 0.058 mmol) in $CDCl_3$ (0.29 ml, 0.2M) and 3-Å MS (3 mm high) were added at r.t. After confirming the generation of enamine by NMR, (*E*)- β -methyl- β -nitrostyrene (9.5 mg, 0.058 mmol) was added. After confirming the generation of **5b**, the mixture was transferred to another dry NMR tube *via* syringe (without 3-Å MS). D_2O (1.8 μ l, 0.088 mmol) and 4- NO_2 - C_6H_4OD (33 mg, 0.234 mmol, D: 81%) were added to the NMR tube. The reaction was monitored by 1H -NMR, and the results are collected in Table 6; they show that there is D incorporation mainly in the α -position of the γ -nitro aldehyde **7r**.

Table 6. Deuterolysis of **5b**. Ratios determined by NMR peak integration.

Time [h]	5b [%]	7r [%]	Diastereoisomers [%]
0.5	89	6	5
1.5	81	14 (D: α > 50%, γ < 10%)	5
3	69	23 (D: α > 50%, γ < 10%)	8
6	57	34 (D: α > 50%, γ < 10%)	9
17	41	49 (D: α > 50%, γ < 10%)	10

6. Formation of the Nitro Enamines **6** and Their Reactions. 6.1. Formation of **6a**, **6c**–**6e**, **6g**, **6r**, and **6s**. (2S)-2-{Diphenyl[(trimethylsilyl)oxy]methyl}-1-[(1E,3R)-2-methyl-4-nitro-3-phenylbut-1-en-1-yl]pyrrolidine (**6a**). Method 1. According to GP, a mixture **4a/5a** 4:1 was prepared from **1a** (32.6 mg, 0.1 mmol), propanal (7.2 μ l, 0.1 mmol) and β -nitrostyrene (14.9 mg, 0.1 mmol), and its composition monitored by 1H -NMR. After 15 h, **6a** formed quantitatively (> 99% conversion). FC purification failed due to decomposition.

Method 2. In an NMR tube, a soln. of **1a** (32.6 mg, 0.1 mmol) in CD_2Cl_2 (0.6 ml) with MS (4 Å) was prepared, and propanal (7.2 μ l, 0.1 mmol) was added; the composition of the mixture was monitored by

¹H-NMR. After enamine formation, β -nitrostyrene (14.9 mg, 1.0 equiv.) was added, and the reaction was monitored by ¹H-NMR again; **6a** formed within 10 min (conversion > 98%).

Method 3. To a flask with 3-Å MS were added benzene (1 ml), **1a** (325 mg, 1.0 mmol) in benzene (1.5 ml), and propanal (79 μ l, 1.1 mmol) at r.t. The mixture was stirred for 5 min at r.t., and an aliquot was taken for NMR recording. After confirming the generation of enamine, β -nitrostyrene (149 mg, 1.0 mmol) was added. The mixture was stirred for 5 min, filtered with a syringe filtration device, the solvent was removed under reduced pressure, and the residue was dried under vacuum for 2 h. CH₂Cl₂ (5 ml) was added to the residue, and the soln. was stirred for 15 min. The solvent was evaporated *in vacuo*, and the residue was dried under reduced pressure to afford **6a** (432 mg, 84%). ¹H-NMR (400 MHz, C₆D₆): 7.56–7.49 (*m*, 2 H); 7.45–7.42 (*m*, 2 H); 7.17–7.03 (*m*, 9 H); 6.72 (*d*, *J* = 6.8, 2 H); 5.97 (*s*, 1 H); 4.26–4.19 (*m*, 2 H); 4.05 (*dd*, *J* = 5.2, 8.4, 1 H); 3.91 (*dd*, *J* = 6.0, 9.6, 1 H); 2.71–2.67 (*m*, 2 H); 1.79–1.65 (*m*, 2 H); 1.35 (*s*, 3 H); 1.23–1.13 (*m*, 1 H); 0.75–0.66 (*m*, 1 H); –0.09 (*s*, 9 H). ¹³C-NMR (100 MHz, C₆D₆): 144.2; 142.9; 140.9; 130.3; 129.9; 129.1; 129.0; 128.6; 127.6; 127.6; 127.3; 127.2; 127.1; 110.3; 84.2; 78.1; 73.0; 55.5; 50.7; 28.2; 24.7; 12.8; 2.2.

(2*S*)-2-[Diphenyl[(trimethylsilyl)oxy]methyl]-1-[(1*E*)-2-[(1*R*)-2-nitro-1-phenylethyl]hex-1-en-1-yl]pyrrolidine (**6c**). According to *GP*, a soln. of **4c** was prepared from **1a** (32.6 mg, 0.1 mmol), hexanal (12.3 μ l, 0.1 mmol), and β -nitrostyrene (14.9 mg, 0.1 mmol); monitoring by ¹H-NMR indicated conversion at r.t. to **6c**. ¹H-NMR (400 MHz, C₆D₆): 5.90 (*s*, 1 H); 4.31–4.26 (*m*, 1 H); 4.18 (*dd*, *J* = 7.6, 11.6, 1 H); 4.12–4.09 (*m*, 1 H); 4.03 (*t*, *J* = 8.0, 1 H); 2.83–2.78 (*m*, 1 H); 2.62 (*dd*, *J* = 7.6, 16.0, 1 H); 2.05–1.97 (*m*, 1 H); 1.78 (*dd*, *J* = 6.8, 14.0, 2 H); 1.73–1.66 (*m*, 1 H); 1.27–1.16 (*m*, 2 H); 1.14–1.07 (*m*, 2 H); 1.05–0.94 (*m*, 1 H); 0.79 (*t*, *J* = 7.2, 3 H); 0.71–0.61 (*m*, 1 H); –0.02 (*s*, 9 H).

(2*S*)-1-[(1*E*)-5-(Benzyloxy)-2-[(1*R*)-2-nitro-1-phenylethyl]pent-1-en-1-yl]-2-[diphenyl[(trimethylsilyl)oxy]methyl]pyrrolidine (**6d**). According to *GP*, a soln. of **4d** was prepared from **1a** (32.6 mg, 0.1 mmol), 5-(benzyloxy)pentanal (19.2 mg, 0.1 mmol), and β -nitrostyrene (14.9 mg, 0.1 mmol); monitoring by ¹H-NMR indicated conversion at r.t. to **6d**. ¹H-NMR (400 MHz, C₆D₆): 7.81–6.85 (*m*, 20 H); 6.01 (*s*, 1 H); 4.32 (*s*, 2 H); 4.29–4.03 (*m*, 3 H); 3.27–3.09 (*m*, 2 H); 3.01–2.91 (*m*, 1 H); 2.77–2.61 (*m*, 1 H); 2.28–2.19 (*m*, 1 H); 1.98–1.17 (*m*, 7 H); 0.77–0.63 (*m*, 1 H); 0.02 (*s*, 9 H).

(2*S*)-2-[Diphenyl[(trimethylsilyl)oxy]methyl]-1-[(1*E*,3*R*)-2-isopropyl-4-nitro-3-phenylbut-1-en-1-yl]pyrrolidine (**6e**). According to *GP*, a soln. of **4e** was prepared from **1a** (32.6 mg, 0.1 mmol), isovaleraldehyde (10.8 μ l, 0.1 mmol), and β -nitrostyrene (14.9 mg, 0.1 mmol); monitoring by ¹H-NMR showed 29% conversion after 24 h at r.t., with formation of **6e**. ¹H-NMR (400 MHz, C₆D₆): 8.00–6.60 (*m*, 15 H); 5.65 (*s*, 1 H); 4.19 (*dd*, *J* = 7.2, 8.8, 1 H); 4.20–4.00 (*m*, 2 H); 2.96 (*dt*, *J* = 6.8, 14.0, 1 H); 2.80–2.60 (*m*, 1 H); 2.55 (*ddd*, *J* = 5.6, 8.0, 9.6, 1 H); 2.0–1.60 (*m*, 2 H); 1.18–1.10 (*m*, 1 H); 0.97 (*d*, *J* = 6.8, 3 H); 0.70 (*d*, *J* = 6.8, 3 H); 1.40–0.40 (*m*, 2 H); –0.06 (*s*, 9 H).

tert-Butyl (2*R*,3*E*)-3-[(2*S*)-2-[Diphenyl[(trimethylsilyl)oxy]methyl]pyrrolidin-1-yl]methylidene]-4-methyl-2-(nitromethyl)pentanoate (**6g**). According to *GP*, a soln. of **4g** was prepared from **1a** (32.6 mg, 0.1 mmol), isovaleraldehyde (10.8 μ l, 0.1 mmol), and *tert*-butyl (*E*)-3-nitroacrylate (17.3 mg, 0.1 mmol), monitoring by ¹H-NMR showed after 40 h > 90% conversion to **6g**. ¹H-NMR (C₆D₆, 400 MHz): 7.63–6.99 (*m*, 10 H); 5.81 (*s*, 1 H); 4.70 (*dd*, *J* = 2.4, 9.6, 1 H); 4.39 (*dd*, *J* = 9.6, 13.6, 1 H); 4.01 (*dd*, *J* = 6.2, 8.2, 1 H); 3.51 (*dd*, *J* = 3.0, 12.2, 1 H); 2.83–2.75 (*m*, 1 H); 2.73–2.61 (*m*, 2 H); 1.82–1.62 (*m*, 4 H); 1.31 (*s*, 9 H); 1.05 (*d*, *J* = 7.2, 3 H); 0.68 (*d*, *J* = 7.2, 3 H); –0.05 (*s*, 9 H).

(2*S*)-2-[Diphenyl[(trimethylsilyl)oxy]methyl]-1-[(1*E*,3*R*,4*R*)-2-methyl-4-nitro-3-phenylpent-1-en-1-yl]pyrrolidine (**6r**). To a soln. of **1a** (18.9 mg, 0.058 mmol) in (D₈)toluene (0.6 ml) with MS (3 Å) in an NMR tube was added nitro aldehyde **7r** [12] (12.8 mg, 0.058 mmol), and the reaction was monitored by ¹H-NMR; **6r** was formed within 10 min (conversion > 90%) at r.t. ¹H-NMR (400 MHz, (D₈)toluene): 7.48–7.45 (*m*, 2 H); 7.40–7.37 (*m*, 2 H); 7.10–6.93 (*m*, 11 H); 5.95 (*s*, 1 H); 4.92–4.84 (*m*, 1 H); 4.11 (*dd*, *J* = 5.2, 8.4, 1 H); 3.65 (*d*, *J* = 10.8, 1 H); 2.67–2.62 (*m*, 1 H); 2.51–2.46 (*m*, 1 H); 1.88–1.71 (*m*, 2 H); 1.27 (*d*, *J* = 6.8, 3 H); 1.19 (*d*, *J* = 0.8, 3 H); 1.23–1.14 (*m*, 1 H); 0.76–0.66 (*m*, 1 H); –0.11 (*s*, 9 H). ¹³C-NMR (100 MHz, (D₈)toluene): 144.4; 143.0; 141.1; 140.4; 130.5; 130.2; 128.8; 128.1; 128.1; 128.0; 127.6; 127.5; 127.4; 111.9; 84.5; 84.4; 73.3; 57.3; 55.9; 28.7; 25.2; 19.8; 13.4; 2.5.

Ethyl (2*R*,3*E*)-3-[(2*S*)-2-[Diphenyl[(trimethylsilyl)oxy]methyl]pyrrolidin-1-yl]methylidene]-2-[(1*R*)-1-nitroethyl]hexanoate (**6s**). According to *GP*, a soln. of **5h** was prepared from **1a** (32.6 mg, 0.1 mmol), valeraldehyde (10.6 μ l, 0.1 mmol), and ethyl (*E*)-3-nitrobut-2-enoate (15.9 mg, 0.1 mmol) in

the presence of MS (3 Å); monitoring by $^1\text{H-NMR}$ showed conversion (t 3 d, >99%, dr 95:5) to **6s**. $^1\text{H-NMR}$ (400 MHz, C_6D_6): 7.47 (d , $J=7.2$, 2 H); 7.41–7.39 (m , 2 H); 7.20–7.09 (m , 6); 6.09 (s , 1 H); 4.64–4.54 (m , 1 H); 4.15 (t , $J=6.4$, 1 H); 3.94 (q , $J=6.8$, 1 H); 3.40 (d , $J=11.2$, 1 H); 2.73–2.64 (m , 2 H); 2.19–2.11 (m , 1 H); 1.75–1.66 (m , 3 H); 1.61–1.55 (m , 1 H); 1.30–1.26 (m , 1 H); 1.13–1.06 (m , 1 H); 1.03 (d , $J=6.8$, 3 H); 0.94 (t , $J=6.8$, 3 H); 0.88 (t , $J=7.2$, 3 H); 0.66–0.58 (m , 1 H); –0.13 (s , 9 H). $^{13}\text{C-NMR}$ (100 MHz, C_6D_6): 172.9; 143.4; 142.3; 140.1; 130.2; 129.8; 127.5; 127.3; 106.5; 83.9; 73.2; 60.9; 54.1; 53.7; 34.4; 27.6; 24.6; 23.5; 18.3; 14.8; 14.1; 2.1.

6.2. *Conversion of 6r to Oxazine 5b*. To the soln. of **6r** (30.7 mg, 0.058 mmol) in (D_8)toluene (0.6 ml) in the presence of MS (3 Å) in an NMR tube was added 4-nitrophenol (3.2 mg, 40 mol-%), and the reaction was monitored by $^1\text{H-NMR}$. The oxazine *N*-oxide **5b** was slowly formed at r.t. (24 h, 30% conversion). For NMR data *vide supra*, *Exper. Part*, *Sect. 5*. We assume that the resulting ratio **6r/5b** 7:3 is a thermodynamic ratio.

6.3. *Deuterium Labeling of 6a*. To a C_6D_6 soln. (0.6 ml) of **1a** (32.6 mg, 0.1 mmol) in an NMR tube were added 3-Å MS (3 mm high) and [2,2- D_2]propanal (7.5 μl , 0.1 mmol) at rt, the mixture was agitated and allowed to stand for 15 min. The $^1\text{H-NMR}$ spectrum was recorded to check the H/D ratio. β -Nitrostyrene (14.9 mg, 0.1 mmol) was then added to the NMR tube, and formation of cyclobutane and oxazine was confirmed by $^1\text{H-NMR}$. After keeping the NMR tube for 20 h at r.t., H/D ratio in the α -position to the NO_2 group of **6a** was determined by $^1\text{H-NMR}$ as 26% D incorporation (*Scheme 6, b*).

6.4. *Diastereoselectivity of the Hydrolysis of 6a to Nitro Aldehyde 7a*. To a benzene soln. (8 ml) of **6a** (257 mg, 0.5 mmol) were added H_2O (9 mg, 0.5 mmol) in benzene (2 ml) and 4-nitrophenol (69.5 mg, 0.5 mmol) at r.t. The mixture was stirred at r.t., and aliquots were taken for $^1\text{H-NMR}$ recordings to check the diastereoisomer ratio of *Michael* product **7a** at 15 min, 30 min, 1.5 h, 16 h, and 40 h. The results are compiled in *Scheme 7*.

7. *Reaction of the Michael Adduct 8 of 1a with tert-Butyl 3-Nitroacrylate*. 7.1. *Formation of 8 in C_6D_6 or in CD_2Cl_2* . *tert-Butyl (2R)-2-[(2S)-2-{Diphenyl[(trimethylsilyl)oxy]methyl}pyrrolidin-1-yl]-3-nitropropanoate (8)*. To a soln. of *tert*-butyl (*E*)-3-nitroacrylate (8.7 mg, 0.05 mmol) in C_6D_6 (0.6 ml) or in CD_2Cl_2 (0.6 ml) in an NMR tube, **1a** (16.3 mg, 0.05 mmol) was added, the mixture was agitated, and the reaction was monitored by $^1\text{H-NMR}$. The adduct **8** was formed (in C_6D_6 : t 30 min, >99% conversion, dr 1.5:1; in CD_2Cl_2 : t 10 min, >99% conversion, dr 1:1). $^1\text{H-NMR}$ (400 MHz, C_6D_6): Major diastereoisomer: 7.63–7.61 (m , 2 H); 7.52–7.47 (m , 2 H); 7.18–7.04 (m , 6 H); 4.88 (t , $J=7.2$, 1 H); 4.78 (dd , $J=2.4$, 9.6, 1 H); 4.40 (dd , $J=8.8$, 13.2, 1 H); 4.13–4.05 (m , 1 H); 2.50–2.44 (m , 1 H); 2.42–2.32 (m , 1 H); 1.99–1.89 (m , 1 H); 1.79–1.74 (m , 1 H); 1.31 (s , 9 H); 1.21–1.14 (m , 1 H); 0.59–0.51 (m , 1 H); –0.07 (s , 9 H); minor diastereoisomer: 7.63–7.61 (m , 2 H); 7.52–7.47 (m , 2 H); 7.18–7.04 (m , 6 H); 4.80–4.74 (m , 1 H); 4.62 (dd , $J=8.8$, 10.0, 1 H); 4.13–4.05 (m , 1 H); 3.93 (dd , $J=3.2$, 9.2, 1 H); 2.42–2.32 (m , 1 H); 2.26–2.20 (m , 1 H); 1.65–1.54 (m , 2 H); 1.37 (s , 9 H); 0.98–0.89 (m , 1 H); 0.36–0.24 (m , 1 H); –0.06 (s , 9 H).

7.2. *Reaction between Adduct 8 and Isovaleraldehyde (= 3-Methylbutanal)*. To a soln. of **8** (24.9 mg, 0.05 mmol) in C_6D_6 (0.6 ml) or in CD_2Cl_2 (0.6 ml) in an NMR tube isovaleraldehyde (5.4 μl , 0.05 mmol) was added, the reaction was monitored by $^1\text{H-NMR}$ to follow the formation of **4g**, **6g**, and **7g**. The results are collected in *Table 7*. For NMR data of **4g** and **6g**, *vide supra*, *Sect. 3* and *6* in the *Exper. Part*, resp.

Table 7. *Reaction of 8 with 3-Methylbutanal*. Ratios determined by NMR-peak integration of the products **4g**, **6g**, and **7g**.

Solvent	Time [h]	8 [%]	4g [%]	6g [%]	7g [%]
CD_2Cl_2	1	81	19		
	18	7	12	23	58 (dr 4:1)
	72			28	72 (dr 1.6:1)
(D_6) benzene	19	63	37		
	96	33	15	7	45 (dr 1.4:1)

tert-Butyl (2*R*)-3-Formyl-4-methyl-2-(nitromethyl)pentanoate (**7g**). ¹H-NMR (300 MHz, CD₂Cl₂) 9.79 (*d*, *J* = 1.5, 1 H); 4.80 (*dd*, *J* = 10.5, 14.4, 1 H); 4.35 (*dd*, *J* = 3.3, 14.7, 1 H); 3.56–3.49 (*m*, 1 H); 2.82–2.76 (*m*, 1 H); 1.64–1.60 (*m*, 1 H); 1.44 (*s*, 9 H); 0.97 (*d*, *J* = 6.0, 6 H).

8. Intermediates **13** and **14** in Tripeptide-Catalyzed Michael Additions. Methyl (4*S*)-4-(((2*S*)-1-((2*R*)-1-[(1*R*,2*S*,3*R*,4*R*)-3-(*tert*-Butyl)-2-isopropyl-4-nitrocyclobutyl]pyrrolidin-2-yl)carbonyl)pyrrolidin-2-yl)carbonyl)amino)-5-(dodecylamino)-5-oxopentanoate (**13**). To a soln. of **11c** [19] (26 mg, 0.05 mmol) in C₆D₆ (0.6 ml) with MS (4 Å) in an NMR tube, isovaleraldehyde (5.4 µl, 0.05 mmol) was added, the mixture was agitated, and the reaction was monitored by ¹H-NMR to follow the enamine formation. When **12b** had been formed, (*E*)-3,3-dimethyl-1-nitrobut-1-ene (6.5 mg, 0.05 mmol) was added, and the mixture was agitated at r.t., and then the reaction was monitored by ¹H-NMR to detect the formation of cyclobutane **13** (t 20 h). Purification by prep. TLC (AcOEt) afforded **13** (19 mg, 52%). ¹H-NMR (600 MHz, C₆D₆): 7.22 (*d*, *J* = 7.8, 1 H); 6.98 (*t*, *J* = 4.8, 1 H); 4.71–4.67 (*m*, 2 H); 4.43 (*dd*, *J* = 4.2, 7.2, 1 H); 3.91 (*dd*, *J* = 7.2, 9.0, 1 H); 3.59–3.53 (*m*, 2 H); 3.36 (*s*, 3 H); 3.35–3.31 (*m*, 1 H); 3.19–3.14 (*m*, 1 H); 2.93 (*td*, *J* = 3.6, 7.8, 1 H); 2.88–2.84 (*m*, 1 H); 2.52–2.46 (*m*, 2 H); 2.42–2.39 (*m*, 2 H); 2.37–2.33 (*m*, 1 H); 2.26–2.19 (*m*, 1 H); 2.01–1.98 (*m*, 1 H); 1.85–1.79 (*m*, 2 H); 1.74–1.66 (*m*, 2 H); 1.63–1.55 (*m*, 3 H); 1.50–1.45 (*m*, 1 H); 1.39–1.21 (*m*, 21 H); 1.13 (*d*, *J* = 6.6, 3 H); 1.10 (*d*, *J* = 6.6, 3 H); 0.92 (*t*, *J* = 7.2, 3 H); 0.76 (*s*, 9 H); ¹³C-NMR (100 MHz, C₆D₆): 174.1; 172.7; 171.4; 170.8; 78.2; 62.0; 61.8; 60.5; 54.0; 51.3; 48.4; 47.1; 47.0; 41.9; 40.0; 32.4; 31.8; 31.0; 30.2; 30.2; 30.1; 30.1; 30.0; 29.9; 29.9; 28.9; 27.4; 27.4; 25.0; 23.3; 23.2; 21.3; 18.5; 14.4. HR-ESI-MS: 720.5269 (*[M + H]*⁺, C₃₉H₇₀N₅O₇; calc. 720.5270 (err., 0.1 ppm)).

Methyl (4*S*)-4-(((2*S*)-1-((2*R*)-1-[(4*R*,5*S*,6*S*)-3,5-Dimethyl-2-oxido-4-phenyl-5,6-dihydro-4*H*-1,2-oxazin-6-yl]pyrrolidin-2-yl)carbonyl)pyrrolidin-2-yl)carbonyl)amino)-5-(dodecylamino)-5-oxopentanoate (**14a**). To a soln. of **11c** [19] (20 mg, 0.038 mmol) in C₆D₆ (0.6 ml) with MS (4 Å) in an NMR tube was added propanal (2.7 µl, 0.038 mmol) was added, the mixture was agitated, and the reaction was monitored by ¹H-NMR to follow the enamine formation. When enamine formation was complete, (*E*)-β-methyl-β-nitrostyrene (6.2 mg, 0.038 mmol) was added, and the mixture was agitated at r.t., and then the reaction was monitored by ¹H-NMR; **14a** was formed with complete conversion within 10 min. Purification failed due to decomposition. ¹H-NMR (400 MHz, C₆D₆): 7.57 (*d*, *J* = 8.0, 1 H); 7.12–6.97 (*m*, 5 H); 6.84–6.82 (*m*, 1 H); 5.27 (*d*, *J* = 10.0, 1 H); 4.72–4.67 (*m*, 1 H); 4.47 (*dd*, *J* = 3.6, 8.4, 1 H); 4.31 (*t*, *J* = 6.8, 1 H); 3.74–3.69 (*m*, 1 H); 3.50–3.44 (*m*, 1 H); 3.40 (*s*, 3 H); 3.39–3.35 (*m*, 1 H); 3.21–3.11 (*m*, 1 H); 3.05–3.00 (*m*, 1 H); 2.94–2.83 (*m*, 2 H); 2.52–2.44 (*m*, 1 H); 2.40–2.30 (*m*, 2 H); 2.20–2.11 (*m*, 2 H); 2.00–1.93 (*m*, 1 H); 1.80 (*d*, *J* = 0.8, 3 H); 1.71–1.52 (*m*, 6 H); 1.36–1.20 (*m*, 21 H); 1.14 (*d*, *J* = 6.4, 3 H); 0.91 (*t*, *J* = 6.8, 3 H). ¹³C-NMR (100 MHz, C₆D₆): 174.5; 172.7; 172.1; 171.1; 141.3; 130.1; 129.6; 129.2; 128.8; 127.6; 122.1; 97.0; 61.7; 60.8; 53.9; 53.5; 51.6; 47.2; 43.7; 41.5; 40.1; 32.4; 30.8; 30.2; 30.2; 30.1; 30.0; 29.9; 29.3; 29.1; 27.7; 27.5; 25.1; 24.4; 23.2; 17.4; 14.8; 14.4.

Methyl (4*S*)-5-(Dodecylamino)-4-(((2*S*)-1-((2*R*)-1-[(4*R*,5*S*,6*S*)-3-methyl-2-oxido-4-phenyl-5-(propan-2-yl)-5,6-dihydro-4*H*-1,2-oxazin-6-yl]pyrrolidin-2-yl)carbonyl)pyrrolidin-2-yl)carbonyl)amino)-5-oxopentanoate (**14b**) and Methyl (4*S*)-5-(Dodecylamino)-4-(((2*S*)-1-((2*R*)-1-[(1*R*,2*R*,3*R*,4*S*)-2-methyl-2-nitro-3-phenyl-4-(propan-2-yl)cyclobutyl]pyrrolidin-2-yl)carbonyl)pyrrolidin-2-yl)carbonyl)amino)-5-oxopentanoate (**14c**). To a soln. of **11c** [19] (22 mg, 0.042 mmol) in C₆D₆ (0.6 ml) with MS (3 Å) in an NMR tube, isovaleraldehyde (4.6 µl, 0.042 mmol) was added, the mixture was agitated, and the reaction was monitored by ¹H-NMR to follow the enamine formation. When **12b** had been formed, (*E*)-β-methyl-β-nitrostyrene (6.8 mg, 0.042 mmol) was added, and the mixture was agitated at r.t., and then the reaction was monitored by ¹H-NMR; **14b** and **14c** were formed in 2 h (conversion > 85%). The two compounds were identified and characterized by 1D- and 2D-NMR (COSY, HSQC, HMBC, and NOESY). The equilibration between **14b** and **14c** 1:1.5 was detected by an EXSY spectrum. Measurement of temp.-dependent equilibrium between **14b** and **14c**, and the corresponding enamine **12b** and nitro olefin: ¹H-NMR (300 MHz, C₆D₆) at r.t.: **12b/14b/14c** 1:7:10.5; at 50°, **12b/14b/14c** 1:1.5:2.5; cooling the sample back to r.t., after further 2 h, **12b/14b/14c** 1:7:10.5. Purification failed due to decomposition.

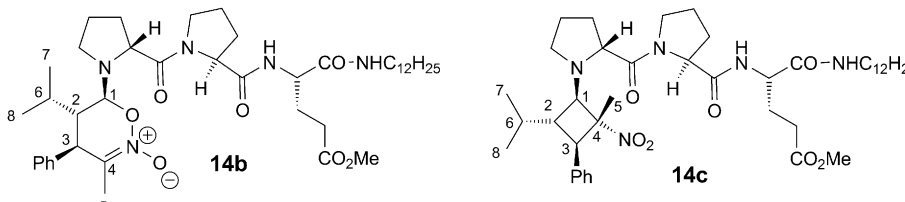
Data of **14b**: ¹H-NMR (400 MHz, C₆D₆): 7.53 (*d*, *J* = 7.2, 1 H); 7.34 (*d*, *J* = 8.0, 1 H); 7.23–6.97 (*m*, 4 H); 6.95–6.93 (*m*, 1 H); 5.36 (*d*, *J* = 9.6, 1 H); 4.73–4.64 (*m*, 1 H); 4.50–4.46 (*m*, 1 H); 4.36–4.32 (*m*,

1 H); 3.50–3.41 (*m*, 1 H); 3.44 (*s*, 3 H); 3.40–2.82 (*m*, 7 H); 2.58–1.98 (*m*, 5 H); 1.81 (*s*, 3 H); 1.72–1.50 (*m*, 6 H); 1.35–1.21 (*m*, 22 H); 1.15 (*d*, *J* = 7.2, 3 H); 0.95 (*d*, *J* = 7.2, 3 H); 0.91 (*t*, *J* = 6.8, 3 H).

Data of **14c**: 7.39 (*d*, *J* = 7.2, 2 H); 7.26–6.82 (*m*, 5 H); 4.82–4.76 (*m*, 1 H); 4.61 (*dd*, *J* = 3.2, 8.4, 1 H); 4.27 (*d*, *J* = 8.8, 1 H); 4.07 (*d*, *J* = 10.8, 1 H); 4.05–4.01 (*m*, 1 H); 3.80–3.73 (*m*, 1 H); 3.38 (*s*, 3 H); 3.40–2.82 (*m*, 6 H); 2.58–1.98 (*m*, 5 H); 1.72–1.50 (*m*, 6 H); 1.35–1.21 (*m*, 22 H); 1.15 (*s*, 3 H); 1.12 (*d*, *J* = 6.8, 3 H); 0.99 (*d*, *J* = 6.8, 3 H); 0.91 (*t*, *J* = 6.8, 3 H).

The most characteristic NMR chemical shifts of **14b** and **14c** are given in Table 8. **14c**: HMBC (400 MHz, C₆D₆): C(1)/H(5), C(3)/H(5), C(4)/H(1), C(4)/H(3), C(4)/H(5). NOESY (600 MHz, C₆D₆): H(2)/H(5), H(1)/H(6), H(1)/H(7), H(1)/H(8), H(3)/H(6), H(3)/H(7), H(3)/H(8). For atom numbering, see Table 8.

Table 8. Comparison of Characteristic NMR Chemical Shifts of **14b** and **14c**



Position	14b		14c	
	$\delta(\text{H})$ [ppm]	$\delta(\text{C})$ [ppm]	$\delta(\text{H})$ [ppm]	$\delta(\text{C})$ [ppm]
1	5.36 (<i>d</i> , <i>J</i> = 9.6)	96.3	4.27 (<i>d</i> , <i>J</i> = 8.8)	62.1
2	2.48 (<i>m</i>)	51.8	2.25 (<i>m</i>)	42.7
3	3.41 (<i>m</i>)	47.9	4.07 (<i>d</i> , <i>J</i> = 10.8)	47.2
4		123.1		91.7
5	1.81 (<i>s</i>)	16.9	1.15 (<i>s</i>)	17.4

9. Reactions with OH-Substituted Nitro Olefins **15** and **19**. (2*S*)-2-[Diphenyl[(trimethylsilyl)oxy]methyl]-1-[(2*R*,3*R*,4*S*)-3,4-dihydro-3-isopropyl-4-(nitromethyl)-2*H*-chromen-2-yl]pyrrolidine (**21**). Prepared according to GP from **1a** (32.6 mg, 0.1 mmol), isovaleraldehyde (10.8 μ l, 0.1 mmol), and (E)-2-(2-nitroethenyl)phenol (**19**; 16.5 mg, 0.1 mmol; *t* 10 min). After completion of the reaction (monitoring by ¹H-NMR), the soln. was filtered and concentrated to afford the crude product. Crystallization from hexane yielded **21** (25 mg, 45%). Pale-yellow crystals, suitable for X-ray analysis. M.p. 101–102° (dec). ¹H-NMR (400 MHz, C₆D₆): 7.55 (*d*, *J* = 7.2, 2 H); 7.48–7.46 (*m*, 2 H); 7.20–6.94 (*m*, 9 H); 6.67 (*td*, *J* = 1.2, 7.2, 1 H); 4.90 (*d*, *J* = 10.8, 1 H); 4.83 (*dd*, *J* = 3.2, 9.2, 1 H); 4.15 (*d*, *J* = 7.2, 2 H); 3.60 (*td*, *J* = 3.6, 7.2, 1 H); 2.52 (*q*, *J* = 9.2, 1 H); 2.19–2.10 (*m*, 2 H); 2.05–2.00 (*m*, 1 H); 1.58–1.53 (*m*, 1 H); 1.41–1.29 (*m*, 2 H); 0.84 (*d*, *J* = 6.8, 3 H); 0.62–0.69 (*m*, 1 H); 0.50 (*d*, *J* = 5.6, 3 H); –0.07 (*s*, 9 H). ¹³C-NMR (100 MHz, C₆D₆): 156.0; 144.4; 144.0; 130.2; 129.8; 129.6; 128.4; 128.2; 127.9; 127.7; 127.4; 127.3; 124.8; 120.4; 116.6; 93.4; 84.8; 77.4; 69.7; 46.5; 44.5; 37.7; 29.7; 27.8; 24.8; 22.2; 19.6; 2.3. HR-ESI-MS: 559.2987 ([*M* + H]⁺, C₃₃H₄₃N₂O₄Si⁺; calc. 559.2987 (err., 0.0 ppm)).

(2*S*)-2-[Diphenyl[(trimethylsilyl)oxy]methyl]-1-[(2*R*,3*R*,4*S*,5*S*)-5-nitro-4-phenyl-3-propyltetrahydro-2*H*-pyran-2-yl]pyrrolidine (**22a**). Prepared according to GP from **1a** (32.6 mg, 0.1 mmol), valeraldehyde (10.8 μ l, 0.1 mmol), and **15** (17.9 mg, 0.1 mmol; *t* 10 min). FC (hexane/EA 10:1) afforded **22a** (44 mg, 77%). Colorless solid. M.p. 145–146° (dec). *R*_f(hexane/AcOEt 10:1) 0.43. [α]_D²⁵ = –141.7 (*c* = 0.50, CHCl₃). ¹H-NMR (400 MHz, CDCl₃): 7.58–7.56 (*m*, 2 H); 7.54–7.51 (*m*, 2 H); 7.35–7.26 (*m*, 9 H); 7.19–7.16 (*m*, 2 H); 4.77 (*td*, *J* = 4.8, 10.8, 1 H); 4.51 (*dd*, *J* = 3.2, 8.8, 1 H); 4.43 (*dd*, *J* = 4.8, 10.8, 2 H); 3.82 (*t*, *J* = 10.4, 1 H); 3.14 (*t*, *J* = 11.6, 1 H); 2.94–2.87 (*m*, 1 H); 2.36 (*td*, *J* = 2.4, 8.4, 1 H); 1.95–1.84 (*m*, 3 H); 1.36–1.18 (*m*, 3 H); 1.02–0.87 (*m*, 2 H); 0.61 (*t*, *J* = 7.2, 3 H); 0.38–0.27 (*m*, 1 H); –0.14 (*s*, 9 H). ¹³C-NMR (100 MHz, CDCl₃): 143.7; 137.8; 130.0; 129.9; 129.0; 128.0; 127.9; 127.5; 127.3; 127.2;

Table 9. Experimental Details for the X-Ray Structures of **4a**, **5b**, **5c**, **5d**, **21**, and **23**

	4a	5b	5c	5d	21	23
CCDC No. ^{a)}	883666	883668	919662	883667	919664	919663
Chemical formula	C ₃₁ H ₄₆ N ₂ O ₃ Si	C ₃₂ H ₄₀ N ₂ O ₃ Si	C ₃₄ H ₄₄ N ₂ O ₃ Si	C ₃₄ H ₄₄ N ₂ O ₃ Si	C ₃₃ H ₄₂ N ₂ O ₄ Si	C ₃₁ H ₃₆ N ₂ O ₄
<i>M_r</i> [g/mol]	522.79	528.75	556.80	556.80	558.78	500.62
Crystal size [mm]	0.20 x 0.12 x 0.03 mm	0.18 x 0.16 x 0.12 mm	0.12 x 0.08 x 0.04 mm	0.26 x 0.18 x 0.16 mm	0.28 x 0.22 x 0.20 mm	0.20 x 0.18 x 0.02 mm
Space group	<i>P</i> 2 ₁ 2 ₁ 2 ₁	<i>P</i> 2 ₁	<i>P</i> 2 ₁	<i>P</i> 2 ₁	<i>P</i> 2 ₁ 2 ₁ 2 ₁	<i>C</i> 2
Crystal shape	Orthorhombic	Monoclinic	Monoclinic	Monoclinic	Orthorhombic	Monoclinic
<i>a</i> [Å]	10.4899(6)	9.5550(3)	9.6978(9)	10.4708(4)	9.1983(3)	23.940(2)
<i>b</i> [Å]	14.9108(6)	10.7941(3)	10.5115(9)	14.1448(6)	15.0166(5)	7.1220(6)
<i>c</i> [Å]	19.2209(10)	14.6652(4)	15.0807(13)	10.6950(5)	21.6324(7)	15.3957(13)
<i>α</i> [°]	90.00	90.00	90.00	90.00	90.00	90.00
<i>β</i> [°]	90.00	92.0530(10)	90.194(6)	98.722(2)	90.00	95.976(7)
<i>γ</i> [°]	90.00	90	90.00	90.00	90.00	90.00
<i>V</i> [Å ³]	3006.4(3)	1511.56(8)	1537.3(2)	1565.69(12)	2988.02(17)	2610.7(4)
<i>Z</i>	4	2	2	2	4	4
<i>ρ</i> _{calc} [g·cm ^{−3}]	1.155	1.162	1.203	1.181	1.242	1.274
<i>μ</i> [mm ^{−1}]	0.111	0.111	0.113	0.111	0.118	0.084
Temp. [K]	100(2)	100(2)	100(2)	100(2)	100(2)	100(2)
<i>θ</i> _{max} [°]	27.52	27.51	27.58	27.63	27.65	27.58
Reflections:						
independent	6908	5576	6311	7206	6806	5523
observed (<i>I</i> > 2σ)	5851	5165	4090	5822	6104	4637
Variables	519	490	537	396	529	478
<i>R</i> (all)	0.0547	0.0332	0.1038	0.0634	0.0439	0.0514
<i>R</i> (gt)	0.0412	0.0284	0.0544	0.0449	0.0356	0.0367
<i>Flack</i>	−0.2(1)	0.0(1)	0.1(2)	−0.0(1)	−0.0(1)	−0.5(8)
<i>Δ</i> / <i>σ</i> _{max}	0.005	0.002	0.001	0.018	0.001	0.001
<i>Δρ</i> _{max} [e Å ^{−3}]	0.267	0.228	0.443	0.275	0.523	0.257

^{a)} Copies of the data can be obtained, free of charge, on application to the Cambridge Crystallographic Data Centre (CCDC), 12 Union Road, Cambridge, CB2 1EZ, UK (fax: +44-1223-336033; e-mail: deposit@ccdc.cam.ac.uk).

127.1; 95.6; 88.6; 84.2; 68.3; 68.1; 50.4; 46.4; 43.4; 29.9; 28.9; 24.1; 14.7; 2.3. HR-ESI-MS: 573.3141 ($[M + H]^+$, $C_{34}H_{45}N_2O_4Si^+$; calc. 573.3143 (err., 0.4 ppm)).

(2S)-2-[Diphenyl(trimethylsilyl)oxy]methyl]-1-[(2R,3R,4S,5S)-3-isopropyl-5-nitro-4-phenyltetrahydro-2H-pyran-2-yl]pyrrolidine (**22b**). Prepared according to GP from **1a** (32.5 mg, 0.1 mmol), isovaleraldehyde (10.8 μ l, 0.1 mmol), and **15** (17.9 mg, 0.1 mmol; t 10 min). FC (hexane/AcOEt 10:1) afforded **22b** (38 mg, 66%). Colorless solid. M.p. 79–80° (dec). R_f (hexane/AcOEt 10:1) 0.50. $[\alpha]_D^{25} = -131.7$ ($c = 1.90$, $CHCl_3$). IR (neat): 2931w, 2955w, 1736w, 1602w, 1548m, 1493w, 1448w, 1382w, 1344w, 1250m, 1215w, 1136w, 1087m, 1061m, 908m, 898m, 878m, 836s, 732s, 700s. 1H -NMR (600 MHz, $CDCl_3$): 7.76 (m, 4 H); 7.31–7.30 (m, 6 H); 7.25–7.28 (m, 2 H); 7.23–7.21 (m, 1 H); 7.18 (d, $J = 7.8$, 2 H); 4.74 (td, $J = 4.8$, 10.8, 1 H); 4.53 (q, $J = 10.8$, 1 H); 4.45 (br. s, 1 H); 4.37 (dd, $J = 6.0$, 10.2, 1 H); 3.77 (t, $J = 10.8$, 1 H); 3.25 (t, $J = 10.8$, 1 H); 2.85 (q, $J = 10.8$, 1 H); 2.32 (t, $J = 6.6$, 1 H); 2.07 (br. s, 1 H); 1.91 (t, $J = 10.8$, 1 H); 1.87–1.85 (m, 2 H); 1.32–1.27 (m, 1 H); 0.61 (br. s, 3 H); 0.41–0.32 (m, 1 H); 0.21 (d, $J = 6.0$, 3 H); –0.17 (s, 9 H). ^{13}C -NMR (100 MHz, $CDCl_3$): 143.8; 138.8; 130.0; 129.9; 128.8; 127.8; 127.3; 127.2; 127.1; 95.0; 89.6; 84.6; 68.0; 67.8; 48.4; 47.9; 46.4; 29.9; 26.7; 24.0; 22.2; 17.3; 2.3. HR-ESI-MS: 573.3138 ($[M + H]^+$, $C_{34}H_{45}N_2O_4Si^+$; calc. 573.3143 (err., 0.9 ppm)).

{(2S)-1-[(2R,3R,4S,5S)-Tetrahydro-3-isopropyl-5-nitro-4-phenyl-2H-pyran-2-yl]pyrrolidin-2-yl}(diphenyl)methanol (**23**). To a soln. of **22b** (27 mg, 0.047 mmol) in EtOH (0.5 ml) HCl (10%, 0.5 ml) was added. The mixture was stirred at r.t., and the reaction was monitored by TLC. After 1 h, the reaction was complete. After addition of AcOEt the soln. was dried (Na_2SO_4) and concentrated. FC (hexane/AcOEt 4:1) afforded **23** (19 mg, 81%). Recrystallization from hexane/Et₂O yielded colorless crystals, suitable for X-ray analysis. M.p. 170–171°. R_f (Hexane/AcOEt 4:1) 0.56. $[\alpha]_D^{25} = -83.6$ ($c = 0.64$, $CHCl_3$). 1H -NMR (400 MHz, $CDCl_3$): 7.76 (d, $J = 7.2$, 2 H); 7.58 (d, $J = 7.2$, 2 H); 7.37 (t, $J = 7.2$, 2 H); 7.31–7.24 (m, 7 H); 7.15 (t, $J = 6.8$, 2 H); 4.78–4.75 (m, 1 H); 4.71 (dt, $J = 4.8$, 10.8, 1 H); 4.28 (dd, $J = 4.8$, 10.8, 1 H); 4.13 (s, 1 H); 3.66 (d, $J = 9.6$, 1 H); 3.34 (t, $J = 10.4$, 1 H); 3.23–3.17 (m, 1 H); 2.99–2.93 (m, 1 H); 2.96 (t, $J = 11.2$, 1 H); 1.96 (t, $J = 10.4$, 1 H); 1.92–1.84 (m, 1 H); 1.78–1.67 (m, 4 H); 0.62 (d, $J = 7.2$, 3 H); 0.25 (d, $J = 7.2$, 3 H). ^{13}C -NMR (100 MHz, $CDCl_3$): 148.0; 146.6; 138.3; 128.9; 128.5; 128.2; 128.0; 127.0; 126.4; 125.7; 125.2; 91.3; 88.9; 67.5; 65.4; 48.1; 47.7; 47.2; 29.6; 27.1; 24.7; 20.9; 18.3. HR-ESI-MS: 501.2752 ($[M + H]^+$, $C_{31}H_{37}N_2O_4^+$; calc. 501.2748 (err., –0.8 ppm)).

(2R,3R,4S,5S)-Tetrahydro-5-nitro-4-phenyl-3-propyl-2H-pyran-2-ol (**16**). To a soln. of **22a** (18 mg, 0.031 mmol) in THF (0.2 ml), 3-nitrobenzoic acid (12.5 mg, 0.075 mmol) and H₂O (5.6 mg, 0.31 mmol) were added. The mixture was stirred at r.t. for 48 h, and then diluted with AcOEt, dried (Na_2SO_4), and concentrated. FC (hexane/AcOEt 4:1) afforded **16** (7 mg, 78%). R_f (hexane/AcOEt 4:1) 0.33. $[\alpha]_D^{25} = +13.3$ ($c = 0.26$, MeOH). 1H -NMR (300 MHz, $CDCl_3$): 7.33–7.28 (m, 3 H); 7.20–7.17 (m, 2 H); 5.32 (t, $J = 3.3$, 1 H); 4.88 (td, $J = 5.1$, 11.4, 1 H); 4.43 (t, $J = 10.5$, 1 H); 4.03 (dd, $J = 5.1$, 10.5, 1 H); 3.52 (t, $J = 11.7$, 1 H); 2.52 (dd, $J = 1.5$, 3.3, 1 H); 2.05–1.96 (m, 1 H); 1.40–1.25 (m, 2 H); 1.17–1.03 (m, 1 H); 0.98–0.88 (m, 1 H); 0.75 (t, $J = 6.9$, 3 H). HR-ESI-MS: 288.1210 ($[M + Na]^+$, $C_{14}H_{19}N_1Na_1O_4^+$; calc. 288.1206 (err., –1.4 ppm)). Data are in agreement with those in [27].

10. *Determination of the X-Ray Structures (Table 9)*. All structures were determined by the X-ray service unit of the Laboratorium für Organische Chemie, ETH-Zürich. Suitable single crystals were analyzed on Bruker Nonius Apex-II (for **4q**, **5d** and **21**) or Bruker Kappa Apex-II Duo (for **5b**, **5c** and **23**) CCD diffractometers with MoK α radiation (λ 0.71073 Å, graphite monochromator). Structures were solved by direct methods with SHELXL97 [53] and refined by full-matrix least-squares on F^2 (SHELXL97) [53]. If possible, the H-atoms were located from a difference electron-density map and refined isotropically or constrained at ideal positions and included in the structure factor calculation. The absolute configurations are determined by X-ray analyses or derived from the known sense of chirality of the chiral auxiliary (for **23**).

REFERENCES

- [1] D. Seebach, X. Sun, C. Sparr, M.-O. Elbert, W. B. Schweizer, A. K. Beck, *Helv. Chim. Acta* **2012**, 95, 1064.
- [2] B. List, R. A. Lerner, C. F. Barbas III, *J. Am. Chem. Soc.* **2000**, 122, 2395; K. A. Ahrendt, C. J. Borths, D. W. C. MacMillan, *J. Am. Chem. Soc.* **2000**, 122, 4243.

- [3] W. Langenbeck, 'Die Organischen Katalysatoren und ihre Beziehungen zu den Fermenten', Julius Springer, Berlin, 1935; G. Bredig, P. S. Fiske, 'Durch Katalysatoren bewirkte asymmetrische Synthese', *Biochem. Z.* **1912**, 46, 7.
- [4] J. M. Betancort, C. F. Barbas III, *Org. Lett.* **2001**, 3, 3737; K. Sakthivel, W. Notz, T. Bui, C. F. Barbas III, *J. Am. Chem. Soc.* **2001**, 123, 5260; J. M. Betancort, K. Sakthivel, R. Thayumanavan, C. F. Barbas III, *Tetrahedron Lett.* **2001**, 42, 4441.
- [5] B. List, P. Pojarliev, H. J. Martin, *Org. Lett.* **2001**, 3, 2423.
- [6] D. Enders, A. Seki, *Synlett* **2002**, 1, 26.
- [7] O. M. Berner, L. Tedeschi, D. Enders, *Eur. J. Org. Chem.* **2002**, 1877; J. M. Betancort, K. Sakthivel, R. Thayumanavan, F. Tanaka, C. F. Barbas III, *Synthesis* **2004**, 1509; W. Notz, F. Tanaka, C. F. Barbas III, *Acc. Chem. Res.* **2004**, 37, 580; O. Andrey, A. Alexakis, A. Tomassini, G. Bernardinelli, *Adv. Synth. Catal.* **2004**, 346, 1147; S. Sulzer-Mossé, A. Alexakis, *Chem. Commun.* **2007**, 3123; D. Enders, C. Grondal, M. R. M. Hüttl, *Angew. Chem.* **2007**, 119, 1590; *Angew. Chem., Int. Ed.* **2007**, 46, 1570; S. B. Tsogoeva, *Eur. J. Org. Chem.* **2007**, 1701; D. Almaşi, D. A. Alonso, C. Nájera, *Tetrahedron: Asymmetry* **2007**, 18, 299; P. H.-Y. Cheong, C. Y. Legault, J. M. Um, N. Ç.-Ölçüm, K. N. Houk, *Chem. Rev.* **2011**, 111, 5042; K. L. Jensen, G. Dickmeiss, H. Jiang, T. Albrecht, K. A. Jørgensen, *Acc. Chem. Res.* **2012**, 45, 248; C. Moberg, *Angew. Chem.* **2013**, 125, 2214; *Angew. Chem., Int. Ed.* **2013**, 52, 2160.
- [8] K. C. Brannock, A. Bell, R. D. Burpitt, C. A. Kelly, *J. Org. Chem.* **1964**, 29, 801; M. E. Kuehne, L. Foley, *J. Org. Chem.* **1965**, 30, 4280; A. Risaliti, M. Forchiassin, E. Valentin, *Tetrahedron Lett.* **1966**, 7, 6331; H. Feuer, A. Hirschfeld, E. D. Bergmann, *Tetrahedron* **1968**, 24, 1187; A. T. Nielsen, T. G. Archibald, *Tetrahedron* **1970**, 26, 3475; E. Valentin, G. Pitacco, F. P. Colonna, *Tetrahedron Lett.* **1972**, 13, 2837; F. P. Colonna, E. Valentin, G. Pitacco, A. Risaliti, *Tetrahedron* **1973**, 29, 3011; F. Felluga, P. Nitti, G. Pitacco, E. Valentin, *Tetrahedron* **1989**, 45, 5667; F. Felluga, P. Nitti, G. Pitacco, E. Valentin, *J. Chem. Soc., Perkin Trans. 1* **1992**, 2331; J. W. Huffman, M. M. Cooper, B. B. Miburo, W. T. Pennington, *Tetrahedron* **1992**, 48, 8213; R. Chinchilla, J.-E. Bäckvall, *Tetrahedron Lett.* **1992**, 33, 5644; D. Seebach, J. Goliński, *Helv. Chim. Acta* **1981**, 64, 1413; S. J. Blarer, W. B. Schweizer, D. Seebach, *Helv. Chim. Acta* **1982**, 65, 1637; S. J. Blarer, D. Seebach, *Chem. Ber.* **1983**, 116, 3086; D. Seebach, A. K. Beck, J. Goliński, J. N. Hay, T. Laube, *Helv. Chim. Acta* **1985**, 68, 162; D. Seebach, M. Missbach, G. Calderari, M. Eberle, *J. Am. Chem. Soc.* **1990**, 112, 7625.
- [9] a) R. Huisgen, *Acc. Chem. Res.* **1977**, 10, 117; b) R. Huisgen, *Acc. Chem. Res.* **1977**, 10, 199.
- [10] R. Häner, T. Laube, D. Seebach, *Chimia* **1984**, 38, 255.
- [11] R. B. Woodward, R. Hoffmann, *Angew. Chem.* **1969**, 81, 797; *Angew. Chem., Int. Ed.* **1969**, 8, 781; R. B. Woodward, R. Hoffmann, 'The Conservation of Orbital Symmetry', Verlag Chemie and Academic Press, Weinheim and New York, 1970; D. Seebach, 'Die 'Woodward-Hoffmann-Regeln'', *Fortschr. Chem. Forsch.* **1969**, 11, 177.
- [12] G. Sahoo, H. Rahaman, A. Madarász, I. Pápai, M. Melarto, A. Valkonen, P. M. Pihko, *Angew. Chem.* **2012**, 124, 13321; *Angew. Chem., Int. Ed.* **2012**, 51, 13144.
- [13] M. Miyashita, T. Yanami, A. Yoshikoshi, *J. Am. Chem. Soc.* **1976**, 98, 4679; A. Yoshikoshi, M. Miyashita, *Acc. Chem. Res.* **1985**, 18, 284; D. Seebach, M. A. Brook, *Helv. Chim. Acta* **1985**, 68, 319; M. A. Brook, D. Seebach, *Can. J. Chem.* **1987**, 65, 836; M. A. Brook, R. Faggiani, C. J. L. Lock, D. Seebach, *Acta Crystallogr., Sect. C* **1988**, 44, 1981; S. E. Denmark, A. Thorarensen, *Chem. Rev.* **1996**, 96, 137; D. Seebach, I. M. Lyapkalo, R. Dahinden, *Helv. Chim. Acta* **1999**, 82, 1829; Y. A. Khomutova, V. O. Smirnov, H. Mayr, S. L. Ioffe, *J. Org. Chem.* **2007**, 72, 9135.
- [14] K. Patora-Komisarska, M. Benohoud, H. Ishikawa, D. Seebach, Y. Hayashi, *Helv. Chim. Acta* **2011**, 94, 719.
- [15] Y. Hayashi, H. Gotoh, T. Hayashi, M. Shoji, *Angew. Chem.* **2005**, 117, 4284; *Angew. Chem., Int. Ed.* **2005**, 44, 4212.
- [16] J. Burés, A. Armstrong, D. G. Blackmond, *J. Am. Chem. Soc.* **2011**, 133, 8822.
- [17] a) J. Burés, A. Armstrong, D. G. Blackmond, *J. Am. Chem. Soc.* **2012**, 134, 6741; b) J. Burés, A. Armstrong, D. G. Blackmond, *J. Am. Chem. Soc.* **2012**, 134, 14264.
- [18] a) A. J. Kirby, 'Stereoelectronic Effects' Oxford University, New York, 1996; P. Deslongchamps, 'Stereoelectronic Effects in Organic Chemistry', Pergamon, Oxford, 1983; b) D. Seebach, U.

- Grošelj, D. M. Badine, W. B. Schweizer, A. K. Beck, *Helv. Chim. Acta* **2008**, *91*, 1999; U. Grošelj, D. Seebach, D. M. Badine, W. B. Schweizer, A. K. Beck, I. Krossing, P. Klose, Y. Hayashi, T. Uchimaru, *Helv. Chim. Acta* **2009**, *92*, 1225.
- [19] J. Duschmalé, M. Wiesner, J. Wiest, H. Wennemers, *Chem. Sci.* **2013**, *4*, 1312.
- [20] M. J. D'Aniello Jr., E. K. Barefield, *J. Am. Chem. Soc.* **1978**, *100*, 1474; N. Zotova, A. Moran, A. Armstrong, D. G. Blackmond, *Adv. Synth. Catal.* **2009**, *351*, 2765.
- [21] H. Ishikawa, T. Suzuki, Y. Hayashi, *Angew. Chem.* **2009**, *121*, 1330; *Angew. Chem., Int. Ed.* **2009**, *48*, 1304; H. Ishikawa, T. Suzuki, H. Orita, T. Uchimaru, Y. Hayashi, *Chem. – Eur. J.* **2010**, *16*, 12616.
- [22] S. Zhu, S. Yu, Y. Wang, D. Ma, *Angew. Chem.* **2010**, *122*, 4760; *Angew. Chem., Int. Ed.* **2010**, *49*, 4656; S. Zhu, S. Yu, D. Ma, *Angew. Chem.* **2008**, *120*, 555; *Angew. Chem., Int. Ed.* **2008**, *47*, 545.
- [23] a) J. Rehák, M. Hut'ka, A. Latika, H. Brath, A. Almássy, V. Hajzer, J. Durmis, Š. Toma, R. Šebesta, *Synthesis* **2012**, *44*, 2424; b) M. Hut'ka, V. Poláčková, J. Marák, D. Kaniánsky, R. Šebesta, Š. Toma, *Eur. J. Org. Chem.* **2010**, 6430; c) V. Hajzer, A. Latika, J. Durmis, R. Šebesta, *Helv. Chim. Acta* **2012**, *95*, 2421; d) E. Veverková, V. Poláčková, L. Liptáková, E. Kázmerová, M. Mečiarová, Š. Toma, R. Šebesta, *ChemCatChem* **2012**, *4*, 1013; e) J. Weng, Y.-B. Li, R.-B. Wang, G. Lu, *ChemCatChem* **2012**, *4*, 1007.
- [24] H. Uehara, C. F. Barbas III, *Angew. Chem.* **2009**, *121*, 10032; *Angew. Chem., Int. Ed.* **2009**, *48*, 9848.
- [25] a) H. Eyring, G. H. Stewart, R. P. Smith, *Proc. Natl. Acad. Sci. U.S.A.* **1958**, *44*, 259; b) R. C. Bingham, *J. Am. Chem. Soc.* **1976**, *98*, 535; c) R. K. Chaudhuri, J. R. Hammond, K. F. Freed, S. Chattopadhyay, U.S. Mahapatra, *J. Chem. Phys.* **2008**, *129*, 064101-1; d) R. Ahlrichs, F. Furche, C. Hättig, W. Klopper, M. Sierka, F. Weigend, <http://www.turbomole-gmbh.com/>, accessed January 12, 2013; e) A. D. Becke, *Phys. Rev. A* **1988**, *38*, 3098; f) J. P. Perdew, *Phys. Rev. B* **1986**, *33*, 8822; g) S. Grimme, J. Antony, S. Ehrlich, H. Krieg, *J. Chem. Phys.* **2010**, *132*, 154104; h) K. L. Brown, L. Damm, J. D. Dunitz, A. Eschenmoser, R. Hobi, C. Kratky, *Helv. Chim. Acta* **1978**, *61*, 3108; i) A. Kümin, E. Maverick, P. Seiler, N. Vanier, L. Damm, R. Hobi, J. D. Dunitz, A. Eschenmoser, *Helv. Chim. Acta* **1980**, *63*, 1158; j) R. Hobi, ETH Dissertation No. 6030 (1977); k) D. Seebach, A. K. Beck, D. M. Badine, M. Limbach, A. Eschenmoser, A. M. Treasurywala, R. Hobi, W. Prikozovich, B. Linder, *Helv. Chim. Acta* **2007**, *90*, 425; l) D. Seebach, R. Gilmour, U. Grošelj, G. Deniau, C. Sparr, M.-O. Ebert, A. K. Beck, L. B. McCusker, D. Šišak, T. Uchimaru, *Helv. Chim. Acta* **2010**, *93*, 603.
- [26] S. Bahmanyar, K. N. Houk, H. J. Martin, B. List, *J. Am. Chem. Soc.* **2003**, *125*, 2475.
- [27] Y. Wang, S. Zhu, D. Ma, *Org. Lett.* **2011**, *13*, 1602.
- [28] L. Wang, X. Zhang, D. Ma, *Tetrahedron* **2012**, *68*, 7675.
- [29] a) L. Guo, Y. Chi, A. M. Almeida, I. A. Guzei, B. K. Parker, S. H. Gellman, *J. Am. Chem. Soc.* **2009**, *131*, 16018; b) B. Stevenson, W. Lewis, J. Dowden, *Synlett* **2010**, 672.
- [30] O. Andrey, A. Vidonne, A. Alexakis, *Tetrahedron Lett.* **2003**, *44*, 7901.
- [31] J. Duschmalé, H. Wennemers, *Chem. – Eur. J.* **2012**, *18*, 1111.
- [32] W. N. Speckamp, M. J. Moolenaar, *Tetrahedron* **2000**, *56*, 3817.
- [33] E. W. Colvin, A. K. Beck, D. Seebach, *Helv. Chim. Acta* **1981**, *64*, 2264.
- [34] E. W. Colvin, A. D. Robertson, D. Seebach, A. K. Beck, *J. Chem. Soc., Chem. Comm.* **1981**, 952.
- [35] D. Seebach, E. W. Colvin, F. Lehr, T. Weller, *Chimia* **1979**, *33*, 1; N. Ono, 'The Nitro Group in Organic Synthesis', Wiley-VCH, New York, 2001.
- [36] V. O. Smirnov, Y. A. Khomutova, V. A. Tartakovsky, S. L. Ioffe, *Eur. J. Org. Chem.* **2012**, 3377.
- [37] a) M. Wiesner, J. D. Revell, H. Wennemers, *Angew. Chem.* **2008**, *120*, 1897; *Angew. Chem., Int. Ed.* **2008**, *47*, 1871; b) M. Wiesner, J. D. Revell, S. Tonazzi, H. Wennemers, *J. Am. Chem. Soc.* **2008**, *130*, 5610; c) M. Wiesner, M. Neuburger, H. Wennemers, *Chem. – Eur. J.* **2009**, *15*, 10103; d) M. Wiesner, G. Upert, G. Angelici, H. Wennemers, *J. Am. Chem. Soc.* **2010**, *132*, 6; e) M. Wiesner, H. Wennemers, *Synthesis* **2010**, 1568; f) Y. Arakawa, M. Wiesner, H. Wennemers, *Adv. Synth. Catal.* **2011**, *353*, 1201; g) M. Messerer, H. Wennemers, *Synlett* **2011**, 499; h) Y. Arakawa, H. Wennemers, *ChemSusChem* **2013**, *6*, 242.
- [38] M. Wiesner, Dissertation, Universität Basel, 2009.
- [39] R. Carlson, T. Hudlicky, *Helv. Chim. Acta* **2012**, *95*, 2052.
- [40] M. Brenner, D. Seebach, *Helv. Chim. Acta* **1999**, *82*, 2365.

- [41] D. Seebach, M. Brenner, M. Rueping, B. Jaun, *Chem. – Eur. J.* **2002**, *8*, 573.
- [42] D. Enders, C. Wang, X. Yang, G. Raabe, *Adv. Synth. Catal.* **2010**, *352*, 2869.
- [43] C. Giondali, M. Jeanty, D. Enders, *Nat. Chem.* **2010**, *2*, 167.
- [44] G. Talavera, E. Reyes, J. L. Vicario, L. Carrillo, *Angew. Chem., Int. Ed.* **2012**, *51*, 4104.
- [45] D. B. Ramachary, R. Sakthidevi, *Org. Biomol. Chem.* **2010**, *8*, 4259.
- [46] L. Albrecht, G. Dickmeiss, F. C. Acosta, C. Rodríguez-Esrich, R. L. Davis, K. A. Jørgensen, *J. Am. Chem. Soc.* **2012**, *134*, 2543; C. Cassani, P. Melchiorre, *Org. Lett.* **2012**, *14*, 5590.
- [47] G. Quinkert, E. Egert, C. Griesinger, 'Aspekte der Organischen Chemie : Struktur', Verlag Helvetica Chimica Acta, Basel, 1995; G. Quinkert, E. Egert, C. Griesinger, 'Aspects of Organic Chemistry: Structure', Verlag Helvetica Chimica Acta, Basel, 1996.
- [48] D. Seebach, B. Lamatsch, R. Amstutz, A. K. Beck, M. Dobler, M. Egli, R. Fitzi, M. Gautschi, B. Herradón, P. C. Hidber, J. J. Irwin, R. Locher, M. Maestro, T. Maetzke, A. Mourilo, E. Pfammatter, D. A. Plattner, C. Schickli, W. B. Schweizer, P. Seiler, G. Stucky, W. Petter, J. Escalante, E. Juaristi, D. Quintana, C. Miravittles, E. Molins, *Helv. Chim. Acta* **1992**, *75*, 913.
- [49] B. Lamatsch, D. Seebach, *Helv. Chim. Acta* **1992**, *75*, 1095.
- [50] U. Grošelj, W. B. Schweizer, M.-O. Ebert, D. Seebach, *Helv. Chim. Acta* **2009**, *92*, 1; D. Seebach, U. Grošelj, W. B. Schweizer, S. Grimme, C. Mück-Lichtenfeld, *Helv. Chim. Acta* **2010**, *93*, 1; D. Seebach, A. K. Beck, H.-U. Bichsel, A. Pichota, C. Sparr, R. Wünsch, W. B. Schweizer, *Helv. Chim. Acta* **2012**, *95*, 1303.
- [51] S. E. Denmark, L. R. Marcin, *J. Org. Chem.* **1995**, *60*, 3221; B.-L. Zhang, F.-D. Wang, J.-M. Yue, *Synlett* **2006**, 567; C.-L. Cao, Y.-Y. Zhou, J. Zhou, X.-L. Sun, Y. Tang, Y.-X. Li, G.-Y. Li, J. Sun, *Chem. – Eur. J.* **2009**, *15*, 11384.
- [52] S. Kobayashi, T. Kinoshita, H. Uehara, T. Sudo, I. Ryu, *Org. Lett.* **2009**, *11*, 3934.
- [53] G. M. Sheldrick, *Acta Crystallogr., Sect. A* **2008**, *64*, 112.

Received February 7, 2013